2010

An investigation of the microwave-stimulated reduction of oxides of refractory metals

Jeffrey John Tanner-Jones
University of Wollongong

AN INVESTIGATION OF

THE MICROWAVE - STIMULATED REDUCTION OF

OXIDES OF REFRACTORY METALS.

A thesis submitted in accordance with subject MATL 957

and in partial fulfilment of the requirements for the award

of the degree of

Doctor of Philosophy

from

The University of Wollongong

by

Jeffrey John Tanner-Jones

BMet (W'gong), DipMet (W'gong).

Supervisors:

Professor Howard K. Worner (deceased)

Professor Noel F. Kennon (retired)

Professor Druce P. Dunne.

Faculty of Engineering,
Discipline of Materials Engineering.

2010

For my father,

JACK TANNER

(23 November, 1922 – 20 March, 1952).

To have known you.

Wishes – not granted, ne'er realised. Hope alone survived

To be with you.

Gentleman exemplar, supervisor and role-model, colleague and collaborator,
mentor and friend.

This thesis is dedicated to the memory of

HOWARD KNOX WORNER, CBE, FAA, FTS

DSc(Melb), HonDEng(Melb), HonDSc(N'castle), Hon DSc(W'gong)

ABSM, CEng, HonFIEAust, HonFAusIMM, FRACI, FIM, FIMM, FAIE, FIMMA, MAIME

3 August, 1913 - 17 November, 2006

PROFESSOR EMERITUS

THE UNIVERSITY OF WOLLONGONG

To one who encouraged me to accept all evidence;
to enquire of all evidence, to observe, to test and evaluate, and
once appraised, to let the facts embolden.
Then ask, *How?* And so,
beyond the obvious, to enquire laterally for the unexpected, for the plausible; to
seek and interrogate all possibilities. Then to re-examine the known.
To reason imaginatively … and, *sans cérémonie,* to never accept an orthodoxy.
And, with euphony of method, … to *know* you are correct.
Then to defend what you know.

Perhaps I have acquired some little of all this.

I hereby affirm that neither this thesis nor the work contained herein have previously been submitted, either in part or in full, at any institution for the award of any degree or testamur. Essentially, the work was carried-out by the candidate in the Faculty of Engineering and other relevant units of the University of Wollongong, Wollongong, Australia.

Jeffrey Tanner-Jones.

SYNOPSIS.

The experimental programme of this thesis project was designed to explore the potential of microwave-stimulated reduction of refractory metal minerals in both "mine concentrate" mineral form and in the "pure" oxide mineral form. Representing the five refractory metals titanium, zirconium, hafnium, niobium and tantalum, the core minesite-derived minerals selected were rutile, ilmenite, zircon and the tantalite-like mineral wodginite, all oxidic minerals, whilst the "pure" standard oxides selected were TiO_2, ZrO_2, HfO_2, Nb_2O_5 and Ta_2O_5. By like means, the minerals of these groups were reduction-processed utilising an innovative plasma technique whose applications and methods are described herein. It was found that, across the range of microwave-stimulated reduction of core refractory metal minerals, both concentrate minerals and pure oxide minerals could be effectively reduced to metallic phases.

Fundamental in this study was that the experimental programme should identify reduction capabilities, alternative extraction route possibilities and process options; this was a keystone study of microwave reduction applied to obdurate minerals. As such, the intention of the study was to underpin further-stage initiatives in advancing microwave-stimulated extractive pyrometallurgy and allied applications. To this end, across the scope of experimentation, the reduction of refractory metal oxides to realise metallic product by means of elementary reduction processes whilst employing such basic reduction procedures suggested the potential for extractive processing routes leading to commercial-grade metal products – outcomes parallel and equivalent to those of conventional routes.

Whilst reduction directly from the metal oxide represents neither a new reduction strategy nor a new production route, the direct microwave-stimulated reduction of thermochemically obdurate refractory metal oxides is novel. Incorporating both carbothermic and metallothermic means of reduction across the experimental programme, the microwave-stimulated reduction method devised was used throughout the core programme of experimental reduction exercises. Being complementary to these core refractory metal results, various instructive "non-core" reduction results are also reported whilst examples of microwave initiated "metal halide" reduction afford comparability with the conventional Kroll and Hunter industrial production processes.

Ultimately, in this foundation project, it was considered that sufficient tangible evidence was accumulated during broader characterisation and analyses of reduction product specimens to contend that essentially pure metal was produced transiently under the experimental conditions before the onset of "over-processing" that produced solid solution and metallic compound phases. And further, system deficiencies and exothermic contributions aside, that refractory metals of good purity can be efficiently reduced from their stable oxide minerals under an extractive metallurgical regime utilising microwave-stimulation to supply the external (or "applied") energy into the system so initiating and sustaining – and generally integral with – its non-equilibrium plasma environment.

CONTENTS.

VOLUME I.

"Truth is never pure, and rarely simple."

Oscar Wilde.

PREAMBLE:

Refractory Metals, Microwave Reduction, Project Concept and Opportunity.

The refractory metals are those nine transition metals presenting in Groups **4, 5** and **6** of the Periodic Table of the Elements and occupying the first, second and third long Periods (representing the **3d**, **4d** and **5d** orbitals (respectively) of the **N**, **O** and **P** electron shells). Dependent upon application-based industry perspectives, vanadium and/or chromium are/(is) sometimes omitted from this general group of transition metals. The refractory metals of interest in this project are the Group **4** metals titanium, zirconium and hafnium and the Group **5** metals niobium and tantalum. In essence, these five elements are represented in three ore-derived mineral groups mined in only two mining-operation types and together represent a disproportionately large (but greatly under-valued and under-rewarded) portion of Australia's export income.

The refractory metals have physical, chemical and mechanical properties that ensure their specification for a diverse range of applications from plain domestic to the specialised and technological. Their high melting point, toughness and strength (particularly at elevated temperatures), strength-to-weight ratio, corrosion resistance and nuclear and electronic properties are among those which ensure that refractory metals are extensively utilised in the aerospace, metals fabrication and manufacturing, construction, chemical, nuclear and electronics industries. Much current, post-primary metallurgical research is aimed at the development of new and performance-improved refractory metal alloys, intermetallic compounds, hard materials and composites to provide advanced high temperature, corrosion resistant materials that will extend the utilisation potential of metals from this group. Accordingly, in order to meet an increasing demand, formerly unproven and obsolete production-route processes must be re-evaluated, established processes reviewed and upgraded, and new extractive metallurgical processing routes and strategies investigated by the refractory metals production industry. This industry is ever pressed to decrease production costs whilst increasing production tonnages in order to supply lower-priced refractory metal products across the range of commercial mill specifications. In acknowledging these factors, this project examines the potential of a new extractive technique; and in doing

so, an intuitive and innovative approach to metallurgical reduction processing is embraced.

The pyrometallurgical reduction of refractory metal oxides using conventional technologies has been a commercial rarity because the extended high temperature processing regimes required are above practicable reactor-vessel lining specifications. Whilst other chemical or electro-winning variations may exist, regular industrial production routes for refractory metals see ore-derived mineral concentrates solution-treated to obtain the "pure" oxide(s), converted to metal halide (normally chloride) followed by fractional distillation to obtain the pure halide, *thence* metallothermically reduced to the pure metal. With variations for the different refractory metals – and if convoluted – the well documented, generally long-established industrial halide-based extractive routes are well proven, as evidenced by their commercial history.

The work described herein will demonstrate that the thermodynamically stable refractory metal oxide minerals sourced from both commercially pure (including laboratory grade) minerals and a range of minesite-derived ore-mineral concentrates can be efficiently reduced to stable metallic phases utilising microwave-stimulated plasma-based pyrometallurgical techniques to drive carbothermic or metallothermic reactions. Similarly, the work will reveal how refractory metal halides can be reduced by thermal decomposition, or "disproportionation", employing techniques that utilise the intricate but versatile thermochemistry of microwave stimulation.

The microwave stimulation techniques employed are essentially novel and, of necessity, are fundamentally simple in experimental character and configuration but show a potential to be gainfully upgraded with respect to reduction product quality, quantity and percentage yield. Process advantages arising from this intimate application of energy are derived from variations in microwave susceptibility in the charge components – that is, the dielectric load in the blend materials – giving rise to a characteristic temperature profile that controls the heating regime and, therefore, the reaction zones in the charge. Pertinently, microwave-initiated reactions are concentrated in the dielectric load centre, so evolved heat (from applied microwave energy plus exothermic energy) is expediently retained centrally in the reactant blend bulk, where its function is best realised at the seat of reaction chemistry and away from refractory

linings or crucible wall. Thus, by design, microwave heating and processing can be strategically configured to extend refractory life and, consequently, to prolong crucible or reactor vessel campaigns whilst facilitating a contained reaction zone requiring reduced process (reaction) time. To an extent, these "physical" aspects of microwave processing are misleadingly consistent with concepts of system equilibrium.

As with comparable microwave systems, however, the metallurgical system (as investigated) is a system operating under conditions of thermal non-equilibrium, or non-equilibrium thermodynamics, and specifically, a system whose thermochemistry is dictated by the reactive species and overall ionisation chemistry of microwave-stimulated non-equilibrium plasma. The plasma chemistry in pyrometallurgical reaction zones is characterised by high populations of highly reactive species in environments of comparably low sensible (bulk) "temperature" and (for plasma environments) at "high" relative reaction-environment pressures up to one atmosphere. These system variables will contribute to successful process outcomes across the microwave reduction programme, particularly in the cases of anatase/rutile, ilmenite, zircon and wodginite – all commercially significant minerals to Australia. Therefore, the research programme will validate the worth of microwave processing to extractive metallurgical applications and, more broadly, to a range of complementary and comparable industrial applications.

AN INVESTIGATION OF

THE MICROWAVE - STIMULATED REDUCTION OF

OXIDES OF REFRACTORY METALS.

VOLUME I

[Introductory sections up to Section 6.]

1

INTRODUCTION.

"There is no unhappier creature on earth than a fetishist who yearns for a woman's shoe and has to embrace the whole woman."

Karl Kraus - 1909.

1 : INTRODUCTION.

The capability to extract, fabricate and utilise metals has represented the technological hallmark of civilisations for thousands of years. Metallurgy has distinguished and identified cultures. It has determined, and is idiosyncratic of, the socio-political achievement of civilisations in the ranking of nations and has exemplified their eventual significance in the flight of history. Empires rose and fell and civilisations flourished or perished in accord with their relative abilities to master the military and commercial arts and crafts of metallurgy. Any reflection upon contemporary history will confirm that little has changed in the making and shaping of the perplexing social and political dynamics of our modern world. The extraction, fabrication and utilisation of metallic and related materials are still as central in the prevailing contemporary technologies as they have been in millennia past. Throughout human history's Ages of Metals - and across cultures and civilisations – the prevalent metallurgical technologies have, in near totality, represented the concept of "advanced technology". Hereunto, that ancient root "metallurgy" yet occupies a substantial portion of the human ingenuity which is perceived to be modern advanced technology.

During the twentieth century and into the dawn of this twenty-first, technical knowledge has accumulated extraordinarily at exponential rates as has our capacity to exploit the power of this body of knowledge; knowledge constantly reviewed, revised and augmented. Consequently, developments in extraction, refinement, fabrication, heat and corrosion treatment and finishing technologies for metals (and materials generally) have stimulated and advanced technical and production capabilities. Today, a broad range of metallic materials is available to provide cost-efficient solutions to satisfy remarkably diverse engineering and general applications.

Modern industrial technologies specify the use of metals in applications where resistance to the effects of corrosion, wear, high or low temperatures, or high-impact loading is required, and in long-term or cyclic applications where high compressive and high tensile load-bearing capabilities are demanded in structural members and general components in manufacture. In particular, metals are used in structural and general engineering applications when service assuredness and longevity are essential. Furthermore, metals are utilised for (either) their low or high mass in density-dictated

applications or where a high strength-to-weight ratio is required; for their electronic properties in electrical and electronics applications; for their nuclear or radioactive properties in nuclear medicine and nuclear power applications; for their liquid properties in sensors or as coolants in high-flux heat transfer applications; for their craft-workability and perceived aesthetic beauty in jewellery and ornamental artistry; for their malleability or ductility in a range of trade and craft applications; for their rigidity in a range of engineering applications; for their durability in coinage; and for a host of other, more obscure physical and chemical applications. Metals can be cast, hot or cold worked, forged, extruded, rolled, formed, drawn, *et cetera* during primary manufacture, and may be punched, swaged, cut, drilled, reamed, tapped, brazed, welded, ground, plated, *et cetera* during subsequent fabrication. Across the spectrum of material families, the metals families are versatile; they provide broad, commonly superior utility in manufacture, fabrication and application. Metals are widely and successfully used.

Some metals, especially those of the refractory metals group, are employed in crystalline conjunction with light elements as compounds or with other metals as intermetallic compounds, or with these light and metallic elements in the non-integer stoichiometric continua of solid solutions (alloys); these find use in technically specific applications. Such specific applications of these compounds and alloys utilise their electronic and physical properties in diverse applications as capacitors, superconductors, thermocouples, hard materials in metal matrix composites, structural and sheet components in aerospace and construction applications, and an extensive list of established and evolving applications – furthermore, these mostly are applications of noteworthy technological consequence. Also, of these materials, the product compounds and solid solutions of metals and light elements are commonly and too easily classified as "ceramics" - that is, as "non-metallic" materials*. Nonetheless, there remains much of the "metallic" about such metal/light-element materials and their grouping here with other metallic materials is relevant, especially so in their inclusion with refractory metals – it is not simply the metallic *elements* which are fundamental in this project, but

* [This strict "ceramics" labelling of such materials has derived from the "incomplete facts" conveniently accorded the scientific definition of "ceramic". This because of the size and strength of the Ceramics Sector, the worldwide numerical strength and influence of integrated and associated professional groups – the momentum of whose predisposition is dictated by industrial agenda, and the inflexible, indoctrinated commercial culture of "standardisation by definition and regulation" which has seen a narrow, simplistic definition of "ceramic" evolve in the Literature.]

the *real metallic materials* of those elements – particularly as they occur as or amongst the real products of reduction operations.

Metallic materials are constantly encountered in general and special applications in everyday life. Quite simply, metals are the backbone of engineering fabrication and of manufacturing generally. Of these, the transition metals of Groups **4**, **5** and **6** - the refractory metals - make prominent, even unique contributions to engineering and manufacturing through their material properties. They have high melting points, high corrosion resistance, high strength (including strength at high temperature) and are ductile in the pure state. The refractory metals have many specialty applications in their pure or near-pure states and lend highly desirable and much sought properties to engineering alloys – most commonly to steels for structural and hard-face applications and to aluminium alloys for aerospace applications. Refractory metals are absolutely central to the materials technologies of intermetalics and hard materials and, consequently, in derivative technologies such as metal matrix composites (or cermets) and ensuing integrated technologies including tooling for cutting and machining operations.

Because of their high thermochemical stability, refractory metal ores provide extractive processors with innumerable process problems in complex and costly extractive production routes. These high cost, highly valued metals are regarded, in both the commercial and military contexts of world commodity economics, as "strategic" metals. This strategic categorisation, and the technical sophistication required for their production, fabrication and utilisation, has ensured that the world production of certain metals including the nine refractory metals has been restricted. World production capabilities for five of the refractory metals central to Australian exports - titanium, zirconium, hafnium, niobium and tantalum - has been limited to a few corporations operating in equally few nations which have collusively manipulated markets, resource developments and raw material supplies to maintain control over the world supply of these metals [1, 2, 77]. Consequently, their production is limited, almost exclusively, to the United States of America, Russia, Japan, China, India and a few European Union nations.

Central in the envisaging of this project was the observation that three of Australia's largest exports, each only minimally value added – denying the great majority of their intrinsic commodity value at export, are represented in three mineral groups mined in only two mining operation types. These three export commodities are titanium, zirconium and tantalum. Of these, two concurrently occur in intimate mineralogical association with minor components hafnium (with zirconium in Australian zircon) and niobium (with tantalum in Australian wodginite and tantalite minerals) and so report in their mineral concentrate products and represent valuable by-products. Of these five refractory metals, titanium, zirconium and hafnium are the three Group **4** elements and niobium and tantalum are two of the three Group **5** elements. Notably, these five elements provide the most thermodynamically stable (most difficult to reduce) oxides of the nine refractory metals, a fact presenting a desirable challenge in the project. So, essentially, from three mineral groups, mined in two types of mining operation, the five refractory metals fundamental in the project are sourced and recovered in complex extractive processing streams. And, other valuable metals such as tin, rare earth elements lanthanum, cerium, neodymium, samarium, europium and others plus the trans-uranic element thorium are variously recovered in these operations processing mineral sands and wodginite/tantalite concentrates.

Australia is the world's largest producer and exporter of mineral-sands-derived ore concentrates, historically these are recovered from quarternary mineral sands deposits along the east and west coasts of Australia. The derived mineral sand concentrates include the principal titanium minerals rutile, ilmenite and leucoxene, the principal zirconium and hafnium mineral zircon, also the valuable rare earth and trans-uranic minerals xenotime and monazite plus several others. [The rutile-like titanium mineral anatase will soon become prominent when exploitation of the deep Murray Basin deposits is realised.] Because (if they are processed at all) Australia processes these concentrate minerals (at best) only to their minimum point of saleability - that is, to the point of *beneficiated* mineral - Australia is also the world's largest exporter of mineral-sands-derived refractory metal and rare earth minerals.

The largest tantalum-source deposit in the world is at Wodgina in north-western Australia. [Of comparable size to the weathered pegmatite deposit of Wodgina are the tantalum reserves of the Mount Weld carbonatite province in northern Western

Australia's Pilbara region – still undeveloped with respect to tantalum/(niobium), and the large but largely expended placer deposits at Greenbushes in southern Western Australia.] From the Wodgina deposit, the largest producer/exporter in the world mines ternary ore to supply wodginite – a principal tantalum/(niobium)/tin ore concentrate which is beneficiated, retrieving the tin, removing the gangue elements and supplying a tin-free synthetic tantalite/(columbite) for export to foreign processors. [Other primary Wodginite gangue elements – principally manganese, iron and minor titanium – could, in future, also be recovered for their significant value.]

These primary products earn Australia enormous export income, however, as primary exports they cost Australia a far greater potential income in lost secondary and tertiary production opportunities – specifically in terms of the loss of a "value-added" component. Not only does this potential value-add greatly exceed the value of primary export earnings from the beneficiated mineral as exported [by between 10 and 400 times (1,000 % and 40,000 %), mineral dependent], but this unequivocally ***lost*** value-added component represents a ***lost*** theoretical export income which is, and has been for many years, considerably greater than Australia's total export income[1]. This massive inequity of realised value-add is earnings forfeited – national opportunities wasted! Even by any modest application of the value-add component, this astonishingly neglectful loss amounts to breathtaking national resource mismanagement. Remarkably few Australians are aware of the fact; and resource companies, bureaucracies and Governments are unwilling, as resource analysts and information outlets are inept, to either highlight or change the fact of this massive multinational exploitation and expatriation of national wealth. In terms of the value-added component of end-product (either actual end-product or theoretical ultimate end-product), far more income is conceded by Australia to those "strategically" sanctioned nations which import Australian refractory metal minerals than is earned by Australia (in exporting those minerals) in either export income or export profit terms. Further exacerbating the loss-at-export inequity is the ultimate cost-premium indignity of initially forfeiting the value-add upon export, then paying for the commodity plus the value-add upon importing the original commodity as a finished product – a very common experience in Australia (although, amongst consumers, a slight of international commerce that is commonly concealed or ignored). [By way of simple example, consider the proportion of iron ore

exports to Japan, South Korea and China which is returned to Australia as motor vehicles and other steel manufactures – a value-add loss of 5.3 (530 %) from high grade haematite (iron ore) to plain carbon steel[1].]

Progress in all fields of broader scientific endeavour and the more specific endeavours of metallurgical investigation - from pure research to product development and from extractive processes to finishing technologies - has advanced the family of metallurgical technologies. Developments in the broad metallurgical field of extractive processing have reflected this burgeoning technological evolution. New processes in extractive pyrometallurgy have kept this age-old extractive method competitively apace with the alternative contemporary process routes of hydrometallurgy and chemical metallurgy (including electrowinning). Microwave-stimulated processes present new and exciting possibilities of very highly populated reactive species environments and/or very-high temperature extractive metallurgical reduction, sublimation, dissociation and decomposition routes in the winning of metallic materials. That is, high populations of highly energetic requisite reactant species leading to thermochemically desirable process outcomes.

The project described in this thesis embraced microwave processing and was conceived and nurtured during several inspired discussions with Professor Howard K. Worner in late 1987. In essence, the project reflects observations of aspects of pioneering experimentation involving complementary microwave-stimulated processes. Professor Worner and others had identified that, amongst other susceptible materials, many minerals and carbonaceous materials were highly receptive of "microwave energy" - this energy being transferred from the microwave field through the dielectric loss characteristic of the load material under irradiation and sensibly registered as heat - and that this energy could be harnessed to stimulate desirable chemical reactions in the irradiated load. It was decided that this concept required testing in the more specific field of reduction reactions of metalliferous minerals and ores. Further, to extend and test the efficacy of microwave-stimulation, the refractory metals were chosen to further challenge and specify the task. [Refractory metals have high melting points and

consequently occur in minerals (both synthesised and naturally-occurring) characterised by high thermodynamic stability and consequently demand complex reduction routes requiring significant energy per unit produced.] Of the refractory metals ores, those of highest thermodynamic stability are also those of enormous economic significance to Australia. So, the project was conceived to investigate the microwave-stimulated reduction of those mineral sands which source the Group **4** elements titanium, zirconium and hafnium, and the tin-rich tantalite-type mineral wodginite that yields the Group **5** elements niobium and tantalum.

In an extension to earlier work, the feasibility of utilising the transferred energy of microwave irradiation to stimulate and thermodynamically catalyse chemical reactions in minerals in an environment of microwave plasma was examined. Particular attention was devoted to the "completeness" of reduction of those thermochemically highly stable pure oxides and principally-oxide minerals of refractory metals which are significant in Australia's export commerce. Whilst these minerals respond to microwave stimulation with a range of dielectric susceptibilities from modest to high, they also exhibit a keen thermal resilience to conventional pyrometallurgical reduction and a high resistance to chemical attack generally.

The rapid and unique thermal processing characteristics of microwave heating, the microwave susceptibilities of both reductant and reactant minerals, and the advantageous thermodynamics and kinetics of non-equilibrium low-temperature plasma chemistry were utilised in this project to produce metallic reduction products from highly stable minerals in reduction systems of low sophistication. Experimental systems employed simple apparatus configurations which produced experimental yields of high conversion percentage and high metallic quality (given the primary extractive nature of most processes investigated). The development of process sophistication and system apparatus was limited (in part by funds and) by a fundamental and deliberate philosophy of simplicity in experimentation which allowed the breadth of scope which was encompassed in the project. It was essential in the project to maintain a degree of flexibility so that the true "survey of the feasibility" of microwave-stimulated reduction processes could be appropriately addressed. In this regard, the final scope of the project

- whilst remaining general - was considerably more limited than the initially envisaged scope. With such a void in the published literature in the overall area of microwave-stimulated reduction there was no real opportunity for a highly specific study; and so a survey was seen to represent the most propitious contribution the project could make to this new body of knowledge.

During the course of the project, the propensity to upgrade process systems used in experimentation was considered, each time with forethought – in light of, and as concession to commercial reality. The possibility of further technical development and scaling-up of systems to pilot plant scale, thence commercial plant scale, was to be deliberated in the context of experimental achievement. The general acceptance of microwave heating technology was challenged by the fact that the hardware of microwave systems and associated application devices required to transform experimental success to industrial reality had not been industrially proven. This lack of technological proven-ness at the industrial scale presented a conceptual dilemma to process development. In particular, the extension of microwave applications into the very high temperature regions of solids and liquids processing and the ultra high temperature regions for vapour, gas and plasma phase processing presented new and persistent problems of process containment as process vessel refractory material melting-points were routinely exceeded.

The thesis addresses both the conventional and the novel aspects of a field in which little has been published or publicly acknowledged – a field which is new and which promises enormous scientific and commercial potential. Section **2** of this thesis introduces the refractory metals, their properties and their utilisation. Aspects of conventional reduction process routes for refractory metal ores are addressed in Section **3** whilst comparable microwave reduction processes are introduced and contrasted with the conventional in Section **4**. Section **5** of the thesis introduces the methodology employed in experimental work, the problems encountered with microwave heating at the experimental scale, the dilemmas of sampling hard reduction product and its heterogeneity, and strategies for analyses. A description of experimental procedures is presented in Section **6**, the results of experimental work are set out in Section **7** and a

discussion of these results in Section **8**. In penultimate Section **9**, a reflective technical overview is followed by recommendations for further process developments and future experimental projects are proposed. Concluding comments are presented in Section **10** in which an assessment is expounded of the worth of microwave-stimulated processes applied to the reduction of minerals in general – the thermochemically stable minerals in particular – and in light of the broad scope of pyrometallurgical production routes to the common metals, the commercially valuable metals, and the high end-value metals.

2

THE REFRACTORY METALS.

"The art of being wise is the art of knowing what to overlook."

William James -
Principles of Psychology, 1890.

2: THE REFRACTORY METALS.

"Refractory metals" refers somewhat loosely to the group of nine transition metals of Groups **4**, **5** and **6** of the first three long periods of the Periodic Table of the Elements (see Figure **{2.1}1**). The refractory metals are titanium, zirconium, hafnium, vanadium, niobium, tantalum, chromium, molybdenum and tungsten. Sometimes chromium and, less frequently, vanadium are omitted from this generalised grouping. Whilst all nine elements are relevant to this study, the project scope was concentrated on titanium, zirconium and hafnium of Group **4**, plus niobium and tantalum of Group **5**. Essentially, the principal commercial ores of these five elements are mined in only two types of mining operations in Australia. In placer deposits, the principal titanium minerals, rutile and ilmenite, plus the principal zirconium/hafnium mineral, zircon, are recovered concurrently in mineral-sand mining operations whilst the principal tantalum/niobium minerals, tantalite and wodginite, are concentrated from ore mined from weathered metamorphic rock and overlying eluvial deposits in open-cut operations. The selection represents three Australian ore groupings as titanium occurs in rutile, ilmenite and leucoxene mineral sands, zirconium and hafnium occur concurrently by mineralogical association in zircon sands, as do niobium and tantalum in tantalite, columbite and wodginite minerals.

Despite their relative under-utilisation and general unfamiliarity in metallic form, the refractory metal elements occur in greater abundance than many of the common and familiar metals in the Earth crust. The prevalence of the more abundant elements and their order of abundance in the Earth crust are shown in Table **{2}1**. Clearly, the table disregards the concentration, dispersion and depth of mineralisation through igneous

Table {2}1 : The abundance of elements in the Earth crust in order of abundance (ppm (g tonne^{-1})) [3].

1	Oxygen	455 000	17	Carbon	180	33	Nitrogen	19	49	Tin	2.1
2	Silicon	272 000	18	**Zirconium**	162	34	Gallium	19	50	Europium	2.1
3	Aluminium	83 000	19	**Vanadium**	136	35	Lithium	18	51	Beryllium	2.0
4	Iron	62 000	20	Chlorine	126	36	Lead	13	52	Arsenic	1.8
5	Calcium	46 600	21	**Chromium**	122	37	Praseodymium	9.1	53	**Tantalum**	1.7
6	Magnesium	27 640	22	Nickel	99	38	Boron	9.0	54	Germanium	1.5
7	Sodium	22 700	23	Rubidium	78	39	Thorium	8.1	55	Holmium	1.3
8	Potassium	18 400	24	Zinc	76	40	Samarium	7.0	56	**Molybdenum**	1.2
9	**Titanium**	6 320	25	Copper	68	41	Gadolinium	6.1	57	**Tungsten**	1.2
10	Hydrogen	1 520	26	Cerium	66	42	Dysprosium	4.5	58	Terbium	1.2
11	Phosphorus	1 120	27	Neodymium	40	43	Erbium	3.5	59	Lutetium	0.8
12	Manganese	1 060	28	Lanthanum	35	44	Ytterbium	3.1	60	Thallium	0.7
13	Fluorine	544	29	Yttrium	31	45	**Hafnium**	2.8	-	- -	
14	Barium	390	30	Cobalt	29	46	Caesium	2.6	66	Silver	0.08
15	Strontium	384	31	Scandium	25	47	Bromine	2.5	72	Platinum	0.01
16	Sulphur	340	32	**Niobium**	20	48	Uranium	2.3	75	Gold	0.004

and sedimentary deposits and neglects ore accessibility. However, it is instructive to note how few of the common industrial, structural and fabrication metals outrank the refractory metals in abundance.

Although its use is entrenched in common terminology, the name "refractory metals" often leads to a degree of confusion as metals of the platinum group (rhenium, ruthenium, osmium, rhodium, iridium, palladium and platinum of Groups 7 to 10 of Periods 5 and 6) also possess excellent, if not superior, refractoriness and corrosion resistance. Further confusion arises from the grouping of "refractory materials" which, whilst usually referring to refractory ceramic materials of high refractoriness, may include metals such as tungsten, rhenium and platinum from the refractory and platinum metals groups. Furthermore, whilst many of these refractory ceramics are minerals of the refractory metal group (ZrO_2, $ZrSiO_4$, TiB_2, HfC, Ta_2O_5, *et cetera*), many - such as Al_2O_3, AlN, SiO_2, SiC, B_4C and graphite - are not. (The common term "refractory oxides", of course, defines just a sub-set of refractory materials. In the not-too-distant past, refractory oxides plus graphite comprised all of the common refractory materials.) "Refractories" refers to those refractory material products which, typically, are pre-formed and fired brick or monolithic fabrications used to line furnaces and reactors so providing chemical and thermal insulation. Refractories are the refractory products as distinct from the refractory materials from which they are made.

The refractory metals have physical and chemical properties that make their selection appropriate for specialised applications, particularly in the increasingly common high technology applications. These elements are central components in the design and fabrication of high performance intermetallic and hard materials. In the pure form, they are ductile and have excellent corrosion resistance, however, "high purity" is difficult to maintain in these light element "getter" metals. As solid solution components, they form alloys that have outstanding mechanical properties – in particular, high temperature strength. As micro-alloying components in modern structural steels, refractory metal additions provide the high strength and associated performance demanded by the specifications of advanced design and technology.

Undoubtedly, three of the central utilisation and consumption routes of the refractory metals, which account for most of production, is their application in the manufacture of intermetallic compounds, hard materials and ceramics. Notably, all of these material end-products are compounds – none are solid solution metals. More than metals from any other elemental grouping, refractory metals are used in the manufacture of the initial two of these processed material types, materials that are so

much in demand in modern technological applications. The aerospace industries have stimulated interest in the development of materials that are strong, ductile and stiff at high temperatures. Many intermetallics, representing compounds with a range of ordered structures, have significant ductility and strength at elevated temperatures – some intermetallics even display increasing yield strength with increasing temperature over a considerable range [4]. Intermetallics tend to be brittle at ambient temperatures, however, because their bonding is tighter than that of their pure components, intermetallics have higher elastic stiffness and melting points at higher temperatures. Consequently, the high strength-to-weight and stiffness-to-weight ratios at elevated temperatures make intermetallics desirable materials for applications in the construction of aircraft and spacecraft.

On the basis of consumption, more than for intermetallics is the utilisation of the refractory metals in the production of hard materials and ceramics. Indeed, a far greater proportion of refractory metal materials production is consumed in the forms of hard material metallo-ceramics, oxide and non-oxide refractory ceramics plus oxides used as paint opacifiers. Up to 90% of high grade titania produced is consumed by the paint production industry – a statistic which infers wasted resource potential and a proportion which should surely ease in future years. Much unprocessed zircon is consumed in cast refractory products whilst a further major proportion is upgraded to high purity zirconia and consumed in specialised ceramics applications.

Of their potential uses, refractory metals are perhaps most widely known for their utilisation in hard materials. Short or diamond, the hardest and most refractory materials known belong to the boride, carbide, nitride and oxide derivatives of the refractory metals. Tungsten carbide, titanium nitride and, in fact, most of the carbides, nitrides and borides of the refractory metals are commonly used in specialised applications in metal matrix composites, or cermets, from which cutting and machining tools are produced. Some, such as titanium diboride, also find special applications as refractory linings because of their refractoriness and corrosion stability. The refractory metal oxides are not usually grouped with the other hard materials, however, some such as zirconia (zirconium dioxide) are used, in the moulded and sintered form, in cutting tools and in extrusion and drawing dies and other applications requiring high wear-resistance with low deformation under load (high rigidity).

The unavoidable facts of outright consumption see that most refractory metals mined, and subsequently reduced or otherwise metallurgically processed, will be consumed as end-products in the material form of either an oxide ceramic or a metal-

like "ceramic" hard material. Despite this, the emphasis of this thesis has *notionally* identified final products of metallurgical reduction operations as metals, and so, without losing sight of other crucially important end-products, reasonable emphasis has been placed on "production routes towards pure metals". This approach then encompasses the conceptual and inclusive principles of production routes towards other end-products. [In addition to the references specifically indicated above, the following sources [3, 4, 5, 6, 7, 8, 9, 10, 11, 12, 13] are referenced for their general consultation reading in the preparation of this section.]

2.1: The Properties and Utilisation of Five Refractory Metals.

The Mendeleyevian relationship of the refractory metals to one another and to the other elements can be seen in the Periodic Table of the Elements which is included as Figure {2.1}1. Some common physical and mechanical properties of pure refractory metals are given in Table {2.1}2. The following brief descriptions of titanium, zirconium, hafnium, niobium and tantalum – the five metals of specific interest in this thesis – are overviews of their brief histories, properties and utilisation and are not intended to be comprehensive. Descriptions generally exclude mention of extractive processing which is discussed in some depth in later sections.

2.1.1: Titanium.

Placed in Group 4 on the first long period of the Periodic Table of Elements, titanium is a lustrous silver-white transition metal whose fracture surface resembles that of steel. Its crystal structure in the α-form is hexagonal close packed (hcp) and above $T_{\alpha-\beta} = 882^{o}C$, in its β-form, is body centred cubic (bcc). Pure titanium is ductile and can be cold worked and cold drawn, however, ductility is easily lost with trace uptake of impurities. Commercially pure titanium is as strong as steel but 45% lighter, twice as strong as aluminium but 60 % heavier. Titanium is a prolific "getter" of oxygen and nitrogen and loses its ductility rapidly upon the uptake of either. The metal burns in air and is the only element that will burn in nitrogen [5]. Titanium has excellent corrosion resistance to seawater and common corrosive substances and is resistant to dilute sulphuric and hydrochloric acids, most organic acids and moist chlorine gas.

Figure {2.1} 1 : The Periodic Table of the Elements as adopted by the International Union of Pure and Applied Chemists (IUPAC) in 1984 on the 150th anniversary of the birth of Dimitri Mendeleyev who in 1869 first proposed this arrangement of the elements. The periodic arrangement shown here was first proposed by Arne Olander in 1958 [3].

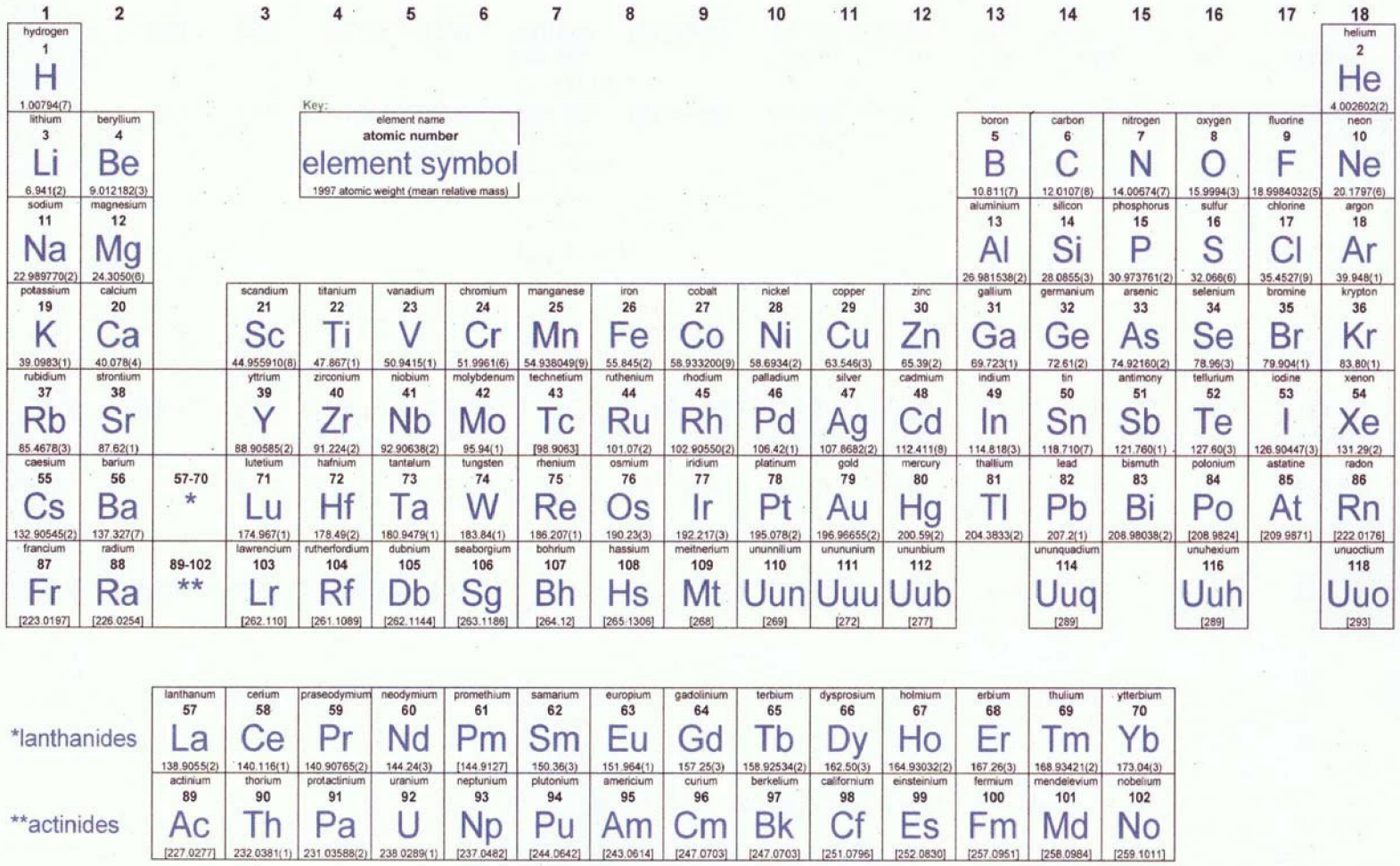

Table {2.1} 2 : Some physical and mecha anical properties of refractory metal s and common metals. Unless otherwise noted, v alues are for pure metals and are in the annealed condition for mechanical property values which are offered as indicative values at 20°C, not as absolute valu es. Note that mechanical property values for pure refractory metals are dra matically affected by the uptake of negligible levels of impurities. (Superscripts: C - commercial purity, MS - mild steel)[5, 9, 30, 131].

Metal	Year Discovered	Melting Temp. (°C)	Boiling Temp. (°C)	Atomic Mass	Density (g cm^3)	Crystal Structure	Electronic Structure	Vicker's Hardness H_V	Poison's Ratio	Young's Modulus E (GPa)	Shear Modulus G (GPa)	Bulk Modulus K (GPa)	0.2 % Yield Strength (MPa)	Tensile Strength (MPa)
Ti	1791	1671	3287	47.90	4.540	αTi: hcp βTi: bcc $T_{\alpha-\beta}$: 882°C	[Ar]3d^{2}4s^2	65-72 70-75^C	0.361	95 115^C	- 105^C	- 44^C	- 150^C	220 240^C
Zr	1789	1852	4377	91.22	6.506	αZr: hcp βZr: bcc $T_{\alpha-\beta}$: 862°C	[Kr]4d^{2}5s^2	93-100 150-180^C	0.35	83 100^C	- -	- -	110 140^C	250 300^C
Hf	1923	2230	5197	178.49	13.310	αHf: hcp βHf:bcc $T_{\alpha-\beta}$: 1760°C	[Xe]4f^{14}5d^{2}6s^2	-	0.37	140	-	-	150	400
V	1801	1887	3377	50.94	6.110	bcc	[Ar]3d^{3}4s^2	180	0.365	125	155	45	220	400
Nb	1801	2468	4742	92.91	8.570	bcc	[Kr]4d^{4}5s^1	80	0.397	110	165	.40	220	280
Ta	1802	2996	5425	180.95	16.654	bcc	[Xe]4f^{14}5d^{3}6s^2	100	0.342	185	190	70	160	200
Cr	1780	1857	2672	52.00	7.190	bcc	[Ar] 3d^{5}4s^1	110	0.210	270	155	115	230	280
Mo	1781	2617	4612	95.94	10.220	bcc	[Kr]4d^{5}5s^1	155	0.225	320	200	135	310	415
W	1783	3407	5657	183.85	19.300	bcc	[Xe]4f^{14}5d^{4}6s^2	200	0.282	405	305	155	200	450
Al	1825	660.5	2467	26.98	2.698	fcc	[Ne]3s^{2}3p^1		0.345	70	70	25	20	50
Fe	c 2500 BC	1535	2750	55.85	7.874	αFe: bcc γFe: ccp δFe: bcc $T_{\alpha-\gamma}$: 810°C $T_{\gamma-\delta}$: 1390° C	[Ar]3d^{6}4s^2	67-70	0.291 0.293^{MS}	205 207^{MS}	165 165^{MS}	80 80^{MS}	45	? ?

[**NOTE**: published mechanical prope erty values for *high* purity metals vary widely.]

Titanium was discovered by Gregor in 1791 and named by Klaproth in 1795. Testament to the stability of its minerals, nearly a century passed before impure titanium was prepared by Nilson and Petterson in 1887. Hunter produced 99.9% pure titanium metal in 1910 by reducing titanium tetrachloride, $TiCl_4$, with sodium metal in a steel bomb – a process that still bears his name. In 1946, Kroll showed that titanium could be commercially produced by metallothermic reduction of titanium tetrachloride using magnesium – a method since known as the Kroll process. As with refractory metals generally, the purest titanium can be prepared by decomposing the iodide – a method devised by van Arkell and de Boer.

Titanium is the ninth most bountiful element in the Earth crust and occurs in common minerals and ore forms more abundantly than do any of the other refractory metal elements. Despite this relative abundance and the established availability of mineral ores to industry, the commercial production of titanium metal did not begin until 1948 [9]. Titanium is a metal of the modern age.

Titanium is produced in greater quantities than any other of the Groups 4 and 5 refractory metals and is produced in comparable quantities to the Group 6 elements chromium, molybdenum and tungsten, all of which are distinctly easier to reduce and refine. The high strength-to weight ratio of titanium and its resistance to oxidation in chemically aggressive environments have been responsible for its enthusiastic adoption and increasing utilisation. Such highly desirable properties make titanium an exploitable necessity rather than a simple, pragmatic choice in applications requiring high temperature utility and chemical resistance in the chemical industries and for high strength alloys in structural applications in the aerospace industries.

In the chemical industries, where it is used in applications requiring resistance to the effects of high temperature and/or chemical attack, titanium is cost-competitive with stainless steels. The initial cost-at-installation of titanium components and equipment is higher than the stainless steel options but the lighter titanium has a significantly longer in-service life expectancy. High resistance to pitting corrosion, general durability and higher strength-to-weight ratio than stainless steels are the attributes of titanium that allow designers of expensive chemical plant to reduce wall thicknesses and component dimensions in process equipment. Once component life expectancy and weight saving aspects of process equipment are taken into account, titanium becomes the desirable alternative for heat exchangers, chemical reactor vessels and other expensive plant installations.

The aerospace industries make use of the same high strength-to-weight ratio and chemical resistance properties of titanium in a broad range of mainly structural applications. In aerospace applications, titanium is principally utilised in applications requiring high strength alloys - particularly those aluminium-based titanium alloys having the accentuated strength-to-weight ratio advantage provided by the lighter metal plus the accentuated strength and stability imbued by titanium. **[**In addition to the specific references, the following sources [3, 5, 7, 9, 10, 12, 14] are referenced in a general sense in relation to the documentation of Section **2.1.1**.**]**

2.1.2: Zirconium.

Below titanium, zirconium occupies the position at Group 4 in the second long period of the Periodic Table. The crystal structure of zirconium in the **α**-form is hexagonal close packed (hcp) and above $T_{\alpha-\beta}$ = 862°C, in its **β**-form, is body centred cubic (bcc). Pure zirconium is ductile, malleable and strong. It is a gray-white lustrous metal that, like titanium, loses its ductility with uptake of trace impurities. Zirconium is a prolific "getter" for oxygen and nitrogen and in finely divided forms will spontaneously combust in air, particularly at elevated temperatures. Bulk zirconium metal is much more difficult to ignite.

Whilst Klaproth is attributed with the discovery in 1789 of the new element, zirconium, the impure metal was first isolated by Berzelius in 1824 by heating a mixture of potassium and potassium zirconium fluoride, K_2ZrF_6, in a small iron tube. Pure zirconium was first prepared in 1914 and zirconium of high purity was prepared in 1925 by an iodide decomposition process developed by van Arkel and de Boer – a process which is still the accepted standard method of production of high purity zirconium and other refractory metals. Modern commercial production of zirconium, which began in 1949, is based upon the Kroll Process – the reduction of zirconium tetrachloride, $ZrCl_4$, by magnesium – or close variations of this most common of all refractory metal production routes.

Almost all of the world production of zirconia/zirconium is derived from the mineral zircon, $ZrSiO_4$, and although zirconium occurs in a diverse range of minerals, the only other commercially important zirconium mineral is baddeleyite, ZrO_2, the naturally occurring zirconia mineral. Synthetic zirconia production for use in ceramic and refractory applications accounts for a large proportion of zirconium minerals

mined. Typically, all naturally occurring zirconium minerals contain 1% to 3% hafnium amongst other, lesser impurities. Consequently, because separation is difficult and expensive, commercial grade zirconium may contain up to 3% hafnium, which does not detract from its utility in most applications. However, like niobium, zirconium has a *low* absorption cross-section for neutrons and is therefore extensively used in control rods for nuclear energy applications – applications which require the elimination of hafnium because of its *high* absorption cross-section for neutrons (making hafnium similarly important in nuclear applications). Commercial nuclear power generation applications consume about 90% of zirconium metal production. Reactor grade zirconium metal is virtually free of hafnium, whilst zirconium-based Zircalloy® is an important alloy range developed for the nuclear power industry.

Zirconium is also used in an extensive range of applications in the chemical industries because of its exceptional resistance to corrosion by most common acids and alkalis, by seawater, and by other common corrosive agents. In micro-alloying proportions, zirconium is used as a grain-refining agent in special steels and to inhibit post-heat treatment and post-fabrication grain growth. Zirconium and high-zirconium alloys are used for the manufacture of special surgical appliances, rayon spinnerets and other equipment for specialised applications. At low temperatures, zirconium becomes superconductive and is used in the production of supermagnets. Zirconium-zinc alloys become ferromagnetic below 35 K. [In addition to the specific references above, the following sources [3, 5, 6, 9, 77] are referenced in a general sense for their use in the documentation of this Section **2.1.2**.]

2.1.3: Hafnium.

Hafnium occupies the Group 4 position in the third long period of the Periodic Table. The crystal structure of hafnium in the α-form is hexagonal close packed (hcp) and above $T_{\alpha-\beta}$ = 1760°C, in its β-form, is body centred cubic (bcc). Pure hafnium is a ductile metal of high density with a brilliant silver luster whose "high-purity" metallic properties are considerably influenced by negligible levels of impurity uptake *and* by any remaining zirconium content. Hafnium always shares the same ore sources as zirconium with which it is inextricably related in the broad Mendeleyevian sense and the metals are (unavoidably) reduced simultaneously in all extractive reduction operation options, and their chlorides (halides) are almost inseparable by distillation.

Predictions of its existence prompted speculation of the presence of hafnium in various minerals but the metal was not "discovered" until 1923 when it was identified by X-ray analysis. Also, it was predicted that hafnium would be associated with zirconium. The confirmation of these predictions was one of many triumphs-of-the-times in science that flowed from the inspired theoretical accomplishments of Mendeleyev, Bohr and others who collectively formulated our modern understanding of the periodicity and electronic structure of the elements. Theoretical science was integral in the development of the Periodic Table of the Elements, a feat that ranks as one of the truly outstanding accomplishments in the history of the sciences and, to a large degree, established Science as a prominent power in the evolution of human society, culture and civilisation.

Metallic hafnium was first prepared by van Arkel and de Boer who thermally decomposed hafnium tetraiodide vapour on a hot tungsten filament to deposit the high purity hafnium metal. Hafnium is commercially produced by metallothermic reduction of the tetrachloride by magnesium or sodium metals (using the Kroll or Hunter processes respectively). Hafnium tetrachloride is a by-product of the fractional distillation of chlorinated commercial or impure zirconium - the $HfCl_4$ being sublimed off the impure chloride leaving the more stable zirconium tetrachloride in pure form. Inherently, the commercial production of hafnium began as a direct consequence of the burgeoning demand for hafnium-free zirconium metal created by the then new and expanding nuclear power industry.

Because they share almost identical chemistry, hafnium and zirconium are two of the most difficult metals to separate after co-reduction and each metal is invariably the greatest impurity in the other after refining. Hafnium is twice as dense as zirconium and this difference has been utilised in a reduction-stage separation technique that is claimed [15] to separate the metals by a liquid metal solvated carbo-nitrothermic process route that produces pure metal nitrides. In this method, hafnium-rich zirconia - which typically may at this stage be 5% to 10% hafnia - is entrained with nitrogen into a carbon-saturated bath of copper at 1500°C. The lighter zirconium nitride product floats to the surface where it accumulates whilst the heavier hafnium nitride product sinks to the bottom Although nitrides, the separated metallic products are claimed to be of high purity having a separation factor of 10^6 in a single stage process. Hafnium nitride is the most refractory of all the metal nitrides having a melting point of 3390°C, whilst hafnium carbide (an honour which it *may* share with tantalum carbide) is the most refractory binary compound known [5] having a melting point of 3930°C. As with all refractory-metal-based non-oxide ceramics of good purity, hafnium borides, carbides

and nitrides are highly valued as hard materials as well as for their refractoriness. Hafnia, hafnium dioxide, finds use in special applications as a high technology ceramic. Hafnium intermetallics, individually and as a group, have outstanding properties – physical, chemical and mechanical. In the family of intermetallic materials they are dense, strong, durable and show high resistance to the effects of very high temperature.

Finely divided hafnium will spontaneously ignite in air. It is resistant to chemical attack by concentrated acids (except hydrofluoric acid) and alkalis but reacts upon direct exposure to halides to form the hafnium tetrahalide. At elevated temperatures, hafnium reacts with oxygen, nitrogen, boron, carbon, silicon and sulphur. Hafnium is alloyed with iron, titanium, niobium, tantalum and other metals to produce a range of special purpose alloys. Because hafnium has excellent mechanical properties, exceptional corrosion resistance, and has a high absorption cross-section for thermal neutrons – almost 600 times that of zirconium – hafnium is used for nuclear reactor control rods. [In addition to the specific references above, the following sources [3, 5, 6, 9, 15, 77] are referenced in a general sense in relation to the documentation of Section **2.1.3**.]

2.1.4: Niobium.

Below vanadium in Group 5 of the Periodic Table of the Elements, niobium, or columbium (Cb), its preferred name in the United States of America, lies between zirconium and molybdenum in the second long period – central in the nine refractory elements. Whilst it has an electronic configuration irregularity in the $[Kr]4d^45s^1$ order of filling of its electron shells which accounts for some individual material characteristics, solid niobium retains the same body-centred cubic crystal structure to its melting point. Niobium is a lustrous silvery white metal that is soft and ductile in the pure state but, like all refractory metals, its pure state properties succumb to trace inclusions of interstitial impurities. When deep-drawn, niobium withstands tearing stresses better than most other ductile metals and it work-hardens at a much lower rate than most metals. At ambient temperatures, it forms a thin, contiguous protective oxide film that is only detectable because of a bluish cast across the exposed metal surface. Generally, niobium is an aggressive "getter" and must be atmosphere-protected as it oxidises rapidly above 200°C. However, a thin oxide film on the otherwise untreated metal is stable enough to resist high temperature corrosive attacks – the exposed metal resists fused alkalis but is attacked by hot concentrated acids. Niobium is used in some

stainless and special purpose steels because of the chemical and mechanical properties it contributes to the alloys. The metal has superconducting properties.

Discovered in 1801, niobium was not isolated in its metallic form until 1864 when Blostrand reduced the chloride in a hydrogen atmosphere. Niobium occurs concurrently with tantalum in ores with a mineralogy ranging from niobium-rich columbite (or niobite), pyrochlor and euxenite to tantalum-rich tantalite. Typically, the metals are co-reduced and separation of tantalum from niobium can be achieved in a number of ways.

Like zirconium, niobium has a low absorption cross-section for neutrons and is extensively used in nuclear reactor applications. Niobium is currently available at about half the cost of zirconium making it economically preferable in cases of choice in the nuclear industries. As ferroniobium, niobium is added as a common micro-alloying element to high-strength, low-alloy steels for use in a wide range of structural applications and, following heat treatment, for fabrication into a range of industrial and constructional components. Niobium acts as a carbide stabiliser and inter-granular corrosion inhibiter when added to austenitic stainless steels, whilst it is added to ferritic stainless steels to improve the high temperature strength for use in turbine blades and comparable applications. Alloys of niobium are creep-resistant at high temperatures and show a high resistance to attack by hot gases. Commercially pure niobium also finds application in special structural frames in the space programme and elsewhere in the aerospace industries. Niobium is utilised in specific-purpose non-ferrous alloys, in welding rods, in intermetallic materials and for the production of hard materials. [In addition to the specific references above, the following sources [3, 5, 8, 9, 10, 13] are referenced for their use in the documentation of Section **2.1.4**.]

2.1.5: Tantalum.

Having twice the density of niobium, tantalum is the Group 5 element lying between hafnium and tungsten on the third long period of the Periodic Table. Like the other refractory elements of Groups 5 and 6, tantalum has a body-centred cubic crystal structure. Tantalum is a silvery-grey metal and exhibits the fourth highest melting temperature of all the known metals. It is heavy and very hard; when pure it is highly ductile and can be drawn into fine wire.

The discovery of tantalum is attributed to Eckberg in 1802. However, confusion and disagreement about the different identities of niobium and tantalum (which usually occur concurrently in minerals) persisted until Rose, in 1844, and Marignac, in 1866, demonstrated the difference between niobic and tantalic acids. Early investigators only produced relatively impure metal – niobium, being difficult to separate, was a common impurity. The first relatively pure ductile tantalum was prepared by von Bolton in 1903. Because of its refractoriness and affinity for carbon, tantalum was adopted for many specialty applications from filament wires to alloying element in special alloys, however, the imperatives of better availability and lower cost have seen tungsten, niobium and other refractory metals replace tantalum in many of its early applications.

As with the other refractory metals, tantalum is easily contaminated by interstitial impurities oxygen, nitrogen, hydrogen and carbon that affect mechanical properties to a pronounced extent. Differences in hardness, a very sensitive indicator of such contamination, can be as high as 200% between 99.5wt% tantalum (at the limit of hot-deformability) and cold-ductile tantalum that is greater than 99.95wt% purity [11]. Tantalum has a very low strain hardening coefficient for a body-centred cubic metal and can be cold deformed to over 99% without stress-relieving or annealing [11].

Typical of the high melting-point refractory metals, tantalum has excellent corrosion resistance and high mechanical strength. The outstanding corrosion resistance of tantalum is imbued by its ability to form a contiguous thin protective oxide film that is tenacious and impervious – retarding further oxidation. This oxide film on tantalum is many times more protective [13] than the comparable oxide film on aluminium – a film whose protective coherency is well appreciated and utilised in numerous applications. Tantalum is virtually impervious to chemical attack below 150°C being attacked only by hydrofluoric acid, fluoride-ion acid solutions and sulphur trioxide; alkalis have negligible effect. At higher temperatures, tantalum becomes much more reactive and is a prolific "getter" for oxygen at elevated temperatures.

Unalloyed tantalum is used in engineering applications for chemical plant components, turbine blades, a broad variety of electronics components including capacitors (in ceramic form); and special applications such as surgical implements, wire and sheet for use in corrosive environments, and spinnerets for artificial fibres. Tantalum is used to produce a variety of alloys with such desirable properties as high melting point and high strength with good ductility. In steels and in nickel, cobalt and nickel-iron based superalloys, tantalum is added to improve corrosion resistance, to stabilise carbon and act as a grain refiner, and to increase strength and hardness.

Niobium is generally more effective in the same microalloying role such that tantalum in steel production has been largely replaced by niobium (as ferroniobium) which is less expensive – world production of niobium is about five times that of tantalum. Tantalum alloys find applications in the nuclear industries, in military ballistics and numerous high-strength at high-temperature applications in the aerospace industries.

As with all of the refractory metals, tantalum is extensively used in the production of hard materials for inclusion in metal matrix composites, hard metals and other applications. Tantalum is usually produced in hard material form as the carbide, and it is commonly deployed with other refractory metals to form mixed carbides [such as (Ta,Nb)C; (W,Ti,Ta)C and (W,Ti,Ta,Nb)C] for specific material design applications in industrial cutting and machining. Whilst hard materials manufacture accounts for about 30% of total tantalum production, almost half of the total world production is consumed in the production of capacitors in the electronics industries. Whilst tantalum foil and wire is used in capacitors, much of the tantalum is consumed as the oxide that has a high dielectric coefficient and good stability. **[**In addition to the specific references above, the following sources **[3, 5, 8, 9, 10, 11, 13]** are referenced in a general sense for their use in preparing the documentation of this Section **2.1.5**.]

3

EXTRACTIVE METALLURGY and REDUCTION PROCESSES.

"A hen is only an egg's way of making another egg."

Samuel Butler (II) -
Life and Habit, 1877.

3 : EXTRACTIVE METALLURGY and REDUCTION PROCESSES.

Primary metallurgy can be divided by function into two general but distinct categories of operation. These are the metallurgical categories of metals extraction and metals refining. Process operations between extraction and refining stages sometimes overlap and metallurgical function may become indistinct in the contiguity of primary metallurgical operations. However, in conceptual terms, the distinction between the primary metallurgy functions of metals extraction and metals refinement should be recognised. Extractive or extraction metallurgy is concerned with the winning of metals from their ores or mineral concentrates. (For the common metals) once this initial bulk reduction is achieved, the typically impure "pig" metal product is then refined to a specified purity in the refining stage process – a stage which may integrally include alloying additions. To distinguish between the functions of these primary processes is elementary and essential – the distinction is fundamental in any understanding of metals production.

Notwithstanding this dictum, primary metallurgy routes for refractory metals depart somewhat in that reduction to metal normally follows purification of an intermediate halide product that, in turn, may follow a mineral processing reduction or other extractive step. Whilst refractory metals are produced at relatively high purity in commercial operations, ultra-high "iodide purity" metal may then be produced from the commercial grade in a van Arkel-de Boer process which is akin to a refining stage. So, whilst primary metallurgy functions may perceivably divert from the stereotypical metallurgical norm, there are identifiable extractive and refining stages in the production of refractory metals.

In metals production industries, extractive operators must remain cognisant of the requirements of refining operations. More by production function than by producer preference, reduction processes are dictated by the intended end-product of the primary metallurgical operations. Minimum assay requirements of input raw material for refining operations limit and determine achievable end-product specifications of extractive processes. (So, price paid for ore concentrate is contingent upon such operational factors.) Extractive end-point specifications, of course, determine which extractive process routes are feasible (for any given raw material) in achieving these

specifications. Furthermore, in the production of refractory metals, the intended end-product for most extractive metallurgical producers may be at any of a number of intermediate points along the numerous, intricate metals production route possibilities. Beyond the ex-mine ore concentrate, end-products may be pure oxide, impure or pure metal halides, impure or pure metal sponge, ferrometals, electro-won electrode metals, pure refractory metal powder, ingot, wire, rolled sheet or manufactured item. Here, of course, one producer's end-product is another's raw material! The logistics associated with producer sophistication and end-product capabilities of production plant has been, in the short history of refractory metals production, open to the combined dynamics of international economic market forces, the politics of multi-nationalism, and (where these remain as strategic commodities) the veto of international strategic and military decision-making.

For the purposes of this review, the reduction processes will refer principally to processes of extraction metallurgy whilst acknowledging that crucial or final reduction stages are conducted during refining or purification operations.

3.1 : Refractory Metal Ores and Reduction Strategies.

Advances in vacuum technology and equipment have made possible the development of successful reduction processes for refractory metals. In all of the many confirmed production route alternatives tested and proved by either laboratory or commercial scale processes, the utilisation of vacuum systems in the reduction and high-temperature stages of processes has been crucial to the success of both extractive and refining operations. Of course, vacuum technology is invoked as an integral means of achieving atmosphere control of processes in systems of metallurgical chemistry. The employment of vacuum systems allows not only the manipulation of the thermodynamic variable pressure – including the chemistry of partial pressures – but allows the flushing or holding of gases introduced for reasons of chemical protection or chemical participation. Gases introduced to control the atmospheric environment of processes may include the inert gases helium or argon or reactive gases such as hydrogen, methane or carbon monoxide. Inert gases provide a reactor vessel with an

atmosphere that ensures acceptable levels of chemical protection against re-oxidation reactions and secondary reactions that may result in unwanted by-products. Reactive gases may be required by process design as active chemical participants.

Historically, during development of extractive metallurgy routes for refractory metals in the mid twentieth century, certain otherwise successful extractive routes failed to be industrially proven simply for the lack of appropriate vacuum technology and incomplete knowledge of atmosphere control systems[6, 7, 8, 9, 30]. This despite the then well established thermodynamic theory and an entrenched acceptance of the chemical processes of metallurgy. Commercially syndicated routes were often initially "proven" by argument of superior funding (which allowed access to better vacuum technology) rather than by superior process efficacy. To some extent, this was true of several of the commercial processes based upon the Kroll process in which, as MILLER [6, 7, 8] points out, process upgrades were subsequently introduced after earlier "failed" process routes were re-assessed with the benefit of more advanced vacuum systems.

Various conventional reduction routes have been utilised commercially over the years in the production of refractory metals from ore concentrates and from the secondary processing of slags (such as the recovery of tantalum from tin slags). In particular, these reduction routes often combine distinctly different reduction strategies. Refractory metal extraction may employ thermal reduction or smelting, thermal dissociation or decomposition, or electrolytic deposition and, typically, these routes include a halidation option as an integral part of their process.

Refractory metal extraction routes are testament to the thermochemical stability of the component ore minerals, and this carries through to the reduction stages. The most obvious statement of this stability is evident in the free energy versus temperature diagrams, or Ellingham diagrams, for the oxide, sulphide, carbide and other comparable systems. Ellingham diagrams for the oxide, sulphide, chloride, carbide and nitride systems are shown in Figures **{3.1}1** to **{3.1}5**.

For refractory and other reactive metals, extractive or refinement routes based upon electrolytic processes require molten salts as electrolytes. These methods are not always commercially substantiated but are capable of yielding product metal of high purity [16].

With some exceptions, such as massive iron ore (haematite), metalliferous minerals are disseminated somewhat randomly through the crustal country rock. Whether a mineral deposit is technically considered an "ore" depends upon several principally commercial factors pertaining to exploitational propensity, which depends upon the economic confluence of production costs and projected metal prices. Huge concentration differences exist across the range of commercially exploited ores. At the mined face, haematite ore contains about 65% iron, nickel ores may contain as low as 1% nickel, and gold ores may be commercially mined as low as 8 ppm (0.0008%) gold.

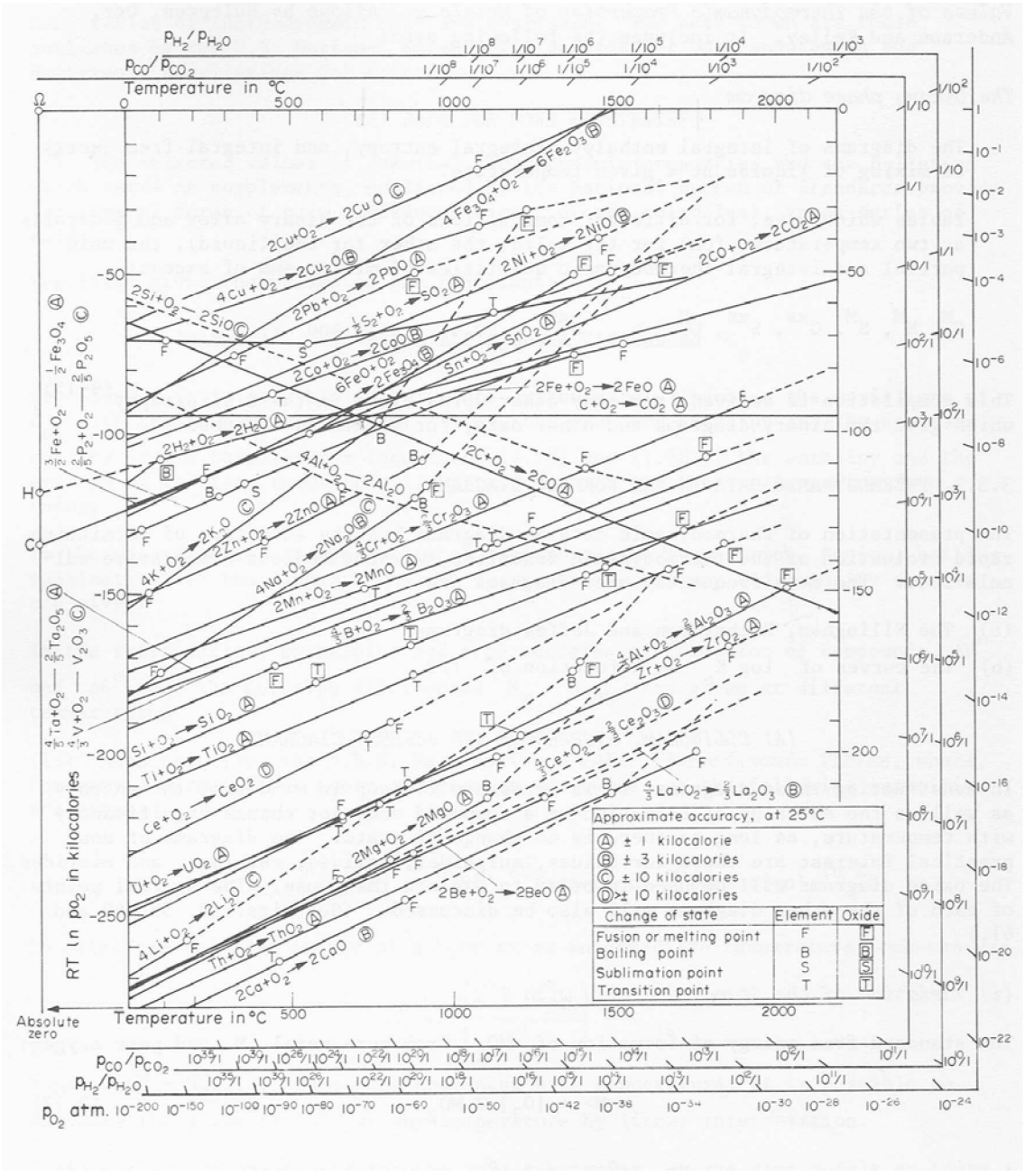

Figure {3.1}1: Ellingham diagram showing the free energies of formation of some **oxides** [17]
(after Ellingham, 1944, and Richardson and Jeffes, 1948).

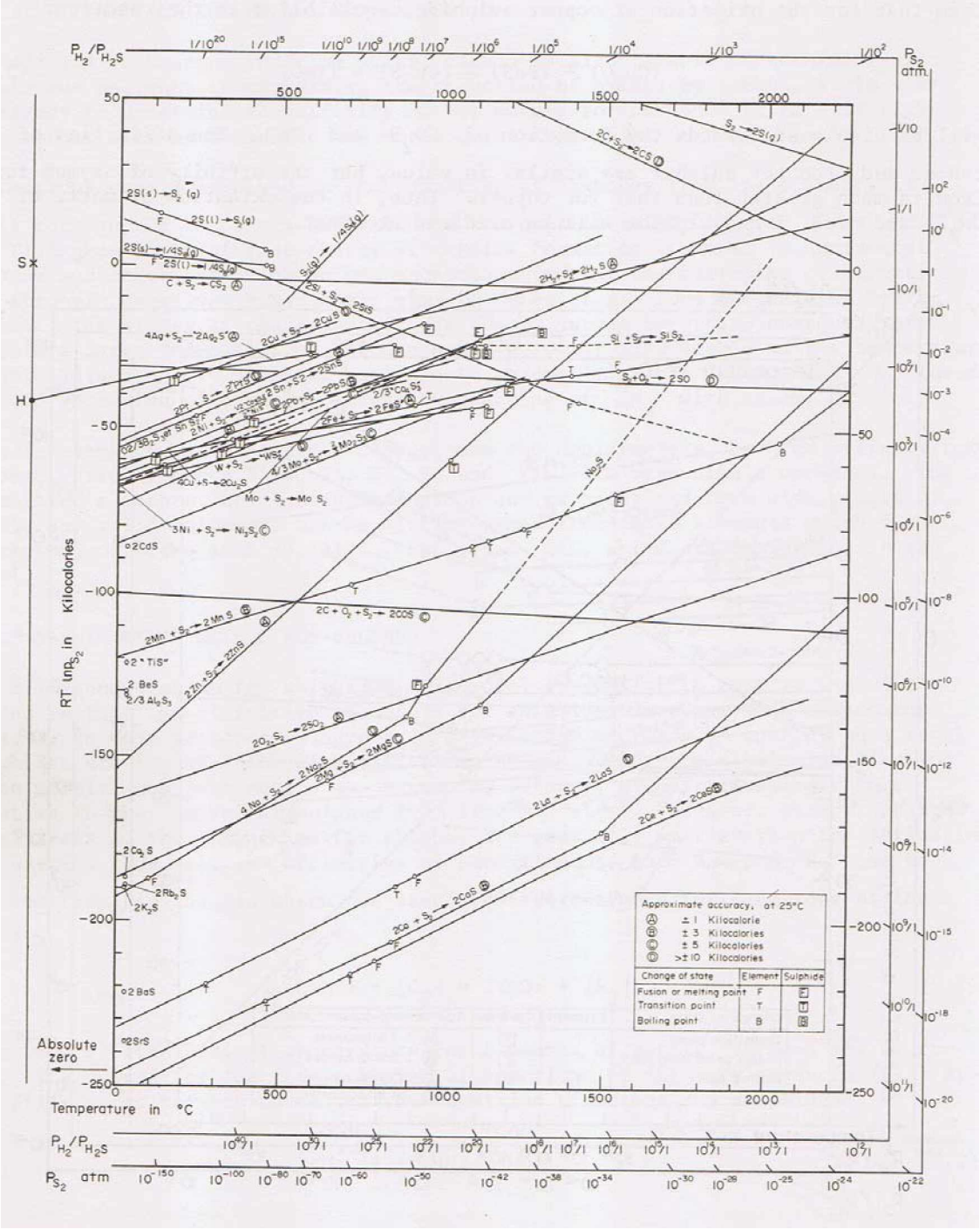

Figure {3.1}2: Ellingham diagram showing the free energies of formation of some **sulphides** [17].

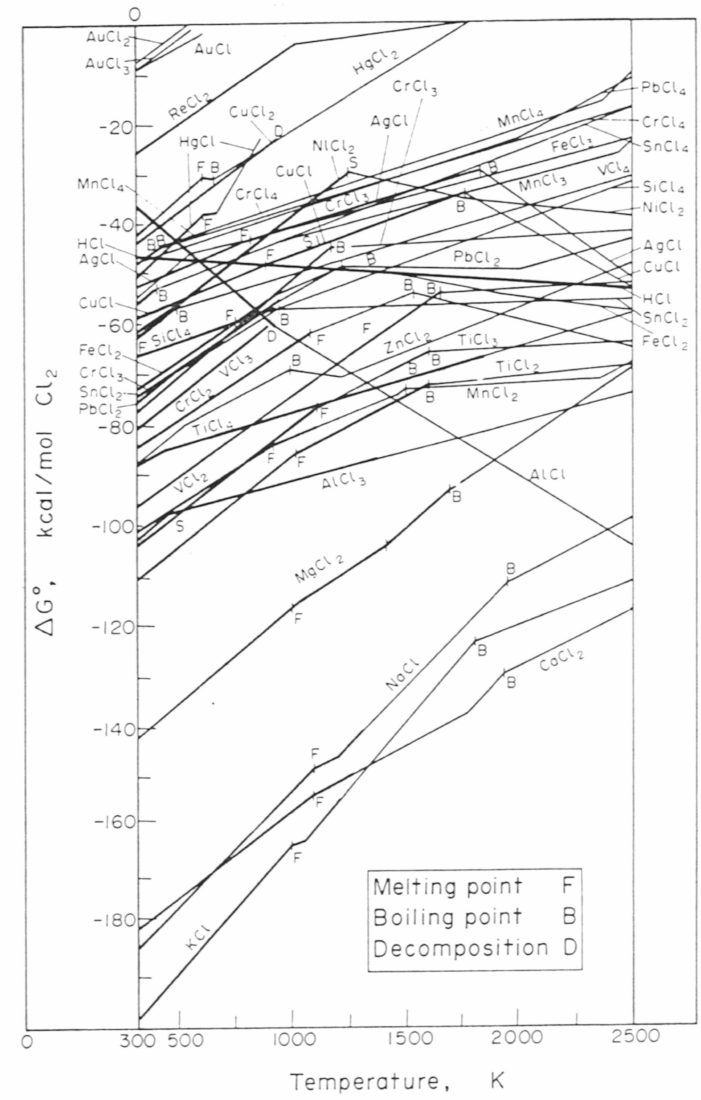

Figure {3.1}3: Ellingham diagram showing the free energies of formation of some **chlorides** [17].

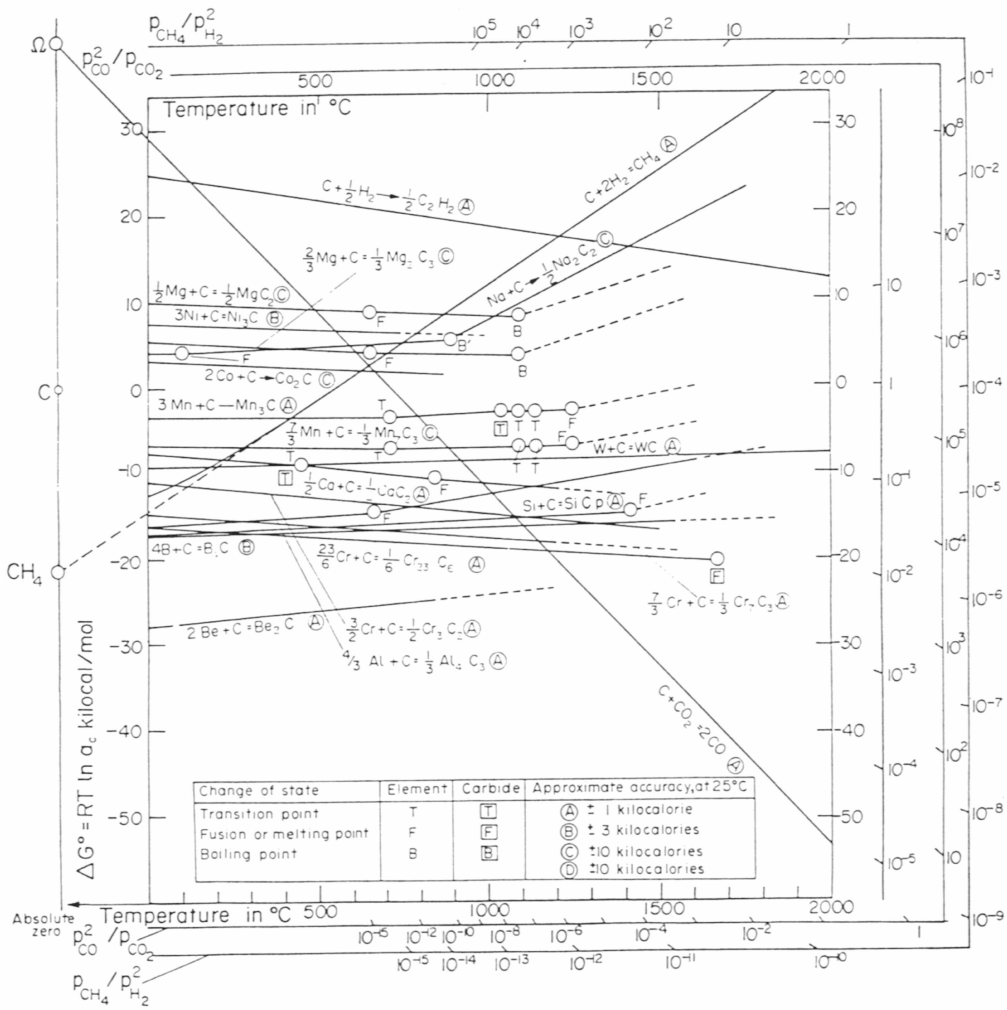

Figure {3.1}4: Ellingham diagram showing the free energies of formation of some **carbides** [17].

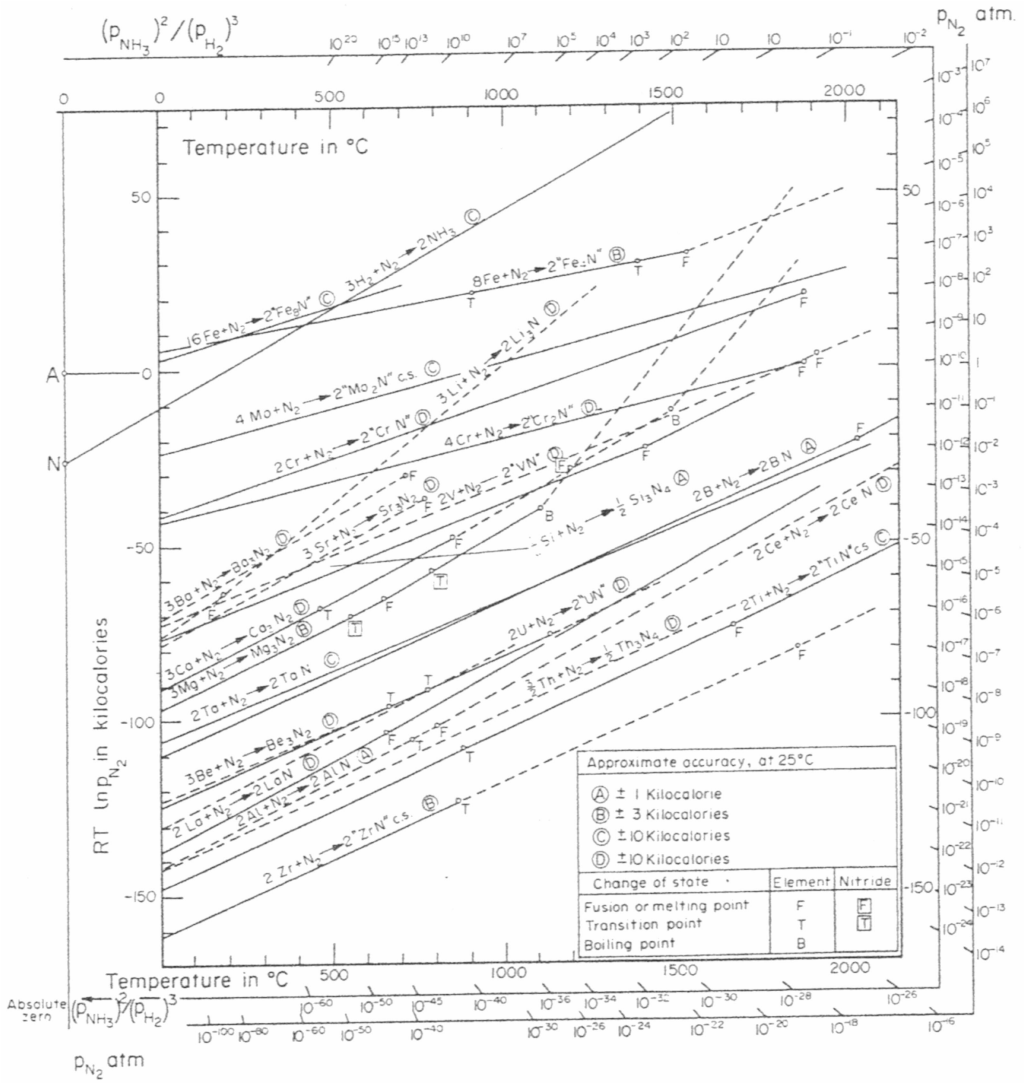

Figure {3.1}5: Ellingham diagram showing the free energies of formation of some **nitrides** [17].

Dictated by the driving force of profit between production cost and metal price, minesite production processes include minesite-remote operations that address the upgrading of ore by mineral concentration, beneficiation and other physical and chemical processes. Upgrading processes encompass ore beneficiation by crushing and grinding to release minerals from gangue and other impurities; separation and concentration of sized fractions by floatation, gravity, electrostatic or magnetic means; calcining, roasting or other chemical upgrading treatment prior to shipping to the metals producer where the selected extractive hydrometallurgical, chemico-metallurgical or pyrometallurgical route is pursued.

The process route(s) followed in the primary production of metals depend upon the mechanical, physical and chemical properties and stabilities of the source mineral, intermediate products and the end-product metal. In realising a final product of maximum purity, all contingent material and process complexities must be dealt with whilst minimising energy consumption, labour, plant and material costs and minimising gaseous, liquid and solid pollutants and waste. By-products must return maximum economic benefit and waste residues must be appropriately disposed-of to overseen and monitored safe stockpiles.

Because of the primordial atmosphere, magma chemistry and solidification conditions prevailing during the mineralisation of the Earth crust, the refractory transition metals principally formed oxides (including oxide derivatives such as silicates, carbonates, titanates, vanadates, tungstates, and so on) or sulphides [17]. The commercially exploited oxide-group minerals include those of iron, aluminium, magnesium, manganese, tin and most of the refractory metals; the important, commercially exploited sulphides include those of copper, lead, zinc, nickel and cobalt, whilst iron occurs commonly but non-commercially in sulphide form [pyrite(FeS_2) and pyrrhotite ($Fe_{1-n}S$) amongst others]. The important refractory metal sulphide is the mineral molybdenite, MoS_2 , otherwise the commercially exploited refractory metal ores belong generally in the broader oxides category.

3.1.1: Mineral Sources of Titanium.

The stable oxide of titanium, TiO_2 (titania), occurs naturally in its trimorphic mineral forms of rutile, anatase and brookite. Brookite occurs sparsely in minor mineralisations and is commercially unexploited whilst anatase is a common gangue mineral of mineral processing in many fluvial-deposit mining operations but has been of only minor commercial significance in Australia, although the huge, deep Murray Basin deposits will imminently reverse this status. Until now, the only straight titania mineral of major commercial importance has been rutile in its mineral sand occurrence. The other predominantly titanium mineral ores of significance are the more abundant but Ti-leaner ilmenite, $FeTiO_3$ (or $FeO.TiO_2$), and the "altered ilmenite" mineral leucoxene which contains about 70% TiO_2. Ilmenite is the most abundant titaniferous mineral mined and comprises the bulk majority of mineral sand concentrate products recovered in sand mining operations - typically ranging from 60% to 90% of yield.

Although rutile and ilmenite were originally formed (frozen) in igneous crustal granites and pegmatites, the minerals are mined in eluvial placer deposits – heavy mineral sand deposits along existing and pre-existing (fossil) beachfronts, particularly along the south-eastern and south-western Australian coastlines. Australia is the largest producer and supplier of both rutile and ilmenite (plus leucoxene) producing approximately 38% and 57% of world production of rutile and ilmenite respectively[1, 14, 18]. Much of the south-eastern Australian ilmenite is trace-rich in the impurity chromium (via chromite, $FeCr_2O_4$) which, because of the difficulties in separation during mineral beneficiation, limits its acceptance for conventional synthetic rutile processing[2, 19]. In Australia, region-specific processes for the conversion of ilmenite to synthetic rutile - the Murso process for eastern-derived concentrates and the Becher process for western-derived concentrates – were developed to accommodate the regional gangue variations in ilmenite[20]. These processes have been propitiously exploited for several decades.

It is appropriate to note that the titanium beach-sand minerals are mined in operations that recover in minor proportions other, more valuable mineral sands in the same operational process. These include the zirconium mineral, zircon ($ZrSiO_4$), and

the rare earth minerals monazite [(Ce,La,Th)PO_4], xenotime [(Y,REE)PO_4] and bastnaesite [(Ca,La)CO_3(OH,F)]. Leucoxene and xenotime are recovered in south-western Australian operations. South-eastern Australia produces a higher yield of rutile (with respect to ilmenite) than do western operations. Not only is Australia the largest producer/exporter of titanium minerals, but Australian producers also account for most of the world production of zircon, of monazite, and of xenotime[1, 20]. The processing of mineral sands is further discussed in the following section.

3.1.2: Mineral Sources of Zirconium and Hafnium.

Zirconium mineral ores are relatively plentiful throughout the world - zirconium being more abundant in the Earth crust than most of the "common" metals including nickel, zinc, copper, lead, tin and the precious metals[3]. Fellow Group **4** element hafnium occurs as the minor co-mineralisation component in all native zirconium minerals, usually from 1% to 3% by weight – and towards the upper end for Australian zircon sands.

Minerals derived from alkaline nepheline syenite rocks show low Hf:Zr ratios compared to the Hf:Zr ratios of minerals derived from acid granitic rocks[6, 14]. Zircon derived from granitic pegmatite (at about 5 wt% Hf) may have a Hf:Zr ratio three times higher than zircon derived from nepheline syenite (at about 1.7 wt%)[6]. Most mined deposits recover alkaline-rock derived zircon. The acid granitic mineral cyrtolite, an altered zircon [(Zr,Hf)SiO_4], contains up to 17 wt% Hf and 50 wt% Zr. Other high hafnium acidic rock minerals are malacon (another altered zircon), naegite (zircon with ThO_2, Nb_2O_5, Y_2O_3 or UO_3); thortveitite, $(Sc,Y)_2Si_2O_7$; and acidic rock derived zircon. Alkaline rock derived zirconium/hafnium minerals which may report with higher Hf:Zr ratios than alkaline derived zircon are catapleiite, $H_4Na_2ZrSi_3O_{11}$; elpidite, $H_6NaZrSi_6O_{18}$; eudialyte, $(Na,Ca,Fe)_6ZrSi_6O_{18}(OH,Cl)$; polymignite, (Y,Ce,Ca,Zr) $(Nb,Ta,Ti)O_4$; rosenbuschite, $(Na,Ca,Mn)(Fe,Ti,Zr)FSi_2O_8$; and woehlerite, $NaCa_2$ $(Zr,Nb)FSi_2O_8$[21, 22, 23].

The zirconium minerals that have been commercially mined are the beach sand mineral zircon and the impure native oxide baddeleyite (ZrO_2) which is mined (as nodules called favas) in alluvial deposits in Brazil. However, current zirconia (zirconium)/hafnia(hafnium) production relies, almost exclusively, upon the common orthosilicate mineral ore zircon, $(Zr,Hf)SiO_4$, commonly written as $(Zr,Hf)O_2.SiO_2$, of which Australia is the largest producer/exporter followed by South Africa, U.S.A. and states of the former U.S.S.R.[3, 14].

Zircon is mined from placer deposits representing current and former (fossil) beachfronts in operations recovering various commercial heavy minerals including rutile, ilmenite and rare earth minerals. Generally, the economics of sand mining is such that mining operations are made viable by the quality and content of the considerably more plentiful proportion of titaniferous minerals in the deposit. Recovery of other heavy minerals (for their own value) from the siliceous sand bulk may be only marginally profitable, if not unprofitable, because of the low percentage fraction in the mineral sand and viable recovery of the other heavy minerals, including zircon, is then justified by the necessity to separate these other heavy minerals from the titaniferous fraction. Variously, Australian mineral sand deposits are relatively rich in non-titaniferous minerals - particularly zircon, xenotime and monazite[1, 2, 20].

Similar to other beach sand minerals, eluvial zircon is derived from the denudation of igneous rocks such as granites and pegmatites. Consequent alluvial zircon deposits are concentrated in stream beds but the richest deposits of zircon (and other heavy minerals) are found high along coastal beachfronts where primary concentration is achieved (over time and the cycle of tides) by energetic wave action of advancing surf depositing bulk sand high along the beach profile, stranding the heavy minerals fraction and returning the less dense, principally siliceous bulk with the less energetic retreating run-off seawater.

Typically, mineral sand deposits are mined by suction dredges floating in the lagging pool of advancing excavation as workings proceed along an existing or fossil beachfront. Sand containing a wide range of heavy minerals is retrieved by the dredge and initial partial separation of the lighter, principally silica bulk is achieved by primary

techniques in this operation. The resulting primary concentrate contains, to degrees varying by locality, the heavy minerals and some light fraction sands. The heavy minerals may include the titaniferous minerals rutile, ilmenite, leucoxene and arizonite, zircon, the rare earth minerals monazite, xenotime, bastnaesite and alanite plus a wide range of other heavy minerals including kyanite, chromite, magnetite, spinel, corundum, sillimanite, staurolite, garnet and cassiterite[24]. These minerals are separated by a series of mineral dressing operations whose sequence is designed to optimally isolate the principal and commercial mineral suite. Mineral dressing options are carried-out on both wet and dry concentrate fractions dependent upon the separation operation which may include screening, spiraling and other gravity jigging, cycloning, and both low-intensity and high-intensity magnetic and electrostatic separation[6, 24]. Routinely, the isolation of zircon from other minerals presents sets of separation criteria singularly characteristic to each heavy mineral concentrate. The sequence of separation of mineral fractions depends upon operational procedure (wet or dry stages) that is dependent upon available equipment, the component blend of the heavy mineral concentrate, and the various commercial constraints of separation thoroughness and end-point splits. Simple physical properties of main fraction minerals which become principal mineral separation parameters are set-out in Table {3.1.2}1.

Mineral	Specific Gravity (approx.)	Magnetic Susceptibility	Electrostatic Susceptibility
Rutile	4.2	non-magnetic	conducting
Ilmenite	4.7	highly magnetic	conducting
Leucoxene	4.5	magnetic	conducting
Zircon	4.5	non-magnetic	non-conducting
Monazite	5.2	magnetic	non-conducting
Xenotime	4.5	magnetic	non-conducting
Kyanite	3.6	non-magnetic	non-conducting
Garnet	4.0	magnetic	non-conducting
Quartz	2.6	non-magnetic	non-conducting

Table {3.1.2}1: Three fundamental physical properties of mineral-sand-derived heavy minerals which are pertinent to mineral processing recovery and separation strategies[28]. Grain size, size range and wet or dry conditions are among other relevant parameters.

3.1.3: Mineral Sources of Niobium and Tantalum.

Like their adjacent Group **4** metals zirconium and hafnium, Group **5** metals niobium and tantalum have strong geochemical coherence and in nature are always found together in oxide minerals. Also like their Group **4** neighbours, niobium and tantalum replace each other isomorphously not only in solid solution metallic form but in the crystalline-chemistry of their mineralogy. Consequently, niobium and tantalum occur in a continuous range of complex oxide minerals – usually including one or more other metals. Niobium and tantalum never occur in nature as sulphides[8].

Most of the world demand for niobium and tantalum ore concentrates is met by the broadly defined, contiguous columbite/tantalite group minerals or by the pyrochlore group minerals. A smaller but significant source of niobium and tantalum is tin slags – a secondary source that may well have been derived from the initial mineral group above. The chemical affinity[29] and co-occurrence of niobium and its higher periodic analogue, tantalum, with the major crust-forming elements iron, titanium, zirconium and others (which acted as carriers) ensured that the formation of niobium and tantalum minerals took place during the late stages of magma solidification. Because of this preferentially late crystallisation in the overall bulk iron/titanium/zirconium-based oxide minerals, the more scarce elements accumulated and differential crystallisation ensured that niobium and tantalum were consolidated in late solidifying minerals[29]. Further, as they occur isomorphously as solutes in crystal lattices, niobium and tantalum minerals are not recovered separately in mineral separation operations.

Prominent in high temperature niobium/tantalum-rich late mineralisation of the principally-oxide titanates, zirconates and tungstates, and the tin minerals - particularly cassiterite, was the pentavalent isomorphism of niobium and tantalum which as Nb^{5+} and Ta^{5+} replaced such quadrivalent ions as Ti^{4+}, Zr^{4+} and Sn^{4+} or trivalent ions such as Fe^{3+}, Mn^{3+} or RE^{3+} [29]. The valence compensation was achieved by simultaneous substitution of other cations (for example, $3Sn^{4+} \equiv 2Nb^{5+} + Fe^{2+}$ in the cassiterite lattice). In such mineralisation the simultaneous admission of significant proportions of niobium and tantalum plus iron, manganese, titanium, *et cetera* led to the formation of discrete minerals. Such selectivity during crustal mineralisation left a complex array of niobium/tantalum-rich minerals displaying comparable mineralogy. Niobium/ tantalum minerals are geochemically consanguineous.

Niobium and tantalum minerals have their origin in rocks of the alkali groups. Columbite/tantalite type minerals are derived from granites (magmatic) or from pegmatitic (intrusive) rocks whilst pyrochlore minerals are derived from nepheline syenite or carbonatite rocks. The proportion of tantalum (with respect to niobium) is higher in minerals of pegmatites and granites than in minerals of the pyrochlore family. Niobium and tantalum ores have historically been recovered from eluvial and alluvial deposits in open-cut placer mining operations. However, as such resources have become depleted, minerals are increasingly being mined from hard rock and weathered rock deposits, often in surface mining operations extended from the overlying placer deposit[8, 29].

Both niobium and tantalum minerals are found in a varied range of rocks in varied geological strata. Correspondingly, from these ore occurrences a complementary range of mineral concentrates is derived. The principal commercial niobium ore minerals are pyrochlore [$(Na,Ca,U)_2(Nb,Ta,Ti)_2O_6(OH,F)$], bariopyrochlore (pandaite) [$(Ba,U)_2(Nb,Ta,Ti)_2O_6(OH,F)$], columbite (or niobite) [$(Fe,Mn)(Nb,Ta)_2O_6$], perovskite [$(Ca,Na,RE)(Nb,Ti)O_3$], samarskite [$(Fe,Y,U)_2(Nb,Ti,Ta)_2O_7$], fergusonite [$(Y,RE)(Nb,Ta,Ti)O_4$] and stibiocolumbite [$Sb(Nb,Ta)O_4$]. The principal commercial tantalum minerals are tantalite [$(Fe,Mn)(Ta,Nb)_2O_6$], microlite [$(Na,Ca)_2(Ta,Nb,Ti)_2O_6(OH,F)$], wodginite [$(Ta,Sn,Mn,Nb,Fe,Ti)_{16}O_{32}$], simpsonite [$Al_4Ta_3O_{13}(OH)$], stibiotantalite [$Sb(Ta,Nb)O_4$], stuverite [$(Fe,Mn)(Ta,Nb,Ti)_2O_6$], euxenite [$(Y,Ce,Ca,U,Th)(Nb,Ti,Ta,Fe)_2O_6$] and ixiolite [$(Ta,Nb,Sn,Fe,Mn)_4O_8$][8, 14, 29, 30].

Generally, because niobium and tantalum occur concurrently in source minerals, each niobium/tantalum source mineral is also a tantalum/niobium source and so mining operations are conducted as dual resource operations. Whilst the pyrochlore minerals (mined for niobium) are only upwards of trace-rich in tantalum, the magmatic/ pegmatitic-derived columbite-tantalite type minerals tend to be relatively rich in the minor component metal. Niobium and tantalum are commonly associated with tin mineral deposits - particularly with cassiterite. In these mineralogical associations with tin, tantalum and, less abundantly, niobium occur both as independent minerals tantalite and columbite *or* as solutes in the cassiterite crystal lattice.

In Australia, niobium/(tantalum) is found as pyrochlore in carbonatite and apatite at Mount Weld. This western Australian ore is the second largest niobium deposit in the world behind the Araxa bariopyrochlore deposit of Brazil. Because of its complex mineralogy and fine pyrochlore dissemination through varied ore bodies, the Mount Weld deposit is awaiting commercial development. Another principally niobium deposit awaiting exploitation is the Brockman deposit in the eastern Kimberly region of Western Australia. Along with zircon, this vulcanogenic sedimentary orebody is rich in columbite and fergusonite which will yield niobium (tantalum) and rare earth elements. Tantalum (and niobium) are recovered as stibiotantalite from the tin-tantalum deposits at Greenbushes in south-western Australia. At Wodgina in Western Australia the ore-body pegmatite is highly weathered, the exposed face occurring as eluvial deposits of tantalum-rich wodginite. Wodgina is potentially the world largest deposit of tantalum and has significant niobium and tin as the minor mineral components[21, 22, 23, 29].

Approximately 10% of niobium is derived from tin and/or tantalum mining operations. Although the proportion of niobium to tantalum varies substantially across the range of ore minerals, the approximate total world production of tantalum is only 10% that of niobium[8, 29, 31].

Minesite production flow diagrams for the Western Australian Greenbushes and Wodgina operations are shown in Appendix **3** as Figure **{3.1.3}1** and Figure **{3.1.3}2** respectively whilst a typical minesite flow diagram for mineral sands production is presented in Figure **{3.1.3}3**, along with other relevant mine and process flow diagrams.

3.2: Established (Conventional) Reduction Processes in Refractory Metals Production.

Terrestrial deposits of alkaline and alkaline earth halide minerals are not uncommon. They report in metamorphic and sedimentary deposits as minerals such as halite, NaCl; sylvite, KCl; sylvinite, NaCl-KCl; carnallite, $MgCl_2.KCl.6H_2O$; fluorite, CaF_2 ; cryolite, Na_3AlF_6 ; plus some naturally occurring bromides and iodides such as those of silver. Unlike the halides of the transition metals that have substantial covalent bonding, the alkaline and alkaline earth halides predominately have ionic bonding and

are readily soluble. The geogony of Earth is such that transition elements, including the refractory metals, generally report in geological deposits as sulphides, oxides or principally-oxide minerals. Terrestrially occurring transition metal halides are essentially unknown. Despite the apparent contradiction, and avoiding any explanation of this geological anomaly, transition metal halides are thermodynamically stable. In almost all cases including all refractory metal halides, they are also freely water-soluble (which to a great extent explains the preceding geo-terrestrial aberration). Chlorides account for most of the naturally occurring halides and most of the industrial halogenation routes involve chlorine as the halogen, so much of the emphasis of industrial extractive processing is on chlorination, or chloridation – the synthesis of chlorides.

In the metallurgy of refractory metals, much is owed to G.L. Miller whose comprehensive work is published in a multiple-volume series which systematically itemises, discusses and analyses the complete scientific knowledge and accumulated industrial experience of the metals extraction, processing, physical and mechanical metallurgies of numerous refractory and other less common metals. Despite some technical obsolescence with respect to modern technological developments, these volumes, by and large, have never been scientifically superseded and are still substantively relevant some five decades after publication. Three of the volumes devoted to titanium[7], zirconium (and hafnium)[6] and niobium and tantalum[8] set-out an all-inclusive series of extraction strategies and describe the system processes and their associated chemistry. *Despite their vintage, these Miller volumes give a comprehensive exposé of possible extraction routes – both commercial and non-commercial. They are recommended as direct augmentative reference sources and no attempt to summarise them will be made here. However, they are specifically referenced where appropriate in the general discussion of extractive processes.*

3.2.1 : Halidation Routes in Extractive Processes.

The following nomenclature has been adopted to provide a deliberate division of emphasis for halogenation processes terms. The denotations may not all be in

accepted usage but have been so defined and used for the sake of succinctness and, moreover, to delineate that the extractive metallurgist remains essentially interested in the halide product rather than the halogenation process.

halogen	*Any of the elements of non-metallic Group **17** of the periodic table - that is, fluorine, chlorine, bromine, iodine or astatine.*
halogenation	*A process which utilises a halogen as a central (principal) reactant species. Emphasis is upon the **reactant halogen** and its associated **reaction process(es)** to define the term (word) – hence chlorination, et cetera.*
halide	*The compound of a halogen and a metal.* *Hence fluoride, chloride, bromide and iodide.*
halidation	*The production of a halide from a halogenation process.* *Emphasis is upon the process' **product halide** and its associated **production** to define the term – hence chloridation, et cetera.*

The numerous franchise variations of the overwhelmingly dominant commercial Kroll and Hunter processes all involve the metallothermic reduction of pure refractory metal chlorides. So it follows that the production of pure refractory metal chlorides is crucial in the production of refractory metals. The other refractory metal halide route, albeit of minor commercial significance and which is crucial in the production of high purity metal, is the reduction of the metal iodide in the van Arkel-de Boer process (see Figure **{3.2.2}3**). This is essentially regarded as a secondary refining process in which any appropriate feed refractory metal from impure metal to commercially pure grade, insitu within a reaction vessel, is halogenated with gaseous iodine to yield an iodide vapour which is reduced by thermal decomposition at a heated wire upon which the pure metal is then deposited. Comparable halide routes utilising bromine as the halogen have been shown to be feasible[6, 7, 8] but have not attracted commercial involvement. Fluoride routes are also feasible[6, 7, 8] in secondary refining, whilst "double fluoride" process routes are well established in primary extractive reduction[17, 29, 35, 39, 40].

The industrial production of refractory metal chlorides typically begins with a mineral oxide or, less frequently, a metalliferous slag or an impure metal source. The relative purity of allowable source raw materials is dependent upon the franchise technology employed in the chloridation and downstream extractive processes and the purity required in the final metal specification. Some fundamental process variations exist in the routes between oxide and pure metal chloride. These variations arise from both the thermochemical requirements of the source material and the particular process requisites implicated by the franchise technology.

The production of a metal chloride (chloridation) is essentially based upon the displacement of oxygen, carbon, or other target non-metallic species by chlorine during chlorination reactions involving chloridising agents Cl_2, HCl or MCl_2 and, where necessary, mixed with O_2 as an augmentative oxidising agent or with C, CO or H_2 as a reducing agent or intermediary[17].

Because it is either not systematically or not thermodynamically feasible to directly reduce the more stable oxide with chlorine or other halogen, the typical chlorination route for the refractory metals, in the most basic terms, is represented by the generalised equations:

metal oxide + carbon $\Rightarrow$ metal carbide$^{\nabla}$ + (CO, CO_2 or O_2)$^{\blacklozenge}$ .... **{3.2.1}1**

[$^{\nabla}$: Or metal carbonitride if processed in air or otherwise in the presence of nitrogen.]

[$^{\blacklozenge}$: Stoichiometry and thermodynamics (temperature) dependent.]

metal carbide + chlorine* + (CO_2 or O_2) $\Rightarrow$ metal chloride + ($CO + CO_2$)$^{\blacklozenge}$

..... **{3.2.1}2**

[* : Chlorine, Cl_2 , or chloridising agent such as hydrochloric acid, HCl.]

However, as they are simultaneously conducted, these process steps are usually portrayed as one and represented by the generalised equation:

metal oxide + carbon + chlorine* $\Rightarrow$ metal chloride + ($CO + CO_2$)$^{\blacklozenge}$

..... **{3.2.3}3**

More expansive descriptions of halogenation/halidation processes are provided in the following sections that address the production of the five refractory metals specific to this study.

The reactivities of the refractory metals titanium, zirconium, hafnium, niobium and tantalum with carbon, nitrogen, oxygen and hydrogen – particularly at higher temperatures – cause considerable difficulties with respect to the production of pure ductile metal. Ductility in metal is required for the fabrication of wire, rod (bar) and sheet products. Even the most negligible content of these ever-present contaminants is detrimental to, if not precluding of, such common and necessary production procedures. Any melting of pure metal to consolidate or further refine must be done in a highly controlled operation and this is typically achieved either by vacuum arc melting or by electron beam melting.

3.2.2: Production of Titanium.

Of the metals production industries producing Groups **4** and **5** refractory metals, the titanium production industry is, by far, the most commercially significant with world titanium output exceeding the output sum of the other metals. Of course, the perception of commodity "significance" is a subjective determination, hence strategic and technological significances may identify the nuclear industry metals zirconium, niobium and hafnium, or the electronics industry may recognise tantalum to be most significant. Be as these judgments may, the Groups **4** and **5** metals, and (indeed) all refractory metals, have been assigned to significant and highly specialised applications in modern technologies. A simplified metal production flow diagram for titanium, the largest production volume metal from Groups **4** and **5**, is shown in Figure **{3.2.2}1** whilst a diagrammatic summary of possible routes to titanium metal is presented in Figure **{3.2.2}2**. The van Arkel-de Boer process is represented in Figure **{3.2.2}3**.

Of the conventional extractive routes, there is no successful commercial process which reduces titanium metal directly from either the rutile mineral concentrate or from refined titania, TiO_2. Primarily, this is because pure titanium metal cannot practicably be obtained from its commercial oxide in a single step process as, even where highly efficient, the process reduces the trace impurity metals along with titanium. (This assured eventuality is generally true in the production of other refractory metals.) The impurity metals would then need to be removed by halidation (halogenation) of the impure metal, separation of the metal halides by fractional distillation, and then re-

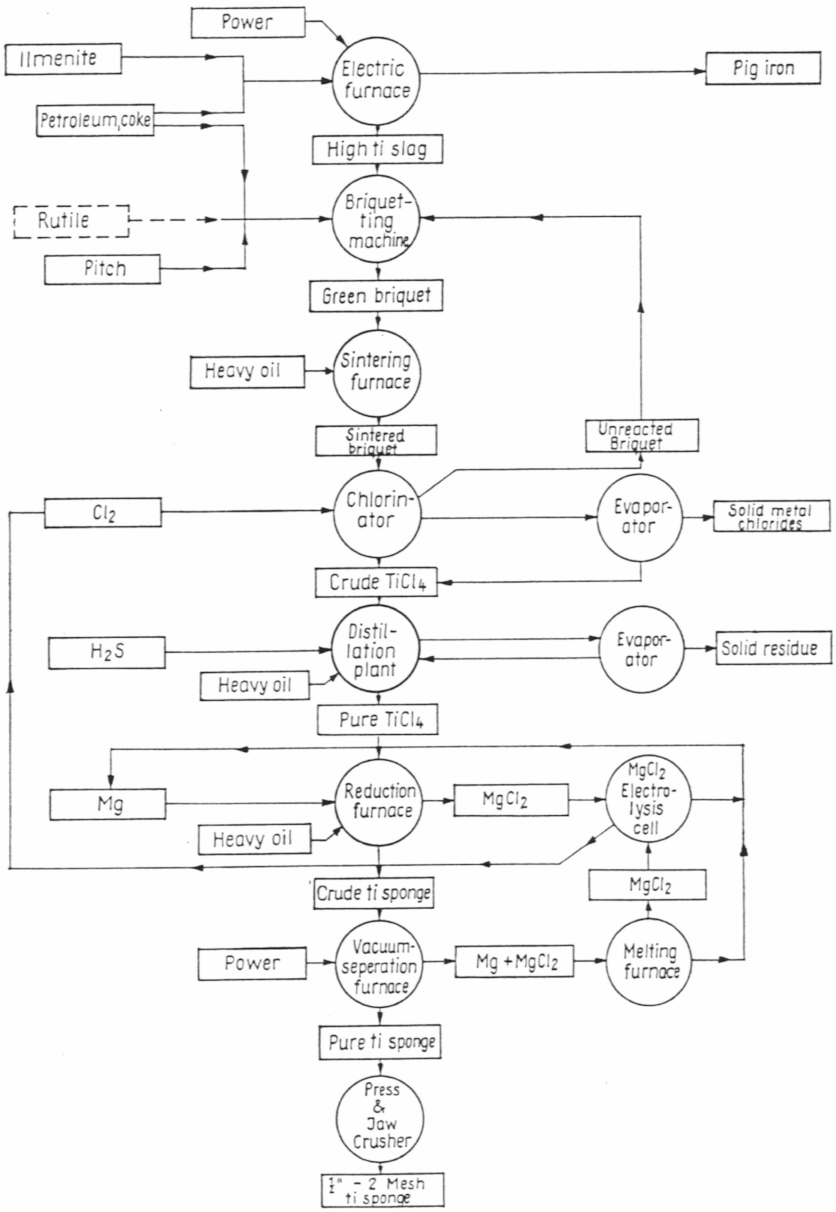

Figure {3.2.2}1: Flow sheet showing the typical production route from ore to titanium metal via chlorination and Kroll reduction[47].

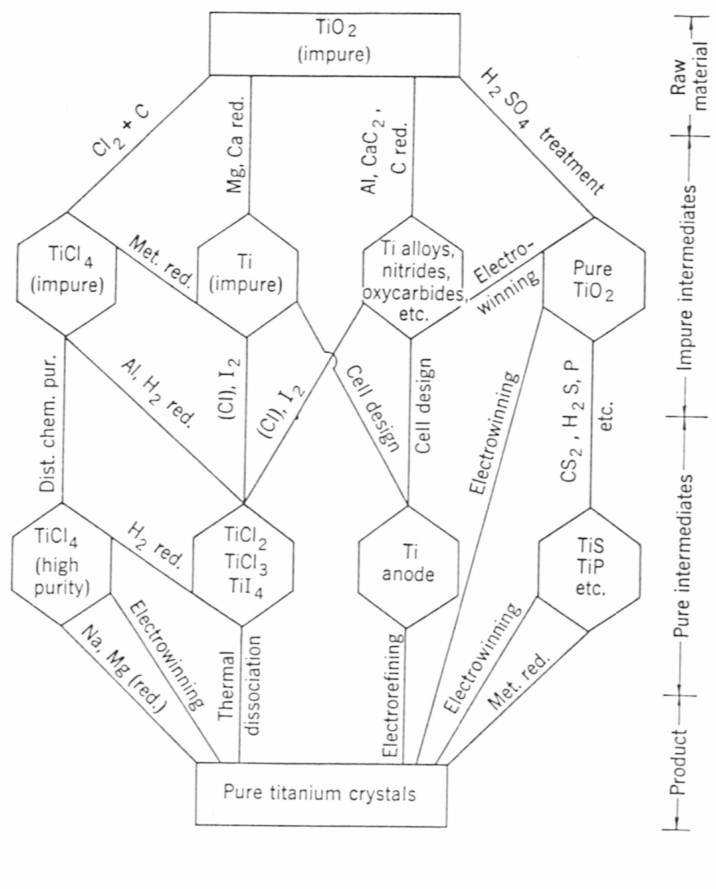

Figure {3.2.2}2: Diagrammatic summary of possible routes to titanium metal[42].

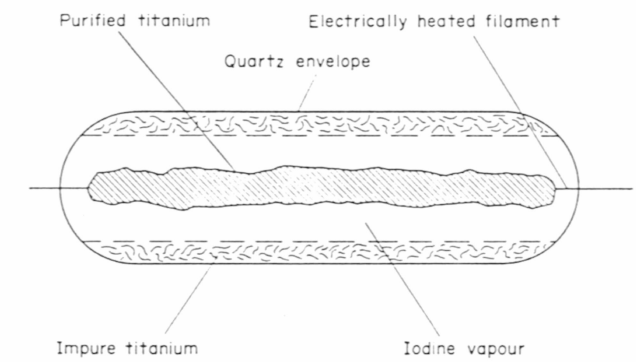

Figure {3.2.2}3: Simplified sketch showing the essential elements of the van Arkel-de Boer iodide process for refining titanium and similar metals[17].

reduction of the isolated titanium halide to yield titanium metal sponge of commercial purity. It is normal in extractive reduction operations producing titanium metal for the commercial "pure" titanium dioxide to be converted to a halide, thence fractionally distilled to separate the pure halide fractions, and finally, the pure metal halide is reduced to yield the commercially pure metal sponge. Titanium sponge produced by such means may then be powdered for specific applications or, more commonly, may be consolidated by vacuum arc melting into ingots appropriate for hot or cold forming.

It must be noted that, for all refractory metals, only metals of high purity are of true commercial value – a fact which sets refractory metals extraction strategies quite apart from those of ferrous extractive metallurgy and most of the common non-ferrous extractive metallurgy routes. Of course, titanium metal of good purity (above 99% titanium but higher in oxygen, nitrogen and carbon than commercial grade) could be reduced direct from refined titania but, because of the property impediments bestowed by such a level of light element contamination, its real value in the current marketplace would be at a level rendering it non-commercial. However, if some common, lightweight compressive-structural or manufacturing applications could be established utilising this grade of titanium (rather than aluminium or steel) then a realistic commercial future might exist for titanium in the sense that aluminium and steel are now accepted.

The impurity conundrum is alleviated in titanium production by the direct carbon-assisted halidation of the "pigment"-grade oxide thence followed by halide separation by fractional distillation, then metallothermic reduction of the pure titanium halide. So refinement precedes reduction in commercial-grade operations. Typically, in titanium extraction routes the halide is chloride and the halogen source is usually gaseous chlorine (Cl_2) or hydrochloric acid (HCl) depending upon the franchise technology of the process route. Most franchise technologies are variations of the Kroll process and the process route chosen is dependent upon several factors that may be related to the process technology available. However, the most fundamental factors relate to the feed material - whether it is native rutile or synthetic rutile, the derivative of the more abundant ilmenite, or the quality of the feed mineral, or indeed, whether the mid-process product, titania (TiO_2), represents a final product or a refined feedstock for re-chlorination and subsequent metallothermic reduction [Kroll (Mg) and Hunter (Na)

processes] or reduction by thermal decomposition. It should be noted that most – over 90% by estimates[14, 41] – of the world production of commercially pure titania is utilised in that form, predominantly as paint opacifier (pigment).

Whilst some routes that reduce ilmenite ($FeO.TiO_2$) to useful metallic forms have been proven[7], the usual first stage process involves the removal of iron (as FeO) to yield what is known as synthetic rutile. Synthetic rutile is a sponge mineral being the product of leaching by partial acid digestion normally after reduction by carbon of FeO to iron. The product residue is a porous solid TiO_2 of good purity which is normally of higher purity than run-of-mine rutile concentrates and therefore of greater value. This process provides the bonus of removing much of the tramp or mineral-impurity elements fraction along with the iron. Typically in synthetic rutile products only minor iron and digestible elements remain in complex stereo-mineralogical association or in tightly bound mineral forms. However, other minor tramp elements survive the acid leach because of their chemical nobility – whilst these fractions routinely remain at trace proportions in synthetic rutiles, their presence may be tolerated in "pigment grade" titania. For high quality titanias of pigment grade, synthetic rutile is re-chlorinated, fractionally distilled and re-oxidised to pure TiO_2. Pigment grade titania is the preferred starting point titania for chlorination to titanium tetrachloride, $TiCl_4$, and thereafter to metallurgical reduction yielding commercial grade titanium metal[1, 41, 42].

The raw minerals used to produce the pure titania common to both major end users of titania, may be rutile concentrate (being 95% to 97% TiO_2), ilmenite concentrate (being about 55% TiO_2), leucoxene concentrate (being above 70% TiO_2) or a titaniferous slag being of variable TiO_2 content. In the case of the iron-rich concentrates, an essential step is taken in producing a synthetic rutile by the digestion of the iron phases plus other minerals from the TiO_2 leaving a relatively pure titania (of higher purity than rutile concentrates). There are various acknowledged commercial processes which reduce ilmenite ($FeO.TiO_2$) minerals to synthetic rutile, however, they all fundamentally rely upon selective reduction and/or acid digestion of the FeO (wustite) phase plus some other tramp oxides and compounds which exist in minor or

trace impurity proportions by intimate mechanical or mineralogical association in the mineral ore concentrate. Older Australian synthetic rutile processes typically followed the digestion route with the decomposition of ilmenite by concentrated sulphuric acid, followed by hydrolysis and precipitation of either rutile and anatase forms of titania[19]. However, newer plants follow the less polluting option of pre-reduction of the wustite phase (FeO) thence digestion in a less concentrated acid process[20].

The direct metallothermic reduction of titania using calcium as the reductant can be achieved and has been commercially attempted, however, the reduction yields a brittle titanium metal containing 0.2% to 0.5% oxygen. The extensive solubility of oxygen in titanium (as in other Groups **4** and **5** metals) ensures that the complete removal of oxygen by calcium is not possible[40].

The commercial production of titanium tetrachloride, $TiCl_4$, typically begins with the chloridation of TiO_2 by gaseous chlorine using petroleum coke as a reducing agent. The titania and carbonaceous reductant are intimately blended and briquetted or otherwise agglomerated before charging into the chlorinator. Because of more efficient reactant contacting, modern chlorination processes utilise fluidised-bed reactors from which $TiCl_4$ has to be separated from other reaction products by spray and condensation techniques. Chloridation reactions are exothermic and the bed temperatures range between 800°C and 1000°C[40]. Further to the generalised equations **{3.2.1}1, {3.2.1}2** and **{3.2.1}3**, and moreover, the basic chloridation reactions (which are dependent upon thermodynamics) are given[50] as :

$$TiO_2 + 2Cl_2 + 2C \Rightarrow TiCl_4 + 2CO \quad \text{..... } \{3.2.2\}1$$

$$TiO_2 + 2Cl_2 + C \Rightarrow TiCl_4 + CO_2 . \quad \text{..... } \{3.2.2\}2$$

An intermediate product of about 94% $TiCl_4$ plus 4% solid and 2% liquid chloride impurities is further refined by fractional distillation and other precipitation methods removing mainly iron, chromium, vanadium, tin, silicon and aluminium chlorides to yield 99.9% $TiCl_4$. This commercially pure titanium tetrachloride is the final product of refining towards commercial-grade titanium metal and the starting

point for industrial extractive reduction processes. Titanium tetrachloride is volatile at ambient temperatures having a melting point of – 23°C and a boiling point of 135.8°C [17] – facts of physical stability which are pertinent to distillation and reduction strategies.

The various franchise reduction routes use minor variations of either the magnesium metallothermic (Kroll) or sodium metallothermic (Hunter) processes. These titanium tetrachloride reduction processes are conducted in steel reactors under an argon atmosphere. In the dominant Kroll process(es), the reductant magnesium metal is charged into the reactor vessel which is subsequently heated to above the melting point of magnesium chloride – a principal reaction product – and maintained at a preferred temperature in the range 850°C to 950°C under controlled atmosphere whilst titanium tetrachloride is metred into the reactor[17, 50]. The Kroll process reduction reaction is given[50] as:

$$TiCl_4 + 2Mg \Rightarrow Ti + 2MgCl_2. \quad \text{..... } \{3.2.2\}3$$

In this typically batch process, the liquid magnesium is initially present as a discrete liquid phase and the reaction proceeds quite rapidly. However, as the precipitating titanium sponge increases in volume, it entraps much of the reactant magnesium and the liquid magnesium chloride must be tapped-off to enable the un-reacted titanium tetrachloride to contact the free magnesium. There may be several such tappings per process batch and excess magnesium is used to ensure near total titanium reduction.

The sponge titanium product may typically contain 20% to 30% $MgCl_2$ plus 10% to 20% magnesium metal[50] which, process dependent, may be removed either by acid leaching or by vacuum distillation. The acid leaching process produces a final titanium sponge having an oxygen content that may leave it suitable for some alloying applications but renders it unacceptable for most further process routes. The preferred process route is by vacuum distillisation in a retort at about 1000°C to remove remnant magnesium materials[7, 12, 17, 40, 50]. The sponge is subsequently vacuum arc melted or otherwise re-melted, processed or further refined by the iodide process.

The other commercially significant titanium metal reduction route is the Hunter process in which titanium tetrachloride is metallothermically reduced using sodium metal as the reductant. The product is comparable and the method largely analogous to the Kroll process. The fundamental reduction reaction is given[50] as:

$$TiCl_4 + 4Na \Rightarrow Ti + 4NaCl. \quad \text{..... } \{3.2.2\}4$$

However, this reaction is more exothermic than the magnesium reduction and external cooling is required during reduction. When stoichiometric proportions are reacted above the melting point of sodium chloride, 801°C, and below the boiling point of sodium metal, 883°C, the high vapour pressure of sodium ensures that the reaction effectively takes place as a gas phase reaction and titanium is produced as a finely divided powder (making this the desirable route where pure, fine metal powder is the required final product). However, titanium dichloride forms a lower eutectic with sodium chloride[40] allowing a greater operating temperature range and thus sodium reduction is often achieved in two steps[50]. The reactions for this option are given as:

$$TiCl_4 + 2Na \Rightarrow TiCl_2 + 2NaCl \quad \text{..... } \{3.2.2\}4a$$

$$TiCl_2 + 2Na \Rightarrow Ti + 2NaCl. \quad \text{..... } \{3.2.2\}4b$$

This two-stage reduction produces much larger titanium crystals that are more stable against the tendency to oxidise during the pursuant water leaching which removes the sodium chloride.

Titanium metal production by the electrolysis of fused titanium-bearing salts has been proven repeatedly across the years in pilot plant scale operations[7, 26, 41, 42, 52]. However, none of the numerous patents generated from these studies has turned into commercial reality for this promising high purity titanium production method of fused salt electrolysis. Also, many thermal arc and similar plasma reduction methods have

been studied, some indicating reasonable feasibility, but none has been successfully tested at pilot plant scale[58].

Whilst commercial grades of titanium are of generally high purity (> 99.9%) they do not meet some metal specifications. However, the production of soft, ductile titanium of very high purity for special applications is met by low volume operations that are not regarded as having a demand, nor a production volume of commercial significance. Titanium of very high purity is obtained by a further refining step which involves the thermal dissociation, or thermal decomposition, of either bromides or iodides which are thermodynamically less stable than are the comparable fluorides and chlorides. The significant refining process for titanium and other refractory metals is the van Arkel-de Boer process, which may be described as a catalytic distillation process with iodine as the catalyst[41].

In the van Arkel-de Boer process, "impure" metal (usually of nominal commercial purity) to be refined is charged into a sealed quartz capsule through which passes a tungsten filament which is isolated from the metal charge by iodine vapour at low pressure (as is shown in Figure **{3.2.2}3**). The iodide formed at the vapour/metal interface depends upon the temperature to which the impure metal charge is heated. In the case of titanium, the synthesis of the tetraiodide is favoured at temperatures around 175°C, whilst the di-iodide is favoured around 525°C. The reactions may be given[17] as:

$$[Ti]^{175°C} + 2I_2 \Rightarrow TiI_4 \Rightarrow [TiI_4]^{525°C} \Rightarrow TiI_2 + I_2 \quad \text{... } \{3.2.2\}5$$

Iodide vapours formed by these reactions pass over the filament, which is heated to 1400°C, and decompose leaving pure metal deposited upon the filament whilst returning free iodine vapour to repeat the cycle. The above di-iodide reaction is effectively trivial under the prevailing thermochemistry and the overriding reaction for the tetraiodide decomposition is given[12, 17] as:

$$[TiI_4]^{1400°C} \Rightarrow Ti + 2\,I_2 \quad \text{..... } \{3.2.2\}6$$

During the process, titanium oxides, titanium nitrides and titanium carbide are not attacked by the iodine and so are by-passed in this closed cycle system. However, co-reduced impurity metals are prone to iodisation and thermal decomposition, so operating temperatures are selected and controlled such that impurity iodides do not become volatile in operational temperature ranges for titanium iodide.

3.2.3: Production of Zirconium and Hafnium.

In varying but minor proportions, hafnium occurs in all zirconium ores. Until the advent of specific purpose, high purity zirconium for nuclear reactor applications, the hafnium content in zirconium was tolerated as its removal, which required sophisticated separation techniques, bestowed imperceptible advantage (if any) to physical, chemical and mechanical properties. Also, because of its high thermal neutron cross-section, hafnium is a preferred commodity for the fabrication of control rods for nuclear reactor installations. The high thermal neutron cross-section of hafnium is the property-reciprocal of the very low thermal neutron cross-section of zirconium that vindicates the use of zirconium in nuclear applications. This reciprocity prohibits even minor hafnium from nuclear grade zirconium, a limitation that consequently dictates production strategies. In recent decades virtually all zirconium and hafnium final products have been derived from the source mineral zircon. So, this industrial reality is the case that is addressed here – the baddeleyite case is but a sub-set of zircon processing.

After zircon sand has been concentrated by mineral processing techniques the concentrate is subjected to chemical processing to digest the mineral prior to separation and reduction of the component metals. There are several acknowledged decomposition route possibilities employed commercially in this initial extractive stage. Amongst these are caustic fusion, chlorination, fluorination, lime sintering, and soda ash sintering[6, 43, 55]. The initial three processes result in full digestion, or "solublisation", of the zircon. The two sintering processes are selective in that they digest only one

minerallogical species from the zircon (either silica or zirconia/hafnia). Other augmentative processes may precede chemical decomposition. One pre-digestive treatment deserving of mention is plasma dissociated zircon (PDZ) which is notable in its effect of separating the post plasma-treatment species of the prior crystalline zircon ($ZrSiO_4$) into distinct crystalline ZrO_2 (both tetragonal and monoclinic) in a matrix of amorphous SiO_2[33, 59]. The glassy silicon dioxide phase is brittle and, by and large, can be physically separated by mechanical methods thus allowing enhanced chemical contacting and more efficient digestion. Where included in extractive operations, digestive processes precede refining processes such as fractional distillation or solvent extraction operations.

In the caustic fusion process zircon is reacted (or "fused") with sodium hydroxide (caustic soda), NaOH, at 650°C for 2 hours. After leaching of the fused product, the residue sodium zirconate, Na_2ZrO_3 , and sodium hafnate, Na_2HfO_3 , are dissolved in nitric acid, HNO_3[55]. The nitrate solution is directly treated with ammonia to precipitate the hydroxide that is calcined to oxide. Whilst this oxide product is relatively free of other impurities, it is a mixture of zirconium and hafnium oxides [$(Zr,Hf)O_2$]. Since minor hafnium oxide is present, the impure zirconium oxide can only be used as zirconia in purity-insensitive applications. Also, in nuclear applications (because zirconium and hafnium have thermal neutron absorption cross-sections of 0.18 and 105 barns respectively [35] which qualifies each for diametrically different specific "capture" applications) nuclear grade zirconium must have a hafnium impurity level (variously specified) below 200 parts per million. In a solvent extraction technique comparable to the Fischer method, this separation level is achieved by acidifying the nitrate solution and (in lieu of ammonia) preferentially extracting the zirconium into an organic solvent leaving behind the hafnium and other impurities in the mother liquor to be stripped separately[6, 55]. High purity zirconium dioxide and hafnium dioxide are recovered from the organic solution by any of several stripping processes. Conversely, by way of its negligible effect upon the thermal neutron absorption cross-section of hafnium in critical nuclear applications, a greater level of zirconium impurity can be tolerated (up to 2 percent[35]) in nuclear grade hafnium.

The direct chlorination of zircon concentrates produces a cocktail of chloride products – including chlorides of the two major components – which have to be separated by fractional distillation. This route is obsolete and modern processes avoid the synthesis of silicon tetrachloride, $SiCl_4$, which is not only costly in terms of chlorine consumption but has to be separated (along with the minor chloride fractions) from the zirconium tetrachloride and further processed or disposed-of in an environmentally acceptable manner[45]. Typically, modern chlorination routes are extractive stage routes that start with the pre-refined pure oxide (as discussed in later paragraphs).

The lime sintering process relies on the selective attack by calcium carbonate on the silica portion of zircon [$(Zr,Hf)O_2.SiO_2$]. The blended reactants are sintered at 1400°C for 2 hours[55] and the sinter product acid leached to remove soluble calcium silicate and leaving insoluble zirconium and hafnium oxides as is represented in the following equation[55].

$$(Zr,Hf)SiO_4 + CaCO_3 \Rightarrow (Zr,Hf)O_2 + CaSiO_3 + CO_2 \quad \text{..... } \{3.2.3\}1$$

In contrast to the above, a soda ash sintering process can be utilised to selectively make soluble the zirconia portion of the zircon [$(Zr,Hf)O_2.SiO_2$]. In this process zircon and sodium carbonate (soda ash), Na_2CO_3, are blended then sintered at 1000°C to 1050°C for 2 to 4 hours and the reaction is described by the following equation[55].

$$(Zr,Hf)SiO_4 + Na_2CO_3 \Rightarrow Na_2(Zr,Hf)SiO_5 + CO_2 \quad \text{..... } \{3.2.3\}2$$

The solid, complex silicate breaks down upon treatment with concentrated hydrochloric acid or, more commonly, nitric acid as represented in the following equation[55].

$$Na_2(Zr,Hf)SiO_5 + 4HNO_3 \Rightarrow (Zr,Hf)(NO_3)_2 + 2NaNO_3 + SiO_2 + 2H_2O$$

$$\text{..... } \{3.2.3\}3$$

Upon filtration to remove silica plus un-reacted zircon, the solution can be directly treated with ammonia to precipitate the refractory metal hydroxide that, after calcining, yields the hafnia-impure zirconia. More typically, to produce the valuable separated oxides, the nitrate solution is reacted with sulphuric acid to separate zirconium sulphate by precipitation[6, 55]. The sulphate is digested in ammonia to produce the hydroxide that is calcined to produce a zirconium dioxide of good purity. Hafnium is precipitated as the hydroxide from the remaining mother liquor and is subsequently calcined to the pure oxide. Typically, zirconium and hafnium hydroxides are calcined in rotary furnaces at 800°C to 850°C with residence times sufficient for the total decomposition of the hydroxide to oxide.

In the fluoride process, zircon and potassium silico-fluoride, K_2SiF_6, (or the alternative, potassium ferric-fluoride, K_3FeF_6[6]) are blended then sintered at 700°C for 4 hours in an electric pit-type furnace. The general reaction is described by the following equation[6, 55].

$$(Zr,Hf)SiO_4 + K_2SiF_6 \Rightarrow K_2(Zr,Hf)F_6 + 2SiO_2 \quad \text{..... } \{3.2.3\}4$$

The sintered product is leached with water to extract the zirconium/hafnium double fluoride leaving the insoluble silica. The small but distinct difference in solubilities between the zirconium double fluoride, K_2ZrF_6, and the hafnium double fluoride, K_2HfF_6, is utilised to separate the Group 5 salts as, during successive crystallisation cycles, the zirconium salt is deposited and the hafnium is retained in liquid solution[6, 30, 55].

The separated double fluorides are each reacted with ammonia to produce zirconium hydroxide, $Zr(OH)_2$, or hafnium hydroxide, $Hf(OH)_2$. The washed, filtered and dried hydroxide precipitates are calcined at 800°C to 850°C to produce the commercially pure zirconia (ZrO_2) or hafnia (HfO_2) that are standard feeds for chlorination routes, direct reduction routes and a well established range of ceramics applications.

In a further refining extractive stage, reactor grade zirconium dioxide and hafnium dioxide can be produced with complete separation of hafnium from zirconium by solvent extraction utilising the Fischer chloride method. This method exploits a two-phase aqueous-organic system in multi-stage, counter-current configuration based upon hydrochloric acid - thiocyanate - methyl isobutyl ketone (HCl – HSCN – *MIBK*) chemistry. This process requires a zirconium/hafnium oxychloride, (Zr,Hf)OCl, free of iron and other metal impurities, in solution with hydrochloric acid to which ammonium thiocyanate, NH_4SCN, is added. After multi-stage contacting of this "aqueous" phase with the organic (*MIBK*) HSCN-containing phase the resulting end liquors are an organic phase containing *all* hafnium plus minor zirconium and a hafnium-free aqueous phase containing virtually all of the zirconium as oxychloride, $ZrOCl_2$, which is converted to ZrO_2. The organic phase is multi-stage contacted with HCL to selectively extract the remaining zirconium content. Finally hafnium is extracted by scrubbing the organic phase with sulphuric acid, H_2SO_4, and is recovered as pure HfO_2. Thiocyanate and MIBK are continually recovered and recycled in this process[35].

Where separation of zirconium and hafnium is not required or where it has already been achieved in a previous step, the oxide can be converted from the chloride using a simple but commercially outdated procedure. In this route zirconium (or hafnium) tetrachloride is reacted with hydrochloric acid to produce zirconium oxychloride octahydrate ($ZrOCl_2 \cdot 8H_2O$) which is crystallised out from the strong acid solution [24, 25]. The washed and dried crystals are decomposed (calcined) at about 1100°C to leave a dense zirconium dioxide product as described by the following equation.

$$[ZrOCl_2 \cdot 8\,H_2O]^{1100°C} \Rightarrow ZrO_2 + 2\,HCl\uparrow + 7\,H_2O\uparrow \quad \text{..... } \{3.2.3\}5$$

As with titanium extractive metallurgy, fractional distillation is commonly and successfully used to separate and refine chloride products of the chlorination chemistry of other refractory metal extractive operations. However, other than chance mineral impurities, titanium minerals have no titanium-analogue element (as zirconium has hafnium and niobium has tantalum) that needs to be separated by fractional distillation

of its chlorides. The tetrachlorides of zirconium and hafnium closely share physical and chemical properties which ensure that they are difficult to separate from each other, however, because of their relatively high sublimation points, they can be conveniently separated (on this basis) from the other pertinent chloride fractions, including titanium tetrachloride, which are present in the cocktail product of chlorination. The melting and boiling points (or sublimation point) at atmospheric pressure of chlorides common to refractory metal chlorination processes are given in Table **{3.2.3}1**.

Table {3.2.3}1: Melting, boiling and/or sublimation points at atmospheric pressure of chlorides common as products of the chlorination process for minerals and ore concentrates of titanium, zirconium, hafnium, niobium and tantalum. Temperatures given are from the *CRC Handbook of Chemistry and Physics - 70th Edition* [5] and are proffered as indicative rather than definative as some range for these values exist in the Literature. Hence, the values here may vary slightly from those given in the text (which have been cited from elsewhere).

Group	Metallic Element	Chloride	Melting Point (°C)	Boiling Point (°C)
1	Sodium	NaCl	801	1413
1	Potasium	KCl	770	subl. 1500
2	Magnesium	$MgCl_2$	714	1412
3	Thorium	$ThCl_4$	-	subl. 770 decomp. 928
4	Titanium	$TiCl_4$	- 25	136.4
4	Zirconium	$ZrCl_4$ $ZrCl_2$ $ZrCl_3$	- - -	subl. 331 decomp. 350 decomp. 350
4	Hafnium	$HfCl_4$	-	subl. 319
5	Vanadium	VCL_4	- 28	148.5
5	Niobium	$NbCl_5$	204.7	254
5	Tantalum	$TaCl_5$	216	242
6	Chromium	$CrCl_2$ $CrCl_3$	824 [(calc.) 1150]	- subl. 1300
6	Molybdenum	$MoCl_5$	194	268
6	Tungsten	WCl_5 WCl_6	248 275	275.6 346.7
7	Manganese	$MnCl_2$	650	1190

8	Iron	$FeCl_3$ (or Fe_2Cl_6)	306	decomp. 315
		$FeCl_2$	-	subl. 670 - 674
12	Zinc	$ZnCl_2$	283	732
13	Aluminium	$AlCl_3$ (or Al_2Cl_6)	190	decomp. 262
14	Silicon	$SiCl_4$	- 70	57.6
14	Tin	$SnCl_4$	- 33	114.1

$ZrCl_4$ and $HfCl_4$ can be effectively separated by fractional distillation at close to atmospheric pressure with NaCl and KCl added to lower the liquidus of the quarternary system. (Without NaCl and KCl fractional distillation is possible in a narrow range in liquid above the triple points of the tetrachlorides (> 435°C) but below the critical temperature (< 500°C) and at very high pressure (> 65 atmospheres)[33].) Extractive fractional distillation can be conducted to high purity standards. The success of such a method avoids the more complex and expensive necessity of the alternative route involving aqueous dissolution of the combined $(Zr,Hf)Cl_4$ followed by multiple-stage solvent extraction to separate the zirconium and hafnium, thence individual precipitation, hydrolysis, calcination to pure oxides, and finally, re-chlorination to pure tetrachlorides for Kroll reduction[8, 33, 34].

Halogenation of oxides is the most common route used in the preparation of anhydrous halides, particularly in the preparation of chlorides[41]. As with fellow Group **4** metal oxide titanium dioxide, the standard oxides of zirconium and hafnium have greater thermodynamic stability than do their chlorides. Consequently, following the titanium example and in a similar reactor, zirconium dioxide or hafnium dioxide is reacted with a chlorine source (usually gaseous chlorine) in the presence of carbon. In a system analogous to the chloridation of titanium dioxide, chlorine reduces an intermediate zirconium carbide or hafnium carbide allowing a favourable overall reaction equilibrium. The reactions reflect general equations **{3.2.1}1, {3.2.1}2** and **{3.2.1}3** and are analogous to titanium equations **{3.2.2}1** and **{3.2.2}2**. The overall thermodynamics-dependent chloridation reactions for zirconium dioxide and hafnium dioxide are given[6, 55] as follows.

$$ZrO_2 + 2C + 2Cl_2 \Rightarrow ZrCl_4 + 2CO \quad \text{..... } \{3.2.3\}6$$

$$ZrO_2 + C + 2Cl_2 \Rightarrow ZrCl_4 + CO_2 \quad \text{..... } \{3.2.3\}7$$

$$HfO_2 + 2C + 2Cl_2 \Rightarrow HfCl_4 + 2CO \quad \text{..... } \{3.2.3\}8$$

$$HfO_2 + C + 2Cl_2 \Rightarrow HfCl_4 + CO_2 \quad \text{..... } \{3.2.3\}9$$

The above overall reactions are exothermic and so, once initiated, take place autogenously. The reaction stoichiometry is dependent upon the process temperature, that is, the thermodynamics - as is reaction rate and equilibrium.

The predominant zirconium tetrachloride, unlike titanium tetrachloride, is a hygroscopic solid and thus requires different processing consideration. Crude zirconium tetrachloride is a loose, light powder that readily absorbs moisture from air to form hydrogen chloride plus zirconium hydroxide (which may be calcined to the oxide and re-chlorinated). Preferably, avoiding this debasing hydration, care is taken to introduce freshly produced zirconium tetrachloride into the reactor in the Kroll reduction to ductile, oxygen-free metal[12].

The metallothermic reduction of zirconium tetrachloride using the Kroll process remains the predominant production route to ductile metallic zirconium. The Kroll reaction is given[6] by the following equation (which is analogous to that for titanium).

$$ZrCl_4 + 2Mg \Rightarrow Zr + 2MgCl_2 \quad \text{..... } \{3.2.3\}10$$

The Kroll process produces ductile zirconium of good to high purity that cover the standard "commercial" purity to "reactor grade" zirconium. However, as for titanium, where a very high purity zirconium is required, the van Arkel - de Boer iodide

process is utilised to produce small-batch production runs. The equation is given as follows[6].

$$[Zr]^{200°C} + 2I_2 \Rightarrow ZrI_4 \Rightarrow [ZrI_4]^{1300\,°C} \Rightarrow Zr + 2I_2 \text{ ..... } \{3.2.3\}11$$

The production of metallic hafnium is generally by Kroll reduction of the tetrachloride that yields a metal of good to high, reactor grade purity. Further refining by the de Boer - van Arkel iodide process yields hafnium of very high purity. Alternatively, Kroll hafnium may be further refined and consolidated by techniques of the electron beam melting process. Pure hafnium may also be produced during direct electrolysis by deposition from molten halide salts ($HfCl_4$ in NaCl-KCl-NaF at 700°C)[25, 44, 46, 53].

In a manner analogous to that for zirconium, the Kroll reduction of hafnium tetrachloride is given by the following equation.

$$HfCl_4 + 2Mg \Rightarrow Hf + 2MgCl_2 \text{ ..... } \{3.2.3\}12$$

Similarly, the following equation indicates the analogous iodide route for the purification of hafnium.

$$Hf + 2\,I_2 \Rightarrow HfI_4 \Rightarrow Hf + 2I_2 \text{ ..... } \{3.2.3\}13$$

Reduction route options (Kroll and electrolytic) are schematically shown in Figure {3.2.3}1 and Figure {3.2.3}2.

A novel technique for the separation of zirconium from hafnium utilising density difference rather than some specific difference in their chemistries has been

suggested by HOWELL, *et al* [15] who maintain that they have achieved a "separation factor better than 10^6 in a single stage" from starting material of mixed zirconium/hafnium oxide being derived from run-of-mine zircon concentrates. The method requires the conversion of the oxides to nitrides by carbothermic reduction of the oxides in a carbon-saturated liquid copper solvent at 1500°C with entrained gaseous nitrogen. The oxide conversions to nitride take the following routes[15].

$$ZrO_2 + 2C + N \Rightarrow ZrN + 2CO \quad \text{..... } \{3.2.3\}14$$

$$HfO_2 + 2C + N \Rightarrow HfN + 2CO \quad \text{..... } \{3.2.3\}15$$

The liquid copper solvent lowers the activity of the reactant refractory metals and, in essence, has a density such that the insoluble nitride precipitates are physically separated in an unequivocal manner as the zirconium nitride floats to the surface whilst the hafnium nitride sinks to the bottom. Of themselves the nitrides are of high value, but they may be decomposed to metallic form or re-oxidised to pure oxide form.

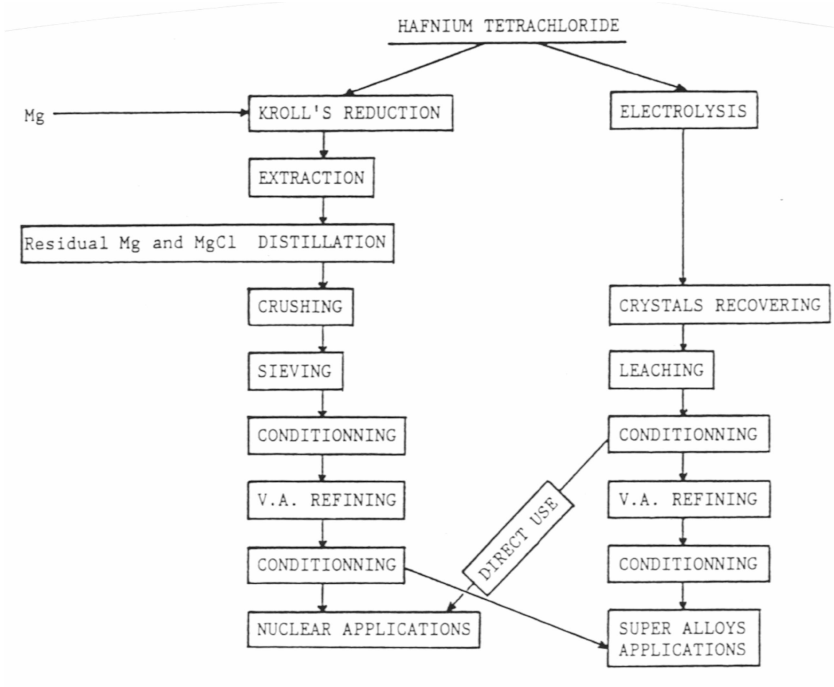

Figure {3.2.3}1: Flow sheets comparing principal steps in the alternative production routes from hafnium tetrachloride to hafnium metal for the Kroll reduction and electrolytic methods [53].

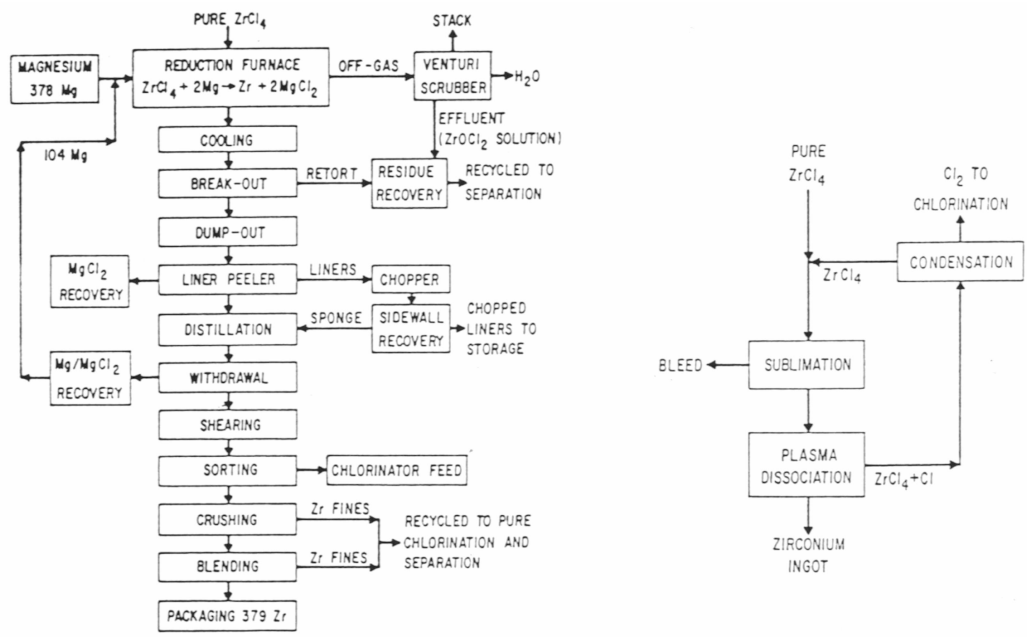

Figure {3.2.3}2: Flow sheets comparing the principal steps in the production of zirconium metal from its tetrachloride via the conventional Kroll reduction route and also by a pilot-proven plasma dissociation (reduction) route alternative [74].

Metallic zirconium (or hafnium) of high purity is not readily produced because of the considerable difficulty in economically separating zirconium(hafnium) from mineralogically associated hafnium(zirconium), titanium, iron, aluminium and silicon (quite apart from the interstitial light impurity elements). Zirconium and hafnium are chemically very similar whilst their Group **4** partner, titanium, displays similar chemical characteristics and only a few separation strategies are available when separating it from zirconium or hafnium. Titanium may be separated by reducing it to its trivalent state so that it remains in solution and subsequently separated. Iron, aluminium, silicon and other elements are separated from zirconium or hafnium by fractional distillation of halides, by precipitation or solubility differences, or by the systematic manipulation of some other minor difference in physical or chemical properties of the species present[6, 25, 33, 34, 36, 41, 53]. Preferred separation techniques for zirconium and hafnium recommended and described in later publications are, in one form or another, essentially described by MILLER in his early comprehensive volume *Zirconium*[6].

3.2.4: Production of Niobium and Tantalum.

Niobium and the less abundant tantalum always occur together in nature in close mineralogical association - always in oxidic minerals which themselves most likely occur with oxide minerals of other metallic elements. With the exception of some pyrochlore minerals (which yield negligible tantalum), all niobium and tantalum minerals produce intimate mixtures of these analogue Group **5** elements upon digestion or reduction. So, similar process separation criteria exist for niobium and tantalum as exist for zirconium and hafnium.

As with other refractory metals, *insitu* ore lodes and their concentrates constitute the primary source of niobium and tantalum - a source overwhelmingly greater than scrap and recycled waste which comprise the secondary source of the metals. Also as with other refractory metals, the initial steps in the production of metallic niobium and tantalum is the refining to pure oxides, chlorides or fluorides from which pure metals

can be reduced[8,29]. Alternatively, refined ferroniobium or ferrotantalum for use in steel alloying may be the desired end-product. [A crude ferroalloy of both niobium and tantalum is commercially produced by aluminothermic reduction as an alternative initial extractive step producing a beneficiated feed for chlorination processes. It is *not* an end-product.]

Niobium-rich pyrochlore concentrates contain an effective equivalent Nb_2O_5 content of 50% to 70% and for Ta_2O_5 about 0.5%[70]. Pyrochlore is chemically more complex but thermodynamically less stable than columbite-tantalite type minerals. The chemical breakdown of pyrochlore concentrates may be accompanied by either chemical conversion or by direct reduction. Chemical treatment may involve either chlorination or dissolution in hydrofluoric acid (or a mixture of hydrofluoric plus sulphuric acids). Direct reduction may be carried-out by metallothermic or carbothermic reduction – but most usually by aluminothermic reduction.

Columbite-tantalite type concentrates are comprised of a continuous series of compositions which are represented generally by the formula $(Fe,Mn)(Nb,Ta)_2O_6$. These concentrates have an effective (generalised) equivalent $(Nb,Ta)_2O_5$ content of 60% to 75% [70] (columbite: 30% to 75% Nb_2O_5, 1% to 40% Ta_2O_5 ; tantalite: 2% to 30% Nb_2O_5, 40% to 80% Ta_2O_5). Wodginite concentrates have an effective equivalent Nb_2O_5 of 1% to 15% and Ta_2O_5 of 45% to 70%. Concentrates of other minerals in this columbite-tantalite group have comparable $(Nb,Ta)_2O_5$ contents and similar chemical and thermodynamic stabilities.

Columbite-tantalite type mineral concentrates are chemically stable and are attacked only by hydrofluoric acid (HF), a mixture of HF and sulphuric acid (H_2SO_4), or by fusion with alkalis (normally sodium hydroxide, NaOH, or potassium hydroxide, KOH) to break-down or digest the minerals. Alternatively, as with pyrochlore concentrates, columbite-tantalite type concentrates may be chlorinated to form fractionally distillable chlorides, or may be directly reduced to crude metallic form[30].

The direct aluminothermic or carbothermic reduction of niobium/tantalum ore concentrates, often with the addition of iron or iron oxides to control the yield of

ferroalloy, is highly exothermic[29], is thermodynamically sound and is therefore commercially attractive as a process for the production of crude ferroalloy feed for the chlorination process[30]. Despite the thermodynamic attractiveness of this route, reduction to metal does not deliver an end-product but a mid process product of limited commercial value.

Chlorination of either crude niobium/tantalum ferroalloy or niobium/tantalum ore concentrates produces a cocktail of metal chlorides which may be separated by their dissimilar water solubilities and/or by utilising their dissimilar vapour pressures in fractional distillation, or by propensity to selectively react with oxygen, steam or hydrogen[29].

The chlorination route provides a decomposition/solvent-extraction inclusive process that allows purification (refinement) with separation. The carbon assisted (after general equations **{3.2.1}1, {3.2.1}2** and **{3.2.1}3**) chloridation reactions expressed for the relevant pentoxides are given[29] as:

$$Nb_2O_5 + 5Cl_2 + 5C \Rightarrow NbCl_5 + 5CO \quad \text{.....} \quad \textbf{\{3.2.4\}1}$$

$$Ta_2O_5 + 5Cl_2 + 5C \Rightarrow TaCl_5 + 5CO \quad \text{.....} \quad \textbf{\{3.2.4\}2}$$

The range of niobium chlorides ($NbCl_2$, $NbCl_3$, $NbCl_4$ and the most common, $NbCl_5$) can all be reduced by the principal metallothermic elements sodium, magnesium, calcium and aluminium. Because of its popular acceptance, a Kroll type magnesiothermic reduction has been the commercially accepted route to niobium where pyro-reduction is the alternative. The principal metallothermic reaction for the Kroll type process is represented by the following equation[29].

$$2NbCl_5 + 5Mg \Rightarrow 2Nb + 5MgCl_2 \quad \text{.....} \quad \textbf{\{3.2.4\}3}$$

The analogous equation exists for tantalum, however, tantalum is commercially produced by other routes. Like titanium, zirconium, hafnium and niobium, tantalum

could be commercially produced by this route in a manner previously described for titanium.

Chlorination/chloridation techniques are industrially well established and their intensive processes systematically provide, with relative simplicity, high purity niobium and tantalum products. However, in recent decades, most producers of niobium and tantalum have used metal extraction processes based upon fluoride chemistry[31].

In the initial mineral decomposition stages of fluoride-based extractive processing, most producers employ an acid digestion route using either hydrofluoric acid or hydrofluoric acid plus sulphuric acid. This strategy can be applied effectively to a broad range of niobium/tantalum mineral concentrates[30]. Decomposition efficiency in the HF/H_2SO_4 digestion system is well suited to, and allows high extraction recoveries in subsequent liquid-liquid extraction[31]. In this chemical extraction step niobium and tantalum are separated from aqueous-retained titanium by reaction with methyl isobutyl ketone (MIBK). The niobium/tantalum solution is then stripped with dilute acid to separate and remove the niobium. Tantalum is then extracted from the liquor with acid ammonium fluoride and the solids calcined to Ta_2O_5, or alternatively are reacted with a potassium salt to crystallise the double fluoride salt K_2TaF_7. The stripped niobium liquor is reacted with ammonia (NH_3), and solids calcined to Nb_2O_5. This convenient, commercially ideal digestion/separation extraction route is shown diagramatically in Figure **{3.2.4}1**. The double fluorides of niobium and tantalum may be further processed in several ways (including electrowinning) or they can be metallothermically reduced by any of several possibilities. The following equations[29] represent the sodiothermic reduction of niobium and tantalum double fluoride salts.

$$K_2NbF_7 + 5Na \Rightarrow 2KF + Nb + 5NaF \quad \text{.....} \quad \textbf{\{3.2.4\}4}$$

$$K_2TaF_7 + 5Na \Rightarrow 2KF + Ta + 5NaF \quad \text{.....} \quad \textbf{\{3.2.4\}5}$$

For environmental and economic reasons, the decomposition of ore concentrates by alkali fluxing is no longer commercially practiced[31]. Similarly, modern solvent extraction techniques have replaced the older Marignac process in which niobium and tantalum were separated by multi-stage fractional crystallisation from fluoride double salts[8, 31].

Commercial chlorination routes offer the advantage of purification (refinement) with extraction whilst using lower cost chemicals in an environmentally more acceptable closed process[31]. Conventionally, ore concentrate or crude ferroalloy is decomposed by contacting with a chlorine source – usually chlorine gas – plus carbon at designated temperature in a fluidised bed reactor. Alternatively, crude ferroalloy may be chlorinated in molten sodium iron chloride from which product chlorides are initially separated into a solid fraction containing niobium chloride, tantalum chloride and other higher boiling point (B.P.) chlorides, plus a liquid fraction containing the lower boiling point chlorides.

Separation and purification of chlorides is efficiently achieved by fractional distillation. In the case of niobium and tantalum chlorides, the loose solid chloride

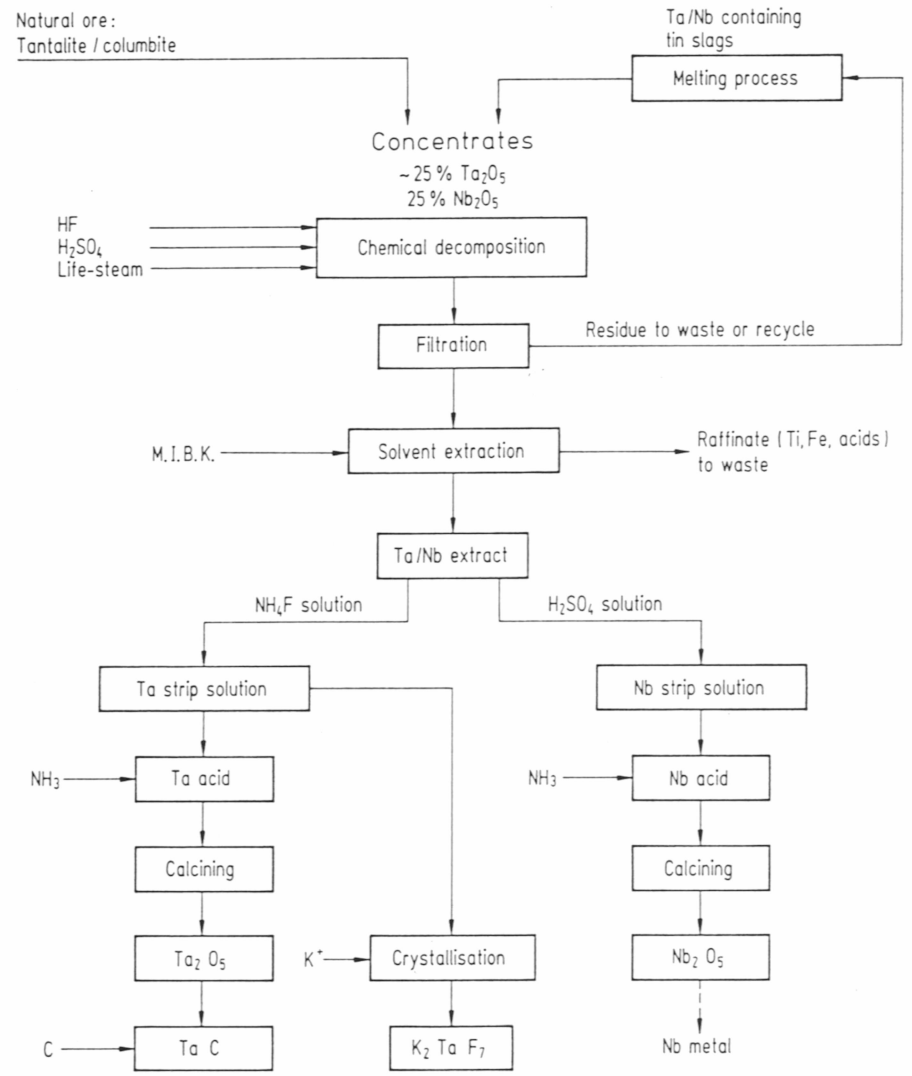

Figure {3.2.4}1: Simplified flow sheet for tantalum/niobium including MIBK solvent extraction and acid separation routes [31].

concoction is heated in distillation columns under a highly controlled regime to separate $TaCl_5$ (B.P. 232°C) from $NbCl_5$ (B.P. 245°C). The pure chlorides are then converted to pure oxides or are used as feedstock for metallothermic reduction (equation **{3.2.4}3**). In general, the chlorination route produces final product of greater purity than does the fluoride route[31]. Tantalum carbide and, to a lesser extent, niobium carbide are produced by intimate and stoichiometrically controlled carbothermic reduction of the pure oxides. Most of the remaining pure tantalum oxide is utilised in the manufacture of capacitor components for the electronics industry, the minor portion of total end-product tantalum is utilised in metallic form. Most end-product metallic niobium is utilised in nuclear applications and in special alloys and high strength steels.

The initial ore concentrate or ferroalloy digestion, chemical extraction and separation stages of niobium/tantalum extractive processing yield the principal intermediate products that are fluoride, chloride or oxide compounds of niobium or tantalum. From these pure compounds, commercially pure metallic niobium and tantalum are reduced by metallothermic reaction in Kroll type processes analogous to those for titanium, zirconium and hafnium. It is important to note that niobium and tantalum have a lower affinity for oxygen than do the Group **4** metals titanium, zirconium and hafnium (which have an affinity for oxygen of "critical" magnitude). So a greater degree of freedom is available in reduction strategies for niobium and tantalum than for the Group **4** metals. Most notable is that it is feasible to carbothermically reduce pure Nb_2O_5 or pure Ta_2O_5 to metal which can subsequently be electron beam refined to reduce (eliminate) oxygen to metallurgically acceptable levels of contamination[29].

Niobium and tantalum chlorides can alternatively be reduced in commercial quantities by reduction with hydrogen[29] (a strategy often accompanied by safety troubles and processing difficulties). Also, the chlorides can be reduced by disproportionation (or decomposition) reactions such as that indicated in the following disproportionation equation[29] for the niobium chloride system.

$$5NbCl_3 \Rightarrow 2Nb + 3NbCl_5 \quad \text{..... } \textbf{\{3.2.4\}6}$$

However, such disproportionation processes have not yet been commercially exploited.

The sodiothermic (Hunter) reduction of the potassium double fluorides of niobium and tantalum are carried-out commercially following the (simplified) reduction routes[29].

$$K_2NbF_7 + 5Na \Rightarrow 2KF + Nb + 5NaF \quad \text{..... } \{3.2.4\}7$$

$$K_2TaF_7 + 5Na \Rightarrow 2KF + Ta + 5NaF \quad \text{..... } \{3.2.4\}8$$

Niobium and tantalum may be electrolytically reduced in molten salt electrolyte processes. Unlike the zirconium/hafnium system in which the electrochemical difference is minute and the metals are co-deposited, the niobium and tantalum electrolyte salts are electrochemically separable and are also chemically separated before electrochemical reduction is attempted – hence the process could be commercially justified[29].

A recently devised reduction route[29] for niobium metal production by the decomposition of the nitride, NbN, has been proven but is awaiting commercial development. The process is summarised in the following equations.

$$Nb_2O_5 + 5C + N_2 \Rightarrow 2NbN + 5CO \quad \text{..... } \{3.2.4\}9$$

Then, by decomposition:

$$NbN \Rightarrow xNb_4N_3 \Rightarrow yNb_2N \Rightarrow Nb \quad \text{..... } \{3.2.4\}10$$

Reduced niobium and tantalum may be refined either to a commercial purity grade or to a high purity grade by a range of process possibilities. Because of the lower oxygen affinity (gettering potential) of niobium and tantalum, the range of process possibilities available to produce high purity (or ultra-high purity) is broader than for the Group **4** metals[8, 30]. Refining operation options largely depend upon the scale or

proportion of impurities to be removed, the range of impurities, and the final impurity level to be attained (that is, the specification). Most modern commercial grade processes utilise electron beam melt refining or a combination of this with pyro-vacuum treatment[29]. Another technique with less commercial acceptance is fused salt electro-refining. The "ultra-purification" techniques which are employed to produce small, non-commercial scale batches of high to ultra-high purity metal are electron beam float zone melting, electro-transport, and the familiar van Arkel - de Boer style iodide refining similar to the processes for titanium, zirconium and hafnium[29, 30].

3.3: The Thermodynamics of (Conventional) Reduction Processes.

All complex, real systems posses a tendency towards maximum disorder - any increase in disorder represents a trend towards thermodynamic equilibrium. Given enough time real, miscible systems increase their degree of disorder by fluid-mixing or by diffusion (time dependent processes) and thus approach equilibrium. (Immiscible phases might be seen to reverse this process and retreat from equilibrium. However, immiscible phases do not voluntarily mix in the first place. In fluids they may be forced to "blend" into many discrete volumes under turbulence – but this blending is transient in that it is linked to the longevity of the turbulence – and the case is trivial.) Classical thermodynamics deals with *equilibrium states.* An equilibrium state is reached when the system is allowed to equilibrate (settle) long enough for quantities such as temperature, pressure, volume and composition to become uniform – so the system displays no evidence of its recent history (energy path).

Quantities that return to the same values whenever the system returns to the same state at equilibrium are called *state variables.* If some of these state variables are known (thus becoming the *independent variables*) then the thermodynamic state of a given system in equilibrium can be defined and the values of all other state variables (the *dependent variables*) may be determined. Classical thermodynamics can only address those states of maximum disorder – those states of *thermodynamic equilibrium.* And, it should be emphasised, these equilibrium states to which systems spontaneously approach when left to settle, and the fact that thermodynamic state variables are

uniquely defined by the equilibrium state, are not conclusions deduced from first principles; they are conclusions drawn from the experience of two centuries of experimental observations[41, 60, 61, 62].

The extractive metallurgist invokes thermodynamics as a tool in the study and control of metallurgical systems and deploys this knowledge in his manipulation of processes that are of interest to him in the extraction of metals from raw materials. Since groundbreaking work published by ELLINGHAM[63] in 1944 and extended by RICHARDSON and JEFFES[64] in 1948, a considerable body of information has been accumulated which describes the chemistry and stability of systems under equilibrium conditions, and systems under pseudo- or near-equilibrium conditions that return to equilibrium during the process under question.

Unlike the configured thermodynamics of physics and mechanics that relates heat and work, the thermodynamics of extractive metallurgy is *chemical thermodynamics* which relates heat, temperature, pressure and chemical composition. Chemical thermodynamics is concerned with changes in these state variables and, specifically, the effects of these changes, tendencies towards reaction and system equilibrium. It is chemical thermodynamics that defines and describes the inevitability of the chemical reactions of extractive metallurgical processes. Without chemical reactions there could be no chemometallurgical, pyrometallurgical, hydrometallurgical or electrometallurgical extractive processes. So, thermodynamics is central in extractive metallurgy, and it is fundamental in any consideration of process possibilities.

Prevalent in chemical thermodynamics is the use of the Gibbs free energy of formation to describe the chemical affinity of the reactants and the stability of the system chemistry. The Gibbs free energy (or Gibbs energy), G, relates the central state functions enthalpy, H, entropy, S, and temperature, T, in the relationship:

$$G = H - TS \quad \text{..... } \{3.3\}1$$

The significance of this simple relationship can be appreciated by an appreciation of its parts. Enthalpy is the heat function identity and it relates other important state functions in the following way:

$$H = U + PV \quad \text{.....} \quad \{3.3\}2$$

Enthalpy, here, is related to U, the internal energy of the system, and to the state variables pressure, P, and volume, V. Parameters representing potential, kinetic and electromagnetic energies, which would otherwise be relevant, are disregarded in chemical thermodynamic treatments of enthalpy. Also it should be noted that few extractive processes are carried-out at constant volume and, correspondingly, most extractive metallurgical processes are carried-out at constant pressure.

Also, at constant pressure, the internal energy can be given as:

$$U = q - PV \quad \text{.....} \quad \{3.3\}3$$

Here q is the heat supplied to, or withdrawn from the system. Heat capacity, C, is the amount of heat added or withdrawn from a system to bring about a temperature change ΔT and is given as:

$$C = q / \Delta T \quad \text{.....} \quad \{3.3\}4$$

This leads to the Kirchhoff equation for systems at constant pressure (such as those "open" to the atmosphere):

$$C_p = \{\delta q / dT\}_p = \{dH/dT\}_p \quad \text{.....} \quad \{3.3\}5$$

Thermochemical considerations arising from heat effects accompanying chemical reactions leads to Hess's law which decrees that, provided that the temperature and either volume or pressure remain constant, the heat content change in a chemical reaction remains constant irrespective of the reaction route or number of stages involved. Further, heat capacity identities can be used to determine the enthalpy change

with temperature. The standard enthalpy change for a reaction can be easily calculated from readily available data for the standard 25°C at which temperature the kinetics may dictate a reaction rate ensuring that the reaction will not go to completion within a reasonable time. Integrating equation **{3.3}6** to equation **{3.3}7** we can solve (for reactions at constant pressure in this case) to determine the enthalpy change at elevated temperatures of typical pyrometallurgical reactions[62].

$$d(\Delta H^\circ)/dT = \Delta C_p \quad \text{..... } \{3.3\}6$$

$$\frac{d(H^\circ)}{dT} = \Delta C_p$$

$$\Delta H^\circ_{T2} = \Delta H^\circ_{T1} + \int [\Sigma C_{p,\,products} - \Sigma C_{p,\,reactants}]dT \quad \text{..... } \{3.3\}7$$

By convention, if the enthalpy change is positive then heat is absorbed by the system; if the enthalpy change is negative then heat is released by the system. From knowledge of the heat of reaction and the heat capacities of reactants and products at temperature, it is possible to calculate the temperature of the system[29]. Enthalpy is deduced from the first law of thermodynamics, which provides no universal criterion as to whether a reaction will proceed or not proceed. However, the second law of thermodynamics introduces the property entropy that provides information regarding the spontaneity of a reaction. Entropy, S, is the other extensive state property in the Gibbs energy equation **{3.3}1** (above) in the product term with the state variable, temperature (T).

From the definition of entropy, in a thermally isolated system, for a reversible process the change in entropy is zero ($dS = 0$), whilst for an irreversible process the change in entropy is always greater than zero ($dS > 0$). The entropy of a thermally isolated system can never decrease. In systems where heat is supplied by an external source, $TdS = \delta q$ for reversible processes and $TdS > \delta q$ for irreversible processes, where δq is the heat supplied by the surroundings.

The entropy change for any chemical reaction is defined as the difference between the sum of the entropies of the products and the sum of the entropies of the reactants. For the reaction:

$$aA + bB + \ldots\ldots\ldots \Rightarrow mM + nN + \ldots\ldots\ldots,$$

the standard entropy change, ΔS^0, accompanying the chemical reaction is given by the following.

$$\Delta S^0 = (mS^0_M + nS^0_N + \ldots\ldots\ldots) - (aS^0_A + bS^0_B + \ldots\ldots\ldots) \quad \ldots\ldots\ldots \{3.3\}8$$

Here S^0_A, S^0_B, S^0_M, ... are the standard entropies per mole of the various reaction participants which must be known at the desired temperature and pressure for entropy change to be calculated. Entropy change of a reaction is generally required at constant temperature and pressure. Where unknown, the entropy values of elements and compounds and the entropy change of reactions can be calculated for any temperature utilising the third law of thermodynamics.

For a reaction, the change in entropy of the system at different temperatures can be evaluated. Changes in standard entropies and heat capacities must be considered for chemical reactions involving reactants and products in their standard states and the entropy change between temperatures T_1 and T_2 is given[62, 65] as:

$$\Delta S^0_{T_2} = \Delta S^0_{T_1} + \int_{T_1}^{T_2} \frac{\Delta C_p}{T} dT \quad \ldots\ldots\ldots\ldots\ldots \{3.3\}9$$

The considerable value in metallurgy of the entropy function is its ability to indicate the direction in which a reaction will proceed and the final equilibrium state of the process[41]. Irreversible change within a real system, such as a spontaneous reaction, will result in an increase in entropy if no heat is supplied by the surroundings. Furthermore, whilst most chemical reactions can be carried-out either reversibly or irreversibly[41], more heat is absorbed from the surroundings if the reaction is carried-

out reversibly than if the reaction is spontaneous. The essential pyrometallurgical reactions are spontaneous.

Finally, for most laboratory and industrial processes, the state variables temperature, volume, pressure and quantity or concentration of reactants and products – and changes to these variables – can be meaningfully and relatively easily measured. Temperature is a measure of the heat or thermal energy exhibited in a system that, for all intents and purposes in the vast majority of cases in common experience, closely approximates the total available energy in the system within any given set of conditions.

Whilst most chemical reactions, including the significant metallurgical reactions, ostensibly proceed under conditions of constant temperature and pressure, and some proceed under constant temperature and volume, few (if any) proceed under conditions of constant energy, even as applied energy. So any criteria for reaction spontaneity based upon entropy becomes impracticable and a criterion for spontaneity based upon another thermodynamic function is required. The thermodynamic function that is appropriate under the applicable conditions of chemical or metallurgical processes is "free energy". The prominent Gibbs free energy identity has been introduced as equation **{3.3}1**, the other important free energy identity in metallurgical thermodynamics is the Helmholtz free energy, A.

$$A = U - TS \quad \ldots\ldots\ldots\ldots\ldots \quad \textbf{\{3.3\}10}$$

The change in free energy for any reaction is the difference between the sum of the free energies of the products and the reactants. For a reaction at temperature T a simple derivation for that most useful identity - the Gibbs free energy change, ΔG - can be written as follows.

$$\Delta G = \Sigma G_{products} - \Sigma G_{reactants}$$

$$= \{\Sigma H_{products} - T\Sigma S_{products}\} - \{\Sigma H_{reactants} - T\Sigma S_{reactants}\}$$

$$= \{\Sigma H_{products} - \Sigma H_{reactants}\} - T\{\Sigma S_{products} - \Sigma S_{reactants}\}$$

or, $\Delta G = \Delta H - T\Delta S$ ..... **{3.3}11**

Equally, the Helmholtz free energy change, ΔA, can be similarly derived and written as:

$\Delta A = \Delta U - T\Delta S$ ..... **{3.3}12**

The criteria for spontaneity based upon free energy for systems at constant temperature and constant pressure (denoted by the subscript "P") and for systems at constant temperature and constant volume (denoted by the subscript "V") are established and are as follows.

(*i*) If ΔG_P or ΔA_V is zero (ie., = 0), then the system is in equilibrium.

(*ii*) If ΔG_P or ΔA_V is negative (ie., > 0), then the reaction will proceed spontaneously (as written).

(*iii*) If ΔG_P or ΔA_V is positive (ie., < 0), then the reaction proceed spontaneously in the opposite direction.

Because most chemical reactions, including the significant metallurgical reactions, proceed under constant temperature and pressure, the Gibbs free energy is the free energy function of more practical use and, consequently, is more often quoted.

As in the case of enthalpy, absolute values of free energies for substances cannot be known – only the free energy difference or free energy change can be known and dealt-with. (Of course, statistical thermodynamics provides a basis for calculating absolute values of thermodynamic functions like free energy by extrapolating from zero kelvin. However, these values are considered "theoretical" and are seldom called-upon in practical thermodynamics.) In order to calculate standard free energy of a reaction, standard free energies of reactants and products must be known. Comprehensive free energy data are widely available – where reactants or products are not in their standard states then corrections can be made to compensate in calculations.

Similar to enthalpy change, free energy change depends upon the initial and final states of the system irrespective of the reaction path followed to bring-about the change[62, 65].

Most standard thermodynamic functions are reported in the literature as values at 25°C (298K). However, most metallurgical operations – including all extractive pyrometallurgical operations – are conducted at considerably higher temperatures. Disregarding intermediate phase transformations, the following equation allows the calculation of standard state Gibbs free energy for a reaction at high temperature.

$$\Delta G^{0}_{T} = \left\{\Delta H^{0}_{298} + \int_{298}^{T} \Delta C_p dT\right\} - T\left\{\Delta S^{0}_{298} + \int_{298}^{T} \frac{\Delta C_p}{T} dT\right\} \quad \text{.....} \quad \textbf{\{3.3\}13}$$

Also, the calculation of ΔG^{0} for a reaction at any temperature and constant pressure is possible using the Gibbs-Helmholtz equation:

$$\Delta G^{\circ} = \Delta H^{\circ} + T\left(\frac{\partial \Delta G^{\circ}}{\partial T}\right)_P \quad \text{.....} \quad \textbf{\{3.3\}14}$$

A useful identity for Gibbs free energy change is expressed in terms of activity, **a**, and can be shown[62] to be:

$$G - G^{0} = RT \ln \mathbf{a} \quad \text{.....} \quad \textbf{\{3.3\}15}$$

For the chemical reaction:

$$aA + bB + ... \Rightarrow mM + nN + ... ,$$

at constant temperature and pressure it can be shown[62, 65] that:

$$\Delta G - \Delta G^0 = RT \ln \left[\frac{a^m_M . a^n_N . \ldots}{a^a_A . a^b_B . \ldots} \right] \quad \ldots\ldots\ldots\ldots \quad \{3.3\}16$$

$$\text{Or,} \qquad \Delta G = \Delta G^0 + RT \ln \left[\frac{a^m_M . a^n_N . \ldots}{a^a_A . a^b_B . \ldots} \right] \quad \ldots\ldots \quad \{3.3\}17$$

When the reactants are in equilibrium with the products, the free energy change is zero. Hence, in equation {3.3} **17**:

$$\Delta G^0 = - RT \ln \left[\frac{a^m_M . a^n_N . \ldots}{a^a_A . a^b_B . \ldots} \right] \quad \ldots\ldots\ldots\ldots \quad \{3.3\}18$$

the term $\left[\frac{a^m_M . a^n_N . \ldots}{a^a_A . a^b_B . \ldots} \right]$ is the "thermodynamic equilibrium constant" and is denoted as K. Then, at equilibrium, the following identity is defined – an identity which is commonly solved for the equilibrium constant, K, with knowledge of the standard Gibbs free energy change, ΔG^0.

$$\Delta G^0 = - RT \ln K \quad \ldots\ldots\ldots\ldots\ldots\ldots \quad \{3.3\}19$$

Chemical reactions in metallurgical or any other operations are only possible when there is a decrease in overall free energy for the process[62]. A reaction may be thermodynamically feasible, but in practice the reaction may not proceed to completion in a measurable period of time. That is, the rate of reaction may be imperceptibly slow. No thermodynamic analysis can provide information on the rate of reaction, nor on the reaction mechanism and reaction path. It is physical and chemical kinetics that provide information on these essential characteristics of reaction processes[17, 66].

3.4: The Kinetics of (Conventional) Reduction Processes.

The reaction direction and final equilibrium state of a chemical reaction can be predicted from thermodynamics, but thermodynamics provides no tangible information about the rate at which this equilibrium will be approached. The reaction rates at which chemical processes proceed are determined by both *physical* and *chemical kinetics*. – each being prominent in the heterogeneous environments of pyrometallurgical chemistry. Accordingly, and moreover, thermodynamics cannot be used to determine the reaction time – the time required to reach equilibrium – nor the mechanism or reaction route by which it is achieved. Like reaction rates, reaction mechanisms are principal determinants of kinetics, each being inter-dependent upon and inseparable from the other. In typical cases where there are multiple possible reaction mechanisms, the mechanism with the fastest reaction rate will dominantly determine the overall reaction rate and will determine the reaction route for which the process will be designed. Such inter-dependencies have often been overlooked in metallurgical operations – particularly in pyrometallurgical operations where initial reactant charge and final product can be easily observed whilst intervening processes and phases may not be directly observable, and so not considered.

The state variables temperature, pressure, volume and composition (or molar fraction) control the direction of reaction and the equilibrium state. In addition to these easily identifiable quantities, reaction kinetics also depends upon other crucial factors such as the physical and chemical forms of the reactants, the possible presence of a catalyst and whether one is required, the presence of external energy sources and the duration of these to initiate reaction or to sustain and accelerate reaction rates.

The rate of reaction may be defined in terms of the rate of decrease in concentration of reactants or, correspondingly, the rate of increase in concentration of the reaction products. The reaction rate remains proportional to the concentration of the chosen reaction participant. The sum of the powers to which the concentrations of the reacting participants must be raised defines the order of the reaction that is required to determine the rate of the reaction[67].

Chemical reaction systems are classified as being either homogeneous or heterogeneous systems. A reaction system is homogeneous if it takes place in one phase (and does not require the presence of another phase to proceed). A reaction system is

heterogeneous if it requires the presence of more than one phase to take place and to proceed at the rate that it does, irrespective of the number of phases in which the reaction takes place. Since, most frequently, metallurgical reactions take place in systems involving two or more phases, *metallurgical kinetics is the chemical kinetics of heterogeneous systems*. Heterogeneous metallurgical reactions may take place between two (or more) liquids as in slag-metal reactions, between two solids as in the solid-state diffusion bonding of two metals or during solid-state reduction between carbon and metal oxide, or between a fluid and a solid as with a reductant gas or a reactive slag and an ore mineral. All extractive metallurgical reactions take place across an interface between phases[17, 67, 68]. Furthermore, most extractive metallurgical reactions such as the burning of fuel, the calcining, roasting and pre-reduction of ores and common reduction operations like the smelting of iron ore are *non-catalytic* heterogeneous reactions[67].

In heterogeneous systems (involving multiple phases), multiple reaction mechanisms are involved and each has its own reaction rate. In such systems rate-controlling mechanisms may be as simple as one relatively slow step controlling the overall reaction rate or a combination of rate-control contributions leading to a complex overall reaction rate. The consuming problem in industrial extractive processes is to determine how each variable affects each of these rate-controlling steps, in what way and to what degree.

In all extractive metallurgical reactions the reactant species occur in different charge components – that is, they occur separately in discrete phases. Reactions in such heterogeneous systems require the mass transport of reacting species in the following generalised steps.

(*i*) Transport of reactant species from the general bulk to the reaction interface at the phase boundary (phase interface).

(*ii*) Single or multiple stage chemical reaction across the reaction interface defined by the phase boundary, or mass transport of reactant species across the phase boundary.

(*iii*) Transport of a product species from the reaction interface into the general bulk, or transport of a reactant species to a reaction site in the general bulk. (The reaction product may need to be transported back to the phase boundary, at least. But, leaving such aside here.)

The slowest of these above steps will overwhelmingly be the controlling stage and will ultimately determine the rate of reaction. Steps (*i*) and (*iii*) are diffusional and/or convectional processes with physical kinetics controlling whilst the chemical kinetics controlled phase boundary step (*ii*) is described by the Arrhenius equation (see equation **{3.4}2** below). In the case of typical industrial pyrometallurgical reactions, where process temperatures are generally very high, thermal dynamics prevailing at the reaction interface ensure high reaction rates across it such that the phase boundary step is unlikely to be the rate controlling stage of the process and diffusion across "macro" charge components becomes rate controlling.

The rate of overall process chemistry can be calculated once the rate law for the process is established and principal controlling parameters are determined. Predictions of a rate-controlling step and the reaction rate can be made when the order of the chemical reaction, the rate constants, diffusion coefficients and distribution coefficients are known or can be realistically estimated, and when a mathematical solution of the rate law is available[69].

It is not appropriate here to give a comprehensive overview of the many nuances of kinetic theory or to summarise the many sub-sections of this subject that rapidly divide into a complex study. Sub-sections split into sub-topics such as reversible and irreversible reactions, order of reaction, interface dynamics and rate-controlling models, reactions in series and parallel, batch and continuous reactors, flow dynamics, stirring and numerous others – each having to be considered with respect to the others. However, in elementary terms, for extractive processes the reaction rate can be proposed as a function of temperature and composition, or as a product of a temperature-dependent term and a function of composition as in the following simple relationship.

$$r_i = f_1(\text{temperature}) \,.\, f_2(\text{composition}) = k \,.\, f_2(\text{composition}) \quad \ldots\ldots \quad \{3.4\}1$$

For reactions of this general type, the temperature-dependent term k, the reaction rate constant, has been found to be adequately represented by the well known Arrhenius expression[41, 67]:

$$k = k_0 e^{-E_{act}/RT} \quad \text{..... } \{3.4\}2$$

Here k_0 is the frequency factor, E_{act} is the activation energy and R is the ideal gas law constant. Taking base 10 logarithms of both sides of equation **{3.4}2** the following expression is obtained[62].

$$\log k = \log k_0 - \left[\left(\frac{0.4342\ E_a}{R}\right)\left(\frac{1}{T}\right)\right] \quad \text{..... } \{3.4\}3$$

The Arrhenius expression can be tested by plotting log k against the reciprocal of absolute temperature, (1/T). Accordingly, from equation **{3.4}3**, a straight line of slope ($0.4342E_{act}/R$) can be drawn through the plotted points. The activation energy, E_{act}, can be calculated from the slope, whilst log k_0 is identified at the intercept (1/T) = 0 from which the frequency factor can be calculated.

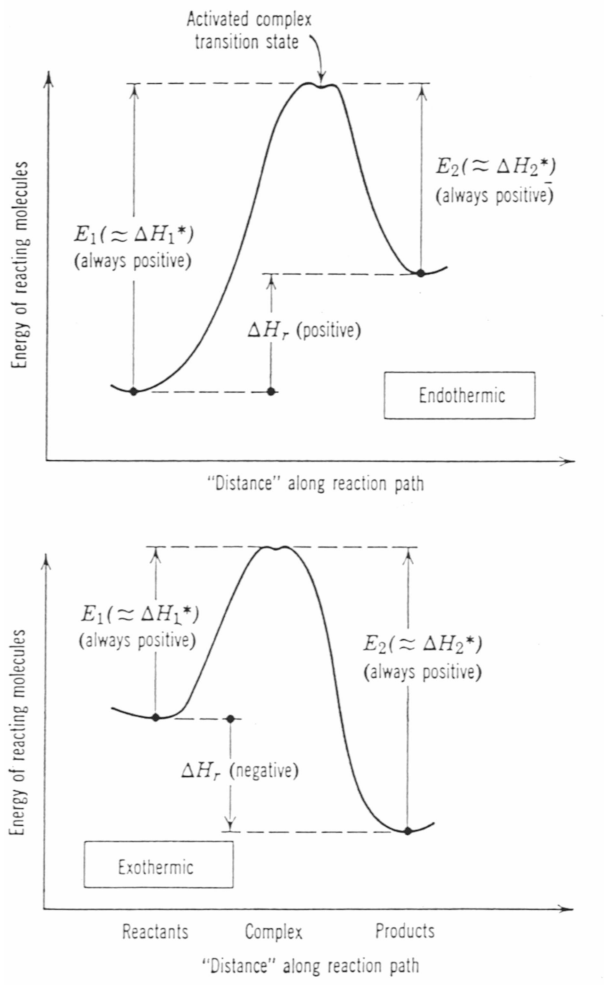

Figure {3.4}1: Diagrammatic representation of energies involved in the transformation of reactants to products in an elementary reaction [67].

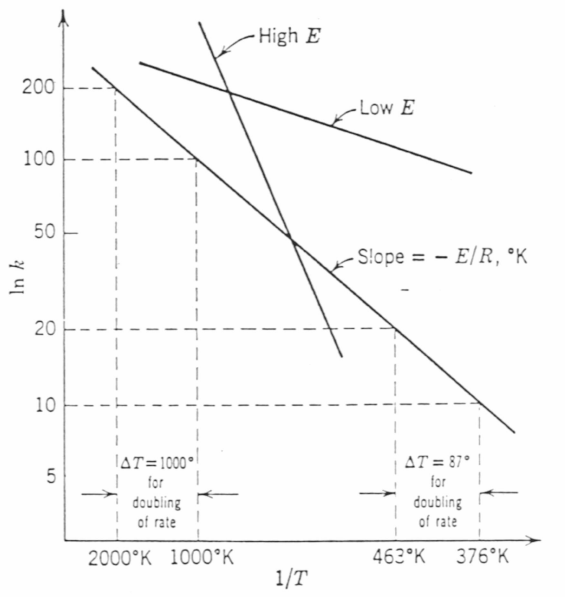

Figure {3.4}2: Representation of the temperature dependence of reaction rate [67].

The Arrhenius model has been modified by Eyring[70] and other workers who have included the notion of activated intermediate complexes in reaction routes and mechanisms. Whilst these additions have undoubtedly introduced an element of reality into the general kinetic mechanisms model, predictions based on the revised model are only marginally different to the original Arrhenius model such that differences cannot be realistically detected by experimental trial[17].

The temperature dependency of chemical reactions is determined by the activation energy and the temperature. This temperature dependency can be clearly seen in the illustrative generalities of Figure **{3.4}1** and Figure **{3.4}2**.

For industrial extractive processes, rigorous studies of system chemistry may go hand-in-hand with a certain measure of serendipitous fortune in divining the design of a metallurgical reactor system. Process and system design are based upon consideration of the reaction stoichiometry, reaction mechanism and reaction rate (kinetics) – each of which is related to the other two. The numerous possibilities of the inter-relationship of these reaction variables affirms that no straightforward experimental programme can be devised to directly predict process kinetics. However, the industrial exploitation of any process depends upon its commercial worth and established economic credibility. Commercial necessities provide the incentive for industrial decision-makers to determine the factors affecting reaction kinetics and the limits of process optimisation. If reaction kinetics delivers reaction rates that are high enough such that the system essentially remains at equilibrium then kinetic information is not required and thermodynamic information alone will be sufficient in the design of an appropriate reactor system. Where this virtual equilibrium is established, the reaction products may be deduced from thermodynamics[41, 67].

Notwithstanding this, the performance of any system configuration of reaction vessels – whether single reactor or series of reactors – is contingent upon the magnitude and inter-dependence of both thermodynamic performance and kinetic performance of

the system. The rate-determining factor of the process may be either a thermodynamic factor or a kinetic factor. The overall rate of chemical conversion for the reactor is then dictated by the rate-controlling step. Such is the case in virtually all kinetically homogeneous systems[62]. However, the great bulk of extractive metallurgical processes involve gas-solid, gas-liquid or liquid-solid phase reactions (including the combination of all three) and, therefore, are heterogeneous systems. Extractive pyrometallurgical processes are high conversion rate, high temperature chemistry processes which are controlled by thermodynamic factors rather than kinetic factors[60, 65].

4

MICROWAVE PROCESSES and MICROWAVE PLASMA.

"The nature of an infant is *not* just a new permutation-and-combination of elements contained in the natures of the parents. There is in the nature of the infant that which is utterly unknown in the natures of the parents."

D.H. Lawrence -
Psychoanalysis and the Unconscious, 1921.

"To accept an orthodoxy is to inherit unresolved contradictions."

George Orwell -
Writers and Leviathan, 1948.

4: MICROWAVE PROCESSES and MICROWAVE PLASMAS.

Microwave discharges generally provide a higher degree of ionisation and dissociation than other discharge types, can be operated over a wider range of pressures and provide a much higher ratio of electron temperature to heavy-species temperature than other discharge types [80, 83]. Further, (for microwave discharges) the absence of in-chamber electrodes removes a possible source of contamination. Microwave discharges are highly efficient generators of electrons, positive and negative ions, excited species (atoms, molecules and ions), and free atoms and radicals [83]. Such efficiency ensures the advanced reactivity capability of microwave plasmas in operations involving ionisation chemistry. In fact, the high level of reactive species in microwave plasmas [80, 86] render them eminently suitable for a range of plasma processing tasks ranging from surface modification to chemical synthesis and reduction.

The wide variety of reactive particles produced in microwave plasmas and the plasma chemistry emanating from the consequent confluence of reactive participant particles and enhanced thermodynamic environment have been widely studied in the contexts of the synthesis and physical treatments of a range of secondary and tertiary materials (plastics, organic and inorganic chemicals, metals and intermetallic compounds, *et cetera*) [74, 76, 80, 83, 86, 87, 88, 89, 90, 93, 99]. However, studies on the process and products of microwave plasma chemistry on primary materials, such as ores and mineral concentrates, is much less frequently published – largely because of the constraints of commercial confidentiality.

Microwave discharge sources are conveniently divided into those that are constrained by applied magnetic fields and those that are not so constrained. Those discharges confined by highly configured magnetic fields are generally operated at pressures between 10^{-3} and 10^{-8} kPa and are utilised in controlled thermonuclear studies in systems such as tokomaks and sterallators. The paths of (charged) ionisation-product particles are controlled by the confining magnetic field that, together with the low particle density, maximises the mean free path of accelerating particles – eliminating wall collisions and virtually eliminating inter-particle collisions [102, 103, 104]. In the

context of conventional fusion configurations, microwave plasmas are employed in two ways. Firstly, microwave plasma is used to provide initial and additional plasma particles by injection into the magnetically confined toroid and, secondly, microwave plasma is used as a medium in microwave diagnostic studies of such phenomena as wave propagation, absorption and conversion, plasma instabilities, diffusion and turbulence in plasma [83]. These phenomenological events are germane to the confined, ultra-high temperature fusion plasmas of high technology, they are not relevant to the un-magnetically confined plasmas pertinent to the area of research of this project. The extension of the literature of fusion and high technology plasmas to describe the plasmas of the comparatively low technology field is avoided.

4.1: Microwave Heating, and Microwave-Stimulated Plasmas and Reactions.

The heart of all microwave heating equipment is the microwave-generating device. Many industrial heating plant installations are rated at over 100 kW [105] represent significant investment and consequently must be reliable, have high generator (conversion) efficiency, be stable of frequency, and must be free of harmonics and spurious frequencies. These requirements are met by the magnetron, a thermionic device, which is robust and durable in application and is also the microwave generator of least cost. The only other microwave generator of possible commercial significance is the klystron which is a driven microwave amplifier device possessing excellent frequency stability but at significantly higher cost. Other generators (such as the gyrotron) are too expensive and inherently too complex for adoption in industrial installations and, almost exclusively, are confined to the relative ether of pure, high technology scientific research. Under international convention*, the common industrial frequency allocations for microwave power generation are (nominally) 2.45 GHz (2450 MHz) and 0.915 GHz (915 MHz) with less common industrially allocated processing frequencies being 433.9 MHz – a "crossover" microwave/RF frequency – plus 27.12 MHz and 13.56 MHz – these being radio frequency nominations [105]. All microwave

* Microwave frequency bands allocated for heating applications are discretely separated from adjacent communications band allocations that are specific to radar, microwave communications, air traffic, civil and military bands. *et cetera*, and are rigidly overseen by national communications authorities.

applicators and reactor equipment used in the course of this project were fitted with 2.45 GHz magnetrons.

Microwaves occupy a band range of the wavelength continuum that is the electromagnetic spectrum and thus are a manifestation of electromagnetic energy. Microwaves have a frequency range of approximately 0.3 to 30 GHz and a corresponding wavelength range of approximately 1000 mm to 10 mm [105] lying between radio waves (or radio frequency, RF) and infra-red, IR, although these divisions are not precise and ranges are often shown merged or overlapping in the literature, as is the case with their use. Significantly for the processing of materials, frequencies that allow dielectric heating occupy a crossover bandwidth between (approximately) 3 MHz RF to 9 GHz microwave and within the combined RF-microwave bandwidth [105]. The electromagnetic spectrum highlighting the microwave range is shown in Figure **{4.1}1**.

In numerous industrial, domestic and scientific operations, processing objectives are accomplished by the application of heat. Heat is a most disordered form of energy and is conventionally applied "externally" to the material under heating [106]. By comparison, electromagnetic energy is a highly ordered form of energy [105, 106] that can be converted into thermal energy (heat) by any of a number of means that employ the direct interaction of the electromagnetic force fields with the electrons and molecular structure (that is, the dielectric properties) of the irradiated material. Typically, microwave-irradiated materials of suitable susceptibility and load size are heated contiguously – that is, "internally" throughout by dielectric heating mechanisms rather than by conduction from a heated surface in solids or by convection or radiation in fluids.

In general microwave heating there are numerous mechanisms responsible for the conversion of electromagnetic energy into thermal energy. However, the principal mechanisms responsible for microwaves' internal heat generation capability are ionic conduction, dipole orientation, various magnetic losses, interface polarisation, molecule twisting and bending, plus a number of resonance phenomena [105, 106]. The initial two of these are the important mechanisms with respect to domestic and commercial cooking and heating operations, however, where loads are more complex, the physics and

chemistry of matter impose their further characteristics (such as changes of state, density, phase and interface, *et cetera*) and other mechanisms become dominant.

Interfacial or Maxwell-Wagner polarisation is optimally important in heterogeneous dielectric loads, particularly when a fraction of the load is of a conducting medium[105]. These conditions are well met by the nature of the experimental charges encountered in this project. Maxwell-Wagner loss relates to the charge particle build-up around load particle surfaces and at interfaces of mixed, heterogeneous dielectrics such that local heating is rapid.

Ideal dielectric materials are electrical insulators, that is, they will not conduct an electrical charge. However, real dielectric materials (such as the minerals in ores) under the influence of an applied electromagnetic field undergo electron/atom or molecular distortion forming networks of dipoles. The dipole moment so created represents a balance between the internal (atomic) forces and the applied field. When

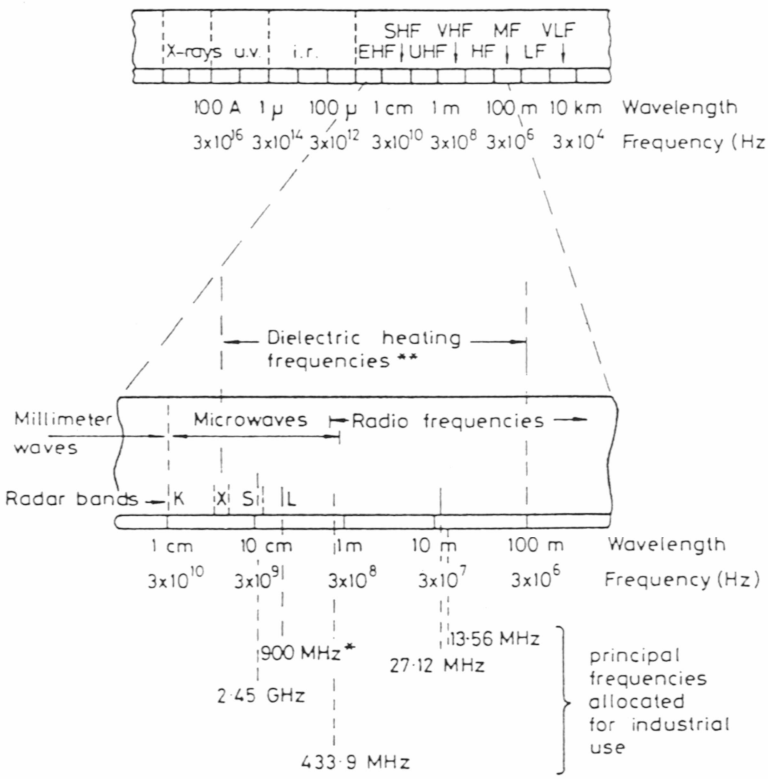

Figure {4.1}**1:** That section of the electromagnetic spectrum indicating the microwave and radio frequency ranges and showing the important frequencies allocated for industrial, commercial and domestic heating applications [105].

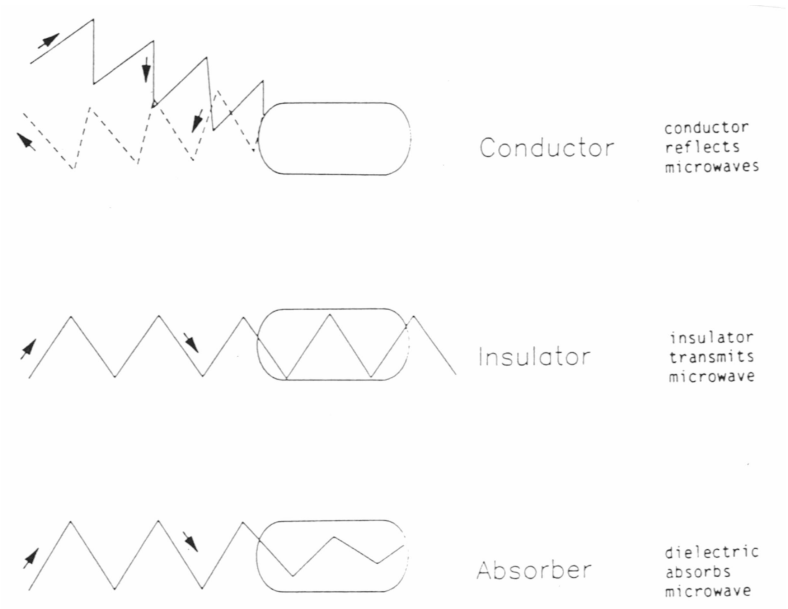

Figure {4.1}**2:** Simple schematic representation showing the classification of materials under microwave irradiation and indicating behavioural characteristics [200].

this force is relaxed – such as when continuously reversed by the alternating current-switching of the typical microwave oven – then a "quantum" of kinetically stored electrical energy is released as thermal energy (heat). The electromagnetic field-induced dipoles reverse their orientation each time the **ac** field reverses. The conversion of electromagnetic energy into heat is referred-to as dielectric loss, and materials exhibiting this as dielectrically "lossy" materials.

The heating mechanisms mentioned above are described in the literature using specific, well-defined parameters. The dielectric constant (permittivity), **ε'**, describes the capability of a molecule to be polarised by the electric field. The dielectric loss factor, **ε"**, is a measure of the efficiency with which the applied electromagnetic energy can be converted into thermal energy (heat). Both the dielectric constant, **ε'**, and loss factor, **ε"**, are frequency and temperature dependent. The ratio of the dielectric loss to the dielectric constant defines the dielectric loss tangent, tan**δ**, where **δ** is the loss angle representing the phase retardation of **ac** current alternation. The dielectric loss tangent, or dissipation factor, determines the capability of a material to convert electromagnetic energy into heat within the material (at a given frequency and temperature)[86, 105].

$$\varepsilon''/\varepsilon' = \tan\delta \quad \text{..... } \{4.1\}\ 1$$

To account for losses arising from polarisation due to the influence of a high frequency field in any real dielectric domain, the dielectric constant requires a complex form, **ε***, defined as follows [105, 107].

$$\varepsilon^* = \varepsilon' - j\varepsilon'' \quad \text{..... } \{4.1\}\ 2$$

Microwave heating requires the conversion of electromagnetic energy into thermal energy and this is dependent upon the "lossiness" of the material being heated. In materials for which dielectric loss is very small, insignificant heating will be induced. Such materials are considered to be *transparent* to microwaves – other properties dependent, it is this group of materials which transmit microwaves, and which provide the "microwave windows and seals" for applicator systems and the "microwave refractories" in which high temperature processes are conducted. As dielectric loss increases, so the dissipation of field energy into the material increases –

this process is known as attenuation and materials that heat in such a manner are considered to be *absorbent* of microwave energy. The other principal material group important in microwave processing is the non-dielectric conductor group that includes carbon forms and metallic materials. (On the proviso that their surface area to volume ratio is not substantial, as it is for fine carbon and metal powders – where a separate absorption effect governs) conductors reflect microwaves and thus are considered *opaque* to microwaves. These three classes of material are figuratively represented in Figure **{4.1}2**.

The delivery of energy through the microwave field is divided into two categories of microwave applicator systems: multi-mode and single-mode applicators. METAXAS and MEREDITH [105] define a multi-mode system as "a cavity, large in relation to the free wavelength, which allows a number of different standing waves to be established". Whilst a single-mode system encloses within its cavity an electromagnetic energy distribution having a specific standing wave pattern being the interaction product of two or more traveling waves [105, 107]. In multi-mode cavities, such as microwave ovens, the electromagnetic field is poorly defined and, by design intention, the "microwave energy" is dispersed or otherwise distributed throughout the cavity. In single-mode cavities – often waveguide sections – a well-defined field distribution can be achieved using tuning devices to focus microwave energy into a specific, confined region. Single-mode applicators are delivery-specific and are utilised where energy is to be maximised in a specific region of the specimen under processing.

The microwave ovens and reactors used in this project were resonant multi-mode systems. Microwaves entering such systems are reflected around the chamber by the metallic walls until the resulting multi-mode field interacts with the susceptible load to convert the microwave energy into heat, whilst modifying the chamber's microwave resonance. Thus, in a multi-resonant system, the utilisation (or conversion) of input energy is optimised and energy reflected to the magnetron is greatly minimised [99, 105]. Unavoidably in microwave systems, some energy is always lost to the metallic chamber or reactor walls (by e-folding or skin depth absorption and the resultant flow of skin currents). Skin depths in the order of picometres are typical for metals, which are

generally categorised as reflectors and otherwise considered to be opaque to microwave radiation.

A common dilemma encountered during the heating of dielectric materials is the phenomenon of thermal runaway. Thermal runaway occurs at discrete sites and is the exponential runaway of temperature that interrupts the uniformity of heating in the bulk load. It is initiated at impurity element or dopant sites (where a dielectric difference exists across a phase boundary or between phases in intimate proximity) by Maxwell-Wagner and other complementary effects, and these effects are greatly magnified where the applied energy is concentrated at the dispersed "dopant" sites of a volumetrically minimal contaminant. The resultant positive rate of change of the effective loss factor accompanying the heating effects leads to an uncontrolled temperature rise in the most susceptible regions of the material being heated by microwave (high frequency) energy [105]. Universally in the literature of communications applications and of bulk heating applications, thermal runaway is regarded as having detrimental if not catastrophic consequences – a phenomenon to avoid by avoiding the causal dielectric circumstances. Nevertheless, thermal runaway was advantageously utilised in the microwave-stimulated reactions of this project to promote regional concentrations of high temperature, to attract further microwave energy, to initiate energy-demanding chemical reactions, to release consequent exothermic energies, and to initiate plasmas – all desired consequences.

High frequency electromagnetic fields of sufficient strength can divide gases into their molecular and smaller constituents producing a conducting medium that will result in an electrical discharge or plasma. Gaseous discharges may be unwanted impositions in radio frequency (RF) or microwave process – often attacking applicator parts or the magnetron itself. Alternatively, by design, such compositional break down and gaseous discharge may be desired in high frequency processes. RF and microwave plasmas are employed industrially in vapour deposition and chemical reaction processes.

Electrode-less discharges such as microwave-induced plasmas have the decided advantage of being independent of electrode effects and are eminently suitable for a range of industrial applications [105]. At pressures greater than atmospheric, microwave-stimulated plasmas are of the thermal plasma type whereas, from very low pressures up to pressures closely approaching atmospheric, microwave plasmas are of the "cold", non-equilibrium plasma type. More common in industrial undertakings, microwave processes are operated to take advantage of the maximum difference in electron temperature to heavy particle temperature ranges – particle parameters that provide unique ionisation or plasma chemistry conditions most suitable for a range of processes [80, 86]. Ions and excited atoms and molecules have far greater chemical reactivity than do their species counterparts in the ground state [80] and so plasma chemistry is a desirable alternative chemistry for a range of industrially important processes.

Generally, microwave-induced discharges provide a greater degree of ionisation and dissociation than do other types of discharge. They can be operated over a wide range of pressures and provide a very high ratio of electron to heavy particle temperatures [83]. Almost universally, these parameters provide greater degrees of freedom in their application to ionisation or plasma chemistry. The theory and application of microwave plasmas and the chemistry arising out of discharge ionisation are pursued and expanded in the following sections.

4.2: Microwave-Stimulated and Other Non-Conventional Reduction Techniques Applied to Refractory Metals Production and Processing.

Whilst the exemplary stability of refractory metal minerals demands intensive thermochemical intervention in the extractive metallurgy stages of metal production, this same stability exists for remnant minerals and secondary compounds which are to be removed utilising similarly rigorous means during the refining stage. Further, and reciprocally commensurate with their gettering capability, the deleterious effect upon mechanical properties in refractory metals imbued by any very minor amount of compound-forming impurity elements requires that extra refining initiative and effort be invested to produce metals of adequate purity. For refractory metals, the commercial

grade purities lie at levels that would for most of the common metals indicate very high purity. High purity in refractory metals is required to ensure ductility and the consequent fabrication utility required to meet the typical range of applications for which refractory metals are specified. (Universally, the problem impurity elements are commonly present in source ores and process refractory materials, and are elsewhere ever-present in processing environments – in particular, these include the pervasive light elements oxygen, nitrogen and carbon.)

So, as a consequence of such thermochemical stability of refractory metal compounds and the impurity intolerance in the reduced metal product, the techniques utilised in the production of the refractory metals extend into the "non-conventional" more so than for extraction and refining processes of other common transition metals. To some extent, the higher end-value of refractory metals permits a greater expenditure allocation for the extractive, refining and other crucial stages of production. However, in the reality of everyday commerce, frugal economic management does not allow *unwarranted* extravagances where commercial competition exists. The pivotal fact that marketable refractory metals cannot be produced without these more expensive, extra-conventional routes is sufficient and necessary justification for their employment. The high affinity of refractory metals for oxygen, nitrogen, carbon and comparable elements – and the great thermochemical stability of their compounds – require more chemically-intensive and/or energetically-intensive reduction solutions. This thermochemical stability is particularly evident in their ore minerals, minerals which have enduring chemical fidelity and high to extremely-high thermodynamic stability (thermochemical obduracy) in their naturally occurring forms (as evidenced by the *in situ* endurance which characterises their geological occurrence and the tenacity that accompanies the devolution of their depositional and environmental history). Accordingly, more intensive, extra-conventional reduction systems in extractive and refining operations are imperative to production feasibility – and to overall economic plausibility.

Typically in commercial operations, such "intensive, extra-conventional reduction systems" constitute operations which are incorporated during the refining stages of refractory metal production where, because of the demanding nature of these purification operations, they are generally slow, tedious, low throughput, costly processes producing metal oxides or chlorides of exacting specification, pre-final

extraction. This is especially so where final metal of highest purity is required. Non-conventional reduction and refining procedures for which an intermediate crude *metal* product is the feed material include, most commonly, processing techniques incorporating arc melting (various methods), electron beam melting, electron beam fractional zone melting, vacuum sintering, ultra high vacuum annealing, gettering, various methods incorporating iodide or other halide refining techniques, and various methods based upon electrowinning or electro-refining. Flow sheets for some of these production routes are depicted in the figures of Appendix **A** of Section **3**.

Non-conventional reduction methods incorporated in the *extractive* stages of production (including "refining" of *metal halide* intermediates by fractional distillation or comparable techniques) are similarly consumptive of "economic" production factors. These methods involve the purification (by separation) of crude *non-metallic* intermediate product – usually metal halides – that are separated by their melting-point and boiling-point differences (fusibility and volatilisation). Such methods are accepted standard practice in the production of "commercial grade" refractory metals and, as such, were addressed in Section **3.2.1**: *Halidation Routes in Extractive Metallurgy*. This level of refining is adequate for standard commercial grades, for highest purity refractory metal grades, commercial grade metal is utilised as a starting-point "crude" metal for *metal* refining processes.

4.2.1: Industrial Refining Processes.

Refining or impurity removal for refractory metals can be accomplished in a number of ways, under varying conditions, and by liquid state *or* solid state refining techniques [29]. Solid state refining was the "standard" purification method for refractory metals such as niobium until the mid 1960s (after which higher metal purities were required by nuclear and other industries). Despite being outmoded, solid state refining has (over liquid state refining) the advantages of not requiring containment and of being spatter-free. In some production lines, however, solid state refining techniques are still employed for partial refinement of crude extraction product metal – this partially refined metal then becomes a superior "crude" metal for subsequent higher intensity liquid refining techniques such as vacuum arc or electron beam [17, 29]. Since solid-state refining reactions occur in the bulk solid, the feed metal should preferably be of sponge or porous texture to facilitate the out-gassing of interstitially trapped gases such as hydrogen and reaction product gases and vapours from the volatilisation of both metallic and non-metallic impurity elements, and the elimination of oxygen by remnant carbon (to yield carbon monoxide) and by sacrificial de-oxidation then volatilisation of the oxide at higher temperatures. Of course, for solid-state refining, bulk metal heating must be universal and well controlled to hold the solid mass within opportune temperature ranges on ramped temperature profiles to facilitate the release of gases and volatiles or the progress of reactions in an integrated manner – the order of this thermal orchestration being significant in the final purity achieved. Heating for solid-state refining is typically accomplished in a purpose-built furnace incorporating resistance heating, self-resistance heating or induction heating [29]. Liquid refining techniques require a heat source capable of melting high melting point metal and keeping it molten in the required temperature range for the duration of processing. Whilst subsequent solidification should not be too rapid, nor should solidification be too slow; so the heated zone must be suitably localised to the pool being processed beneath the heat source. The following liquid refining methods may be employed for refractory metals.

The pyro-refining of metallic primary products or the pyro-reprocessing of intermediate products requires the incorporation of melting and hot-processing techniques that afford the thermochemically susceptible metal the assurance of vacuo-atmospheric control and protection. This is particularly so for reactive metals –

including the refractory metals. In cases where an unreactive crucible refractory is available*, vacuum induction melting provides a commonly available means of melting small to large quantities of metal for processing. Vacuum induction furnaces provide a continuously atmosphere-evacuated environment in which metals can be melted, compositionally adjusted or processed (utilising the stirring of induced currents within the melt to assist the establishment of thermodynamic and compositional equilibria leading to homogeneity of castings) and control-cast into ingots or shapes specific to further processing. Induction heated systems are limited by the maximum temperature attainable in any load (via the susceptibility of the load metal at load size) and the melting point of the load metal. Where, prior to refining, the load metal was somewhat impure, its melting point may be sufficiently lower allowing melting to be achieved where it otherwise would not in the highly pure state. (Levitation melting is normally a specialised case of induction melting. Refractory metals are common subjects of this containerless technique that is principally intended for melt/solidification exercises rather than purification operations [57, 109].) Moreover, refractory metals of high purity typically need the benefit of more controlled techniques of intensive processing.

Vacuum arc melting has been the common method of melting high melting point metals for further processing. As a technique it approaches ideal because (*i*) the arc provides the high intensity heat source required to melt refractory metals, (*ii*) it provides atmospheric protection and impurity evacuation through high vacuum, and (*iii*) melting is typically contained in a solid metal "skull" (of the metal to be melted) or a water-cooled copper hearth or mould – either option offering protection from contamination by reaction with refractory material. The metal to be melted will most likely be fabricated into anode and/or cathode and arc melted in what is known as the consumable electrode process. Alternatively, the non-consumable electrode process can melt refractory metals that cannot be formed into an electrode. To facilitate the arc, the melt metal will be required to have low vapour pressure above the melt [108].

The very high temperatures of the molten pool (at the anode spot for **dc** electrode negative configuration – the most common method) ensure high impurity element volatilisation and high gas removal in the vacuum. Consequently, vacuum arc

* Refractories or ceramic crucibles may not be available for the more reactive metals, particularly at low pressures where reactions between refractory or ceramic crucible and hot liquid metal proceed much

melting is used as a simple, straightforward method of melting *and* molten refining for refractory metals. However, by comparison, electron beam melting is an analogous technique that (reputably) produces higher purity molten-refined metal than arc techniques and is more amenable to the system-inclusion of zone refining.

(Always minute but) varying in magnitude across the block of refractory element groups, as little as a few parts per million of impurity can embrittle otherwise pure refractory metals and, at these levels of impurity, hardness measurement is extremely sensitive as a predictor of ductility [108]. At such high levels of requisite purity, the technique and system employed to melt and purify the objective metal load may well be crucial in determining whether the specification can be attained. Electron beam melting provides the capability of producing higher purity metal than vacuum arc melting or, of course, vacuum induction melting where this is compatible. As the name implies, electron beam melting utilises a beam (or stream) of electrons projected from a fine cathode onto either the melt metal which acts as anode or through a ring anode and onto the earthed melt metal [110].

The principal advantages which are claimed for electron beam melting over vacuum arc melting are (*i*) the extended molten-state time of the melt pool, (*ii*) the much higher vacuum over the molten pool, and (*iii*) the considerable superheats which are possible in the melt thus allowing some desirable reactions to proceed much faster than otherwise [108, 111, 112].

The principal industrial methods which utilise the water-cooled hearth technique of melt solidification are the vacuum arc melting, the electron beam melting and the thermal plasma (plasma torch) melting methods of processing – the initial two under high vacuum and the last under controlled atmosphere. The cold hearth technique utilises a designed series of water-cooled copper hearths that guide and direct the solidifying melt metal into the appropriate cooling mould [110]. Such cooled containment and casting techniques minimise the pick-up of contaminants and inclusions.

---

more rapidly than at atmospheric pressure [108].

Essentially, as a melting procedure - and like the induction melting and arc melting processes, zone melting does not fundamentally require a vacuum. However, where zone (or float zone or fractional zone) melting is utilised as the processing configuration in a purification or refining operation, then high vacuum becomes mandatory in volatile removal from the melt zone. In zone refining one end of a bar of good purity material is melted and the molten zone is moved along the length of the bar. Generally, the impurities are progressively and accumulatively confined to the molten "float" zone ahead of the re-solidifying refined material as the molten zone progresses along the bar. To be more concise, zone melting techniques are normally vertical operations - bar and melt zone size, advance rate, and other parameters are controlled by the melting point, viscosity, surface tension, and other physical properties of the material. The specified final purity determines the number of "passes" the initial feed bar will require – the zone refining method is normally a multi-pass operation. Zone melting/refining techniques are used not only for "pure" metals, but also for "pure" alloys. The technique may also be used to re-solidify a material under more controlled conditions to dictate or redistribute microstructure and adjust the physical properties of the material.

Metallurgical pyro-processes are energy intensive, however – kJ/kg – conventional combustion flames deliver far less energy intensity than is the case for the techniques described above. However, plasma torch systems, and the range of plasma heating devices which are analogous to or hybrid of these, can deliver optimum energy density at required temperature and achieve this heat with as little as five percent of the gases (mass) required to deliver the same thermal energy by combustion [116]. The temperature and energy density of thermal plasma heaters are multiples of those of combustion systems. Plasma torches not only involve the continuous processing of matter of insubstantial mass, but because oxygen-based combustion reactions are *not* required, the plasma chemistry can be designed to be compatible with the process chemistry and offer extended chemistry options through the creation of activated chemical species through ionisation. Under thermal ionisation, either inert or chemically active gaseous species at pressures varying from 10^{-2} to 10^{7} Pa (but normally at the higher end for torches), operational plasma temperatures are usually in

the range 9,000°C to 20,000°C for typical commercial torches and similar plasma devices operating over a wide range of extractive and refining applications worldwide [58, 116].

Thermal plasma techniques delivered through torch-type plasma devices have opened-up entirely new chemical and metallurgical processing possibilities [58] by offering extremely high concentrations of thermal energy, and by association, (with increased reactive components) accelerated fundamental metallurgical reactions. Typically, reaction rates are known to increase by one or more orders of magnitude under plasma processing – for both thermal and cold plasmas. Along with this kinetic augmentation is the crucial thermodynamic observation that, for heterogeneous systems under plasma stimulation, "the heats of reaction are shifted towards the exothermic range, and the role of the entropy factor increases" [58].

Plasma torch devices are often RF induced and are operated in a controlled atmosphere environment at pressures above or below atmospheric. The plasma torch is a "high pressure" arc and, as with evacuated arc systems, is operated in either the transferred or non-transferred arc modes. Whilst the transferred torch configuration is more efficient, each mode has its advantages for specific applications and most plasma torch systems are hybrids; one such system is the non-transferred arc, thermal plasma cyclone reactor described by TAYLOR, *et al.* [118], and used for ore beneficiation and mineral reduction to metal. Thermal plasma torches and analogous devices are employed where a controlled atmosphere environment is preferred to an evacuated environment in furnaces and reactors from bench scale apparatus to blast furnace tuyere. Because of their plasma chemistry capabilities as well as their heating capabilities, plasma torch devices are well suited to extractive reduction applications and to chemical and evaporative refining techniques. As a straight heating technique, plasma torch heating using an inert gas thermal plasma is highly effective but may not produce a re-solidified product with the equivalently retained high purity of any of the continuously evacuated high vacuum methods.

Ultimately, ultra-high purity refractory metals are most commonly prepared by a combination of complementary techniques. Whilst plasma torch melting produces metal of very high purity, it does so at "high" system pressures making it incompatible for in-line application with systems incorporating vacuum-dependent operations such as zone refining. Typical ultra-high purity system configurations are based upon electron beam melting feeding into a zone refining sequence of single or multiple passes, and possibly incorporating electro-refining steps between passes. Both electron beam melting and zone refining are processes requiring controlled, high vacuum environments.

4.2.2: Microwave and Other Techniques Reported in the Literature.

There have been published in the literature of the past three decades a modest number of significant articles reporting work on microwave-based and RF-based processes akin to extractive processing or otherwise of relevance to this project. Only a minority of these reports were explicitly extractive metallurgy articles, and furthermore, virtually all of these articles reported results of laboratory-based research rather than recorded actual pilot plant or industrial applications. It is known, however, that several groups working in Canada are quite advanced in the area of microwave-stimulated extractive metallurgy but do not openly publish because of the constraints of commercial confidentiality considerations. Such restraint of publication, even at a fundamental research level, has denied this project valuable technical information and insight into real, practical development applications. However, these groups *have* published some information and, whilst such has been of interest, this author suspects that the material released was quite dated at publication and/or technically innocuous.

Perhaps the most general grouping of published articles is of those which document the mineral processing and/or reduction of run-of-mill sized mineral concentrate down to fine-powder sized mineral particulates in variously generated plasmas of diverse chemistry, kinetics and thermodynamics. Although some groups claimed "imminent scale-up to commercial scale operation", generally these articles recorded the outcomes of speculative research projects. Furthermore, it was often difficult to identify a "learning curve" which might have been common across projects

in this field (as is normally quite clear in retrospect upon any overview of research accomplishments across research groups in any field of "cutting-edge" research and development). Some reported research "accomplishments" appeared to be regressive with respect to well-reported similar work (conducted years earlier). [Re-inventing the wheel but ending-up with a stone disc to replace the pneumatic tyre!]

In-flight reduction of ore minerals or their synthetic-mineral equivalent has been trialed by numerous investigators (particularly in Japan) with varying levels of success. Whilst adopting considerable process sophistication in terms of experimental procedure and equipment – especially reactor evacuation and atmosphere control, plasma generation, and "temperature" monitoring and assessment – few displayed in their reports and descriptions of experimental apparatus any real attempt to overcome the crucial dilemma of *residence time* of reactants. However, most authors acknowledged, measured and modeled the extremely brief in-flight time (in the order of microseconds) of reactant particles in the plasma plume and the associated transitionary thermochemistry of this brief and transitory reaction path. No experimental group was able to "fix" the reactant particles in the plasma environment – all were limited by the flight trajectory across or otherwise through the temperature profile of the plasma plume and the in-flight time for the system. The general approach of investigators was that system in-flight times were calculated and matched with theoretically acquired estimates of reactant particle feedstock size and condition that were invoked from conventional thermochemistry values and known mineral reducibilities. Where the brief residence time was sufficient to complete the reduction, the operation was deemed to be successful; however, in the typical case, these metallised minerals could have been reduced efficiently using less energy-intensive, less expensive methods. The minerals whose reduction would justify such energy-intensive extraction techniques were not reduced, or were only partially reduced, within such limited residence times (even at ultra-fine size fractions). These generally well conducted, often technically advanced studies were almost always "inward-looking" scientific studies (of definite individual worth) rather than pre-pilot investigations looking towards industrial application.

Possible extraction routes to titanium are summarised by HENRY [42] as shown in Figure {3.2.2}2, however, high purity refining techniques are not indicated. OJEBUOBOH and MARTINS [51] examined the upgrading of various ores and the conversion of solid feed to titanium metal utilising both transferred arc and non-transferred arc plasmas. They were not successful in full reduction of ores to metal but did find a measure of success in the disproportionation (decomposition) of the iodide TiI_4 in a laboratory apparatus.

WAN, *et al*,[120], used a 2.5 kW RF source with pulse controller with which they adjusted pulse width and repetition rate over experimental charges of various transition metal minerals including molybdenite (MoS_2), molybdic oxide (MoO_3), magnetite (Fe_3O_4) and ores of zinc, lead and nickel using carbon as the reductant. Their results were modest with only small amounts of metal being reported. M^{c}GILL and WALKIEWICZ [121] also investigated a suite of ore minerals and laboratory chemicals reporting various aspects of their heating under microwave irradiation but did not constructively produce any metallic product.

KITAMURA, *et al* [119, 122], undertook the in-flight reduction of Fe_2O_3 , Cr_2O_3 , TiO_2 and Al_2O_3 employing an RF plasma torch and Ar-H_2 plasma. They succeeded in reducing the first two oxides to metallic iron and chromium respectively, however, the more stable oxides of titanium and aluminium were reduced only to oxygen-depleted-oxides, not to metallic forms. REID, *et al* [75] used an in-flight technique in a conical expanded plasma torch to reduce oxidic ores chromite and taconite plus sulphide ores of copper and nickel. They were able to achieve metallisation in particles up to "99.7%" in minerals that are comparatively easy to reduce by conventional, lower intensity means. In advanced work reported by TYLKO, *et al* [37], lean chromite ore was successfully reduced in-flight to an iron/chromium metallic form in a sustained shock wave plasma reactor in which a pulsating plasma arc was made to spin at up to 60 000 rpm – a modest result from a highly developed system.

Oxides of iron, manganese, vanadium, nickel, lead, chromium and copper were successfully reduced in-flight under a reducing plasma in a carbon arc. This work by PICKLES[123] qualitatively reported good metallisation over the range of reduction

products, none of which, however, represented any significant accomplishment in metallurgical terms. Fine particulate Al_2O_3 was successfully reduced by RAINS and KADLEC [124] who reported conversion rates ranging from 3% to 30% aluminium metal plus Al_4C_3 in unconverted alumina quenched from a variety of Ar - (H_2, CO or CH_4) thermal plasmas. Their work represented a significant achievement in this field.

Although conducted over fifty years ago, developmental work by GIESEN and DAUTZENBERG [125] (and earlier work upon which they reported) on the aluminothermic reduction of ilmenite to yield ferrotitanium is still highly relevant – if not more relevant – because of the subsequent development and adoption of plasma systems in extractive metallurgy. Considerable work has been invested in the development of primary extraction routes involving the halide metallurgy of crude ferroalloys, as distinct from the "pure" ferroalloys produced either for straight refining to pure refractory metals *or* for alloy additions to steel melts to produce high strength or otherwise special steels. Addressing aspects of the halide extraction of ferroalloys, GROSS [126] described the development of a continuous process based upon the well established principle of disproportionation of halide intermediate products.

Whilst aluminothermic reduction of ilmenite to ferrotitanium has proved feasible, the general extractive route-preference for titanium ores has been to by-pass the production of intermediate ferroalloy products. The aluminothermic reduction of pure TiO_2 has never been truly competitive with halidation routes on grounds that reduction product purity is not comparable – crude titanium halides are fractionally distilled to high purity levels, the aluminothermically reduced metal would need to be subjected to a halidation process and thence fractionally distilled. So generally, in the typical industrial route, titanium ores are all digested to synthetic rutile, nominally "pure" TiO_2 , thence carbothermic assisted chlorination, fractional distillation, and then to metallothermic (Kroll or Hunter) reduction. In light of the earlier comprehensive works on titanium extraction by MILLER [7] , RODGERS [12] , OGDEN and GONSER [129] and others, HOCH [132] critically reviewed the (then) current state-of-the-art techniques employed industrially in the winning and refining of titanium – a constructive reference work from ore to high purity metal.

Proposed improvements or variations to existing established technologies, new technologies, or investigations into raw material variations have regularly been addressed in published technical articles. STANDISH and WORNER [133] investigated systems of microwave-stimulated carbothermic reduction of metal oxides and compared the evident advantages of microwave-stimulated reduction with conventional reduction routes. This comprehensible and practical work evaluated a successful experimental programme and proposed purposeful adaptations of microwave energy onto new metallurgical applications. Nonetheless, orientated towards real applications of metallurgical reduction, this more objective work of review is industrially practicable in scope, the work bears favorable comparison with that more scientifically orientated study (reported above) by WAN, *et al* [120] who used high powered pulsed RF with carbon to "decompose" metal oxides.

Kinetics of the solid state carbon reduction of ilmenite was studied by EL-TAWIL, *et al* [134] whilst EL-GUINDY and DAVENPORT [135] studied the kinetics and mechanism associated with the solid state reduction of ilmenite using graphite as the reductant. PAJUNEN and KIVILAHTI [136] provided a relatively comprehensive overview in their study of the thermodynamics of the titanium-oxygen system. The influence of prior weathering (geological environment) on the carbothermic reducibility of ilmenite ore was investigated by GUPTA, *et al* [137]. BONSACK [138] reported on a process utilising the entrained-flow chlorination of ilmenite to produce titanium tetrachloride plus metallic iron. Aspects of the supercritical interaction between titanium tetrachloride, $TiCl_4$, and CO_2 – a crucial stage of the titanium chlorination route – was investigated by TOLLEY, *et al* [139] .

The alternative to pyrometallurgical reduction of ilmenite is the conventional industrially accepted option of digestion to synthetic TiO_2 . A proposed system revision for the acid sulphidisation of ilmenite to produce TiO_2 was reported by JAIN, *et al* [140]. Various patent applications are worthy of mention because they indicate the broad sweep of developmental directions currently dominating industry upgrades in the quest to produce the most commercially acceptable highest purity "pigment" grade titania which also supplies the feedstock for metallurgical chlorination routes (this "pigment" actually being paint *opacifier*). In their patent application, HALL and GLAUM [141]

claim a process for the treatment of titaniferous ores and slags using sulphuric acid to recover solid titanium compounds for further processing. This process is an extension of existing established processes which digest titaniferous mineral ores to produce synthetic rutile – bound for further processing to paint opacifier or chlorination feedstock. A similar system is claimed by RAHM and COLE [142] for the sulphuric acid digestion of titaniferous mineral ores to produce synthetic rutile. A hydrochloric acid based digestion process for titaniferous ores was claimed by TOLLEY and LAUGHLIN [145] . In their chemical process, the digestion product is treated with organophosphoric acid leaving titanium in solution from which it is precipitated for further processing. MAGALHAES [143] in his patent application proposed a new route to pure TiO_2 by the chlorination of anatase (TiO_2) ore, an ore commercially uncommon or avoided on impurity grounds. In a proposal to bypass the conventional acid digestion stages, BONSACK [144] claimed a new *low* temperature fluidised-bed process for the chlorination of titaniferous mineral ores. In a parallel and interesting proposal, HARD and PRIETO [146] claim a direct fluorination route for raw titanium mineral ores, whilst MEYER [147] claimed a system for the recovery of hydrofluoric acid – a major impediment to the adoption of fluorination routes because of environmental considerations. Although none of these primary metallurgical routes are essentially *pyro*metallurgical, they are fundamentally precursor to the extractive pyrometallurgy of titanium and of refractory metals generally.

A system that bears comparison (thermodynamically) to the titanium system – that is, to the reduction of titanium minerals and the synthesis of titanium compounds – is that of the reduction of silicon minerals and synthesis of silicon compounds. Although not directly relevant to this project, the silicon system is worthy of mention in that similar numbers of articles have been published presenting various strands of research into aspects of reduction to and processing of silicon – much of which is analogous to titanium. Methods which utilise microwave-stimulated plasma, other plasma, and other processing techniques have been employed experimentally and commercially to reduce minerals of silicon and/or synthesise various silicon intermetallics (silicides) and other compounds – prominent among these are the industrially important silicon nitride (Si_3N_4) and silicon carbide (SiC) and several

strategically important intermetallics such as V_3Si, Ti_5Si_3 and $MoSi_2$ plus other, refractory metal intermetallics TiNi, ZrNi, $HfIr_3$ and $Be_{12}Ti$, plus TiB_2 and other refractory metal compounds addressed in the literature [4, 149].

TAYLOR and PIRZADA[150] investigated the synthesis of silicon carbide from silica in a non-transferred arc thermal plasma reactor, whilst TANAKA, *et al* [151], employed an analogous plasma device to produce an ulta-fine silicon powder from molten bulk silicon. Silicon nitride films were produced in a "large volume" microwave plasma by TESSIER, *et al* [153]. YOSHIDA[164] reported on the plasma-based systems possibilities for synthesis of silicon carbide and silicon carbide, whilst HAGGERTY and FLINT [173] also investigated aspects of the combustion synthesis of these compounds. COSTANTINO and HOLT [174] reported on the synthesis of silicon nitride. The combustion-syntheses of refractory metal intermetallics, *pre se*, be it microwave-, plasma-, or shock wave-stimulated, were investigated by KAIEDA, *et al* [157]; YI and MOORE [159]; WORK, *et al* [160]; WARD, *et al* [162]; OTANI, *et al* [163]; YOSHIMURA, et al [167] ; KNITTEL and RISBUD [168]; and MOORE [171].

Reduction of ores of the geologically associated metals zirconium and hafnium, which occur concurrently although in greatly varying proportions (although, Zr >> Hf typically) across all of their ore minerals, bears many similarities to the reduction of the titanium minerals – along with which they are normally mined [24]. Zirconium and hafnium have similar "chemistry" to titanium but greater thermochemical stability. These properties dictate that commercial reduction strategies for zirconium/hafnium minerals are comparable to those for titanium minerals. The nearly identical chemistries of zirconium and hafnium dictate that the two analogue metals are not separated until the otherwise pure "raw zirconia", $(Zr,Hf)O_2$, has been produced. Almost all Zirconium and hafnium is derived from mineral sand zircon, $(Zr,Hf)SiO_4$, a double oxide which may be more meaningfully written as $(Zr,Hf)O_2 .SiO_2$ in keeping with initial plasma beneficiation of contemporary mineral processing operations.

In earlier high-intensity primary processing systems for the conversion of zircon to zirconia, large quantities of zircon sand were melted with sodium hydroxide in arc

furnaces fitted with carbon electrodes. Having a lower boiling point, the product sodium silicate was boiled-off leaving zirconium dioxide (zirconia) that was cooled leaving crystalline zirconia of good purity [58]. The system was highly consumptive of energy, could be polluting, and became obsolete on economic grounds.

In the various plasma dissociation processes, zircon is fed through the plasma torch of a top-fired plasma shaft furnace. The short thermal exposure is sufficient to melt the falling fine sand but subsequent rapid quenching, which occurs as the descending droplets exit the plasma plume, physically separates the prior-melt material into single oxide components SiO_2 and ZrO_2 in a two-phase solid. (Zircon is thermodynamically unstable above 1676°C where it "decomposes" into the discrete components, silica and zirconia [175].) The significant separation of silicon and zirconium, bound with oxygen in crystalline form in the zircon mineral lattice, is accompanied by different solid-phase transitions – zirconia crystallites first re-solidify whilst the silica freezes into an amorphous matrix. This split second of plasma mineral processing represents a major portion of the mineral ore beneficiation *en route* to the valuable pure zirconia plus silica by-product. The considerable benefit bestowed by this plasma process is that the pure separate phases can be *mechanically* separated to an advanced degree and the reactive glassy silica phase remaining can be effectively leached from the zirconia crystallites using a 50% sodium hydroxide solution to yield high purity (better than 99%) $(Zr,Hf)O_2$ plus sodium silicate, a useful by-product. The simplified equation [58] is shown below because it has tangible relevance to this thesis project – as described elsewhere, phase separation was achieved as an intermediate step in reduction of zircon to zirconium.

$$[\,ZrO_2 + SiO_2\,] + 2NaOH \Rightarrow Na_2SiO_3 + ZrO_2 + H_2O \quad \text{.....} \quad \textbf{\{4.2.2\}1}$$

Beyond plasma dissociation of zircon, the greater thermochemical stabilities of zirconia and hafnia have excluded these oxides from the same speculative realms of experimental and developmental expectation which drove the research and development of plasma and comparable extractive/reduction systems for the higher demand, lower stability titanium oxides. Consequently, and given the relative efficiency and process-committed nature of commercial production, little attention has been afforded the plasma reduction or comparable high-energy extraction of zirconium and

hafnium from their minerals. Further, separation of hafnia from zirconia has still to be achieved in the raw zirconia that might be intended as plasma feed, a circumstantial conundrum that lends itself to the "wet" chemistry solutions prominent in current commercial routes. No plasma-type method has been proposed which includes a zirconium/hafnium separation solution.

It is worth noting that, beginning at a cautious rate, zirconium has only been commercially produced since 1945 [43], and hafnium much later (once *its* potential for nuclear applications was recognised). Following other authors [35, 36, 12, 25, 27, 127, 130], GUPTA and KRISHNAN [55] described the typical set of production stage possibilities in the route to reactor grade zirconium and hafnium.

A fusion-leach-fractional crystallisation method was developed by ELGER and BANNING [44] in a project directed at producing high-hafnium concentrate from zircon for feed material for further extractive halide processing towards hafnium metal production. LAMAZE and CHARQUET [53] reviewed the production possibilities for reactor grade zirconium and hafnium. In particular they proposed a single-step system for the reductive electrolysis of hafnium tetrachloride to produce high purity hafnium crystals suitable for nuclear applications and equivalent to the alternative route of Kroll reduction plus refining by either the iodide route or electron-beam melting. In earlier work, STEINBERG, *et al* [26], established the chemical and physical parameters of fused salt electrolysis for zirconium extraction whilst GOODRICH and SPINK [46] had shown through comprehensive feasibility trials in a half-scale production plant that molten salt electro-refining of hafnium tetrachloride to reactor grade hafnium in one stage was achievable. In the development of system improvements for the electrowinning of both zirconium and hafnium at high reactor grade purities, MARTINEZ and COUCH [176] followed the work by Steinberg, *et al*, Goodrich and Spinks, and others.

The fluidised-bed chlorination of zirconium-bearing materials (carbide, pure oxides and zircon) was successfully accomplished by SPINK, *et al* [45] in a resistance-heated system essentially comprising a cylindrical graphite wall and central graphite

electrode. The resistance heating was induced using an **ac** power supply and contact between the electrode wall and central electrode being maintained by the fluidised particles - the bed temperature being easily manipulated to initiate and control process chemistry. Once stimulated, the exothermic nature [45, 177] of the chlorination reactions of these batch processes produced considerable heat in the reactor shaft, however, the heat so produced was efficiently contained by variable flow rate and the mass transfer properties of the fluidised bed operation which yielded high conversion rates. The promising characteristics of fluidised-bed technologies have been matched with plasma technologies by many research and development workers with varying degrees of success [58, 74, 180, 181].

In an attempt to circumvent some of the complexities of the conventional separation route, SPINK and JONASSON [33] devised and built an extractive distillation system for the separation of zirconium and hafnium tetrachlorides using a molten "carrier" salt (NaCl:KCl) and distillation by vapour pressure difference. In parallel and concurrent work, PICKLES and FLENGAS [34] achieved the same success in separating hafnium tetrachloride from zirconium tetrachloride utilising the vapour pressure difference to distil from a range of molten alkaline salts. In a significant new technique circumventing even the "tried and true" chlorination route is that proven by Howell, *et al* [15] who used a liquid-metal solvated carbothermic reduction process to reduce commercial zirconia and separate the hafnium and zirconium fractions in one metallurgical operation. In a carbon/nitrogen-saturated copper solvent at 1500°C the activities of zirconium and hafnium are lowered and the following parallel reactions [15] proceed stably.

$$ZrO_2 + 2C + N \Rightarrow ZrN_{(s)}\uparrow + 2CO_{(g)}\uparrow \quad \text{.....} \quad \textbf{\{4.2.2\}2}$$

$$HfO_2 + 2C + N \Rightarrow HfN_{(s)}\downarrow + 2CO_{(g)}\uparrow \quad \text{.....} \quad \textbf{\{4.2.2\}3}$$

This novel metallurgical process represents significant developmental initiative. Because the chemistries of zirconium and hafnium are almost identical they are extremely difficult to separate chemically. However, the metal nitrides formed as products of carbothermic reduction in copper solvent are unambiguously separated by

clear density difference – the hafnium nitride sinking in copper and the zirconium nitride floating – with an extremely high separation factor of 10^6 reported (and that in a single stage). Other exceptionally high stability oxides of magnesium and uranium can be efficiently processed using similar liquid-metal solvated carbothermic reduction techniques [15].

Considerably diminished thermodynamic imperatives governing the thermochemistry of Group **5** metals niobium and tantalum allow a greater degree of freedom in reduction and processing operations for these metals. Pertinently, the relevant oxides of niobium and tantalum are notably less stable than those of the Group **4** metals, titanium, zirconium and hafnium. Although a generality, this essential thermochemical trend away from the highly reactive metals and extremely stable compounds of Group **4** towards "more moderate" metal reactivity and compound stability affords a comparable shift in reduction and processing options for niobium and tantalum. A greater number of production route options are available in the extraction, refining, consolidation and processing of these metals.

Typically, the principal oxides of niobium and tantalum, pentoxides Nb_2O_5 and Ta_2O_5 , are chlorinated and the chlorides metallothermically reduced in operations similar to those for the Group **4** metals. (Also, the ore minerals are often designated by their "pentoxide-equivalent".) However, the direct metallothermic or carbothermic reduction of the pure oxides is a realistic option for the oxides of niobium and tantalum – an option which, provided the metal produced is of adequate purity for further processing, avoids the resource-consuming and lengthy halination process stage – thereby circumventing a major portion of production cost and environmental burden. GUPTA and SURI [29] describe three working systems utilising calciothermic, aluminothermic and magnesiothermic reduction routes to niobium metal from the pure Nb_2O_5 . Similarly, tantalum pentoxide can be successfully reduced. The authors describe various techniques used in commercial production including co-reduction with the relevant metal carbide to yield pure metal plus carbon monoxide. Solid-state carbothermic reduction of niobium and tantalum pentoxides to metal or carbide can be carried-out in the laboratory or industrially with notable success. Compacts of the finely

blended solid reactants – as shown for niobium in the following equations [29] – are pyro-vacuum treated (around 1800°C under continuous evacuation) and the evolving reaction product carbon monoxide is removed leaving good purity solid end-product.

$$Nb_2O_5 + 5C \Rightarrow 2Nb + 5CO \quad \text{..... } \{4.2.2\}4$$

$$Nb_2O_5 + 7C \Rightarrow 2NbC + 5CO \quad \text{..... } \{4.2.2\}5$$

A nitride decomposition process for the production of ductile niobium and tantalum by pyrovacuum treatment was described by Gupta and Suri [29]. The metal nitrides can be produced by either of two ways; by the direct reaction of the metal pentoxide with ammonia, or by carbothermic reduction of the pentoxide in the presence of nitrogen after the following reaction [29].

$$Nb_2O_5 + 5C + N_2 \Rightarrow 2NbN + 5CO \quad \text{..... } \{4.2.2\}6$$

The decomposition process essentially involves the pyro-vacuum treatment of the metal nitride and de-nitridation follows the following sequential steps.

$$NbN \Rightarrow Nb_4N_3 \Rightarrow Nb_2N \Rightarrow Nb \quad \text{..... } \{4.2.2\}7$$

As for Group **4** refractory metals, the highest purity, lowest oxygen niobium and tantalum is produced by the reduction of metal halides. Most commonly, a chlorination route is chosen for pure niobium and tantalum pentoxides and the resultant chloride is magnesiothermic (Kroll) or sodiothermic (Hunter) reduced to sponge which, once distillation cleansed, is typically electron-beam zone refined to required purity. Alternatively, disproportionation (decomposition) techniques can be effectively utilised to yield pure niobium or tantalum from their chlorides, or their fluorides. Both the trichloride and pentachloride of each niobium and tantalum can be decomposed at low temperatures to yield the metal plus an attendant more stable chloride which is re-processed [17, 29]. A perennially encountered problem in the reduction to oxygen-free metal is the presence of oxychloride impurity in the chloride feed – the oxygen tending to remain in the reduced sponge metal. BOESINGER and STEVENSON [182] reported

on aspects of the use of phosgene, $COCl_2$, to reduce remaining niobium oxychloride, $NbOCl_3$, to $NbCl_5$ prior to metallothermic reduction.

Niobium and tantalum fluorides can be metallothermically reduced by calcium, aluminium, magnesium or sodium, however, the Hunter route is chosen because the product sodium fluoride salt is readily water-soluble and can be separated from the niobium and/or tantalum powder reduction products by simple aqueous washing. Further, the double fluoride complex salt required by some processing routes can be produced by the addition of potassium fluoride. The niobium double fluoride salt, K_2NbF_7, in the principal KCl-NaCl mixture, is the electrolyte reported by Gupta and Suri for the successful electrolytic extraction of niobium; the tantalum system being analogous. PASHEN and KOECK [52] developed a fused salt electrolysis process for the deposition of high purity tantalum dendrites from an analogous salt mixture (K_2TaF_7 in alkaline metal halides) with continuous supplements of Ta_2O_5 directly to the salt to replenish the tantalum in the electrolyte.

An attractive route for the extraction of niobium from ore concentrate was developed by GUSTISON [36]. His method required the hydrofluoric acid leach followed by drying, "complete" recovery of the acid remnant leaving NbO_2F, thence aluminothermic reduction to a vacuum-grade ferroniobium or, with higher heat system, aluminothermic reduction to a good purity niobium metal. Gustison's method avoids the attendant pollution problems by deleting the ammoniated precipitation of the pentoxide, but is ore-specific in that it does not contend with the separation of tantalum where this is significant in the non-pyrochlore ores (that is, in concentrates of most ores). The thermodynamics and practical aspects of niobium/tantalum separation, particularly in eletrolyte-type metal chloride salt mixtures, was investigated and defined by SADOWAY and FLENGAS [38]. The mandatory recovery of hydrofluoric acid from niobium/tantalum-bearing material was outlined in a patent application by MEYER [147]. By comparison, the treatment of tantalum/niobium ore concentrates with sulphuric acid was proposed in a patent application by TAMARU and KITSUNAI [148]. The relative merits of the modern conventional routes was outlined by KOCK and PASCHEN [11] who addressed the more accepted new-technology methods utilised in these industrial routes.

The recovery of niobium-bearing and tantalum-bearing phases from tin slags and other industrial sources has occupied much research attention but little other than basic conventional processes has been adopted in either research strategies or industrial application. Materials recovered from such sources enter the extractive processing chain along with the ex-mine concentrates and represent a large proportion of primary niobium and tantalum minerals that proceed to halination and separation (purification). Amongst many authors, GABALLAH, *et al* [54] reported on the leaching of tin slags and subsequent chlorination of niobium and tantalum concentrates and current practices incorporating slag-derived minerals.

The production of ferroniobium or ferrotantalum is not normally conducted as a recognised standard step in the extraction from mineral to metal. Because of the high degree of purity required to optimise its unique alloying properties, the direct application of ferrotantalum as an alloying addition is not possible; although alloying additions are desirable in the form of the other refractory metal ferroalloys [31]. Most ferroniobium produced is produced for, and used as an alloying addition in the production of high strength, low alloy (HSLA) steels. Niobium can be extracted from its ferroalloy by a nitriding process in which crushed ferroalloy is nitrided, acid leached, and pyro-vacuum treated leaving a niobium sponge of good purity which is electron-beam melted and zone refined [29].

The various extraction and refinement options for niobium and tantalum were comprehensively addressed by early authors such as MILLER [8] and JAMRACK [30], whilst others (such as MOLLER, *et al* [78]) have since contributed as technologies and techniques developed. Whilst primary niobium/tantalum digestive extraction has broadly remained unchanged, purification by electron beam and zone refining have largely replaced vacuum arc technology for niobium and tantalum, as for other refractory metals. RERAT [48] investigated systems of purification under inert gas rather than vacuum protection for the sintering of niobium and tantalum compacts. Explosion generated shock-compression waves were used by WORK, *et al* [160] in the shock synthesis of niobium aluminides Al_3Nb and $AlNb_2$ and other transition metal aluminides. In comparably rapid syntheses, Yoshimura, *et al* **[110n]** used an arc-image heating reactor to synthesise refractory metal carbide and nitride powders. NbC, Nb_4N_3, TaC and Ta_2N were reductively synthesised from the pentoxides Nb_2O_5 and Ta_2O_5.

Whilst reminding the reader that transferred arc furnaces of up to 100 tonne capacity have been and are being operated over long campaigns producing refractory metal ferroalloys, GAUVIN and CHOI [74] describe dedicated transferred arc plasma reactors which have been operated in Canada to produce the range of refractory metals in operations from "bench" scale to production "pilot" scale. Of course, plasma torches have long been fitted to blast furnace tuyeres and, along with coal injection systems, are standard equipment for many of the world-largest production units. DEMBOVSKY [58] asserts that, for large transferred arc plasmas, the confined thermal energy supplied to the charge represents between 10 000 and 15 000 times the *concentration* of thermal energy attainable from conventional combustion heat sources. Such thermal intensity has provided technologies with thermodynamic and kinetic potentials not previously available nor fully understood in the purely theoretical sense, and much of the formerly thermochemically "unachievable" has become achievable.

In Dembovsky's words, "plasma metallurgy offers uncommonly flexible and precise control of process temperatures and pressures" and "affords equally effective control of the chemical composition in the reacting plasma" [58]. There may be no combustion products to contaminate a plasma atmosphere as there are by necessity with chemically generated flames. Also, being electrically conductive, plasmas can be compressed and contained by magnetic restraint thus keeping the highest temperatures away from refractory walls – even allowing the employment of water-cooled metallic (usually copper) hearth casting arrangements in conjunction with extremely high processing temperatures. The benefits and the possibilities of plasma processing options are still being realised – in both industrial and research applications.

The above reported investigations represent a fair representation of the spread of success in microwave stimulated and other plasma reduction trials sighted by this author during the course of this project.

Quite apart from the above technical reports describing specific investigations into extractive processing, many papers have been published describing aspects of the thermal physics, kinetics and characteristics of the full range of plasmas, plasma generating systems, and RF and microwave systems. Such distinguished contributors as Julian Szekely [71, 263], Emil Pfender [72, 85, 169, 180], Maher I. Boulos [90, 180], W.G. Davenport [115, 117, 135], Charles B. Alcock [60], Nagy El-Kaddah [113, 165] and Zuhair A. Munir [154] have written enthusiastically about the research and commercial achievements to date and the industrial potential of these new-technology, high-temperature systems. Szekely [71] provided an overview of plasma processing of materials with reference to the various discharge types, their characteristics, temperature profiles with respect to plasma composition, pressure and other variables, and industrial applications arising from research. He postulated that the various categories of industrial plasma application will be increasingly utilised by industry with the plasma melting and refining of refractory metals becoming process-dominant, and predicting "the emergence of plasma technology as a vital component in extractive metallurgy". This view was clearly supported by Pfender [72] who described more fully the characteristics of plasma types and the generating system possibilities available whilst the kinetics and thermal physics of the plasma types generated in different systems was competently discussed by KHAIT [76]. BULLARD, LYNCH and DAVENPORT [117], and BULLARD and LYNCH [99] extended these principles for microwave-induced plasmas to the processing of ores, whilst MacDONALD and TETENBAUM [83] described the processing possibilities presented by microwave and other high frequency discharges.

The industrially based melting/remelting technologies that utilise plasma are exclusively thermal plasma technologies (including arc). In his comprehensive account of the then current state of development of industrial equipment and plant exploiting thermal plasmas in industrial applications in the field of extractive and refining metallurgy, ROMAN [73] reviewed the principles of heating by thermal plasma and the benefits of the principal industrial installations. He compared RF arcs to **dc** arcs, transferred versus non-transferred mode arcs, **ac** arcs, ignition and delivery and other aspects of practical application. Roman presented prominent plasma reactor types, plasma torches and examples of plasma melting reactors and furnaces. He described the extended plasma arc flash reactor, a Soviet production scale hollow-electrode melter, a

production scale plasma reactor for the continuous casting of commercial grade titanium, plus various other reactors with dedicated purpose including skull casting, nuclear waste processing and refractory metal scrap consolidation. Another purpose-specific plasma reactor was presented which was capable of mono- or single-crystal growing and this type of reactor/synthesiser was used to grow mono-crystals of refractory metals, directionally solidified eutectic alloys and high melting point carbides including TiC, HfC, TaC and NbC [73].

Apart from their high electrical to thermal efficiency, thermal plasma furnaces are used to process refractory metals because of the degree of atmosphere control which can be attained - particularly at the associated gas temperatures which are magnitudes above those achievable in resistance heater or chemical combustion (flame) systems. Equilibrium or thermal plasma furnaces can offer high melting and throughput rates in a highly controlled atmosphere and deliver a dense ingot product. Being at "elevated" pressures, these systems minimise metal vapour losses to mandatory high vacuum pumping procedures in vacuum arc and electron beam type systems [58, 73, 90, 110]. Conversely, non-equilibrium plasma reactor systems (such as adopted for this project) provide high relative populations of reactive species and associated augmented reaction propensities to extractive metallurgical applications – applications that fundamentally are chemical processes. Thermal input levels for these systems are more comparable with flame combustion chemistry reactor systems.

4.3: The Thermodynamics of Microwave-Stimulated Reduction Processes.

Real conventional pyrometallurgical processes take place in heterogeneous systems where there are no significant temperature differences between the various reacting components. In microwave plasma and other plasma metallurgy processes, however, the temperature differences between reaction components constituting the plasma and the reaction components of the solid charge are very large and may be of several orders of magnitude difference. In non-equilibrium plasmas this high-order-of-magnitude temperature difference is attained in the gaseous species alone. (The temperature gradient across gaseous, plasma phases is always considerably greater than those across liquid or solid phases present in plasma-driven reaction processes.) In microwave-heated systems, *per sé*, temperature distributions are large and this is especially true of systems operating under microwave-induced plasma. Plasmas are consequential, if not unavoidable, in systems heating by the various dielectric mechanisms initiated under microwave-stimulation – and particularly so in systems involving chemical reactions, or where reactions are imminent.

Keeping in mind that a plasma is a mixture of excited molecules, atoms, ions, electrons and recombined particles in a host gas (neglecting "solid state" plasmas), and in view of the high particle energies characteristic of these plasma components, it is intuitive that the physical and chemical behaviour of component particles in plasma differs markedly from their equivalent's behaviour in the "ground state". Furthermore, microwave plasmas proceed under conditions in which the energy levels and temperatures of free electrons differ widely from the other, heavy particles. Of course, energy quanta define discrete energy levels, and "discrete" energy photons are also represented in the light particle types. Consequently, systems under microwave plasma are in a state of advanced non-equilibrium – a state in which the physico-chemical reactions proceeding in the system may be profoundly different from their "equivalent" ground state reaction analogue [58, 80, 178].

Statistical thermodynamics enables the calculation of thermodynamic properties of any substance only if the distribution is known of the energy levels of particles

which make-up the system. For a system in equilibrium the distribution of particle energies will conform to the thermodynamic probability governing the distribution such that entropy is maximised. The number of possible alternative modes by which this thermodynamic distribution can be achieved is determined by the partition function that defines all of the thermodynamic properties of a substance [66]. The partition function accounts for the energy of translational motion, vibrational and rotational energies, and associated with plasma, the excitation and ionisation energies in electrons and nuclei, *et cetera*, or any combination of these energies. The energy of translational motion of particles is not a quantum energy and its partition function is pressure dependent, whilst vibrational and rotational energies are only applicable for molecules (that is, for particle units of two or more atoms) [60, 66, 184, 185].

Irrespective of the physico-chemical composition of the charge, most industrial plasma-metallurgical processes proceed under conditions of thermal non-equilibrium [58] – so the laws of thermodynamics, or more succinctly, equilibrium thermodynamics, and chemical kinetics do not apply. Metallurgical reduction processes typically are heterogeneous systems that, by the very nature of the physical complexity of the reactor charge, are disinclined toward chemical and thermal equilibria [95]. When this disinclination due to heterogeneity is imposed upon the disinclination toward equilibria imposed by plasma reduction processing then the non-equilibrium regime in the system persists such that equilibrium may not be reached during the process (particularly for batch processes). Non-equilibrium is characteristic of microwave plasma reduction processes generally and especially where the microwave plasma is imposed upon a heterogeneous load as was typical of reduction operations in this thesis project.

Whilst it is true that irreversible changes play a fundamental role in classical thermodynamics, the characteristic restriction in classical theory is that all system changes that can be treated quantitatively are *reversible* changes between *equilibrium* states. And where reversibility is common to equilibrium phenomena, irreversibility is common to non-equilibrium phenomena [186]. It can be shown that, as a consequence of the second law of thermodynamics, without irreversibility it would not be possible to define an *absolute* temperature scale (which is so essential to reversible processes) [185].

Despite this theoretical constraint, the introduction of temperature (and, of course, other thermodynamic variables such as enthalpy and entropy) depends upon the concept of thermodynamic equilibrium. So, what is the outcome when "temperature" is measured in a system operating under non-equilibrium conditions? A number of different types of thermometer could be employed to "measure" the temperature in a non-equilibrium system – however, it is likely that they would (significantly) disagree with one-another as to the temperature **[66, 184, 185]**. In his comprehensive treatise on plasmas [187], FRANK-KAMENETSKII of the USSR Academy of Sciences recorded that "there are many cases in which temperature measurements by different methods on the same plasma yield results which disagree by a factor of ten". Thus, without standard means of measurement, there is no conventional way of defining temperature in a non-equilibrium system and a "new approach in thinking" of the importance and "meaning" of such measurement is appropriate – in fact, the *sum of energies* is relevant, rather than the dogged, "spontaneous" measurement of *thermal* energy.

For low-density (low pressure) plasmas, which are not in thermal equilibrium – and in which the various particle species move with different energies – the concept of "temperature" is not defined [58, 187]. Under the imposed stimulation of microwave irradiation, species' energies in low-density plasmas undergo further excitation disparity and the concept of plasma "temperature" becomes even less meaningful.

Every measurement of plasma or in plasma is a problem. Methods for determining the temperature, particle density and particle concentration of plasmas are the subject of essential operations in experimental plasma physics, which are collectively called plasma diagnostics. Plasma diagnostics presents a powerful means of characterising plasma properties – but again, the requirement of thermodynamic equilibrium to define a "temperature" is mandatory [187, 188].

Whilst total energy is conserved in any closed system, the same is not true for entropy in systems not at equilibrium. The principle of the conservation of energy notwithstanding, the entropy of an isolated system will continue to increase whilst there are any changes proceeding within the system [184, 185]. In classical terms, this apparent contradiction raises quite a theoretical conundrum for systems such as microwave plasma operating at steady-state non-equilibrium.

Entropy is not measured directly, rather it is defined in terms of other quantities. Generally, the assumption made in using the Gibbs equation is that entropy always depends upon these quantities in the same way whether or not the system is at equilibrium. Boltzmann defined the entropy of gases in terms of their molecular structure [185] – the definition is applicable to systems under equilibrium or non-equilibrium conditions. However, rigorous experimental analysis [185] has shown Boltzmann's definition to hold true only where the "non-equilibrium" condition was not far removed from equilibrium. Again, this amplifies the conundrum of the steady-state system operating in clearly unambiguous non-equilibrium.

It should be stressed (again) that this thesis project was not an exercise in analysis of the thermodynamics and kinetics of microwave-stimulated systems. However, the idiosyncrasies of these complex, expansively non-equilibrium systems are acknowledged and discussed here and elsewhere in this thesis.

4.4: The Kinetics of Microwave-Stimulated Reduction Processes.

As any system under processing approaches thermodynamic equilibrium it fluctuates between and through transient states of equilibria. The rate of this transition is determined by the kinetics of the process. The physical kinetics of the process determines the equilibrium distribution of energy whilst the chemical kinetics determines the rate at which equilibrium chemical composition is attained [86, 80]. These rate-dependent kinetic processes are further complicated in plasma processes in general, and even more so in microwave-stimulated systems through direct microwave coupling and/or microwave plasma, which is inherently non-equilibrium in nature [80]. At temperature regimes typical of plasma processes (microwave or otherwise) chemical reaction rates are rapid and, generally, are limited by physical kinetic reactions such as diffusion and fluid-phase turbulence.

Section 4

A feature of plasma pyrometallurgy processes is the predominance of reaction chemistry occurring at the plasma-solid or plasma-liquid interface. Whilst this feature is characteristic of pyrometallurgical processes generally, reaction kinetics (rates) across these interfaces is greatly enhanced by plasma chemistry and by microwave stimulation generally [58, 80]. The overall rate of any chemical reaction is dictated by the rate of the slowest step. For many reactions this slowest step is the diffusion of reactants through an un-reacting medium. It is established [86, 105, 181] that mass transport (diffusion) is greatly enhanced by dielectric heating mechanisms during microwave processing and, thus, microwave processing in the sub-plasma and plasma temperature regimes must enhance chemical kinetics. So, the rate-controlling phenomena of mass transport of reactants through "un-reacting" media (phases) and the rates of reaction in reaction zones are both stimulated by the impost of microwave energy - particularly in the presence of a microwave plasma.

In reaction environments dominated by, or determined by plasma chemistry the equilibrium status of the system is of over-riding importance with respect to reaction dynamics (including kinetics).

Equilibrium plasmas – that is, plasmas exhibiting kinetic equilibrium between constituent particles – are characterised by low field voltages, high bulk temperatures,

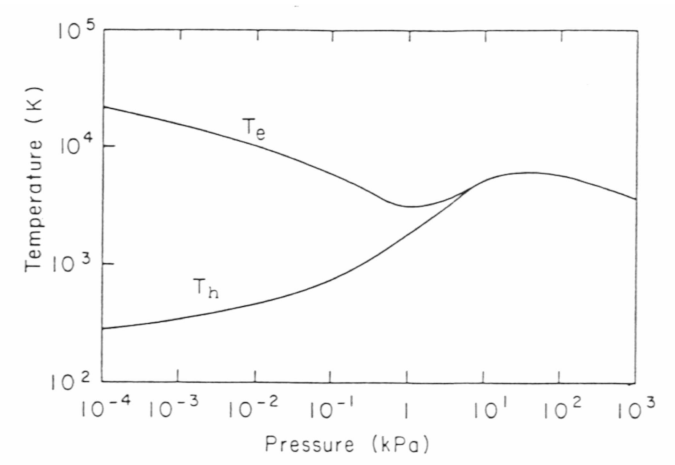

Figure {4.4}1: Diagram showing the separation of electron temperatures with respect to heavy particle temperatures at low pressures in non-equilibrium plasma (note that 1 atm ≈ 10^2 kPa)[72].

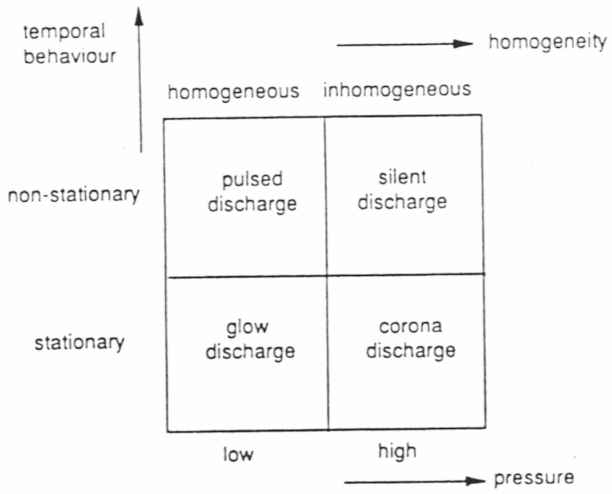

Figure {4.4}2: A simple representation of the classification of various discharge types according to their temporal behaviour, discharge pressure and appearance [80]. [Note that microwave discharges are grouped in the "pulsed discharge" quadrant.]

and "high" pressures (upwards from atmospheric). The strict validity of thermodynamic expressions holds only for these high pressure discharges as is evident by the low pressure separation of particle temperatures and consequential non-equilibrium portrayed in the particle temperature versus plasma pressure plot of Figure **{4.4}1**.

Equilibrium plasma is characterised by approximate "equivalence" between electron temperatures (T_e) and heavy particle temperatures (T_h). In truth, such plasma only approaches equilibrium and is often more appropriately and usefully defined as being in "local thermodynamic equilibrium" (LTE). As with full equilibrium plasmas, the LTE of high pressure plasmas is characterised by kinetic equilibrium ($T_e = T_h$) and, because electron and heavy particle concentrations are effectively equated by the temperature equivalence of particle species, by effective chemical equilibrium [72].

Non-equilibrium plasmas, which exist for low-pressure discharge regimes, are characterised by particle temperature non-equivalence with $T_e >> T_h$. Non-equilibrium plasmas can be generated by a number of means under a range of conditions. The factors governing these means – the generation mechanism, electrode geometry, initiation and operating pressure ranges, *et cetera* – are typically evoked in their classification and/or nomenclature. The common non-equilibrium plasmas are the glow discharge, corona discharge, silent discharge, radio frequency or RF discharge, and microwave discharge plasmas [80]. These discharge groups are summarised according to temporal behaviour, pressure range and appearance in Figure **{4.4}2**.

The concepts of equilibrium and non-equilibrium in systems and the consequential inter-relationships of thermodynamics and kinetics are pursued and expanded in the following Sections **4.5** and **4.6**.

4.5: Plasmas, Microwave Plasmas and Ionisation Chemistry.

For any material, a given amount of energy is required to transform it from one physical state into another. This energy is the bonding energy or latent heat and is characteristic of the material and its phase (and absolutely independent of activation

energy, the requirement for *chemical* change). Because the kinetic energy of ionising particles must exceed their ionisation energy for matter to form a plasma state, *plasma* has been called the fourth state of matter [187]. This may be true for the thermonuclear environment of stars in which all matter exists as totally ionised hydrogen (deuterium, tritium) and helium. However, in interstellar space and in our Earthbound experience where partially ionised gases are categorised as plasmas, this fourth state is not strictly true as there is no clearly defined state boundary between gases and plasmas. However, a distinguishing characteristic is that, unlike gases, all plasmas respond to electromagnetic forces. Charged particles in plasma are affected by externally applied electric and magnetic fields. Otherwise and moreover, for glow discharge plasmas (in which perhaps 10^{18} ion-electron pairs are produced and re-combined per second) the degree of ionization is typically of the order of 10^{-4}, which (statistically) closely approximates a ground state gas [189]. In fact (not surprisingly), plasmas obey the gas laws. Indeed, the gas-to-plasma shift of our experience is more analogous to change of *phase* rather than change of *state* – different discharge types representing different phases of one state (gas).

4.5.1: Gaseous Plasmas and Solid State Plasmas.

Recognition must be made, at this point, of the other class of plasma that may play a minor but real role in microwave-stimulated reduction of solid reactants. Like gaseous discharges, electrons and holes in semiconductors and electrons in metals and semi-metals are requisites of systems which display plasma-like behaviour in solids. "Solid state plasma" is the term used to describe the phenomena arising from the interaction of any collection of mobile charge carriers in such solids [190]. However, not all charged-particle systems in solids display plasma-like characteristics; ionic salts are a case at point. For example, in sodium chloride the Na^+ and Cl^- ions are too tightly bound to allow free movement about the lattice.

The term *solid state plasmas* suggests substantive similarities with *gaseous plasmas*. Whilst this is notionally true, there are definitive quantitative differences that characterise the two classes of plasma. An obvious example is, by comparison with

solid state lattices, the largely unimpeded mean free path of particles in a gaseous plasma – such free path is often comparable in magnitude to the dimensions of the reaction chamber. Consequently, the solid state plasma is effectively an infinite medium in which boundary conditions play little role whereas, in gaseous plasma, they can be crucial [190]. As with gaseous plasmas, the concepts of equilibrium and non-equilibrium hold true for solid state plasmas [191]. A comparison of the orders of magnitude of some characterising parameters of gaseous and solid state plasmas is shown in Table **{4.5}1**.

Table {4.5}1: The orders of magnitude of some characterising parameters of gaseous and solid state plasmas (after Hoyaux [191].

Parameter.	Gaseous Plasma.	Solid State Plasma.
Plasma density.	10^{6} to 10^{24} (m^{-3})	10^{18} to 10^{29} (m^{-3})
Negative carrier mass.	1 (electron mass) [Except negative ions.]	10^{-3} to 1 (electron mass)
Positive carrier mass.	10^{3} to 10^{5} (electron mass)	10^{-3} to 1 (electron mass) [Except uncompensated plasma.]
Plasma temperature.	10^{2} to 10^{9} K	0 to 10^{3} K [Although degeneracy possible.]
Plasma frequency.	10^{3} to 10^{13} Hz	10^{8} to 10^{15} Hz
Dielectric constant (low freq.).	essentially 1	1 to 10^{3}
Average time between collisions.	10^{7} to 10^{-10} sec	10^{-10} to 10^{-14} sec

Whilst acknowledging the *probable* likelihood of enhancement of the overall reduction kinetics afforded by solid state plasma, the probable secondary nature of any real contribution to total reduction flux directly attributable to solid state plasma ascribes this topic to a "mention only" status in this thesis. Unless otherwise specified, further references to "plasma" should be understood to mean *gaseous* plasma.

4.5.2: Residence Times in Plasma Processing.

Another essential digression is to identify the fundamental distinction between the processing concepts of "in-flight" and "continuous" plasma processing. In-flight processing, which is normally carried-out in a plasma torch, is characterised by the time-limited nature of the residence of particles in the plasma plume, whose plasma exposure is determined by their in-plasma flight time. That is, residence time within the plasma proper as particles pass through, or from the torch nozzle to the plume (flame) limit. Typically in torch processes, particles are injected with the plasma-forming (ionising) gas into a plasma torch system and are processed during the extremely brief in-flight time as, in the flame, they pass through the continuously changing temperature

profile representing several sets of thermodynamic/kinetic conditions. Residence times for in-flight systems, which are typically measured in milliseconds, are virtually always insufficient being far short of required processing times (even for super-fine powdered reactant particles) whilst thermochemical processing conditions are most likely unsuited or, at least, inefficient (as numerous sets of published experimental data and micrographic evidence bear witness [75, 92, 117, 119, 120, 121, 122, 151]). Some types of arc processing techniques have similarly brief residence times, however, these essentially are not techniques orientated towards ore processing or reduction.

By comparison, continuous plasma processing is carried-out in a contained, standing-wave plasma and therefore is bestowed with the overwhelming processing advantage of *control* over residence time. Because the constrained plasma has a predictable (possibly pre-determined) temperature profile, the reactant materials can be introduced into the appropriate plasma zone, processed to completion, and removed as desired. Alternatively, the desired plasma can be generated around or within the reactants in such a way as to envelop the reactant charge or to occupy a zone discretely within the charge. Control over residence time and greater degree of control over thermochemical parameters ensures a far superior processing or reduction result. Microwave plasma processing is representative of this continuous processing class and is arguably the system offering the greatest degree of control over process variables [80, 99]. Experimental results over a range of ore and mineral reduction operations certainly support this claim.

4.5.3: Plasma Initiation, Maintenance and Stability.

In the laboratory, as in nature, plasmas can be produced by various techniques or initiating processes. The important and more prevalent of these are ionisation by heating (thermal stimulation), ionisation by irradiation, and ionisation by electrical discharge [187, 192, 193]. All substances will become ionised if they are heated to sufficiently high temperatures (above their lowest ionisation energy equivalent) and this process is known as thermal ionisation (as distinct from the unrelated term "thermal plasma"). Ionisation energies of elements reflect their position in the periodic table –

the mono-valent elements of Group **1** alkali metals provide the weakest bound outer electrons with ionisation energies increasing across each period and decreasing down each group. Consequently, alkali metal vapours are often utilised to initiate plasmas. In plasmas that are fully ionised (star cores and magnetically confined fusion plasmas) all electrons are stripped from all orbitals of all atoms of the gas (inevitably a light gas, especially hydrogen, *deuterium*, *tritium* or helium; only light nuclei are stable under these conditions).

Ionisation by irradiation fits into two discrete categories. Firstly, irradiation ionisation is important in astrophysics because the ultraviolet radiation from stars (such as the Sun) causes ionisation in interstellar gases and in the outer layers of the Earth atmosphere. The other category encompasses the irradiation ionisation induced by the adjacent bands of the spectrum of electromagnetic radiation, RF and microwave, and is indirectly fundamental to this project.

In industry, and in the laboratory, the most universally employed method of generating plasma is the gaseous electrical discharge method. Gaseous electrical discharges are commonly observed as electrical sparks and arcs, and in nature the phenomenon is commonly observed in electrical storms as lightning (in various manifestations). Electrical discharge ionisation depends upon the generation (across the plasma-target-gas) of an "electron avalanche" induced by the potential difference between anode and cathode (normally plate or rod electrodes). The necessary presence of electrodes characterises gaseous electrical discharge systems, whilst RF-generated and microwave-generated discharges are often described as electrode-less discharges. Hybrid discharges are often operated where RF generation is augmented by electrode (**dc**) generation.

The plasma of our Earth-bound experience can be described (if somewhat simplistically) as a partially ionised gas consisting of equal numbers of positively and negatively charged particles in a much larger number of non-ionized neutral atoms and/or molecules (~ 1 in 10^3 for glow discharge). More generally, plasma is a mixture of excited atoms and molecules, ions, electrons, photons and "recombined particle"

species in gaseous atoms and/or molecules at "ground state". "Recombined particles" are produced when an atom, molecule or ion recombines with another particle, usually an electron, to form a product that will typically possess energy above ground state for that species. Given the high energies of free electrons, the increased energies of ions, the elevated energies of recombined particles, plus the energies associated with the promotion of electrons to higher orbitals in excited atoms, molecules and ions, the physicochemical behaviour of such a mixture is comparably quite removed from that of the same gaseous matter at ground energy state [58, 193].

A nuclear species is said to be in a state of excitation when a weakly bound electron is promoted to a higher energy orbital by the absorption of the appropriate quantum of energy. This excitation can be achieved by electron impact excitation, photo-excitation, or (in high temperature discharges) by thermal excitation. (Thermal excitation is of greater significance in thermal plasma processing where heavy particle species also have high energy.) The most commonly successful of these excitation events is that provided by free electron impact, although, photo-excitation can be a significant contributor in high-energy photon fields. The excitation of an argon atom by electron impact is written as follows [58].

$$Ar + e^- \Rightarrow Ar^* + e^- \quad \text{..... } \{4.5.3\}1$$

In this case the electron has, by inelastic collision, lost a quantum of energy (kinetic) to the argon atom which now has an electron promoted to a higher orbital (but has **not** lost an electron).

Like excitation, ionisation can be achieved by free electron impact when energy transfer exceeds the species ionisation energy. Electron impact ionisation is fundamental in the sustenance of plasma in that it creates charged particles – a positive ion plus an electron (negative), or a negative ion. The standard ionisation of an argon atom by electron impact is written as follows [58].

$$Ar + e^- \Rightarrow Ar^+ + 2e^- \quad \text{..... } \{4.5.3\}2$$

A more comprehensive list of plasma ionisation and other principal plasma reactions is presented in Table **{4.6}1**. The equations are central to the chemistry of plasma processing.

Collision theory stipulates that both excitation and ionisation represent inelastic collisions in that both the kinetic and internal energies of participating particles change. The energy-depleted but more abundant electrons leaving the above reactions (right hand side of Equations **{4.5}1** and **{4.5}2**) are subsequently accelerated by the prevailing electric field until they produce further excitation or ionisation, or recombine with a heavy particle.

Photons are discrete energy quanta that are released when recombined particles or other excited species give-up energy in dropping back to a lower energy level – which may be ground state energy; and noting that all energy transfers are transacted in well-defined energy quanta which are characteristic to the species and the energy band, or level, at which that particle currently exists (see Lymon, Balmer, Paschen, *et cetera* series). Highly energetic photons provide the impact energy for photo-ionisation which may provide a significant proportion of ionisation in some systems. Thermal ionisation is not significant in "low temperature" plasmas (glow type discharges) but becomes important in "high temperature" thermal plasmas (such as high pressure arc discharges) **[58, 193]**.

The prospect of ionisation by *ion impact* on neutrals (atoms or molecules) in a glow discharge is infinitesimal in the glow region of the discharge but improves its chances of occurrence to negligible in the cathode sheath region of electrode generated discharges and similar in electrode-less discharges such as microwave plasma **[58]**. So, whilst ion impact ionisation can occur, its likelihood remains highly improbable because ion energies are generally low for low-pressure discharges.

Direct current (**dc**) discharge characteristics are described graphically in Figure **{4.5.3}1**. *Townsend* or *dark discharge* is unstable at low current intensities and requires an electric field plus an external source of electrons to persist. As can be seen (in Figure **{4.5.3}1**), potential difference increases with increasing current and, at a critical value, dark discharge spontaneously transforms to *glow discharge*. Glow discharge is stable

over a comparatively wide and useful current intensity range until, at higher current intensities, the potential difference begins again to climb. At a very high, critical current intensity the glow discharge transforms into an *arc discharge* whereupon the potential difference is spontaneously relieved. Further increase in current sees an enhanced propensity to arc – and to sustain the arc – as required voltage decreases [58]. The transformation from glow discharge to arc discharge may represent a shift in the non-equilibrium status of the local thermodynamics operating within a system – such a shift must be recognised.

Of course, the above description is of an electrode-generated discharge producing glow discharge plasma – a system with several essential comparable attributes characteristic of the electrode-less microwave-generated discharge – and arc discharge at higher potential difference.

The generation (initiation) of plasma, and the sustaining of it, is dependent upon a number of probability-based processes involving the interaction of gaseous particles either by the coincidence of collision or by the emission or absorption of radiation. Collisions between particles are either *elastic*, in which there is an exchange of kinetic energy without a change to the total kinetic energy of the particles, or *inelastic*, in which some kinetic energy is transformed into other energy forms. Such energy transformation may result in the excitation of particles, in their ionisation, in the

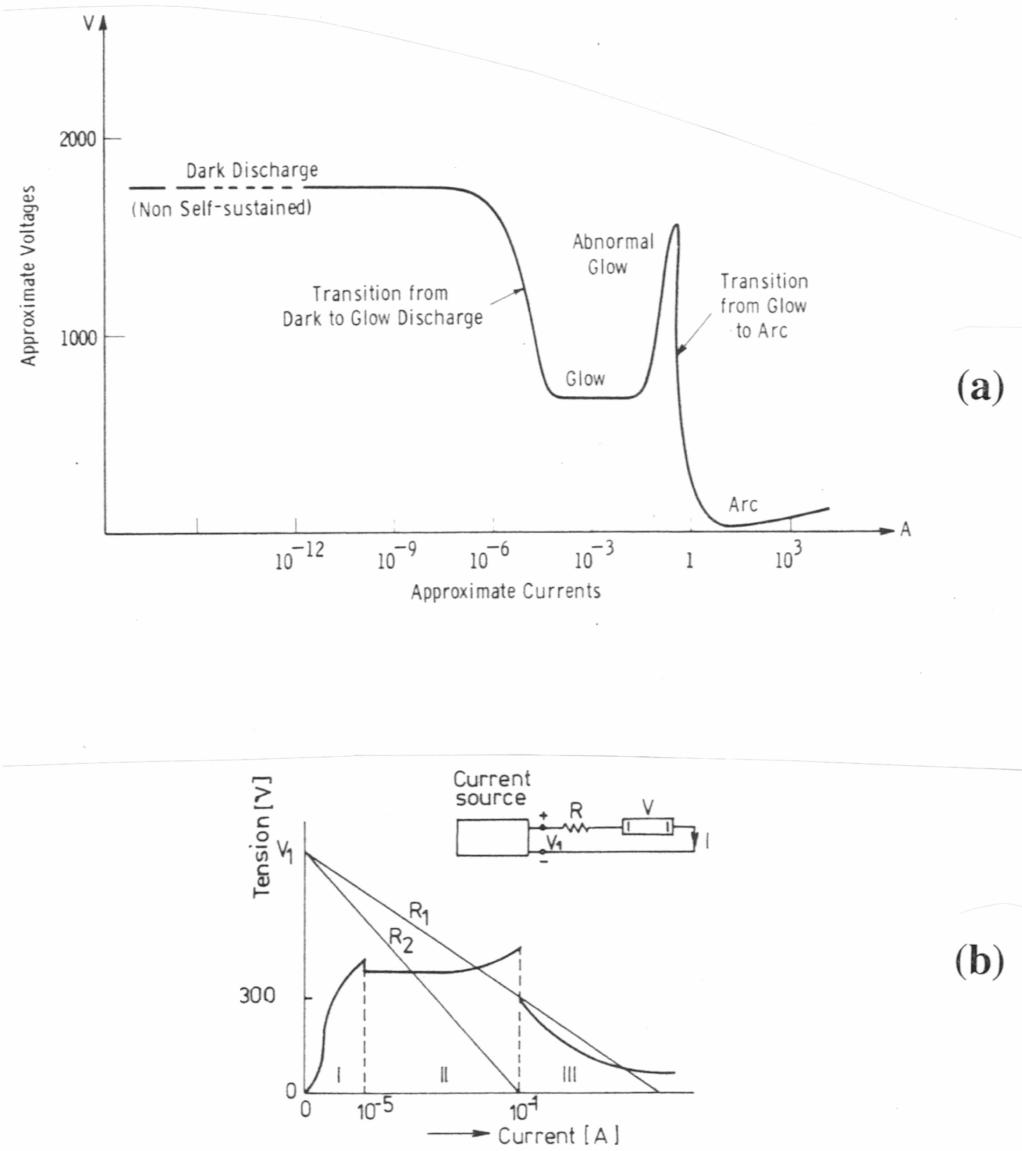

Figure {4.5.3}**1:** Voltage – current characteristics of electrically-induced discharges showing **(a)** approximate voltage versus current characteristics of electrical discharge without tips or edges [195], and **(b)** voltage versus current characteristics of **dc** discharges where: I – dark discharge region, II – glow discharge region, and III – arc discharge region [58].

transfer of their electrical charges, or in the release of photons as energy quanta are satisfied [189].

Ionisation, that is, the separation of an electron from its host atom or molecule, is the most essential of the plasma-forming processes. An atom or molecule can be ionised by the nett input of energy: by the inelastic impact of an electron, an ion, or a neutral atom or molecule, or by the absorption of a photon or similar quantised "energy package". This is achieved in electrode-less systems by absorption of radiation of a suitable wavelength (both microwave and radio frequency are highly suited to the promotion of this outcome). The ionisation of some molecules (such as CO, N_2 and CH_4) produces molecular ions which may, by design, play a prominent role in plasma chemistry, and that they produce composite particles which will draw both rotational and vibrational energies. Under further excitation, molecular ions may dissociate into atomic ions plus neutral particles and so extend ion chemistry beyond the simple Group or valence shift of atomic ions.

Energy changes in system thermochemistry tend to disrupt and divert the system from thermodynamic equilibrium. Plasma discharges, being comprised of charged particles, supplement their energy by absorbing energy from an applied electric field. The electrical energy being continuously converted to kinetic energy of the plasma particles – particularly the free electrons. This is the means by which free electrons replenish their kinetic energy after losing some portion of it (by inelastic collision) to other, heavy particles in the plasma – and (outside of energy supplied by exothermic chemical reactions) it is the regulated means by which the total system energy is increased. The kinetic energy of the accelerated free electrons is rapidly converted into thermal energy by their collisions with the various heavy particle species. The proportion of its kinetic energy an electron will transfer to the heavy particle with which it collides is dependent upon the ratio of the particle masses: $2m_e/m_h$, where m_e is the electron mass and m_h is the mass of the heavy particle [58, 193]. A quasi-equilibrium state is reached in the collision processes when the energy imparted by the applied field to the electrons equals the energy lost by electrons to the heavy particles in inelastic

collisions. Of course, as total energy is continuously increased, the system is in retreat from kinetic equilibrium.

Also, the difference between the free electron temperature and the background gas temperature does not solely depend upon the ratio of the energy absorbed from the electric field by the electron and the base thermal energy of the electron. The temperature difference also varies with the mass ratio of the colliding plasma particles, that is: m_h / m_e [58, 189].

In the (0.3 – 10 GHz) microwave region of the electromagnetic spectrum the magnitude of irradiation wavelengths become comparable to the dimension of the discharge vessel. Typically, microwave fields and their consequent microwave-induced plasmas are produced within a dedicated waveguide section or in a waveguide-fed resonant cavity. The required dimensions of the waveguide and cavity decrease as the microwave frequency increases, and for practicability, microwave frequencies used for discharge applications are preferred at the higher frequency end of the spectrum - the very common domestic, commercial and industrial frequency being 2.45 GHz. Whilst not the highest frequency possible in the microwave band, the nominal 2.45 GHz is especially well suited because water, water-based and organic materials are particularly susceptible to this frequency and consequently heat readily rendering the frequency ideal for domestic, commercial and industrial applications [105]. All allocated microwave-heating frequencies are band-slots in the greater continuum of microwave communications bands. Other (non-allocated) frequencies are only available by rare license arrangement – a hindrance to industry and to legitimate, fundamental scientific research as frequency "tuning" to load susceptibility would be enormously advantageous to peak processing strategies (particularly for continuous tuning to maintain optimum susceptibility in the dielectric load as dielectric properties vary with changing temperature).

At microwave frequencies only the ultra-light charged particles in the ionised field – that is, the electrons – can follow the oscillations of the electric field. This alone is sufficient to establish from theory that microwave plasmas are never in local

thermodynamic equilibrium, and are normally far from local thermodynamic equilibrium (LTE) [80]. Microwave plasmas can be induced and operated over a large pressure range, from below $1x10^{-3}$ atm (~0.1 kPa) to about atmospheric pressure, sustaining "large volume" non-equilibrium plasmas of reasonable homogeneity [80, 189].

In the context of microwave discharge (as with other discharge regimes), the essential mechanisms in the plasma are ionisation followed by recombination such as to maintain a steady state of ion and electron densities, plus excitation and relaxation. To avoid plasma extinction, the recombination process must be balanced by an ionisation process. Thus an external energy source is required. In practice that energy source is conveniently provided by an electric field that will act directly on charged particles.

The work done by a microwave-generated electric field transfers energy to the ions and electrons in that field. As established previously, because the mass of electrons is much, much less than that of ions or atoms or molecules, the action of the field is primarily to give energy to the electrons. The nett result is that electrons have a high average kinetic energy whereas ions, because they absorb little energy from the electric field, have an average kinetic energy only modestly higher than equivalent uncharged (neutral) species. At the risk of over-simplification, essentially the ion temperature remains in the "ambient" range close to the temperature of neutral species (and the "bulk" or measured temperature in the plasma chamber), whilst the electron temperatures accelerate into the extremely high range of tens of thousands of kelvin for low pressure (low density) plasmas. As thermal energy is reflected in the "mass bulk" as temperature, the measured temperature of the mass bulk does not intelligibly reflect the electron temperature in these non-equilibrium plasmas. Of course, in high-density (equilibrium) plasmas, the high frequency of electron collisions limits electron temperatures to a heavy particle temperature equivalent.

It is not possible to heat plasma that is in contact with solid walls or any other substantial solid part of the enclosing chamber (particularly conducting or metallic sub-structure) because of the "heat sink" effect [187]. The containing vessel will not melt as the heat capacity sum of the colliding electrons is too small. However, reaction

chemistry will be greatly affected because particle temperatures are effectively restrained.

In the chemistry of discharge-induced plasmas it is the electrical discharge that provides the energy required to initiate and (where necessary) sustain chemical reactions. In the case of non-equilibrium plasmas this energy is largely, and very often solely, transferred by the electrons [31, 80, 189].

4.5.4: System Equilibrium and Non-Equilibrium in Plasma Processes.

In plasmas not generated by electrical discharge nor irradiation, such as in many large metallurgical operations (blast furnace tuyere plasma injection, for example), the thermochemical characteristics of the plasma environment are most acutely determined by the thermal ionisation mechanism prevailing in the high plasma temperature. The gas pressure in the reactor vessel determines which ionisation regime, equilibrium or non-equilibrium, will be controlling in the reactor. Plasmas stimulated by the thermal ionisation mechanism at reactor pressures above 10^4 Pa* are distinguished by possessing an array of charged particles which conform to the Maxwell-Boltzmann energy distribution and are characterised by a narrow temperature band across charged plasma particles. Such plasmas are said to be in a state of *thermal equilibrium.* Chemical reactions conducted in plasmas at thermal equilibrium obey the general laws of thermodynamics, as do the kinetics describing those reactions [58, 189].

Generally, low-pressure plasmas are sustained by either electrical discharge or irradiation ionisation (or both). However, it is possible to generate low-pressure discharges with thermal ionisation. By comparison with the high pressure plasmas noted above, industrial plasmas stimulated by the thermal ionisation mechanism at reactor pressures lower than 10^4 Pa display significant departures from thermal equilibrium – particularly in that the plasma cannot be described by a single mean

* Note that 1 atm = 760 mmHg = 101 325 Pa or, more simply, atmospheric pressure approximates 10^5 Pa. Under certain conditions, "low pressure" non-equilibrium microwave plasmas persist up to ~ 10^5 Pa [80].

thermodynamic temperature nor by a single temperature profile [58]. This is typical for low-pressure plasmas generally. Electron temperatures are much higher than the temperatures of much heavier particles in plasmas at these pressures. Such systems are said to be in *thermal non-equilibrium*. As the plasma cannot be described by a single thermodynamic temperature, chemical reactions conducted in such a plasma cannot easily be described by the general laws of thermodynamics [189]. In fact, such plasmas *appear* to blatantly disobey the laws of thermodynamics. (An observation that was repeatedly noted early in experimental work of this project was that reactions utilising microwave plasmas appeared to disregard the laws of thermodynamics. Such a tempting notion, apparently repeatably "confirmed" by experiment, had to be assiduously resisted. Several authors [86, 97, 100, 101, 181, 194] also allude to having considered this notion and many report well-known reactions as "apparently" occurring at "lower temperatures than predicted by the literature". However, it is comforting to realise, in hindsight, that the observed effect was real, has been observed by others, and can be explained by a more rigorous and "legitimate" application of thermodynamics.) Not only has temperature (representing sensible bulk thermal energy) been regarded as total energy and therefore predictive of equilibrium thermodynamics, but where $T_{electrons} >> T_{ions} \approx T_{neutrals}$, there is scope for various chemistries to be operating concurrently in the same material bulk.

The kinetics of reactions in plasmas under thermal non-equilibrium depart from the Arrhenius equation which holds only for the kinetics prevailing in thermal equilibrium (equilibrium thermodynamics). DEMBOVSKY [58] suggests that, in this non-equilibrium mixture, electrons, ions, atoms and molecular fragments are excited to different relevant electron, vibrational and rotational quantum levels. He postulates that component energies of each compound particle exhibits its own distinct vibrational "temperature" and rotational "temperature" and that these temperatures should coincide (as they will with the bulk temperature) at thermal equilibrium. This proposal is generally accepted in later literature as the accurate model for non-equilibrium plasma thermochemistry.

Section 4

In the plasma processing of materials, low-pressure (or cold) plasmas are utilised in industry for chemical processing and surface modification operations such as plasma etching and plasma deposition processes. The processing effectiveness of low pressure, non-equilibrium plasmas is imbued by the reactivity of the chemically active species present rather than by the total energy available in the plasma. In contrast, because of their high-energy densities (thermal mass), thermal or equilibrium plasmas are commonly utilised in materials processing for their capability to heat, sinter, melt or vaporise solid particulate materials [80]. Thermal plasmas are also used to *thermodynamically stimulate* chemical synthesis reactions. In such processes reactions are initiated by the provision of thermal energy (heat) to stimulate the chemical thermodynamics of the reaction rather than by the provision of chemically active species to stimulate the (chemistry of the) reaction. Same outcome, essentially different means! As a generalisation, non-equilibrium plasmas are used in the *chemical processing* of materials whilst equilibrium plasmas are used in the *physical processing* (of properties) of materials [58, 80, 90, 92].

As has already been identified, plasma consists of a mixture of electrons, ions, excited and fragmented species, other charged particles and neutral species existing in local electrical neutrality. In contrast to the uncharged, ground-state gas, the free electric charges in the plasma-state gas allow high electrical conductivities which can approach those of metals [80]. Plasmas produced by electrical discharge (such as microwave generated plasmas) are classified into the categories of equilibrium or thermal plasmas – which exist above one atmosphere pressure – and non-equilibrium or cold plasmas – which persist only at low pressures.

Thermal or equilibrium plasmas are characterised by their high energy density (incorporating high "thermal mass") and by the relative parity of the electron temperatures (T_e) and the heavy-particle temperatures (T_h). That is, $T_e = T_h$ ideally, but for "real" thermal plasmas, $T_e \approx T_h$. (Heavy particles include ionised particles (ions) plus recombined and neutral particle species.) In such cases the thermodynamic state of the plasma is said to be in equilibrium, or given the temperature profile across the plasma section, the plasma is more realistically and more accurately regarded as being

in local thermodynamic equilibrium (LTE). Whilst LTE implies both kinetic and chemical equilibrium throughout the plasma, local deviations in LTE must exist in thermal plasmas whereby conditions are met in accommodating the steep temperature gradients which so essentially exist across any plasma profile [90].

Non-equilibrium plasmas are characterised by their significantly lower energy densities (compared to thermal plasmas) and by the conspicuous difference between electron temperatures and heavy particle temperatures – with electron temperatures being orders of magnitude greater than temperatures of the various heavy particle species ($T_e >> T_h$). These high electron temperatures (typically of the order of several electron volts (eV) or 10^4 to 10^6 K) represent low electron and particle densities (less than 10^{20} m^{-3}). By contrast, equilibrium plasmas have relatively high electron and particle densities (10^{23} – 10^{28} m^{-3}) and low electron energies which represent electron temperatures in the range 0.1 to 2 eV (where each electron volt is equivalent to a temperature interval of approximately 11,600 K) and being close to heavy particle temperatures [58, 76, 80, 90, 178, 189]). A comparison of the relative characteristics of equilibrium and non-equilibrium plasmas is presented in Figure **{4.5.4}1 (b)** and Figure **{4.5.4}2**.

In the reduction operations of this project, the first ionisation phenomenon to appear in all arrangements of experimental heterogeneous loads under microwave irradiation from very low vacuum to atmospheric pressure was the phenomenon of "micro-arcing". It was assumed that these very small, short-lived "micro-arcs" were typical low-pressure arc events displaying pseudo thermal equilibrium. Moreover, the observed micro-arc discharges displayed the typical thermal plasma characteristic of delivering thermal energy to their immediate region at a rate that ensured rapid heating. Micro-arc events are the energetic culmination of local thermal runaway heating phenomena in conductive and dielectric load-components where conductive pathways

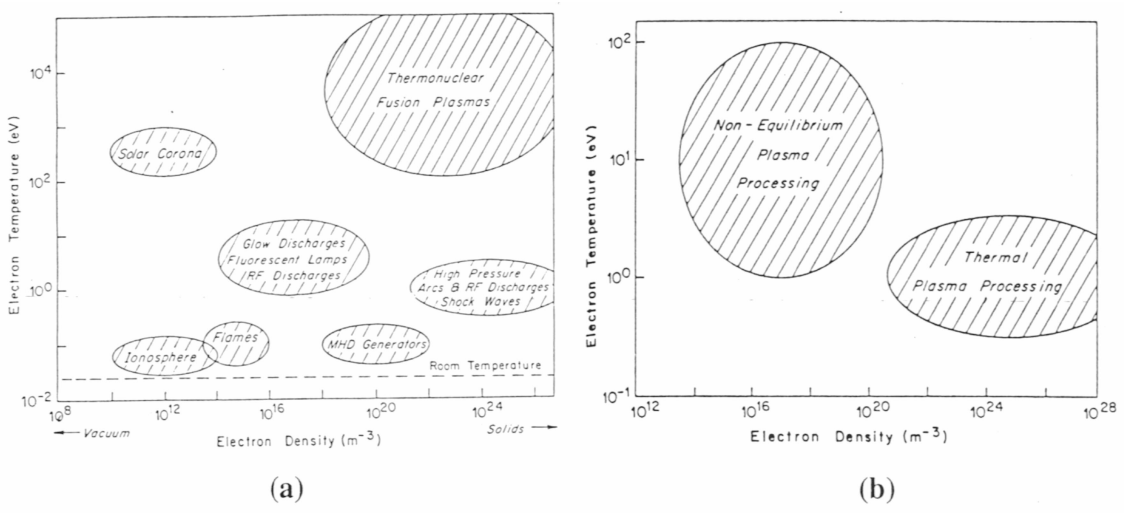

Figure {4.5.4}**1:** Typical ranges of plasmas defined by electron temperature versus electron density fields indicating **(a)** the classification distribution of natural and man-made plasmas [72], and **(b)** the typical ranges of operation for industrial and domestic application of thermal (equilibrium) and non-equilibrium plasmas [90].

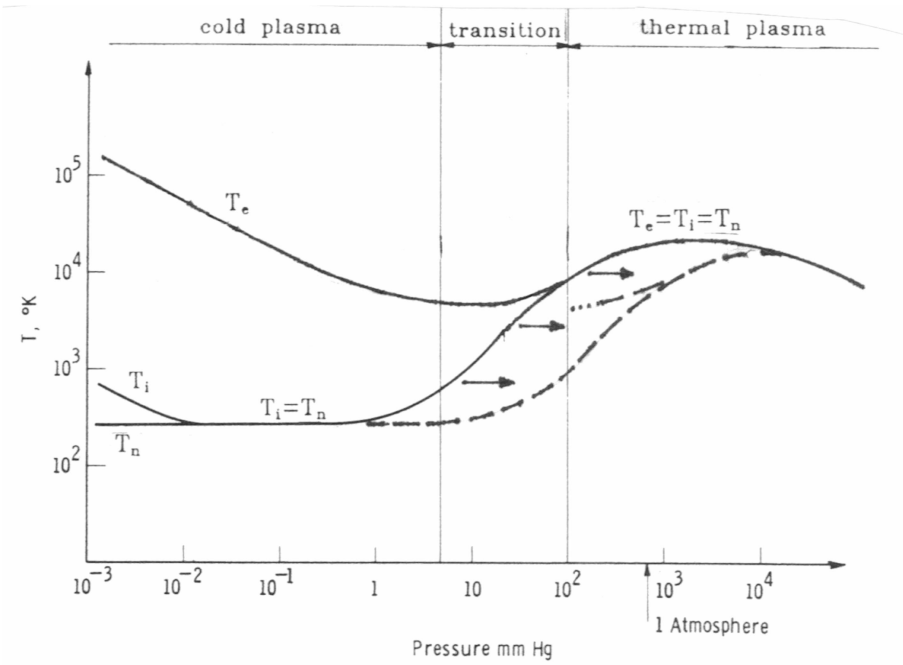

Figure {4.5.4}**2:** Diagram showing the separation of electron temperatures, and ion from other heavy particle temperatures at low system pressures (after Figure {4.4}**1**) and indicating the evident extension of this "separation" as non-equilibrium conditions shift to the right into the atmospheric pressure range for microwave-stimulated plasmas [58, 71, 72, 80, 117]. [T_e – electron temperature(s), T_i – ion temperature(s), T_o – neutral and other heavy particle temperature(s); cold plasma – non-equilibrium plasma, thermal plasma – equilibrium plasma, and atm pressure $\approx 10^2$ kPa $< 10^3$ mm Hg, and temperature in kelvin, K.]

are formed through heterogeneous (granular) materials [105]. This predictable feature was utilised always as the initial means of heating the reactants to a temperature at which chemical reaction was stimulated, especially the generation of atmospheric CO – process reaction that, in turn, provided exothermic stimulation to further progress the desired reaction route. However, there exists here a theoretical conundrum around the "thermal equilibrium" nature of non-equilibrium, low-pressure arc-type plasmas. The subject of "low pressure arcs" is avoided in the literature relevant to this project – normally totally unmentioned, let alone conceded or discussed. (Along with the discharge regime transposition between "full thermal equilibrium" and "local thermal equilibrium") low pressure arcing is incompletely understood and one of the least agreed-upon plasma topics; Hoyaux [195], however, gives good insight into the phenomenon of micro-arcing.

Micro-arcs provide the initial heating (*via* dielectric mechanisms) and stimulate the initial chemistry within the microwave load or charge. In experimental work it was not ascertained when or whether micro-arcs finally give way to glow-type plasma discharge before the final melting of solid phases extinguished the micro-arcs. It was always observed that micro-arc discharges persisted after the initiation of the gas phase glow-type discharge (which the arcs were undoubtedly instrumental in initiating), however, the duration of this "persistence" was lost in the rapidly increasing intensity of the visible radiation of volumetric plasma (towards and through white heat). Also, for reasons of practicability, direct "line-of-sight" observations into "mobile" reaction zones through heavily insulated apparatus was not possible and, further, was deemed unnecessary with respect to reduction outcome.

By convention, arc discharges are defined in terms of voltage drop versus current. Shown in earlier Figure **{4.5.3}1** was a typical voltage versus current plot for an unspecified electrode-initiated discharge. The characteristic domains correspond to the dark or Townsend discharge, the glow discharge and the arc discharge. These characteristic domains, separated by their discharge transitions, remain remarkably recognisable through variations to specified conditions [58, 189, 195]. However, voltage drop and current tell little about the prevailing thermodynamics in the discharge.

The density of the discharge medium and the medium (or matter) itself, which control such critical parameters as the "mean free path" of ionised particles and electrons in the applied field, is crucial in determining the thermochemistry of the discharge. For gaseous plasmas, density is tantamount to (gas) pressure. As has elsewhere been discussed, the gas pressure in which the discharge has been generated predominantly determines the equilibrium or non-equilibrium status of the system thermodynamics, kinetics and related chemistry. Other factors which arise from the chemical species and irradiation field type collectively play a role of varying significance – and, as it happens, a prominent role for microwave-stimulated plasmas [80, 195].

For gaseous plasmas, the determining difference between low-pressure and high-pressure discharges is the length of the mean free path of free electrons that equates to a measure of the acquired kinetic energy of the electrons. The increase in mean free path with decreasing system pressure enables free electrons in low-pressure plasma to acquire a mean energy greatly in excess of the mean random kinetic energy of the heavy particle species [195]. Particle temperatures are kinetically defined by the following equation.

$$^3/_2kT = {}^1/_2mC^2 \quad \text{..... } \{4.5.4\}1,$$

where k is the Boltzmann constant, T the temperature of the relevant particle species, m the relevant mass, and C the root mean square velocity.

In high-pressure discharges (including arcs) the plasma is characterised by the temperature equivalence (to within a few percent of difference) of all of the particle species (including electrons) [193, 195]. Consequently, ignoring heat fluxes associated with temperature gradients, at each point in the plasma there can be defined a unique temperature - and the system is said to display local thermal equilibrium [195].

In low-pressure discharges (including arcs) the large mean free path of free electrons ensures that they attract a large proportion of the available energy from the applied field. This is not the case for the slow heavy particle species that (even disregarding particle mass non-equivalences) attract significantly less energy from the

applied field. The highly energised electrons lose relatively little energy to heavy particles in elastic collisions, considerably more in the less frequent inelastic collisions, and a nett imbalance between electron and heavy particle energies exists – increasing with decreasing pressure. Whereas, by comparison, the exchange of energy between heavy particles is highly efficient thus maintaining the equi-partition of energy between ions and neutrals and ensuring temperature equivalence down to very low pressures where the mean free path for ions becomes large enough to overcome the energy transferred in the decreasing number of ion-heavy collisions.

The conventionally utilised low-pressure microwave-stimulated plasmas are non-stationary glow-type homogeneous discharges that, in the case of restricted (lower) power generation (as in this project), operate as non-equilibrium plasmas up to pressures approaching atmospheric [80]. Also, effectively, in gas mixtures (such as air) not all gas fractions are ionisation participants (until the available energy *per capita* from the imposed field equals the ionisation energy of the most stable species). This suggests a possible partial role or link between the concept of partial pressures and the generation of non-equilibrium discharge.

There is a genuine lack of published information (certainly of that provided in "plain" English) about the upper limit region of the electron temperature – heavy particle temperature ($T_e - T_h$) separation in the particle temperature versus pressure diagram for microwave discharges (see general separation of temperatures diagram of Figure {**4.5.4**}**2**). Consequently, the precise field boundary between equilibrium and non-equilibrium thermodynamics is not available for microwave discharges – likely because theoretical work in this field has not been experimentally determined and validated. However, various prominent authors – experts in the applied science of plasmas – have proffered informed and useful comment (as follows) about the likely extension of the non-equilibrium field up to atmospheric pressure for microwave plasma.

ELIASSON and KOGELSCHATZ [80] state that (for low temperature plasmas) "it is possible to have transient non-equilibrium discharges" at higher pressures "since it takes a certain time or a certain number of collisions to establish equilibrium between

electrons and heavy particles". This is particularly true for non-stationary, pulsed discharges such as microwave and RF. Furthermore, in systems comprised of heterogeneous mixtures such as those that constitute the experimental materials of this project, equilibrium may not be attainable (HELIODORE, *et al* [95]; EVES and SNIDER [97]; and SCHULTZ [196]).

For the common low temperature, non-equilibrium discharges – glow discharge, corona discharge, silent discharge, RF discharge and microwave discharge – only the microwave discharge can be efficiently operated at pressures approaching atmospheric pressure whilst remaining in the non-equilibrium state. The reasons for this are further elucidated in the following paragraphs.

Glow discharges (**dc** and **ac**) only operate in low-pressure regions up to 1 kPa (or 0.01 atmosphere). Whilst corona and silent discharges are more stable at very low operating pressures, they can operate up to atmospheric pressure [84]. However, glow, corona and silent discharges are stationary discharges and are increasingly *inclined away from non-equilibrium* at higher pressures as atmospheric pressure is approached. Glow, corona and silent discharges are electrode-derived discharges, unlike pulsed discharges. And, it is the pulsed, electrode-less discharges that have the propensity to more greatly stimulate free electrons (thus extending the non-equilibrium range) [83]. Significantly, it is in the higher frequency microwave range that the light free electrons can follow the oscillations of the microwave electric field (as discussed elsewhere) [80, 83] – oscillations that are small enough to be contained within the confining dimensions of the discharge vessel or reactor and, in turn, support non-equilibrium. This microwave characteristic is <u>*not*</u> shared by the lower, radio frequencies (RF) which consequently do not accumulate such high levels of energy in electrons but lose it more frequently to containing walls and, particularly at higher particle densities toward atmospheric pressure, to other particles [178]. And so, with increasing pressure, RF discharges are less inclined (than microwave) towards non-equilibrium.

Under microwave irradiation, when the applied field direction changes (reverses), the direction of the force on the electron changes. Consequently, at microwave frequencies, when changes in the field direction are cycled and because the electron can still follow the field reversals at microwave frequencies, the electron will

oscillate. Where the chamber design is empathic with physical parameters of the microwave frequency, the free electron will oscillate *within* the volume of the reactor-confined discharge [80, 83]. For frequencies lower than microwave, the reversal of direction of the accelerated electron does not (realistically) take place within the physical constraints of the discharge chamber or reactor. Such low-frequency-excited free electrons too frequently lose energy to the chamber walls (as well as to heavy particles), whereas comparably, microwave-frequency-excited electrons lose only a small proportion to chamber walls and more to heavy particles thus promoting ionisation and other stimulation mechanisms. Hence, microwave discharges can operate under non-equilibrium conditions up to greater particle densities – or *higher pressures* – than lower frequency discharges. This is the essential characteristic that distinguishes microwave discharges from lower frequency RF and **dc** discharges [80]. And, this is the characteristic feature of microwave frequencies that enable them to generate non-equilibrium ($T_e >> T_h$) plasmas at higher system pressures than RF discharges and other, electrode-generated plasmas.

In essence, discharges initiated by microwave or high frequency fields differ significantly from **dc** or low frequency discharges [81]. Amongst others, these differences include the fundamentals of discharge initiation and maintenance. There are a large number of independent variables required (by theory) to describe gaseous electronic phenomena including the interaction of the applied field with electrons, ions and the array of other particle species, the containing walls, ionisation potential of the gas(es), electron density, collision dynamics in the discharge, field frequency, reaction vessel dimensions and geometry, *et cetera* [82, 83]. The set of variables is greater for high frequency microwave breakdown than for **dc** and other low frequency discharge breakdown. In fact, by way of explanation [83], (for typical constant wavelength cases) the required number of dimensionless proper variables for low frequency systems can be reduced to two and can therefore be represented in two dimensions – that is, an area plot – whereas, for microwave frequencies, a three dimensional space would be required to represent all variables. So, in short, microwave (high frequency) discharge systems are more difficult to model and it follows that (theory-based) predictions are less available in the literature.

In plasma generation and maintenance, energy (or power) from the applied electrical field is most efficiently coupled to free plasma electrons in low-pressure discharges. In contrast, the transfer of energy from electrons to heavy species by collisions is comparably inefficient [178]. The electron energy distribution is generally (Maxwell-Boltzmann)-ian with proportionate distortions to the curve's "bell" depending upon the degree of separation from equilibrium displayed by the discharge. Also depending upon the state of equilibrium in the system, plus the type of discharge generation, the four types of electron heating mechanisms: ohmic heating, stochastic heating, resonant wave-particle interaction heating, and secondary electron emission heating. Although it is present in all discharge categories, ohmic heating is the heating mechanism of importance for low-pressure microwave plasmas. Ohmic heating arises from the transfer of kinetic energy, acquired by electrons during their acceleration in the applied electrical field, to heavy species in electron/heavy particle collisions – the transferred energy reporting as thermal energy, or heat [178, 189].

Each chemical species in the ionising gas ("pure" or mixture) possesses a characteristic collisional-energy loss which arises from electron collision with the species and is crucial to plasma generation and maintenance dynamics. Whilst they have a higher ionisation energy requirement, monatomic gases such as argon and the other noble gases, have a collisional-energy loss considerably lower than the molecular gases whose additional collisional-energy losses include the excitation of vibrational and rotational energy levels, molecular dissociation, and negative ion formation (in electronegative species). The most pertinent outcome of this quite intuitive thermodynamic requirement is that, for the same resultant electron temperature, different species will require a different kinetic input [178]. Molecular gases such as CO, CH_4 and N_2 may commonly be present as reactant or product gas components in plasma processing operations.

In respect of the microwave processes of this project, one simple, fundamental characteristic of microwave plasma-generation is worth repeating. In practice, when a microwave field is applied across a gas, charged particles in that gas are accelerated. Because of the difference in magnitude of their masses, electrons are affected to a far

greater degree than the heavy particle species and are duly accelerated at a rate representatively proportional to the inverse of the mass difference ratio of electrons to heavy particles. (Recalling from earlier passages that, unlike the heavy particles, the light electrons can follow the oscillations of the microwave field – continuing to build-up energy from the applied field between collisions.) Thus, energy transfer from the applied field to the free electrons is proportionally greater than that to heavy particles (ions) to such a magnitude that the contribution of energy transferred to ions and other heavy particles can be disregarded (which it invariably is in the literature of plasma processing).

4.5.5: Discharge-Catalysed Reactions and Ionisation Chemistry.

Described in preceding passages were phenomena encountered in low-pressure plasma created by electrical discharge in gases with pressures ranging from low to atmospheric. These processes involved the excitation or ionisation of particle species and the subsequent interactions of product electrons, ions and excited particles with each other and with the neutral species. The affiliated reactions involving these reactive, energetic species comprise one category of processes. The other category of elementary processes reflected in plasma metallurgy includes those reactions involving "neutral" participants. This category of reactions is further identified by the transfer of vibrational energies that takes place in reactions notable in that they maintain a close identity with the "conventional chemistry" associated with their species. The following equations are representative of this second category [58].

$$AB \Rightarrow A + B \quad \text{.....} \quad \{4.5.5\}3$$

$$AB + C \Rightarrow A + BC \quad \text{.....} \quad \{4.5.5\}4$$

$$A + A + B \Rightarrow A_2 + B \quad \text{.....} \quad \{4.5.5\}5$$

The first of these, Equation **{4.5.5}3**, is a general equation representing chemical dissociation. When, in Equation **{4.5.5}3**, the dissociation involves the decomposition by

heating of a solid to produce both a solid plus a gaseous product then the process is more commonly called thermal decomposition. So equation **{4.5.5}3** might usefully be re-written as follows.

$$AB_{(s)} \Rightarrow A_{(s)} + B_{(g)} \text{ ..... } \textbf{\{4.5.5\}3a}$$

Thermal decomposition reactions are always endothermic, and therefore proceed more readily with increasing temperature [58]. They also invariably involve the expansion of the system volume or pressure, so that a concurrent reduction in pressure, or partial pressures, will maintain and/or intensify the shift in equilibrium in favour of the reaction products. Techniques involving microwave processing are particularly well suited to thermal decomposition operations [83, 86, 105]. Many economically important extractive metallurgical operations (and others which would become economically important) could be re-designed to utilise the capital and technical economies of microwave-stimulated thermal decomposition (or disproportionation, as the industrial process is commonly called). An obvious example would be the thermal decomposition of metal halides to yield metal plus gas – each of good to high purity.

Element transfer and recombination reactions shown respectively as Equations **{4.5.5}4** and **{4.5.5}5** are neutral recombination reactions – comparable (reverse) reactions to the thermal decomposition reactions. They also have relevance to many commercial operations that are currently carried-out under more conventional chemistries.

Process conditions in the microwave-stimulated reactor determine the type of plasma discharge that will prevail in the reaction zones. The discharge type that will arise is dependent upon pressure and the dielectric excitation in the load with respect to process conditions and the current-voltage characteristics of the discharge itself [58]. Electrode-derived arc discharges occur at relatively low voltage but very high current intensities and are usually operated in high-pressure environments. Similarly, microwave micro-arcing between charged load granules occurs at low potential differences and, relatively, at very high induced current intensity. This micro-arcing

phenomenon acts to rapidly increase temperature in the granular reactant load and is pervasive in the granular, dielectrically heterogeneous loads typical of this project. Because micro-arcing was observed consistently (with no apparent shift nor variation between regimes) from low pressure up to atmospheric pressure, it could be inferred that it is a low pressure phenomenon whose stability extends to atmospheric pressure. Alternatively (and in keeping with theory), there exists a transition between low pressure arcing and arcing at atmospheric (high) pressure – with the implicit changes to system equilibrium and perceived temperature which such a shift entails – but with no observed variation in appearance nor apparent rate of heating (which, it must be conceded, remained un-measured). The phenomenon is described more completely in later sections.

The other obvious plasma form present in microwave processing is analogous to glow discharge. Such a low-pressure discharge may be a complex environment involving both physical and chemical aspects of process reaction. Not only do plasmas consist (in part) of physically energetic electrons and ions but these ions may behave as chemically active species. Species can completely change their chemical nature upon becoming ionised. The chemistry of the diffuse, glow-type discharge is more pervasive through a (heterogeneous) charge load than is the arc-type discharge. This and the subsequent particle species interactions is the basis of *ionisation chemistry* or *plasma chemistry*. Consider the earlier Equation **{4.5.3}2** the electron impact ionisation of atomic argon – a noble gas (here reproduced and re-numbered).

$$Ar + e^- \Rightarrow Ar^+ + 2e^- \quad \text{..... } \{4.5.5\}6$$

Whilst the argon atom has a closed outer shell configuration its ion, Ar^+, now has the electronic configuration of atomic chlorine and, despite the fact that it retains the one more neutron/proton pair than chlorine, may behave chemically with comparably high activity under certain conditions [58, 189]. Similarly, the other noble Group **18** gases can each be promoted to chemical activity comparable with their Group **17** halogen neighbour. The implications of this notion need (at least) to be stated. The first implied possibility of the existence of highly active positive ions of noble gases and ensuing plasma chemistry is the obligatory extension to product compounds, that is, to metal "argides", "helides", *et cetera*. Whilst such compounds are feasible [181], no un-

identified phases of this project were "explained away" into this ethereal category. The second possibility is that, in their persistent compulsion to return to a highly stable noble monatomic state, "noble" ions may strip the required electrons from less stable, "non-noble" elements reducing the latter to negative or positive ions – so providing a *catalytic* effect in the overall plasma chemistry. The third and most likely possibility is that, in the nano-timescale of ionisation events, the newly ionised "noble" ions immediately recombine with free electrons to form noble recombination products such as is shown below where the monatomic product is a gas above ground state energy.

$$Ar^{+} + e^{-} \Rightarrow Ar^{*} \quad \text{.....} \quad \{4.5.5\}7$$

4.6: Chemical Reactions in Non-Equilibrium Plasmas.

A characteristic feature of plasma processing which has important implications in plasma-stimulated chemical synthesis reactions is that, because energy is supplied to the system by means of electrical coupling rather than by conventional combustion within the system, independent and isolated system-control over input energy, reactant species and reaction chemistry is achievable. The specific enthalpies of gaseous species in plasma vary depending upon whether the gas is monatomic, molecular or a mixture. Because of the molecular dissociation step, plasmas of molecular gases have (relatively) a higher specific enthalpy and a more complex array of participating particles than do plasmas of monatomic gases [80, 178]. Thus, the reactions of plasma chemistry proceed in environments having very high temperatures (energies), a mixture of reactive species having higher specific enthalpies and higher thermal conductivities than those of comparable conventional systems, and heating and quenching rates in reactant species up to the order of 10^{7} Ks^{-1} [90]. The very high reactivities of participating species and the stimulated reaction kinetics of chemical systems under plasma excitation ensure dynamic chemistry – new reactions, new reaction routes, new reaction products – often quite dissimilar to the chemistry of parallel conventional systems. The complexity of participating species co-existing in discharges can be seen in Figure {4.6}1 and {4.6}2.

Section 4

Within the pressure range and temperature regimes characteristic of low-temperature plasma processes, chemical reactions proceed under either quasi-equilibrium or non-equilibrium thermodynamics. Quasi-equilibrium conditions apply in systems where low-temperature plasma is discharge-induced at pressures close to atmospheric pressure and above $\sim 10^4$ Pa. In such cases there is minor variation in the temperatures of the various component particles (including neutrals) in the plasma. Systems which posses such minor temperature profiles across component particles could be described as "approximately isothermal" and the system's thermodynamics is described as being in quasi-equilibrium [58], that is, above the pressure range where

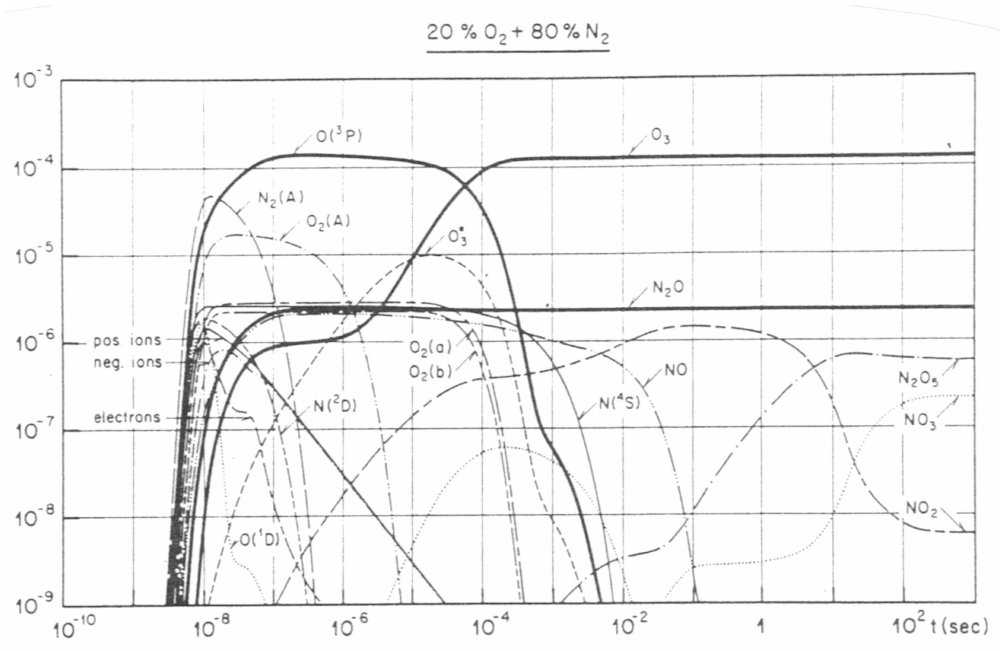

Figure {4.6}1: The generation sequence and species density with time showing the complexity and transient nature of species in a micro-discharge induced in an "air" mixture of 20% oxygen – 80% nitrogen [80].

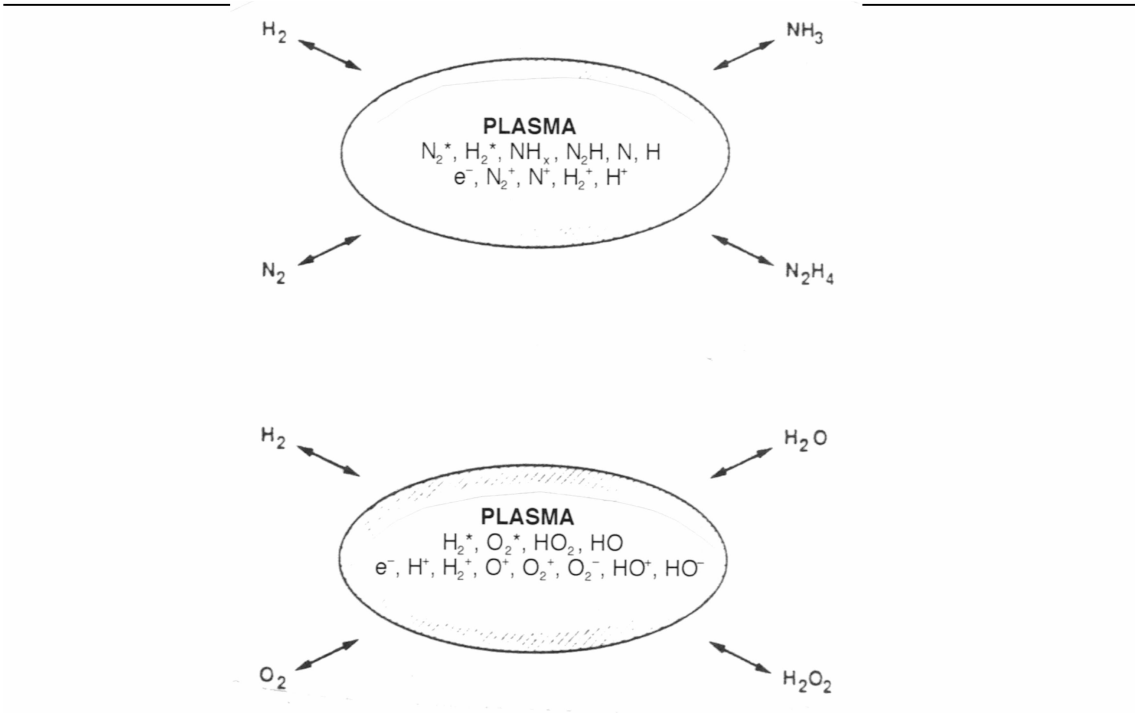

Figure {4.6}2: Schematic representation showing the complexity of transient species possibilities existing in plasma generated in a hydrogen – nitrogen mixture (top) and a hydrogen – oxygen mixture (bottom) [80].

$T_e >> T_h$ and, as it approaches local thermal equilibrium, at $T_e \approx T_h$. (In systems under *microwave* irradiation at "quasi-equilibrium pressures", this quasi-equilibrium is quickly driven into thermodynamic non-equilibrium by the capture and stimulation of free electrons by the applied field.)

In general cases of quasi-equilibrium, elementary processes are typified by reactions that involve the transfer of vibrational energies, and that primarily involve the participation of electrically neutral particle species. Fundamental chemical equations which typify quasi-equilibrium reactions include the three groups representing dissociation, element transfer and recombination given (respectively) as Equations **{4.5.5}3**, **{4.5.5}4** and **{4.5.5}5** in an earlier section.

Quasi-equilibrium plasma reactions are affected by the presence of excited particles with their attendant individual thermodynamic properties. These excited particles impose a catalytic effect upon quasi-equilibrium plasma reaction rates. The degree of catalysis is not only dependent upon the basic chemistry but is largely dependent upon the degree of ionisation in the plasma and the magnitude of departure from isothermal conditions of the excited and ionised particles, that is, the temperature difference between free electrons, other heavier excited and ionised particles, and neutral particles in the plasma.

Beyond some point in the thermal dynamics of quasi-equilibrium systems, with decreasing density, Maxwell-Boltzmann predictability breaks down and the system shifts into non-equilibrium thermodynamics. For low-temperature plasmas this point of transition is commonly associated with, and is most easily described in terms of, a decrease in system pressure.

As system pressure decreases in a low-temperature plasma the further the system departs from isothermal and there is an increasing frequency of reactions controlled by elementary processes which involve excited electrons and excited and ionised heavy particles or, more specifically, the interactions between these particles and other excited, ionised or neutral particles. With decreasing pressure, the temperature difference between particle species becomes more marked (as described elsewhere) and, in particular, free electrons attain much higher temperatures (by orders

of magnitude) than the heavier particles. As a consequence of their much higher particle energies, a correspondingly higher proportion of reactions involve free electrons as suppliers of activation energy. To a lesser extent this is true also for the other excited and ionised particles whose greater masses, despite complimentarily elevated particle energies, ensure only a comparatively modest temperature increment above the temperature of the background neutral atoms and molecules. Consequently, as this particle energy disparity increases, elementary processes controlled by thermal quasi-equilibrium are increasingly joined and supplanted by elementary processes devoid of thermal equilibrium. Accordingly, thermodynamic non-equilibrium is characteristic of low-pressure, low-temperature plasma processes [189] – with or without microwave-stimulation, but "arriving" at non-equilibrium far more directly under such irradiation.

As for equilibrium systems, particle energies in thermal quasi-equilibrium systems exhibit a Maxwell-Boltzmann distribution. For the translational motion of particles in chemical reactions under quasi-equilibrium, the activation energy, E_{act} , exceeds the mean energy, kT. By definition, chemical reactions are processes out of thermal equilibrium but moving toward thermal equilibrium with the progress of the reaction. Inherently, whilst E_{act} remains greater than kT, the equilibrium distribution of particle energies in the plasma remains substantially unaffected. Hence, the reactions of quasi-equilibrium plasma chemistry can be adequately described in terms of the general laws of (equilibrium) thermodynamic theory and chemical kinetics.

By comparison, in non-equilibrium processes where chemical reactions proceed under conditions devoid of any thermal equilibrium, the translational, rotational and vibrational energies of the plasma particles differ widely between particle species and vary between similar particles. Consequently, apart from neutrals, the different plasma components – free electrons, other excited particles, ions, and decomposed fragments, each with its own range of particle energy possibilities – and, subject to particle complexity, can be said to possess their own translational temperatures, rotational temperatures and vibrational temperatures [58, 117, 178]. Obviously, such a complex distribution of temperature ranges has its complimentary number of Maxwell-Boltzmann distributions of particle energies. So we can no longer apply simply the general classical concepts of equilibrium thermodynamics, nor the Arrhenius equation,

nor any other of the general relationships founded upon equilibrium thermodynamics and/or statistical mechanics.

Deviations from the equilibrium state where the Arrhenius equation holds true become more pronounced with increasing reaction rate and as kT approaches E_{act}. At the point where kT is equivalent to E_{act}, the kinetic disposition of chemical reactions cannot be predicted by the Arrhenius equation and such chemical processes can only be thermodynamically categorised as non-equilibrium processes [58]. Knowledge of complex inter-related sets of data would be needed in order to thermodynamically describe chemical processes proceeding under such non-equilibrium conditions. We would need to know the distributions of reactant and product particle species participating in the reaction and their Maxwell-Boltzmann inter-relationships, their effective cross-sections for the various reaction type possibilities, the inter-dependent relativities of particle motion energies and their effect upon distribution cross-sections, and how (with respect to each other) these inter-related factors and distributions alter with time. Such a description set quickly becomes exceedingly complex – even in statistical thermodynamic terms [58, 76, 193]. Constantly varying chemical outcome possibilities make it impracticable to pursue description as a routine operation, and for typical non-equilibrium plasma chemistry, process description in thermodynamic or kinetic terms may well be a practical "impossibility" – although, statistical thermodynamics practitioners may choose to differ! Some empirical system outside thermal physics (thermodynamics) and kinetics may be required to "practicably" describe "Earthbound" non-equilibrium plasma events – physical and chemical – a system based, like thermodynamics, itself, upon the long-term results of collected data from assiduously observed experimental outcomes [185, 189].

In extractive metallurgy endeavours and related fields of industrial application, plasmas have principally been used as high enthalpy heat sources – heat sources capable of generating gas-phase temperatures of 3,000 K to 6,000 K consequently delivering high thermal energy to entrained solid or liquid particles, or to underlying molten phases in reaction vessels, or into packed beds as in blast furnace tuyere injection. Such plasmas are thermal or equilibrium plasmas and, recounting for

emphasis, their primary function is to raise the sensible temperature of the reactants until their chemical potential is pushed far enough into the negative so as to ensure rapid reaction rates [58, 117]. Steadily receiving more industrial attention is the alternative procedural strategy for enhancing chemical kinetics in which non-equilibrium low-pressure plasma is utilised to generate highly reactive particle species from the reactant components and, within the designated reaction zone, confine the non-stimulated with the stimulated species within the plasma.

Whilst much of this subject matter was addressed in the previous section, there are aspects of low-pressure plasmas that must be recounted here because they are central in any understanding of the enhanced standing of chemical reactions in so-called "cold" plasmas. Specifically (for microwave plasmas), upon their discharge ignition, the applied field generates free electrons, ions and free radicals – all of which have a higher chemical potential and greater energy than their comparative (original) gaseous precursor components. Because of their insignificant mass and wavelength compatibility, electrons most easily respond to the applied electric field and consequently accumulate the significant majority of transferred electrical energy, which is revealed in the accelerating electrons as kinetic energy. That energy, ε_e, is related to the electron temperature, T_e, by the Boltzmann equation (where k is the Boltzmann constant).

$$\varepsilon_e = {}^3/_2 kT_e \quad \ldots\ldots\ldots\ldots \quad \{4.6\}1$$

Despite their charge-induced inclination to do so, the comparably large mass of ions inhibits their capability to respond to the applied electric field, however, a similar identity exists for ion energy, ε_i, and ion temperature, T_i. Essentially, it is conceded in plasma physics that ions in plasma do not sensibly gain energy directly from the applied field but indirectly through collisions with energetic electrons.

The frequency of particle collisions decreases with decreasing pressure, so free electrons experience a greater increase in energy, accelerating more between collisions with heavy particles (and other electrons). Also, each free electron experiences a greater share of the energy from the applied field – but not enough to cause electron acceleration to the point where the resultant increase in collision frequency would

compensate for the collision frequency decline due to the loss of particle density in the decreasing pressure of the plasma medium. Consequently, the difference in particle temperatures increases with decreasing pressure and is substantial below about 10 kPa, as was shown in Figure **{4.5.4}2** of a previous section. Low-pressure plasmas operate in non-equilibrium and are often called cold plasmas because the sensible temperature of the thermal bulk – that is, the neutrals plus ions – may lie in a relatively ambient range. At pressures upwards from about atmospheric, the particle density is high enough to ensure that the increased frequency of collisions between particles equilibrates the resultant range of particle temperatures such that $T_e \approx T_i \approx T_n$ or, to within a few percent, $T_e = T_i = T_n$ [83].

Ionisation, dissociation and the general absorption of energy into internal states of heavy particle species arise from *inelastic* collisions in plasma – and for these, the greatest unit energies transferred are from those electrons having the greatest mean free path. Hence, it is to be expected that species created in low-pressure plasmas will be more highly active – or more reactive – than those comparable species stimulated in higher-pressure plasmas. In monatomic gases (such as the inert gases), electron-neutral collisions are principally elastic (involving only kinetic energy) because the electron energy made available in the collision is typically less than that quantum required to promote the neutral to an excited state, or (further) to an ionised state. Despite this, under microwave stimulation, inert gases such as argon readily form low pressure plasmas because of the efficiency of energy transfer from microwave irradiation. Conversely, polyatomic gas species typically have energy level requirements for excited and ionised states within the available energy range supplied by random electron collisions. Consequently, more energy is transferred in the collision leaving a more highly de-energised electron, the transferred energy is absorbed internally (by a change of state), and the collision is *inelastic*. These characteristics are portrayed diagrammatically in Figure **{4.6}2**.

It is the accepted consensus that plasma chemistry operations, whose reaction mechanisms rely on the presence of reactive radicals and ions in the plasma, benefit by the presence of polyatomic gaseous reactant-components [117]. The chemistry that takes place in plasma is complex. A mere glance at Figure **{4.6}2** will confirm this statement. Under different conditions chemical reactions proceed differently. Typically, chemical

systems in plasma not only proceed differently from systems not in plasma but also from other plasma systems under different plasma stimulation. (Given that some degree of freedom exists for possible chemistries) systems with identical reactants will proceed differently and may have different product outcomes depending upon the discharge-generating mode and, more importantly, whether the system is operated in equilibrium or non-equilibrium. In non-equilibrium plasmas the transferred electron energy is directed into the production of active radicals, ions and free electrons (rather than the generation of heat). The associated reactions are classified into groups that typify their function. These groups are the electron/molecular reactions [which importantly include *ionisation* (the creation of an ion and an electron), *dissociative ionisation* (the creation of an ion, a neutral and an electron), *attachment* (the creation of a negative ion), *detachment* (the creation of a neutral plus an electron), *dissociation* (the creation of radicals), and *recombination* (the creation of neutrals) amongst others], the atomic/molecular reactions [which include *atom* or *neutral recombination* (the recombination of radicals into neutrals) and *ion recombination* (the recombination of ions into neutrals) amongst others], decomposition, and synthesis [80, 117]. These groups and their more prominent sub-groups are set-out (over page) in Table {4.6}1 – a complete list (which would contain a great number of extraneous and rare reaction possibilities, conferring little insight for this project) would occupy many pages.

Equilibrium between charge-carrier creation reactions and charge-carrier loss reactions is essential in the electronic sustenance of the plasma and the maintenance of the steady state concentration of active species in the plasma. Active ions and radicals (which do not recombine first) are available for reaction with gaseous *and* solid particulate reactants in systems such as those typical in this project.

Table {4.6}1: The principal plasma reactions which occur in volume plasmas are set-out below by type or classification [80]. Symbols A and B represent atoms, A_2 and B_2 represent molecules, and e represents a free electron. M represents a temporary or transitory collision partner, species superscripted $^+$ or $^-$ represent ions, and excited particle species are superscripted with an asterisk (*).

Electron/Molecular Reactions.			
Excitation	$e + A_2$	$\Rightarrow$	$A_2^* + e$
Dissociation	$e + A_2$	$\Rightarrow$	$2A + e$

Attachment	$e + A_2$	$\Rightarrow$	A_2^-
Dissociative Attachment	$e + A_2$	$\Rightarrow$	$A^- + A$
Ionisation	$e + A_2$	$\Rightarrow$	$A_2^+ + 2e$
Dissociative Ionisation	$e + A_2$	$\Rightarrow$	$A^+ + A + e$
Recombination	$e + A_2^+$	$\Rightarrow$	A_2
Detachment	$e + A_2^-$	$\Rightarrow$	$A_2 + 2e$
Atomic/Molecular Reactions.			
Penning Dissociation	$M^* + A_2$	$\Rightarrow$	$2A + M$
Penning Ionisation	$M^* + A_2$	$\Rightarrow$	$A_2^+ + M + e$
Charge Transfer	$A^\pm + B$	$\Rightarrow$	$A + B^\pm$
Ion Recombination	$A^- + B^+$	$\Rightarrow$	AB
Neutral Recombination	$A + B + M$	$\Rightarrow$	$AB + M$
Decomposition.			
Electronic	$e + AB$	$\Rightarrow$	$A + B + e$
Atomic	$A^* + B_2$	$\Rightarrow$	$AB + B$
Synthesis.			
Electronic	$e + A$	$\Rightarrow$	$A^* + e$
	$A^* + B$	$\Rightarrow$	AB
Atomic	$A + B$	$\Rightarrow$	AB

Theory decrees that, at the micro-scale, energy and momentum must be conserved during chemical reaction. For systems where monatomic species are dominant – cases pertinent to much plasma chemistry – recombination of monatomic species is exothermic and the following atomic recombination reaction (where A may be oxygen, hydrogen, chlorine, nitrogen or fluorine) yields an energetically activated product [117].

$$A + A \Rightarrow A_2^* \quad \ldots\ldots\ldots\ldots \quad \{4.6\}2$$

The so-created activated species must lose some of its heat (energy) or it will have sufficient energy to decompose by the reverse reaction. There are several mechanisms by which energy may be dissipated, however, for plasmas the accepted means is by photon emission unless there is energy loss intervention by collision with

cooling walls or other bodies. The species can be stabilised by the emission of a photon leaving behind a ground state molecule as by the following reaction (where h is the Plank constant and υ is the photon frequency).

$$A_2^* \Rightarrow A_2 + h\upsilon \quad \text{.....} \quad \{4.6\}3$$

Further to this, research [117] has shown that the decomposition frequency, υ_d, of an activated complex is given as follows and that this equates to a mean life expectancy for an activated complex of the order of 10^{-13} seconds at room temperature.

$$\upsilon_d = \frac{kT}{h} \quad \text{.....} \quad \{4.6\}4$$

Further, and most significantly for the potency of plasma chemistry, it has been shown that this life expectancy translates to 10^4 to 10^5 dissociations of activated complexes to radicals (by the reverse route of equation **{4.6}2**, that is: $A_2^* \Rightarrow A + A$) for every photon emission (that is, energy dissipation by equation **{4.6}3**). BULLARD, LYNCH and DAVENPORT [117] also reveal that a large proportion of absorbed electromagnetic energy is engaged in the production of radicals that are then available for reaction with entrained particulate reactant species. Manipulation of the levels of reactive radicals in low-pressure microwave plasma can be achieved to concentrations far in excess of that available by other methods.

In the volume plasma chemistry of non-equilibrium microwave plasma operations a central processing objective is to manipulate the plasma parameters such that desired reactions are favoured and undesired reactions are suppressed. Moreover, and fundamentally, process objectives have to be assessed with two underlying aspects of chemical plasma processing in mind: the physical requirement of plasma initiation and sustenance, and the chemical requirement of supplying and replenishing plasma chemistry participants. However, these conditions are typically met totally and concurrently by the satisfaction of the chemical requirement. The physical requirement is simply a proviso that the plasma, having been generated, will receive sufficient input energy stimulation such that the recombining charge-carrying particles will at least be

matched by newly created charge-carriers (ions plus free electrons created by ionisation events). The plasma's chemical requirement ensures that, irrespective of the physical requirement, there be available the required chemical participants – particularly those which are products or by-products of ionisation events – and that they be supplied by the process in the required quantities and at the required stage of the chemical process. This stipulation is synonymous with the chemical kinetics of the process.

Ionised, excited or otherwise energised species have a much greater reactivity [80] than they do in their ground state. In the discharge volume these energised and charged particle species react with other chemical species (atoms, molecules and radicals) to form new species. Molecules (both charged species and uncharged, neutral species) may dissociate as their bonds are broken; whilst, with these new reactant species, others may create new bonds and synthesise new chemical species. It is obvious from both circumstantial and chemical logistics that many chemical reactions run concurrently in plasma chemistry processes (as is in evidence in Figure **{4.6}1**).

The inherent advantage of non-equilibrium plasmas in volume plasma chemistry is that low pressure plasmas can provide particles with the high energy required to stimulate and complete reactions – the inherent drawback is the low reaction-mass-flow because of the low active plus neutral particle densities present in low pressure plasmas. The range of electron energies in microwave plasmas, that is 1 - 10 eV, is the ideal energy range for the excitation of atomic and molecular species, ionisation and the breaking of chemical bonds [58, 80].

Bullard, Lynch and Davenport [117] have shown that, albeit for a *hybrid* microwave-stimulated non-equilibrium system, the floating potential (of the voltage potential of the plasma) can be manipulated so as to promote chemical reactions and enhance process kinetics. The manipulation of such a variable was found to produce active radicals at the plasma-solid interface in concentrations that cannot be achieved by other methods and, furthermore, that such plasma chemistry positively revised the chemical kinetics of the overall process – promoting new reaction paths limited by new rate-controlling mechanisms.

As has already been presented, much of common plasma chemistry hinges upon the dissociation of molecular species, and (neglecting other structural complexities) to achieve this, the energy delivered to that molecule must exceed the bond energy (of the bond which is to be broken). Also, it is mainly the fast, energetic electrons created by the discharge of non-equilibrium plasmas that initiate chemical reactions in plasma chemistry – either by ionisation or the lesser excitation events. So, the downloading or

transfer of inelastic energy from fast electrons to heavy particles (thus raising internal energies) is indirectly responsible for the spectrum of reactive species, the chemical activity of the environment, and the actual reactions and their sequence in the plasma chemistry. Consequentially fundamental in plasma chemistry is that the transfer of energy from electrons to heavy species be efficient with effective subsequent transformation of these energised species into reactive species, and that the energy-depleted electrons are efficiently replenished by the applied field **[80]**.

Recounting that, essentially, plasma is comprised of non-ionised gas, excited particles, and electrically charged particles that can be affected by electric, electromagnetic and magnetic fields. In low pressure, non-equilibrium plasmas, energy distributions of plasma electrons, $f_e(\varepsilon_e)$, and ions, $f_i(\varepsilon_i)$, can differ significantly from the Maxwell-Boltzmann distribution. The mean energy, $\bar{\varepsilon}_y$, of charged particles is given by the following general equation.

$$\bar{\varepsilon}_y = \int \varepsilon_y f_y(\varepsilon_y)\, d\varepsilon_y \quad , y = e, i. \quad \ldots\ldots\ldots \quad \{4.6\}5$$

$\bar{\varepsilon}_y$ can exceed kT_g, where T_g is the temperature of the un-ionised gas; in many cases by orders of magnitude. KHAIT [76] and others give the example for typical ranges of values for these energies as $\bar{\varepsilon}_e$ = 1 to 5 eV (but up to 10 eV) and kT_g = 0.04 to 0.1 eV (but up to 2 eV) (where 1 eV ≈ 11,600 K).

Excited and ionised particles in plasmas have non-equilibrium populations (relevant to particle complexity) of their rotational, vibrational and electronic levels because of the influence of charged particles with non-equilibrium $f_e(\varepsilon_e)$ and $f_i(\varepsilon_i)$. This "biasing" of thermodynamic functions can influence both the thermodynamic and kinetic possibilities of chemical reactions. New reaction route possibilities can also be affected by the participation of electrically charged particles in chemical reactions [76]. Processes including plasma-stimulated chemical reactions increase in a non-linear manner with increasing energy input since, as imposed field strengths increase, the electron and ion concentrations increase – the effect of which is to further increase the field strength parameters, and so on.

The following facts are recounted here to generally summarise the salient points governing the ionisation chemistry of plasmas. In plasma-stimulated chemical reactions proceeding under equilibrium or quasi-equilibrium conditions – systems which exhibit a Maxwell-Boltzmann distribution of particle energies – the activation energies, E_{act} , exceed the mean energy (equivalent to kT) for the translational motion of the particles. In systems governed by "conventional" chemistry, chemical reactions are essentially processes devoid of, but approaching thermodynamic equilibrium (until reaction end) and, whilst E_{act} is greater than kT, the equilibrium distribution of particle energies remains substantially unaffected. The reaction "driving force" is related to the degree of non-equilibrium exhibited – which is never far from equilibrium at any point. Like equilibrium plasma chemistry, quasi-equilibrium plasma chemistry, as was suggested at the beginning of this section, can be described tangibly by applying the basic general laws of chemical kinetics.

When chemical reactions proceed under conditions of non-equilibrium where translational energy, and rotational and vibrational energies of relevant (molecular) particles, differ greatly both across these categories and within these categories, then temperature becomes indeterminable and the dictates of chemical kinetics become nonsensical. Hence, as addressed in an earlier section, each of the various plasma components (such as electrons, ions, decomposition fragments and other particle species excited through the range of quantum levels – each distinguished by a discrete energy) may be considered as having its own specific temperature. Furthermore, there likewise exists the distinction between translational temperature, rotational temperature and vibrational temperature for each relevant plasma component [58, 80]. Where systems so obviously depart from a Maxwell-Boltzmann distribution of particle energies the classical concepts of equilibrium thermodynamics, statistical thermal physics, and the Arrhenius equation (Equation **{3.4}2**) and all ensuing kinetics can no longer be applied.

In non-equilibrium plasma, as kT approaches E_{act} the Arrhenius equation fails to describe the kinetic characteristics of chemical processes [58]. To adequately describe non-equilibrium processes such as low pressure plasmas, the distributions of the reaction participants and the reaction products by their effective cross sections of the various reaction path possibilities, the dependence of the cross sections on the energies of the particle motions relative to other particles, and the variation of distributions with reaction progression (time) all must be known. Moreover, the degree to which systems diverge from predictability also depends upon the divergence from homogeneity of the system, or the degree of heterogeneity comprising the system. Such heterogeneity is common for the reactant charges of this project, and such non-equilibrium plasma is

typical for the reaction environments generated under microwave-stimulation throughout the experimental programme.

For conventional chemistries, an equilibrium distribution of energy among the various degrees of freedom is established at a rate determined by the *physical* kinetics of the process, whilst an equilibrium chemical composition is attained at a rate dependent upon the *chemical* kinetics of the process. In plasma chemistry, reactions are advanced by prominent interaction between the physical and chemical kinetics [58, 83]. Further, at plasma processing temperatures, chemical reaction rates are high and these are strongly influenced by the high rates of physical reactions – particularly diffusion.

5

EXPERIMENTAL METHODOLOGY.

"When the torrent sweeps a man against a boulder, you must expect him to scream, and you need not be surprised if the scream is sometimes a theory."

Robert Louis Stevenson -
Virginibus Puerisque, 1881.

"To think is not enough; you must think of something."

Jules Renard - *Journal,* 1899.

5 : EXPERIMENTAL METHODOLOGY.

It is appropriate at this point to reiterate the goals of the project. Central among project objectives was to establish whether various minerals and ores could be pyrometallurgically reduced to useful unrefined *"pig"* metallic forms or to "refinement pure" metallic forms utilising microwave energy as the initiating and ongoing principal thermodynamic stimulant of the reduction process. Source minerals and ore concentrates were to be representative of the refractory metal minerals – particularly those oxides of Groups **4** and **5** elements titanium, zirconium (plus hafnium) and tantalum (plus niobium) – which are so prominently represented in Australian mineral exports. The degree of reduction completeness was deemed important but only in the indicative sense that could be adequately represented in qualitative analytical results and micrographically recorded. It was found that reduction product complexity precluded the acquisition of meaningful results at a fully quantitative level.

Generally, experimental reduction trials were batch processes conducted with a view to extending to continuous processing where appropriate, if possible or, at least, recommending the implementation such extension where suitable for future work. Because of the inherent advantage in the adopted microwave processing technique of providing the capability to dictate the residence time of reactants in the microwave field (microwave plasma), the required contacting time for optimum reduction under prevailing thermodynamic conditions (once established) can be routinely attained (unlike the severe contacting constraints imposed by in-flight plasma reduction techniques). Also, whilst acknowledging the importance of experimental reproducibility, reproducible exactitude was not to become an over-riding nor determining criterion upon which experimental success was to be adjudicated (given the ever-present likelihood of erroneous phenomenological events associated with the smallness-of-scale of the experimental apparatus, and of experimental "heats" and their brief duration, the uncertainty of quenching and heterogeneity, and because of other peculiarities arising from small-scale microwave reduction processing).

The reduction route was not to be of issue, nor was the reductant, nor system chemistry – although each was fundamental in extractive process options. The precise chemistry of highly ionised environments under microwave-stimulation, in particular, high temperature plasma environments having non-equilibrium thermodynamics and complimentary kinetics, leaves much room for conjecture as to process chemistry and is an extensive field of research in its own right. [Similarly, outside microwave conditions, systems under equilibrium plasma impose their particular chemistries that are considerably removed from the non-equilibrium of microwave thermochemistry.] In

this project, reduction products were related to reactants in a general, chemically non-specific way with respect to known process parameters. Given availability (of course), the experimental configuration, reactor type, reactor materials, support apparatus and infrastructural configuration, and the process generally was to be limited only by the proviso that microwave energy be the sole applied (initiating and ongoing) external thermodynamic stimulant to reduction; inevitably, exothermic energies of reaction would, of course, supplement total system energy and would be acknowledged where and when such augmentation occurred. Concurrently with the recording of experimental progress, observations of process characteristics were noted and pursued if it was felt that the incorporation of deductions might lead to process augmentation or refinement. It should be noted that many possible process permutations* were not, in the final outcome, pursued in this project simply because of the constraints of time and, to a lesser or greater degree, because of constraints of access to, and availability of equipment and facilities. Put simply, the logistics of pursuing these permutations in this project precluded their inclusion.

Further, it was deemed unnecessary, if not inappropriate, to pursue the electrical power-use efficiency of the process because of the relatively incomparable nature of "sensible" temperature (or thermodynamic energy) between microwave-stimulated processes and conventionally heated processes. Also, power drawn at the magnetron (via the microwave field) changes constantly with the varying dielectric properties of the heating charge – quite unlike the constant, partly superfluous power slavishly drawn by conventional heating systems. So, any comparison of electrical power use between microwave-stimulated and other systems would prove to be an imponderable criterion for process assessment or justification.

How plasmas are created and sustained, what they are and how they function, and how they affect physical and chemical change *was <u>not</u> to be of issue in the conduct of experimental objectives*. Although unavoidable in any study of microwave applications, and necessarily acknowledging their primacy in every microwave operation, the processing consequences of these plasma characteristics were to be confronted empathetically, learned and constructively considered in experimental endeavours, and substantively addressed in the reporting of experimentation. However,

* Process permutations included top and bottom submerged lancing using various gases, injection of solid fines, mechanical vibration of charge during the reduction process to assist consolidation either by melting or by solid-state agglomeration of reduction products, manipulation of slag chemistry by fluxing, manipulation of process chemistry and kinetics via catalysis, *et cetera*. Process permutations were reliant upon the campaign type implicit in the reactor design – that is, principally, whether the specific operation was a batch or a continuous process. Ultimately, the procedures adopted in the final experimental method were a simple assemblage of options described in a later section as the "microwave oven set-up method".

the project was not to become a study in ionisation physics nor plasma processing although both of these pure and applied fields were crucial to an understanding of plasma-dominated microwave processing. Nor was it to become a comparative study of microwave-stimulated plasma processing versus other plasma processing techniques. The project was to be a study of microwave-stimulated reduction possibilities for thermochemically stable minerals – a study that, accordingly, must acknowledge the central role played by microwave-induced plasmas in the reduction processes under investigation.

From the evidence provided by initial experimental trials when this project was a mere concept there was tantalising promise of success for mineral reduction under modest physico-chemical conditions in the simplest crucible configurations and using the most basic of experimental microwave apparatus. In standard domestic and commercial microwave ovens good reduction results were achieved for a range of common minerals and ore concentrates of commercial importance. A Sharp R2370 microwave oven of nominal 1300 W rating was adopted as the "standard" commercially available oven for early experimental investigations. In later experimental work a Sharp R2380 microwave oven (an equivalent model superseding the R2370) of similar rating and specification was used as standard providing comparable results. These models utilised two counter-posed 650 W magnetrons effectively providing 650 W of continuous power on a "one-on, one-off" switching basis (at 100% input power). The ovens allowed timing control of experimental runs and adequate control over input power – 100% power input was generally employed in experimental work. [Noting that in the commercially available ovens, and by way of example, a programme setting of (say) "40% power" was delivered by employing 100% power for 40% of the programmed time, that is, at 4 seconds in each 10 seconds of the programmed duration. However, being un-required in formal experimentation, such power settings were not used in experimental trials.]

In light of high temperatures to be generated within the oven cavity, a practical but essential concession to "chamber" integrity was that the oven's plastic ceiling shield was removed along with the mode-stirrer* fan and its spindle mechanism situated

* Intended by design to disperse and distribute the microwave field through the oven chamber, the mode-stirrer is the functional equivalent to the rotating plate in domestic microwave ovens. It was found that

above this microwave-transparent ceiling so that neither melting nor microwave arcing would disrupt trials. After such removals the oven was essentially a stainless steel chamber with a high-density, high temperature-rated ceramic floor and "interrupted" only by the dual waveguide ports and the "microwave leak-proof" window in the oven door. Also, some "minor" modifications were made to experimental ovens to allow (in preliminary studies) for the provision, through microwave choke inlets, of inert gases (for some measure of atmosphere control) and reactive gases (for lancing) to the crucible/reactor arrangement. Microwave leakage at chokes, the oven door and at other points around the oven was monitored using appropriate microwave leakage detection equipment to ensure that microwave radiation did not become a safety hazard. Leakage from ovens was generally negligible and gave little cause for concern, although low "safe" level radiation leakage proved to be unpredictable at any potential leakage point in the oven system – varying with the imposed microwave load in the oven and shifting emphasis between leakage points due to fluctuating field manifestation with changing load susceptibility. Under constant scrutiny of advanced leakage monitoring, the microwave ovens used throughout the experimental programme were shown to represent negligible microwave leakage danger. The ovens proved to be reliable and durable under the "rigorous" and unorthodox treatment received in the high-temperature, corrosive environment of experimental "reactor chamber" application.

Typically, reactant charges in a standard crucible configuration were positioned centrally in the oven cavity for processing (see diagram of Figure {5}**1**). With oven durability enhanced by the above-mentioned chamber modifications, the available chamber volume was suitably enlarged to accommodate the insulation-wrapped "crucible configuration" containing the reactants charge. Given that the removed mode-stirrer was superfluous when processing strategy predominantly relied upon the thermal runaway that these devices were designed to overcome, predictability of "heating times" was ascertained such to ensure some measure of confidence in the planning of the experimental programme. Microwave processing times were planned, initiated and then monitored with respect to the observed progress of test reduction trials. With cavity light removed and laboratory lighting low, evidence of heating and chemical reaction in the charge could be observed through the borosilicate glass of the oven door.

---

removal of the mode-stirrer did not subjugate uptake of applied power as the load-susceptibility of experimental charges was sufficient to draw the applied field – and because the thermal runaway alternative was arguably beneficial to process.

experimental programme. Microwave processing times were planned, initiated and then monitored with respect to the observed progress of test reduction trials. With cavity light removed and laboratory lighting low, evidence of heating and chemical reaction in the charge could be observed through the borosilicate glass of the oven door. As thermocouple and optical pyrometer temperature measuring techniques were not employed (refer Section **5.1.5**) visual observations of radiation intensity, origin and spread of heating through the insulated crucible configuration, the beginnings and extensiveness of plasma activity, and chemical change indicators (exit-flame and fume start points, plasma colour shifts, *et cetera*) were recorded against process time. These observations would be used to build a thermal and chemical record of events that would finally be physically validated in the reduction remnants (reduction products plus crucible and insulation material remnants). This assemblage of a general, overall sense of experimental expectations in conceptual reduction process testing and following

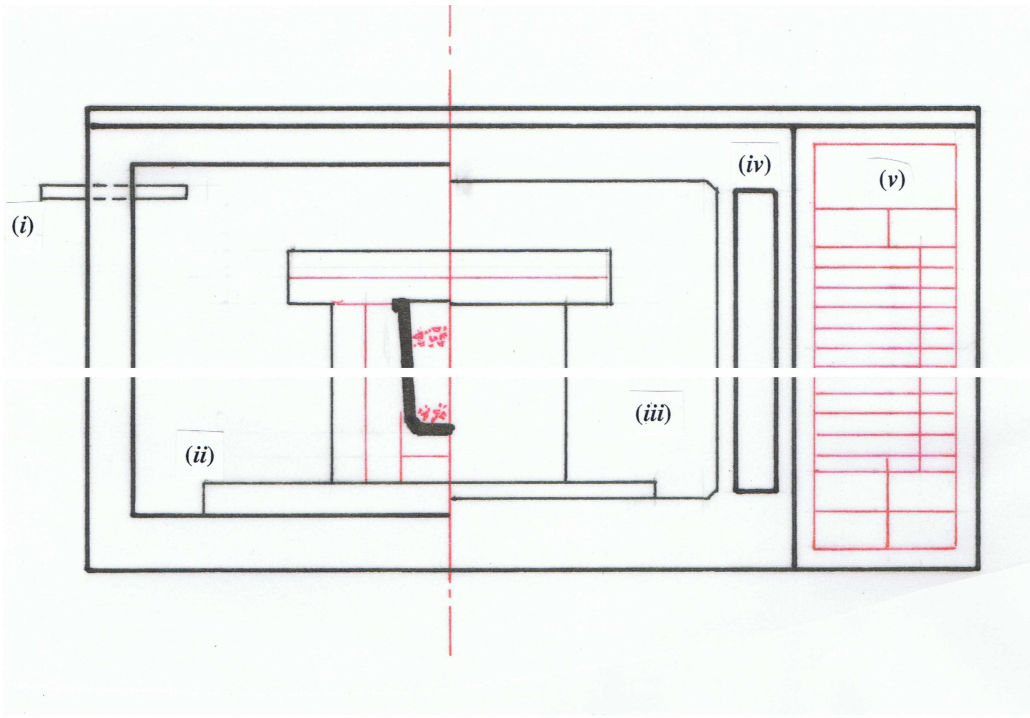

Figure {5}**1:** Schematic drawing representing the microwave oven set-up arrangement with insulated crucible configuration as employed for the more common carbothermic reduction trials. Other principal features shown are (***i***) outlet choke for the escape of gases and fume from oven cavity, (***ii***) insulation base, (***iii***) oven window (with integral mesh choking), (***iv***) handle of oven door, and (***v***) standard operation and control settings and read-out panel. [The tube length (length/diameter ratio) and mesh aperture for microwave choke applications are determined by the wavelength of the applied irradiation.]

preliminary experimental work was employed to build an experimental programme for the final, core thesis experimentation.

Observations of an extended range of microwave-stimulated reduction experiments were noted through the early, preliminary work. These experiments were carried-out over several years across a range of minerals (predominantly oxide based) of both laboratory chemical and minesite ore derivation, employing a range of reductant options, and conducted in reactor vessels of varying process sophistication and process methodology. Light optical examination of the post-process crucible containment (normally crucible plus insulation) and its solidified reduction product contents were made stereoscopically in all cases with supporting scanning electron micrography and energy dispersive spectroscopy (EDS) analyses in relevant cases prior to specimen recovery from reduction remnants, often under stereomicroscopic examination. Mounted and polished reduction product specimens were examined light optical microscopically and, where relevant, electron optically in a scanning electron microscope (SEM) utilising EDS for analytical support of light optical and electron optical micrographs. X-ray diffraction (XRD) analyses were selectively conducted for comparison with EDS output and, on a few fortunate occasions, wavelength dispersive spectroscopy (WDS) analyses using a Cameca microprobe was employed to provide indicative (comparative) support to EDS light element analyses.

[Covered in some detail in a later section, an evacuable, atmosphere controlled microwave reactor was trialled to yield impressive reduction products but at the cost of reactor process and equipment failure (which led to its experimental obsolescence).]

5.1: Microwave Heating and Processing.

Microwave heating is just that, heating by microwave irradiation of dielectrically susceptible material. In the sense of "bulk" temperature, it normally does not exceed the task of raising the irradiated load from a lower to a higher temperature by means of raising its internal energy, that is, its thermal energy (as directly represented by the temperature rise) without registering other non-equilibrium phenomena such as excited speciation or ionisation. In microwave processing of particulates, this "heating" by microwave irradiation invokes both the dielectric

susceptibility of the solid load material and of interstitial gas(es), by way of dipoles between particles of dielectrically different charge for solids and "across" molecular ions of dipole (vibrational and rotational) moment in ionised gas(es), to higher levels of excitation and ionisation thence chemical interaction. So, primary heating is the fundamental initiator – the essential precursor – of all subsequent processing. Because of the innate nature of microwave and near microwave wavelengths of electromagnetic irradiation which generate excited and ionised species in the target load, such subsequent processing is always conducted in an environment above its "ground state" (determined by the pre-irradiation load temperature) and rising rapidly through excited states into the realms of partially ionised states (partial plasmas) towards full ionisation. Typically, the pre-irradiation ground state (often at ambient temperature) is representative of equilibrium thermodynamics so the load will exhibit constant temperature through its profile and within its particles or species. Upon further heating in particulate loads, microwave irradiation rapidly gives rise to excited and augmented speciation, newly independent species (such as ions, electrons and photons, *et cetera*) and re-combined species, hence these different species exhibit different energies – different "temperatures" – and the environment moves from equilibrium towards non-equilibrium which is characterised by quasi-equilibrium plasmas moving to non-equilibrium plasmas – both micro-arc and volume discharge – at relatively high system pressures by comparison with other, non-microwave plasma-generation methods (as comprehensively discussed elsewhere).

Whilst microwave reduction produces novel but undeniably sound and regularly impressive experimental results, it is not necessarily a method that yields predictably reproducible results at laboratory scale experimentation. To this point, best results have been attained using the simplest experimental methods in the most basic laboratory apparatus. However, this lack of experimental sophistication was tantamount to a concession of some degree of process control. Such a concession of process control of itself concedes a level of control over the vital reproducibility factors of reaction time, temperature profiles and compositional consistency of reactants during reduction.

5.1.1: Mineralogy, Particle Size, Dielectric Doping and Susceptibility.

The variability of mineralogy within mineral grains and between mineral species of the ore concentrate under reduction, the mix of mineral reactants and reductants, the intimacy (relative size, surface area, contact potential, state, *et cetera*) of the reactant blend, and the mean particle size and size distribution within the reactant blend, or

charge, are all factors which affect microwave susceptibility as well as reactivity – both within each charge species and of the bulk charge. The microwave susceptibility of any naturally occurring mineral species varies significantly due to impurity content, temperature change and state or crystallographic (phase) change due to thermodynamic change. Even the most indiscernible impurity levels promote physical dielectric interaction far beyond their chemical importance. Mineral impurities act as dielectric dopants promoting heating locally around these inhomogenieties, then extending regionally through the charge. Of itself, rising temperature acts to continuously vary the dielectric properties of materials such that the overall propensity to heat generally increases with increasing temperature of the material (whilst it retains its crystal or molecular structure – state and phase changes set new dielectric ground rules for the material). Phase changes occurring during heating may or may not bring with them dielectric properties that imbue increased microwave susceptibility. Also, localised heating promotes thermal stresses with associated local volumetric changes. Volumetric change is also associated with phase change within solid phases.

The phenomenon of *thermal runaway* is brought about by the collective effects under increasing temperature upon microwave susceptibility (increased susceptibility due to the temperature-dependent term in the dielectric identities, see Equation **{5.1.3}1**) of bulk physical properties (packing density in the charge, particle size, size distribution, blend intimacy of reactant species – both physical and chemical, and blend stoichiometry) and specific physical properties of participant species (dielectric coercion of and between blend component species and the variability of mineralogy and impurity components (doping effect) within species). Trends arising from all of these phenomenological effects and events are expanded-upon in the following sections.

5.1.2: Load Size and Charge Configuration.

Whilst microwave susceptibility is dependent upon the dielectric properties of the charge components, the heating rate is further facilitated by the optimisation of the microwave load size (with respect to the power input) and charge configuration. The effective microwave energy available and the cavity's microwave field configuration (field manifestation) were not quantifiable. This field manifestation may be visually ascertained by setting-up a grid system of LED's that display their pulsing interaction with the prevailing electric field in the cavity – but this is mere display and is not directly measurable. Current drawn at the magnetron can be measured and quantified – but this is not necessarily equivalent to the power, or energy, available in the

microwave field – the "microwave energy". Also, the microwave field sees loads other than the intended load and some energy is dissipated in the cavity walls, insulation and other unintentionally targeted loads (including the magnetrons – self-targeting by magnetrons may cause self-destruction). The "keying-in" of the microwave field to the load is attributable to a load-matching factor quite separate to (although not totally independent of) susceptibility. If the microwave load is too small it will see only a fraction of the available microwave energy. If the microwave load is too large it will see the whole energy in the microwave field but will heat very slowly. So, in any given microwave cavity there will be an optimum microwave load that, moreover, will vary as the collective susceptibility of the charge varies with temperature.

Superimposed upon microwave load size, and linking load size with susceptibility and other physical properties, is *charge configuration.* Charge configuration is the arrangement of the charge components with respect to each other, with respect to the crucible or reactor vessel, and with respect to the bulk microwave load itself. Within the reaction vessel, charge configuration is the arrangement of the charged reactant (mineral and reductant) components – whether layered or blended – and granular carbonaceous material providing both atmospheric protection and heating stimulation. (The trivial case of charge configuration would be a charge consisting only of a uniformly sized and blended mix of reactants, whilst a typical complex configured case might be one in which the reactant components were independently charged, perhaps layer upon layer, with varied particle size distributions and independent protective granular or lump carbonaceous underburden and overburden.)

The configuration of the component reactants within the microwave load affect the bulk heating regime through thermal runaway and associated dielectric heating effects plus evolved heat from consequently initiated exothermic chemical reactions. Heating is enhanced by the intimacy of charge components that have dielectric difference such that dielectric loss factors promote local heating. Also, charge intimacy is essential in the contacting of chemical species to ensure chemical reaction (given adequate thermodynamic stimulation).

5.1.3: Bulk Heating and Microwave Irradiation.

Upon irradiation, bulk heating is initiated by a network of microwave arcs between component particles of charge-difference or of different charge in the most susceptible regions of the charge. These minute microwave discharges between

susceptible particles are commonly referred-to as "micro-arcs" in deference to their diminutive character being of the order of micrometers in length and milliseconds in duration, but continuously re-generated between charge points along "micro-arc paths". Despite their miniature size and longevity, micro-arcs are brilliantly radiant and regenerate locally with rapidity that, in real time, defeats the eye's resolution. The naked eye, however, registers the track of the averaged micro-arc path; the heating associated with such micro-arc paths sinters local material forming "skeletal structures" – proof of the phenomenon – as shown in the stereomicrographs of later Figures **{5.1.3}1** and **{5.1.3}2**. Heat radiating from these micro-arcs rapidly heat the immediate region and the continuously repeated phenomena combine to heat the charge bulk quickly and efficiently, if somewhat erratically – generally from the load centre outwards.

As materials heat, their dielectric properties change – generally they become increasingly microwave susceptible with increasing temperature, although this is not always the case within specific phases, across (allotropic) phase changes in solids, nor in changes of state (which can be unpredictable in un-established cases). It is well described and recorded in the literature [83, 86, 96, 105, 121, 133, 198, 199, 200, 201, 202] that this increasing dielectric interaction (susceptibility) is to be expected given the temperature dependent terms ε' and ε" in the dipolar heating expression (as Equation **{4.1}2**).

Complex relative dielectric constant, $\varepsilon^* = \varepsilon' - j\varepsilon''$ **{5.1.3}1**

where: ε' is the relative dielectric constant, and
ε" is the dielectric loss factor (the heating factor).

In fact, this temperature-determined propensity to heat was the case with all materials pertinent to this project – not only for *susceptor* materials (most ore minerals, gases and carbon forms) but also for microwave *transparent* materials such as crucible and insulation materials. State and phase transformations occurring in experimentation during heating or further processing resulted in corresponding changes to the dielectric properties of the transformed phases. The most obvious example of this phenomenon occurs when a solid exceeds its melting point and becomes liquid. It was observed repeatedly through the course of this project that materials (usually minerals) "lost" their susceptibility upon melting – visibly cooling, its interrupted chemistry often "captured" at solidification. In such cases of melting there was for most materials a sudden drop in the material's dielectric lossiness (equivalent to its microwave susceptibility – or its ability to heat in the microwave field) and the liquid tended to plunge back beneath the melting point and re-solidify unless it was augmented by local radiant and/or conductive heat energy from adjacent materials. Where re-solidification

occurred before quenching then "revised" susceptibility characteristics dictated heating in the new solid phase. Thus, microwave heating can be "less than predictable" as a straight heating method. [The ice/water duality is a notable exception to this "rule". In fact, both water and steam are vastly more microwave susceptible than ice. Being a bipolar molecule and capable of "vibrational" switching about its bonds, H_2O is highly susceptible in the liquid and gaseous states but far less so in the solid state where the molecule is "fixed".] Phase transformations in the solid state also impose changes to dielectric properties between the phases as do state transformations representing boiling and sublimation (during heating), and condensation and precipitation (during cooling).

Typically (even at the high temperature ranges of microwave processes) where relevant project minerals became molten – both simple melts and spongy liquid/solid mixtures – the "melts" displayed low microwave susceptibility. Of course, as previously mentioned, not all liquids behave in this way. Aqueous solutions are well suited to microwave processing techniques because water is highly susceptible at the common, commercially important 2450 MHz microwave frequency. By comparison, reduced metals in either liquid or solid state become microwave reflectors rather than the susceptors they were in the un-reduced mineral. In contrast, many of the gases common to reduction and/or plasma processes displayed high susceptibility to microwave irradiation. So much so that chemical dissociation was standard for larger-moleculed gases such as methane, CH_4 , as was ionisation for such vitally important gases as nitrogen, N_2 , carbon monoxide, CO, and the monatomic argon, Ar, as they reproducibly displayed their characteristic plasmas in reactor vessels. Microwave plasmas are created when a suitably susceptible gas "ionises" by absorbing appropriate quanta of microwave band electromagnetic energy in promoting an outer shell electron(s) to an orbital(s) in a higher electron shell(s) (thus creating the "ionised" state of the gas). Plasma is realised when this absorbed quanta of energy is released (as thermal energy in the forms of *heat* and *light*) upon the dropping-back of the promoted electrons to their original or other lower energy state orbital – and it is sustained by the repeated cycling of these ionisation phenomena.

As specific regions in a charge experience the intense localised thermal stimulus of repetitive micro-arcing those regions undergo rapid local heating, the intensity distribution visibly displayed indicating a pronounced temperature profile across the point of thermal concentration. The susceptible region will, in keeping with the temperature profile, exhibit rising dielectric properties and, thus, this locally enhanced microwave susceptibility will attract a greater proportion of available applied energy,

and a greater rate of heating. Hence, circumstances feed upon themselves as this local region's propensity to attract an even greater share of the available microwave energy increases. In what might be thought-of as a "thermal flywheel" effect, the increasing concentration of attracted energy equates to an accelerated rate of local heating. This normally avoided heating phenomenon is known as ***thermal runaway*** and is fundamental in microwave reduction processing – it is initially paramount in that it is responsible for rapid temperature increases to the requisite high temperatures (energies) which initiate chemical reactions and where characteristic microwave processing is conducted. Micro-arcing is symptomatic of thermal runaway, and this transient arc discharge is ultimately expressed as volumetric discharge – in concert (at least initially) with the micro-arcing between charged points in the microwave "load". Locally, thermal runaway continues unarrested until the material undergoes a phase or state transformation, usually melting, or reduction – at which point susceptibility is (normally) spontaneously lost or curtailed such that the temperature rise is halted and the microwave field is captured by a new region of peak susceptibility, transposing the point of thermal runaway. Also, thermal runaway may be retarded by the initiation in carbonaceous reductant of the endothermic Boudouard reaction.

$$C + CO_2 \Rightarrow 2CO \quad \text{..... } \{5.1.3\}2$$

This reaction has an increasingly significant quenching effect as reactor temperature increases. Carbon monoxide, CO, is stable at temperatures above ~ 900°C, and the Boudouard reaction proceeds rapidly above 950°C [17] [Less relevant at this stage of process is that, below ~ 900°C, CO_2 is the stable gas and CO oxidises in the exothermic reverse reaction.]

In the initial stages of heating, thermal runaway in random, isolated regions throughout the charge give rise to an unusually complex stereological temperature profile, or topograph. It is in this thermodynamic environment that the thermal and chemical stabilities of the charge components are first put to test. The first solid state sintering (the self diffusion of like species providing mass transport between, and thus fusing, particles of like reactants and products) and the initial liquid state sintering (the liquid mass transport of matter around surfaces to fuse particles) begins at temperatures below the melting point, $\mathbf{T_m}$, of the blend particles. Thermal runaway, which is the primary initiator of heating in the charge bulk, is promoted by micro-arcing between dielectrically susceptible particles in close proximity which have discharged releasing micro-current. The discharge repeats and frequently the resulting micro-current joins with adjacent discharged micro-current events to form arc pathways or tracks.

Micro-arc tracks are formed when micro-arcing persists along an approximate path en-route between dielectrically interacting particles. Each track is the prominent mean arc path – a corridor which is marked by a continuum of fused particles which form a skeletal structure when (as they commonly do) the tracks intersect at particles representing points of enhanced dielectric potential.

The degree of "fusedness" along the skeletal limbs depends upon the degree of micro-arcing along the tracks, that is, the temperatures reached along the tracks. Where micro-arcing has persisted to a greater degree along these tracks the degree of sintering or fusion between particles is greatest and the skeletal framework is correspondingly thickest. Where micro-arcing has been less persistent along arc tracks, or has only briefly been initiated, the related temperature profiles have been less pronounced with lower maxima and, thus, the skeletal limbs are finer and the structure more delicate. Typical skeletal structures can be seen to advantage in the SEM stereomicrographs of Figures **{5.1.3}1** and **{5.1.3}2**.

The charge regions represented by the skeletal interstices are the last regions to heat and represent the temperature troughs. Nominally, these regions are heated not by direct arcing but by the extreme radiated heat of adjacent micro-arcing. They are last to sinter and last to melt (where melting temperature is exceeded). So, these skeletal interstices contain the least converted phases where these are preserved by reduction process incompletion in quenched reduction products. But, correspondingly, they also contain the most extensive record of reduction process stages from initial reduction to advanced reduction. These stages present clearly in multi-phase fields of polished sections of the solidified reduction products.

Overlooking the likelihood that mineral phases of different melting point may be present in the reactant charge, and knowing that the carbonaceous solids will not melt, and despite the unknowns of surface tensions and local gasification and other chemical reactions, the molten phases may flow into the interstices of the still solid agglomerate regions. With increasing temperature, liquid phase viscosities drop and minor volumetric contraction accompanies the oxygen depletion of advancing oxide phase reduction. Each of these phenomena acts to assist the flow of molten phases into interstitial regions. However, with the melting comes a dramatic drop in local microwave susceptibility (effectively dousing any micro-arcing), and so, these newly liquid regions may no longer experience direct micro-arcing thus retarding local heating and reduction, and "locking-in" existing reduced metal. (Such regions are identified in colour micrographs of Figures **{5.1.3}3** and **{5.1.3}4**, and extensively in those of Section 7, *Results*).

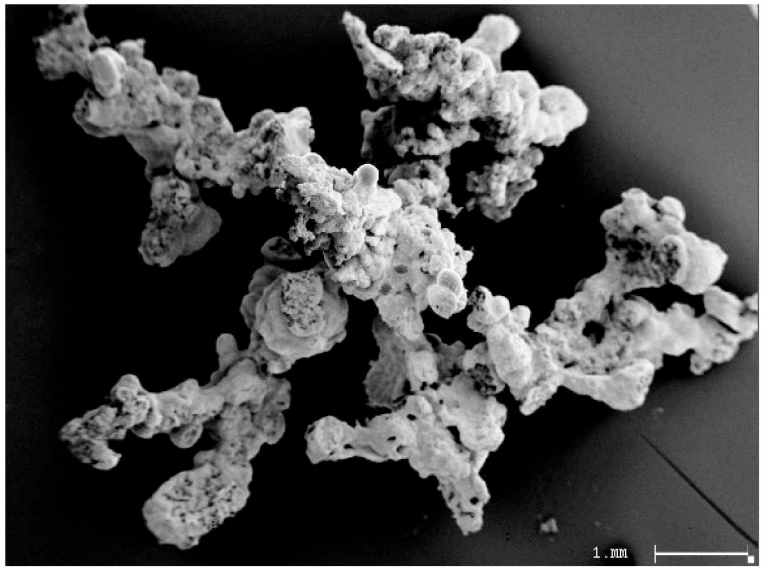

Figure {5.1.3}1: SEM stereomicrograph of a typical skeletal structure as excavated from the reduction product remnants of a crucible. Note the brittle fracture surfaces where skeletal continua have broken, whilst local "brightness" is from charging in the non-conducting specimen under the HT excitation beam of the SEM. [Note the 1 mm bar providing scale to this micro-arcing thermal record.] As below, note the randomness of the micro-arc-induced structure which was recovered from the partially reduced particulate charge of a prematurely terminated experimental trial in which the friable remnant charge remained largely loose allowing recovery of these fragile structures. Advanced intact structures could be up to 1 cm "long".

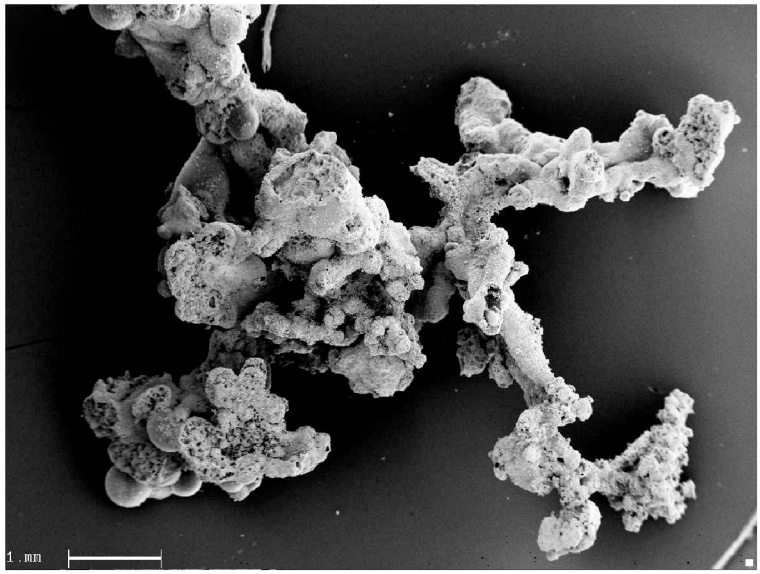

Figure {5.1.3}2: SEM stereomicrograph of an advanced skeletal structure (at the same scale as above) and again excavated from the remnants of a prematurely terminated reduction trial. The advanced structure is extensively fractured, the brittle-fracture surfaces show possible signs of porosity.

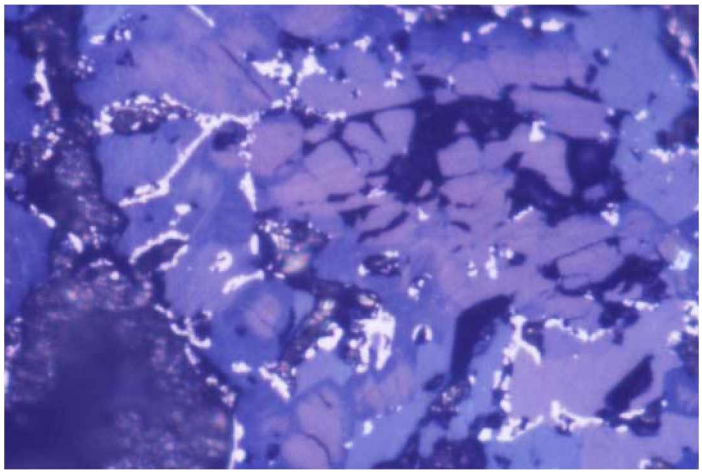

(a) [fov: 0.16 mm]

(b) [fov: 0.05 mm]

Figure {5.1.3}3: Detail of Ti-metallisation along remnant micro-arc tracks in prematurely terminated reduction remnants of anatase reduction processing. Because of the unlikely conditions (by-passing LN_2 quench) at termination/solidification, the reduction product "specs" that reported in quenched specimens were here provided with the opportunity to coalesce, with distinct phase separation between metal and un-reduced mineral (blue-grey), along the micro-arc tracks where they were initially reduced.

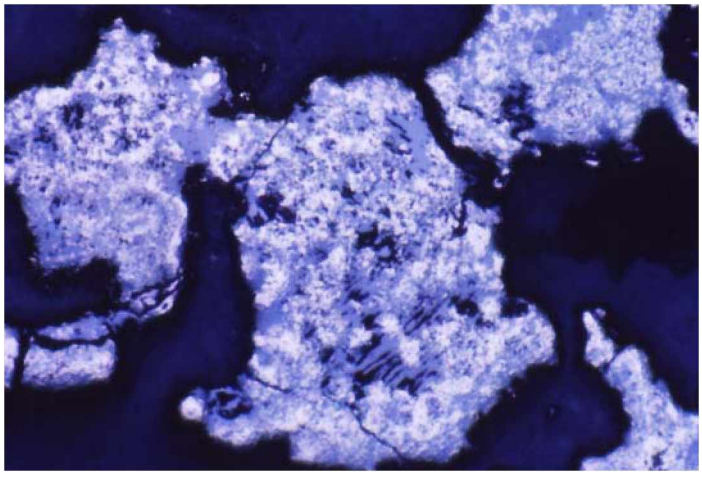

Figure {5.1.3}4: Distribution of Ti-metallic specs in an anatase reduction product remnant which has been LN_2 quenched in the usual manner. Metallisation is concentrated along remnant micro-arc tracks – zones of initial reduction. [LOM; Ektachrome; fov: 0.75 mm.]

Whilst complete skeletal frames representing sintering along micro-arc tracks can be excavated from prematurely terminated reduction product remnants, other compelling evidence of subsequent reduction stages – even reduction as advanced as metallic phase – along micro-arc tracks can be seen in polished section across a range of phase fields reporting in reduction products of reduction processes for all minerals, although more commonly recorded for anatase products. Note further that, as discussed in Section 7, the physical expression of the reduction mechanism sees the development of reduction product "spots" at reduction initiation point-sites along the *mean* tracks of the recurrent micro-arc "events", extending outwards with increasing overall degree of reduction into the cooler interstitial material. This reduction trend can be seen in the selection of micrographs of Section 7. In particular, Figures **{7.2.1}3** and **{7.2.1}5** show regions in anatase reduction product remnants where Ti-metallisation along micro-arc track "hot-zones" indicate the concentration of metallic "point-reduction specs" into visible "pathways" which undoubtedly follow micro-arc routes, zones of initial thermal activity and reduction. Correspondingly, and especially obvious in the micrograph of Figure **{7.2.1}5**, as shrinkage associated with reduction and the local thermal profile takes effect along micro-arc tracks, voidage is created by volumetric contraction centrally in cooler, still-friable interstitial regions between micro-arc metallisation as the last non-rigid volumes of material are "pulled" towards the shrinking, reactive regions. So, microscopical observations of polished sections reveal the enhanced degree of reduction in phases present along micro-arc tracks (reduction phases are post "sintered skeletal frame" stage) with respect to that reduction evident in adjacent skeletal-interstitial regions (as in Figures **{5.1.3}3** and **{5.1.3}4**, plus later Figures **{7.2.1}3** and **{7.2.1}5**).

Skeletal "arms" that are subjected to the highly reactive "dry" zones of glow discharge plasma high in the crucible sinter into agglomerate clusters of high melting point phases. These clusters invariably capture interstitially some remnant lower melting point phases that have failed to drain to lower zones. Note that whilst electron temperatures in the plasma are exceedingly high – perhaps rising into the tens of thousands of kelvin – their contribution to the thermal mass of the local bulk temperature is in keeping with their relative mass. So, whilst these exposed phases react in the plasma's reactive ionisation chemistry environment, they may not acquire enough thermal energy to exceed their melting points (which are typically very high). Consequently, the reduction phases of such exposed regions are frequently solid state reduced phases of advanced conversion.

Upon microscopic examination, re-oxidation and reversion products can be identified in phases at and near the surface regions of reduction remnants – whereas,

comparable reduced and incompletely-reduced phases occur in remnants away from surface regions or, more particularly, away from exposure to highly reactive plasma. Duly, however, the ultimate importance to reduction in this project of the micro-arcing phenomenon should not be over-stated; it is simply ***the*** *mechanism* "in the right place, at the right time" to initiate the ionisation process and to instigate the reduction process. Upon reduction, retaining the composition and general metallic "integrity" of phases from the reduction-process environment to the quench-frozen reduction product was a particular challenge that is addressed in following sections.

5.1.4: Process Phenomena, Process Completion and Reproducibility.

Because of the random nature of microwave-stimulated reactions imposed upon the generally rapid rate of reduction where microwave-stimulation occurs evidently *without* commensurate changes to physical parameters such as chemical contacting of charge components, melt fluidity and heat conduction in solid phases, a high degree of experimental reproducibility cannot be routinely expected in high-temperature pyrometallurgical reduction processes of such short duration and of such small scale. (Generally, experimental reduction trials were batch processes conducted with a view to extending to continuous processing where appropriate – however, this latter contingency, despite its desirability, did not eventuate during the course of project experimentation, although, where fitting, adoption of a continuous option to specific processes is contemplated.) Process thermodynamics and kinetics become complex and quite unclear because of the vagaries of microwave heating. However, the microwave-stimulated reduction of minerals produces certain general process characteristics or trends whose results can be identified in the reduction products across a range of comparable experimental runs. These "general process characteristics", which are representative of local reaction paths and local regions of reduction completeness (introduced in the previous section), are well recorded in the physical evidence that the solidified reduction products represent.

During microwave processing two types of process events take place in the load charge. Conceptually, these process events – which are governed by the material properties of the charge – may be complimentary or they may be competitive. The material properties give rise to the *thermal* or *physical stability (instability)* at temperature of phases present, and the *chemical stability (instability)* at temperature of phases present. The thermal and chemical stabilities, in concert, dictate the sequence and magnitude of events in the microwave reduction process.

"Reduction process completion" has been an ambiguous and, at times, difficult concept to define as it was determined not simply by the specification of a desired end product but by the chemical "reactor" capabilities that are determined by the process sophistication inherent in the reactor design. That is, process sophistication may allow a reduction product having a greater degree of reduction; for example, a reduction product being a metal rather than a metal carbonitride, or perhaps, a reduction product representing 95% conversion rather than 85% conversion of reactants. Also, in the trivial case, reduction process completion may be the chosen termination point in an experimental run (but this sense will be disregarded). Significantly, however, the most successful experimental results were attained using the simplest microwave "reactor" configuration and the simplest process methodology.

The general case addressed is of the simple but successful reactor system of an insulated crucible containing a charge of blended reactants beneath charcoal (which affords simple but effective atmospheric protection to the reduction reactions until solidification of the reduction products) and processed in a minimally modified 1300 W microwave oven. Because the crucible and insulation materials are nominally microwave transparent, the initial microwave irradiation "sees" the crucible's microwave-susceptible charge of reactants as the *microwave load* and heating is initiated in the charge. Heating within the charge depends upon the spacial configuration of the charged reactants and upon the degree of susceptibility of each charge component group and the dielectric interaction between charge components. Dielectric interaction occurs not only between charge components of different chemical species but also between components of the same chemical species. Further, dielectric interaction between charge components is enhanced by increased particle size difference (as described in earlier Sections **5.1.1** and **5.1.2**).

As previously established, because of the random nature of microwave-stimulated reactions, a high degree of experimental reproducibility cannot necessarily be expected in microwave reduction processes – particularly in small operations of short duration. Moreover, the likelihood of reproducibility increases with increasing processing time. Initially, process thermodynamics and kinetics are complex, indeed unclear, because of the vagaries of microwave heating. However, the microwave-stimulated reduction of minerals produces certain general process characteristics or trends that can be identified in the reduction products across a range of comparable experimental runs. These "general process characteristics", which are representative of

local reaction paths and reduction completeness (as was earlier affirmed), are well recorded in the physical evidence that the solidified reduction products represent.

The experimental programme was carried-out at intervals over several years. In a formative manner, the microwave-stimulated reduction exercises were conducted on relevant minerals as they became available. Fittingly, as the kernel of the project developed, "lead-in" preliminary experimental trials were conducted on many minerals of metals from across the periodic table during a learning period of "non-core" experimentation during which experimental procedures were refined (including the trialing of the later-described evacuable microwave reactor). An established routine of experimental procedure was in practice by the time the "core" refractory metals and their relevant minerals were identified, the microwave oven set-up method confirmed. The suite of "pure" single oxide minerals (of commercial or laboratory grade) was assembled to accompany the complementary suite of minesite-derived mineral concentrates, concentrate products of importance in the Australian mining industry – and of considerable commercial significance in view of their recurrent proportion of Australian export earnings.

Upon consideration of the accumulated evidence, the following scheme of process events was proposed to describe the reduction of minerals in intimate association with a reductant and utilising the primary energetic stimulation of microwave irradiation to initiate and drive the process reactions. (It should be emphasised again that a process stage representing "reduction process completion" may be difficult to define as it was determined not only by the specification of a desired reduction product but also by the system capabilities which were determined by the process sophistication allowed by the "reactor" design.) The general case addressed is of the simple but successful system of an insulated crucible with a charge of blended reactants beneath char (which afforded simple but effective atmospheric protection to the reaction process and until solidification of the reduction products). This crucible configuration was placed in minimally modified 1300 W microwave oven where the reduction operation was carried-out. Pertinently, descriptions hereafter follow-on from those describing the initiation of microwave reduction processing given in Section **5.1.3**: *Bulk Heating and Microwave Irradiation*.

By providing heating to the reactant charge the input microwave energy thereby provides the thermodynamic stimulus for the reduction reactions. Reduction begins by solid state diffusion of carbon (by contact with charcoal) into the mineral(s) to be

reduced forming non-stoichiometric oxycarbide regions at surfaces and lowering local melting points. The process is of comparatively minor importance and probably short lived as it is rapidly overtaken by other more significant reduction events.

As the atmospheric protection charcoal and/or the carbon portion of the charge-blend heat above about 900°C the available energy becomes adequate to provide a stable reducing atmosphere of carbon monoxide, CO, throughout the reactant charge and the mass transport of reductant carbon becomes predominantly controlled by the CO gas phase reduction reaction. As the reaction environment's temperature is driven higher by the net release of exothermic energy *plus* the continuing applied microwave energy input the gas phase reduction reactions become the overwhelming rate controlling reaction steps. The following schematic equations are intended only as indicative – as starting points to conceptualise the chemistry of microwave-stimulated reduction – and, of course, (neglecting integral plasma chemistry events here) are chemically complemented by the carbon monoxide regenerating Boudouard reaction (C + CO_2 $\Rightarrow$ 2CO … Equation **{5.1.3}2**).

oxide mineral + CO $\Rightarrow$ oxygen-depleted mineral phase + CO_2 ….. **{5.1.4}1**

oxygen-depleted mineral + CO $\Rightarrow$ metal + CO_2 ..... **{5.1.4}2**

reduced metal + CO $\Rightarrow$ metal carbide + CO_2 ..... **{5.1.4}3**

reduced metal + char (+ N_2) $\Rightarrow$ metal carbide (carbonitride) ..... **{5.1.4}4**

The above reactions are, unfortunately, too simplistic to adequately describe the reduction reactions even for the general case. However, a fifth equation might be added to allow the proposal to develop.

oxygen-depleted mineral + [N*] $\Rightarrow$ oxygen depl. mineral nitroxide ... **{5.1.4}5**

Excited or ionised nitrogen, [N*], in the plasma also seems to deposit an authentic plasma vapour deposition (PVD) bronze coloured nitride coating to the surface of metal-rich phases. Much of the uptake of nitrogen seems to be through the oxygen-depleted oxide phases as suggested (stoichiometry ignored) in equation **{5.1.4}5.** Evidence also suggests that a similar proportion of carbon is taken-up in these oxygen-depleted oxide phases, both as carboxide or carbide phases, or with nitrogen as oxycarbonitride or carbonitride phases. [Each of carbon, nitrogen and oxygen may be chemically active in their gaseous, excited or ionised states.] So, perhaps the true

chemical nature of these depleted oxides might be a non-stoichiometric, oxygen-rich metal oxycarbonitride. Moreover, under observation and analysis in the University of New South Wales's Cameca SX50 microprobe the more heavily reduced metallic "nitride" phases in various titania derived reduction products where actually titanium oxycarbonitride compounds of close but varying composition and tending towards the straight titanium carbonitride where there was evidence of increased reduction intensity. X-ray diffraction analyses over several reduction product specimens have revealed the majority phase presences of (separately) both titanium nitride and titanium carbide in a phase spectrum including carbonitride and a continuum of un-resolved complex oxycarbonitride phases.

Visual information in micrographs show nitrogen-rich "nitride" phases which appear as "nitride spots" which could arguably have been original reactant powder, solid state reduced and converted to nitride then encapsulated in an oxide phase of lower **Tm**. However, it is the contention of this author that these phase fields of nitride spots in oxide phase actually represent a solidified eutectic structure. This claim makes sense as the more reduced phases would be further from the oxide corner (ternary) or end (binary) of the relevant phase diagram and this is the case in micrographs where such highly reduced phases are highly populated by bronze nitride spots.

5.1.5: The Resolution of "Temperature".

Determination of temperature by direct measurement is standard practice for conventional thermodynamic systems and is considered mandatory in establishing a fundamental thermochemical understanding of the system. The precept is well established and is conditional upon two simple and, for the conventional case, reasonable assumptions. These are that the temperature sampling point can be accessed such that the measurement can be made, and secondly, that the thermal energy (heat – represented by and indicatively measurable as temperature) is essentially equivalent to and, therefore, representative of the total energy available for thermodynamic change in the system. So, for traditional pyrometallurgical systems, temperature – which can be practicably and systematically measured – (by precedent of a long history of prior recorded experience) is predictably related to thermodynamic state and is therefore worth knowing.

However, as described earlier in Section **4** (specifically **4.3**, **4.4**, **4.5.3** and **4.5.4**), in systems under microwave-stimulated plasma the prevailing non-equilibrium thermodynamics controls matter in an ionising environment having a range of temperatures. In such an environment each particle type is distinguished by its own temperature which, in turn, governs its (ionisaton) chemistry. So, different thermochemistry sets are active in the system. In addition to thermal energy, these particles – particularly excited and ionised particles – have significant other energies that participate in thermochemistry but which are otherwise evident – and so are not necessarily available as thermal energy and accordingly are not measurable as "temperature" until they break down from other forms and are expressed as thermal energy. Consequently, in an environment of many component "temperatures" – each capable of its own impact upon system chemistry, the measurement of a single mean "bulk temperature" with which to define non-equilibrium system thermochemistry would provide an imprecise and relatively meaningless quantity. Furthermore, if energies which are not manifest as thermal energy (heat) take part in chemical change without first breaking-down or converting into thermal energy (as is suggested in earlier-cited literature), then thermodynamics, as it is defined, is incomplete and the "temperature" term, **T**, needs to be replaced by several energy term equivalents. Statistical thermal physics addresses non-equilibrium thermodynamics [66, 192, 203] but non-equilibrium microwave plasma thermochemistry is not specifically defined – this is, in part, because statistical thermodynamics still defines energy in terms of temperature, **T**, and therefore carries the same general flaw as the long-evolved Gibbsian thermodynamics.

There exists a prevalent doctrine encoded into scientists and engineers by their education and subsequent vocational training which insists that "experiments dependent upon thermodynamics cannot be proceeded-with without the measurement and monitoring of temperature" and "little can be known about a system without knowledge of system temperature". In general, where temperature is a sufficient indicator of total available energy, this prevailing credo has provided the initiating rigour required in experimental operations governed by the usual equilibrium or near-equilibrium thermodynamics of conventional metallurgical and comparable operations. However, simple (bulk) temperature measurements in non-equilibrium plasma actually provide a "temperature" which suggests that *the laws of thermodynamics are being contravened* when, in fact, such is not the case. This bulk temperature is a false mean temperature that may be magnitudes below that range of temperatures possessed by the highest energy, most chemically active plasma particles – the particle species bringing-about

the chemical change. Consequently, reaction events are observed to occur at apparently-lower temperatures than predicted or are "known" from conventional (equilibrium or near- equilibrium) systems. Temperature is an indicator of total thermal energy, not (necessarily) total available energy.

Alternatively, other legitimate and illuminating observations of system parameters can be acquired during a process – observations leading to measurements of meaningful quantities that may be made on a reproducible basis. So, for non-equilibrium systems, the lack of temperature measurement does not proscribe the legitimacy of other philosophically different approaches to system monitoring and definition. Amongst the central quantities (such as *time, mass* and *pressure*) that define a system's operating parameters, *temperature* may well seem the most pertinent quantity measured, but temperature measured for measurement's sake is a dangerous quantity. Considerable effort may be invested in acquiring a record of system temperature, therefore operators and experimentalists alike must understand what this record represents and the limits of its legitimate application. Where, as in this project, (*if* a measurement sighting can be achieved) it is unclear what the measured temperature may represent, then another philosophical approach to system definition is required. Such a philosophical shift in system assessment was required for this project.

The other primary thermodynamic variable, pressure, was not measured for the project-significant majority of experimental trials (which, co-incidentally, were carried-out at room pressure). Local partial pressure variations were suspected within the plasma sheath – variations, real *or* virtual, which might be due to particle speciation, differences in particle ionisation characteristics, or other ionisation phenomena in the plasma environment. As proposed in Section **4**, any *perceived* drop in partial pressure may provide some contribution to an induced, tentative shift in system thermodynamics towards non-equilibrium plasma. To experimentally pursue this hypothesis was beyond the scope of this project despite it being implied and supported by the evidence of experimental reduction products.

5.1.5.1: The Preclusion of Direct Temperature Measurement.

Notwithstanding the relative meaninglessness of such an exercise in terms of the range of plasma particle temperatures, there were several idiosyncrasies of microwave

heating and processing which precluded the feasibility, practicability and effectiveness of any endevour towards direct temperature measurement in the pyrometallurgical operations of this project. Beyond the *"what"* of the theoretical *what temperature was being measured?* (as addressed above), the peculiarities on the practical side of microwave processing which, in their own right, adequately and necessarily refute any justification of physical measurement were the *"where"* of *where within the microwave stimulated charge would provide a meaningful measurement (given processing time)?* and the *"how"* of *how can this possibly changing measurement point be accessed and a consistent reading taken over time with varying parameters (such as corruption of emissivity from optical pyrometer measurement surface, or field interference and corrosion of thermocouple tip)?* To these "what", "where" and "how" could be added, especially for batch processes, the *"when"* of *when during microwave processing should temperature measurements be taken (assuming such are meaningful)?*

The "where" and "when" conundrums are relevant to the positioning of the proposed measurement point with respect to the temperature profile through the reactant charge (come microwave load) with progression of processing time. As has been described in earlier sections, and unlike typical conventionally heated and processed operations, peak heating positions within microwave-stimulated charges vary with time. The typical temperature profile across the section of a microwave-stimulated (heated) body, as indicated in Figure **{5.1.5.1}1**, indicates the sensitivity of the vertical and radial (or horizontal) positioning of the temperature measurement point to the actual measured "temperature" (reading) – that is, of course, if the desired measurement point could be identified and accessed, and a technically legitimate measurement acquired. Figure **5.1.5.1}1** also indicates the variance of the temperature profile with processing time.

The "how" relates to the virtually insoluble problems arising from the "siting and sighting" of any measurement device at any (presumably varying) position within the radiantly dynamic thermochemistry of the pyrometallurgical process in progress. This elementary conundrum of experimental methodology presented the more fundamental difficulties that proved to be the most challenging to solve (when "solution" was a viable, practicable option in early experimental heating operations) and which, in essence, was not solved for high temperature reduction operations. Direct sighting of the target emissive surface was a conceptually simple task for optical pyrometry cases, although the equivalent of "sighting" for thermocouple devices might better be considered as "cable access" (through reactor from measurement apparatus to thermocouple tip). Ultimately, both methods of temperature acquisition presented

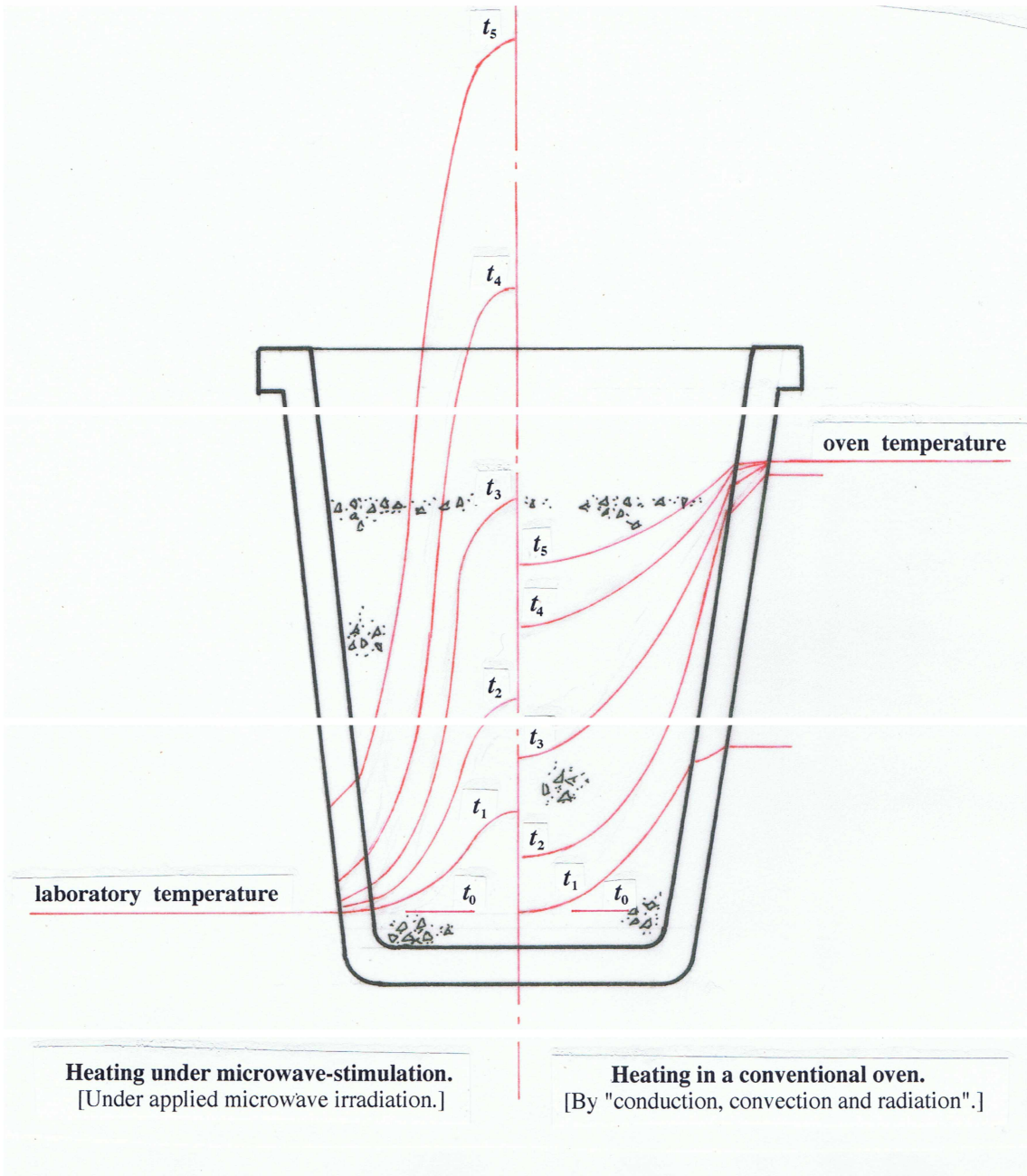

Figure {5.1.5.1}**1:** Schematic representation of temperature profiles as they might manifest in a crucible heating under either simple microwave irradiated heating or conventional closed oven heating. The charge is assumed to be both microwave susceptible and thermally conductive (that is, conducive to heating for each system of heating) – perhaps reaction-neutral Fe_3C in granular form. The system is assumed independent of any thermal contributions from reactions (endothermic loss or exothermic gain to profiles, *et cetera*). Nominal heating times are represented above the point of initiation (t_0), increasing from t_1 to t_5 , these "times" are not necessarily equal for both systems of heating.

insurmountable practical problems in the dynamic thermochemistry existing even in such small plasma pyrometallurgy operations as those that characterised this project.

Inside the microwave cavity, thermocouple cable must be shielded from the interference of imposed electromagnetic field plus insulated in the usual manner from the heat of the oven or furnace environment. Where a thermocouple device was used during this project, insulation-wrapped stainless steel tube sheathing the insulation-bead-clad thermocouple wires was found to be an adequate thermocouple-shielding configuration for the intermediate, in-cavity cable. However, one major drawback remained that, in the reactive pyrometallurgical environment and extremely high temperatures, the crucial thermocouple exposure point, the thermocouple tip, could not be shielded without loss of temperature sensing accuracy. The imposed microwave field, with its electric and magnetic components, was known to (was seen to, and was shown to) interfere with the electric circuit of the thermocouple loop. The principle that makes the thermocouple work (the temperature-dependent current flow across a potential drop induced between two close alloys) makes it fail in a microwave field. The dielectric difference between its wires, as exists at the exposed bead (tip), presents a natural arc point under microwave irradiation. Further, any section of thermocouple wires, particularly the exposed tip, which was open to field interference was therefore open to degradation by arcing and by corrosion due to chemical reaction and thermal runaway effects. Shielding with a microwave reflecting metallic tube close up to the thermocouple tip afforded some protection from field interference, and coating or chemically protecting the tip afforded a measure of corrosion resistance, however, no combination of measures guaranteed satisfactory long-term service for thermocouple devices. The electronic integrity of the thermocouple circuit was at the mercy of the effects of microwave field interaction. Over short-term use, this had the effect (which was observed and recorded) of distorting the thermocouple current in a "hounds-tooth" pattern following the magnetron switching, hence the reading and therefore the converted "temperature measurement" – in part at least, this distortion could be allowed-for in calibration – it must otherwise be seen as routine inaccuracy leading to systematic error.

Keeping in mind that thermocouple-type devices needed to be comprehensively shielded from field interference plus chemical attack and insulated from the extreme temperatures generated, the siting of a thermocouple tip at a fixed point or moving along a locus (descent, ascent or radial) would require, besides a benevolent choice of positioning, a good knowledge of the predicted heating and reaction regimes expected

to prevail dynamically and internally in the reactor. Again, the risk of error is extenuated.

Because the temperatures of interest on the temperature profile exist inside the reactor vessel, the measurement points are blind to operators using either thermocouple or pyrometer devices. The various optical pyrometry techniques require the satisfaction of two essential provisos: firstly that there be a clear and unhindered sighting of a surface at the measurement point, and secondly, that the measurement surface remains unsullied, has a known emissivity range over the measured temperature range, remains intact and, of course, does not melt. Despite considerable efforts to incorporate sighting-aided pyrometry, including purpose-built sealed high purity ceramic sighting tubes inserted into reaction centre, pyrometry methods failed generally on considerations of lack of positioning options, size of device, and unavailability of high melting point materials with both neutral (nil) reaction propensity and known emissivity over the required temperature range (emissivity being calibrated to temperature). High temperature ceramic slumping also negated the sighting requirement, and even *inside* inverted ceramic sighting tubes, the emission surface always discoloured or developed a film that rendered illegitimate the emissivity conversion factors.

In plain terms relating to heating under external stimulation, and as is well known, simple heating of a body under microwave irradiation heats that body from the inside outwards, depth of microwave penetration dependent – the cause arising from the geometry of re-radiation summations relating to the bulk susceptibility or "microwave load" centroid. Whilst for conventional heating, a body will heat from the outside inwards – by thermal radiation, conduction and/or convection (for example, items in ovens or furnaces). So, it follows by intuition that for homogeneous, concentric or otherwise geometrically uncomplicated bodies simply heating by any conventional heating technology, certain minimum facts can be known about the series of temperature profiles between the beginning of heating at time, t = 0, and the end of heating when the set temperature of the oven is reached by the body, when $\mathbf{T}_{\text{BODY BEING HEATED}} = \mathbf{T}_{\text{OVEN}} = \mathbf{T}_{\text{MAX}}$. Accordingly, the hottest point ($\mathbf{T}_{\text{MAX}}$) of the conventionally heating body will always be at the surface exposed to the oven environment, and the minimum temperature ($\mathbf{T}_{\text{MIN}}$) will always be at the body centre. $\boldsymbol{T}_{MAX}$ *can always be sighted* and the position of $\mathbf{T}_{\text{MIN}}$ can be predicted with greater certainty for conventionally heated bodies than can the position of $\mathbf{T}_{\text{MAX}}$ in the profile-reversed microwave heated bodies. Also, for bodies heating under microwave irradiation, the

surface value of $\mathbf{T}_{MIN}$ is relatively trivial as it is not the transport interface controlling the heat transfer into the heating body (as with the conventional case). Consequently, the siting of temperature measurement points and the sighting of them by temperature measurement devices for temperature acquisition is considerably more straightforward for conventionally heated cases. Fundamental to the above was that the penetration depth of radiation was at least equal to the charge radius, thus the temperature peak was central, or near-central in the charge. The case of larger charge sizes, having twin peaks across the temperature profile, remained trivial for this project.

Also, for all cases of this microwave-stimulated project, where chemical reaction was integral with process conception, heat from exothermic chemical reactions ("internal" in the body, or charge) generally increased $\mathbf{T}_{MAX}$ well beyond the realms of simple heating operations and otherwise complicated temperature profiles. The magnitude of the impact on the temperature profile (and the unpredictability of its point of release in process time) of the heat released by exothermic reactions (most reactions) should not be underestimated.

5.1.6 : Reduction Process Termination, Cooling and Solidification.

A major problem associated with the reduction of refractory metal minerals was the cooling of the reduction products from process completion temperatures to stable, ambient temperature without re-oxidation of metallic reduction products. The reactive refractory metals of Groups **4** and **5** form highly stable oxides, sulphides, halides and other mineral compounds. Their propensity to re-oxidise is high to extreme (particularly at reduction process temperatures) in that these metals will themselves reduce most other oxides which may be inadvertently present by experimental misadventure or by impurity in reactants or reactor vessel (crucible) and insulation material. The substantial silica (SiO_2) component in the aluminosilicate fibre blanket used as wrapping and other crucible-intimate insulation, and the similar mullite [$3Al_2O_3 . 2SiO_2$] refractory products was particularly prone to reduction by any of the five core refractory metals.

For such reasons, the cooling of reduction products to stable, ambient temperature must ideally be conducted in a controlled, inert atmosphere or vacuum and reduction products contained within stable refractory material. Whilst cooling rate (of itself) was not identified as being of fundamental conceptual importance in the project, the high reactivity of these metals dictated that high cooling rates would minimise that proportion of reduced phases which would otherwise re-oxidise. Slow cooling of

reduction products under vacuum and/or controlled atmosphere, in all cases attempted, led to appreciable re-oxidation of reduction product phases (even, in accord with visual evidence, by reduction of less stable oxides in crucible and insulation materials).

A method which proved to be successful in avoiding this re-oxidation during cooling was to rapidly cool the reduction process remnants by immediately and totally immersing the terminated-reduction vessel in liquid nitrogen and thence keeping it under a nitrogen atmosphere until cooled. Significantly, this method utilised the compatible joint benefits of an oxygen-free gaseous nitrogen blanket, intimate to and surrounding the reduction product, and rapid cooling rates – which more truly approached *normalisation* rates than the more rapid quench rates – thus minimising the reduction product's exposure to elevated, re-oxidising temperatures. Typical cooling times for this method were in the range 5 to 8 minutes (to sub room-temperature) for average reduction product remnants and largely dependent upon the thermal mass contained in the insulation material attached to the reduction vessel configuration. All indications from the in-crucible products of the fading red-heat glow being dissipated after ~ 3 min of cooling. Oxidation of metallic phases to nitride products was certainly possible during "quenching", however, from evidence of non-liquid-nitrogen cooled products, most nitride phases produced were so formed during high temperature processing under "prior-air" atmosphere (basically $CO/(CO_2)$ in 80% N_2 – plasma adjusted).

Typically for refractory metal reduction product remnants (of reduction experiments conducted in the common crucible configuration), sintered and solid state reduced phases occurred high in the crucible where maximum exposure to the plasma environment was reflected in the product phases remaining. Any (extraneous) liquid phases drained from these upper-level phases into the lower reduction zone – sometimes retarding reduction at lower levels (depending upon the prevailing reduction mechanism). In its descent some of these extraneous liquid phases became entrapped in solid phases, but most of the liquid produced high in the crucible became part of the lower crucible reduction product. Where such "extraneous" liquids existed in the preliminary "pre-core" stages of reduction trials they were likely to represent lower melting point reduction product metals, and so produced, liquid metal pooled in the crucible bottom, displacing the less dense liquid slag and solid phases. All of these physical tendencies combined to accentuate reduction product heterogeneity, which then presented that perennial conundrum of sampling for subsequent microscopical studies and analyses options.

5.2: Heterogeneity and Sampling.

Somewhat exacerbated by the individual idiosyncrasies of small-scale microwave processing, and of overall experimental reproducibility, heterogeneity was a feature characteristic of all experimental products throughout this project. Moreover, the fact that experimental products were, indeed, reduction products of extractive pyrometallurgy – usually rapidly cooled – only served to guarantee a pronounced degree of heterogeneity throughout the frozen product. This degree of heterogeneity was evident both macroscopically in the observed post-reduction vessel and across polished sections of all specimens sampled from all experimental reduction procedures. Not only was there found to be heterogeneity across phases within contiguous agglomerate solids, but also there was found (using EDS) to be compositional heterogeneity across identifiably singular phases, particularly in material from liquid nitrogen cooled product.

5.2.1: Reduction-Product Heterogeneity and Sampling.

Experimental reduction products were typically multi-phase agglomerate masses, even extending identifiably into reaction product of crucible material. Typically for reduction products of refractory element minerals, there were no distinct regional or phase boundaries conveniently separating the major phases existing across the reduction products. This reduction product complexity owed itself largely to solid state reduction mechanisms and to the high melting points of ceramic and metallic phases present in the reacted charge. For strongly solid-solution-metal forming reduction products (such as iron) this was generally not the case as two or more liquid phases existed at reaction temperatures. Upon freezing, large beads or single buttons of metal were produced and were separated from the slag phase by a phase boundary obvious to the naked eye and easily separated by mechanical means. However, for the reactive refractory metals having high melting points and thermodynamically stable oxides, sulphides and other minerals that were difficult to reduce and hold in metallic form, the typical products of small-scale microwave reduction experiments were reduction-phase agglomerates exhibiting both chemical and physical heterogeneities. This general heterogeneity reflected both the lack of process sophistication at laboratory scale and both a degree of incompleteness of reduction and a degree of over-processing (re-

oxidation) as various reduction phases (typically) were evident locally and adjacently in the agglomerate cross-section. Some minor incidental reduction products were "surface coated" products of microwave plasma vapour deposition (PVD). Whilst these PVD phases were indicative of the ion chemistry in the plasma environment of the crucible's reaction zone, the (nominally) metal nitride PVD coatings were regarded as "incidental" products to the more fundamental reduction process.

For this fact of reduction product complexity, then, sampling was a major consideration. In reality, for the more heterogeneous reduction products, analyses such as "percentage total conversion" might nominally require the whole reduction product as "the sample" to yield an accurate result. As the unlikely recovery of 100% of reduction product phases was impracticable (if not impossible because of adhesion to crucible and diffusion into refractory material) and because of the need of some specimen preservation of a portion of reduction products (some for mounting), there was a need of some rationalisation of both sampling and specimen analyses required. The emphasis in specimen analyses favoured *qualitative* analyses rather than *quantitative* analyses because of the complexity of heterogeneity in the reduction products. Quantitative analyses for such heterogeneous specimens (particularly those containing phases having continuously varying stoichiometry as was displayed by some oxycarbonitride (light element) compounds) would have been a pointless exercise offering little insight into process events not already available from qualitative results (and more readily so).

It might seem that a post-microwave-process homogenisation of specimens by vacuum arc re-melting could have circumvented this significant problem (of heterogeneity) by delivering a two-phase specimen (metal plus slag). However, after trialing this approach – with reasonable success, it should be noted – it was found that all "reduction history" locked into the frozen primary reduction product was eliminated, so that *both specimen forms still required characterisation and analyses* in the reporting of experimental results for this formative programme. And further, the creation of a phase-simplified, homogeneous metallic "sum-of-products" specimen did not improve the truth *that the single requisite fact of "reduction accomplished" was neither changed nor advanced.* Consequently, it was decided that such an apparently "desirable" upgrade to specimen "simplicity and integrity" was more likely a luxury at this investigative stage of experimentation. The concept of re-melt homogenisation is re-visited in a later section.

The rationale of "sample collection to suit analysis" had, in response, placed an emphasis on the need to minimise reduction product heterogeneity either by reduction

process extension (time) to minimise phases present and maximise their degree of reduction, or by the post-reduction homogenisation by in-vacuo arc re-melting of agglomerate phases into a consolidated specimen having a simplified distribution of phases. [Microstructural and phase simplification was contingent upon such a re-melt amalgamation of agglomerate phases such that there was a distribution of the ***n*** phases into ***n*** phase fields rather than the **X*n*** phase fields of the agglomerate.] In terms of producing a representative specimen, an unfortunate aspect of vacuum arc re-melting was, beyond phase simplification, that it further processed the composition of the phases present in the solid – not only did it allow some reactions to proceed further in the new liquid mixture under the arc, but vacuum degassing also changed the composition of some light element phases. In certain cases this consolidation and/or compositional simplification might be used to advantage as a stratagem but such an approach was not utilised in this project.

A *sample* must be representative of the body of material to be sampled with respect to the information sought from the sample and the analysis route intended for the sample. If the sample was required for an absolute, statistically accurate quantitative analysis then it must reflect this and be statistically representative of the material body to be sampled – that is, proportionally representative on a compositional basis (physical and chemical, as needs be). The criteria for such sampling would depend upon the degree of heterogeneity existing across the specimen to be sampled and the ease with which each phase could be sampled (where this affects phase proportion taken). In the trivial case of a specimen known to be homogeneous the sampling decision would be simple as all possible samples would be identical. However, as the degree of heterogeneity increased toward the typical reduction product in this project, the "philosophy" of sampling had to be evaluated so that the sampling method provided samples that would be representative. "Representative" was an increasingly difficult criterion to satisfy as the degree of heterogeneity increased in the specimen – and fully quantitative analyses became somewhat meaningless and tended towards the unachievable as the scope of quantitation became quite implausible, forcing a downgrading of required analyses to qualitative, and then only of central metallic product phases (they being relevant to the distinction of "accomplished reduction").

Where, however, at the other spectral end of sampling criteria, a simple "YES/NO" distinction was required – perhaps as to the presence of a phase in a reduction product – then a sample could be selected which was biased toward the presence of such a phase. In reduction product analyses the testing for metallic phases was an obvious starting point when testing for reduction success. However, an equally informative test was to optically inspect or analyse for the starting refractory mineral

remnant in the reduction product – and for the range of intermediate reduction phases. This approach yielded information on the degree of conversion at process termination and on the reduction stages in the process and was generally employed to qualify and recommend further analyses and to review experimental parameters of subsequent experimental trial procedures.

Generally, because of specimen heterogeneity and sampling difficulties, the *sufficient* level of analyses required in this microwave reduction project was at the qualitative level (although quantitative level analyses were performed where possible). From qualitative results – supporting macroscopic and microscopic observation of the reduction product – a meaningful assessment was made of the overall reduction accomplishment (conversion products, the completeness of conversion, and other process factors). Qualitative EDS plus XRD confirmation (where possible) of the presence or absence of phases and the range of phases existing in cooled reduction product was found to reveal much about the process. A physical representation of process events was contained in the *sequence* of phases of the reduction product range evident in polished section – particularly the *intimacy of phases* and the apparent *order of their occurrence* with respect to neighbouring phases.

X-ray diffraction (XRD) analyses of reduction product phases – randomly sampled from reduction product remnants – were conducted to substantiate energy dispersive X-ray spectrometry (EDS) and other results. XRD results were compared with EDS output, corroborated with macrstructural and microstructural detail, and matched to known and predicted metallurgical chemistry. Because of reduction product complexity, XRD analyses were necessarily general in nature with fundamental and dominant phases identified. Some trace to minor phases remained un-identified or were not identifiable as no index records could be matched. The extensive range of possible synthesised carbon forms (with attendant unremitting continuum of peaks) was a major contributor to this conundrum, whilst further contribution was undoubtedly attributable to the presence of amorphous phases and chance artifacts. However, XRD contributed "fresh" possibilities to a general, broad accrual of information about "phases present" – and contributed considerably to knowledge of (or constructive inference about) the essential microwave-stimulated plasma reduction process.

5.2.2: Specimen Preparation for Micrography and Analysis.

For the purposes of mounted specimen preparation, sampled lump and fine material was "split" and a representative sub-sample was isolated for mounting. Where a specific phase present in the reduction product remnants (perhaps metal only) was to be selectively separated for mounting and specific analysis and photomicrography, the fraction was selected under stereomicroscopic examination of a sample split. Specimen phases were occasionally inspected in a sputter-coated but un-mounted condition and cursorily analysed in the SEM. Such exercises were conducted on "first specimens" simply to gain an understanding of the particulate nature of particular reduction products, particularly with respect to their frozen in-crucible position indicating apparent reduction history, and to indicate choice of specimen material and reveal the range of possible material types which should be included in, or precluded from, each specimen mount (with respect to the effects of variable phase hardnesses and friability upon specimen preparation and polishing).

Selected reduction product materials were mounted most commonly in a clear mounting medium – either a clear thermoplastic (Lucite or Transoptic) or a clear volume-constant cold-setting resin. A clear mounting medium was preferred as it allowed visual sub-surface inspection and monitoring of agglomerated material during grinding and polishing thus optimising the choice of exposed material and its final polished surface. Clear mounts also allowed greater control over the grinding reduction of the surface in stages to achieve the best exposed-surface selection possible. Where an electrically conductive mounting medium was warranted for electron microscopy of poorly conductive specimens, or where a superior edge-retentive medium was required for more friable materials, an appropriate thermosetting mounting medium was used (although these were opaque). In the general case, however, sputter (gold or nickel) or evaporative (carbon or aluminium) coatings on inspection surfaces proved adequate for electron beam conduction in the electron microscope and, under appropriate technique, the several clear mounting media alternatives provided adequate edge-retention qualities. In particular, the tough, volume-constant cold-setting epoxy resins assuaged concerns regarding this latter stipulation, although the "next day" setting and curing time was always a drawback with resin-mounted specimens. Elements selected as the conductive coating medium for mounted specimens were so chosen as to avoid EDS spectral peak interference with reduction product components.

Although geological specimen grinding and polishing techniques were often desirable they were infrequently employed, metallurgical grinding and polishing techniques were generally employed with appropriate compensation for the mineralogical (ceramic) nature of that considerable portion of mounted material that was non-metallic. Indeed, some of the "metallic" reduction products were, by some

definitions, "ceramic" – however, by other yardsticks, they (variously) were solid solution metal alloys associated with metallic compounds ranging into the hard material and intermetallic categories. Because components in the specimen material were usually magnitudes harder than the mounting medium, a preparation policy of "rapid cutting" (fresh grinding and polishing media under high specimen contact pressure) was employed to minimise the deleterious metallographic consequences of surface relief between specimen phases and between specimen and mounting material. Generally, grinding of specimens was accomplished on fresh carborundum papers – or a diamond-impregnated disc when required – before polishing on selected papers or napped cloths charged with a diamond paste, spray or suspension down to 1 µm (micron) specification. Final polished state was assessed by naked eye and confirmed by microscopical examination (in the usual metallographic manner).

Polished specimens were extensively examined and relevant details recorded photomicrographically with supporting notes. Some details of certain phases benefited from etching and, where etching techniques were utilised, detail evident in microstructure and microtexture in the as-polished condition was corroborated and contrasted by recording that feature in the identical field after etching. 5% nital was used on ferrous alloys, otherwise, where relevant, alternative etchant details are noted in photomicrograph annotations.

5.3: Strategy of Analyses.

Because of the heterogeneous nature of reduction products the general approach to classification tasks – the characterisation and analysis of reduction product phases – was to be *generally* descriptive in a useful and meaningful way (to support or confirm microscopical observations and interpretations) rather than *definitively* descriptive in a fully quantitative manner. Although fully quantitative analyses were possible, and their execution within the scope of allotted resources and capability of available facilities*, *in virtually all analytical tasks the employment of quantitative level analyses to corroborate results would presume to confer an excessive degree of "certainty" upon the composition of reduction product specimens which, indeed, were highly variable throughout the reduction product remnants.* Consequently, "quantitative" results (which may have been highly accurate at the relevant points of analysis) were deliberated-upon

* Although a "fully quantitative" capability in analytical facilities was generally available, crucial facilities were incapable of fully quantitative analytical work for extended periods on several occasions during the course of this project. The "qualitative" capability was not so compromised.

with due caution and forethought when extrapolating to a "general case" result representative of that phase across the specimen proper. *For this project, where a goal of equilibrated reduction product phases was not an open objective and outright "purity" was not at issue, any pretence to a fully quantitative approach to analyses was regarded as unwarranted.*

Generally, assessment of specimens through this project was accomplished in two mutually supportive stages. The initial stage of assessment encompassed that group of microscopically-based procedures involving the matching of visual (microscopic and macroscopic) evidence, intuitive interpretation of phases and their spacial and apparent physical or chemical inter-relationship (given the starting materials and their positional circumstance in reduction product remnants). The second stage of assessment was the analytical or confirmative stage. This stage might have involved any of several chemical or spectral analytical methods but SEM-based EDS was deemed to be the most appropriate means of providing a level of analytical support of the required adequacy – and, with some constraining exceptions, was usually available as a means of spectral analysis throughout the project. WDS analyses via microprobe were sought on few occasions to confirm EDS results, and XRD analyses also were sought for ground particulate samples of reactant minerals and reduction products to establish "conversion" and to confirm mineral phases present. [For reasons of variable inter-phase bonding and heterogeneity (which are covered elsewhere), reduction product materials could not be easily sampled in a manner that yielded a sample "truly representative" of the reduction product. XRD analyses on reduction product materials yielded complex spectra – a complexity revealing the range and compositional continuity of reduction product components.]

During the course of this project, hope was entertained of a comprehensive level of analyses for all specimens – promise of requisite analytical capability would be met by available facilities and contemplation of successful accomplishment of such a level of analyses was a reasonable expectation. Notwithstanding the above discussion, a programme of qualitative and quantitative analyses was planned to support extensive black and white plus colour light-optical micrography, backscattered and secondary electron-optical micrography, and light-optical stereomicrography. X-ray diffraction was to be utilised to introduce a separate, independently sufficient measure of phase

confirmation, and other complementary analytical techniques were to be convoked where required.

In keeping with experimental objectives and the discussion above, the broad plan of characterisation and analyses for experimental reduction products followed the outline presented below. In general, characterisational and analytical procedures reflected this original plan, however, where experimental practice deviated from that outlined below, the relevant variations are noted with experimental results and/or described in micrographical annotations.

1. Once the cooled crucible was dry, and under guidance of ongoing assessment of the condition of reduction remnants (whether sinter-bonded, agglomerated or friable and loose), "excavation" type recovery of reduction product remnants was carried-out. Recovered materials were set-aside to be split and stored (as described below) whilst phase regions indicating process-significance were set-aside for mounting, preparation and microscopic inspection leading to analyses.

   Under stereomicroscopical inspection, and with selective micrographical recording of reduction product and general remnant details, specimen samples representing the continuum of reduction phases were selected, labelled and set aside in vials for further microscopy and analyses. From these, representative samples of reduction product phases were chosen for metallographic preparation. The chosen samples were duly mounted (in a clear plastic or resin medium which allowed best preparation of exposed area by visual discretion), ground and polished down to a 1 μ diamond finish on an appropriate paper or cloth medium. After initial microscopical inspection and micrographical recording in the as-polished condition, if and where appropriate, some specimens were etched and microscopically inspected and recorded to support the un-etched evidence.

   Mounted specimens typically contained both metallic and ceramic (slag) phases having a wide range of physical properties – particularly hardness and brittleness – and metallographic preparation had to account for these anomalies.

2. Each mounted and polished specimen was objectively inspected across all phases and fields representative of reduction product phases were selected and recorded micrographically, nominally in colour (Ecktachrome colour positive film) and in black and white (where micrographically appropriate). Where etching was employed this micrographical procedure was repeated and emphasis

was placed upon recording the same fields-of-view as were recorded in the un-etched condition. Wherever possible, re-locating and recording of particular fields-of-view was pursued through all inspection stages in order to optimise knowledge of reduction product characteristics and the reduction process.

Some light-optical micrographs of prominently featured areas were taken specifically to be used as references to relocate features under electron optics - a system which proved to work effectively on most occasions. Other reference marker stratagems were deemed to be inappropriate in such complex heterogeneous, particulate fields where introduced reference points, such as microhardness indentations, were not readily re-located and were easily confused with morphological features – especially ceramic chipping and fracturing, and other imperfections attributable to specimen preparation. Despite the initial care taken to identify specific features of significance, some such features could not be re-located under electron optics.

3. Directly after light-optical microscopy, the mounted and polished specimens (with nil or negligible further polishing) were sputter coated (with gold or nickel) or evaporative coated (with carbon or aluminium) in preparation for subsequent electron microscopy. Coated specimens were inspected objectively in the scanning electron microscope (SEM) under both secondary electron and backscattered electron modes of operation and appropriate fields were micrographically recorded in both secondary electron and backscattered electron modes (with image storage to optical disc in the case of the Leica S 440 SEM and later to hard disc storage). Particular attention was given to re-locating and recording, at comparable magnification at the final reproduction, those fields that had been recorded on the light-optical microscope – a task that proved to be more demanding than expected.

4 (i) Selected electron-micrographic fields were X-ray mapped providing a series of area-identical elemental maps (one for each chosen element tested) on each of the selected fields. (Being area-orientated information, X-ray maps were regarded (at best) as qualitative level analyses.)

A system comprising Moran Scientific software through an Oxford Link EDS detector fitted to the Leica S 440 SEM was used to collect and assemble EDS spectra for X-ray maps, line profiles and point spectra. At a later stage, the Moran Scientific software was replaced by Oxford Link software (resulting in some discontinuity in output formatting of results – for uncertain gain). Some

WDS X-ray maps, line profiles and point spectra were performed on a Cameca microprobe and these results, whilst of higher analytical power and presumed higher accuracy, because of their incompleteness in terms of the entire experimental range, were only used to compare with and gage the relevant likely accuracy of EDS results.

(ii) Appropriate elemental line profiles through chosen inter-phase boundaries were generated during X-ray mapping procedures and recorded to support the evidence of X-ray maps. (In league with maps and spot acquisitions, the semi-quantitative line profile process was utilised to confirm "change of composition" variations across phase interface regions.)

(iii) Appropriate EDS point spectra were quantitatively collected from identified points in characteristic reduction product phases in the X-ray mapped regions to identify the phase compositions at those points and to confirm phase identifications interpreted from X-ray maps and line profiles. Spectra were collected to an acceptably high level of quantitation with a good cross-referencing against acknowledged analytical standards or (later) to established software-based standards. This "sufficient" level of quantitative acquisition was considered greater than experimentally warranted for such specimen materials, and therefore adequate when straight qualitative was believed broadly sufficient in the context of its routine "matching" against other means of verification.

Remaining reactively dynamic (in continuing plasma) and phase-diverse prior to cooling, and having been solidified under non-equilibrium cooling conditions of the "LN_2 quench" method, the reduction product phases under analysis were known to be heterogeneous and display continuous (if close) ranges of composition across any section. Such disparity of composition was expected to reflect the state of reduction at reduction termination or subsequent re-oxidation during and after "quench" cooling. So, points of analysis for point spectra collection were chosen in regions apparently representing main phases and away from apparent phase boundaries to best avoid the ever present possibility of disparities arising from phase boundary overlapping of the excitation beam's "Monte Carlo bulb".

Whilst the analysis of each acquired spectrum was quantitative for that point only, it was also regarded as correct and representative of that phase locally identified – and generally representative of that phase throughout the reduction product. It was expected that the collection of point spectra from

discerningly selected regions of discrete phases would suppress or, at least, minimise the effect of local phase-inhomogeneity. The analyses of these spectra were compared with similarly collected spectral analyses and any degree of compositional variation noted. Generally, spot acquisitions from comparable points on similar phases returned analyses in good agreement.

Because of the nature of the liquid nitrogen "quench-cooling" subsequent to termination of the experimental reduction process (under a carbon monoxide atmosphere), the degree of compositional heterogeneity was accentuated, and this trend particularly so in central reduction phases present in the reduction remnants. This accentuating trend was a methodological compromise (versus massive re-oxidation); increased heterogeneity an acceptable alternative outcome given the cooling/solidification methodology. It was an unavoidable consequence of an atmosphere-controlled cooling method whose profound advantages outweighed the lesser disadvantage of accentuated heterogeneity – a disadvantage that could ostensibly be "overcome" by vacuum arc re-melting if required. Also, rapid solidification "freezes-in" reduction-stage phases thereby capturing irrefutable evidence of reduction processes. However, EDS spectra were, at times, complex and spectral analyses were assessed with appropriate analytical vicissitude.

Phases were checked using windowless or ultra-thin window EDS for the presence of light elements (retained (unreduced or re-oxidised) oxygen plus carbon and nitrogen pickup in the reduction chemistry). Lower excitation voltages were used to sympathetically excite light element emissions thus promoting light element K-series spectral peaks and, as an unavoidable consequence, co-incident low energy L-series peaks of other elements present. These low energy peaks were used to correlate with, and contrast against beryllium window EDS spectra of the same field.

5. As a cross-reference for the determination of reduction change and to provide a final confirmative measure of characterisation analyses, a limited programme of X-ray diffraction was carried-out on reduction product materials. To both sustain and monitor this technique, XRD was also conducted on starting reactant minerals (laboratory-grade and commercial-grade "pure" minerals and ore-concentrate minerals), and these core reference spectra used to corroborate "change due to reduction". Changes in mineral phase and/or composition could not only be clearly seen and verified in spectral shifts, but the new mineral phases could be identified by reference to known, indexed values.

This stage of analyses provided proof of pyrometallurgical reduction and, although not exhaustive, analytical confirmation of this was established by identification of actual reduction product phases present in reduction remnants. This proof of reduction was two-fold in that any spectral shift to the reference spectrum (of starting mineral material) represented "chemical change due to reaction under a reducing environment", and secondly, that those identified reduction product phases confirmed to be present in the reduction product spectrum represented reduction product phases (both intermediate and final) which were predicted by relevant reduction chemistry. [Ultimately, some minor peaks – representing peak sets – could not be identified either by automatic machine analyses or by exhaustive manual searching of PDDF files. These peak sets were relatively insignificant, probably represented a minor phase with a trace element component, or were a more convoluted representation of an "unknown" amorphous phase having some limited-range crystallographic order and being the product of the unusual "quench" process.]

It was fitting (also) to acknowledge the impact of the other principal variables of system pressure and "power" absorption upon processes exploiting plasma-solid reactions. Issues concerning system pressure were addressed in an earlier section, suffice to mention here that the pertinent experiments in this project were conducted at atmospheric pressure. Due to resources insufficient to construct further evacuable reactor systems or parts and repairs thereof, the extensive investigation of this important variable was forestalled until a future project. The measurement of absorbed "microwave power" and "reflected power" in microwave systems is typically regarded as crucial in the assessment, characterisation and justification of microwave systems and processes. However, this project was motivated by factors beyond the simple "cost of process" basis of assessment to be centrally concerned with the quality and range of possible products – or to equate, "the cost of processes saved". Moreover, the project was motivated by the possibilities of *products* rather than the economics of the *processes*. Also, it must be noted, microwave power absorption and reflected power are largely inconsequential with respect to the value of resultant reduction products. Consequently, the assessment and characterisation of power absorption and reflected power with respect to systems operation was deferred for this project. Further, had it been adapted into "reactor" designs and experimental methodology, measurement equipment and diagnostic support for such system assessments would not have been readily available to this extraction metallurgy project.

All in all, only so much of the accumulated recorded micrographical and analytical output can reasonably be included with associated discussion and duly presented in any document. In the assembly of the material (argument and evidence) for this thesis most of the acquired data of microscopy and analyses was brought-together for corroboration and confirmation in the formulation and justification of argued discussion; in the development of observations into ideas, and experience into understanding and know-how. Ultimately, some small portion of recorded micrographs and analyses found their way into the sections of this thesis in support of *contention*, *argument* or *discussion*; such selected output was considered pertinent to the thesis. And generally, the project objectives were realised with the support of these co-ordinated offerings of complementary evidence that allowed development of discussion towards fair and reasoned conclusion.

6

EXPERIMENTAL PROCEDURES.

"When everyone is against you, it means that you are absolutely wrong – or absolutely right."

Albert Guinon - *c.*1900.

6: EXPERIMENTAL PROCEDURES.

Section **5** addressed the practical and technical backgrounds of process parameters; the generalities and the intricacies of both heating and reactive processing under microwave irradiation; the gradations of physical and dielectric (electronic) charge characteristics with respect to processing; and the theoretical circumstances against which the experimental methodology was structured. Such ordering of the basics of microwave processing in Section **5** allowed in this section the more open depiction of process principles as they developed from early, exploratory reduction work and, essentially, as they pertained to the core project. This "more open depiction" permitted review and discussion of aspects of procedural experimentation, whereat, such delineative documentation comprises Section **6**. The "early exploratory work" generally included descriptions of particular non-refractory-metal and non-core refractory metal reduction processing trial experimentation that (whilst recounted here) fell outside the scope of this project and is only cursorily covered in Section **7**, *Results*. However, the carriage of such trials formed the bulk of formative experimental reduction processing – providing the foundation for experimental "means and expectations" along the way – and whose reduction outcomes were precursor to process expectations and to key experimental procedure, ultimately crucial to the conduct of this project.

Of pivotal importance in the conduct of the project were the fundamental choice of experimental reduction apparatus and its configuration with respect to the designated mission of the project and the means of achieving that goal. It was anticipated that a microwave reactor featuring controlled atmosphere, an adequate rate of evacuation and high-vacuum capabilities would be developed and utilised throughout the core experimental programme, however, such well-intentioned plans were not to be realised. Nonetheless, a working reactor *was* designed, constructed and experimentally trialled over a range of reduction tasks with notable, if qualified, success whilst the system remained intact. Certain conceptual flaws in the operational capabilities of the reactor were not to be overcome during the experimental "life" of the evacuable microwave reactor. These "flaws" were contained principally in apparatus ancillary to the central reactor chamber, and whilst foreseen at the design stage, proved to be too pervasive to overcome. Concurrently, a deceptively simple, experimentally acceptable system of reduction was perfected which utilised the familiar, well-performed 1300 W microwave oven in conjunction with carbon monoxide atmosphere control supplied by an *excess* of char in the system. Char, of course, also supplying the essential reductant carbon to carbothermic reactions, and the necessary supplementary reductant to aluminothermic reactions – or more correctly, carbo-aluminothermic reactions. The necessity and

attributes of these fundamental processes are described and discussed fully in later sections, as is the crucial but unavoidable decision to bypass the reactor system in favour of the efficient oven set-up method.

The nature of this project determined that the process outcomes as represented in the quenched experimental products would be dissimilar to any equivalent product of a conventional pyrometallurgy route. [Where detected, gaseous by-products were noted as was (if such was the case) their subsequent combustion once vented to air; no post-quench liquid phases where produced during the core experimental programme.] The experimental programme investigated the pyrometallurgical reduction of refractory metal minerals to reduction product phases by microwave-stimulated reduction processing. Such microwave-stimulated processing inescapably included microwave plasma, so reduction events were plasma-pyrometallurgical incorporating the associated plasma-chemistry derived from particle-speciation and the broader phenomenological events typical of ionisation. [Microwave plasma imposed certain system benefits, particularly the sustenance of non-equilibrium thermochemistry that controlled and delineated the reduction process and its products – this most defining circumstance is discussed at length elsewhere.] The solid, post-quench reduction product phases ranged through ceramic to metallic and presented in the reduction remnants as partially reduced (the continuum of partially-reduced phases), reduced (end-point phases) and reversion products, including secondary products (end-point plus post end-point and new reduction product phases). Inevitably, the least complex reduction products were the end-point outcomes of "simpler" pyrometallurgical reduction tasks that were commonly represented in the formative earlier project work. This preliminary period in the experimental programme saw the evolution of procedural protocols during experimental reduction processing under microwave irradiation. Thus developed, procedural protocols were subsumed within the broader edicts of schedule and routine; whence, experimental procedures were well established and understood by that advanced juncture in the programme when the more challenging reduction of stable refractory metal minerals was experimentally addressed.

As suggested in earlier sections, the experimental approach to the microwave-stimulated reduction of minerals varied through the course of this project. These variations to experimental procedure represented fair expression of the responsive interaction between observation and analysis of experimental trials and the application of improvements in experimental technique. Such a "learning curve" relationship between prior observation and next implementation was characterised by a cautious relaxation of "scientific rigidity" in the plain experimental techniques employed, with experimental rigidity progressively succumbing to procedural simplicity as reduction

"expertise" was realised. Of course, progressive changes to experimental method were not only brought about by the consideration of lessons learned from experimental operations but also by unadorned trialing of new ideas and new techniques in the method. The methodologies so described in this experimental procedures section were the simple, best methodologies utilised during the final experimental reduction trials for each mineral case. Where process improvements were determined and instigated during experimental trials, the essential details were recorded and are noted herein and/or in the following Section 7. Such improvements tended to be variations in processing time, ratio of solid reductant to reactant mineral and their distribution within the charge, insulation configuration (thickness and type), and the degree of atmosphere control employed (the means of carbon monoxide blanketing leading into LN_2 "quench" cooling). Inevitably, such variations were necessary concessions to the "thermodynamic (or thermochemical) stability" of each mineral in terms of its reduction propensity as represented in Ellingham diagrams.

6.1: Experimental Materials and Equipment.

Minerals of refractory metals and other minerals used in this project were either raw mineral-processed ex-mine minerals, or were commercial or laboratory grade refined minerals of "good" to high purity and known composition. Raw minerals being either minesite-derived ores (such as haematite and magnetite) or ore-derived mineral concentrates (such as rutile, ilmenite, zircon and wodginite) with assigned assays. Refined minerals were commercially available minerals of specified purity or commercially available high purity oxide minerals used in the production of guaranteed purity ceramics or other products, or were laboratory grade minerals used for analytical and laboratory syntheses purposes, both groups of good to high purity and having guaranteed quality control over composition (specification). Compiled in Appendix **6.1** are the source and geographical origin (as provided and/or to the best of knowledge) of each minesite-derived mineral listed together with its chemical analysis (assay) *if and as provided to the project* (that is, variably specific and not necessarily exhaustive) whilst, similarly, each commercial and laboratory grade mineral is provided with relevant specified purity and principal minor and trace impurities. It was decided that the expense of seeking further, independent specific analytical assays for "mine-derived" and "commercially available" minerals was not justified given the fundamental character and intent in the project's "primary reduction" mission.

The greater emphasis during this project was on accomplishing and verifying the fact of extractive reduction under microwave-stimulated processing more so than on the absolute degree of that reduction. Also, the "degree" of reduction was invariably complicated by an unavoidable proportion of re-oxidation and related over-processing in the reduction product. So, as such, concise knowledge of trace elements in starting minerals and analytical precision to the same degree in reduction products (which, without melt consolidation, displayed marked heterogeneity) was regarded as somewhat excessive – particularly given the degree of possible contamination afforded by the very high temperatures in the reduction zone, the minor scale of the operation and the novel nature of the process. Main contamination possibilities were from refractory materials, gangue content of starting minerals, char and the pervasive gaseous nitrogen, N_2 plus ionisation species.

Auschar®, a low mineral-matter Victorian brown-coal-derived charcoal was used as principal reductant in early, exploratory experimentation. In some preliminary work when intimate reactant compacts were reviewed as a reduction strategy, a brown coal slurry (supplied by the Morwell operation of the Victorian Brown Coal Board) was used to create a paste of the reactants which was extruded or shaped and dried before reduction (to prevent the compact from explosively exfoliating when steam was generated rapidly under microwave irradiation). These reactant compacts were typically reduced in the presence of loose Auschar as carbon monoxide producer for the atmosphere protection blanket around the reaction zone until quench. The mineral matter in both the char and the dried coal (slurry), about 1% to 1.5% (variable) in total of Fe, Si, Al, Mg, K and S -bearing clay and rock minerals, had the potential to introduce a proportionally greater percentage of impurities into the reduction product. Consequently, to eliminate this impurity potential, activated charcoal – being a high purity carbon form – was utilised as the sole carbonaceous reductant in all core experimentation in the project. Whilst highly microwave susceptible (dopant and surface area effects aside) the brown-coal-derived carbon forms were found to be, if anything, modestly less reactively susceptible than the activated carbon forms.

During the project, two activated charcoal products were used. The first employed (and used through from the early experimental campaign pre-dating the core experimental campaign) was a Dupont™ product which (until it ran-out) was used exclusively through all of the core experimental tasks except for the anatase reduction sequence when an equivalent Norit® charcoal product was used in replacement. The extremely high surface area to volume ratio of these activated charcoals must unquestionably have provided a reactivity benefit to the rate of gasification of carbon during reduction operations (to provide CO at reaction interfaces on/in the mineral

being reduced), plus the miniscule amount of $BaCO_3$ activation agent minimised surface tension on reduction-evolved liquid-metal prills thus allowing the growing prills to coalesce and flow into liquid metal beads, thence to drain and "pool" in the bottom of the crucible where, thus consolidated, to be quenched to a metallic button. In practice, this repeatedly was the liquid consolidation path for the easily reduced metals such as Fe, Ni, Cu, Sn plus most others, and for incidental reduction product alloys such as bronze, for the higher melting point refractory metals. However, for reduction products of the core refractory metals, even with the efficient surface tension attenuation assistance of $BaCO_3$ – and with perceptible "temperature" presumably adequate to melt solid-state reduction products or to keep liquid-state reduction products molten – this "grow and flow" procedure did not characteristically progress past the *in situ* formation and growth of tiny metallic prills. Indeed, sinter-agglomeration (of reduced-phase specs) seemed to by the consolidation route followed by the key reduction products of experimentation. This particularly so where reduction products were found to be metal/light-element solid solutions or compounds as was the case for reduction products in each of the three classes of refractory metal minerals and as can be seen to advantage in numerous of the micrographs presented in Section **7**.

The charcoal products were utilised in both "as received" form (< 1.5 mm; cylindriform to equiaxed granular) and as a very fine powder as ring milled from the as received form to 100% < 5 μm for blending or, for greater reactant-intimacy, ring mill blended *with* reactant mineral to 100% < 1 μm. This ring mill blending was restricted to limited duration to avoid process-supplementation by any possible "incidental process consequence" that might be derived from the corresponding chemistry of "high energy milling". The blend-milled charges, enhanced by carbon smearing and the creation of common interfaces, were destined to allow a more beneficial reduction regimen once under microwave processing.

Generally, the reactant charge blends were prepared by the stoichiometric proportioning of milled char with each mineral reactant (plus aluminothermic-Al where appropriate) then blend milling enough fine intimate blend to supply the whole experimental campaign for that core mineral. This allowed consistency of blend stoichiometry in each charge, the details of stoichiometric proportions for all principal mineral blends are provided in Appendix **6.2**. Loose granular char charged below and above the reactant blend charge was also weighed before charging (details in Appendix **6.2**) to keep consistency of overall microwave load (for each mineral) as "seen" by the microwave field and drawn through the magnetrons. In all cases, and to a consistent degree, more reductant than was stoichiometrically (theoretically) necessary was assigned to each experimental charge to assure reduction (thermochemistry permitting)

plus to provide more than adequate CO atmosphere to the reaction zone environment until quench. [This excess C was present in blend powders at 120% of stoichiometry plus that overwhelming excess as CO from granular char.] That is, CO adequate to massively overwhelm any tendency towards oxidation (or re-oxidation), and as was discussed in Section **5** (and in Section **6.2** below), this seemingly inelegant solution (to the problem of oxidation prevention during processing and prior to quenching) actually worked very effectively. It was presumed that, partly because of its simplicity, and because of the reductive capacity of gaseous CO and its complementary plasma species, this unadorned method out-performed other more technically rigid attempts (involving argon atmospheres, evacuation and vacuum procedures in varying stages of devolution towards this simplest procedure) to achieve the same result and, comparatively, at minimal expense and effort.

The equipment used and the configuration of that equipment and materials during microwave reduction processing was as described in previous sections, especially Section **5** and as represented in Figure **{5}1**. Further to note that, by the inception within the overall programme of initial core experimentation, the relatively simple experimental apparatus configuration within the microwave oven (as Figure **{5}1**), and the established experimental procedure were adopted as the "default standard" which was to be utilised across all core microwave-stimulated reduction operations. The only process variations across core experimental reductions were the variables relating to process initiation and duration and the thermochemical (physical and chemical) properties of the reactant minerals, reductant(s) and gaseous participants (reactants and inerts), and reduction products. These entities include such obvious aspects as processing time (both within and across reactant species); the variation in charge mass between reactant species (due to variation in densities between reactant minerals and to process stoichiometry); the relative microwave susceptibilities and dielectric interactivities within the charge (dielectric "lossiness" and the microwave load); the variations between reactant minerals due to their reactive reducibility and the relative in-crucible reduction process "temperatures" reached by each reactant charge type – including reactant type; the partial pressure characteristics of participant and product species; and most centrally to overall process chemistry were the collective properties of the physics and chemistry of the induced plasma in the reaction zone of the process. Of essence in this plasma environment, its population and distribution of numerous excited, ionised and recombined particles (ions, atoms, molecules, electrons and photons) all at energies above ground state, and superimposed upon the lesser "background" chemistry of species in their ground state – the numerical bulk of the "environment". Whilst fundamental to reduction processes throughout the project, it was necessary to consider *ad valorem* the thermochemical properties of these collective

energetic states, however, their specific investigation was not within the scope of this project – but must be in the scope of any "next generation" study.

6.2: Oven Setup Versus Reactor Vessel Systems.

In recognition of the degree of thermochemical intransigence associated with project reduction tasks – and as commitment to that same primary metallurgical undertaking of the reduction of very stable minerals under microwave irradiation in the presence of plasma – early in the life of the project considerable emphasis was placed upon, and effort assigned to conceiving and fabricating an evacuable reactor which met the quite demanding requirements of such a mission. Much, of course, was already known (from initial investigative activities in the standard R2370 microwave oven) about the task of microwave-stimulated reduction and what might be expected when the processing parameters were changed by introducing such a controlled atmosphere system as the reactor represented. It was decided that, given reasonable scientific diligence during procedures in the working reactor, such a controlled atmosphere reactor would add rigour to the experimental method and acceptability of investigational procedure and results.

In proceeding with design of the reactor vessel, the overriding problems that had to be resolved before design could proceed to fabrication were manifold – and each anticipated solution tended towards mutual exclusion of another. Moreover, for this fundamental concept to become the reality, reactor and process parameters were re-visited, reciprocal ideas regarding component functions were re-examined, process expectations were challenged and contending solution-alternatives weighed-up and prioritised so that a functional reactor with genuine if modest capabilities evolved – pragmatically rather than idealistically – from realistic, practical compromises. Such options, however, precluded certain equipment alternatives-of-choice whose quite reasonable inclusion might more credibly come into the ambit of a vanguard, "next generation" reactor development.

6.2.1: The Reactor: Concept, Development and Trials.

The initial microwave reactor – for there was a second reactor built and tested but in which no project work was performed (covered briefly in Section **6.2.3**) – was

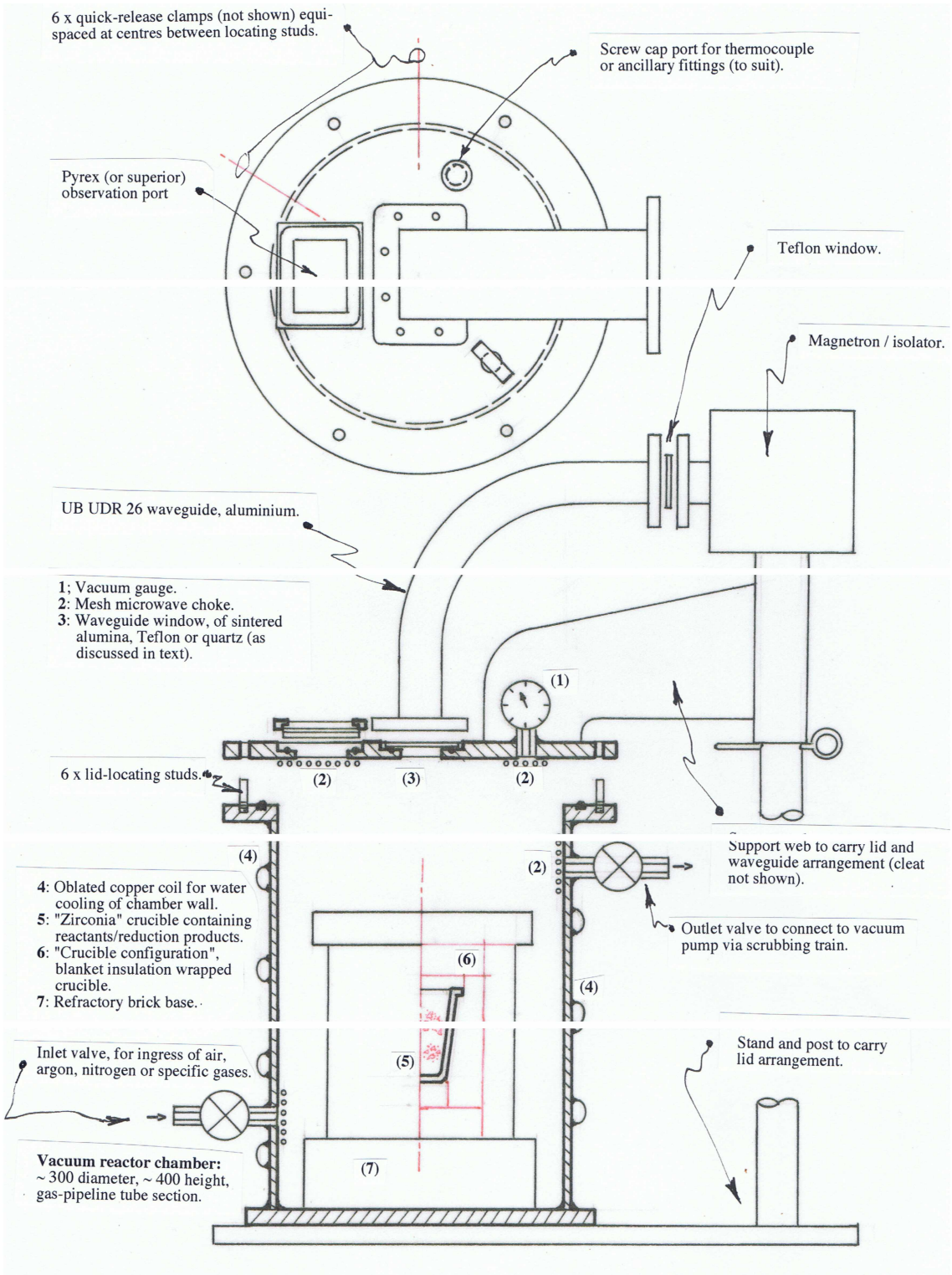

Figure {6.2.1}**1:** Drawing showing the evacuable, atmosphere-controlled microwave reactor with crucible configuration as operated prior to its "abandonment" – rather than by failure of concept or results – because of the endemic malfunction during preliminary trials of under-developed ancillary systems necessary to its essential functioning.

serviced by a standard 2450 MHz, 650 W magnetron system which delivered microwave energy by means of a waveguide and introduced into the upright cylindrical chamber through a central waveguide port in the reactor chamber lid. [A less successful, 5 kW variable power unit replaced this 650 W unit during the latter stages of the reactor campaign (refer to Section **6.2.2**).] Also incorporated in the lid, in functional arrangement about the waveguide port, the chamber's pressure gauge, cleat connection for radial support arm, a screw-cap port through which a sheathed thermocouple (or other) could be inserted and sealed, and an observation port (quite apart from clearance for the clamping devices with which the lid was secured). The central waveguide entry port was so located to suit the in-chamber wave-form manifestation of the microwave field, and the overall layout was configured in such a way as to be practical for the other services, but was otherwise not specifically crucial and is shown in Figure **{6.2.1}1**. [The chamber dimensions (diameter and height) in relation to its expressed microwave field and the waveguide entry were subject to fabrication availability (of pipe section) and consequent design advice provided by the University's microwave group of electrical engineers [107].] Near the base of the chamber, an inlet tap-valve was provided for the ingress supply of inert or other gases into the chamber's atmosphere or to flush after and/or in league with evacuation. Also in the chamber wall, and radially opposite the inlet valve, but sited close to the top of the chamber just below the lid-line soffit, was the all important outlet valve – key to basic chamber evacuation and the in-process pumping of off-take gases and volatiles, all by means of a standard rotary vacuum pump through "expansion bellows" to capture off-take solids (also refer later). Generally, the number of appendage ports and valves was kept to a minimum to minimise the possibility of random leakage into the chamber (whilst under vacuum) at vacuum seals and at fabrication points on and around the reactor vessel.

Once at atmospheric (room) pressure and whilst the chamber lid was un-clamped, to facilitate access to the chamber and maintenance therein, the lid could be swung aside by means of the cleat/radial arm arrangement which was centred in the same vertical plane which contained the centerline of the waveguide and shared the same vertical axis contained in that plane. Hence the lid and waveguide could quickly be swung aside clearly to an adjacent support thus allowing attention to in-chamber post-reduction recovery matters, maintenance and subsequent experimental preparation. Later, with minimal inconvenience, the lid with intact peripheral accoutrement was swung back into position and clamped for next use. To assist with chamber cooling, oblated copper tubing was coiled around the chamber's exterior vertical surface and, providing comprehensive contact, brazed into position such that when cooling water was run through the tube during reactor use a maximised heat sink effect was achieved.

[Heating of the reactor vessel chamber and components was considered to be detrimental to process wellbeing and to the longevity of reactor components (seals, windows, valves and tubing, welds and brazes, vacuum gauge, vacuum pump, *et cetera*). Of course, peripheral cooling such as this was acknowledged as essential to good experimental management of the reactor system (as plant), but concurrently was considered non-pivotal to the process and its thermochemistry.]

During fabrication and pre-trial testing, once the "theoretically reasonable" reactor was developed beyond draught idea towards a working concept, perceived problems in processing needed to be addressed-in-review and various crucial elements in component design and specification were to be resolved to advance the reactor concept into a working reality. As it transpired, finalisation of reactor design hinged crucially around certain recurrent, familiar concerns – concerns quite common in elevated temperature microwave applications and related processes.

Firstly, as microwave power was delivered into the reactor chamber by means of a standard 2450 MHz waveguide conduit (British Plain UDR 26), an impervious and microwave-transparent waveguide window was required which, whilst remaining impermeable to gases, was capable of withstanding the lateral stress (bending moment deflection leading to catastrophic crack propagation) induced by the pressure difference between waveguide and chamber, and by local thermal stresses. Here a compromise was required as microwave transparency recommended window thinness, whereas, window rigidity (strength) and impermeability demanded window thickness. And further, noting that the chamber would rarely be at greater pressure than the waveguide's (general external) atmospheric pressure (and even then, minimally so), but operated generally with positive pressure on the waveguide side whilst the chamber was being pumped-down.

Secondly, and as the complementary property to ambient strength, strength (including toughness) at elevated temperatures was, in its absence, the property most preclusive in material selection. Not only was the selected window material to be able to withstand high temperatures, but also resilience to thermal strain under the high gradients of temperature (across any window profile) was crucial to window durability (including "multiple-use" longevity). Material durability here was defined as its capacity to resist in-service catastrophic failure under the combined torque loading of a deflection-induced stress-disparity continuum plus the counterpart stress-disparities induced by local thermal expansion discrepancies conjointly leading to unconstrained crack propagation. Material toughness was required for the window.

In addition to thermal resilience and durability, and thirdly, the chosen window material was to be reactively inert, or at least chemically "durable", under exposure to the range of reactive contaminants and reduction products to which it variously was to be exposed during the process range of the reactor environment. Accordingly, and being nominally both chemically "inert" and microwave "transparent", the three materials considered for fabrication and use as waveguide windows were the oxide ceramics alumina (sintered Al_2O_3) and re-crystallised quartz (silica, SiO_2) and the polymer PTFE (polytetrafluoroethylene, or Teflon®). Although commonly and successfully utilised in many low-to-mid range thermal applications, of these the stabilised quartz was rejected because, at high temperatures, the quartz became disposed to phase changes, grain growth and accompanying softening at high process temperatures. In such state the silica was quite vulnerable to the impinging of contaminants upon its surface, sites and regions that then became microwave susceptor centres – the window, no longer microwave transparent, would progress rapidly towards failure. [Phase transformations (at 1 atmosphere of room pressure) in crystalline silica follow the following changes: low-quartz transforms into high-quartz at 573°C; high-quartz transforms into tridymite at 867°C; tridymite transforms into cristobalite at 1470°C; cristobalite melts to liquid at 1713°C [219]. Also, and separate from the "impinging contaminants" liability, because the window was sufficiently removed (thermally) from the reactive environment of the contained reactants and associated plasma, silica reactivity to CO, *per se*, was not a problem at the window sites. However, silica reactivity was a reality in the reaction zone for exposed refractory insulation materials containing silica species, and reflection on this plasma-based phenomenon is offered below (in Section **6.2.2**) as resultant fume was a principal source of window fouling during microwave processing.]

Although extra in-chamber protection against radiant heat was provided, predictably, Teflon windows were found to soften in the high temperature reactor environment and also thinned by corrosive pitting – particularly in the hotter, structurally crucial window centre (indicative of waveguide node point heating) – and were found to have a campaign life of two to three experimental procedures. Further, points of "reactant impingement" represented sites of chemical or thermal failure. However, a Teflon window was employed successfully as the waveguide window at the top of the radial waveguide elbow between the radial elbow and the waveguide section connecting the magnetron microwave source.

In terms of in-service rigidity, the thermally best-performed windows were of alumina. However, these sintered alumina windows (whose manufacture required individual casting to size prior to sintering of the "green" ceramic) were imported from

the U.S.A. and were considerably more expensive than either of the other window types (which could be more readily fabricated). Alumina windows were used in the initial experimental reactor trials and were found to be well suited to the less than ideal, non-pristine operating conditions. However, despite their overall superiority, after a number of experimental procedures, and given the gradual thermal and contaminant-driven deterioration of the cast ceramic window surface, lack of strain-toughness under differential thermal expansion caused each waveguide/reactor window to catastrophically fail, thus releasing the vacuum and resulting in the termination of the process to minimise further system damage. [Upon a suggestion from the microwave engineering group, a laminate composite of Teflon sheet clamped intimately between two alumina plates to form a waveguide window was trialled in an actual microwave reactor reduction. However, the benefit derived from the composite-sandwich window was actually less than the sum of its perceived advantages rather than greater as was the intended bestowed benefit. Dielectric interactions between the erstwhile microwave transparent materials were exacerbated by the reactor-side corrosive nature of the process and the different physical properties of the ceramic and the polymer components. Also, separately trialled, waveguide-side air-cooling of the window caused its own stresses in the window material – separate to existing process-derived stresses – and was found to be, at best, of limited benefit.] It should be noted that each window failure required window replacement, vacuum seal testing, and repetition of the experiment. After the few available alumina windows were expended, Teflon windows were fabricated and used with reasonable success, although, because of softening, corrosion pitting and thinning, Teflon windows had a usable life of only two or three experimental runs of limited duration before pre-failure replacement. This "anticipated failure" strategy evaded unwarranted "failed" outcomes and saved a number of experimental results of that preliminary trial programme.

The fourth prominent consideration regarding waveguide windows was the vital consideration of vacuum seals around the waveguide port and other port types in the reactor lid. It was, however, the waveguide window port seal that proved most problematic and, in system failure and seal replacement inconvenience, presented the most common disruption to in-service seal application. The waveguide seal (alone) was subject to the material property foibles associated with the transmission of microwave energy via standing waves in the waveguide and the consequential effects of that energy and its transmission upon an imperfectly transparent window and imperfectly reflecting waveguides and associated metallic components, all of which heat, testing the thermal resilience of the Vitor high-temperature compound seals used. Wherefore, with a few exceptions, seal replacement typically accompanied waveguide window replacement.

In comparison to the waveguide window and seal, the seals, materials and application selection considerations for other service ports and valves were, over the course of the reactor programme, of little trouble both in use and at recurrent reactor maintenance. The observation port window was, initially, a compromise between size (area) and structural strength of the thick, thermally resilient borosilicate (Pyrex®) glass viewing port – which proved to be thermally durable in service – but between each use, to retain window transparency, needed to be cleaned of the contamination tarnish resulting from process fume. Integral with the window glass was the absolute requirement of a fine mesh "microwave choke" to eliminate the passage and escape of microwaves through the viewing port. Such mesh or gauze application can, upon close inspection, be seen in the viewing window of all domestic microwave oven doors. [Similar to other human organs, but genuinely more vulnerable, the eye is particularly prone to attract incidental or stray microwaves – to great detriment.] Where required, such borosilicate windows and mesh chokes were easily replaced. A Vitor O-ring seal was used in the removable dummy cap of the thermocouple port, the seal also supported the un-used thermocouple cap fitting. [In the relatively short period over which the reactor was utilised, a thermocouple was not employed during microwave processing (because of the previously described microwave interference phenomenon).] Being unlikely to fail or be otherwise affected during reactor use, the vacuum gauge spigot was a welded and brazed fitment as shown in Figure **{6.2.1}1**. Inlet and outlet valves were also soundly brazed fitments. The containment of microwaves exclusively within the waveguide system and reactor chamber was of absolute importance. As with work throughout the project, the system was continually monitored for microwave "leakage" using appropriate microwave leakage detectors – with particular emphasis being given to perceived leakage "weak points" around windows, doors or lids and chokes, plus brazes, welds and other points of fabrication.

With waveguide window, observation port, and other valves and service port seals and materials selection criteria decided, reactor process matters could be more closely considered. Because the reactor concept was contingent upon evacuation-based atmosphere control during experimental reduction processes, it was fundamental to initially examine, thence continually assess, the atmosphere control capability, the evacuation limit of the system, and the vacuum recovery response of the system under actual reduction processing and consequent generation of off-take gases, volatiles and fumes (smoke and other ultra-fine precipitate solids). Under such conditions, system evacuation was captive of the limitations set by both the vacuum pump capacity and its inevitably diminishing pumping capability due to gradual, unalleviated (by adequate filtering) vacuum oil contamination by off-take gases, fumes and vapours (including

H_2O from both system moisture (including humidity) and as incidental reaction product). Even the (un-recommended but fraught) inclusion along the outlet tube between the reactor and the vacuum pump of a bubble bottle, as expected, did not fully eliminate the problem off-take fumes and volatiles, but more than replaced these with the predictable water vapour which was just as debilitating in the vacuum oil as the fume and volatiles. [Alternatively, other spirits and oils were considered to replace water in the bubble bottle, however, all practicable possibilities were no less volatile than water. The bubble bottle apparatus did not work using vacuum oil, which was too viscous to be effective as such, but may support a real alternative if a revised bubble system is devised. Alternative in-line pre-pump gas scrubbing options were not available to this project.] A plausible alternative solution to the contamination of vacuum oil (and/or its continual replacement) was to replace the rotary pump with either a diaphragm vacuum pump and/or a higher-vacuum-rated turbo molecular type pump, both of which are non-oil based in principle. However, the former alone may have too low a vacuum capability whilst the very costly latter may be too damage-prone to particulate ultra-fines in the off-take gases – and neither option was available to the project. Also, an in-line cyclone apparatus may solve *most* of the off-take gas problems. [No matter how successful the outcome of any experimentation may have proven during the project, it was understood that the experimental programme would remain constrained by its pre-pilot bench-scale status, and as such, (realistically) was limited in its access to desired facilities.]

The vacuum pump available to the microwave reactor programme was a quality mid-range rotary vacuum pump in excellent repair and capable – as established in evacuation tests – of efficiently evacuating and holding system vacuum in the empty, un-irradiated reactor vessel in the range 20 to 30 Pa [~ 2.0×10^{-1} torr, or ~ 2.64×10^{-4} atm] The vacuum range was "independently" verified by colleagues and repeatable over several trials. And, further noting that exactitude in vacuum measurement was not an outright requirement here as will necessarily become clear in following paragraphs. Under reduction processing conditions – and acknowledging processing variations between reduction assignments – the vacuum status changed predictably with chemical interactions between charged reactants and with reactive plasma species heralding the generation of process gases, volatiles and fume and consequently increasing the system pressure in the reactor. Typically, under reduction processing – and dependent upon the gas-make rate – the reactor pressure rose into the processing pressure range (by interposition from gauge pressure) of from 8,000 Pa down to 200 Pa under continued evacuation. This processing range of pressure proved to be as ideal as it was favoured in sustaining the non-equilibrium CO plasma that characterised reduction processing in the microwave reactor (as it does in microwave reduction processing generally). [The

population of reactive plasma species was known to increase with increasing overall species population (or increasing pressure) in the reactor or equivalent environment – an argument for processing at the maximised pressure that also provided no loss of non-equilibrium. A marked population loss of reactive species was known to accompany any transition from non-equilibrium to equilibrium at given temperature and pressure (refer to Section **4.5**) although the fact of microwave-stimulation would stave-off such transition until about atmospheric pressure.] Once reduction processing was terminated (by desisting with irradiation at the adjudged reduction end-point) the continued evacuation steadily returned the chamber to maximum attainable vacuum. Ideally, maximum vacuum was required during cooling when quenching was not employed, and/or when repeated Ar-flushing was used (in league with evacuation) to displace reactive gases and volatiles. However, when liquid nitrogen (LN_2) quenching was employed in later experiments, the evacuation was ceased and valves opened at the LN_2 introduction point when N_2 gas evolution required its constrained but adequate escape. The reactor lid was not immediately opened but left to thermally equilibrate until it was reckoned that the reduction product had been cooled to ambient temperature above the remnant boiling pool of LN_2 – now below the reduction product level and still cooling the system. [Cooling below zero degrees was not desired, but could easily be achieved as the temperature of boiling LN_2 is about –196ºC (77.4 K)[219].]

Heat generated both by simple microwave heating of the reactor and reactor contents (including experimental materials) and by exothermal reaction chemistry, plus (where relevant) energy released at plasma relaxation (photons) as the excited and ionised states of species decay to lower energy states, was (without quench intervention) dissipated eventually through the heat sink bulk of the reactor walls or, to a minimal degree, was transported out of the reactor chamber in flushing inert gases via the vacuum pump. The initial reactor concept stipulated reduction product cooling by cooling the entire reactor chamber and contents under vacuum, or Ar-flushed vacuum, which (it was understood) would take several hours with the crucial reduction product being last to cool. The shear length of time this cooling necessitated, even under tight vacuum and with no observable "misadventure", invited incidental re-oxidation in some refractory metal reduction products (Ti and Zr), even (as observationally suspected) by oxygen exchange with adjacent oxide ceramics – in the silica component and particularly where fireclay crucibles were used. The solution, it was hoped, would be interventional "quenching" using liquid nitrogen (LN_2) – initially introduced through the inlet valve, thence through the opened thermocouple port until room temperature was reached.

The obvious advantage of LN_2 quenching was the cooling rate, but it was also recognised that the rapidly cooling mass was quickly enveloped in cold gaseous N_2 thus displacing any remaining oxygen-based oxidising gases. It was also acknowledged that N_2 was "oxidising" in the strict sense, so the formation of nitride "reduction" products in the evacuated reactor could, it might reasonably be inferred, only occur in metals that had been "fully" reduced prior to LN_2 quench. However, the more important advantage was the outright rate of reduction product cooling, which "modestly" approached a true quenching rate, but could reasonably be categorised as a normalising rate of cooling.

Despite the vagaries of "temperature" measurement [220] throughout the project, some informed estimation was required. So, consequently, whilst the "bulk" reaction zone temperature for the typical experimental reduction was known* to be in the range 1700°C to 2000°C (with localised temperatures around arc perturbations reaching magnitudes higher [58, 80] reflecting the upward temperature discrepancies of ionised and excited species), for the purpose of estimation, the upper temperature of the reduction product (the "hot spot" in the charge) was assumed to be 1700°C at the onset of the LN_2 quench. Also, for the typical case, the mean quench time to "room temperature" was consistently close to 8 minutes for the oven set-up and about 20 minutes average for the bulky reactor configuration. Whilst this gave a simple linear quench rate of 3.5 C°/sec for the oven set-up and 1.4 C°/sec for the reactor – of course, for these systems under rapid cooling, the overall linear cooling rate was shallower than the sub-linear quench curve during high quench rates over the initial stage of cooling, thence flattening-out as the limited LN_2 was incessantly depleted and the remnant thermal bulk became a "thermal millstone" – the final "ambient tail" of the curve approaching the horizontal at a low rate of cooling. There was no realistic possibility of deliberating a "precise" quench rate curve as there was no exact knowledge of the terminal temperature prior to quench nor any "guarantee" that the quenchant LN_2 had direct and unrestricted access to the reduction product being cooled (especially considering N_2-gas-blanketing around hot solids). Nor was there "infinite" pooled LN_2 quenchant as there was no possibility of unfettered supply of LN_2 into the cooling reactor chamber. Also, little was "pre-emptively" known about the precise nature and thermal conductivity of the heterogeneous reduction product over the temperature range of the quench. Also, there was resolute impracticability in attempting to site and hold a sheathed thermocouple arrangement near reduction product location at temperatures exceeding "sheath melting-point" – firstly through irradiation arcing, thence through the

* From experimental evidence both by reference to thermodynamic and chemical data, and in keeping with reference to actual physical evidence of captured phases existing in the reduction products and evident by interpretation from light-optical characterisation studies and/or by weight of various radiation-based analyses. [This important aspect is covered elsewhere and again addressed in Section 7.]

quench sequence – this exercise would embody a thesis topic in its own right. And, as it was of marginal impact upon the project objectives, any further quench information gained would not have justified the endeavor.

Generally, the quicker the reduction product could be brought (down) to room temperature in the controlled atmosphere of the chamber, the less the possibility of attendant incremental re-oxidation (by reclamation from oxide ceramics and system leakage (as distinct from CO or N_2 "oxidation")). Depending upon the total thermal "mass" of the insulated crucible arrangement plus the enclosed reduction product (charge remnant) and the hot reactor chamber (under water cooling), the cooling of the reduction product to a temperature approximating room temperature took between two and four hours *under vacuum or inert gas flow and without LN_2 quench*. As previously intimated, and by confirmation of experience, such cooling times allowed too great a magnitude of opportunity for re-oxidation for such slow cooling to be experimentally acceptable. The same (reactor) system cooling under LN_2 "quenching" took upwards of fifteen minutes, depending upon the quantity of LN_2 available, its "coolant proportion" to the cooling mass and the provisional capacity to allow the boiling-expulsion of N_2 gas from the chamber through open-able valves prior to lid-release after sufficient cooling. However, and by any order of introduction of LN_2 into the reactor, the larger size of the chamber plus the relative inertia of its combined thermal mass meant that the cooling time to room temperature of reduction products was considerably longer for the microwave reactor than for the LN_2 quenching of a comparable reduction product in the smaller, already cool quench chamber used integrally within the microwave oven reduction procedure.

6.2.2: Reactor Trials: Evaluation and Comparison with Oven Set-up.

Although the project intention was to develop and utilise the controlled atmosphere microwave reactor for the purpose of achieving the declared goal of microwave-stimulated reduction of refractory metal minerals under essentially controlled conditions, by the time of the reactor trials much more was understood about the capabilities and experimental integrity of the deceptibly simple alternative, the "microwave oven set-up" method. Whilst the microwave oven set-up allowed a modicum of atmosphere control, it conceded any real prospect of true atmospheric evacuation and vacuum control, conversely, the reactor could not realistically deliver such control during the crucial processing period because of the integral, unavoidable "gas make" – essential in the case of CO – once the microwave reduction process was

in progress. Although conducted at atmospheric pressure, the oven set-up was operated with an evidently very efficient, effective CO-atmosphere "blanket" which proffered sufficient protection until the similarly efficient LN_2 "quench" in the LN_2 quench chamber (as represented in Figure **{6.2.2}2**). Despite this unexpected good fortune conferred upon the programme by the quintessential fundamentality of the simple oven set-up in both operation and outcome(s), it was conceded that any future extension of this primary, concept-based reduction experimentation was undeniably linked with an improved vacuum-based or (at least) evacuable, controlled atmosphere reactor system which might become available in a next generation project.

Of the two systems, comparatively, when processing analogous reduction tasks, it was easier to attain correspondingly successful experimental results using the simple oven set-up. Although technically comprehensible, reproducibility including the retention of reduced metals of such "noble" oxides through such rudimentary processing was not expected. Indeed, the sidelining (and hitherto, the abandonment) of the controlled reactor concept in favour of the oven set-up method was, both as methodological means and as project direction, an outcome which was not foreseen when the reactor was being developed. In its demise, as bold as the reactor may have presented – for it *was* moderately ambitious (in keeping with the project) – the basic reactor system held greater potential (than the oven set-up) at all levels of technical consideration and process consequence. Irrespective of any "learning curve" effect, some trial outcomes implied a degree of validation of this potential.

Despite the not unreasonable number of system and operational "hiccups" for the new reactor – *most* of which were duly dealt with without notable down-time – some significant results were achieved over the relatively few experimental trials. A strategy of varied trial reductions was implemented to attempt to assess the likely true capabilities of the newly commissioned reactor – both reductive (plasma-chemical) capabilities and operational capabilities. In the initial trial run a composite blend of zircon ($ZrSiO_4$) and "red mud" – an intractable, problematic Fe-rich waste by-product of the bauxite to alumina production stream – was carbothermically reduced to yield, after vacuum cooling only, a carbon-saturated re-oxidised mass containing discrete prior-zircon grains of silica (SiO_2) shielding partially reduced zirconia (ZrO_2) zones. Significantly, these partially reduced zirconia zones contained reduced, metallic phase flecks – minute but easily observable in both light optical and electron optical microscopes and large enough to yield accurate windowless EDS results certifying the

near total absence of oxygen in the metallic phases and near total oxygen allocation in the clearer (LOM) or darker (EOM) zirconia remnant – signifying (in the latter) either

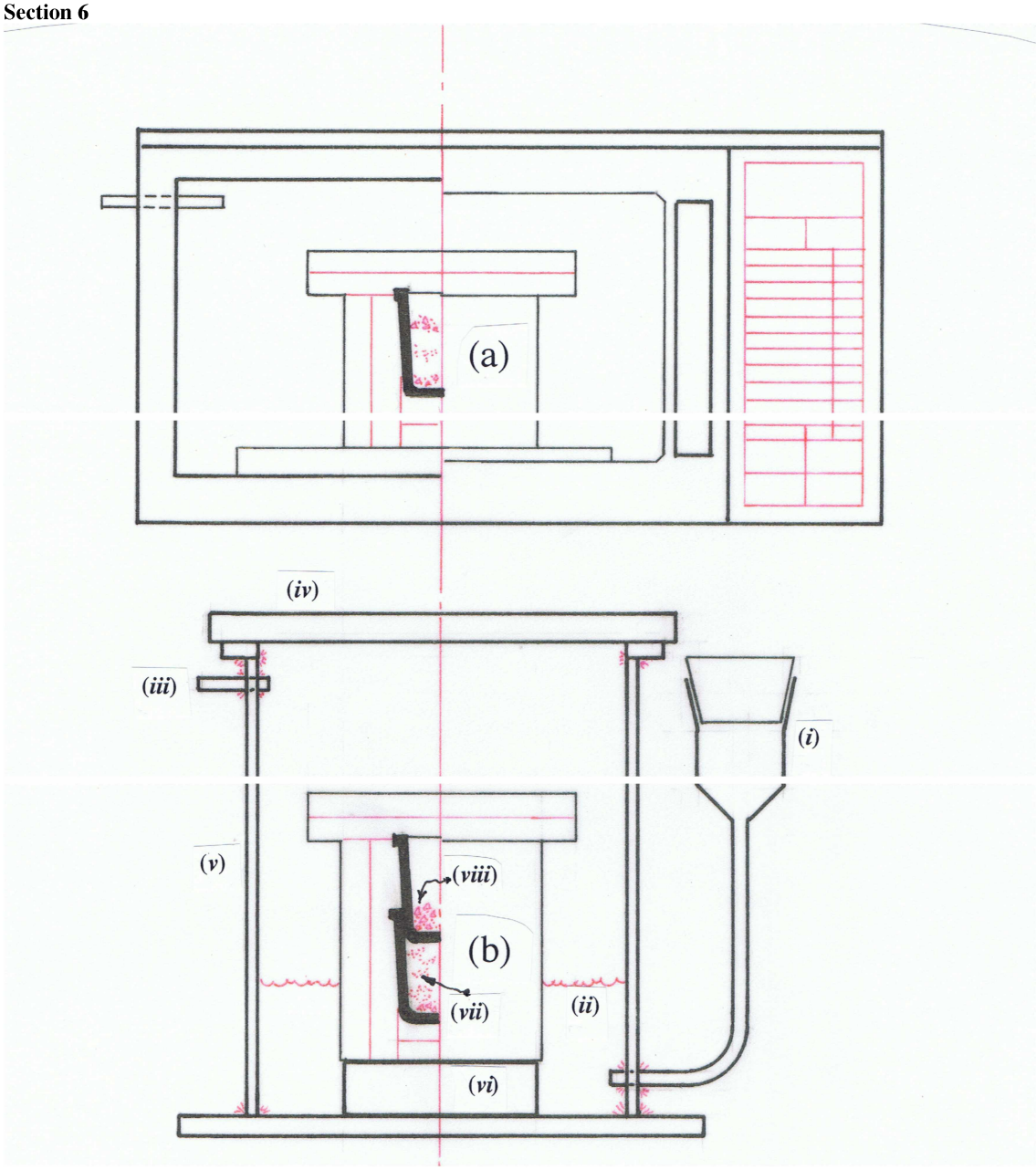

Figure {6.2.2}**1:** Drawings schematically representing the microwave oven set-up and the LN_2-"quench" chamber indicating "quench"-cooling procedure. The ***carbothermic*** crucible/insulation configuration, **(a)**, is shown in the oven, whilst the crucible/insulation configuration for ***aluminothermic*** operations, **(b)**, is shown in the quench chamber. Where still "freely removable" after processing, outer layers of blanket insulation were quickly removed before quench immersion (to minimise thermal load, and thus "quench" time to ambient temperature). The oven set-up is as per Figure {5}**1**, otherwise (***i***) is the fabricated copper thistle-funnel (with rubber bung) inlet arrangement for LN_2 introduction into chamber (all Cu-Cu and Cu-steel connections silver-soldered), (***ii***) boiling liquid nitrogen "quench" bath to generate extended gaseous N_2 – so to displace air, O_2 , CO_2 , and other oxidising gases, (***iii***) gas outlet, principally N_2 , (***iv***) heavy steel lid, loose for quick placement and adjustment, (***v***) cylindrical tube-section chamber (steel components welded), (***vi***) solid stainless steel block (of high thermal mass) to provide an efficient conductive "heat sink" close to reduction remnants, (***vii***) aluminothermic reactant blend, and (***viii***) reactant-isolated char granules for initial heating and to supply additional CO-atmospheric protection during microwave processing.

lack of reduction or, more likely, of re-oxidation – especially as the reduced phase was contained centrally *within* the plasma dissociated prior-zirconia. [A comparable outcome, of sorts, was later achieved in the oven set-up.] The second reactor trial reduction was a carbothermic reduction of anatase (TiO_2) which yielded a high degree of reduction from the oxide to the metallic and metal carbide phases thence evidence of reversion re-oxidation by both oxygen (during initial "vacuum" cooling) and by nitrogen (belatedly during LN_2 trial quench from moderate temperature). Both initial trials employed the intimate blending of finely divided reactants, although the zircon was not fully milled (powdered) from the as-received mineral sand starting size. For the fine zircon grains, the resulting plasma dissociation tended to effectively further attrite the grains by separating multiple SiO_2 and ZrO_2 fractions (as described elsewhere).

For the third reactor trial the extremely stable mineral monazite ($(REE,Th)PO_4$) was chosen to further test the reactor system's capacity to reduce thermochemically highly stable minerals. [Again, as with all reactor trials, the reduction route was carbothermic – for safety reasons, and to protect the constructional integrity of the reactor vessel and its configured system during the "learning stages" of reactor use, thermite and metallothermic reactions generally were considered too risky – exothermically and explosively – to conduct in the enclosed, thermodynamically enhanced environment of the chamber.] The monazite was intimately mill-blended with activated charcoal and charged into a crucible under excess course charcoal, well wrapped in blanket insulation and secured in the reactor.

The reactor was evacuated to vacuum pump limit and then irradiated at the full 650 W of magnetron-delivered power for a lengthy 30 minutes – well past the observed peak of thermal radiation emitted from the reaction zone through the encasing insulation and with gauge-indicated vacuum returning towards maximum (vacuum) suggesting that the process gas make had effectively terminated. With the termination of irradiation, the chamber was flushed with high purity argon (Ar) gas (to atmospheric pressure thence evacuated), the Ar-flush repeated, thence the chamber kept under evacuation during a 2.5 hour cooling period until the reactor was touch-cool when the reactor chamber was again filled with Ar gas. The Ar inlet rate was then equilibrated with the newly decreased evacuation rate and (under Ar at 1 atmosphere) further heat was removed with the evacuated Ar through the vacuum pump. After 30 minutes the "heat flushing" process was terminated and the system allowed to further settle for an hour whilst reduction product recovery arrangements were attended-to. Here it should be noted that, during the last stages of reduction and early cooling, the observation port window was gradually coated in a dark, opaque substance with ensuing gradual loss of visibility and even the premature loss of transmission of red-heat radiation from the

insulation bulk. It should also not go un-remarked that this trial reduction was cooled without the aid of liquid nitrogen (LN_2).

Upon opening the reactor it was found that the entire exposed surface areas inside the reactor chamber – including the external surfaces of the wrapped insulation, the exposed base of the reactor, its wall from base to lid, and the lid including the observation and waveguide windows and the chamber-side details of all valves, gauge and similar – were uninterruptedly coated in up to 1.5 mm thickness of lightly deposited, tan to brown labile phosphorous (later confirmed to be pure, untainted P). Whilst much of this vaporous, miasmal P was evacuated with off-take volatiles (and was a devastating contaminant in the pump oil), what remained as precipitate coating of this intriguing reduction product of the phosphate group (PO_4) was recovered before the crucible and contents could be accessed. Contained within the remains of the largely melted crucible was the reduction product remnant of the rare earth element/thorium (REE/Th) plus gangue mineral balance. In the case of this particular monazite, the principal metallic elements involved were Ce, Y and Th with gangue elements Si, Al, Zr, Ti, Fe and Mn in ranging percentages. [Group **3** element yttrium, Y, is often found in co-occurrence with REE's in mineralisation exhibited by resource ore minerals.] The contained reduction product was a complex heterogeneous oxycarbide mass of the combined metallic elements for which EDS analyses provided two essential phase types – both oxycarbide – the minor phase being of Ce, Y, Th and Zr and the major phase was comprised of the metallic element balance.

After three "successful" experimental runs using the reactor, further experimentation saw the onset of system problems and failures of ancillary elements (waveguide windows, seals, *et cetera*). Consequently, trials in the remaining period of the reactor campaign were conducted somewhat intermittently as maintenance allowed the return of the reactor into the programme. Further to the maintenance tribulations, the originally intended (and long promised) but belated addition to the reactor of a more powerful microwave system delivered a variable power supply (designed specifically for the reactor by colleagues from the electrical engineering group) which did not enhance reactor performance. Consequently, the exchange of the reliable 650 W microwave power supply for a nominal 5 kW variable power 2450 MHz magnetron-delivered microwave power supply saw an upper limit of 2200 W available for delivery into the reactor vessel. Whilst delivered power could be varied up to 2200 W for processing use in the reactor vessel, power level settings above 2200 W were contra-indicated by microwave diagnostics conducted during in-chamber tests (by others from the electrical engineering group). This "contra-indication" could be simply observed by surveillance of "reflected power" on the relevant indicator gauge of the power supply

unit, and was also easily detected by quite noticeable, undesirable waveguide heating. For whatever reason, at any power setting – even 650 W – the 5 kW variable power system did not apparently possess the synchrony of wave manifestation in the waveguide and then as expressed in the chamber; nor the power delivery efficiency inter-relationship between wavelength and chamber as did the original 650 W system.

The variable power microwave supply was installed (and replaced the 650 W system) mid-way through the following experimentation. Nominal evaluation of the new unit had not been fully realised before the reactor itself was sidelined pending project re-assessment, then abandoned, because of the intractable nature of the vacuum oil problem and *its* terminal effect on the reactor programme (within this project). No attempt to amend the 5 kW system, nor to revert to the 650 W power supply, was pursued as neither could reinstate reactor function without the evacuation problem being realistically solved.

Input microwave power aside, the remaining reduction experimentation in the reactor was centred on carbothermic TiO_2 reduction exercises including reduction in the presence of Fe_3C which, it was expected, might capture reduced titanium in solid solution or as TiC particles contained in C-saturated iron. A varied range of experimental outcomes was achieved depending upon whether the functional elements of the reactor remained intact for the course of the experimental trial. In summary, when the system maintained its integrity for the course of the trial, the reactor produced encouraging results on (straight) anatase reduction – results comparable to those of the equivalent oven set-up experimentation – and TiC rich iron products from anatase/Fe_3C carbothermic reduction. In the cases of carbothermic anatase reduction, the various acceptable reduction product outcomes all presented TiC as the dominant phase with evidence of Ti metal in the silvery metallic product as distinct from the bronze metallic lustre of the comparable reduction product of reduction in the presence of N_2 as was the case with the oven set-up or, to a much lesser extent, when LN_2 quenched from reduction temperatures. Reduction exercises carried-out using the new variable power system seemed to be inseparable in process event, time and product from the equivalent reduction carried-out using the 650 W unit. Ostensibly, this was thought to be simply the outcome of the lower power 650 W system's greater efficiency acting to roughly equilibrate the results of the two power configurations but, in hindsight, was largely to be expected in terms of process outcome. Thereinafter, despite patient persistence with the reactor's foibles, its increasing maintenance demands and the ultimately insoluble vacuum pump oil maintenance conundrum, and after re-appraisal of the oven set-up "strengths and weaknesses" and their impact upon project objectives, the decision was taken to move the project's experimentation from the controlled atmosphere microwave

reactor to the microwave oven set-up with relevant acknowledgement of the minor variation in experimental aims and outcomes. The project duly advanced utilising the microwave oven set-up, with few setbacks and results improving with experience.

It must be reaffirmed that, for reasons of continuity-of-method (and outlined in Section 7), none of the reactor-derived reduction product specimens form part of the formal specimen suite(s) contained in, and defining this thesis; although, they are contiguously representative where reduction task-equivalence exists. However, the above brief overview is proffered because of the significance of their reactor-sustained syntheses and, where relevant, their comparability to the adopted, lesser microwave oven set-up system.

Even more so than was quite visibly evident in oven-based experimental work, and as covered in Section **4**, the reactor process outcome of the gasification of silicon was not only easily observable through the observation port, but was of genuine nuisance value as it was a prime contributor to the steady contamination of the observation port window (as white SiO_2 precipitate fume condensed there). Also, because the gasification reaction was dependent upon *both* adequate available energy (temperature) in the reaction zone *and* the random or incidental presence of silica in that zone, the generation of SiO gas did not always take place. The following equations become relevant in and above the upper cristobalite silica phase at about 1700°C (non-equilibrium thermodynamics dependent) in the presence of CO plasma, plus immediate reversion as the SiO gas and oxidising CO_2 escape the reaction zone plasma and drop below 1700°C.

Above ~ 1700°C: [here CO* represents CO in either excited or ionised state.]

$$SiO_2 + CO^{*}\uparrow \rightarrow SiO\uparrow + CO_2\uparrow \quad \ldots \quad \{6.2.2\}1$$

Below ~ 1700°C:

$$SiO\uparrow + CO_2\uparrow \rightarrow SiO_2\downarrow + CO\uparrow \quad \ldots \quad \{6.2.2\}2$$

Or, alternatively, if and where relevant:

$$[\ SiO\uparrow + \tfrac{1}{2}\,O_2\uparrow \rightarrow SiO_2\downarrow\ ] \quad \ldots\ldots\ldots \quad \{6.2.2\}3$$

(For Equation {6.2.2}**3**, being more energetic, monatomic O may replace the molecular O_2 in air under initial microwave irradiation.)

6.2.3: Abandonment of Reactor for Oven Set-up.

In the relatively short campaign life of the microwave reactor, vacuum oil contamination and the related limitation to pump efficiency, continual oil maintenance and, in due course, anticipated damage to the vacuum pump and integrated system, proved to be the most intractable ongoing system problem-set. Without access to other, non oil-adsorption based evacuation technology, the contamination conundrum (alone) proved to be necessary and sufficient reason to discard the reactor programme in favour of the apparently inferior but better performed microwave oven setup. Other significant factors which mitigated towards support for this decision were the greater operation time in the reactor with less control over freezing of the reduction product at process end-point; the higher level of down-time including process-to-process maintenance, cost and replacement availability of windows, seals and repairs; the higher requirement for consumables (bottled high-purity Ar, insulation and larger crucibles, and cryogenically supported LN_2); and the need for greater monitoring, safety and security of and over the reactor vessel whilst in use. Furthermore, without the oil contamination problem, these operational disadvantages could have been tolerated within an ongoing otherwise-successful reactor programme. Ultimately, sooner rather than later, and with some disappointment, the pragmatic and obvious decision was taken to discard the controlled atmosphere microwave reactor in favour of the simpler oven setup method for the remainder of this extractive metallurgical reduction project.

The early indications of success of the initial microwave reactor gave rise to the commitment to, and subsequent design and fabrication of, a second, larger "improved" reactor that was to be used also by other groups whilst remaining available to this project. The new reactor chamber included decidedly improved features which addressed chamber rigidity (convex lid and thicker, stainless steel construction) and better seal facilitation to the larger chamber which was designed to better suit the microwave power supply (a new 10 kW variable power unit). Whilst the new reactor vessel displayed a propensity to actively "heat" target test loads positioned appropriately in its polished stainless chamber, its allocated vacuum pump, similar to that on the original reactor system, was of insufficient capacity to evacuate and hold the chamber at a metallurgically meaningful level of vacuum. [Also, it must be recalled that the original reactor "failed" as a compounded result of the process chemistry and its off-

take gaseous products and their detrimental effects, whereas it "heated" well and could sustain good vacuum prior to and outside of reduction processing.] Whilst a few trial "heating-only" tests were conducted with a view to utilising the new reactor system for project work, it transpired that reduction experimentation in the pristine chamber was not to be allowed by edict of the majority experimental interests who, requiring the chamber to remain "pristine", were separately to go on and conduct chemically neutral sintering trials and to measure electrical field dynamics and perform related microwave diagnostics. The new reactor system would similarly have had the same off-take gas and vapour evacuation shortcoming which eliminated the original reactor system and, significantly, by the time of the "replacement" reactor trials, this microwave reduction project had moved-on fruitfully to the oven set-up programme of experimentation and initial real project results were being generated.

In review (and with the deliberation of "20/20 hindsight"), the evacuable, controlled atmosphere microwave reactor gave way to the conceptually inferior but functionally superior microwave oven set-up utilising atmosphere control (of reactant species dominated by N_2 and CO and their energised derivatives) at atmospheric pressure and engaging the thermochemistry of microwave-derived non-equilibrium plasma. Such efficiency of microwave energy delivery was attributed to the highly effective oven cavity design and microwave delivery of the conventional Sharpe R2370 and R2380 commercial microwave oven models. The further significant advantage the oven set-up possessed (with respect to the reactor) was the separate quench chamber which had the great advantage of being pre-cooled at quench inception, plus it allowed a more effective liquid nitrogen quench and reasonable monitoring of that quench process. Ultimately, for the reactor system, the project-bound shortcomings (as discussed in the preceding sections) were not regarded as insurmountable when projected onto any future reactor development, probably with in-line cyclone(s) and cooling options to filter off-take gases before the vacuum pump. Without doubt, the development of a "next generation" microwave reactor holds exciting prospects – it was seen to be the only real, aspirational option for future, expanded experimentation in this field.

6.3: Crucible Setup and Processing Parameters.

The crucible setup as configured within the microwave oven (as shown in Figure **{6.2.2}2**) was configured about a resilient, high-temperature-rated zirconia/

alumina crucible (of ~ 50 mm overall height, ~ 18 mm internal base diameter, ~ 32 mm at internal top, ~ 3.5 mm wall thickness and realising ~ 16 ml holding capacity – the fired crucible being materially comprised of fine zirconia aggregate in a filler/binder of ultra-fine alumina). As previously described, the crucible was double wrapped in Fiberfrax™ Durablanket® 25 mm thick aluminosilicate blanket with double base and lid pieces to suit. The zirconia/alumina crucibles used commonly and with considerable success throughout the formal experimentation were about as tall as, but volumetrically smaller than, the (nominal 50 ml) fireclay assaying crucibles which were used for the lower temperature early reduction work.

The blanket form of insulation was ideal for this wrap-application as it could be easily cut, shaped, wrapped and generally formed to suit the tapers and curves of the bound crucible into which the protective granular-reductant layers plus reactant blend would be charged. Whereat, as an unavoidable consequence of this "fabricating to suit", the aluminosilicate blanket insulation underwent a degree of compression when deformed by the curvature of wrapping and when secured by tying such that the compression (with its decreased thickness with increased density) had the effect of reducing the nominal insulation rating of the blanket product. However, the insulation as secured for each crucible – and which was equitably comparable for each experimental trial – performed satisfactorily, if no more than adequately so, under thermochemically difficult and unusual conditions (atypical of insulation specifications) for most applications of the experimental trial series. [Where the (collective) insulation and/or crucible were/was deemed to have failed during experimental processing, that trial was rejected and the experimental procedure repeated. Such "failure" was, of course, a subjective-based decision and much depended upon the stage in the reduction process at which insulation failure occurred, the apparent effect upon the reduction product (if at a late stage), and/or whether the failure should otherwise be adjudged to disqualify the reduction product result for any reason.]

Recorded trial profiles inevitably included cases of varying product performance including "thermal hollowing" in insulation depending upon both local and overall thermal history of each experimental trial. When local process temperatures exceeded its temperature rating, the blanket material was disposed to "hollow-out" and recede from the affecting hot zone. This hollowing-out came about because the loose, matted-

fibre insulation's molten volume collectively occupied only a small fraction of the initial fibrous blanket volume. Insulation hollowing was a constant feature of the underside of blanket lid-pieces, this being the blanket surface which saw the greatest direct heat radiation and which (outside of the crucible) was most intimately exposed to chemically reactive species and the ionisation chemistry of the plasma. Whilst blanket insulation crucible lid-pieces thermally and chemically eroded, rigid crucible lids of various specifications generally failed abruptly (and terminally for that trial) by the mechanism of thermal-stress-derived failure, or "thermal shock", delivering collapsed ceramic fragments into the crucible. It serves to reiterate here that, despite the nominal thermal (temperature) rating of any ceramic material, rather than to (its) chemical stability and refractoriness, its resilience to thermal shock was found to be correlated more so with the actual porosity of the ceramic and its apparent density. This presented the allusion of circumstantial dependence of longevity upon porosity – where the higher the proportion of porosity – typically presenting in the material as interconnected vesicular structure – the longer its in-service life under microwave irradiated heating. In future design work for microwave systems, such an uncannily direct relationship between service life and porosity could over-ride the need of, and the correlation difficulty associated with, the application of any coefficient of expansion calculation across the complexity of a porous continuum.

Once the crucible was securely wrapped in insulation the configuration needed to be fixed in such a manner that the insulated configuration held secure through the experimental procedure. Contrary to prevailing opinion and unsolicited advice, the most successful method of fixing the insulated configuration was found to be the use of electrical wire, independently looped twice around the body of insulation – one upper, one lower – then twist-tied and "nipped-off" in such a way as to tighten the loop thus squeezing the outer insulation blanket swathe. This pair of electrically conducting loops, on each occasion and to varying degrees, drew much of the initial applied microwave field energy – carrying in the loop an electric current captured from the electric phase component of the imposed "electric/magnetic" microwave field and concurrently attracting significant electrical arcing because the loops were not grounded to the metallic oven walls. The arcing phenomena persisted until such time as the wire, once exceeding red heat, finally fused into a series of molten beads over a short "hot spot" length and breaking the loop circuit. Thus broken, the circuit wire drew

no more current and rapidly cooled, attracting less and less arcing as the intended load – the reactant charge – began to heat and overwhelm the wire remnants as the primary susceptor of the applied microwave energy.

The whole "wire arcing-to-failure" process extended up to about one minute, but typically the wire loop arcing process was over in less than 20 seconds – before the charge had had time to significantly heat. [It was known from observations of charcoal "test heats" in the standard crucible set-up, that the level of observable micro-arcing immediately and expansively increased once the securing wire loops had fused allowing the reactant charge to receive the majority of the applied microwave energy.] At the section of fused wire where the loop was broken, the fused metal also reliably fused itself to the adjacent insulation material thus (evidently) adequately securing the wrapped blanket insulation for the duration of the experimental trial. Also, once heated beyond a certain point, the insulation blanket tended to "bond" to its adjacent like-kind material. Almost no un-raveling of insulation wrapping took place on insulation-configured crucibles whilst reduction processing was under-way.

Essential and prevalent amongst the processing parameters were the charge configuration, the choice of reductant and its form; the type and level of atmosphere control through to cooled reduction product including the quench process; the degree of microwave irradiation and the control over consequent plasma in the reduction zone(s) of the charge; and the duration (elapsed time) of the reduction process (campaign). Fundamental amongst these was the choice of reductant and the projected reduction route – defined by and including the reduction processes, including pre-plasma and plasma thermochemistry, and whether the reduction route required manipulation in view of desired reduction product(s). Also, the choice of reductant was known to influence all other parameters. As each of these factors is appropriately and sufficiently addressed elsewhere, they are only briefly addressed here in the context of their inter-relationship as processing parameters in this microwave-stimulated reduction project.

Of course, once a reduction route was tested and confirmed in operation, the reduction products found to be acceptable and desired, and the process corroborated as

reproducible, then process-to-process manipulation became obsolete and precise monitoring of en-route thermochemistry, whilst essential, became superfluous to process-to-process needs. However, laboratory notes were made of each experimental exercise with particular emphasis on a time-interval based assessment of observed thermal and ionisation phenomena including a "temperature" assessment of the reaction zone and a prediction of the stage of the reduction process.

In the reduction of such thermodynamically stable metal oxides as are subject of the project, the list of possible reductants must include elements which can, at some temperature and pressure, form oxides of greater stability than the oxide being reduced. For the refractory metal oxides of this project, two choice types were plausible. Firstly, at the very high temperatures (> 1700°C) available in this novel reduction technique, reduction processing could be carried-out with any of a number of carbon forms in carbothermic reaction; or secondly, at lower reduction temperatures in metallothermic reactions utilising metals of the "*even more* stable" oxides. These metals could nominally come from the list of the more common highly-reactive metallic elements: Ca, Ce, La, U, Li, Th, Mg and Al – of these, only Ca, Mg and Al were at all viable in context of this project. [U and Th are toxic and dangerously radioactive; Be is toxic and carcinogenic; Li, La and Ce are relatively scarce – and all are dangerous in finely divided form.] Of the three possible candidates, finely divided pure Al powder was chosen as the metallothermic reductant – and even then it was employed in conjunction with char so to provide the thermite-initiating heat of reaction plus the reducing atmosphere control of CO until quench.

Because of the use of carbon as the direct or indirect reducing agent in the project, some understanding of the "oxidation of carbon" and the fundamental importance of carbon as reductant was required before further account. To this end, it could be readily demonstrated from plots of relevant free energy changes involved in the oxidation of C, that CO_2 was more stable than CO below ~710°C (at atmospheric pressure) and that the reverse is true above that temperature [17]. [The imposition of plasma chemistry upon the CO_2/CO balance imposed some degree of variation that is discarded here in the context of this exposition.] Also, it is recalled that gaseous CO_2 was an oxidising agent whilst CO is highly reducing. Further, CO formation was especially important because it took place accompanying a considerable increase in entropy that delivered, with increasing temperature, increasing thermodynamic stability of CO [17, 58]. Ultimately, for this project investigating the microwave-stimulated reduction of refractory metal oxides, process outcomes could be prudently interpreted by reference to the relative Ellingham diagram(s) (see Figures **{3.1}1** to **{3.1}5**) – essentially, such interpretation was contingent upon the inferred reduction of their

oxide(s) by carbon or another metal or species having a higher affinity for oxygen under process conditions. Concurrently, the metal being reduced may also have a strong affinity for carbon and, if so, a metal carbide (MC, MC_2 , *et cetera*) may be formed rather than the "pure" metal (M). The five refractory metals central to the project were all strong carbide (and nitride) formers and, in the exploratory work of the broader project, copper and tin were the sole examples of a post-reduction "pure" metal product.

Without exception, susceptible extractive metallurgical charges and comparable chemical systems under microwave irradiation heated faster and from the centre outwards, a dual advantage that, of itself, would provide sufficient process benefit to warrant adoption over conventionally heated systems. Moreover, microwave processing in such systems was not to remain a mere analogue of the conventional process-series of physico-chemical events – there was a shift from the "conventional" process-equilibrium into non-equilibrium. This divergence was because of an idiosyncratic confluence of physical properties and scale between electrons and the applied field. Because of the wavelength (at 2450 MHz frequency) of microwaves utilised in this project (and as they were over the range of wavelengths common in microwave processing), the susceptible light electrons in outer orbitals plus free electrons followed the oscillations of the electric field vector of the applied microwave field and were captured by that electric field as increasingly energetic free electron particles. Whilst continuing irradiation maintained this electric field component, the free electrons continued to receive the electrical energy, storing it as internal energy. These increasing energy levels were interrupted by elastic and inelastic collisions with other gaseous particles whose energy was thus increased, and the overall system was driven further and further from local equilibrium into non-equilibrium – the degree of non-equilibrium being the disparity between particle energies in a system with respect to those in the system at equilibrium. Because of this means of stimulation, microwave-stimulated plasmas can operate over large frequency and pressure ranges and can typically produce homogeneous, large-volume non-equilibrium ionised gaseous environments that are ideal for chemical processing [80, 226]. In such non-equilibrium plasma chemistry it is the electrical discharge (manifest as gaseous micro-arcing) that delivers the activation energy to initiate plasma-chemical reactions; and for non-equilibrium plasmas, energetic free electrons may exclusively deliver that energy. Free electrons acquire their energy by two mechanisms – universally, (as above) by exposure to the electric field component of the applied microwave field, and by interaction with other energetic particles. In non-equilibrium plasmas such as microwave-stimulated plasmas, the free electrons were known [80, 90] to acquire electron energies of up to 10 eV – an intensity of

particle energy that freely supplied the stimulation for excitation and ionisation of heavy species and, notably, was sufficient for the breaking of chemical bonds.

For the non-equilibrium plasmas of the project, the highly energised free electrons, particularly at microwave generated micro-arc discharges, act to initiate plasma-chemistry reactions. The fast, energetic electrons do this by collisions with gas atom and molecule species hence exciting these species to higher energy levels, thereby losing portion of their energy. Whilst the electrons replenish their energy from the electrical field, the collision partner (now with higher energy) is able to dissociate or otherwise participate in reactions. Thus energised above ground state, the plasma-constrained species are available and energetically favored for process-chemical reactions *beyond* the purely intra-plasma ionisation reactions – that is, the gas/solid phase and solid/solid phase reactions representing the intended process chemistry of reduction. To over-simplify this, **energetic free electrons replenish the plasma and largely supply activation energy of reactions, whilst energetic heavy particles are accountable for the substance of process chemistry**. Also, where energetic enough, photons were capable of initiating chemical reactions (as represented in the three Equations **{6.3}1**, **{6.3}2** and **{6.3}3** following). The branch of chemistry dealing with photon-initiated processes – often referred to as photo-chemistry – is not dissimilar to electron-initiated reactions, however, in microwave-generated non-equilibrium plasmas, the advantage of electron plasma chemistry over photo-chemistry is that electrons are generated at much higher efficiencies than photons could be generated [58, 115].

The idealised partially ionised plasma present in the system at any time is a mixture of atomic and molecular particles in their ground or basic states (the overwhelming majority) plus excited, dissociated, recombined and ionised states plus free electrons, the nascent essence of any plasma process – independent of its equilibrium standing. The excited, dissociated, recombined and ionised states differ from their basic energy state principally in the configuration of their electron orbits; and since the chemical properties and associated behaviour of atoms and molecules are governed by this electron shell configuration, these energetic particles are disposed to influence the course of reactions in which they participated [58]. In non-equilibrium plasma, where the population of these energetic particles is proportionately high (with respect to equilibrium or near equilibrium systems) the propensity for augmented process chemistry was high [58, 80, 83, 87] (although in low population environments). It is in this light that the following discussion is intended.

For reduction processes, the physical and chemical interactions between plasma-generated active particles and the solid surface of the mineral being reduced are concentrated in the low temperature plasma (gaseous) proximity of the reaction interface of the solid [58]. Where solid-state diffusion conducted the reactant(s) to an internal reaction site (that is, where the reaction interface was away from the solid's surface), the energetic particles promoted an enhanced diffusion rate.

For the specific cases of this project where a particular char-augmented reactant charge was microwave heated from room temperature in the presence of air at atmospheric pressure (1 atm), numbers of activated particles (as excited species) were possible from the onset of the initial low temperature plasma. Even at "high" 1 atm pressure, it was known that being under constant irradiation from the applied microwave field the field-energised electrons and their interim inter-particle collisions guaranteed that the system quickly retreated from equilibrium and moved more and more into the non-equilibrium [80]. Being approximately 78 vol% of the initial gaseous mixture (air), nitrogen as molecular N_2 was available from low temperatures to dissociate, ionise and provide a population of ground state plus active particles of species N_2, N_2^*, N, N^*, N^+, N^{2+}, N^{3+} and e^- which varied with increasing "temperature" – or increasing energy available in the system. In higher temperature nitrogen plasmas such as existed above ~ 1000°C where much of the reduction processing took place, N_2^+ and N^- became available as supplementary active species. Nitrogen was central in the syntheses of various less important, transient species that emerged in the initial plasma chemistry. Of these, NO, NO_2, NO^+, NH_x, OH and other of their energetic particle derivatives were a few of the numerous species possible for air mixture plasmas [58, 80]. These energetic particles were available to take part in both plasma and process chemistry, subject to the greater reduction desirability and availability of other available particles present or becoming available in the system. At atmospheric pressure, the minor (~ 1%) argon proportion contributed the activated distribution of Ar, Ar^*, Ar^+, Ar^{2+} and e^- to the plasma. Notably, gaseous oxygen was not as readily ionised and, whilst some of the molecular O_2 was expected to dissociate to the monatomic O, before oxygen could expansively ionise it was consumed totally by gasification reactions involving carbon and, to a lesser extent, nitrogen. The heterogeneous reaction of oxygen with carbon proceeded rapidly at the solid carbon surface [17, 58] – and noting that the activated charcoals used in project experimentation had high surface area to volume ratios. As previously established, at atmospheric pressure, thermodynamics favoured the maintenance of CO_2 below ~ 710°C and CO above that temperature – with temperature dependent compositional self-adjustment between these gases in the presence of charcoal. At process temperatures, reduction

took place by the gas phase reactions involving CO and its ionised derivatives; direct oxide reduction by solid carbon was possible given solid-to-solid contact, however, the mass transport of carbon to the reducing mineral interface was generally assumed to be by gas phase to interface, thence by solid state diffusion to the reduction site. Under the conditions of the project experiments, it was repeatedly observed that CO formed plasma at a slightly higher temperature than N_2 or Ar being shortly after the initial, principally nitrogen air plasma had established itself. CO ionised in the presence of red-heat char, presumably in the CO stability temperature range, and its ignition could be identified by the significant spectral shift – a change to deeper colour in the plasma accompanying increased plasma intensity. The significant CO-derivative species in this reducing plasma were CO^*, CO^+, CO^{2+}, CO^- and e^-, all excited and ionised particles being of higher energy than the ground state CO and thus more reactive in reduction operations having increased kinetics and thermodynamics but having the same ultimate reduction product outcomes as conventional pyrometallurgical systems [17, 58].

This abundance of chemically active particles – which was evident and predictably reproducible – advanced the propositional temptation of a multitude of notional and actual reduction route possibilities. It was not the purpose of this project to investigate and propose plasma reduction mechanisms, although such was thought highly important. It was, however, recognised that the project's plasma-assisted end-point reduction products were essentially equivalent to those of "conventional" pyrometallurgical chemistry. And further noting that **the project placed emphasis on the *fact of reduction* more so than the *means* or *mechanism of reduction* contained in the reduction route**. Also, because a suite of export-prominent refractory metal minerals was selected in redress of a national economic impasse, the usual scientific imperative of reduction route exactitude was of less consequence than was highlighting the collective affront of national resource neglect of mineral commodities – or, more insentiently, the consequence of unrealised commercial exploitation.

Accordingly, it was decided that rudimentary, generalised equations such as those presented in Appendix **6.2**, although basic, were sufficient to represent the overall reduction equations for the reduction processes central to the project. Whilst these equations were deemed adequate for their purposes in the project overall, they do not represent the range nor the intricacy of the equation set which might purport to fully represent the phenomenological chemical events taking place over the range of non-equilibrium thermochemistry present in the reduction processes of this project. It is also acknowledged that the various systems' kinetics and thermodynamics were accentuated by the collective impact of the range of non-equilibrium particles such as excited atoms and molecules, ionised atoms and molecules, negative ions, recombined atoms and

molecules, dissociated radicals (atoms) plus free electrons and photons whose impacts upon system chemistry were all more highly energetic than the ground state precursors of those particles. Together with their modes of formation, a generalised summary of activated particles was previously presented in Table **{4.6}1**. Supplementary to Table **{4.6}1**, because their impact upon the continuum of particle and system energies and chemistries has been too frequently overlooked, photo-chemical reactions involving the energy quanta of released and absorbed photons were duly acknowledged. Representing energy transfer between plasma particles, plasma reactions involving photons played a defining role in ionisation thermochemistry both during the relaxation of ionised particles and the excitation of other, recipient particles as represented in the following equations [115, 221, 222].

$$e^- + X^+ \rightarrow X + h\upsilon \quad \ldots \quad \textbf{\{6.3\}1}$$

$$X^* \rightarrow X + h\upsilon \quad \ldots\ldots \quad \textbf{\{6.3\}2}$$

$$X + h\upsilon \rightarrow X^* \quad \ldots\ldots \quad \textbf{\{6.3\}3}$$

For these three equations, which describe events that are common in plasma, X represents any molecular species, e^- is any free electron, h is the Plank constant and υ is the frequency of the photon (and noting that the energy change (quantum) is proportional to the frequency, $\Delta E \propto \upsilon$). The reactions suggest that energetic changes which prescribe chemical and energy changes in plasma occurred in discrete energy quantum sets as embodied in quantum mechanics (see energy levels: Lyman, Balmer, Paschen, *et cetera* series), expressed and evident as electronic orbitals, and both positively and negatively imposed upon the specific system energy in terms of multiples of such discrete quantum sets [223, 224, 225, 229].

6.4: Early Experimentation and Experimental Programme for Ti, Zr/(Hf) and Ta/(Nb) Minerals.

The experimental programme which marks this thesis was derived during pre-project experimentation which ranged across a broad spectrum of laboratory minerals, ore concentrate minerals and their ores, carbonaceous materials (including the influence of maceral groups upon susceptibility in coals and their carbonised derivatives), and in gases and liquids. Because of their importance in the formulation of project sense and procedure, included in this thesis are microwave-processed examples which lie outside

the ambit of those chosen mineral *"oxides of refractory metals"* which delineate the core minerals of the project. The planned order of the experimental programme and the presentation of such are outlined below. It should be noted that the project was a foundation area of research and, as such, the study contained that element of being an overall "unrestricted" topic. However, such a tendency towards the indefinite was averted as progress through the early experimental and analytical programme instructed the appropriate final plan of experimentation.

In earlier experimental work intended to investigate the primary and obvious characteristics of microwave-stimulated reduction, an instructive range of run-of-mine minerals (as mineral concentrates or as high purity ores such as haematite and molybdenite) were reduced to metallic products utilising various carbonaceous reductants, typically the reduction products were water-quenched. These simple but instructive experiments were normally carried-out in small fireclay gold-assaying crucibles securely wrapped (including base and lid) in aluminosilicate blanket insulation. Both the crucibles and the aluminosilicate wrapping proved universally to be thermally adequate for most of the early, moderately high-temperature reduction operations on the relatively common minerals, whilst the simple but brittle fireclay crucibles proved to be resistant to catastrophic failure by the thermal shock of high heating rates and acute temperature-profile-induced stresses (unlike the more expensive, higher density, high purity ceramic crucibles which were less successfully trialed in exercises where higher temperature-rating was required). Unencumbered by configuration complexity or process sophistication, certain straightforward thermal and physical processing variables (such as consolidation tamping, fluxing, inert and active lancing, layering of reactants, charge permeability traits and bed behavior, cooling rates and their effect on reduction products, *et cetera*) were tried and adopted or learned, or otherwise, were discarded during this period.

Dependent upon availability, and as with later work, minerals commercially significant to the Australian economy were favoured for the unrestricted early microwave-stimulated reduction exercises. Along with these run-of-mine minerals, some laboratory grade minerals were chosen for reduction as they (*i*) would provide additional information of significance in that they would more closely represent raw mineral feed in any pilot process up-scale which could purport to precede a real industrial operation, (*ii*) would give comparative reducibility information against their counterpart impure run-of-mine concentrate mineral, and (*iii*) would fill any availability gap for an important mineral group which might be otherwise unobtainable (ultimately,

a concern that was unwarranted). The following account is written in summary of the key and primary aspects of the early experimentation. The early or introductory experimentation was conducted both with a view to discovering the potential (as distinct from the limitations) in microwave-stimulated reduction and with a view towards defining that portion which was to become the subject of this project. Thus, what follows is abridged for the sake of current "relevance", it is an overview of initial work as it developed in both promise and expectation along with process and system sophistication.

Reduction experiments began in the staple iron minerals group, including iron-dominant minerals. Haematite (Fe_2O_3) and the highly microwave susceptible magnetite (Fe_3O_4) were successfully and rapidly reduced in minimally atmosphere-protected conditions producing either high carbon grey or white iron (method and cooling rate dependent). In fact, in all but a few of these carbon-reduced smelt products the carbon uptake tended heavily towards the saturated end of the spectrum – a trend which was of little consequence in the light of the project aims, and for which no counter-measure was deemed necessary at the early stages of experimentation (and if at all through later stages). [Thereto, as an exercise, indurated Whyalla blast furnace feed pellets were, under microwave irradiation in a stream of natural gas, CH_4, reduced to a near pure Fe steel – the only impurity detectable being minor Si at grain boundaries. So, controlled reduction *could* be accomplished to yield a "refinery grade" pig product. Whyalla and similar indurated pellets were also easily reduced to cast iron.] The presence in the quenched metallic product (iron bead or button) of alloy carbide or carbonitride compound particles or as solid solution phases in alloys was interpreted as proof of reduction (typically from the oxide) of transition metal elements contained in the mineral reactant.

Supplementary to working with iron oxides, iron carbide (> 99% Fe_3C) – the product of a discontinued (1989) pilot plant operation at Wundowie, Western Australia – was found to be highly susceptible to microwave irradiation and was therefore used to augment reduction where the intended product was iron or iron-based. Uneconomical on its own as a primary resource, Fe_3C was found to be highly desirable when blended with minor char and any of the range of iron-based oxides and microwave reduced. Of itself, iron carbide is a reduction product, however, it is mentioned here for its processing potential as a microwave susceptor and reduction process catalyst.

Further to this initial set of reduction successes, iron-rich minerals chromite ($FeCr_2O_4$) – in various grades of concentrate, ilmenite ($FeTiO_3$), wolframite ($(Fe,Mn)WO_4$), a New Zealand titano-magnetite, and a V-rich magnetite were all

successfully reduced under reductant carbon to yield iron products which captured virtually all of the alloy metal as carbide or carbonitride contained within the iron smelt-product beads. At this point it was noted that certain of the captured phases and compounds, and their presumed transition forms, would have extremely high melting points – higher than the melting points of the containment refractory materials – and it was recognized that some of the prevailing reduction characteristics were apparently at odds with those of conventional pyrometallurgy.

Molybdenite, the significant ore of molybdenum – mined from vein-deposits formed upon massive intrusion of the sulphide into basal country rock and occurring as the triclinic MoS_2 phase at high purity – was incompletely reduced to form an indefinite $MoS_xC_yO_z$ phase whilst issuing copious sulphurous fume, detectable (by smell) in the off-gases. Failure to completely recover Mo from molybdenite in metallic form was reversed when molybdenite was blended intimately with magnetite, wolframite and char and microwave reduced to yield a complex white iron plus, significantly, only trace quantities of W, Mo and S in the remnant slag. Intriguingly, one specific WMo non-carbide, solid solution phase in the iron was assessed by composition to have had a minimum melting point of 3,300°C [assessment by Professor H.K. Worner, interpretation from Mo-W, Mo-C and W-C binary phase diagrams] and that the phase had been frozen from its *liquid* state. This result was interpreted as further evidence of unconventional thermochemistry if only because the deformed but not melted crucible with which the iron bead was in intimate contact before and after quenching, was only rated up to a temperature of about 1,500°C melting point. When laboratory grade MoO_3 was intimately blended with magnetite and char and microwave reduced the resulting iron was full of molybdenum carbide particles, whilst negligible Mo was detectable in slag phases.

Other microwave carbothermic reduction exercises on ferruginous-dominant mineral blends were attempted with varying degrees of success. As a trend, however, those metallic elements that were strong carbide formers and were, in Ellingham diagram terms, relatively easily reduced by carbon were found to report in carbide or carbonitride form in the iron bead or button reduction product. The strong carbide forming elements such as the transition elements (including lanthanides and actinides) Ti, Zr, Y, Th, Ce, La and Nd, plus Mg, Ca, Al and similar, all of which form oxides of even greater "nobility" – as is attested by their extremely stable mineral forms (both physically and thermochemically) – are recognisably stable in Ellingham diagrams for carbothermic reduction routes, and for other possible reduction-element routes, and remained un-reduced whether blended with ferruginous minerals or otherwise.

Where it occurred as a gangue element in mineral concentrates or integral in complex minerals, the observation was made that Si was reduced and reported as carbide particles in the resulting iron product. Minerals unsuccessfully (or minimally) reduced included laboratory grade alumina (Al_2O_3), yttria (Y_2O_3), cerium oxide (CeO), barium oxide (BaO_2), and minesite-derived minerals bauxite [boehmite/diaspore (AlO(OH)) + goethite (FeO(OH))], scheelite ($CaWO_4$), calcite ($CaCO_3$), gypsum ($CaSO_4.2H_2O$), fluorite (CaF_2), dolomite ($CaMg(CO_3)_2$), rutile (TiO_2), baddeleyite (ZrO_2), zircon ($ZrSiO_4$), monazite ($(Ce,La,Th)PO_4$), xenotime ($(REE,Y)PO_4$), bastnaesite ($(Ca,La)CO_3(OH,F)$), uraninite (UO_2) and commercial grade neodymium oxide (Nd_2O_3).

Aluminium, magnesium, titanium, zirconium, thorium and several of the rare earth elements were successfully reduced from their minerals *later* in the project when certain "experimental proficiencies" were more advanced. Although scientifically noteworthy, reduction of several of the non-core metals in subsequent stages of the project was not reported beyond this mention as the exercises, which fell outside the project core, were conducted purely to edify the project expectation that learned expertise and the configured system had improved from earlier experimentation. And, in no small way, their reduction satisfied bare curiosity.

Whilst, under modest reduction conditions, some metals proved to be too difficult to extract from their minerals, under similar conditions other important oxidic minerals proved to be easy to carbothermically reduce, yielding economically important base metals. Mn was microwave reduced from pyrolusite (MnO_2) to yield a manganese "cementite" solid solution, and franklinite $\{(Fe^{2+}, Zn, Mn^{3+})(Fe^{3+}, Mn^{2+})_2O_4\}$ yielded an FeMn solid solution plus zincite (ZnO) crystals deposited from the fume of Zn sublimed from the smelt (see Figures **{7.1}5** and **{7.1}6** in Appendix for Section 7). Laboratory zincite (ZnO) itself was reduced in a CO/inert reducing atmosphere to yield zinc metal. The laboratory chromium oxide Cr_2O_3 was reduced to yield chromium metal. Both cerussite ($PbCO_3$) and minium (Pb_3O_4) were rapidly reduced to lead metal under a CO/inert atmosphere. Similarly rapidly, cassiterite (SnO_2) was reduced to tin metal; also (see later) the cassiterite fraction in the tantalum mineral wodginite was rapidly reduced. The black copper oxide, tenorite (CuO) was rapidly reduced to a near pure copper metal (Cu does not take-up C to form carbide phases or compounds). The laboratory mineral vanadium pentoxide (V_2O_5) was substantially but incompletely reduced when blended only with reductant char (greater atmospheric protection would have rendered this operation complete).

A significant proportion of Australia's export mineral concentrates are sulphide minerals mined in massive sulphide lodes in iconic regions such as Broken Hill, Mount Isa and Kambalda. Significantly successful results were produced in microwave reduction operations using carbon forms as reductants on a range of sulphide minerals. Predictably, and deleteriously (as industrial environmental cases avow), copious noxious sulphurous gases (principally SO_2 with SO and H_2S) are evolved from any pyro-reduction processes of sulphide ore or laboratory minerals.

In relatively straightforward carbothermic microwave-stimulated reduction exercises, prominent Australian sulphide minerals were experimentally reduced to their metallic products plus matte and/or slag phases plus the aforementioned sulphurous off-gases. Galena (PbS) was rapidly reduced to lead metal. Similarly, sphalerite (ZnS) was reduced to zinc metal. Chalcopyrite ($CuFeS_2$) was reduced to copper containing distinct iron dendrites plus a Cu-matte and slag. Stannite (Cu_2SnFeS_4) was reduced to a primary CuSn bronze followed by the reduction of iron. Chalcocite (Cu_2S) reduced to copper metal plus a stubborn matte. Millerite (NiS) was reduced to nickel metal. Stibnite (Sb_2S_3) was reduced to antimony metal. Pentlandite ($(Fe,Ni)_9S_8$) was reduced to a high carbon iron/nickel alloy plus a pyrite-rich slag.

As an aside to conventional reduction approaches, simple experimental trials were conducted following a concept to utilise sulphur in simple sulphides to reduce or replace oxygen in simple oxides, with some assistance from char to provide – albeit a reducing atmosphere – a protective CO atmosphere to prevent re-oxidation. To test this concept, and it was acknowledged that, of itself, sulphur is neither a strong reductant nor a particularly desirable one, pyrite (FeS_2) was intimately blended alone with magnetite (Fe_3O_4) and, beneath char was quickly reduced to iron with no slag or remnant reactant, with SO_2 principally comprising the off-gases. Also, sphalerite (ZnS) and zincite (ZnO) were similarly reduced to zinc metal, whilst more complex combinations were reduced to metallic alloys – the higher the reduction temperature required the more problematic the mechanism. In these sulphide plus oxide cases it is probably best to describe the process as a replacement rather than a reduction exercise because, in the same way that C is the necessary chemical intermediary in the conversion of refractory metal oxides to refractory metal chlorides in the one process, here C is probably the catalytic agent reducing both oxide and sulphide whilst the S and O are removed gaseously as SO and SC_x thence through rapid stages to the more thermodynamically stable SO_2 and CO_2 as the off-gases leave the high temperatures of the immediate reaction zone.

In a complementary set of experiments it was established that, in the absence of any reductant, run-of-mine sulphide concentrates could be partly if not fully sublimed when heated under microwave irradiation. To this end, and in similar configuration to reduction exercises, galena (PbS) was (totally) sublimed to lead metal and sphalerite (ZnS) to zinc metal. It was established that other common mine-site-derived sulphide minerals [chalcocite (Cu_2S), chalcopyrite ($FeCuS_2$), stannite (Cu_2FeSnS_4), pyrrhotite ($Fe_{1-n}S$), stibnite (Sb_2S_3) and molybdenite (MoS_2)] could be sublimed – most of them only in part-sublimation at this experimental level – then, once conceptually demonstrated, the experimental exercise of sublimation was sidelined for more central work. Apart from conceptual matters of project direction, simple process containment for sulphide operations was also an underlying problem.

The less dense, higher porosity oxide crucibles that were found to perform suitably under microwave irradiated heating/processing conditions were, however, vulnerable to chemical attack during sulphide processing. Whilst catastrophic failure (by mechanical disintegration) of any of various types of these porous, basically oxide crucibles was uncommon, fluxing attacks during reduction operations involving some minerals – especially sulphides – resulted in failure by lower-temperature melting of the crucible. During the processing of various sulphides, fluxing failure of crucible and insulation materials was both predictable and common as sulphurous radicals impinged upon the chemical integrity of these refractory oxide systems, locally converting them to sulphite or sulphate systems, consequently lowering local melting points. Liquid so formed acted aggressively to flux adjacent material thus leading to extensive refractory failure that resulted in configuration failure (of crucible set-up) and premature quench-termination of the reduction trial. Along with the noxious nature and by-product intransigence of products of sulphide processing, attack by chemical fluxing upon crucible and other crucial refractory items provided the last of a trio of indisputably prohibitive experimental events which concordantly led to the early termination of any possible experimental programme involving sulphides and related minerals. This collective magnitude of process negatives was so much so that the notion of a sulphides reduction programme was set aside *despite* impressive reduction successes arising from the considerable degree of susceptibility of sulphides to microwave irradiation. Furthermore, and cogently so, to avoid any Occupational, Health and Safety directive, the generation of labile sulphur (vapour) and other noxious sulphurous gases during experimental reduction processing became an unequivocal disincentive to the continuation of this section of work whilst the simple configuration of experimental apparatus was employed, devoid of any off-gas handling, containment and/or scrubbing equipment.

Further complicating any proposed processing of the sulphide minerals of real ores is that they frequently include fractions of the more environmentally problematic arsenic (As) and/or antimony (Sb) in place of sulphur, arsenopyrite (FeAsS) and cobaltite (CoAsS) are examples in the Australian experience – or they may be more complete arsenides or stibnides as S is replaced by Group **15** elements As or Sb in minerallogical continuum from the sulphide, also, both As and Sb may replace either metal or non-metal in minerallogical association. One such example, stibnite (Sb_2S_3) was carbothermically reduced in simple microwave processing configuration to antimony metal. Arsenopyrite (FeAsS) was similarly reduced to yield iron plus a matte phase accompanying slag. From Western Australia, a complex cobaltite/pentlandite {(Co,Fe)AsS/$(Fe,Ni)_9S_8$} mineral concentrate was successfully reduced to yield a high CoNi alloy (with minor Fe and As) beneath slag only.

Despite significant results in microwave-stimulated reduction of sulphides, arsenides and stibnides, the noxious nature of off-gases (which alone provided sufficient reason) plus the requirement, should this line of research continue, for considerable off-gas scrubbing (quite a resource allocation) determined that sulphide and associated minerals reduction was a limited concept in this otherwise oxide mineral project. Whilst further sulphides investigation was terminated, there was identified a considerable potential in this technique which recommended itself regarding an investigative study into the desirability of microwave-stimulated reduction of sulphide and associated ores and minerals. Otherwise, work on sulphides and other non-oxide or non-principally-oxide minerals was relegated to the mantle of instructive encounter once the project-proper was defined.

Other more removed microwave experimentation was conducted out of earnest, scientific curiosity – work such as the melt-destruction of asbestos (chrysotile and crocidolite) with associated mineralogical reassignment by melt-chemistry adjustment to yield a safe solid product suitable as lightweight aggregate for the building industry; the ultra-charring of black coals to create pyrolytic carbon phases of interest for their hardness and their low reactivity; the microwave-sintering of metal matrix composites (supplied by Sandvik™ and others) to yield high density sintered compacts; and the recovery from mine wastes and slags of valuable metals thus rendering the processed materials environmentally safe for disposal to unmonitored sites and for unfettered use as fill. It was established that calcining operations could be achieved under modest microwave processing and, to this end magnesite, $MgCO_3$ was calcined to MgO. A further experimental outcome was the successful aluminothermic microwave reduction of MgO to yield magnesium plus alumina. Further, by invoking certain outcome-determining machinations, a degree of processing success was attained using TiC, TiN,

TiB_2 and B_4C to assist in the manipulation of reaction routes towards simplification of reaction product(s). These and other experimentally appealing but un-associated process developments are not otherwise reported in this thesis, but much was learned about the possible permutations of processing of materials under microwave irradiation and in the associated presence of non-equilibrium plasma and its activated, species-rich chemistry.

Once the scope of the microwave reduction project had been narrowed to its final, current topic, the "early work" was re-assessed for mention with formal experimental outcomes in Section **7**: *Results*. It was decided that certain of the early reduction accomplishments and any significant stages of progress in the microwave reduction process should be sufficiently covered so as to demonstrate the evolution of the project as a developing research entity. A coherent point of reference in the evolution of the project was that nascent moment of decision when the five chosen refractory metals – titanium, zirconium, hafnium, niobium and tantalum, representing three ore mineral groups, and mined in as few as two mining operation types – were, for the purpose of final project topic identification, separated from the remaining refractory metals vanadium, chromium, molybdenum and tungsten, all metals of commercial significance. Of these, by way of comment (because the more difficult reduction tasks were favoured so to better substantiate microwave reduction capabilities), Group **6** elements chromium, molybdenum and tungsten were least difficult to reduce from their oxides whilst Group **5** metal vanadium was easier to reduce than any of the selected five (as can be determined from the relevant Ellingham diagram for oxides).

Consequently, and by way of brief overview, the following is an outline of the structure of those results reported in Section **7**. The iron-based reduction of the deleted refractory metals was included: of vanadium (from V-rich magnetite and V_2O_5), of chromium (from various grades of chromite and Cr_2O_3), of molybdenum (from molybdenite and MoO_3), and of tungsten (from wolframite and scheelite). Also included were a limited number of microwave reduction outcomes (products) which exhibited some significance or reflected some processing relevance which could prove pertinent in the experimental programme overall – or beyond the project altogether.

The microwave-stimulated reduction of titanium minerals was addressed next with all reduction operations conducted in the established wrapped crucible configuration under a CO atmosphere until liquid nitrogen (LN_2) quench. Two strategies of reduction were attempted for each mineral, these being (*i*) straight

carbothermic – with char and mineral reactants mill-blended to a fine intimate consistency and blend carbon exceeding the stoichiometric requirement by ~ 20 at%, plus excess granules of char below and atop the reactant charge to effectively provide a reducing CO atmosphere in the reaction zone from reaction initiation to quench, and (*ii*) aluminothermic – with fine pure aluminium powder (exceeding stoichiometric requirement by ~ 20 at%) intimately mill-blended with the fine mineral plus minor fine carbon (as assurance against local re-oxidation) and (as in (*i*) above) an excess of char granules below and atop to provide the protective CO atmosphere. The titaniferous minerals anatase, rutile and ilmenite were selected for microwave reduction. The anatase (TiO_2) used in all anatase experiments was a finely divided commercial grade TiONA® > 99.9% pure and equivalent to any starting raw material for either paint opacifier or titanium metal production. The rutile (TiO_2) used in all relevant experiments was a mineral concentrate derived from an undisclosed northern New South Wales sand mining operation. The rutile (~ 99% pure) had the expected trace element impurities including chromite in intimate mineralogical association. The ilmenite ($FeTiO_3$) used in microwave reduction experiments for this project was also a mineral concentrate from the same northern New South Wales source, was ~ 96% pure and similarly contained chromite ($FeCr_2O_4$)) in intimate mineralogical association in the minor impurity range approximating 3%, plus other elements in trace proportions. The following is a brief experimental programme outline of the microwave reduction of titaniferous minerals with some indicative commentary.

(a) Anatase. (*i*) **Carbothermic reduction.** [Section **7.2.1**]
[Initial significant results set and principal titanium result.]

(*ii*) Aluminothermic reduction. [Section **7.2.2**]
[Few results only.]

(b) Rutile. (*i*) Aluminothermic reduction. [Section **7.2.2**]
[Few results only, covered in the section with anatase.]

(c) Ilmenite. (*i*) Carbothermic reduction. [Section **7.2.3**]
[Few results only.]

(*ii*) **Aluminothermic reduction.** [Section **7.2.4**]
[Second significant set of results, thermite reaction suitable for industrial application, few results only.]

The second mineral group in this project was the zirconium/(hafnium) group. Of all of the selected core minerals in this project, minerals representing this group were expected to be, and were subsequently found to be, by far the most obstinately problematical to reduce to metal from their oxides – as reference to the Ellingham diagram for oxides will attest. Almost all zirconium metal produced around the world finds it way to that final reduction product from the source mineral zircon ($ZrSiO_4$), often described as a silicate mineral, but in other quarters as a double oxide, $ZrO_2.SiO_2$ – which, mineralogy aside, presented a more sensible representation in this project for several reasons. Firstly, the element silicon is almost as thermodynamically stable in its dioxide form, silica (SiO_2) as is titanium as titania (TiO_2) (refer to the Ellingham diagram for oxides). Silicon "metal" is reductively extracted from clean quartz (SiO_2) minerals such as quartzite and sandstone concentrates or ore from deposits of massive quartz in extractive metallurgical operations quite similar to refractory metals extraction. Also, the mineral zircon can be preparatorily processed (including by microwave processing) by passing the fine zircon through a high temperature plasma such that, upon their exit, the molten zircon droplets re-solidify by initially re-crystallising the zirconia fraction, thence amorphously freezing the silica remnant. This quenched product is such that the glassy silica fraction is distinctly separate from the re-crystallised zirconia fraction and, largely, can be physically separated by mechanical attrition of the brittle glassy phase, any remaining silica is removed with sodium hydroxide [see Section **4.2.2**, Equation **{4.2.2} 1**] leaving a zirconia product > 99% ZrO_2 – or, acknowledging the hafnium content, $Zr(Hf)O_2$ – known as plasma dissociated zircon (PDZ). Zr is replaced by Hf in the Australian east coast zircon to the extent of ≥ 2 $_{at}$% Hf, which is slightly above world average – and in some "altered" zircon minerals originating in acid igneous rock types can contain Hf percentages well into double figures, however, these altered zircon minerals are extremely rare in the alluvial mineral sands deposits mined around the world which typically exhibit maximum Hf levels < 3 $_{at}$% as Zr-replacement in zircon concentrates. This plasma dissociation phenomenon is mentioned here because it was a principal accompanying feature in the microwave reduction of zircon during this project. The zirconia and hafnia minerals used in

secondary microwave reduction experimentation were both laboratory grade minerals with specified purity > 99.5 % $(Zr,Hf)O_2$.

The following is a brief experimental programme outline of the microwave reduction of zirconium and hafnium minerals (specific to this project) with some indicative commentary.

(d) Zirconia. (*i*) Carbothermic and aluminothermic reduction. [Few results only.] [Section **7.3.1**]

(e) Hafnia. (*i*) Carbothermic and aluminothermic reduction. [Few results only.] [Section **7.3.2**]

(f) Zircon. (*i*) Carbothermic reduction. [Section **7.3.3**] [Few results only.]

(*ii*) **Aluminothermic reduction.** [Section **7.3.4**] [Third significant set of results. Separation of metallic Zr/(Hf) from Si phase.]

The third mineral group of the project was that group of tantalum/(niobium) minerals which currently (and will into the future) represent such a huge export income to Australia. Unlike most world ores, the Australian tantalum/niobium ores are heavily biased towards the tantalite end of the "content spectrum", with the niobium-bearing columbite (niobite) content of processed ores being comparatively low by world standards, and as low as 3 at% in the wodginite used in this project. The near expired Greenbushes ore concentrate, the current Wodgina ore concentrate, and the concentrates of the upcoming Mount Weld ores are all mineralogically different, however, the export products of all of these (as of recent years) is Ta_2O_5 and Nb_2O_5 which generally go to metals extraction operations, at least in the first instance. The mineral concentrate chosen for microwave reduction processing in this project was wodginite $[((Fe,Mn)Sn(Ta,Nb))_{16}O_{32}]$, partly because it is the current primary tantalum

mineral, and partly because the high tin (cassiterite-like) content bound mineralogically in the wodginite concentrate presents particular minerals processing and beneficiation problems – representing costs – to miners and processors *en-route* to their primary export product.

It was found that microwave processing of the unaltered concentrate would yield Sn which, as irradiation persisted, "mopped-up" the subsequently reduced Fe and Mn into a form of Mn-hardhead (hardhead* being a mixture of intermetallic Fe-Sn compounds). This ternary solid solution could thence be solvated away leaving the remaining, modified oxide mineral as a Ta/(Nb) concentrate having a trace to minor content of titanium, Ti. Generally, these two metal groupings, the Mn-hardhead and the Ta/(Nb,Ti) metal/carbide, were found to be broadly represented in the reduction products. Also, the two relevant oxides, Ta_2O_5 and Nb_2O_5 (as laboratory grade oxides) were carbothermically reduced to metallic form. Because these Group **5** metals were known (by Ellingham diagram) to be considerably easier to reduce than the preceding Group **4** metals, carbothermic reduction was presumed (and proved) to be adequate and no aluminothermic reduction was attempted, however, metallothermic reduction could plausibly play a desirable role in any pyro-extraction strategy for these metals.

(g) Niobia [Nb_2O_5] (*i*) Carbothermic reduction. [Section **7.4.1**]
[Few experimental runs only.]

(h) Tantala [Ta_2O_5] (*i*) Carbothermic reduction. [Section **7.4.2**]
[Few experimental runs only.]

(i) Wodginite. (*i*) **Carbothermic reduction.** [Section **7.4.3**]
[Fourth significant set of results. See comments below.]

(*ii*) **Aluminothermic reduction.** [Section **7.4.4**]

---

* Hardhead is a mixture of impure intermetallic Fe-Sn compounds typically resulting as an infusible residue during the refining of crude smelted tin by liquation [241]. The intermetallic Fe-Sn compounds that may comprise hardhead are FeSn, $Fe_{1.3}Sn$, Fe_3Sn_2 and Fe_3Sn. As was qualitatively evident from project EDS analyses, intermetallic Mn-Sn compounds in minor Mn-Sn alloy phases were present as a comparable Mn-hardhead. Mn exhibits similar physico-chemical properties to Fe when in solid solution with Sn or other metal, known Mn-Sn intermetallics are Mn_9Sn, Mn_3Sn, Mn_2Sn and $MnSn_2$.

[Fourth significant set of results. (Along with the carbothermic results) the most "metallic" refractory metal reduction products of the project. Found that tin could be employed to "mop up" other major impurity metals, manganese and iron.]

It was believed that a short extension into halidation of refractory metal minerals and the subsequent disproportionation (decomposition) of those halides to yield metallic products of high purity was a logical and instructive progression of the microwave minerals-reduction work. Whilst numerous reference sources [17, 34, 42, 45, 49, 50, 51, 61, 74, 80, 86, 89, 92, 99, 132, 177, 216, 207, 217] expound the use of microwave and/or non-equilibrium plasma enhancement in halogenation operations and their like, it was felt that full experimental confirmation of this non-core, ephemeral aspect would extend the experimental programme beyond the resources of the project. However, as it could undoubtedly be achieved, "indicative" demonstration of the disproportionation process was cursorily conducted on two common, simple salts to expound the capability embodied in this concept. The "concept" represents the plausibility of an alternative class of reduction processes: reductant-free routes to pure metal product.

It is noted that this halidation and decomposition extension may be viewed as more than extractive processing and has much in common with conventional refining stages of production – thereunto, it must be borne in mind that the refining and extractive stages are routinely reversed for refractory metals production. This extension was conducted to test and clarify certain experimental observations and trends whereby to establish the "developmentally lateral" technological potential of microwave-stimulated processing. An ultimate microwave reduction accomplishment here would have been to disproportionate titanium tetrachloride ($TiCl_4$) [or any of the refractory metal tetrachlorides] to yield metallic titanium plus gaseous chlorine which could be collected for storage or by-product reprocessing, or could be indirectly looped into re-use for halogenation processes leading again to metal tetrachloride. However, as with the above "full" disproportionation proposal, this exercise would have required considerable further fabrication of equipment and associated expense plus safety approval because of the liquid form of the reactant and the perceived "nasty" nature of such chlorides. However, disproportionation of common salt and other solid salts and

minerals drew no such restrictions and, even if in a "rough and ready" manner, the processing principle (of disproportionating refractory metal and other halides) could at least be unambiguously demonstrated with minimal changes to the common processing configuration.

(j) Cobaltous Chloride Hexahydrate	(*i*)	Disproportionation of the hydrated cobalt(II) chloride, $CoCl_2.6H_2O$, by a two-stage decomposition to yield cobalt metal. [Section **7.5.1**]
(k) Halite [NaCl]	**(*i*)**	**Disproportionation of common salt to yield sodium metal (combusted to oxide) plus chlorine gas.** [Section **7.5.2**]

Of the fifteen assignment tasks identified above (and covered in fourteen later sub-sections), the *core substance* of the project was contained in just five of these: **(a)**(*i*); **(c)**(*ii*); **(f)**(*ii*); **(i)**(*i*) and **(i)**(*ii*); whilst task **(k)**(*i*) was significant in the implications contained in the result for its possible impact upon next generation industrial processing – incorporating refractory metal production. It would be easy to extend the scope and intent of the chosen experimental programme outlined in assignments (a) to (k) above. However, tasks outlined above already pushed the boundaries of possibilities of experimental scope. Save to say that this body of work was essentially novel and, being thus unique, it was felt that it should be seen to represent a raft of experimental information upon which future research extensions could be constructed and might reasonably profit (with respect to process direction and experimental intent).

6.5: Constraints and Limitations Imposed by Analytical "Availability".

During the somewhat extended life of this thesis project, access to certain facilities was interrupted from time to time. These interruptions were typically during

periods of planned maintenance including the occasional upgrading, both hardware and software, of various items of essential equipment, plus various periods of unplanned "down-time" whilst repair or recurrent maintenance was conducted (particularly with the SEM and its appendage equipment). Furthermore, it was inescapable that the period of the project spanned the technological changeover from the era of pre-computer, manual-controlled equipment to the computer-controlled equipment era. Consequently, much of the utilised equipment moved with this revolution and was either rendered obsolete and replaced or was upgraded by appending computer-interfaced hardware with requisite controlling software. Both hardware and, more frequently, software were generally subjected to the predictable, inevitable sequence of "version amendment" upgrades before "application efficiency" was either established or restored. Whilst some equipment down-time intervals were somewhat lengthy, and the inconvenience of unanticipated disruptions could be frustrating, negligible real time was lost as other gainful activities were always pending. In terms of project planning, such occasions were accounted-for by task re-organisation and/or, where possible, preparation for the next stage of experimentation.

Hardware and software system upgrades to analytical and microscope (characterisation) equipment imposed fundamental output changes, especially with respect to the permanent shifts in output format (information- and image-capture) that manifested as differences in presentation and appearance of data printout and micrographic images. Of course, unarguably, all such system upgrades represented system improvements. Of the hardware/software installments and revisions that most affected the analytical and characterisation output of this project, a range of upgrade variations to the SEM/EDS and XRD had ongoing impact. In terms of the presentation of variously acquired data and images, the change to output appearance represented minor nuisance variation which duly was either accepted despite disparity or transformed by legitimate discrete format manipulation to overcome the changes in presentation form if and where they were reported herein.

Also, although the reproduced photomicrographic format may appear identical through this thesis document, the inevitable technological shift from chemical photographic film to digital photographic storage was instituted during the course of the project. Across this generational shift in image-capture technology, virtually all of the

light optical photomicrography and most of the electron optical photomicrography were recorded to chemical storage means (photographic film). Only belatedly after hardware upgrades across photographic facilities were images recorded digitally. Consequently, in the preparation of this thesis document, many images were transferred via scanner from photographic negative (or photographic positive in the case of the colour Ektachrome slides) to electronic image and, it must be said, there was some loss of resolution, contrast and (where relevant) colour accuracy. However, best efforts were afforded to retain the image quality during such transfers. Further, noting that on top of such loss of resolution during transfer, (despite polishing caution) inter-phase hardness differences contributed towards depth-of-field focus perturbations in many polished specimens – as is covered elsewhere in Section **5** – and (where recorded) this flaw may have contributed by exacerbating any such transfer discrepancy.

6.6: Experimental and Post-Experimental Analyses.

To provide suitable rigour to the project, a programme of post-experimental analyses was devised to most adequately assess and represent the reduction product specimens and to descriptively encapsulate and instruct on the reduction process followed. The key post-experimental programme was both to exhibit a suitable thoroughness of analyses and to summon concise and meaningful reporting of analytical results as supportive portion of the broader results base (which included characterisation observations). Such post-experimental analyses, referenced to relevant micrographic characterisations, would be the basis for determination of success of the reduction product and subsequent evaluation of the microwave-stimulated reduction process. Quite independent of the post-experimental investigation of solid reduction products and their implied level of accomplishment was the intended imperative of dynamic sampling during the reduction process. Whilst sampling from the gaseous off-take was planned, access to requisite analyses was not made available. Also, no sampling from within the limited and vaguely defined reaction zone was planned (given that much of the interim reduction history was inadvertently captured in each final quench product). Such "experimental" sampling and consequent "experimental"

analyses – either directly or indirectly conducted – would reveal more about the reduction process than inform about the reduction product.

To add completeness to process evaluation, then, and to assist in the supposition and determination of reduction processes involved in the various reduction routes employed through the project, it was intended to provide select, experimentally concurrent, in-time analytical support. This real-time analytical support, contemporaneous with experimental progress, was to take the form of quite conventional in-line, in-time (direct) analyses by mass spectrometry of off-take gases continuously sampled from the reaction vessel outlet. This of course meant bringing together the microwave reduction system with the mass spectrometer, whereunto, early assurances advised that such was logistically reasonable. By such direct in-time analyses the reduction process could be monitored and process adjustment could be instigated by controlled feedback (if such was required). If direct in-time sampling or analysis could not be instituted, then it was planned that indirect in-line samples from the off-take stream would be acquired for later (indirect) mass spectrometry analyses of gaseous and gas-borne off-take products of the reduction process. Also, specifically for indirectly sampled off-take specimens, alternative or supplementary analyses were contemplated as complementary to mass spectrometry. Being cognisant of the lack of procedural constraint of any processing feedback requirement, indirectly sampled off-take specimens (gases, volatiles and gas-borne precipitates and other solid matter) could be submitted to more lengthy evaluation routes, and so could be submitted for spectrographic analyses by atomic absorption spectrophotometer, gas chromatograph, total elemental analyser or appropriate other analytical means such as to contribute information of maximum benefit to the reduction project. However, such per-experimental process evaluation ambitions were reliant upon the development and successful operation of a suitable vessel within which the controlled reduction process would take place.

During the formative stages of the project when it was expected that the project-proper would be conducted in the controlled environment of the then-heralded microwave reactor, emphasis was fittingly placed upon the consequent suitability and ease of facility which in-line sampling and analyses of off-take gases, volatiles and entrained solids would entail; and of resultant information, the process significance

such assessments would afford. Off-take gas analyses are standard procedure in comparable process-metallurgical operations (from experimental to full-scale). In the context of the proposed reduction operations of this novel but small-scale project, off-take gas analyses would provide beneficial process information. Notwithstanding this procedural norm, however, such information was not of "make-or-break" significance; the existence or absence of off-take analyses would not alter the *fact of reduction*, nor the *composition and form of the crucial reduction products*, features that were the centre-piece objectives of the project.

However, as is well documented in earlier Section **6.2**, the reactor concept was abandoned for the course of this project, and with its abandonment and the adoption of the experimentally-minimal microwave oven set-up, any pragmatic, functional plan to gauge and evaluate gaseous by-product compositions from a now nebulous off-take stream was forfeited. Whilst not only allowing plausible interactive reduction processing, the possibility of process feedback with direct in-time analyses would have provided a desirable record of process history (for later scrutiny). By comparison, a proportionate benefit could reasonably be expected from the fallback indirect analytical route that had the propensity to provide reserve specimens suitable for further, more rigorous analyses. However, as a fortuitous outcome of its adoption, the microwave oven set-up method brought with it a more predictable consistency in both reduction process and reduction product that, in a thermal stimulation process that was so influenced by thermal runaway phenomena, was an experimental blessing.

The plan for analytical evaluation of post-experimental reduction product specimens was comprehensively discussed in earlier Section **5.3**, *Strategy of Analyses*. The following summary re-affirms those elements of analytical endevour described in Section **5.3**, whereupon, where descriptions expand upon those of the earlier account, they hereinafter do not supersede nor replace those described in that Section.

In formulating the assemblage of investigative means by which to assess, differentiate and describe the metallic products of microwave reduction processes, the two broad elements of description identified as necessary were *visual characterisation* and *elemental (or chemical) analyses*. Unfortunately, the routine determination of phase hardness – that typically complementary, obvious and available means of categorisation

– was eliminated because it was found that reliable, reproducible micro-hardness or hardness measurements could not be attained from indentations at the inconsistent sites available across the variable oxide-nitride-carbide metallic phases present in refractory metal reduction products. (Although, good and consistent hardness readings could be taken from indentations across the predominant phases in alloy iron and comparable solid solution reduction products of the "early" microwave reduction work summarised in Section **6.4**.) Other analytical or descriptive methods were deemed unsuitable given the general heterogeneity of the reduction product specimens.

After "desiccation" and excavation, the solidified reduction product remnants of each experimental trial were inspected under a stereomicroscope and, accommodated by some physical probing, the remnants visually assessed for apparent range of reduction stages represented in the reduction product solids; their apparent state of agglomeration and degree of (fused) conglomeration; and the steps which might be required in recovering material samples from the typically fused reduction product mass then best presenting them in terms of specimen preparation for both micrography and analyses. Stereomicrographs were taken if they were particularly instructive or if record was required, and at this stage of visual evaluation, specimen materials were sampled and (*i*) representative specimens mounted, polished and otherwise prepared for micrography plus EDS and, where appropriate, (*ii*) a representative sample taken for mill-blending thence XRD analysis. Being generally representative of the broad chemical suite of advanced reduction product phases, X-ray diffracted specimen powder blends produced complex spectral output. Against these complex output spectra, the foreseen peak sets (of predicted compounds) were further complicated by the background presence of broad spectral peaks of remnant carbon forms – some undoubtedly amorphous – plus peak set additions and accentuations due to the unwanted incidence of certain non-reduction product compounds and other, redundant non-refractory metal reduction products. Once resolved from the mire of such spectral complexity, XRD results were compared, balanced and equated with final determinations of the more mainstream light- and electron-optical micrography plus results from SEM/EDS output before assessment could be finalised and reduction performance conclusions reached.

Mounted and polished specimens were extensively inspected both prior and post etching and light optical micrographs recorded over a range of magnifications using air lenses, some oil immersion microscopy was carried-out early-on to determine whether any advantage was to be gained by this method. However, given the ease of inter-element contrast that was available utilising backscattered electron excitation through the SEM, both the etching of specimens and the use of oil immersion optics (as means of phase delineation by contrast) became effectively un-necessary. Generally, the etching of polished specimens was sidelined to some light-optical evaluations, thence the etched surface re-polished before conductivity coating for SEM investigation.

As identified in Section **5.3**, various coating elements were trialled and used during EDS analyses. Generally, the common diffused carbon coating was used for samples, however, carbon coating was avoided where light element EDS analyses were performed under thin-window or windowless conditions. [Noting that, with the full beryllium window, light elements spectral k-peaks were eliminated.] Carbon coating imposed unwanted carbon k-peak intensity when those very k-peaks for the central light elements carbon, nitrogen and oxygen – all closely congregated – were what was sought for analyses. And, even under low voltage excitation (desired for highlighting such light elements), the k-peaks for these crucial elements were yet complicated by the presence of spectral l-peaks of such other important element presences as titanium, zirconium and niobium and those spectral m-peaks of hafnium and tantalum, plus the various spectral presences of tin, manganese, iron and other elements contributing unwanted, complicating k-, l- and m-peaks to a congested section of the of spectral band. Whilst gold sputter coated specimens yielded very clear visual images for micrography, gold consequently provided far too complex a range of peaks to the spectral background – particularly the many m-peaks, an array of lines spanning the necessary k-peak region of elements of interest. As a coating, silver was similarly masking, whilst diffusion coated aluminium provided reasonable spectral clearance but, as a coating, was inclined to opacify, burn or peel under the accelerating voltage and typically did not perform well under the accelerating voltages of the SEM, resulting in loss of image clarity. The coating element which was found to provide a thin and reliable sputter coating for both clear SEM micrography and EDS analyses (for any window) was nickel. Nickel has both k- and l-peak spectral lines which proved to be

only minimally coincident with the spectral lines-of-interest for the range of central elements of this project.

Electron-optical micrography for each mounted specimen was employed to support light-optical micrography, and where possible, the same specimen fields of view were recorded. Within these fields of view, extensive spot and area EDS analyses were performed on prominent features identified as meaningful and/or significant reduction product phases. To assist the developing order of the sequential ranking of reduction product phases and their inter-relationship in the evolving understanding of the reduction process, elemental mapping (X-ray mapping) was undertaken on fields of view which were adjudged to represent important reduction product phases and/or characteristic microstructure. Line scans (that is, one dimensional scans) traversing between phase regions to assist in the phase demarcation across phase boundaries or other artifact of interest were used to assist and confirm the compositional change and integrity across such phase boundaries. Such qualitative line profiles were principally of supportive function when affirming what seemed visually evident. Although also qualitative (only), the two dimensional elemental maps allowed "categorically affirmative" alternative representations of micrographic images, the maps were more compelling than the simpler line scans.

As was expressed previously, the consuming objective of analyses through this reduction metallurgy project was to demonstrate the relative state of reduction of a reduction product by emphasising the relative absence of oxygen (in the oxide mineral remnants) rather than the presence of metal and its relative purity. (Of course, EDS output reflect the results in the usual order of components: from major to minor.) For refractory metals, it was the oxygen remaining that determined the further utility of the reduction product metal. Also, paradoxically, in assessing analyses through this project, the assay-presence of carbon and/or nitrogen in reduction product metallic phases actually represents reduction, that is, the replacement of oxygen by either carbon or nitrogen (by way of some level of reduction "success"). With tighter process control over the reduction process, such un-wanted presences could be largely or totally eliminated. The high proportion of refractory metal in reduction products generally was both highly desirable and an incontestable affirmation of the results. Additionally, there were various established refining and "further processing" techniques that could be

applicable to de-carburising and de-nitriding of impure metals such as the reduction products of this project. Further, with regard to impurities in starting refractory metal oxides – as with current industrial halidation production routes – for future commercial microwave-stimulated reduction routes, the production sequence should include refining of ore-derived minerals to pure oxide mineral form *prior* to the actual extractive reduction stage. Again, in reduction products, the absence of oxygen in prior oxide mineral reduction remnants proved reduction; alone, the presence of metal did not. Nonetheless, somewhat paradoxically, it was upon this metallic product that assays were conducted and conclusions reached.

AN INVESTIGATION OF

THE MICROWAVE - STIMULATED REDUCTION OF

OXIDES OF REFRACTORY METALS.

VOLUME II

[Section 7: Results.]

7

RESULTS.

"Success is relative:
It is what we can make of the mess we have made of things."

T.S. Eliot -
The Family Reunion, 1939.

"When in doubt, tell the truth."

Mark Twain -
Following the Equator, 1897.

7: RESULTS.

In presenting the results of this project's experimental campaign it is relevant to acknowledge several fundamentals and precursor conditions which distinguish the project and which characterise its experimental novelty. In addressing the experimental aims, method and achievements of the project and consequent implications for future development and industrial application, important fundamental concepts ought be re-visited for their relevance to Section **7**, *Results*, and to the commentary of Section **8**, *Discussion.* In particular, the experimental (process) design and requisite equipment, its configuration and operation, and the consequences realised in experimentation all bear reflection and amplification. Such experimental fundamentals are discussed in the following paragraphs. Of themselves, the concepts were simple in essence and were (of necessity) interactively implemented by way of operator discretion consequent upon ongoing experimental observations during relevant periods of experimentation (as outlined in previous experimental Sections **5** and **6**); the outcomes were self-evident in experimental results.

Furthermore, at this point of introduction to *Results*, it is apposite to recount that, for each and any reactants charge, the imposed "microwave heating" (or dielectric heating) by mechanisms of dielectric interaction in and between the charge solids (the load) readily transformed into "microwave plasma processing" derived largely and increasingly from the newly ionised attendant gases (predominantly air plus CO_2 and CO generated at micro-arcing sites on the char). This transpositional mechanism-shift from solids-borne dielectric heating within and between solid component particles to – and although still intimately associated with the charge solids – the generation of non-equilibrium thermochemistry broadly within the gaseous mixture was decidedly beneficial to the target reduction metallurgy. The uptake of the applied microwave energy gradually shifted from the dielectric heating mechanism of the solids, through the subsequent transient micro-*arc* ionisation which initiated the primary bulk plasma ionisation, to the sustenance and further promotion of (wholly) gaseous ionisation (bulk plasma). This *mechanism transformation* was openly regarded as a bountiful *process progression* and, being so considered, the mechanism shift was systematically promoted and exploited in the process chemistry of reduction. Therein, from the early stages of irradiation, during these thermochemically interactive stages of microwave-stimulated

processing, processing was *always* and *concurrently* accompanied by non-equilibrium, low-temperature increasing to high-temperature microwave plasma – the unavoidable but beneficial consequence of the microwave irradiation of enclosed gaseous systems. From its generation early in processing, such microwave-stimulated plasma was non-equilibrium; was increasing in "apparent temperature" (energy) with mechanism shift; was contained within and around the reactant charge; was reaction-rate controlling in application to heterogeneous systems; and re-generatively retained high populations of highly energetic reactive particles, including those desired species demanded by the stoichiometric and speciation requirements of both "conventional process chemistry" and, moreover, by plasma- or ionisation chemistry.

In determining the conceptual merit and particular process efficacy of specific experimental microwave-stimulated mineral-reduction procedures, it is emphasised that the key processing objective was that ***reduction*** was achieved – and, specifically underscored, that the ***degree of reduction*** attained was of overriding importance in any assessment of process success and comparative worth. [Also, it was observed in a previous section that appraisal of "reduction success" for such an experimental programme ought be concentrated on the degree of *absence of oxygen in the reduced mineral* rather than the *presence of oxygen in the reduction product metal* should be seen to be the *sufficient* proof of process reduction. A moot point, perhaps! Consistently, however, metallic reduction products were plainly metallic, with typical analyses *clearly* exceeding 90 at% of *target* metal, plus mineralogically associated metals, plus carbon and nitrogen from processing, and with << 2 at% oxygen – and the second approach was sensible.] Such a degree of reduction could be directly equated with the degree of process efficiency. The project was therefore an investigation of a set of *extractive* processes as distinct from *refining* processes.

Although undeniably desirable, the "purity" of metallic reduction product, its actual elemental composition and the quantitative spread and identity of minor compositional components were of lesser importance when determination of process success was to be assessed. As a concession to the above distinction, it was ascribed that the *degree of reduction* (in the reactant oxide-mineral remnants) reflected the *relative absence of oxygen in the reduction product* with respect to the *abundance of oxygen in the starting mineral*. Furthermore, as well as any straight "reduction" removal of

oxygen by carbon in carbothermic or carbo-aluminothermic reduction, other possible reactions were by chemical exchange replacement of oxygen (in substitutional solid solution) by reductant carbon; or by nitrogen from the entrained, nitrogen-rich process "atmosphere" of the oven set-up (or from the subsequent nitrogen "blanket" during liquid nitrogen quenching); or by interstitial solid solution of carbon or nitrogen. The last case is relevant to the refractory metals that are significant "getters" of the light elements. The compositional assessment for C, N and O in reduction products was deemed to be of fundamental importance in any process assessment. Also, being refractory metal reduction products, the presence of oxygen, carbon and nitrogen (and their partial and total compositional fractions) was of primary relevance when attributing the reduction product as nominally "metallic", and as to whether and how the product could be further processed or whether the product would require or could (economically) justify a subsequent refining-stage process.

Distinct from the light elements, some principally metallic elements were found in the refractory metal reduction product phases in trace to minor concentrations as well as being present as distinctly separate secondary metallic reduction product phases (such as the manganese hardhead [$Mn_xFe_ySn_z$] by-product of wodginite reduction). Trace elements were essentially incidental and their presence in analytical results reflects two principal factors. Firstly, for all cases the fundamental simplicity of process conception and operation resulted in complexities of composition derived from the unavoidable melting, mixing and subsequent reduction of gangue minerals and partial reduction of molten refractory material and other, incidental contaminant minerals. Secondly, and recalling that *refining* ***precedes*** *extractive reduction* in industrial refractory metals production as a consequence of disposition towards gangue-mineral reduction, where a minesite-derived concentrate mineral was the object of reduction, then a broader suite of reduction products was expected. Consequently, a trace to minor range of reduced impurity elements was derived from the often compositionally significant gangue minerals fraction in the mineral concentrate. Wherein, during the reduction process, most trace to minor element components in ore minerals (because of their lower thermodynamic stability) were reduced before the refractory metal elements and so were predisposed to report in analyses of metallic phases (whether in solid solution or as compound). This precursory reduction occurred whether the "impurity" element was (*i*) contained incidentally within the mineral in mineralogical (chemical)

inclusion [as with Si and Zr in the single phase zircon ($SiZrO_4$ or $SiO_2.ZrO_2$) or as with Fe and Ti in ilmenite ($FeTiO_3$ or $FeO.TiO_2$)] or (*ii*) co-incidentally coupled across a grain boundary in intimate (physical) association brought about by its gangue co-mineralisation [as with chromite ($FeCr_2O_4$ or $FeO.Cr_2O_3$) attached to rutile (TiO_2) in the same duplex mineral grain as pervasively occurs in the east-coast Australian rutile concentrates, and even more so for chromite, magnetite (Fe_3O_4) and haematite (Fe_2O_3) in co-occurrent east-coast ilmenites ($FeTiO_3$ or $FeO.TiO_2$)].

Because of the nature of the specimen materials (that is, sampled reduction product materials as prepared and analysed) the EDS results reflected certain apparent "incongruities" between field acquisition results and spot acquisition results. As can be seen in the range of photomicrographs presented herein of any and all reduction product remnants, reduction product materials exhibited inhomogeneous fields down to a generally sub-field-scan magnitude. This meant that (*i*) field scan EDS acquisitions reflected this inhomogeneity with reduction products of non-target species replicated in results, and (*ii*) only where the electron beam interaction volume (the "Monte Carlo bulb") was contained wholly within a single reduction product phase did spot EDS acquisitions reveal the "true" composition of the intended target phase. (Both field and spot techniques were subject to and within the accepted limitations pivotal to those operational parameters contained in the analytical approach employed.)

In common with the above revisited fundamentals of experimentation, aspects of background regarding the scope and conduct of the project's programme of analyses and supporting photomicrography necessitate further expansion or explanation. Certain characteristic elements of the project imposed specific experimental difficulties that were atypical even for comparable conventional pyrometallurgical experimentation. In the typical refractory metal case for this project, "metallic" products representing the experimental reduction product remnants were not the clearly defined metal buttons plus discrete slag phases – each easily separated from the other and from the crucible – as were products of the early iron, tin and copper oxidic-mineral smelts. Reduction products of this refractory metal mineral reduction programme were heterogeneous, with reduction product metallic phases and spent slag(s) included with primary regions of incompletely reduced multi-phase material plus remnant char. Typically also was that these phases were generally physically inseparable, being delineated by complex

boundaries and commonly exhibiting an indistinguishable interface between the crucible wall and the reduction product(s) proper (the crucible contents). Not all quenched phases exhibited evidence of fully liquid melting, surface-minimisation-driven coalescence of liquid beads, puddling accretion or associated liquid flow. High melting point metallic phases commonly appeared to be the product of solid state reduction (through diffusion from a gas phase reaction interface), possibly followed by softening and fusing or sintering agglomeration before a melting point was realised, if melting was reached at all.

Notwithstanding the non-equilibrium status of the thermal regime exhibited by the experimental microwave set-up, the characteristic "bell curve" type thermal profile of "bulk temperature" for microwave heating (in charge loads such as typified this project) tended to broaden or flatten out under extended processing. Unlike the flat (level) temperature profiles of extended, externally applied conventional heating (under radiation, conduction and convection modes of heat transfer), and with the irradiated microwave penetration depth and load size used in this work, a thermal maximum always occurred at or near the centre (the crucible axis) with temperature profile dropping with increasing radial distance – a flat, constant temperature profile being approached but never being realised in the campaign scope of the project. Further to this thermal profile of the charge solids, non-equilibrium plasma was stimulated by the microwave irradiation of gaseous particles and indeed, as generated, manifested as "low temperature" plasma, perhaps at several hundred degrees Celsius. This newly imposed heat input further modified the "temperature" profile through the charge. Subsequently, with the constant application of microwave energy into such a volume-limited system of increasing susceptibilities and the associated steadily increasing degree of excitation and ionisation in the plasma, the low temperature non-equilibrium plasma steadily ascended into non-equilibrium plasma of "high 'bulk' temperature". [Just to recount, this bulk temperature was the sensible or apparent temperature which (although imprecisely) could be recorded by sheathed thermocouple as a "weighted average" temperature of the "thermal mass bulk" of all particle temperatures.] For the sake of discussion, by crudely equating this bulk temperature with an equilibrium temperature equivalent, sensible plasma processing temperatures at process termination for the typical experimental trial peaked in the range of 2000°C to 2400°C (circumstance-dependent) by consensus of physical evidence of colour and intensity of plasma emission, molten phases and

thermodynamic history captured in frozen reduction products of the process's reduction remnants. By "flywheeling" the applied energy by means of further stimulation of system susceptibilities through process extension, system energy was increased and it was established that process temperature could be driven above 3000°C. (One such "thermal marker" phase *which was known to have been in the liquid state at quench* was assessed by Professor H.K. Worner for a tungsten, 10 at% Mo, 1.5 at% C metallic constituent phase of an early wolframite/molybdenite microwave smelt product as being at minimum 3300°C.)

As mentioned above, large portions of reduction products were unavoidably so hard and their fusion (bond) with contiguous material, including refractory containment material, so intimate and strong – even where clearly delineated – that any attempt to quantitatively separate for sampling collection was inevitably unsuccessful. A more "judicious", qualitative approach to sampling was instigated to yield more-subjective samples, samples which presented their own traits, and from which specimens were prepared for the various analytical requirements. Where suitably sampled reduction product material *was* recovered from post-reduction zones, the material attribute of hardness presented a challenge in respect of routine attrition during preparation of specimen materials, and for grinding and polishing of mounted specimens. After advice sought and upon intervening instruction, apparently less friable, larger very hard pieces of recovered material were not attrited for fear of damaging available milling apparatus. Nevertheless, selected material perceived to be representative of the reduction product was successfully reduced to an assayable size range using a ring mill. [Mounted specimens were successfully prepared utilising hard media and diamond wheels to grind followed by polishing on diamond media using quick stages under heavy pressure (to both cut the hardest phases but leave minimal polishing relief around phase interfaces and particle edges.]

Whilst milled material as prepared was suitable for "small or part sample" specimen analyses, photomicrography and characterisation studies, "all-of-reduction-product samples" such as would be essential for meaningful mass balance studies could not legitimately be prepared nor "all-of-sample" analyses conducted. Had the retrieval of reduction products been rudimentary, a mass balance study element to process evaluation would have been wholly desirable and, accordingly, would have been

enthusiastically pursued as an "essentially quantitative" means of ascertaining reduction process completion and substantiating process success. However, the nominal mass balance approach was otherwise compromised in its ultimate merit due (*i*) to the imprecise process chemistry and (*ii*) to the elusive stoichiometry and composition of final products – wherein minor quantities of the persistent light elements in reduction product metallic phases were the determining factor of the product metal's worth. Moreover, this element of diagnostic compromise plus the incapacity for complete reduction product reclamation (together) pre-determined that the mass balance element of total assessment was not available as a quantitative option; consequently, process verification by mass balance evaluation was just not possible within the scope of the project.

Similarly, notions of other "whole of reduction sample" strategies and comparable methods were eliminated, as were methods requiring in-vacuo arc re-melting of the total recovered sample (that is, equilibration and re-consolidation). Such re-melting provided a neat, consolidated, phase-simplified button but, by tendency towards vacuum de-gassing and phase-modification, also had the drawback of expunging physical and chemical evidence of reduction process history routinely captured in LN_2 solidification. Traditional "wet chemistry" techniques were regarded as inappropriate at such an emergent stage of process development, particularly due to complexity of product chemistry and the chemical stability of phases. Also, this family of analytical techniques was not readily available.

Despite the distended "trial and error" element of this fundamental and deceptively simple experimental programme, a high proportion of experiments yielded successful and edifying results. And, whilst the thrust of this thesis project was always to investigate the propensities and characteristics of microwave-stimulated reduction of refractory metal minerals, much was learned from early forays into the reducibility of minerals and ores of other metals – and, indeed, from microwave processing incursions into technical areas-of-interest related only indirectly to extractive metallurgy. [For point of interest, such microwave processing "areas-of-interest" included combustion synthesis; synthesis of intermetallic compounds; synthesis of ammonia; melt-syntheses of oxide ceramics and blend-specific materials; melt-process despoliation of asbestos types and conversion into safe ceramic options (including lightweight aggregate for

concrete construction); microwave-driven diffusion of metallic elements into steel substrates; sintering of metal matrix composites; metal/metal and metal/ceramic bonding; and the extractive-related microwave method of solid-state reduction (metallisation) of indurated ore pellets (such as blast furnace pellets) to low-carbon metal product.]

Inevitably important in the project was the management and conduct of experimentation and consequent reporting of results. Central then to the carriage of the programme of experimentation were the adopted task-specific points of procedural practice, the reporting of measured and/or assessed experimental results, and on presentation of observational and related corroborative experimental evidence and supporting material. Issues representing these aspects are addressed in the following, closing passages of this introduction to Section 7.

Certain relevant administrative matters regarding the organisation of results, their presentation (assemblage, scale, annotation, abbreviations and overall depiction), reporting (description and characterisation) plus co-ordination and categorisation of analytical means versus results (grouping, inter-relationship and explanation) and associated concerns are hereby dealt-with to best enable interpretation of this *Results* section. The notes prefigure the presentation of core results through the remainder of Section 7.

Where micrographs and similar figures are addressed or otherwise noted in the text then they are included nearby to that referral in the text, conversely, they are duly listed as "in Appendix **7".** Also, commonly for micrographs, the abbreviation **LO** means light-optical, and dependent upon context, **LOM** indicates light-optical microscope, _scopy or _graph. Original colour micrographs were captured on Kodak Ektachrome slide positives, and where un-attributed, an air lens optical configuration was employed, otherwise **oel** indicates oil emersion lens optics was employed. Colour images were transferred from slide medium to digital (electronic) storage by scanner for reproduction in this document; any loss of resolution was minimal, however, reproductions herein exhibit marginal loss of colour integrity and image sharpness

(delineation of features). [This option was an undesired concession to the combined cost of, and lack of control over, colour photographic prints.] The abbreviation **EO** means electron-optical, and **EOM** was similarly indicative of electron-optical microscope, _scopy or _graph. Where it is not written in full, **B/s** means backscattered and indicates that the electron-optical micrograph has been generated by back-scattered electron acquisition – almost all electron-optical micrographs in this document were acquired using the back-scatter detector. The alternative electron-optical format utilised was the more common secondary electron emission where, under bombardment by the incident beam, secondary electrons escaped from the target surface and were acquired through the secondary electron detector. **Sec** indicates the use of this secondary electron emission acquisition in capturing micrographs. Secondary electron images were generally clearer with superior resolution but lacked that atomic mass dictated "phase contrast" definition which allowed phase delineation in backscattered electron images. Such phase contrast delineation was of considerable benefit to this project *.

Nominally, for micrographs, the notion of magnification is meaningless without a frame of reference; therefore, electron-micrographs were nominally supported by the automatic superimposition of a labelled bar-scale. Alternatively, for light-optical and other micrographs where this facility was *not* available, noted with the annotation is the *page-wise* width of the photographical field of view (**fov**), albeit the photograph's "length". (The photograph's "width" being the page-wise height.) It was thought that this ambiguity, no matter how unlikely, might promote misunderstanding if not avoided. Consequently, the common annotation abbreviations of **wof** (for "width of field") or **fw** (for "field width") were not adopted, and field width presented in the annotation represented the page-wise width of the field of view (**fov**) of the photograph (micrograph, stereo-micrograph, macrograph or other). Thus, "fov: 0.12 mm" represents

* Along with the generation of other particle types, both secondary and back-scattered electrons are produced in the "near-surface" bulk of the specimen under excitation by the microscope's high voltage electron beam. Defined by their electronic origin and characteristic relative energies, (once they escape the specimen surface) the particles of interest are detected and electronically configured to produce the electron optical image [257, 260]. Of specific relevance, particularly for the ore-derived minerals of later sections, is the imaging feature of phase contrast (or atomic number contrast). Plainly evident in back-scattered images, phase contrast across specimen fields is facilitated by the sheer number of back-scattered electrons generated from within phase volumes of greater density – the greater the unit mass of the phase, the greater the counts registered, hence, the greater the phase brightness. Such a phenomenon provided not only a useful means of phase delineation, but was held to be analytically compelling when asserting phase differentiation [256, 258, 259].

the distance 0.12 mm from the left edge to the right edge of the photograph (or field) at the magnification captured at the photographic print. Such field width dimensions were converted from reference photographic prints taken of a commercial graticule (1mm divided into 100 equal divisions: 1 division equal to 10 μm or one hundred thousandth of one metre) on each microscope used to produce micrographs, for each lens used, and with the same focal train from lens to camera as used for the capture of micrographs. Typically, as specimens were examined intermittently through the project, such graticule recordings were routinely conducted when specimen micrographs were being recorded and so exist on the same film stock. [One such routine recording of the graticule is shown in the micrograph of Figure **{7.2.1.1}26**.]

Energy Dispersive Spectrometry (EDS) was carried-out on "metallic" phases-of-interest in the selected fields on chosen specimens and EDS counts were set at 100 sec live time acquisition for all spot and area acquisitions. [Live time exceeded 80% for all accepted counts. "Live time" = {(total acquisition time) – (dead time)}, where "dead time" was that system-measured acquisition time during which ***no*** counts were registered. A high dead time was considered representative of poor quality acquisition reflecting proportionately unreliable data – hence poor reliability of result. Also, as is generally acknowledged for this type of work [256], 80% live time was considered amply acceptable.] On occasions the hardware-to-software inter-relationship exhibited the distinct problem of being incapable of returning legitimate EDS results calculations, with neither at% or wt% totals equating to 100%. Strictly speaking, this predicament would demand that the results be disregarded as "flawed", however, on these few protracted "occasions" of machine (software) malfunction the problem was endemic and a modified approach was conceded. Consequently, for some EDS acquisitions on some specimens (including certain of those included later), where required, the EDS output was software-adjusted to total 100at% to facilitate some comparability between results. Whilst it was conceded that such adjusted results were *inaccurate* and effectively *incorrect*, they were "acceptable enough" to be *indicatively* employed when characteristic comparisons were required (and they were preferable to *no result* for the specimen). [Although quite obvious because wt% ≠ at% = 100% (adjusted total), where EDS spectra are accompanied by adjusted results in later figures of EDS spectra, the

figure annotations are accompanied by the suffix **å%** to indicate that the result should be viewed with prudent discretion.]

During primary examination, (to protect the otherwise exposed detectors against potential depositional contamination from the specimen in the central chamber) the more cursory EDS acquisitions and micrographical image acquisitions were collected through a beryllium detector window (**BeW**) – consequently denying the detection of the crucial Period **2p** light elements. Where collected, these **BeW** acquisitions were employed to locate ideal fields and, thus identified, formal EDS counts were acquired utilising the preferred windowless detector (**NoW**). Failing the availability of the windowless facility, ultra-thin (Be) window (**UTW**) detection could be employed for quantitative acquisition, generally inclusive of the crucial light elements O, C and N. Thereunto, it was noted that EDS **K**-spectral lines for these three light elements were inopportunely close or over-lapping with **L**- or **M**-spectral lines for the refractory elements of interest; **K**-, **L**- or (where applicable) **M**-spectral lines could be utilised in analyses of these metals [255]. However, **K**-spectral lines (energies) were mandatory for machine calculations of light element percentages in phase compositions (as light elements do not generate the higher peak-sets). Generally, the Leica Stereoscan 440 SEM (with integral Oxford Link EDS/detector system) software was calibrated and well capable of dealing with such contentious calculations when determining component percentages – the author alert to potential erroneous computations. Further, note that SEM/EDS studies (representing the various campaigns of mineral reduction) were conducted intermittently through the various programme-stages of the project – consequently, some minor variations in machine performance were recognised and accounted for where necessary. Also, (after system "upgrade" modifications) minor differences in output presentation were evident. On any occasion, the detected count of any acquisition was dependent upon machine (detection) performance. And, machine performance (itself) was a function of the working and material variables of accelerating voltage, beam current, specimen and coating conductivity, coating uniformity and stability, detector cleanliness and reliability, window cleanliness and stability (where relevant), chamber evacuation and environment, *et cetera*.

Unless noted otherwise (with each relevant reported instance), throughout this *Results* section all reported EDS acquisitions (counts) were collected using the windowless configuration. Although machine-output of the very many individual EDS-count analyses recorded, the overwhelming majority were overlooked for direct inclusion in this thesis document – and (excepting examples) those included are in summarised form. This was because, for each actual spot or area spectral count acquisition, the SEM printout of EDS analyses occupied one full page – or two pages for longhand information output. Consequently, whilst presenting as highly credible – even impressively informative – such full machine print-output were no more than selectively included in the thesis for purpose of example, and then only in Appendix **7**. [Many hundreds of SEM or other output pages could not realistically be included.] Where they are included in *Results* because of their importance in substantiating claims on newly reduced Ti-metal, to maximise the breadth of reporting, actual summarised results of EDS analyses are presented in condensed form as Table **{7.2.1.2}1** in Section **7.2.1.2**. [Also, where interim unavailability of electronic storage hindered documentation, early EDS results from Ti-metal were hand recorded directly into a log. In such cases, and as presented in Table **{7.2.1.2}1**, the last "significant" integer was rounded to either the nearest half or the nearest whole significant number.] Conversely, where an overview of the *range* in reduction product phases was required (to substantiate claims regarding "process" rather than "product"), phases generally representative of the broad scope of reduction product remnants were chosen to illustrate, if somewhat anecdotally, the complexity in typical process output. These explanatory results, configured as *"spectrum plus short analysis"*, were presented as an integral part of presentation in Section **7.2.1.3**, they should be interpreted in concert with the colour micrographs of Section **7.2.1.1**. In addressing these process-wide reduction product phases (aside from the product-specific "proof of concept" Ti-metal results of Section **7.2.1.2**), light was shed upon the overall microwave-stimulated reduction process under the oven set-up method – and to the relationship of the intended "pure" Ti-metal product to that range of concurrent phases within the breadth of the process. Where variously employed, XRD studies were used to support the results of these broader EDS surveys across the array of reduction product phases whilst identifying the target reduced "pure" metal existing within this process-wide array. In brief, the results strategy was to identify the target reduction product metal in its reduced, near-pure form, and then (with a view to process history) establish and account

for the process-wide range of phases captured with this "pure" metal at the process termination quench. Overall, reduction product complexity (through sinter agglomeration rather than melt consolidation) was a constant feature through the core experimental programme and the above approach to presentation of results was retained throughout Section 7, *Results*. Where departure by morphological deviation from this reduction product regulus-type defied the generality – such as for the consolidated product of the thermite reduction of ilmenite – the variations to coverage were duly noted with relevant descriptions.

Comment should be made at this point that microwave irradiation exposure times for experimental trials – commonly referred to as *processing times* or *campaign times* – seem quite long considering the size of the charge with respect to the input microwave energy. However, it must be understood that some minutes of irradiation exposure was spent on raising the temperature of the charge from ambient into its reaction temperature-zone. It was learned in preliminary work that when such a charged crucible configuration was raised to, in extractive metallurgical terms, a relatively modest 500°C in a temperature-controlled oven, thence wholly transferred into the microwave oven set-up and irradiated as per normal, then the same reduction result (in ~2000°C plasma environment) would be attained in about 3 min less than the same charged crucible irradiated in the oven set-up starting from room temperature. Whilst providing the desired boost (to new base properties at 500°C) for dielectric susceptibilities within the charge materials, this targeted heating did not wholly account for the nominal heat-sink debt of cold recipient refractories in the oven set-up system at the point of transfer, nor for the appreciable further thermochemical input required to lift the charge into the realm of reaction thermochemistry. Consequently, where an estimation of relative pre-process heating time has been established for a charge or system under batch process, then experimental "processing times" ought be viewed in context of such a "relative processing time reduction". [Of course, such allowances would not be required for systems operating on a *continuous process* basis; an ultimate aspiration in the further development of such metallurgical operations.] Also, whilst the reactants charge was "seen" by the magnetron as the susceptible microwave load (as reflected by its imposed microwave field), the "microwave transparent" crucible and insulation (at many times its mass, and directly heated only minimally by the

microwave field) were almost wholly heated by conducted heat plus radiated heat "robbed" from the heating reactants charge. Thus, heat energy input into the total system was accommodated by way of the charge's microwave susceptibility – quite an extra thermal load (heat sink) upon the small reactants-charge mass. Further, as substantiation of this thermal millstone effect of the collective insulation, it was also found in preliminary work that a charged crucible configuration with only one thickness of insulation blanket wrap could be heated considerably faster into the very high temperature range required for processing. However, an energy input limit was reached whereupon heat lost by radiation from the outer wrap surface equalled the heat produced internally by the combined consequences of dielectric heating (the "absorbed" microwave energy as distinct from the applied microwave energy) plus that liberated in exothermal process chemistry, and no higher system temperature could be reached. By comparison, a doubly wrapped, equivalently charged crucible could, with a plainly lower exponential rate of temperature increase, reach temperatures clearly in excess of the singly wrapped version – ultimately, of course, constrained by the same energy "input/output" proviso. Reduction product and melt remnant outcomes (phases present, degree of consolidation, *et cetera*) of these pilot "heating" trials were confirmation of this "not unexpected" result. Unfortunately, calibration of microwave-stimulated heating profiles (temperature versus time) for known charges was never narrowed beyond the subjectively notional "*expected*" into the more tangible "*predicted*" heating profile; an unavoidable tendency for microwave processing in random loads of uncertain dielectric consistency. Accordingly, in any assessment of this microwave processing, when projecting process energy efficiencies, the ranges of processing times at constant (full) microwave power recorded against each of the project's diverse experimental reduction trials should not be construed so minimally as to be a simple "*mass processed* versus *power expended*" deliberation.

7.1: Early Reduction Programme.

*[Foreshadowing the core refractory metal results of Sections **7.2** to **7.5**, this Section **7.1**:* Early Reduction Programme *(incorporating Sections **7.1.1** to **7.1.5**) is included because of its relevance to the formulation and development of the project –*

both in methodology and in subject scope. It also provides some insight into the choice of topic and, as such was necessary, the narrowing of project scope from more obvious, if less challenging, process-metallurgy options. Fittingly, augmentative Section ***7.1*** *represents a project foundation, a provisional reference set for the ensuing core programme; its inclusion is intended to introduce and illuminate the nature of the project.]*

In the "early experimentation" period of process development leading towards the experimental programme which was to become the essential core of this project, many minesite-derived and laboratory grade minerals were reductively processed using the evolving microwave oven set-up method. This microwave method became more defined and process orientated (*vis-à-vis* equipment orientated) during the course of the project. The rudimentary reduction assignments covered in this Section **7.1** were fleetingly cited in the overview of the broader early reduction work described in Section **6.4**. Any reference in the earlier section was for the want of completeness in *that* summary; and where described in Section **6.4**, the earlier accounts do not override nor obviate those presented in this section. The accounts herewith feature since-deferred (residual) experimentation involving refractory metal minerals and, preceding (as they did) the core experimentation, the execution and consequences of this work proved to be relevant.

Generally, early reduction product aspirations were quite modestly configured around ferruginous co-reduction strategies – many of the minerals in early work being ferruginous. Hereto, whether of ferruginous origin or not, cited reduction examples do otherwise include minerals of the refractory metal elements – including the "core" elements. Moreover, being commercially important in the Australian mining sector (and resource investment and development generally), minerals in this section also represent the four omitted refractory metals, vanadium, chromium, molybdenum and tungsten (which, once discarded, left those five that are core to this project). Even where refractory metals were co-reduced with iron their smelt reduction was instructional, and their appropriate inclusion was supplementary to the evolving procedure of *specific mineral* reduction that was common across the core programme. In addition, their

example offered valid insight into the possibilities of further beneficiation techniques and procedures, and into alternative reduction route gambits. Inevitably, in industry generally, such "next generation" process possibilities are routinely developed into real applications under the illumination of exceptional "new technologies". Such innovation is the case for microwave processing generally and, fittingly, will in future be so for microwave-stimulated reduction processing.

The simplicity of the reduction procedure and its reduction product can readily be seen in the photograph of a sectioned crucible with reduction product iron button and slag remnant still intact, presented as Figure **{7.1}1**. This bare standard, an example of the most straightforward of reduction assignments was, throughout later work, only to become more complex explicitly in that the operational reduction chemistry shifted more into the realm of ionisation chemistry, thermal regimes became more aggressive and consequent reduction products more differentiated. Reduction products of the straight refractory metal minerals were heterogeneous, usually with an entrained by-product "slag" component, and commonly were intimately fixed or fused to the crucible wall, were atop and beneath the layers of "atmosphere protection" char granule remnants, and were interspersed by displaced char granules. Such reduction products were characteristic both of reactant minerals possessing pronounced thermochemical stability (requiring higher reduction "temperatures") and of reduction product materials of high melting point; each in contrast to those of the more easily reduced, often ferrous-based smelts of the "early work".

A constant feature of reduction smelts of lower melting point base metals such as iron, copper and tin was the solidification of phases as dendrites, laths or other distinguishing morphological habit. This outcome presenting a noteworthy trait in quenched irons where solidification of highest melting point liquid together with the draining (of subsequent-phase liquids) associated with volume contraction left the initial solid exposed at either an internal or the external surface of the metallic button. Dependent upon surrounding thermal conditions at initial solidification, the continuity of the initially frozen outer surface determined whether exposure of initial-phase solid would be contained internally around a cavity or exposed as a solely external feature.

Figure {7.1} **1:** Macrograph of a sectioned fireclay crucible with reduction product intact minus the loose char remnant that, at smelt termination, surrounded and covered the frozen slag cap. The smelt product was a slowly cooled (in insulation wrapping, here removed prior to sectioning) grey cast iron button being the microwave-stimulated carbothermic reduction product of a simple haematite smelt. [LO photograph, 90% of full size. Flat crucible base: 42 mm diameter.]

Figure {7.1} **2:** Dendrites exposed (by retreating liquid after volume contraction) at the button surface of an air cooled high carbon iron smelt product of the microwave-stimulated carbothermic reduction of Mount Newman haematite. [EO stereo-micrograph, fov: ~3 mm]

Such exposed crystals feature in nearby Figure {7.1}**2** and in later Figure {7.1.1}**1** showing V-rich phase needles atop the reduction product button. Additional supportive stereo-photographs (Figures {7.1}**3**, {7.1}**4**, {7.1}**5** and {7.1}**6**) plus further informative macrographs (Figures {7.1}**7** and {7.1}**8**) are included in Appendix **7**. Unless otherwise noted, the microwave reduction examples presented in Section **7.1** (including **7.1.1** to **7.1.5** inclusive) were carried-out in small fireclay or alumina crucibles charged with up to 35.0 g (mineral density dependent) of reactants plus loose char, and in the configuration and conditions of the "oven set-up" at its contemporaneous (then-current) stage of evolution. Also of methodological significance, the reduction product "buttons" as solidified were never the products of deliberate cooling-curve strategies, nor their microstructures ever the deliberate intention of such strategies; microstructures as attained were merely the chance product of random *physical* events at reduction process termination. The later liquid nitrogen (LN_2) quench strategy was devised, not to arrive at a specific microstructure, but to *chemically* protect cooling reduction products from re-oxidation (by oxygen most particularly). The LN_2 quench provided an acceptably high rate of cooling thereby minimising the chance of re-oxidation (by both contact opportunity and species denial) in a purpose-designed LN_2 quench chamber system that, although simple in concept, was of sufficient design to guarantee the method. (Also, return to Figures {5}**1** and {6.2.2}**2** for schematic drawings.)

This abridged Section **7.1** was included to afford some visual narrative, some sense *of* and feeling *for* the formative early work, and to round-out the refractory metal elements (with respect to microwave reduction). Above all, its inclusion was intended to impart an awareness of the wider potential of microwave reduction processing applications for refined source-minerals and mine-derived mineral concentrates of the thermochemically ***less-stable*** transition elements. [The method also has relevance to processing and reduction of the geochemically enduring minerals of those rare earth (**4f**) and transuranic (**5f**) elements of the long periods.] *Because of the supplementary, "thumbnail sketch" nature of Section 7.1, reduction products are presented photographically or micrographically and (for this Section 7.1)* ***no analytical corroboration is provided to accompany descriptive*** **annotations**, *because these plainly are illustrative examples compositional verification was considered to be superfluous.*

7.1.1: Reduction of Vanadium-Bearing Magnetite and Vanadium Pentoxide.

Vanadium does not occur in mineralogically massive deposits (as do iron, copper, lead, and other more common metals) but is sparsely distributed both geologically and geographically as patronite (VS_4), vanadinite [$(PbCl)Pb_4(VO_4)_3$], carnotite [$K_2(UO_2)_2(VO_4)_2.3H_2O$] and roscoelite, a vanadium-bearing mica[14]. However, most vanadium (as a minor, "contamination" component) is won from vanadium-bearing magnetites and recovered in the form of the pentoxide, V_2O_5 . As with many other lower-output refractory, rare earth and transuranic metals, mine and subsequent extraction output is designated in the *oxide equivalent* (that is, as V_2O_5 – in longer-term tonnages). The Savage River (Tas.) vanadium-bearing magnetite used in this project contained$\leq$ 1.5 wt% V in Fe_3O_4 and, at the time of its acquisition, was no longer being sourced to supply vanadium production operations. Gangue content of the concentrate from Savage River was very low at ~1%, whilst the vanadium was present in substitutional solid solution in the magnetite lattice rather than as intimate gangue co-mineralisation (of, perhaps, roscoelite or a vanadate).

In carbothermic reduction trials, the Savage River magnetite was reduced without difficulty to an iron product, and despite the ready reduction – and as no V reported in the slag remnant – apparently all V was retained in the iron as either a V-carbide (or carbonitride) compound or as a component of an Fe/V/C solid solution phase. Whether water quenched or air cooled in the crucible, the carbon saturated smelt products cooled rapidly enough such that the resultant metal buttons cooled as white iron rather than grey iron, although the morphological habit of these irons varied between the two cooling rates. At variance with typical grey irons of this project, and atypical of comparable white iron smelt products, it was observed that (upon quenching) particulate char inclusions were captured at sites of initial freezing, possibly initiating the precipitation of the initial primary carbide needles radiating through the white iron microstructure, as seen in Figure **{7.1.1}2**.

Under varying experimental conditions, carbothermic reduction of the pentoxide was partially successful, leaving either an oxygen-depleted oxide form (V_2O_{5-n}, $0<n\leq2$) or

Figure {7.1.1} **1:** Iron button shown above was the solidification product of the air-cooled (moderate cooling rate < quenching) smelt product of the reduction of Savage River V-bearing magnetite mineral concentrate, a concentrate which contained only ~1% gangue with the <1.5% V magnetite. The stereo-micrograph shows a ~15 mm diameter button exhibiting needles of primary carbide well delineated by the volume contraction of freezing – here exhibited externally – but in water quenched iron buttons (generally) this shrinkage (where such was expected) was more commonly exhibited internally as a similarly adorned central void, whilst the "smooth" button surface revealed little of the immediate sub-surface phase morphology. [LO stereo-micrograph.]

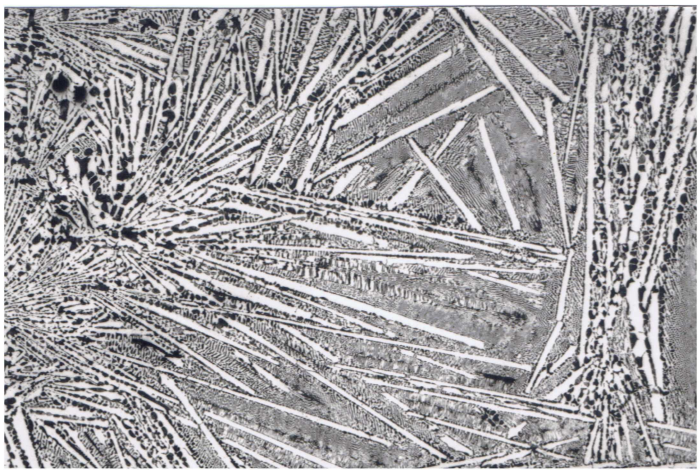

Figure {7.1.1} **2:** Micrograph of the iron smelt product of carbothermic reduction of V-bearing magnetite showing acicular carbide phase (possibly $(FeV)_3C$) in a eutectic matrix. Note those regions of first solidification being the points of radiation of the primary carbide needles bounding the balance of pearlite plus excess ferrite. The field of view was representative of an air-cooled iron button specimen similar to that shown in Figure {7.1.1} **1** above. [LOM, fov: 1.28 mm]

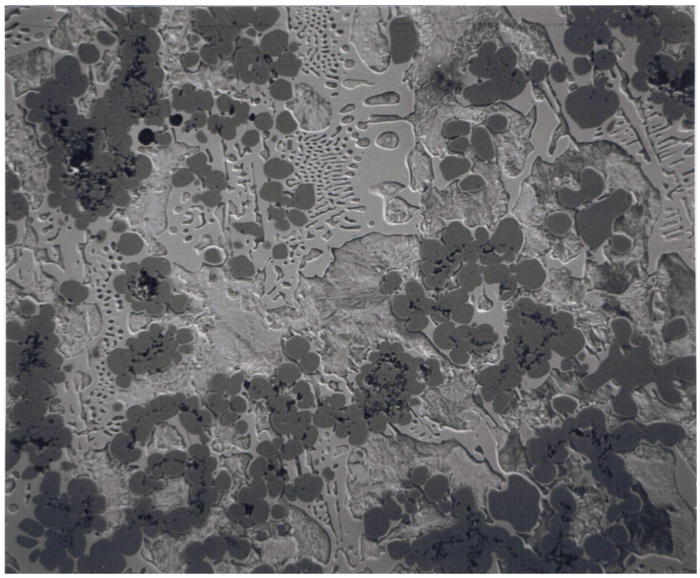

Figure {7.1.1} **3:** White iron smelt product of the carbothermic reduction of vanadium pentoxide (V_2O_5) with intimately mill-blended char plus co-reductant/solvent iron carbide, Fe_3C. The iron button so produced contained an overall 32 at% V in a water quenched iron. Precipitating around black remnant carbon inclusions, the darker plain "bunched" V-oxycarbide phase was initially solidified within the matrix of ledeburite [$(Fe,V)_3C$ + transformed γ-phase]. [B/s EOM, fov: 0.06 mm.]

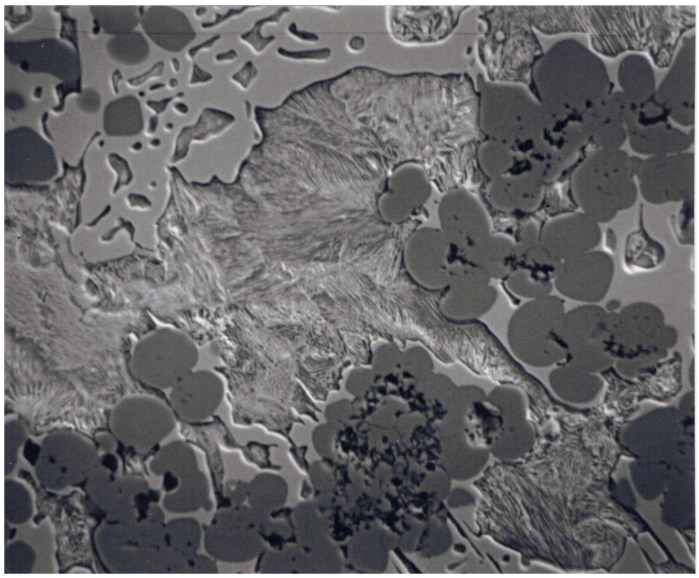

Figure {7.1.1} **4:** Micrograph shows detail of the above white iron smelt product of the carbothermic reduction of intimately mill-blended vanadium pentoxide (V_2O_5) with char plus co-reductant/solvent iron carbide, Fe_3C. [B/s EOM, fov: 0.02 mm]

a comparable oxycarbide. It was noteworthy also that, without reductant, the pentoxide bonds could be broken under microwave irradiation, effectively reducing the pentoxide to a similarly-depleted oxide form. However, reduction of the pentoxide was accomplished by intimately ring mill-blending V_2O_5 with char and iron carbide, Fe_3C, as co-reductant/solvent under CO-atmospheric protection, the resultant white iron is micrographically presented in Figures **{7.1.1} 3** and **{7.1.1} 4**. Clearly, this experimental result has particular synergy with the industrial production of ferrovanadium, most of which is destined for the iron and steel industry. In steelmaking, vanadium as an alloying component is introduced into the ladled molten steel by lump additions of ferrovanadium such as to adjust the melt to alloy specification before slab-casting operations, or the casting of billets for conventional rolling. Ferrovanadium is produced by the arc-furnace reduction of iron and vanadium oxides with carbon yielding a ferrous alloy of 50 - 60% V and up to 3.5% C [241].

7.1.2: Reduction of Chromite.

Although modestly less abundant than vanadium in Earth's crust (136 versus 122 ppm), in terms of resource mineralisation chromium occurs in deposits which are more chromium-abundant than is vanadium in its deposits. In these chromium-abundant deposits, the chromium presents in minerals of high chromium content in high ore-mineralisation concentrations (compared to the relatively more sparse vanadium minerals). As a primary mineral formed in ultramafic plutonic igneous rocks and serpentines derived from them, chromite ($Fe^{(2+)}Cr_2O_4$) and the lesser magnesiochromite ($MgCr_2O_4$) are geologically obdurate and consequently survive in detrital deposits. Chromium also occurs in silicates and rock forming minerals such as picotite (chrome spinel), uvarovite (chrome garnet), chrome diopside, chrome zoisite and crocoisite, lead chromate ($PbCrO_4$)[14]. However, chromite is the only commercially important mined chromium mineral and mineral concentrates are produced in the nominal range from Cr-lean low-grade chromite to the higher value Fe-lean high-grade chromite (which is close to nominal $FeCr_2O_4$ stoichiometry), all chromite mineral concentrates have nuisance levels of mineralogically associated gangue components. Broadly, the three utilisation

routes into which chromite may be destined are (*i*) for use as a high-value refractory sand; or for direct arc-furnace reduction to ferrochrome and assigned thereafter (*ii*) to steelmaking, or (*iii*) to solution separation or electro-winning of chromium metal. Dependent upon both the source chromite and subsequent mineral dressing and/or pre-reduction processing, ferrochrome compositions may vary widely and will typically assay in the range: 60 - 75% Cr, 1 - 8% C for arc-carbothermic method, (or 1 - 7% Al if by arc-aluminothermic method) with balance Fe [241].

Generally, chromite concentrates proved to be readily reducible. Two grades of chromite were used in microwave reduction trials in the preliminary experimental programme. A low-grade ex-mine chromite mineral concentrate from the Philippines (Minpro) was successfully reduced under a range of conditions, with accompanying minerals, and with various reductants. Of passing importance (and for reasons which remain somewhat unclear and were only envisaged speculatively as being attributable to the serendipitous confluence of dielectric interactivity between entrained mineral fractions) high-grade chromite concentrate proved to be both more microwave susceptible and more readily reducible than the lower grade concentrate. Charges of lower grade concentrate retained some degree of refractoriness through a more extended lower temperature range of microwave processing (relative to charges of high grade chromite concentrate). Typical of all highly reducible ore concentrates, under reduction the N.S.W.-sourced high-grade chromite quite promptly formed primary metallic beads, which ultimately coalesced, drained and accumulatively pooled into (what was to become upon quenching) a final metal button. Such an intermediate coalesced metal bead, mounted and polished, with an atypically high average (overall) composition of 87at% Cr (by EDS area acquisition) is shown in Figure **{7.1.2}1**. The accompanying micrograph of Figure **{7.1.2}2** shows an air-cooled button product of high-grade chromite mill-blended with char, and in an experimental trial, carbothermically reduced under microwave irradiation for a brief 4 minutes from room temperature – many processes required similarly short exposure to process irradiation, but most were extended beyond their perceived end-point to ensure reduction completion and/or melt consolidation.

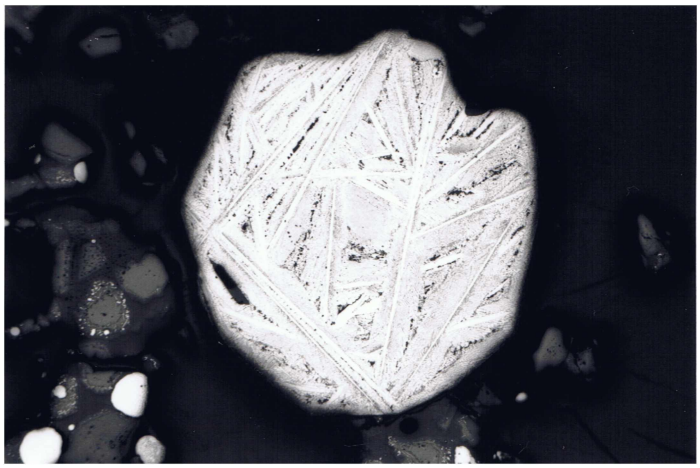

Figure {7.1.2} **1:** The micrograph shows a metal bead formed in the upper region of a partially reduced high-grade chromite charge and frozen prior to consolidation pooling. The polished and etched section was found (by EDS area acquisition) to have (C disregarded) a mean composition of 87 at% Cr with balance Fe. This bead presented an anomalously high Cr:Fe ratio and was representative of the wide compositional range represented in such initially formed beads of metal. The average ratio in the final cast metal button for reduction smelts of high-grade chromite was close to 2:1 (Cr:Fe) by atomic percentage for each relevant microwave smelt reduction trial. [LOM, bead diameter ~1.5 mm.]

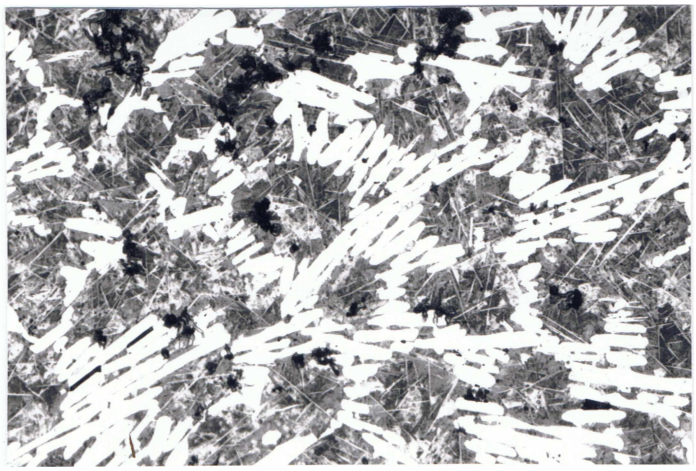

Figure {7.1.2} **2:** The micrograph shows the air-cooled white iron microstructure of the reduction product of a microwave reduced high-grade chromite/char mill-blended charge, in this case the processing time from room temperature to irradiation termination was a brief 4 minutes. The micrograph shows a complex microstructure in which γ-phase dendrites (dark regions) form ahead of the carbide - γ-eutectic (white parallel plates and interspersed γ-plates), the carbide was $(Fe,Cr)_7C_3$ (or possibly, $(Fe,Cr)_{23}C_6$). Cooling between 1200°C and 800°C, Widmanstätten M_7C_3 plates form in γ. Below 800°C, eutectoid decomposition of γ occurs yielding α + M_7C_3 , [with $M_7C_3 \equiv (Fe,Cr)_7C_3$ here.] [LOM, fov: 0.32 mm.]

[Coalescence, draining and pooling agglomeration phenomena were universally aided by the trace presence in activated charcoal of $BaCO_3$ – added in miniscule proportion to such char products as an activation stimulant and modifier. This agent had the desirable effect in project work of lowering surface tension on liquid metal entities, allowing said coalescence and flow in liquid phase metallics. Therein – fundamental even for such surface-minimised volume-types as the near-spheroidal reduction product beads – underlying the physics of containment and flow for liquid micro-volumes was the principal that the smaller the liquid bead, the higher the surface area to volume ratio and, consequently, the greater the surface tension restraint on the bead and the greater its resistance to either coalescence or flow. So, initial growth of primary metal beads was both a limiting factor to flow and essential to resultant pooling agglomeration. Further, different liquids exhibit different surface tension under the same prevailing conditions. By way of example, in cassiterite reduction, liquid Sn (whilst dense, of low melting point and high fluidity) forms beads that have high surface tension (relative to liquid beads of other metals). The surface tension restraint to coalescence and flow of primary Sn beads was overcome by the surfactant presence of trace $BaCO_3$ from the reductant char, consequently promoting the pooling agglomeration of clean metal. Tamping and/or vibration techniques also assisted high temperature agglomeration of lower melting point metals. (Tamping, vibration and other physical accumulation techniques became irrelevant for "sticky", high melting point reduction products.) In the cases of chromite reduction, because of easy reducibility, an evenly distributed array of fine metallic beads (representing the universal distribution of reaction sites, and reflecting microwave susceptibility sites) was evident in prematurely quenched charge remnants representing the range of chromite charges subjected to reduction. In chromite reduction exercises, reduction was compliant and prompt yet (in contrast) corresponding accretion was retarded. Here, the surfactant assistance of $BaCO_3$ was necessary for coalescence and flow in the transitional accumulation from fine molten beads to liquid metal pool awaiting quench to ferro-chrome button.]

Several strategies were employed in reduction processing of low-grade chromite. As revealed above, compared to the high-grade concentrate, low-grade chromite was less readily smelted under microwave-stimulated reduction, however, even the low-grade Minpro chromite was efficiently and gainfully reduced on every occasion. Figure **{7.1.2}5** shows typical microstructure evolved in a smelt product ~21 at% Cr iron,

initially cooled slowly to solidification *in situ* in its undisturbed crucible, thence the hot button turned-out, freed of char and detritus and allowed to "air-quench" on a cool surface. The specimen was the smelt product of microwave reduction under loose char of a charge of mill-blended 50/50 wt% low-grade chromite concentrate and iron carbide, Fe_3C. Also smelted under char in a similar manner, the same blend was reduced and water quenched to produce a white iron containing ~23 at% Cr. For chromite reduction trials, as for repeated reduction exercises generally throughout the project, reproducibility of overall alloy compositions was broadly consistent in replicated smelting experiments. The Minpro low-grade chromite was prominent amongst minerals used in multiple-mineral blends that, for a period of broader exploratory reduction experimentation, were tested for *"dielectrically-catalysed mutual reducibility"* in the microwave plasma environment of the reduction process. Resultant reduction products (metals and slags) were of considerable interest when assessing process parameters and outcome possibilities – and the concept raised some plausible process advantages in favour of reductively processing mineral *blends* integral within an *extractive processing* stream.

Figures **{7.1.2}3** and **{7.1.2}4** present micrographs of the air-cooled microstructure of the smelt product of microwave reduced charge of the ring-milled mineral-concentrates-blend of low-grade chromite/ilmenite($FeTiO_3$)/pentlandite[$(Fe,Ni)_9S_8$]/char (8:8:3:1 by wt) under loose granular char. It was intended with such a blend to investigate the use of, and respective impact upon, oxides possessing different reducibilities in process-permutation with a co-reductant sulphide (to validate or to lay bare an old reduction concept). In this case the sulphide nickel concentrate was completely reduced along with the oxide concentrates to produce the alloy iron plus an aggressive dark sulphurous slag that retained minor Ti (~4 at% Ti) from the ilmenite. As with the mineral-bound O, most of the mineral-bound S (in the pentlandite) escaped the reduction zone (and the reduction configuration proper) in gaseous form, principally as SO_2 (by detector). Derived from the minerals' gangue contents plus O and S portions not gaseously released, the smelt slag was considerably supplemented by the sulphur-fluxed molten erosion-portion of fireclay crucible. Although variously allowed-for in smelt work – for there was always sufficient slag-forming material (indirectly) available by proxy of the nature of such

operations – the *intentional* inclusion in mineral blends of specific slag-forming mineral additions (dolomite ($CaMg(CO_3)_2$), limestone ($CaCO_3$), *et*

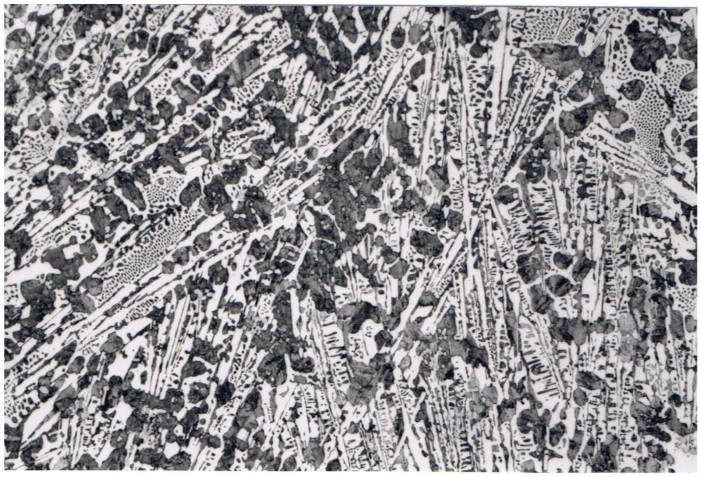

Figure {7.1.2} **3:** The micrograph shows the slowly cooled microstructure of the reduction product of a microwave reduced charge of mill-blended low-grade chromite($FeCr_2O_4$)/ilmenite ($FeTiO_3$)/pentlandite[$(Fe,Ni)_9S_8$]/char (8:8:3:1 by wt) under loose char and cooled *in situ* to room temperature. The field of view (fov) shows the resultant hypo-eutectic microstructure in which pro-eutectic austenite (γ) formed prior to ledeburite eutectic, whilst carbide laths may be due to local eutectic divorcement. [LOM, fov: 0.32 mm.]

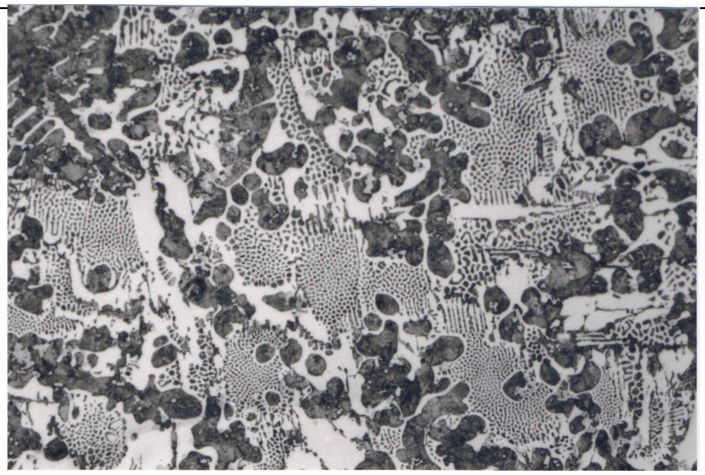

Figure {7.1.2} **4:** The micrograph shows to some advantage microstructural detail of the specimen presented above in Figure {7.1.2} **3**. TiC particles can more clearly be seen in the prior austenite – these particles may have acted to nucleate the pro-eutectic γ-dendrites. [LOM, fov: 0.16 mm.]

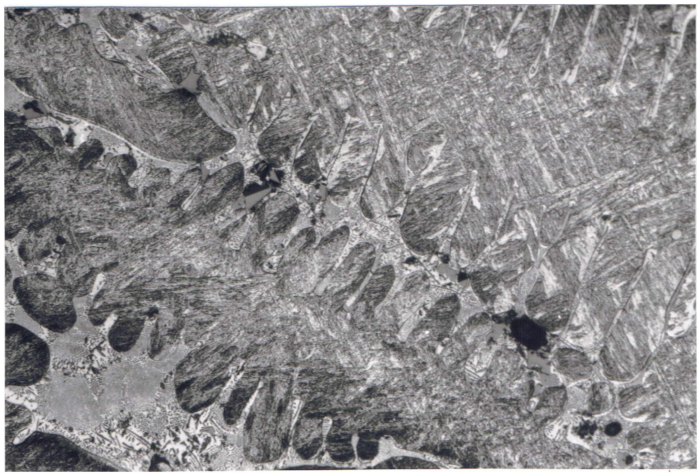

Figure {7.1.2} **5:** The micrograph shows the microstructure of the air-cooled white iron reduction product of a microwave reduced charge of mill-blended low-grade chromite($FeCr_2O_4$)/Fe_3C (1:1 by wt) beneath loose granular char. The air-cooling in this case was both slow enough during initial solidification to allow the development of expansive austenite (γFe) dendrites, thence upon exposure to air, sufficiently rapid during further cooling to allow the solid-state transformation of γFe to martensite and/or bainite. The inter-dendritic structure was carbide–austenite eutectic, this austenite has also transformed upon cooling. [LOM, fov: 0.32 mm.]

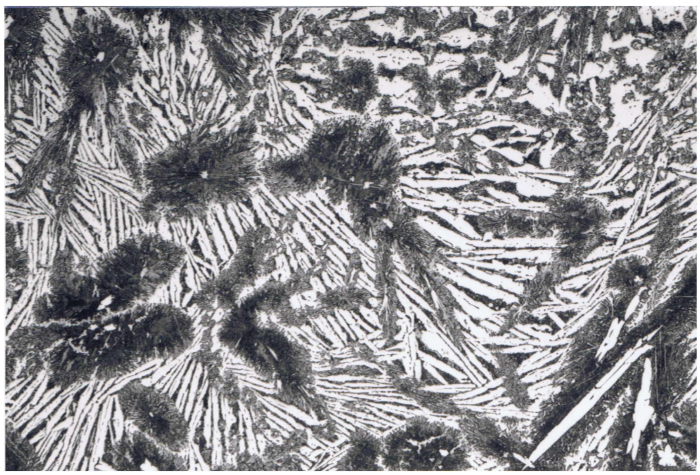

Figure {7.1.3} **1:** The micrograph shows the water quenched white iron microstructure of the reduction product of a microwave reduced charge of mill-blended MoO_3/Fe_3C/Fe_3O_4/char (4:4:4:1 by wt) beneath loose char. The specimen, having a mean ~12.5 at% Mo, exhibited a high alloy microstructure quite typical for the hypo-eutectic alloy irons of this reduction work. Pro-eutectic γ-dendrites were here transformed to fine pearlite and the eutectic consisted of alloy carbide laths interspersed between regions of transformed austenite (pearlite – appearing dark at this magnification). The specimen was not over-etched despite its appearance at low magnification). [LOM, fov: 1.28 mm.]

cetera) was, beyond the occasional trial, still not systematically instituted by the time of the termination of this preliminary phase of project experimentation.

The green laboratory grade chromium oxide, Cr_2O_3 , which is reductively obdurate amongst the chromium minerals, was reduced using the microwave-stimulated reduction method with inconsistent results – and varying degrees of completeness in those trials that satisfactorily progressed to a reduction product outcome. However, this exercise remained incomplete; it was not pursued once the scope of the project was narrowed – chromium thereafter discarded from the core refractory metals. Notwithstanding promising early results, other refractory metals of initial interest, molybdenum and tungsten, presented hereafter in Sections **7.1.3** and **7.1.4**, were also excised in the same narrowing of project scope. The remaining five refractory metal elements identified to become the project core were so chosen because, despite their minimal value-add component, they represent major Australian export streams and were contained in as few as three ore minerals from just two types of mining operation.

7.1.3: Reduction of Molybdenite and Molybdenum Trioxide.

The principal commercially mined ore mineral of molybdenum is the more common sulphide, molybdenite (MoS_2), which occurs as late-stage mineralisation in acid igneous plutonic rocks, as mineralogically varied high-temperature hydrothermal veins and as intrusions in quartz pegmatite deposits. Because of its lower frequency of occurrence, the oxide ore mineral wulfenite ($PbMoO_4$) is of lesser importance and occurs as oxidised outcroppings associated with other lead-bearing and molybdenum-bearing deposits. Molybdenum also occurs as the hydrated (and misnamed) molybdate mineral, molybdite ($Fe_2O_3.3MoO_3.8H_2O$) [14]. The sulphide was difficult to fully reduce and earlier reduction attempts yielded incompletely reduced matte-type solids. However, molybdenite was successfully reduced in blend-association with Fe_3C, excess char plus other, oxidic ferruginous alloy minerals (such as chromite and wolframite) in longer campaigns of more intense microwave irradiated thermochemistry. The laboratory grade oxide mineral molybdenum trioxide, MoO_3 (molybdite), was

microwave reduced in the presence of ferruginous co-reductants with relative ease (when compared to the sulphide) and with apparent completeness as no Mo reported in the slag material.

Laboratory mineral MoO_3 was mill-blended with iron carbide (Fe_3C) and magnetite (Fe_3O_4) plus char [MoO_3/ Fe_3C/ Fe_3O_4/char (4:4:4:1 by wt)], and the blend charge microwave reduced (beneath loose granular char) to yield a white cast iron button upon water quenching. Both Fe_3C and Fe_3O_4 are highly microwave susceptible (to approximately the same degree), consequently, smelt reduction was rapid, and Mo was not lost to slag. The microstructure of this ~12.5 at% Mo (area-acquisition average, C not assessed) reduction product is presented in the micrograph of Figure **{7.1.3}1**. By comparison, the microwave reduction of mill-blended molybdenite/Fe_3C/char (6:6:1 by wt) under loose granular char yielded the air-cooled white iron whose characteristic microstructure is presented in Figures **{7.1.3}2** and **{7.1.3}3**. The alloy iron microstructure was complex and the distinctive "herringbone" eutectic was pervasive across the full microstructural field of the button.

Both MoS_2 and MoO_3 were commonly blended with other charge minerals during the "exploratory extractive processing" phase of early project experimentation (see Section **7.1.2**). Particularly with the molybdenum minerals, wolframite was a favoured blend component because of its complementary ferruginous base when matched with a singularly-iron oxide or carbide with a view to generating a liquid-metal solvent hub into which reduction product alloy components would quickly (and irreversibly) be contained. Presented in Figures **{7.1.3}4**, **{7.1.3}5**, **{7.1.3}6** and **{7.1.3}7** are micrographs of the arc-remelted alloy white iron button which was melt-consolidated from sintered solid-state reduction product remnants of the microwave reduced charge of mill-blended molybdenite/wolframite/magnetite/char (6:6:3:1 by wt) blend. The porous reduction product was a solid-state reduced, sintered metallic sponge containing remnant sulphur-rich black oxide slag (which, upon arc-melting, was released from sponge pores and separated as a less dense immiscible liquid layer, capping the button upon quenching). [A typical solid state reduction product sponge is shown in Figure **{7.1.4}1**.] Also, metallic compound particles were not evident in sponge microstructures or, at least, were not detected – possibly because of sponge morphology. The iron microstructure represented in the first three figures, Figures **{7.1.3}4**, **{7.1.3}5** and **{7.1.3}6**,

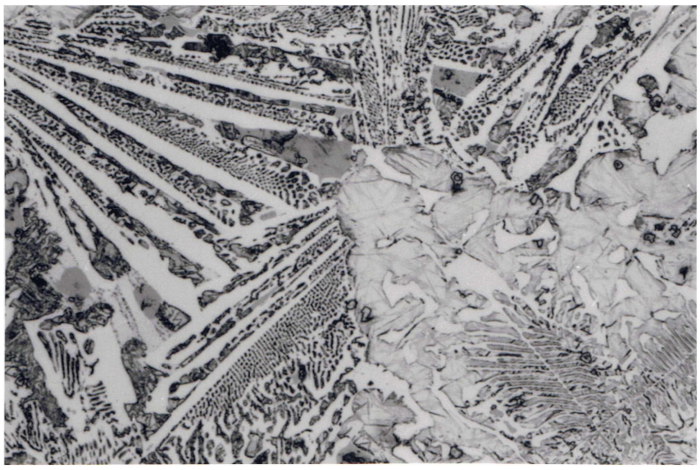

Figure {7.1.3} **2:** The micrograph shows the air-cooled hypo-eutectic white cast iron microstructure of the air-cooled reduction product of a microwave reduced charge of mill-blended molybdenite(MoS_2)/Fe_3C/char under loose granular char. The field shown presents two dominant phase regions. The upper and left field shows pro-eutectic carbide plates with ledeburite eutectic – here the Mo has segregated to the carbide leaving the liquid Mo-depleted such that it has formed a "normal" eutectic upon freezing. The phase field of the lower right quadrant shows pro-eutectic γ-dendrites plus divorced carbide and γ plus carbide "herringbone" eutectic. The formation of γ could have rejected Mo back into the melt thus influencing eutectic morphology. Also, as can be more easily identified in the following micrograph of Figure {7.1.3} **3**, austenite (γ) appears to have partially decomposed into martensite plates. [LOM, fov: 0.14 mm.]

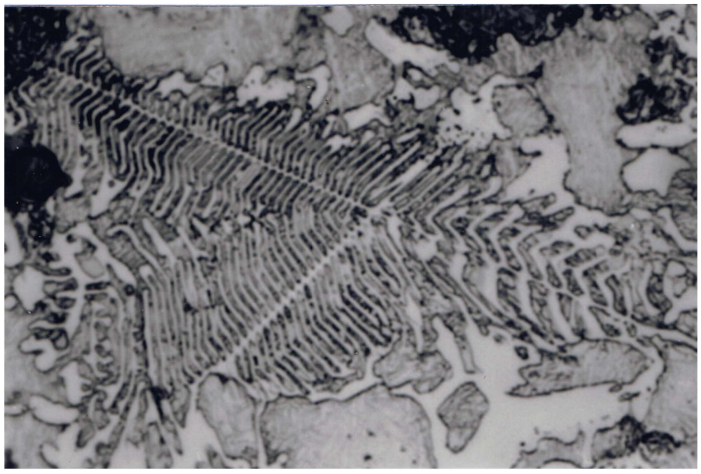

Figure {7.1.3} **3:** The micrograph shows further detail of the herringbone faceted-, non-faceted eutectic in the high C alloy Mo white cast iron reduction product of the molybdenite/Fe_3C/char microwave smelt shown in previous Figure {7.1.3} **2**. [LOM, fov: 0.07 mm.]

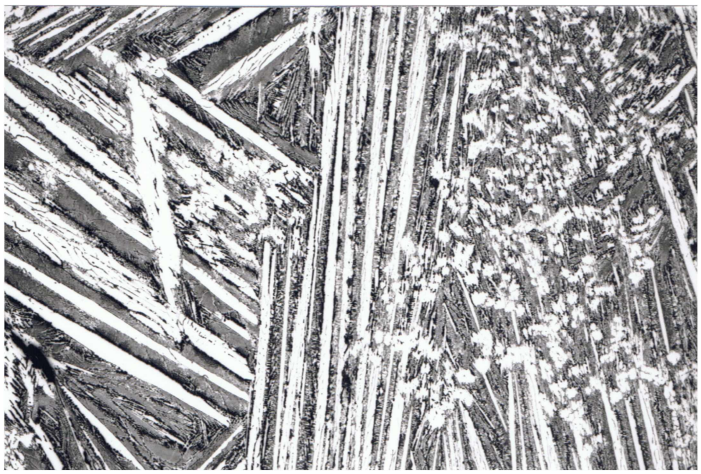

Figure {7.1.3} **4:** The micrograph shows microstructure of the vacuum arc re-melted button product of a sponge-metal reduction product. The sponge was the solid state reduction product of the microwave reduction of a charge of mill-blended molybdenite/wolframite/magnetite/char (6:6:3:1 by wt) beneath loose granular char. The melt-consolidated white cast iron was solidified on the water-cooled copper hearth of the arc melter – the typical quenched microstructure was evident in this micrograph and those of Figures {7.1.3} **5** and {7.1.3} **6**. Figure {7.1.3} **7**, however, shows elemental segregation in material of the final solidification region of the button. [Further description is provided in the accompanying text and with following Figures {7.1.3} **5**, {7.1.3} **6** and {7.1.3} **7**.] [LOM, fov: 0.32 mm.]

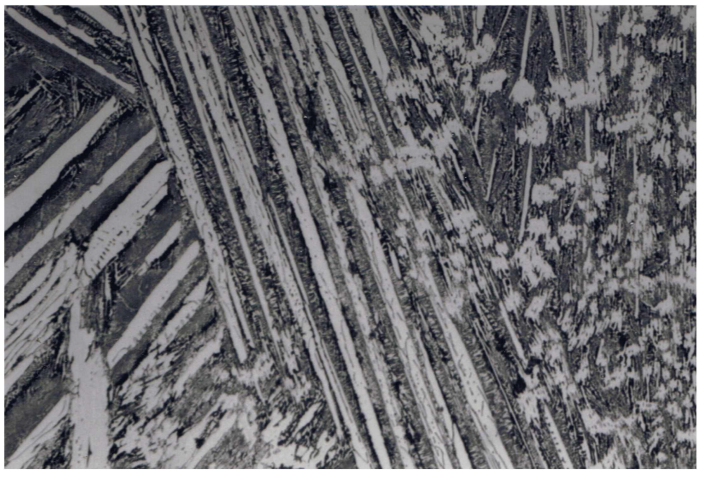

Figure {7.1.3} **5:** The micrograph shows further detail of the vacuum arc re-melted button product of the sponge reduction product metal identified in the above Figure {7.1.3} **4**. The average composition (by EDS area acquisition over a broad general field) of the melt-consolidated white cast alloy button was: 42 at% Mo, 9 at% W and 49 at% Fe (C not assessed). [LOM, fov: 0.16.]

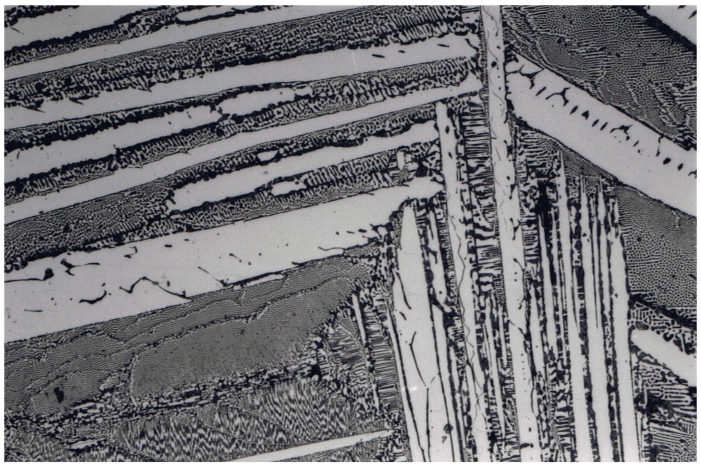

Figure {7.1.3} **6:** The micrograph shows detail of the quench microstructure in the vacuum arc re-melted button product identified in previous Figures {7.1.3} **4** and {7.1.3} **5**. The field presented shows typical detail of primary carbide plates or needles and eutectic matrix as they manifest in (majority) quenched regions of the button. [LOM, fov: 0.08 mm.]

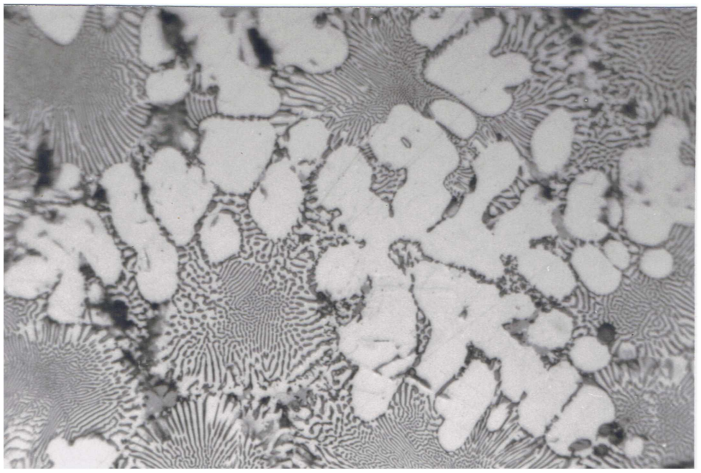

Figure {7.1.3} **7:** The micrograph shows detail of the "cap" microstructure atop the vacuum arc re-melted button of the previous Figures {7.1.3} **4**, {7.1.3} **5** and {7.1.3} **6**. The microstructure shows evidence of elemental segregation with non-faceted carbide phase interspersed by eutectic "rosettes" characterising this last frozen region which was more slowly cooled beneath a slowly cooling slag cap, the slag derived from the sponge interstices. [LOM, fov: 0.025mm.]

are indicative of the button region frozen against the water-cooled copper hearth of the arc-melting furnace whilst the region less rapidly solidified beneath the more slowly cooled slag cap provided the "segregated" microstructure of Figure {7.1.3}7. Of course, this and other mineral blends incorporating tungsten minerals, and their reduction products, could have been incorporated in the following tungsten section, however, the higher atomic percentage of Mo (over W) in both the blend mineral and the reduction product iron warranted its categorisation in this brief molybdenum section.

7.1.4: Reduction of Wolframite and Scheelite.

The Group **6**, Period **5d** occupant, tungsten, possesses physical and chemical similarities to its Period **4d** chemical analogue, molybdenum; tungsten (W) even occurs in Earth's crust in the same 1.2 ppm abundance as molybdenum (Mo). However, these metals rarely co-exist in any given ore-body mineralisation (unlike their counterpart Group **4** pairing of Zr and Hf, and Group **5** pairing of Nb and Ta which (respectively) do co-habit the same ore minerals (refer to Section **3**). Occurring in close contact with acid igneous rocks, the main tungsten minerals are the tungstates: scheelite ($CaWO_4$), hubnerite ($MnWO_4$), ferberite ($FeWO_4$) and the more common composite of these, wolframite [$(Fe,Mn)WO_4$], all of which occur as primary minerals associated (from rock to alluvium) with the principal tin mineral cassiterite.

The commercial minerals wolframite [$(Fe,Mn)WO_4$] and the calcium tungstate mineral, scheelite ($CaWO_4$), were microwave reduced both individually (with char) and in mineral blends with quite mixed results. It was found, at the preliminary stages of reduction system development that, of all minerals tested, scheelite was likely the most difficult mineral to reduce of all minesite-derived minerals trialled. This reduction intransigence presented no surprise and is testament to the thermochemical stability of hypabyssal and plutonic calcium minerals. However, carbo-aluminothermic reduction was relatively successful, and a scheelite/Fe_3C/char mill-blended charge was microwave reduced to yield a quenched white iron exhibiting tungsten carbide particles as proof of reduction. Greater smelt success was realised in numerous wolframite blend microwave reduction operations; as with the molybdenum minerals molybdenite and molybdite,

wolframite [(Fe,Mn)WO_4] was a common mineral blend choice for the exploratory mineral blend reduction work. To this end, Figures **{7.1.4}1** and **{7.1.4}2** present the solid-state reduction product sponge metal of the microwave reduction of a mill-blended charge of wolframite/MoS_2/Fe_3C/ char (8:4:4:1 by wt) beneath loose char. The sintered iron sponge reduction product* was water quenched. In a microwave reduction trial of comparable duration (15 minutes total irradiation) a niobium-bearing wolframite was reduced in the charge of mill-blended Nb-wolframite/Fe_3C/char (6:3:1 by wt) and the reduction product water quenched. The resultant iron button was "layered" in that the upper portion exhibited a multi-phase white iron (Figure **{7.1.4}3**) which extended the full thickness of the button whilst the lower portion contained the great bulk of tungsten carbide (WC) particles [actually (95%W, 5%Nb)C, by stoichiometry (of at%), C not assessed] plus minor niobium/titanium-rich [(W,Nb,Ti)(C,N)] carbonitride particles shown in Figure **{7.1.4}4** [actually (35at%W, 24at%Nb, 41at%Ti)(C,N), light elements not assessed; carbonitride because of their salmon pink colour under LOM inspection]. Micrographs presented in the seven Figures **{7.1.4}1** to **{7.1.4}7** are back-scattered electron-optical micrographs [B/s EOM] which, by "phase contrast", highlighted the constituent phases and compounds by virtue of atomic weight of elements and the proportion of elements in those phases and compounds, the higher the net atomic weight (or atomic number) of the phase the lighter (brighter) the phase (or compound).

The electron-optical micrograph of nearby Figure **{7.1.4}5** shows representative microstructure exhibited by the air-cooled iron smelt product of microwave reduction of a mill-blended charge of wolframite/Fe_3C/char (8:4:1 by wt) under loose granular char. The typical microstructure of a similarly reduced but water quenched iron smelt product of mill-blended wolframite/magnetite(Fe_3O_4)/char (8:4:1 by wt) is presented as Figure **{7.1.4}6**. The accompanying Figure **{7.1.4}7** shows principally faceted primary carbide in a microstructure of complex morphology resulting from its quinary "eutectic" and the

* Where reduction processes were by diffusion-driven solid-state reduction, that is, where diffusion of reactive radicals from and to the reaction interface was carried-out generally below the melting points of the starting mineral, intermediate phases and the final metal, then a sintered "sponge" metal was the reduction product at reduction end-point. However, where such sponge metal products received ongoing input of microwave energy, the melting point of the sponge conglomerate could be reached and a metal button subsequently quenched from the liquid. Where the melting point requirements of the metal sponge was beyond the energy attained during processing then the "sticky" sinter paste stubbornly persisted and was consequently quenched as a sponge metal, the degree of sintering in the sponge structure varying with processing time and input energy. Sponge metals were arc melted when "phase consolidation" was required, however, such compositional amalgamation could be informatively contra-notional.

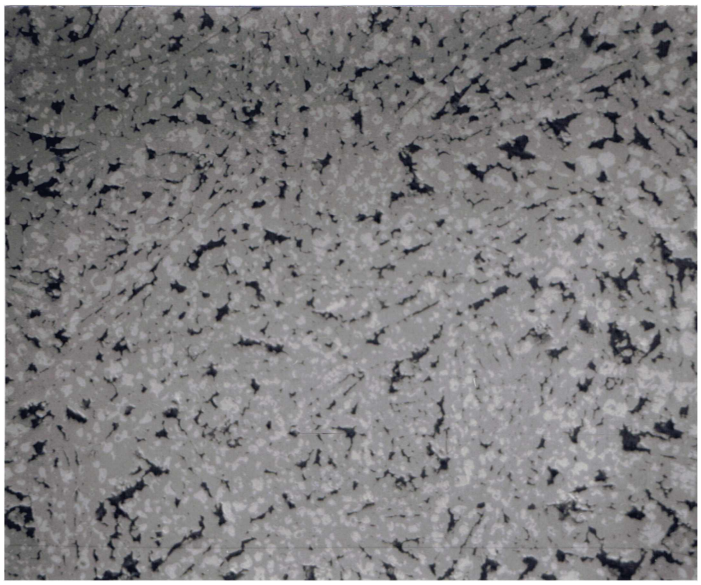

Figure {7.1.4} **1:** The micrograph shows the sponge microstructure of the solid-state reduction product of a microwave reduced charge of mill-blended wolframite[$(Fe,Mn)WO_4$]/molybdenite (MoS_2)/Fe_3C/char (8:4:4:1 by wt) beneath loose granular char. The sintered alloy iron sponge (whose detail is better viewed in Figure {7.1.4} **2** below) was comprised of two metallic solid-state reduction product phases plus attendant slag in interstices. The brighter metallic phase was a 10 % Mo, W carbide whilst the grey phase was an iron-rich phase comprised of ~ 30 % (Mn,Mo,W) in iron. [B/s EOM, fov: 1.0 mm.]

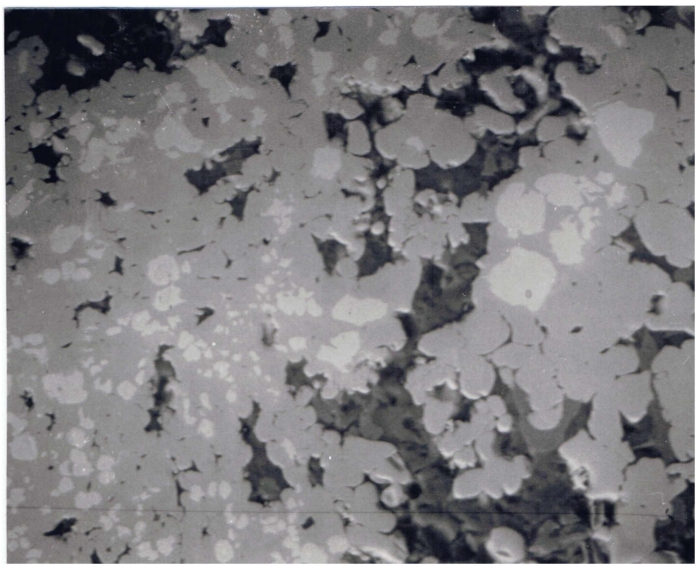

Figure {7.1.4} **2:** The micrograph shows in more detail the sponge iron microstructure of Figure {7.1.4} **1** above. Shown more clearly here as dark grey was the slag phase, the black regions were voids. The solid-state reduced and sintered sponge was an emergent "alloy in progress"; almost totally reduced, diffusion modified but not melt-consolidated before termination of microwave processing. [B/s EOM, fov: 0.25 mm.]

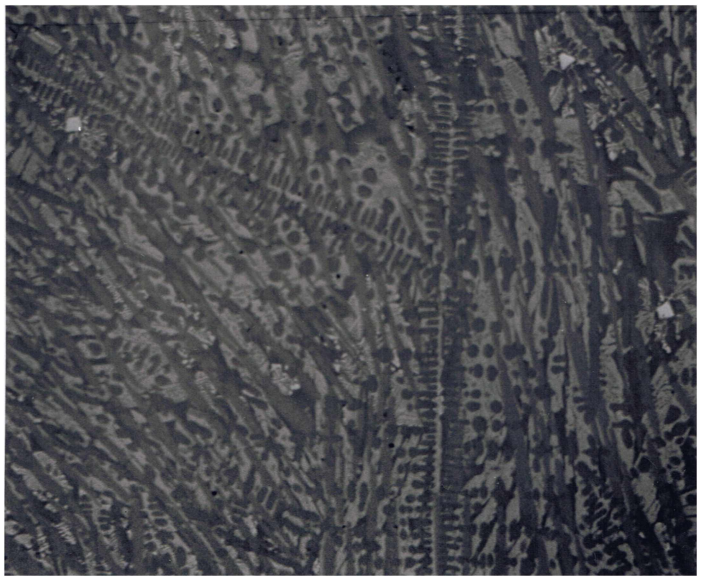

Figure {7.1.4} **3:** The micrograph shows the microstructure of the white iron reduction product of a microwave reduced charge of mill-blended Nb-bearing wolframite/Fe_3C/char (6:3:1 by wt) beneath loose granular char. The alloy iron so-produced was comprised of the solid solution matrix (shown here near the centre of the quenched button) that extended throughout the button. Such "particle-free" matrix material assayed as 10 at% W, 0.5 at% Nb iron (C not assessed) and, whilst not determined, was most likely a complex quarternary eutectic of γ plus $(W,Nb,Fe)_3C$. The preponderance of incorporated compound particles was contained within this matrix in the bottom stratum of the button (see Figure {7.1.4} **4** below). [B/s EOM, fov: 0.80 mm.]

Figure {7.1.4} **4:** The micrograph shows typical detail of the microstructure in the particle-rich bottom region of the microwave reduced white iron reduction product shown in Figure {7.1.4} **3** above. Amid other minor phases, the large white particles were (95at%W,5at%Nb)C whilst the smaller hexagonal pale grey particles were (35at%W,24at%Nb,41at%Ti)CN (pink under light-optics); the average overall composition of the iron button was: 22 at% W, 3 at% Nb, 75 at% Fe, (trace Ti and Mn, C not assessed). [B/s EOM, fov: 0.20 mm.]

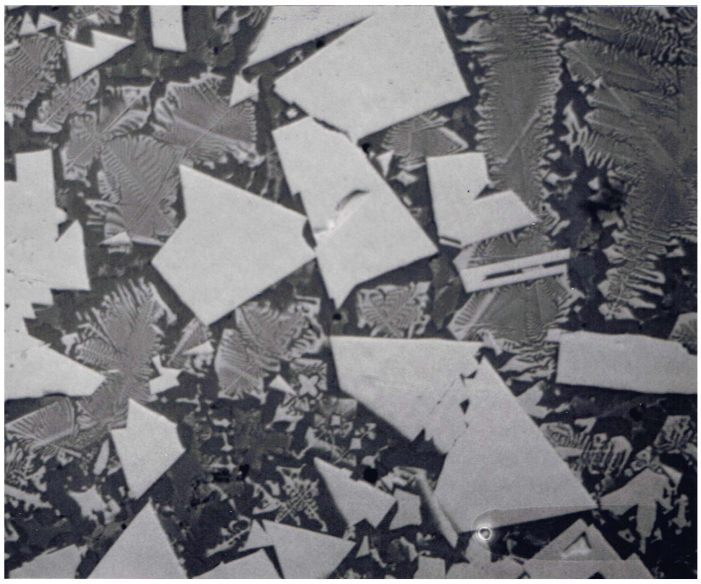

Figure {7.1.4} **5:** The micrograph shows the air-cooled white iron microstructure of the reduction product of a microwave reduced charge of mill-blended wolframite/Fe_3C/char (8:4:1 by wt) beneath loose granular char. Most prominent in the field were the bright primary WC particles plus complex multi-phase eutectic structure, possibly WC, γ (transformed) plus $(W,Fe,Mn)_3C$ in this 16 at% W iron (by EDS, C not assessed). [B/s EOM, fov: 0.80 mm.]

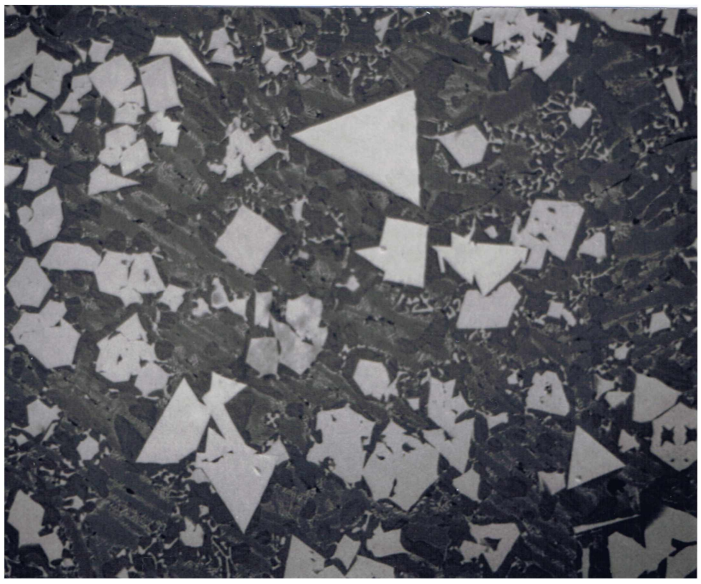

Figure {7.1.4} **6:** The micrograph shows the water quenched white iron microstructure of the reduction product of a microwave reduced charge of mill-blended wolframite[$(Fe,Mn)WO_4$]/ magnetite(Fe_3O_4)/char (8:4:1 by wt) beneath loose granular char. The field shown was representative of the typical microstructure in which the bright primary carbide (WC) particles were prominent in a quarternary eutectic of γ plus $(W,Fe,Mn)_3C$. [B/s EOM, fov: 1.20 mm.]

Figure {7.1.4} **7:** The micrograph shows the air-cooled white iron microstructure of the reduction product of a charge of mill-blended wolframite[$(Fe,Mn)WO_4$]/ilmenite($FeTiO_3$)/Fe_3C/char (8:5:4:1 by wt) microwave reduced beneath loose granular char. The complex field shows faceted primary carbide polymorphs (which have been affected by the presence of Ti) in a quinternary eutectic of γ plus $(W,Fe,Mn,Ti)_3C$ phase. The average button composition was: 22 at% W iron with trace/minor Mn and Ti; with the large primary carbides: (45 at % $W,Fe)_n$ C; with possible γ transformation product: Fe_7W_6 (by stoichiometry), light elements not assessed. [B/s EOM, fov: 0.60 mm.]

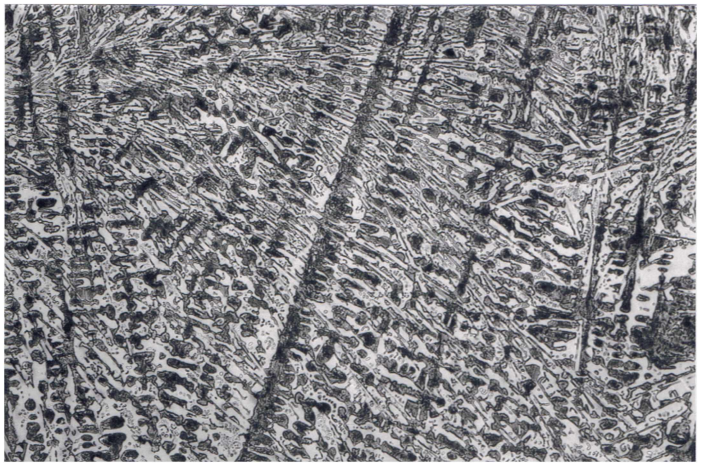

Figure {7.1.5} **1:** The micrograph shows the water quenched white iron microstructure of the reduction product of a microwave reduced charge of mill-blended haematite(Fe_2O_3)/char (8:1 by wt) beneath loose char. The iron was close to the binary eutectic composition of 4.3 wt% C (17 at% C) in which dendrites of transformed austenite (γ) present in a matrix of ledeburite γ plus Fe_3C. Figures {7.1.5} **2**, {7.1.5} **3** and {7.1.5} **4** also present this specimen, but in greater detail by virtue of higher magnification. [LOM, fov: 0.64 mm.]

fact of its ultimate arrival at a minimal overall liquid consolidation point of an initially sponge smelt product of the microwave reduction of a mill-blended charge of wolframite/ilmenite($FeTiO_3$)/Fe_3C/char (8:5:4:1 by wt) under granular char.

The commercially dominant and common ore minerals molybdenite, MoS_2, (for molybdenum) and scheelite, $CaWO_4$, (for tungsten) – both chemically obdurate – were notably difficult to reduce. Nonetheless, for other important Group **6** minerals, where the microwave-stimulated reduction method was pyrometallurgically utilised, the oxide minerals of the Group **6** metals were easier to smelt-reduce than the corresponding oxide minerals of the metals of Groups **4** and **5** (from which the core project metals come).

7.1.5: Other Reduction Products.

This section briefly covers microwave smelt products (*i*) plain high-C irons, (*ii*) high-C iron alloys or composite irons incorporating core refractory metals Ti, Zr(Hf) and Ta(Nb), and (*iii*) some noteworthy non-ferrous reduction products.

The earliest microwave reduction products smelted using the then evolving microwave oven set-up with CO-atmosphere control were straight carbothermic haematite (Fe_2O_3) or magnetite (Fe_3O_4) smelts. These rudimentary operations on metallurgically key iron ores were used to gauge the reduction propensity of the simple system and to investigate experimental parameters and establish operational procedure and limits, and to determine the degree of reproducibility and other necessary experimental variables. A central intention of "early experimental work" was to determine whether, as the sole energy input, microwave energy *alone* could drive the metallurgical thermochemistry of the then-evolving microwave reactor and, in parallel, whether the simple microwave oven experimental system (the "oven set-up") could provide the requisite metallurgical thermochemistry and, if so, what experimental boundaries would define the project for refractory metals. The microstructure presented

in Figure {7.1.5}**1** is a water quenched white cast iron smelt product of microwave reduction of a charge of Mount Newman haematite blended with fine char and processed beneath granular char. The irradiation time was 8 minutes, reduction was complete and formed a cleanly pooled liquid which, upon quenching, produced a well-defined iron button with minor slag – much like the sectioned crucible example shown in Figure {7.1}**1**. Further micrographical detail of this reduction product iron is presented in Figures {7.1.5}**2**, {7.1.5}**3** and {7.1.5}**4**. The same blend of haematite plus fine char was microwave reduced to yield the grey iron which is micrographically presented as Figures {7.1.5}**5**, {7.1.5}**6** and {7.1.5}**7**.

Amongst other interesting hypotheses variously tested with a view to developing new microwave processing projects, and which were (consequently) jointly investigated with colleagues, was the utilisation of sewerage plant "sludge" as a pyrometallurgical reductant. To this end, haematite was blended with the sewerage sludge, dried and then ground to a fine consistency, charged into a crucible and, without the standard CO-atmosphere-controlling loose char topping, microwave reduced to produce liquid metal which was slowly cooled *in situ*, but with a *loose char topping quickly added* post microwave and re-covered with insulation. The reduction product grey iron button was sufficient "proof of concept" for others to successfully proceed with this project. The result was a phosphorus-containing grey cast iron and typical micrographs of its microstructure are presented in Figures {7.1.5}**8**, {7.1.5}**9**, {7.1.5}**10** and {7.1.5}**11**.

An early and continuing interest was the carbothermic reduction of the titanium minerals rutile and ilmenite. During these preliminary stages of system evolution, whilst rutile proved difficult to co-reduce with iron minerals, the ferruginous ilmenite proved to be readily reducible with respect to both Fe and Ti constituents. Notwithstanding that the significant aluminothermic (thermite) microwave reduction of ilmenite is specifically addressed in Section **7.2.4**, and the carbothermic microwave reduction of ilmenite addressed in Section **7.2.3**, the carbothermic microwave reduction of *mineral blends* incorporating ilmenite received specific attention during early trials. Notable in formative experimentation, elementary mineral blends (incorporating Fe plus Ti) and compound mineral blends (incorporating Fe, Ti plus other metal) provided worthy smelt results, some of which are presented in the following cursory outlines. In one elementary case a charge of mill-blended ilmenite ($FeTiO_3$)/magnetite(Fe_3O_4)/char

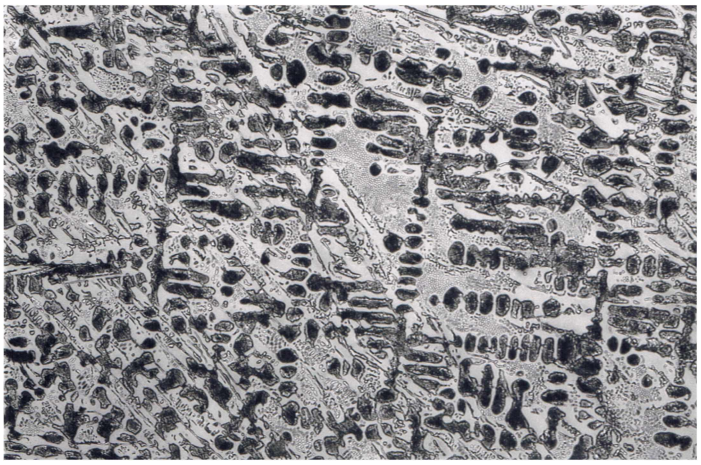

Figure {7.1.5} **2:** The micrograph shows the water quenched white iron microstructure of the reduction product of a microwave reduced charge of mill-blended haematite(Fe_2O_3)/char (8:1 by wt) beneath loose char. The iron was a high-C iron of approximately eutectic composition with primary austenite (γ) dendrites that have transformed by eutectoid reaction to a fine aggregate of ferrite (α) plus cementite (Fe_3C). The variation in contrast within the prior γ regions was a reflection of the local fineness of the aggregate structure (see Figure {7.1.5} **3** below). [LOM, fov: 0.32 mm.]

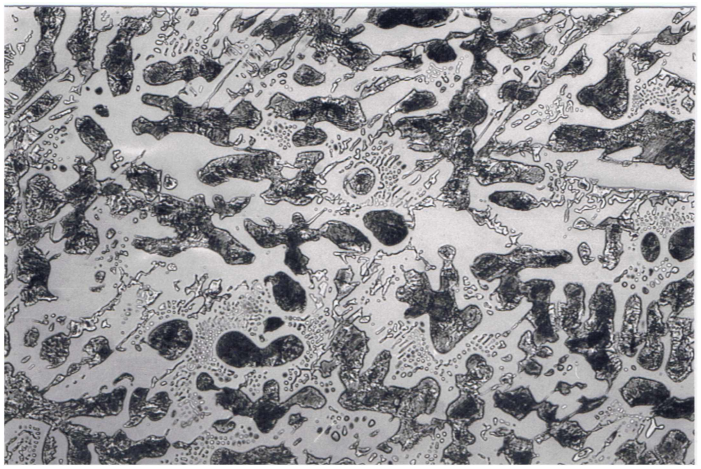

Figure {7.1.5} **3:** The micrograph shows detail in the water quenched white iron microstructure of the reduction product of Figure {7.1.5} **2** above. Eutectic ledeburite surrounds the transformed prior austenite dendrites. [LOM, fov: 0.16 mm.]

Figure {7.1.5} **4:** The micrograph shows detail in the water quenched white iron microstructure of the reduction product of Figure {7.1.5} **2** (on previous page). The eutectic and prior austenite regions (of Figure {7.1.5} **3**) typifying the interior of the metal button were here interspersed by prominent cementite laths in regions representing higher quench-rate near the button's surface. The different structure here (versus Figure {7.1.5} **3**) was attributable to compositional segregation in regions of higher cooling rate where the eutectic microstructure expected would be dominated by the lath-like Fe_3C. [LOM, fov: 0.16 mm.]

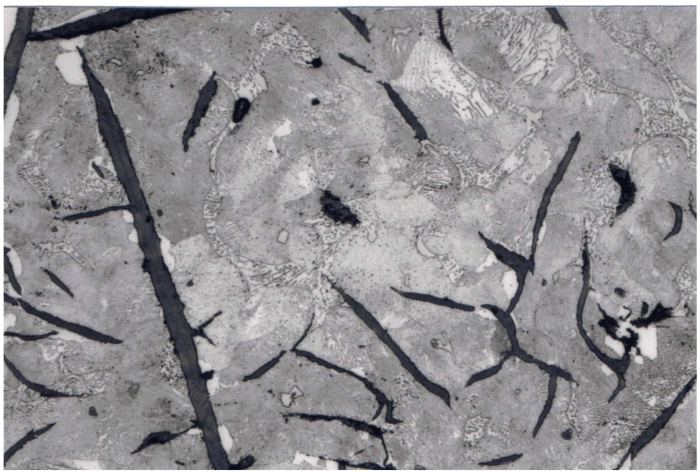

Figure {7.1.5} **5:** The micrograph shows the crucible-cooled grey cast iron microstructure of the reduction product of a microwave reduced charge of mill-blended haematite(Fe_2O_3)/ char (8:1 by wt) beneath loose char. (This was the grey iron equivalent of the preceding white iron.) The specimen button was a high-C iron which, post reduction. was slowly cooled *in situ* in the undisturbed crucible. The resultant microstructure is described (to greater effect) with the following, higher resolution micrographs of Figures {7.1.5} **6** and {7.1.5} **7**. [LOM, fov: 0.32 mm.]

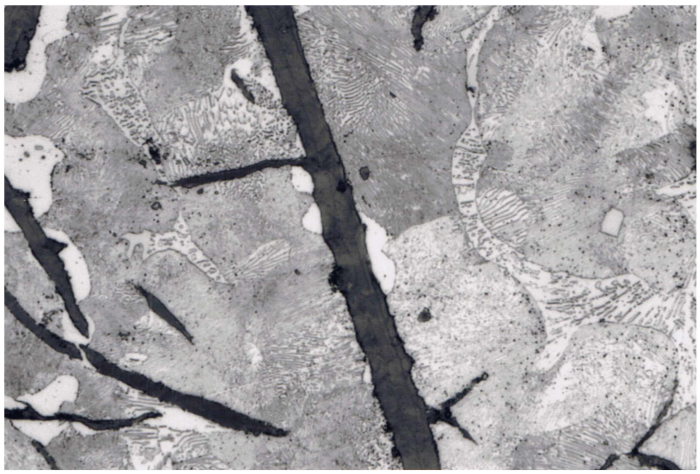

Figure {7.1.5} **6:** The micrograph shows detail in the crucible-cooled grey cast iron microstructure of the reduction product of a microwave reduced charge of mill-blended haematite(Fe_2O_3)/ char (8:1 by wt) beneath loose char (and presented in previous Figure {7.1.5} **5**). Upon slow cooling, primary γ formed ahead of transformation of eutectic liquid to γ plus graphite flakes, whilst ternary eutectic steadite formed in remnant liquid and the γ has subsequently transformed eutectoidally to pearlite. The non-etching white phase attached to graphite was α-Fe formed by γ-decomposition to α plus graphite *at* the graphite flakes whilst, remote from the flakes, the eutectoid product was α plus Fe_3C. Further detail is presented in Figure {7.1.5} **7** (following). [LOM, fov: 0.16 mm.]

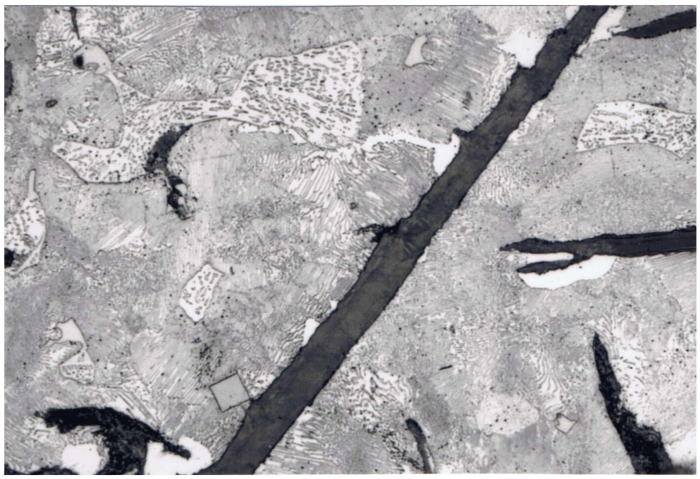

Figure {7.1.5} **7:** The micrograph shows further detail in the crucible-cooled grey cast iron microstructure of the reduction product presented above in Figure {7.1.5} **6** and in Figure {7.1.5} **5** on the previous page. [LOM, fov: 0.16 mm.]

Figure {7.1.5} **8:** The micrograph shows the crucible-cooled grey cast iron microstructure of the reduction product of a microwave reduced charge of blended haematite (Fe_2O_3) plus sewerage plant "sludge", dried and smelted *without* the loose char atmosphere control until post reduction cooling. The microstructural evolution exhibited by this reduction product iron was similar to the previous iron of Figures {7.1.5} **5**, {7.1.5} **6** and {7.1.5} **7** except that rosette graphite (Type B) has formed in this specimen. A faster cooling rate has promoted the formation of Type B rosette graphite rather than the more evenly distributed flake graphite (Type A) as typified the previous specimen. [LOM, fov: 0.16 mm.]

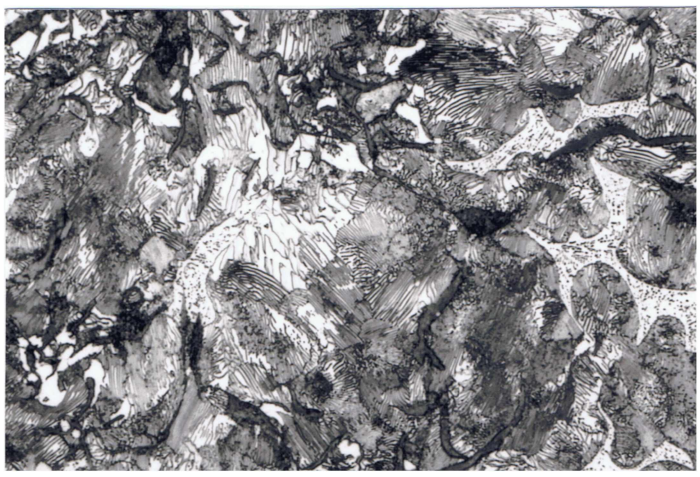

Figure {7.1.5} **9:** The micrograph shows further detail of the microwave reduced iron presented above in Figure {7.1.5} **8**. The micrograph shows the grey cast iron microstructure in a typical field with α-Fe in-filled graphite rosettes distributed in pearlite (transformed primary γ) and ternary phosphide eutectic. Greater detail is presented in the following Figures {7.1.5} **10** and {7.1.5} **11**. [LOM, fov: 0.16 mm.]

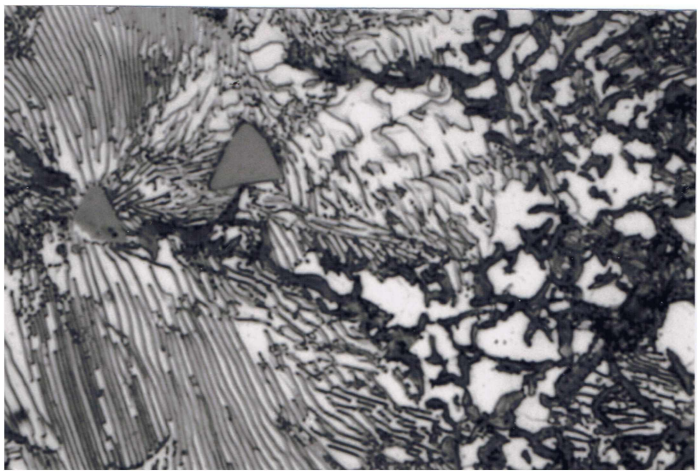

Figure {7.1.5} **10:** The micrograph shows detail of the grey cast iron microstructure of the same reduction product presented in Figures {7.1.5} **8** and {7.1.5} **9** (previous page). The iron was the crucible-cooled reduction product of a microwave reduced charge of haematite using sewerage plant "sludge" as the sole reductant and *without* loose char atmosphere control until the point of process termination and post reduction cooling. The generally sparse alloy carbide particles were set in pearlite (transformed primary γ) adjoining a graphite rosette harbouring α-Fe, itself a γ-transformation product along with graphite (in lieu of Fe_3C) which has deposited onto the pre-existing rosette folds. [LOM, fov: 0.06 mm.]

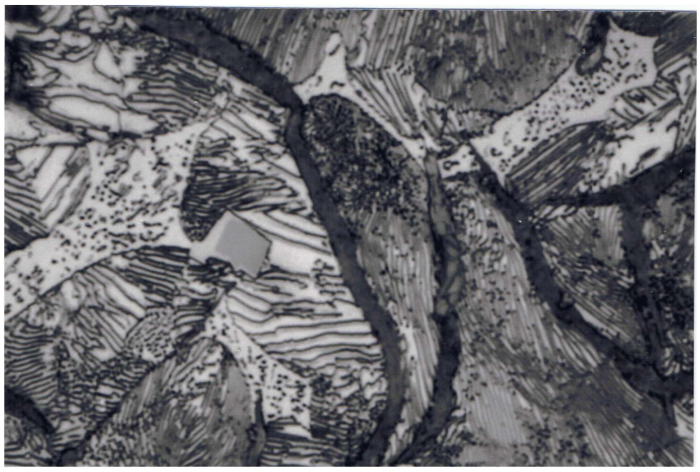

Figure {7.1.5} **11:** The micrograph shows detail of the grey cast iron microstructure of the reduction product presented in Figure {7.1.5} **9** (previous page). The idiomorphic particle is set in pearlite, adjacent to a region of steadite eutectic and beside the extremity of a graphite rosette. [LOM, fov: 0.06 mm.]

(4:4:1 by wt) beneath loose granular char was microwave reduced thence cooled *in situ* under char in the process crucible to yield a grey iron. Micrographs of the etched microstructure of this reduction product are presented in Figures {7.1.5}**12** and {7.1.5}**13**.

Various other core refractory metal minerals were co-reduced successfully with iron in the early reduction work, however, the final such ferrous example presented here is that of the (minor) Group 5 core metal, niobium. (Whilst being the minor Group 5 constituent partner in Australian tantalite [$(Ta(Nb))_2O_5$] ores, niobium is predominantly the major partner in the counterpart columbite [$(Nb(Ta))_2O_5$] ores. Columbite ores are more orogenically prevalent (than the complementary tantalite analogue) in commercial deposits and undeveloped outcrops around the world.) In the standard oven set-up, a charge of mill-blended niobia(Nb_2O_5)/magnetite(Fe_3O_4)/Fe_3C/char (4:6:1 by wt) was freely reduced by the microwave method to yield, upon air-cooling, the white iron presented in Figures {7.1.5}**14** and {7.1.5}**15**.

The scope of the early, exploratory reduction programme diverged once general process parameters were understood and before the microwave reactor was a work-in-progress reality. Reduction of non-ferrous minerals, both singularly and in mineral blends, presented many possibilities for the microwave reduction system. Notable reduction outcomes were attained for elements across the Periodic Table and, as for the ferrous-based smelts (from which the above were chosen), most non-ferrous examples are left simply summarised in Section **6.4**. The few examples chosen for inclusion here are indicative of microwave reduction possibilities broadly.

Smelted in an oxygen-depleted air/argon atmosphere under loose granular char, a charge of Kambalda (W.A.) Ni/Co mineral concentrate [as ~50/50 vol% cobaltite ((Co,Fe)AsS)/pentlandite ($(Fe,Ni)_9S_8$)] mill-blended with char was microwave reduced to yield three phases of primary reduction product featuring a highly metallised phase, an intermediate matte/(speiss) phase plus a black sulphurous glassy slag (a minor phase) which, to some extent, reported also in the numerous voids of the porous metal/matte agglomerate. In fact the two reduced phases were metallic dendrites of NiCoSi (with ~1 wt% S impurity) in an impure matte/(speiss) matrix of NiCo(SiFe) with ~35 wt% S and ~2 wt% As – (in this prematurely terminated specimen) this phase was an intermediate reduction product in a staged extraction process. Principally oxidic, the dark sulphurous

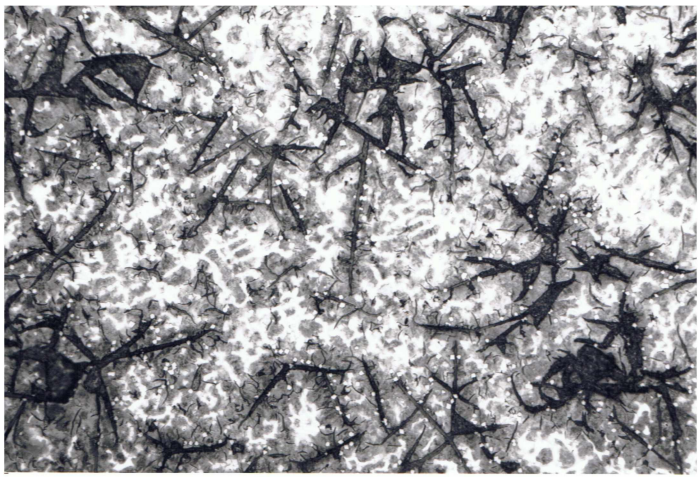

Figure {7.1.5} **12:** The micrograph shows the crucible-cooled grey cast iron microstructure of the reduction product of the microwave reduction of a charge of mill-blended ilmenite ($FeTiO_3$)/magnetite(Fe_3O_4)/char (4:4:1 by wt) beneath loose granular char. The etched iron was liberally scattered with TiC particles, formed initially from the liquid, and associated with coarse flake graphite prior to the engulfing solidification of primary eutectic (γ plus further graphite). The primary austenite (γ) surrounding graphite flakes and particles has transformed to pearlite, excess liquid solidifying last as ferrite (α). Further detail can be seen in Figure {7.1.5} **13** below. [LOM, fov: 1.20 mm.]

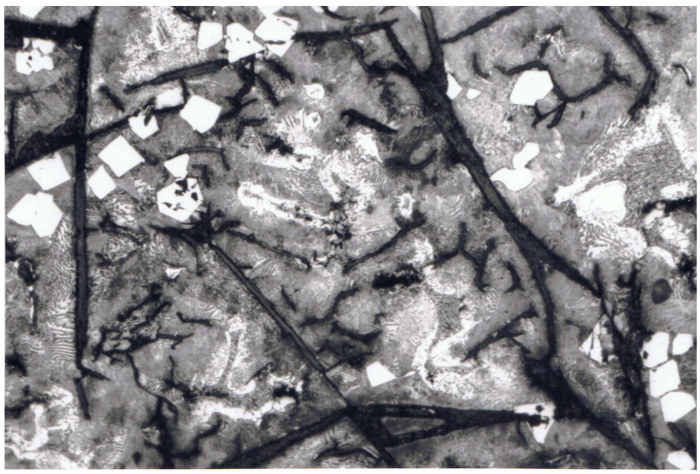

Figure {7.1.5} **13:** The micrograph shows detail of the crucible-cooled grey cast iron microstructure presented above. The particles were confirmed by windowless EDS to be TiC particles, most Ti from the ilmenite reported in the metal in this compound form, negligible Ti reported in the slag. Very fine transformation product pearlite was separated by transformation product excess, ferrite (α). [LOM, fov: 0.16 mm.]

Figure {7.1.5} **14:** The micrograph shows the air-cooled white cast iron microstructure of the reduction product of a microwave reduced charge of mill-blended niobia(Nb_2O_5)/magnetite (Fe_3O_4)/char (4:6:1 by wt) beneath loose char. The solidification/formation sequence is somewhat unclear because of final transformation products, however, dominant austenite (γ) dendrites formed ahead of the γ – NbC eutectic (white prismatic phase). Widmanstätten carbide needles [$(FeNb)_3C$] formed in the γ prior to the majority remaining γ transforming to fine pearlite. [LOM, fov: 0.08 mm.]

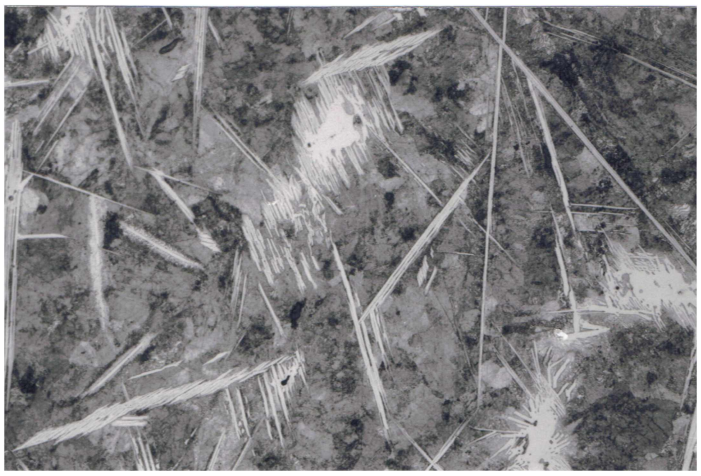

Figure {7.1.5} **15:** The micrograph shows further microstructural detail of the air-cooled white cast iron reduction product presented above in Figure {7.1.5} **14**. [LOM, fov: 0.08 mm.]

glassy slag phase retained ~5 wt% Fe, but (somewhat inexplicably) retained negligible Co or Ni. Broadly, this reduction achievement was regarded as noteworthy and of plausible value with a view to an industrial precursor stage of extraction, a micrograph of this "first stage" reduction product is presented in Figure {7.1.5}**16**. [The use of char both blend-intimately and loosely as CO-producer was intentional on different levels. Firstly, char was intended to draw microwave energy and thus provide rapid heating in the projected reaction zone – even though the sulphides themselves heated quite responsively. Secondly, as was briefly addressed in Section **6** and previously in this Section **7**, it was experimentally established in preliminary work that, under microwave reduction conditions (and independent of the disproportionation effect of microwaves discretely breaking molecular bonds), some sulphides can "reduce" certain oxide minerals (only partially in most cases) in the *absence* of carbon. Therein, with respect to "process efficiency", the said reduction proceeded more directly and, prospectively, more irreversibly towards process completion when reductant char was employed in the process*. Char also provided the protection of a reducing CO atmosphere "blanket" to secure the reduction (that is, to prevent re-oxidation or other reversion).]

In thermochemical terms, the reducibility of silica (SiO_2) was known to be substantially analogous with that of the refractory metal oxides. For this reason silica was occasionally of particular nuisance consequence in the reduction of refractory metal minerals where it was commonly co-occurrent in the ore-mineral charge and/or was introduced to the system upon insulation material "malfunction". This comparability presented a direct challenge when reducing the Zr-silicate, zircon ($ZrSiO_4$), where pre-reduction separation (of ZrO_2 and SiO_2) was desirable because silica is much more reducible the zirconia. Separation was otherwise (physically rather than chemically) achieved during cooling by a solidification rate phenomenon (as addressed elsewhere) which thence invited either physical and/or solution removal of amorphous silica from crystalline zirconia. Also, pure silica forms were shown to be microwave "transparent" (hence its use in insulation applications) so, even blended with highly susceptible char,

* Not to second-guess the chemistry of such a limited S-based reduction process, it is worth recording for comparison that the common industrial chlorination process of TiO_2 to $TiCl_4$ proceeds (under suitable thermochemistry) through the aegis of C-reduction via the transient intermediate carbide state. Essentially, C reduces the oxide and fleetingly holds the Ti as TiC*, thence Cl replaces the C in what is basically a preferred dual reaction (as Cl "reduces" both Ti (of C) and C (of Ti) to form the two tetrachlorides); Cl alone will not reduce the oxide – the conversion process requires the transient carbide state. [And independently, in the straight reduction process, C requires quite advanced thermochemistry to complete the reduction of TiO_2 to Ti-metal in *that* separate chemical environment.]

the reduction chemistry was suppressed until very high net temperatures, and (dependent upon the degree of reduction) a ceramic oxycarbide form approaching SiC was generally the reduction product. However, clean quartz river-sand was impure enough to ensure that a dielectric dopant effect was evident upon microwave irradiation and the un-blended sand heated freely. Blended with reductant char the blend charge behaved (heated and reduced) comparably to the moderately high reduction rate of a haematite/char blend. One such mill-blended quartz-sand/char (4:1 by wt) charge was reduced to metallic Si exhibiting low C (~6 at% C) – the reduction product was solid state reduced and sinter-bonded enough to metallographically prepare and examine. For lack of a suitably edifying micrograph of this relatively featureless specimen, no micrograph is presented of this otherwise instructive reduction achievement – an achievement which alone validates this mention and sets apart the technique, its capabilities and prospective possibilities before an industry-based extraction science rooted in *conventional* method.

In early work prior to the core microwave reduction programme being convened, various approaches were adopted pursuant to the reduction of mineral blends incorporating refractory metal minerals with a view to both (*i*) dielectrically catalysing the reduction, and (*ii*) retaining the reduced refractory metal as solute in a co-reduced solvent metal. This "solvent" metal was usually iron, however, non-ferrous solvents were investigated in pursuing the concept. To this end, and to test the upper bounds of process possibilities, a charge of mill-blended ZrO_2/TiO_2/SiO_2/char (5:5:3:1 by wt) was microwave reduced under granular char and in an oxygen-depleted air/Ar-atmosphere to yield a non-coalesced solid-state reduction product composite of the three oxides in their various stages of reduction. Although this task was somewhat beyond the atmosphere control capability of the then pre-reactor oven-based system, and the desired final solid solution was not reached, the under-processed resultant sinter was arguably more instructive for its quench-captured record. This reduction product specimen was a sinter-bonded agglomerate of three discrete reduction product phases and, again for the lack of a clearly instructive representative micrograph, is not micrographically presented herein. However, to cursorily describe the reduction product agglomerate, incompletely reduced Ti-phase particles were partially sinter-coalesced with their like-kind; the largely reduced Si-phase regions had softened most, had coalesced with like regions and had in-filled void interstices between the more rigid

phases; and mottled Zr-phase regions showed distinct signs of initial solid-state reduction. (At the quench-point of processing) phase boundaries were distinct around the Zr-phase regions, and less so between the Si- and Ti-phases of this premature reduction product. [Light element EDS was not available at the time of analyses, however, independent XRD analyses (by Dr B. Chenhall, Department of Geology, University of Wollongong) revealed (*i*) the presence of TiN (osbornite) in the salmon coloured, partially reduced Ti-phase, (*ii*) SiC in the silvery, partially reduced Si-phase, and (*iii*) ZrO_2 still to be the dominant presence in the Zr-phase. It should be noted that, being un-referenced complex compounds, the broad range of "partially reduced" oxides were un-resolvable under the auto-analytical "data-bank of minerals" available to the XRD system employed. Hence the "machine uncertainty" with respect to mineral assignations across the varying array of the unresolved, "possible minerals remainder" generated by such auto-analyses. Also, as a point of interest, the EDS examination of reduction processed ZrO_2 phase regions indicated an infusion of Ti (up to ~5 at% Ti, light elements un-assessed) in relevant phase boundary regions.] In this exercise, Si and Ti were (upon their reduction) the intended co-solvent elements and the more reduction-resolute Zr the intended solute to be captured in the lately reduced solvent alloy. In retrospect, it is reasonable to extrapolate from this incompletely processed case that more advanced thermochemistry and atmospheric protection would have produced complete reduction. Nonetheless, the result was a sentient *expression of possibilities* towards a more highly developed microwave reduction-route option in extractive processing and, by extension perhaps, for composite fabrication (by routes such as combustion synthesis).

The final "blended minerals" microwave reduction outcome addressed here is that of an easy thermochemical challenge, the microwave reduction of a mill-blended charge of high grade mineral concentrate cassiterite(SnO_2)/CuO/char (10:2:1 by wt) smelted beneath loose granular char. In the standard oven set-up configuration, the reduction proceeded rapidly and the smelt product was slowly cooled *in situ* in the process crucible which, to aid cooling, had been stripped of its outer insulation. A slag (substantially of an un-reduced cassiterite portion) accompanied a bright metal button, this button was sectioned and metallographically prepared. By EDS area count acquisition (and in agreement with area estimation of solidified phases across the specimen) the reduction product was an Sn, ~20 wt% Cu alloy, the typical

microstructure of which is shown in micrographs of Figures **{7.1.5}17**, **{7.1.5}18** and **{7.1.5}19** where solidifying first was the lath-type ε-phase (Cu_3Sn), followed by deposits and dendrites of η-phase in a matrix of βSn – all in accord with the back-scattered phase contrast of the electron-optical micrograph. Carbon has nil to negligible solid-solubility or compound potential in either tin or copper and the inclusion-free microstructure of the alloy appeared C-free – a metallic product virtually alone amongst the often C-saturated reduction products of this project. In separate reduction operations (noted in Section **6**) other, *un*-blended Sn and Cu reduction product metals produced analyses close to refined or commercial metal purities.

Notwithstanding the relative success realised under the procedurally evolving method of preliminary trials, for the remainder of this thesis project the solvent/solute approach to microwave reduction processing plus the numerous previously described "early" experimental elements were sidelined once the core programme was ultimately identified. However, during this formative work much was learned about dielectric "lossiness" and consequent heating in minerals; dopants and dielectric interaction between minerals; and the reactivity of both commercially "pure" minerals and ore-derived "real" minerals. Also, correspondingly, much was learned about the reactivity between mineral reactants and reductants; the behaviour of non-carbonised and carbonised carbon forms, of macerals, chars and maceral derived components (MDC's) in carbonised composites under microwave irradiation; and about gases and the reaction environment of microwave plasmas.

Although the preceding microwave reduction examples represent preliminary, non-core experimentation, it was felt that their inclusion at modest length in this Section **7.1** was vindicated because of the instruction their collective example provided in the development of the adopted microwave oven set-up. (And recalling that, once the microwave reactor was discarded as "un-achievable within the project interval", and so reverting to the remaining tangible option, processing expectations resided solely with the oven set-up method.) The microwave oven system as devised, the integral

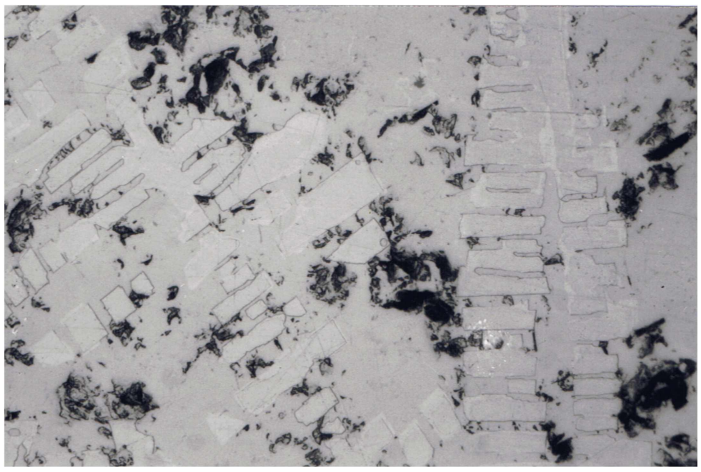

Figure {7.1.5} **16:** The micrograph shows the sponge reduction product of a microwave reduced charge of mill-blended Kambalda Ni/Co (~50/50%) concentrate/char (8:1 by wt) smelted in an air-depleted Ar-atmosphere beneath loose char. (Kambalda concentrate assayed as cobaltite [(Co.Fe)AsS] . pentlandite [$(Fe,Ni)_9S_8$] with minor silicate gangue.) The microstructural field shows an incompletely reduced primary metallurgical composite "sponge" featuring metallic dendrites (lightest phase) of 46 wt% Co, 40 wt% Ni, 13 wt% Si and 1 wt% Fe (C not assessed) in a matte/(speiss) phase of 44 wt% Ni, 16 wt% Co, 2 wt% Si, 1 wt% Fe, 35 wt% S and 2 wt% As. Evidently removed during specimen preparation, the dark void regions contained some brittle black sulphurous slag which retained ~5 wt% Fe but negligible Ni or Co. [LOM, fov: 0.64 mm.]

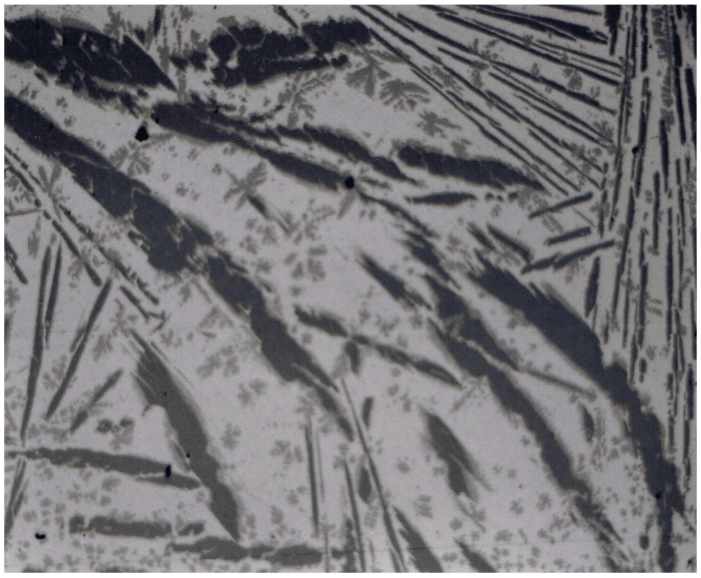

Figure {7.1.5} **17:** The micrograph shows the crucible-cooled microstructure of the tin-rich reduction product of a microwave reduced charge of mill-blended high grade cassiterite (SnO_2)/ CuO/char (10:2:1 by wt) beneath loose char. The microstructural evolution for this metal button (whose overall composition was assessed to be Sn, ~20 wt% Cu) is described in annotation with Figures {7.1.5} **18** and {7.1.5} **19** (on the following page). The negligible slag "make" which accompanied this reduction product retained minor Sn, the bright metal was C-free. [B/s EOM, fov: 0.64 mm.]

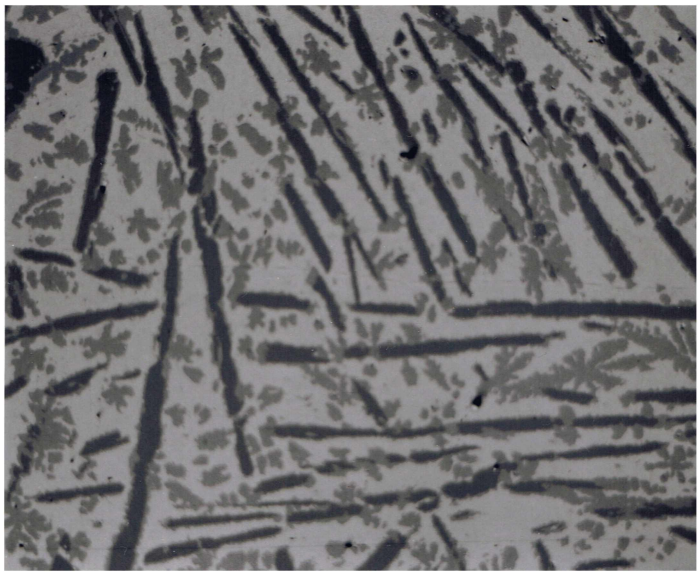

Figure {7.1.5} **18:** The micrograph shows an alternative but more typical field of view of the crucible-cooled microstructure of the microwave reduction product presented in Figure {7.1.5} **17** (on the previous page). Upon cooling through the liquidus at ~560°C, the dark primary ε-phase (Cu_3Sn) laths were solidified down to the 415°C peritectic, below which these ε-laths were "encased" by initial deposition of the peritectic product, η-phase. The deposition was incomplete when, below 227°C, the remaining Sn-rich liquid decomposed to yield eutectic products of η-phase "dendrites" captured in a matrix of βSn (the bright phase). (Also, below 186°C, the transformation: η → η' was expected, if not observed.) Microstructural phase delineation from this sequence of solidification events can be seen to advantage in Figure {7.1.5} **19** (below). [B/s EOM, fov: 0.32 mm.]

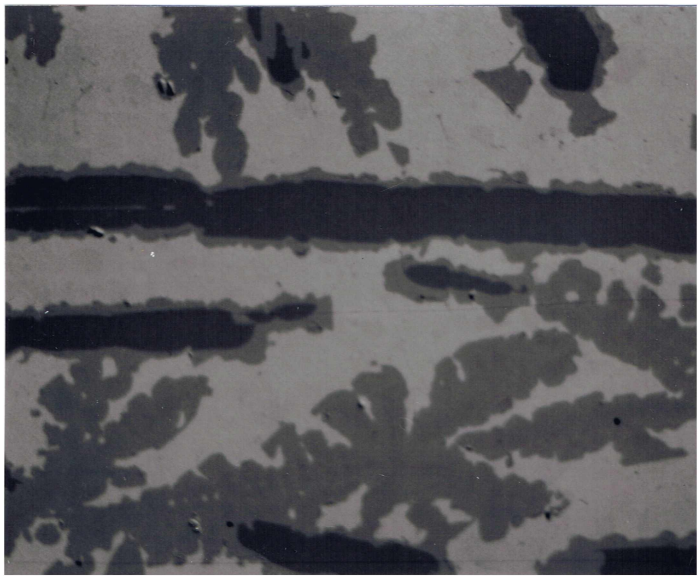

Figure {7.1.5} **19:** The micrograph shows microstructural detail in the crucible-cooled Sn, ~20 wt% Cu reduction product presented in Figures {7.1.5} **17** and {7.1.5} **18** above. [B/s EOM, fov: 0.08 mm.]

microwave plasma with its non-equilibrium environment, and microwave reduction processing were all learned and honed during this early period. Moreover, within the restrictions of this provisional oven method, process shortcomings and limitations (of insulation thickness, crucible performance, charge configuration, reductant quantity, blend intimacy, adequacy of charcoal-derived atmospheric protection, processing time and apparent "temperature", *et cetera*) were identified along the learning curve of "experimental persistence". Once such process inadequacies were acknowledged, then adjustments to system and/or process were implemented and the revised system tested in ensuing work. As these adjustments were successfully adapted into the method, the established technical system parameters – of both equipment and process – evolved into the fundamental, successful though simple microwave oven set-up method of reduction that then progressed to the core experimental programme. Further to this development of the "microwave-stimulated reduction process", in conjunction with the in-process re-oxidation protection afforded by the carbon monoxide (CO) atmosphere control, the introduction of liquid nitrogen (LN_2) quench-cooling extended this protection. (From the peak-heat of the reaction zone at process termination through solidification to the cold, stable reduction product) the extension of atmosphere protection by LN_2 quenching both supplemented and consolidated the feat of gainful reduction for the microwave oven set-up system, thereby assuring the success of the experimental programme. Without the crucial sufficiency of this broad but ample atmospheric protection method the refractory metal project could not have proceeded.

7.2: Reduction of Titanium-Bearing Minerals Anatase, Rutile and Ilmenite.

Through recent decades titanium has retained the aura of marketplace "flavour of the moment" magic for a widening range of retail consumables in addition to the traditional technological and industrial applications for which they have, it might be said, more "material properties based" legitimacy. (Titanium golf clubs and cookware are sales orientated products, manufactured goods whose material choices were fashion driven rather than needs driven.) Accordingly, (irrespective of intent or utility) titanium production has great currency in the mercantile deliberations of the broader production and fabrication industries. Because of this unequivocal commercial trend, a keener…

previously described charge configuration of the definitive microwave oven set-up method incorporating the LN_2 quench (refer to Figure {5}1). Between the excess blend char and the generous granular char blanket, it was conceded that – and as was the intention – an abundant over-supply of reductant CO gas was available to system chemistry (including plasma chemistry). Beyond the fundamental "reactant function" of the reductant, and generally afforded by gasification of the non-intimate granular char, this CO excess efficiently provided the system's atmosphere control. The atmosphere control extended from pre-reduction through reduction processing and post-irradiation into the process-termination phase of the LN_2 quench procedure, whereupon, CO-protection shifted through CO/N_2 mixture to N_2-protection at sub-ambient quench-termination temperature. During the period approaching quench end-point, because of the lagging thermal mass of the residual intact crucible configuration, the metallic reduction product was commonly subjected to a sub-zero (C°) holding period before turning-out to "air", thence material recovery of reduction products from the crucible remnants. This freezing into the sub-zero range was neither anticipated nor observed to have detrimentally affected the product outcome. Overall, and irrespective of means, this ultimate method was more a triumph of intuitive "experimental know-how" than of the culmination of prudently planned, orderly incremental shifts in experimentation towards such a functional and sufficient "definitive" method.

Encompassing a practicable range of experimental processing times, twenty seven experimental microwave-stimulated carbothermic reduction trials were carried-out on anatase. In these campaign trials the individual processing times covered operations upwards from six minutes (in specimen sets with intervals of "nominal" two minute progression) to process times that ultimately represented the melt-limit of the crucibles' thermal capacities. (In addition, it is noted that *fluxing* attack on crucibles was not an overt concern for this and other carbothermic/aluminothermic, oxide to metal or metallic carbide/(nitride) systems.) As discussed elsewhere, the general raising of the total energy of the charge (and that material intimate to its containment) from ambient into the broader thermochemical range of more pervasive* process reactions occupied

* Because of the nature of microwave heating in solids (that is, the concentration of "heating" at point centres of dielectric lossiness and along corridors approximating micro-arcing paths between these doped

the bulk of the initial six minutes of microwave processing. These twenty seven microwave-stimulated carbothermic reduction products of anatase provided the sets of reduction product materials as remnant specimens ANAT**01** to ANAT**27**.

By way of the central assessment methods employed, Table **{7.2.1}1** presents a comparative overview of the experimental outcomes grouped by processing time (and) representing the specimens ANAT**01** to ANAT**27**. The intention of the Table **{7.2.1}1** format was to provide a provisional means by which, illustrated by this representative first experimental set, simplified procedural assessments could be cross-referenced in a generalised but meaningful way thus providing a corroborated *summary of trends* in reduction-phase speciation. Contingent upon such condensed summary, the *succession of process chemistry* is reflected in the specimen series – so providing insight into the process-progression of results (of the carbothermic microwave reduction processing of anatase). Whilst seemingly pre-emptive at this introductory stage of anatase results presentation, the tabulated summary is presented early because (*i*) it anticipates project-wide reduction trends and therefore assists in developing an overall appreciation of process characteristics and capabilities, and (*ii*) out of this first, most investigated core project task, it offers a helpful and edifying introduction to the separate complementary studies of this Section **7.2.1**.

Also, being a "template" section indicative of subsequent reduction sub-sections, the procedure and results of this key *carbothermic reduction of anatase* sub-section are more thoroughly addressed than are those in following reduction categories (sub-sections) of the wider *Results* section. Whilst this Section **7.2.1** presents the routine of experimentation and assessment of carbothermic reduction products of anatase, the experimental approach described epitomises the typical procedure for experimentation and evaluation of each reduction trial (individual experiment) in each reduction task (reductant route and mineral) in following work. [In that work described in following sub-sections, where specific reduction campaigns were

centres) random concentrations of energy (by "thermal runaway") promoted early random reduction reactions pre-emptive of process procedure and which occurred before the bulk energy ("temperature") allowed this general "pervasive" extension of reduction reactivity spreading throughout the charge.

Table {7.2.1}1: Summary of generalised variations to phase speciation with processing time in anatase reduction products ANAT**01** to ANAT**27** as characterised by light optical microscopical evaluation and after review of SEM/EDS and XRD analyses. In order to support the plainly evident "pattern and relationship" between assessment procedures, the overview presents commentary of an intentionally generalised nature in order to highlight any reduction commonality or any trend in process indicators. The table provides an introduction to reduction processing trends in ensuing documented (formal) results.

Experimental Specimen Number	**Processing Time** (min)	**Principal Reduction Products (indicated by):** **LO Microscopy**	**EDS**	**XRD**
ANAT**01**	6	Minor nitride regions at crucible wall extremities in a sintered mass. No distinct metal.	Depleted Ti-oxides (with some C & N) in varying degrees of reduction. Some evidence of metal.	TiO_2 in a range of ill-defined principal oxide phases representative of reduction stages. Some TiC & TiN, no Ti-metal.
ANAT**02**	8	External carbide/ nitride regions in variable, fractured, sintered mass, minor silver metal regions internally.	Depleted Ti-oxides, increasing C & N within advanced exposed Ti(O)CN outer rim. Minor metal in reduction product.	Range of Ti oxides plus increasing CN-principal oxides. Minor Ti metal, increasing TiC & TiN & intermediate phases.
ANAT**03**	8	"	"	"
ANAT**04**	8	"	"	"
ANAT**05**	8	"	"	"
ANAT**06**	8	"	"	"
ANAT**07**	10	Ext. bronze nitride regions becoming more prominent. Plasma-exposed internal regions now all metallic: nitride appearance externally but carbide internally.	Ext. phases higher in C and N. All internal regions of varying Ti-OCN phases. Now a gratifying number of spot-assayable Ti-metal features for clear EDS acquisitions.	The range of oxides shifts more towards the ill-defined Ti-oxycarbonitrides. TiC and TiN peaks also now clearly discernible, as are Ti-metal peaks.
ANAT**08**	10	"	"	"
ANAT**09**	10	"	"	"
ANAT**10**	10	"	"	"
ANAT**11**	10	"	"	"

Table 7.2.1 (continued)

Experimental Specimen Number	Processing Time (min)	Principal Reduction Products (indicated by): LO Microscopy	EDS	XRD
ANAT**12**	12	Ext. bronze nitride interface (surface) regions densify. Int. regions largely Ti metallic, Ti carbide or Ti carbonitride in partly reduced balance. First signs of over-processing.	Bronze phases range from minor carbon Ti-nitride to Ti-carbonitride. Int. phases being Ti-oxycarbonitride. plus other metallic Ti solid solution & intermediate phases.	Remaining oxides shift further towards a range of leaner and still ill-defined Ti-oxycarbonitrides, plus Ti_2N, TiN, TiC & other suspected compounds, plus Ti-metal.
ANAT**13**	12	"	"	"
ANAT**14**	12	"	"	"
ANAT**15**	12	"	"	"
ANAT**16**	12	"	"	"
ANAT**17**	14	Bronze phases were now pervasive, but this external rim material now quite fissured from consolidation shrinkage. Internal partly reduced, part metallic regions were largely spent with increasing metallisation.	Bronze phases were both increasing in N (& C) & decreasing in O and were more pervasive into internal regions. Remnant principal oxide regions mostly absent. Broad Ti- metallic regions internally through specimen.	Principally oxide phases evidently decreasing as carbide/nitride phases emerge as dominant. Ti-metal still a minor peak set as Ti proceeding to compound balanced by newly reduced Ti-metal.
ANAT**18**	14	"	"	"
ANAT**19**	14	"	"	"
ANAT**20**	14	"	"	"
ANAT**21**	14	"	"	"
ANAT**22**	15	Bronze nitride rim was now showing definite indications of over-processing as fissuring widens & "skull" features develop at rim extremities. Silver metal and carbide regions decrease in favour of bronze coloured regions.	Rim and similar plasma-exposed regions increasing in N & C. Where solid solution Ti regions could be found (internally), they exhibited low C & N with negligible O.	XRD scans reveal continuing decrease in intermediate phases concurrent with increasing proportions of full, stable metallic compounds TiC & TiN, with fewer hybrid compounds ($TiN_{0.26}$, $TiC_{0.7}N_{0.3}$, $TiC_{0.3}N_{0.7}$, *et cetera*)

& Ti solid solution.

Table 7.2.1 (continued)

Experimental Specimen Number	Processing Time (min)	Principal Reduction Products (indicated by): LO Microscopy	EDS	XRD
ANAT**23**	16	As ANAT**22**, but Ti-metal regions are more difficult to identify as they become more restricted.	As ANAT**22**, but, where found, new Ti-metal quite free of light elements. Increasing metallic compound regions.	As ANAT **22**, but solid solution Ti-metal noticeably decreasing.
ANAT**24**	17	As ANAT**23**, plus more prominent skull densification & related voidage.	As ANAT**23**.	As ANAT**23**.
ANAT**25**	18	As ANAT**24**.	As ANAT**23**.	As ANAT**23**.
ANAT**26**	18	As ANAT**24**.	As ANAT**23**.	As ANAT**23**.
ANAT**27**	18.5	As ANAT**24**, but notably, trial was terminated by thermal failure of crucible. Highly developed skull densification in a high voidage reduction product. Negligible solid solution regions remain.	As ANAT**23**. Bronze extremity regions approximate compound status for Ti(C,N). Minor internal Ti-metal as solid solution.	As ANAT**23**. [Note apparent contradiction between the Ti(C,N) of EDS and the XRD distinction of Major TiC *plus* major TiN phases – presumably as rim type material. (*Discussed elsewhere*.)]

curtailed or were otherwise less central to the broader project, their experimentation and subsequent reporting of procedure and results were suitably truncated. (Refer to *précis* of experimentation in Section **6.4**.)]

Therein, for its bare worth, Table **{7.2.1}1** presents nub observations of process trends and material variations across the central result outcomes of light-optical (microscopical) characterisation, EDS analyses and XRD analyses for each of the anatase reduction products from ANAT**01** to ANAT**27**. Whilst the table's summary of process trends was not intended to formally present results, it does, by way of recorded experimental observations, provide a condensed but clear preview of process events which fundamentally unfold in the following primary presentations of microscopy, EDS and XRD. Also germane, upon comparisons within the table, if and to what degree any correlation exists between observer-based (subjective) characterisation studies and the results of machine-based (objective) diagnostic methods. [Some inconsequential "interpretation derived" differences exist between the EDS and XRD assessments in accrediting phase or compound types to their *actual* or *exact* species. Component elements comprising species could be complex throughout remnant reduction product phases – particularly for the interim species of intermediate phases. (Here, in the trivial case, a single species may be equated with a single phase; alternatively, a reduction product phase may be comprised of more than one identifiable chemical or physical species.) In such cases of uncertain species identification, where "reasonable doubt" overrode "attributional exactitude", absolute ascription of phase or compound species was left unresolved between analyses, consequently, counterpart EDS and XRD descriptions may appear "at variance" in Table **{7.2.1}1**.]

Based upon their propensity to represent the full suite of reduction-stage phases, representative sections of material from the range of retrieved anatase reduction product remnants were selected for metallographic preparation. Material selection was more frequently conducted under the low magnification light-optics of a stereomicroscope, however, un-aided inspection was adequate for obviously representative phases (where they existed discretely). As was obvious from the summary table, the outer, rim material (adjacent to the crucible) and that of charge-top and similarly exposed material were

found to exhibit higher N-proportions overall (as could be inferred upon un-aided visual inspection). Some sections of material removed from the crucible base, adjacent to the bottom char during processing, revealed themselves to be silver metallic or carbide phases rather than the distinctive bronze of the nitride-dominant phases (or compounds where relevant). Some C- or N-prevalent regions in shorter-term processed specimens were sufficiently conversion-advanced to be allocated the status of stoichiometric compound, and moreover, the proportion of compounds increased with processing time as later X-ray results corroborate. There again, it was a source of confusion in initial investigations that some apparently solid solution metallic phases, wherein the N-uptake was found to be relatively minor, exhibited in polished section a bronze metallic sheen that was characteristic of TiN and comparable compounds. For each reduction product specimen, sampled materials were selected such as to include the apparent and representative range of reduction product phases which were retrieved from the shrinkage-fissured, part sintered, sometimes friable crucible contents. [As is discussed elsewhere and in the following passages, sample splits for microscopical studies and for EDS and XRD analyses were not intended as *quantitative* samples. To ensure *qualitative* relevance across examinations, however, it was intended that sampled material should include the range of phases in the remnant specimen – and in proportionate quantities such as would secure their analytical identification.]

As was indicated in earlier sections, the absence of a neat "whole" metallic button product, and moreover, the nature of the sintered bond between crucible wall and the typical solid-state sintered reduction product ensured that, within reason, recovery of the reduction product as an *integral whole* was not possible. Consequently, vacuum-impregnated full cross-sections of *wholly* retrieved reduction products were not mounted and prepared for micrography and EDS analyses. (Also, the crucible material was too hard to practicably grind and polish *en masse* – a prohibitive reality had preparation of "included-crucible" sections been contemplated as a metallographic option. As mounted, the comparatively lesser quantities of hard reduction product material were already a hindrance in specimen preparation.) Furthermore, knowing the inhomogeneity of the post-reduction "charge remnants" zone, it was generally felt that there would be too much variability from potential cross-section to cross-section (both horizontally and vertically) in any single reduction product to assert outright representational legitimacy in any one (cross-section). Overall, given the point of

process development in this exploratory pilot project, notional broad-analysis studies on representative cross sections *per se* were considered a "next stage" study option where whole quenched crucible or reactor chamber reduction remnants (intact) could be investigated by sectional analyses (point count, image analysis, *et cetera*), progressive excavation logging and other relevant means. In addition, and of tangible concern during the course of project experimentation, recovered reduction product remnants equivalent to those mounted were required also for selection (sampling) of material for XRD plus reserve for contingencies. Although reduction product remnants were small in quantity across the range of project experimentation, adequate material was produced, reclaimed and available in each case for characterisation and analytical needs leaving a modest quantity in reserve.

For material characterisation studies on titanium and other reduction products it was decided that for light optical capture, although both media options were nominally employed, colour micrographic images conveyed more and different visual information than did black and white micrographs – in particular, the primary visual perception of *metallic lustre* was more accurately conveyed in colour. [Metallic lustre was, for this project, a fundamental marque (attribute) underlying the innately contentious distinction between *ceramic* and *metallic* for metallic compounds and their like.] Especially for titanium reduction product phases, the visual difference between bronze and silver metallics was better represented by colour-contrast rather than the grey-scale contrast of monochromatic micrographs. To this end, Kodak Ektachrome colour positive slide exposures were recorded principally through a Leitz Orthoplan microscope using both oil immersion and air lens systems over a range of conditions and settings (illumination, daylight blue filter (to compensate for Ektachrome film), polariser/analyser, quarter-wave ($\lambda/4$) plate, *et cetera*) found to be beneficial to the captured image. Few black and white micrographs were recorded for titanium reduction product specimens; however, such images can be found accompanying the output of elemental mapping exercises, although these were EO micrographs.

Resisting the temptation of faux-colour EO micrographic images (be they meaningful or cosmetic) – which was possible for images re-created from electronically acquired data – all SEM pictorial images were acquired and stored as "black and white" monochromatic micrographs. Notwithstanding this edict, colour was sometimes

meaningfully employed as a visual descriptor (for elements) in X-ray mapping exercises. Individually such "maps" were not strictly micrographs but monitored-element survey reproductions which mimicked a selected micrographic "template image" (which, with fellow elemental maps, it accompanies in presentation). X-ray maps, or elemental maps, were acquired over representative phase fields for each of a suite of elements relevant to the reduction product composition. The forte of elemental mapping as an assessment facility was that maps indisputably showed the partitioning of elements to their component phase(s) and therefore distinguished the phase boundaries and defined the extent of components within the mapped field. Such elemental maps were employed to provide support to EDS spot and/or area analyses on specimen fields and to lend legitimacy to the claim(s) of projection or extension of such EDS results across other like but un-tested phase-fields. However, as with all mapping techniques, this method requires inhomogeneity to provide map detail – in this case, chemical inhomogeneity of phases across the field. Again, for anatase reduction products and for others of "pure" starting-point minerals (zirconia, hafnia, niobia and tantala) elemental mapping was a trivial exercise unless stable windowless field-acquisitions could provide variation in light element detection where such phase or compound discrimination existed. To successfully accomplish such light element maps, the multiple (element-by-element) acquisition exercises required long-term exposure of the detector to the chamber environment. This "exposure", at high chamber vacuum, included indiscriminate near-surface volatility from the random instability of quench-termination specimens – specimens primarily of process-terminal material but also including that fraction of transitional phases acquired upon quench-interruption of process chemistry. Consequently, the successful acquisition of stable light element maps was subject to the foibles of both specimen preparation plus the sealant property of its conductive coating, the conductive capacity of this coating and, more importantly, the stability of the beam current, image drift, detector and other machine parameters, limitations and ponderables over the length of the acquisition period. A number of potentially informative prospective map-sets were belatedly lost to image drift phenomena when performing late stages of windowless field scans, at a cost of considerable machine time. Usually, the full machine time allocated to those drift-affected maps and consequently lost could not be *pro rata* re-scheduled, hence machine access was not fully redeemed. However, whilst the total number of successfully acquired maps suffered, a number of "lost" map acquisitions were subsequently

repeated satisfactorily. Also, and pertinently so for the reduction products of the laboratory grade minerals such as anatase, elemental maps were of solitary metallic composition with (if at all) only faintly perceptible inter-phase detail delineated by scans of the light elements O, N and C. Consequently, these relatively featureless map sets represented quite "trivial" results unless oxide-dominant areas could be distinguished from carbonitride-dominant and principally-metal (alloy) areas. Typically, however, this light element discrimination of phase-categories was not sufficient to discernibly image phases on maps scanned across phase fields of "pure" mineral reduction products. In contrast, scans on reduction product remnant specimens of minesite-derived mineral concentrates produced X-ray maps of elements which were more structured and meaningful, even light element discernment of phases was more marked (although somewhat redundantly so because partitioned metallic elements also identified these phases). Separate to the principal metal(s), these maps featured the light element distribution plus secondary metallic elements, usually partitioned from the principal metal(s). This fact ensured that X-ray maps were utilised to greater effect and more commonly (as presentations attest) for those elemental component studies of reduction products of ex-mine mineral concentrates.

Ostensibly unrelated to the reactant anatase, the presence of impurity metals and, in particular, the recorded proportion of these elements in reduction products across the suite of carbothermic anatase reduction output was as unexpected as it was unwanted. However, considering the mode of oven set-up experimentation and after reflection upon possible material sources of such contamination, the following appraisal seems wholly reasonable.

Irrespective of source, taking into consideration the *presence* of impurity metal in reduction products from anatase – a nominally pure titania – it was reasonable to assume that, where and when they occurred, the more easily reduced tramp elements would report in the reducing charge as metal *from the onset* of reduction under microwave processing. Bearing this out, microscopic entities (specs or micro-beads) of reduced Fe, Si, Cr and/or other more easily reduced contaminant elements were evident in newly reducing regions of reduction product specimens from the least processed

cases through (sometimes) to lagging regions in the most processed. The recorded variation in the *proportion* of these impurity elements in reduced metal with increasing processing time is accounted for in the following passages.

Under microscopical examination of reduction products it was also universally noted (and evident in the included micrographic record) that where specs of initially reduced tramp metals existed in the fabric of the charge agglomerate, they commonly were intimately accompanied by latterly-reducing Ti-metal. Whereafter, upon further processing in these primary reduction regions, evidently, the separately-reducing micro-entities subsequently coalesced into small alloy liquid beads. Such small beads of alloy liquid had a greater propensity to grow and coalesce into more expansive beads than did those near solid-state reduced Ti-metal entities which were in any way isolated from lower melting-point alloy entities (beads). It has to be assumed that it was from the alloy beads – more prominent and more visibly metallic than those adjacent reductively-evolving "untainted" Ti-phases of higher melting-point – that EDS spot sites were selected and counts acquired, the results subsequently compiled as Table **{7.2.1.2}2**. Consequently, this compositional delineation in beads inadvertently presented an EDS specimen selection quandary: that dilemma being an aversion from equivocal acquisitions off the ill-defined phase-fields of small Ti-metal beads towards the cleaner acquisitions off definite phase-fields of larger, low-alloy beads. [Although suspected, this distinction was not so abundantly clear at the time of analyses – or was not sufficiently so to then revise spot site selection.] It followed that results were skewed towards the impurity content of low-alloy Ti-bead compositions rather than towards the desired "pure" Ti-metal of latterly reduced micro-beads, this diagnostic idiosyncrasy (arising from otherwise "reasoned" choices of EDS sites) needed to be borne in mind in interpretation of those results. [Notably also, in Table **{7.2.1.2}2** the area acquisition results show Al prominently as a tramp element. This presence of Al may have been factual, but its presence as *reduced Al-metal* in this case was implausible (given its greater thermodynamic stability and the still incomplete stage of Ti reduction). Even the notion of "retained" Al-metal bears the implication of initial reduction; reduced Al-metal was certainly plausible in some intensity-specific ex-programme exercises and in the few microwave reactor trials. However, if Al-metal was ever achieved during experimentation, it almost certainly re-oxidised upon cooling and once outside microwave plasma environment. The assignation of Al under area acquisition must be

attributed to detection of Al in an un-reduced ceramic (oxide) phase intermingled with the reduced metallic phase(s), possibly around grain boundary/phase interface regions where (say) finely disseminated Al_2O_3 may be the by-product of the reduction of Si from alumino-silicate refractory material. Such a presence would not be readily detected visually, and may in fact be contained *beneath* the polished surface where it might be easily detected under back-scattered electron examination. Also, as discussed elsewhere, spot EDS acquisitions from those volumetrically smallest beads (of any composition) sometimes yielded an exaggerated proportion of extraneous elements (including Al) in results because the excitation bulb was not contained within the bead. (In later XRD studies, and observing that greater dispersal of minor components could be expected in X-ray powders after ring-milling of sampled material, suspected major spectral peaks of Al_2O_3 were noted breaching the background trace of *some* individual specimens. Moreover, these otherwise unaccounted peaks (*i*) were (at best) indicative of trace proportions in individual specimens, (*ii*) were not detected in composite spectra and so, (*iii*) (beyond a conjectural recognition of "*suspected present*") occasional suspected peaks did not comprise *confirmation* of the presence of alumina in reduction product remnants.)]

In further deliberation of the mixing mechanism and convergence of components into alloy micro-beads, bead growth, cumulative drainage and pooling capacity, the following plausible mechanisms and trends are here discussed. It was proposed (anticipated) above that elements more easily reduced were present in the reducing charge from the instigation of processing specifically because they were reduced from their contaminant source more readily than was Ti from titania. And, importantly, as is observed in the following *Micrographic Record*, these entities of initial metal reduction product – evident as miniscule liquid metal specs – acted (more or less catalytically, as centres of energy and chemistry) to actively attract and absorb adjacent newly reduced Ti-metal into an alloy liquid droplet. This "*absorption*", or amalgamation by simple liquid mixing, liquid metal into liquid metal, may alternatively or initially have been instigated as an *adsorption* mechanism: solid metal onto liquid metal, thence by diffusion to an alloy liquid droplet – the liquid bead growing with time. Also, as elsewhere mentioned, this "newly reduced Ti-metal" was not pure Ti, but merely approached "pure" during the final, "near O-free" metallic stage of reduction. It was loosely categorised as the "reduced metal" stage Ti-metal before it "over-processed"

into Ti-carbonitride by "re-oxidation". Beyond the light elements, the presence of the tramp elements was derived from a trace tramp component incorporated in either the reactant mineral or reductant char of the charge (the reactants) or, more likely, were intrusively introduced to the charge during processing by means of thermally failed or mechanically failed refractory materials. Of the several containment and insulation sources, such failed refractory material collapsed and/or drained into the reaction zone to join the reducing charge, intimately intermingling with the reactants – especially when in the molten state. The majority of refractory items which were charge-intimate enough to contribute such detritus were fabricated from alumino-silicate of reasonable purity (with respect to trace contaminants), although, the presence of trace Fe was noted universally throughout the fibrous blanket product and in some rigid refractory material (fireclay crucibles and lids). Trace components aside, the composition of the alumino-silicate blanket material was typical of that commonly specified refractory material (synthetic) mullite ($[3Al_2O_3.2SiO_2]$ or $Al_6Si_2O_{13}$) although, for certain specimens as selected, the silica portion tended to drift marginally higher. This "drift" was affirmed in instances of EDS analyses during random "quality monitor" checks of materials *incidental* to the process. Of note, regarding the "zirconia" crucibles universally used as intimate containment in the core experimental programme, the zirconia (aggregate) and alumina (cementitious fines) portions evidently contributed negligibly towards the "trace impurity component" of the reduction products.

In some respects the tendency of initially Fe/Si-metallic specs to grow more quickly (than their un-seeded, reductively emerging Ti neighbours) through alloy succession into larger "predominantly-Ti" liquid beads mitigated against the veracity of their subsequent selection (as sites) for EDS analyses to *verify reduction* and, crucially, leading to *proof of concept*. Their neighbouring, rather size-limited and non-equilibrated Ti "beads" – which may have been the straight product of solid-state through to liquid-state titania reduction – remained comparatively small. Accordingly, in regions of advanced reduction, eventual coalescence of these small entities fortuitously provided a large enough "clear" specimen volume to permit successful EDS acquisition. Moreover, in anatase specimens across the processing range, the thermal conditions did not come about which, for the composition of phases produced, permitted liquid metal pooling to occur *en masse* in the usual "liquid draining" sense of melt-aggregation and button formation.

Cognisant of the above circumstances, in selecting specimen fields from which to acquire EDS data it was mandatory to find a site having sufficient volume to assure an un-contaminated acquisition (regarding clearance to nearest neighbouring phases of Monte Carlo bulb excitation). Particular care was taken for counts on fields of least-processed reduction product – such fields typically exhibiting sparse, un-aggregated metallic beads in groups having varying size ranges and inconclusive reduction status. EDS spot sites were selected within fields of the "most metallic" bead-sections and these, inevitably, were those larger metallic features representative of the impurity-seeded alloy-Ti beads identified above. Consequently, the significant presence of minor proportions of impurity elements, especially Si and Fe, was recorded across the range in spot acquisitions on specimen fields of specimens from ANAT**01** to ANAT**27**. Supportive of the case that straight reduction to Ti would be amplified with greater processing time and "temperature", (in their EDS data) the suite of anatase specimens duly demonstrated that the degree of alloy impurity levels decreased with increasing processing time. This experimental "sleight-of-hand" was simply explained, and was of negligible consequence in terms of the microwave reduction process. Generally, then, impurity proportions in evolving beads fell both (*i*) with the increased thermochemistry of evolving reduction, and (*ii*) incidentally as the increasing proportion of newly-reduced metallic-Ti diluted the original proportion of initially-reduced impurities.

Furthermore, the same was true of the corresponding fractions of contaminant components in reduction products of other nominally pure oxides that were microwave processed over the course of the extended experimental programme. Of course, reduction products of minesite-derived mineral concentrates exhibited noteworthy compositional quantities (generally in the trace to minor range of magnitudes) of tramp metals reduced from gangue mineral components in the mineral under experimental examination. Smaller in proportion than these gangue impurities, and not always determinable in the concentrate minerals, incidental impurity metals were also present in reduction products of minesite-derived minerals as a result of those lesser contaminant sources, the reductant and refractory material contributions (as described for the "pure" oxide cases). Despite progressive improvements to the refractory configuration and other measures devised to lessen such contributions, and although latterly a minimised contributor, refractory material "failures" remained, throughout the

core project, an unwanted and relatively constant component-fraction contributor of total impurity elements to reduction products.

In general, all carbothermic anatase reduction specimens displayed some proportion of metallic conversion. Predictably, the least processed specimen, ANAT**01**, displayed the most extensive range of partially converted principally-oxide phases over which spot windowless EDS spectral analyses indicated an extensive, possibly continuous range of Ti-oxycarbonitrides ($TiO_xC_yN_z$). This range of phases reflected the on-going state of reduction of the incompletely processed anatase (TiO_2) in, as later became plain, the (still) evolving thermochemistry of the microwave system, including the conversion of O_2 into CO/CO_2 (with ratio dependent upon thermodynamics). Upon carbonisation of the gaseous O_2 , the CO, CO_2 plus the remnant balance of the air mixture, principally N_2 and Ar, are open to increasing excitation, ionisation and re-combination under the input microwave irradiation. Whilst not the most chemically active species-set in the ionising post-air mix, N_2 and its sub-sets of activated diatomic and monatomic species form the most numerous particle family in the ionisation mix of the developing plasma[58]. This consequently ensures the relative prominence of activated N-family species in the plasma chemistry, and in the composition of products of the microwave reduction process (that is, nitrides, carbonitrides, *et cetera*). Because of detection software idiosyncrasies which, from time to time, would clearly under- *or* over-calculate the light elements' percentages, procedural caution was employed in EDS evaluation of light elements in the different reduction product phases. Suitably employing windowless EDS detection to investigate compositions of light element "phases", results for the full range of mounted specimens were assessed. [Where such idiosyncratic computational deviations were presumed, their inconsistency was evident by visual inference (estimation) from the acquired spectral peaks (given allowances for peak-suppression – inverse to atomic number – being accounted-for).] Assessment of reduced metallic-Ti was carried-out on representative internally located metallic phases-of-interest across the range, and because in all cases for the generalised "metallic" reduction phase $TiO_xC_yN_z$: $2 >> (x+y+z) \Rightarrow$ minimum, where $x \neq y \neq z$. With further processing as "metallic (carbonitride) compound" was approached: $x \Rightarrow 0$, whilst y and

z increased with time. [In over-processed rim material, (y + z) $\Rightarrow$ 0.5, 1, 2, *et cetera* as metallic phases receded from the "solid solution" and approached "compound" status for various common stoichiometries.] Pleasingly, EDS results on the metallic phases-of-interest indicated that actual reduction had taken place and that straight substitutional O-replacement by C or N was not the overriding chemical mechanism at work in the plasma chemical environment of the microwave reduction experimental trials – progression to metallic compound was via the reduced state, that is, via Ti-solid solution comprising minor light elements.

Whilst acknowledging their inescapable presence across the range of reduction products, the most broadly identifiable metallised regions – the nitride coloured "rim and other exposed surface" regions, which with processing time tended more and more towards the metallic compound and away from the Ti solid solution – were not regarded as representing the most *fundamental* reduction product metallic regions. The experimental programme hinged on this "fundamentality" of reduction product, that the product should represent the simplest, most basic metallic product (the pure metal or dilute solid solution which might be achieved under the ideal conditions of an atmosphere-controlled reactor); it was a project informing the *primary reduction of oxide minerals* as distinct from the *secondary processing of metals*. The essential windowless EDS point counts were conducted on such unexposed, basically silver-metallic phase fields located in the sectioned specimen and sub-surface in the remnant specimen and evidently representing *Ti-solid solution* material, rather than on fields which were apparently representative of the more advanced, "over-processed" post-reduction bronze nitride *rim and other exposed* material. Thereunto, whilst it is stressed that the nitride rim type material was unquestionably regarded as successfully reduced material, it was, however, processed beyond the point which might be representative of the desired reduction product of a successful *atmosphere controlled reactor* – a sometime supplementary pinnacle of project aspirations. Whilst this system ideal of an ultimate *working reactor* was not experimentally realised within the project, its more material counterpart ideal of a desired metallic-Ti product could universally be found embedded in remnants of the more diverse reduction product output of the microwave oven set-up.

Although (as previously indicated), once reduced, such desired reduction product metal tended beyond the solid solution towards the metallic compound. In fact, it was an entirely likely projection that over-processing continually transformed "pure" metal through solid solution alloy towards the carbide/nitride metallic compound. And further, that new reduction saw that newly reduced metal continued until the incompletely reduced mineral was fully spent – save for an unaccounted fraction which by-passed true, oxygen-free "metallic" to proceed to an oxycarbonitride final phase. Such concurrent phase-steam diversity within the broader complexity of the process left the identification of an ideal processing time somewhat indecipherable for the oven set-up system. Furthermore, where conducted, vacuum arc-melting of reduction product material(s) did consolidate the remnants into a simpler two-phase metallic-Ti button – a product form far easier to contend with, to verify and to support in dissertation. Although desirable, such consolidation buttons provided no direct information with respect to the sequence and mode of actual reduction processes. Consequently, this controlled re-melting approach was notionally promoted into a "future experimental" programme where, perhaps, larger microwave reduced specimens might be produced with a sizeable portion committed to arc re-melt consolidation and appropriate follow-up studies.

7.2.1.1: Micrographic Record.

Micrographically presented in Figures **{7.2.1.1}1** and **{7.2.1.1}2** are typical fields representing early stages of carbothermic anatase reduction. What is captured in these micrographs is the essence of initial reduction phenomena affecting the visible physico-chemical changes to the initial TiO_2 reactant material. It can be observed in the former micrograph that initially coalesced regions are bounded by planar perturbations of the former micro-arc pathways – partially reduced to different degrees by the partly expended (by both reduction and gasification), partly adsorbent blend char. These initially coalesced regional entities (in micro-arc interstices) have, upon further

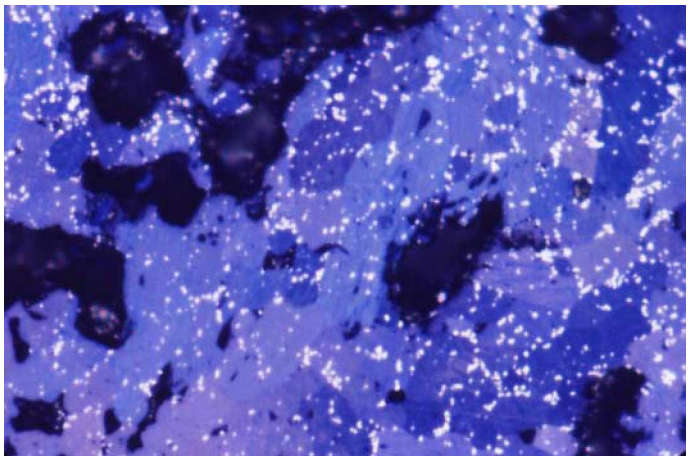

Figure {7.2.1.1} **1:** Micrograph of a typical field on specimen ANAT**01** (6 min.) showing voidage from initial contraction (before melt-consolidation stage) as anatase particles coalesce into a solid continuum. Note that the bright Ti specks represent the earliest reduction phenomena, here beginning to fuse, highlighting the original microwave derived micro-arc tracks which were integral with the initial dielectric heating mechanism. Also, these Ti particle-defined "tracks" tend to define the phase boundaries of secondary reduction in the anatase as it begins its reduction path from $TiO_2 \Rightarrow Ti_2O_3 \Rightarrow TiO \Rightarrow Ti$ for T < 735 K, and $TiO_2 \Rightarrow Ti_3O_5 \Rightarrow Ti_2O_3 \Rightarrow TiO \Rightarrow Ti$ for T > 735 K [117], the varying shades of blue could represent changed phases in re-solidified oxide rather than indicate optical activity. [LOM oel, Ektachrome, fov: 0.53 mm.] *{As per Section **7.2.1**, all colour images compensated through daylight blue filter, whilst this and certain other images captured using λ/4 plate and partially crossed nicols.}*

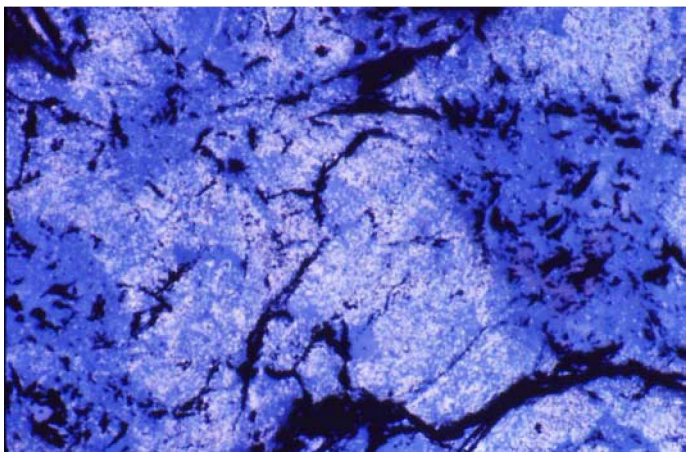

Figure {7.2.1.1} **2:** Micrograph of a typical field on specimen ANAT**01** showing voidage and shrinkage-induced fissuring from initial contraction (before melt-consolidation stage) across a broader field than in Figure {7.2.1.1}**1** (above). The field is expansive enough to show contracted "as-charged anatase" regions of low reduction and high voidage that, despite their appearance, were not to be confused with granular char particles from the adjacent blanket char zones (which can be seen in later micrographs). The field was representative of regions in the central charge where, ultimately, most of the contraction voidage was contained as material was contracted outwards towards the more reduction-advanced, rigid rim material. [LOM (air), Ektachrome, fov: 1.05 mm.]

thermally induced softening or melting, undergone further consolidation by secondary coalescence – ultimately, an event responsible locally for extinguishing the micro-arcing phenomenon. Before its termination, the system of micro-arcs was responsible for the initial instances of reduction and consequent Ti-metallic particles delineating these pathways (or tracks). Once subsumed by the enveloping softened or liquid phase coalescence, the dielectric "lossiness" heating mechanism – requiring an ionising gaseous environment and being defined as the constrained gaseous micro-*arc* plasma between solid dielectric extremities – was replaced by the elsewhere emergent thermochemical mechanism of the gaseous *volumetric* plasma. With micro-arc discharges being increasingly lost in the intensifying radiant glow of the volumetric plasma, this incoming principal processing mechanism progressively overwhelmed and is believed to ultimately replace the dielectric mechanism for the remainder of the reduction processing operation. As elsewhere described, the incoming plasma mechanism functioned by creating a high population of energetic, highly reactive particle species and driving reduction from the energetic plasma through the plasma/solid (or plasma/liquid) reaction-interface, thence by microwave-enhanced diffusion of active species to and from the interface, from and to lattice sites.

Also, for the 6 minute processed specimen, ANAT**01**, the latter Figure **{7.2.1.1}2** shows the inter-relatedness of gasification zones, the initial CO-producer zones, and diffusion-driven reduction concentration zones – metallised regions favoured by their proximity to (*i*) a local energy concentration, and (*ii*) proximity (and exposure) to a reaction interface. Different modes of shrinkage attest to their initially different regional functions, and noting that both regional types were compositionally equivalent and neither regional type contained large granular char particles (despite appearances, in this instance the fissured regions are not incorporated charcoal features).

Micrographs in the sequence of five Figures **{7.2.1.1}3** to **{7.2.1.1}7** present the evolving synthesis and accretion of metallic particles, and their amalgamation into sintered clusters throughout internal fields in shorter-processed specimens and featuring material not directly exposed to the enveloping plasma; plasma within the crucible but external to the charge. [The term "exposed" is frequently used herein to indicate both (*i*) *position* within the charge (and with respect to the crucible), and (*ii*) the *proportion of remnant air* (N_2 + Ar + CO) – that is, after C-gasification and above CO stability (over

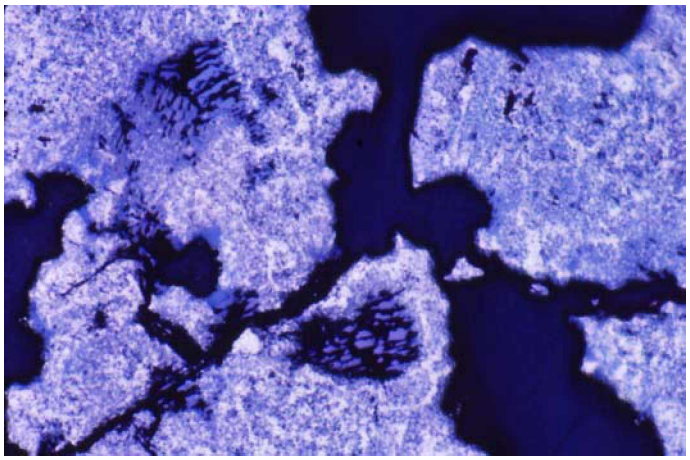

Figure {7.2.1.1} **3:** Micrograph of a broad field on mounted specimen ANAT**03** (8 min.) showing independent sections of similarly reduced material. Evidence remains (in this still under-processed example) of the further development (from the 6 min. specimen) of reduction along the primary micro-arc tracks. By this stage of processing, dielectric arcing was a "primitive" and largely overwhelmed heating phenomenon as the plasma mechanism increasingly drew the dominant share of the total attenuated microwave energy. Those various metal-free areas were, in this case, charcoal granules, showing considerable associated solution loss (reaction) by way of increased voidage, and showing some indication of accentuated reduction local to the char, plus increased carbon content in intimate oxycarbonitride regions. [LOM, Ektachrome, fov: 1.05 mm.]

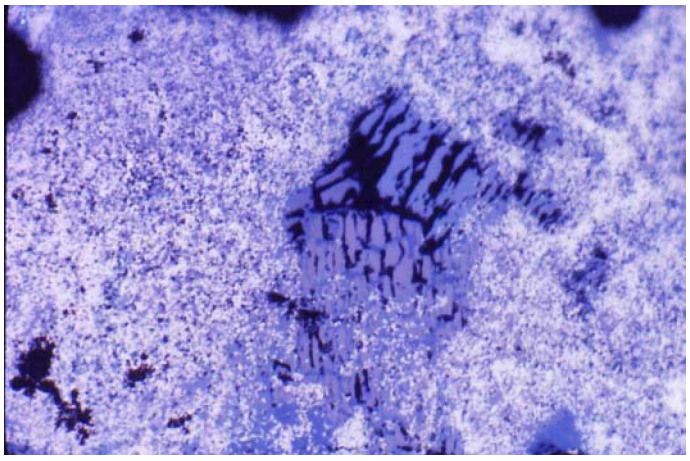

Figure {7.2.1.1} **4:** Micrograph representing a field existing in Figure {7.2.1.1} **3** of specimen ANAT**03** (8 min.) showing in greater detail the above-described elements of the carbothermic reduction of anatase. The metallic phase(s) were Ti-solid solution with low C and N, these light elements increasing in regions of greater exposure to gases CO and N_2 and their ionisation derivatives where plasma was the pervading environment. [LOM, Ektachrome, fov: 0.53 mm.]

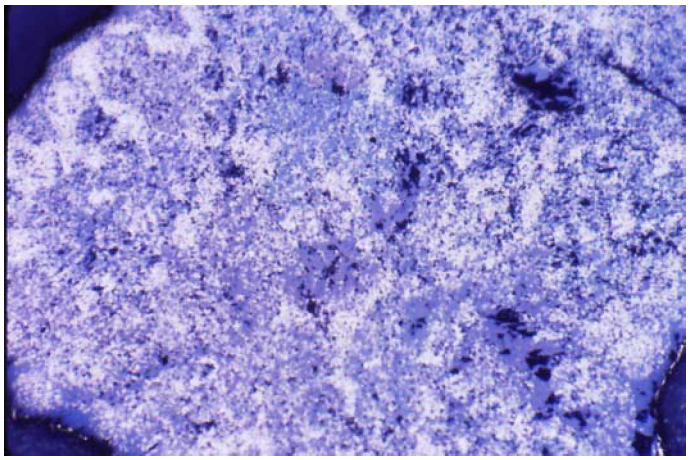

Figure {7.2.1.1} **5:** Micrograph on mounted specimen ANAT**04** (8 min.) showing typical field-of-view representative of central specimen with developing metallisation across the field. The comments with Figure {7.2.1.1}**3** are similarly appropriate for this field and for this specimen broadly. [LOM, Ektachrome, fov: 0.53 mm.]

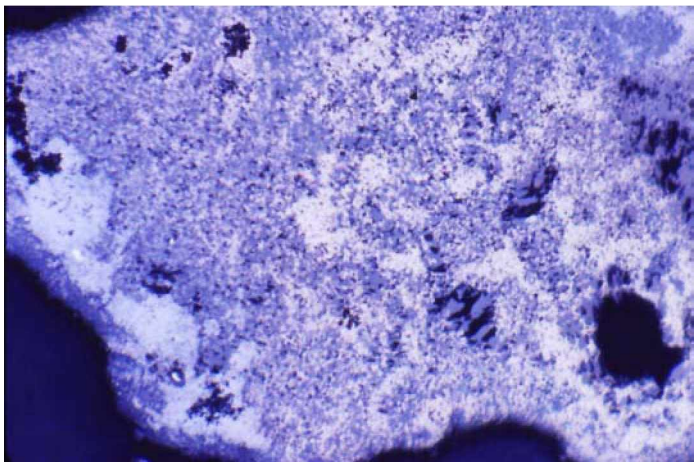

Figure {7.2.1.1} **6:** Micrograph of a broad field on mounted specimen ANAT**07** (10 min.) showing the colour differentiation of local carbide and carbonitride regions over a continuous but quite intimate field of reduction product. Some small bright (white) areas in the silver "carbide" phase region were found to be Ti-metal with virtually no light element component whilst both the silver carbide and pale bronze carbonitride regions contained minor components of C and N, and were virtually O-free. Generally, the silver-grey carbide regions were restricted to zones central and/or bottom remnants of the crucible. [LOM, Ektachrome, fov: 0.45 mm.]

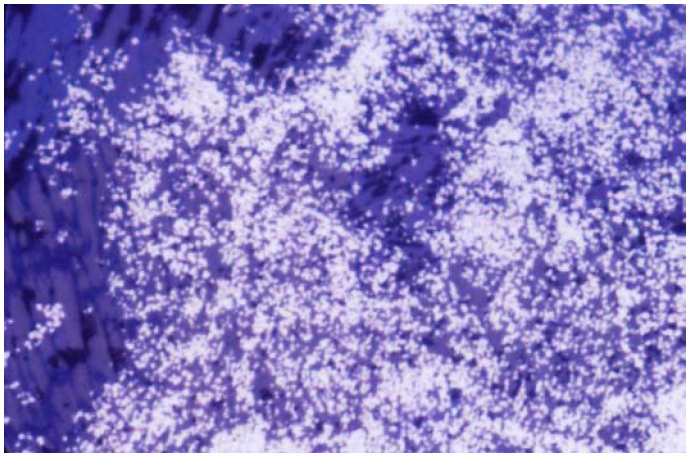

Figure {7.2.1.1} **7:** Micrograph showing detail of the "random" occurrence of reduced metal prills in the multi-phase oxycarbonitride anatase/char remnant charge material. Attention is drawn to the mode of aggregation and subsequent coalescing (sintering) of these reduced metallic specks, which constitute the mode of solid-state growth of metallic regions. The specimen was ANAT**09** (10 minute processing time). [LOM oel, Ektachrome, fov: 0.21 mm.]

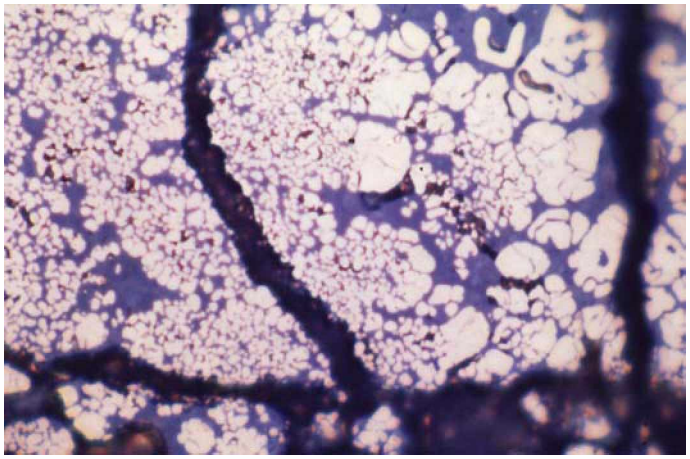

Figure {7.2.1.1} **8:** Micrograph presenting the typical "rim and similar" nitride phase in oxycarbonitride matrix material, the field representative of shorter processing times, in this case for ANAT**07** (10 min.).Such shorter processed rim material was characterised by the still significant proportion of un-reduced, C-rich grey matrix material, molten during processing and from which the nitride phase was deposited, at this stage the "nitride" phase was still in the loose solid solution compositional range. [LOM, Ektachrome, fov: 0.21 mm.]

CO_2) – which constituted the intimately local plasma associated with an element of charge (Δ(charge)). Correspondingly, "unexposed" regions were defined to be localised regions exposed only to CO-plasma and its associated chemistry (yielding metal and carbide phases), and not to any significant proportion of N_2-plasma (which led to the synthesis of nitride phases).] Annotations accompanying the figures adequately describe the developing metallisation as it proportionally accumulated with processing time upwards from the raw evidence of those figures of the 6 min specimen, ANAT**01**. The metallisation trend in 8 and 10 minute processed specimens (ANAT**02** to ANAT**11**) tended to favour the reduction synthesis to yield solid solution Ti-metal presenting as carbide "silver" or pale nitride "bronze" in colour through the volumetric majority of the specimen which could still be classified as "internal" material. This internal material, basically unexposed to nitriding plasma, was found to retreat (inwards and downwards) within the crucible with each increase in processing time, and that the "inner" nitride coloured metal presented as deeper bronze in colour with increased processing. Whilst these rudimentary changes were occurring to internal regions of specimens, the most exposed (to external radiant energy and N-rich plasma) regions of the reactants charge – that toroid of material against the crucible wall plus the charge top – continued to increase as the depth of remnant-air plasma penetration increased with increasing fissuring of the outer charge. This "increasing fissuring" equated to the volumetric contraction accompanying phase conversion and reduction to metallic state.

The external case, or rim material, plus the more friable top material (the "rim and other exposed" material) were, from the outset shortest process, the most bronze nitride regions of any produced during processing. The quite shallow nitride surface on oxide ceramic phase of ANAT**01** (6 min) progressed markedly in effective thickness and metallisation with each increase in processing time. Each progression in reduction processing, however, brought with it an increment of over-processing to previously reduced material as solid solution phases moved (for the oven set-up system) irrevocably towards metallic compounds, with attendant volume shrinkage and simplification of phase diversity. Figure **{7.2.1.1}8** presents a typical rim material commonly evident in shorter processed specimens (ANAT**07** (10 min) in this case) complete with substantial incompletely-reduced grey matrix phase (into which the metallic conversion phase was growing) plus pre-existing fissuring. The following Figure **{7.2.1.1}9**, from a similarly processed (10 min) specimen, shows rim material

which was considerably more advanced in both reduction (with only minor grey oxide phase) and in further processing (by evidence of densification and "skull feature" formation with accompanying polishing relief). The characteristics displayed in Figure {7.2.1.1}**9** were instructively typical of metallic "rim and other exposed" regions which were inexorably moving towards the end stoichiometric metallic compound. Such material was to be found in all later cases of specimens with longer processing times, albeit with more accentuated densification phenomena for the over-processed specimens in the last group.

Figures {7.2.1.1}**10**, {7.2.1.1}**11** and {7.2.1.1}**12** further review aspects of reduction stages in depleted oxide phases and their relationship to metallic conversion clusters in exposed regions of processed charge. Of considerable significance was that quench-captured reduction phenomenon shown to great effect in Figure {7.2.1.1}**13** presenting the sharply defined, clearly recognisable demarcation between heavily reduced solid solution zones of carbide metallic and nitride metallic phases in 12 minute processed specimen ANAT**12**. Whilst both phases were subsequently found to be Ti-solid solution, in this field the "carbide" (silver) metallic reduction product was formed near the charge base, as corroborated by the particle inclusions of loose bottom char, where it was accessed only by CO-plasma. The "nitride" metallic phase in right field was reduced in a "remnant air" (N_2 + Ar + CO)-plasma and, consequently, along with C-species, activated N-species became commonly involved in the microwave-driven diffusion from the reaction interface. As well as diffusion-driven N-substitution, in such ionised and associated states of activation, N* may have been directly responsible for a minor proportion of actual reduction, producing NO and NO_2 gases.

The micrographs of Figures {7.2.1.1}**14**, {7.2.1.1}**15** and {7.2.1.1}**16**, also of 12 minute processed specimens, depict well developed nitride solid solution metallic regions which represented a moderate range of post-reduction processing, however, all were classified as "rim and other exposed" material. Figure {7.2.1.1}**17** shows a complete rim of over-processed nitride coloured metallic compound phase formed when the perimeter of a limited agglomerate of reactant oxides was fixed in size by its outer shell. Converted to carbonitride, this fixed outer shell supported subsequent internal volume contraction (in common with void creation) pulling the inner oxide material onto the

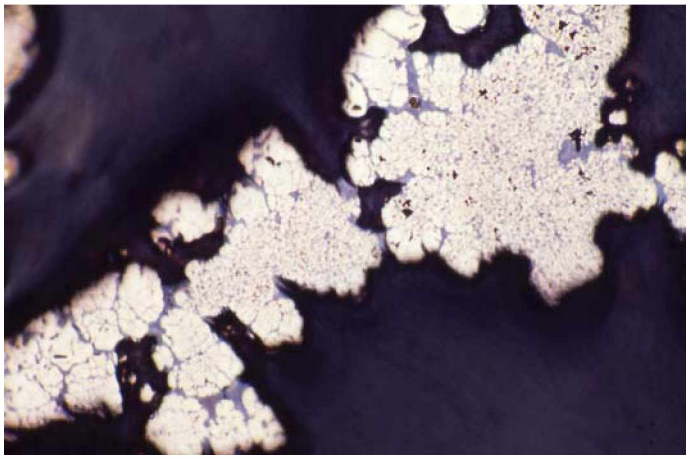

Figure {7.2.1.1} **9:** Micrograph of specimen ANAT**11** (10 min.) showing rim nitride material at a similar stage of development to that of previous Figure {7.2.1.1}**8**. The developing compact nature of such rim material can already be seen, as can the hardness of the phase which is indicated by the polishing relief evident across the plastic mounting medium after polishing on diamond media down to 1 μm. (For this and other phases throughout the specimens, micro-hardness testing was not conducted because the indentations were likely to fracture the immediate region of the agglomerate continuum and because the target fields were generally too small to support the indentation size.) [LOM, Ektachrome, fov: 0.53 mm.]

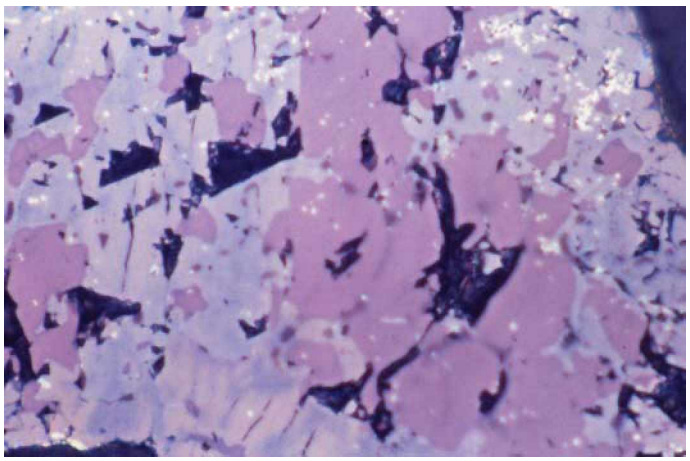

Figure {7.2.1.1} **10:** Micrograph captured through partially crossed nicols highlighting various regions of crystallographic orientation which (it is proposed) largely coincide with reduction stage phases in the oxide – diffusion modified by the presence of active C and N – as TiO_2 progresses towards Ti through the chain of principally oxide phases, some minor Ti-metal can be seen across the field of view. The field captured on specimen ANAT**06** (8 min.). [LOM, Ektachrome, fov: 0.21 mm.]

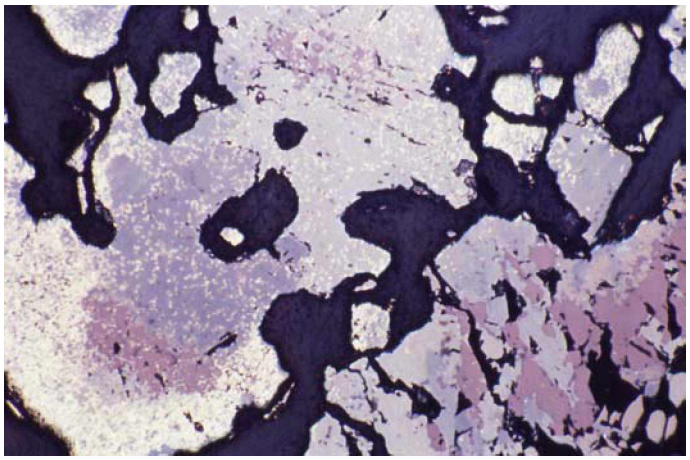

Figure {7.2.1.1} **11:** Micrograph captured on specimen ANAT**14** (12 min.) again using partially crossed nicols to highlight regions within the fused or re-solidified, partially reduced anatase material (for which further description appears with Figure {7.2.1.1}**12**). The field presented was of lesser reduced regions in a specimen of otherwise quite advanced reduction. [LOM, Ektachrome, fov: 0.53 mm.]

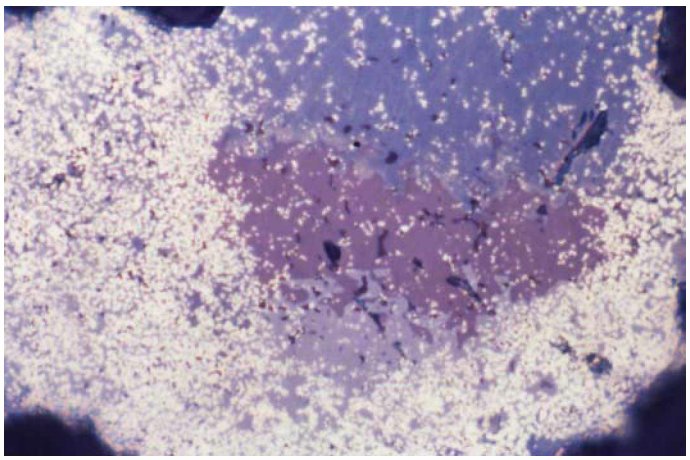

Figure {7.2.1.1} **12:** Micrograph (with partially crossed nicols) showing detail in Figure {7.2.1.1}**11** (above), specimen ANAT**14** (12 min.). The bright phase is Ti-solid solution metallic with minor C and N (and O, variably). If not wholly optical activity, it is possible that the three oxide regions in this re-solidified former-anatase material may approximate to: TiO (grey-mauve); Ti_2O_3 (mauve); and Ti_3O_5 (blue-mauve). The Ti-O binary phase diagram is quite complex and the numerous phase possibilities and many phase transitions, which cover a wide temperature range of transition and melting points, are spread over multiple crystal systems defined by an even larger number of space groups. (Originally powder) the principally-oxide phases have re-solidified from the fused, if not fully molten, reactant mass. The inclusion of minor C and N into this reducing oxide mass further complicated the phase possibilities frozen from the "melt"; any confirmation of composition by windowless light element EDS analyses was unfeasible for these oxide regions. [LOM, Ektachrome, fov: 0.21 mm.]

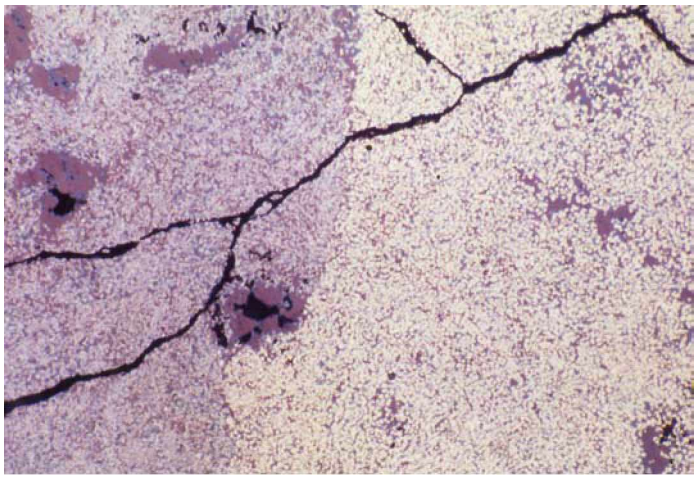

Figure {7.2.1.1} **13:** Micrograph on specimen ANAT**12** (12 min.) showing clear delineation between carbide and nitride phase fields across a continuous reduction product field. Note that the fissure, which crosses the "inter-phase" boundary, provides no evidence of process-impact by way of introducing N into the adjacent silver carbide region, so the fissure was a post-process event – possibly by thermal stresses upon quenching. [LOM, Ektachrome, fov: 0.53 mm.]

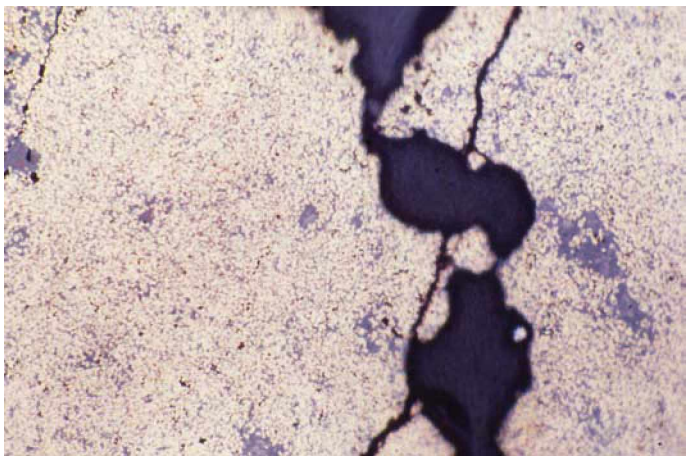

Figure {7.2.1.1} **14:** Micrograph (also on ANAT**12** (12 min.) showing an adjacent and typical field of view through the central reduction product remnants, by now processed throughout to an advanced degree of reduction. The typically "nitride bronze" coloured metallic phase was, however, still in the solid solution range of compositions, but rim type material (not shown here) was compositionally shifting inexorably towards metallic compound status for all specimens of 12 minutes and upwards. [LOM, Ektachrome, fov: 0.53 mm.]

outer shell as it, too, converted to carbonitride. Whilst this example was of a localised unit of charge reducing to a local "rim" perimeter, it was typical of rim material in the more inclusive sense of "rim and other material" which originally identified the outer rim of the charge initially against the crucible wall. Figure {7.2.1.1}**18** shows the development of the "skull" feature common at extremities of rim and other exposed regions in specimen groups of advanced process times, and representing the most compacted, over-processed material which most approached metallic compound status.

Various aspects of specimen densification are represented in the micrographs of Figures {7.2.1.1}**19**, {7.2.1.1}**20** and {7.2.1.1}**21** including growing metallisation and increased voidage in 14 minute specimens ANAT**18** and ANAT**20** plus, in ANAT**20** and in the 17 minute specimen ANAT**24**, evidence of increasing coalescence and densification internally (that is, away from extremities). Likewise, regions characteristic of greater densification and related phenomena in specimens of extended process times are presented in micrographs of Figures {7.2.1.1}**22**, {7.2.1.1}**23**, {7.2.1.1}**24** and {7.2.1.1}**25**. However, it must be emphasised that material of such over-processed regions was regarded as post-reduction phase metallic material, consequently, those scarce regions on each specimen of the most recently reduced solid solution phases were sought for windowless EDS analyses. Analyses on the belatedly reduced Ti-metal in the most processed specimens proved to contain the lowest percentages of O (oxygen) and, thus, these phases were nominally the "most reduced" Ti-metal produced by the microwave oven set-up method. (The latterly reduced Ti-metal was also least affected by dilution of the easier- and earlier-reduced gangue metal impurities, impurity components that so subjugated the newly reduced Ti-metal in earlier specimens.) The phase groupings within and between the regions of reduction product along with the compositional deviations imposed by processing time, thermochemical intensity, the contact co-incidence of reactant species and consequent reciprocal interactivity between activated species are discussed and further clarified in the following assay sections.

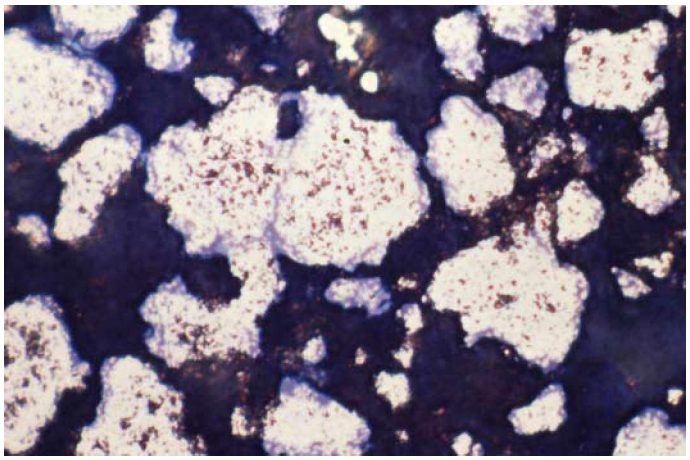

Figure {7.2.1.1} **15:** Micrograph of an array of typical loose or otherwise freed particles (and) being a mounted portion of the sampled material bound for further attrition and integral blending by mortar and pestle for XRD analysis. However, the intent of this micrograph was to present the typical range of reduction product phases in specimen ANAT**15** (12 min.) in that each particle being representative of a separate phase field, some from the central reduction product region, the remainder representing the more "exposed" rim material – the two types essentially indistinguishable here, but the larger, less friable pieces being from rim-type material. [LOM, Ektachrome, fov: 0.21 mm.]

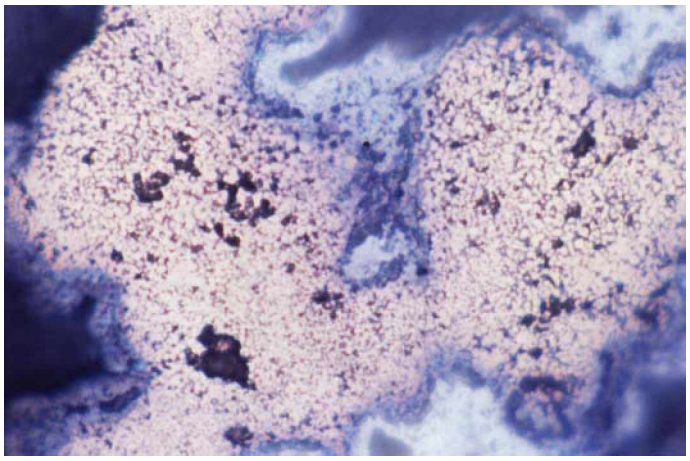

Figure {7.2.1.1} **16:** Micrograph on ANAT**16** (12 min.) showing a field quite typical across both cental and rim materials of 12 min. processed specimens for its degree of reduction and characteristic for its metallic nitride "colour" of phases which were, at this processing time, still displaying minor C- and N-content in solid solution Ti rather than the shift towards metallic compound(s). [LOM, Ektachrome, fov: 0.21 mm.]

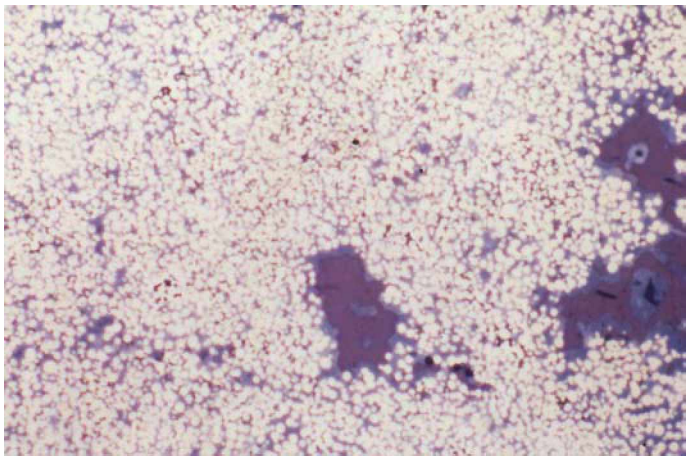

Figure {7.2.1.1} **19:** Micrograph showing the degree of reduction through a lower-central crucible region of specimen ANAT**18** (14 min.). Note that not mounting medium but C- and N-rich prior-anatase material still involved in the reduction process that, as liquid, had drained to the lower zone of reactants. Also notable is the evident reality that this field could be said to be typical of certain fields of view in any reduction product across the range, and it is evidence that real densification (by sinter or melt) does not *rapidly* progress until the last of the reactants matrix liquid has been reduced or otherwise expunged. [LOM, Ektachrome, fov: 0.21 mm.]

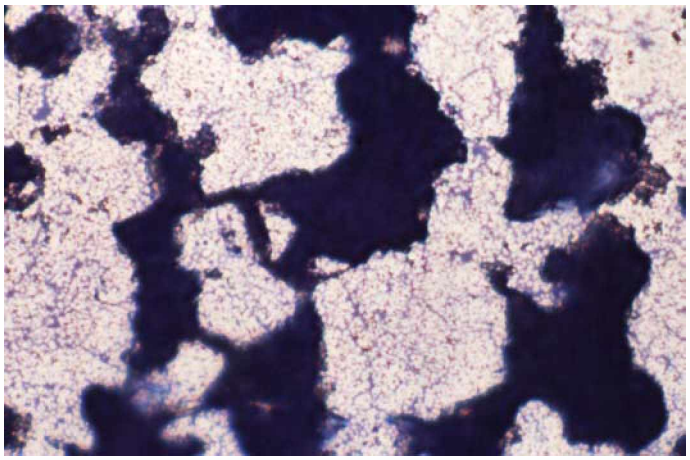

Figure {7.2.1.1} **20:** Micrograph showing the degree of voidage (from both volume contraction towards rim and liquid drainage to lower regions) in the upper-central region of an advanced processed reduction product, in this case ANAT**20** (14 min.). As distinct from that in the above Figure {7.2.1.1}**19**, (complete with some "give-away" internal reflection) mounting medium plastic fills voids which characterise an undisturbed, *in situ* field of view representative of the upper-central region of longer processed specimens. [LOM, Ektachrome, fov: 0.21 mm.]

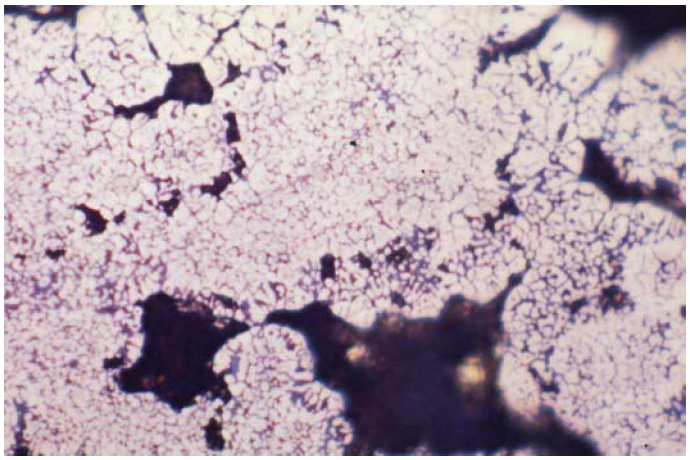

Figure {7.2.1.1} **21:** Micrograph showing the developing densification of over-processed, post-reduction Ti-phases in specimen ANAT**24** (17 min.). A grain growth phenomenon was evident in this field that was typical of other fields across this specimen – for both rim material and central material phases. Windowless EDS-detected O was negligible in metallic phases by this advanced stage of processing, but both C and N were noticeably increasing. [LOM, Ektachrome, fov: 0.21 mm.]

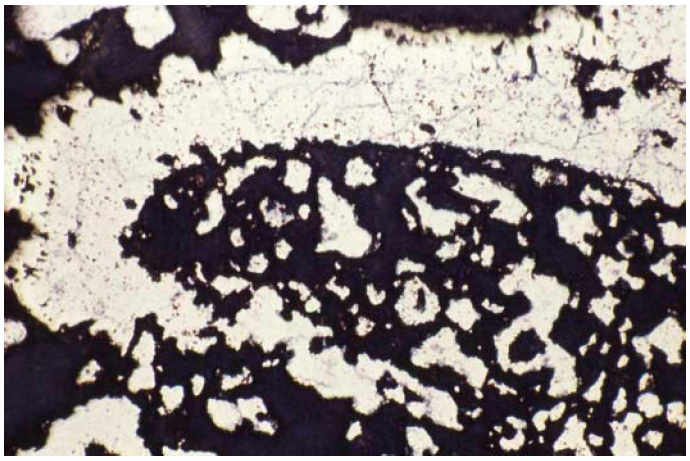

Figure {7.2.1.1} **22:** Micrograph on ANAT**26** (18 min.) showing massive rim material development with internal particles *in situ* with respect to the rim (all particles here were inter-connected). There was significant sintering of carbonitride particles forming these structures of near continuous phase aggregation. A major proportion of these features were found (by XRD analyses) to be TiC, TiN and inter-related carbonitrides, carbides and nitrides, a minor portion was more closely related (still) to the Ti-solid solution continuum. [LOM, Ektachrome, fov: 0.53 mm.]

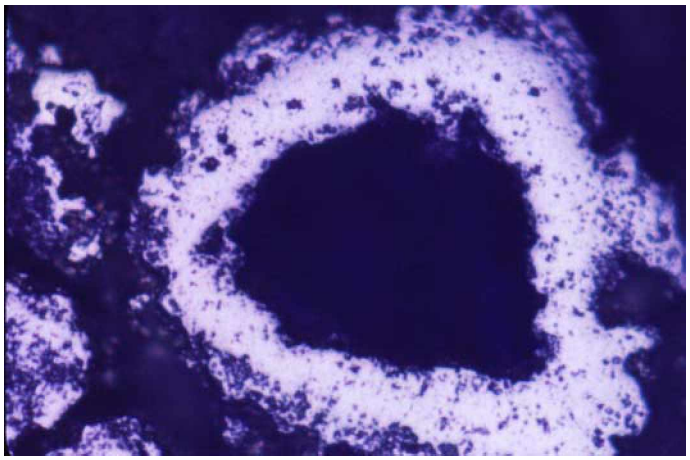

Figure {7.2.1.1} **17:** Micrograph quite instructively showing a "rim" of highly processed metallic phase rim material in the reduction product of ANAT**17** (14 min.) – such process artifacts were common, but larger rims were frequently broken during mechanical and thermal stress events. This quite small rim was formed in a local agglomerated particle of reactants where the initially reduced material remained stiff enough to draw the continuously reducing material outwards to consolidate the rim and leaving the particle's centre as void. Such phenomena could be found across the range of specimens, however, the longer the processing time, the more advanced the post-reduction metallic processing of the rim and the more likely the occurrence. [LOM oel, Ektachrome, fov: 0.21 mm.]

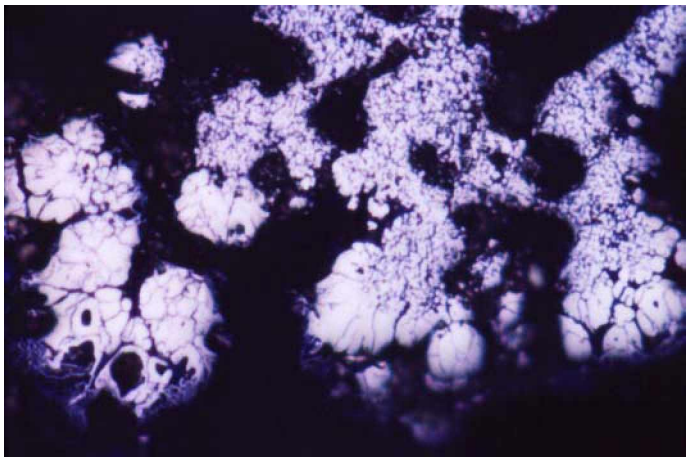

Figure {7.2.1.1} **18:** Micrograph on ANAT**23** (16 min.) of outer rim material, adjacent to crucible wall, showing over-processed nitride material featuring the characteristic "skull" formations at "process extremities" of outer rim material. Such formations, often accentuated by polishing relief, were highly sinter-compacted and characteristically fissured by accompanying volume contraction both with reduction and as the Ti-solid solution stoichiometrically progressed towards the metallic compound form. Both this skull feature and the rim feature (common in such process metallurgy and where volumetric shrinkage accompanies chemical or physical change, as in coal carbonisation) were usual features in anatase reduction and can generally be seen throughout the micrographic record (here) and in micrographs accompanying X-ray maps. [LOM eol, Ektachrome, fov: 0.21 mm.]

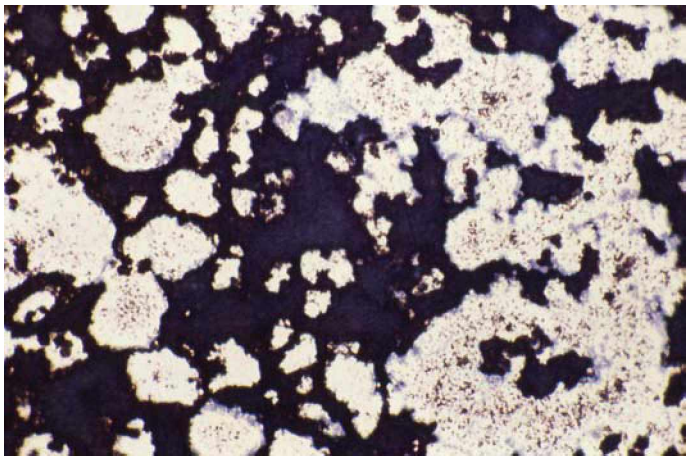

Figure {7.2.1.1} **23:** Micrograph showing developing densification in rim-type material from upper crucible region of extended-term processed specimen ANAT**22** (15 min.). Those plain nitride coloured phases in the lower and left field areas of the micrograph were closest to the crucible wall whilst, moving inwards from the wall, the metallic phase was interspersed by minor incompletely reduced oxycarbonitride matrix material (grey). [LOM, Ektachrome, fov: 0.53 mm.]

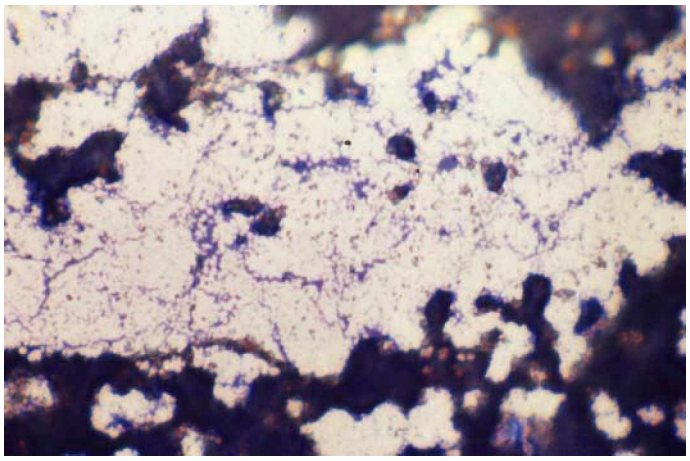

Figure {7.2.1.1} **24:** Micrograph showing massive local agglomeration and densification of metallic phases retrieved from the outer region of reduction product, adjacent to crucible wall. Some minor incompletely reduced matrix material was evident in this and adjacent fields on this specimen ANAT**25** (18 min.) although some quite minor portion of matrix inevitably remained in all highly processed (and other) specimens which might, not unreasonably, be termed "slag", although a true slag was not expected at a detectable level without contingent thermal failure of insulation or unaccounted fluxing. [LOM, Ektachrome, fov: 0.53 mm.]

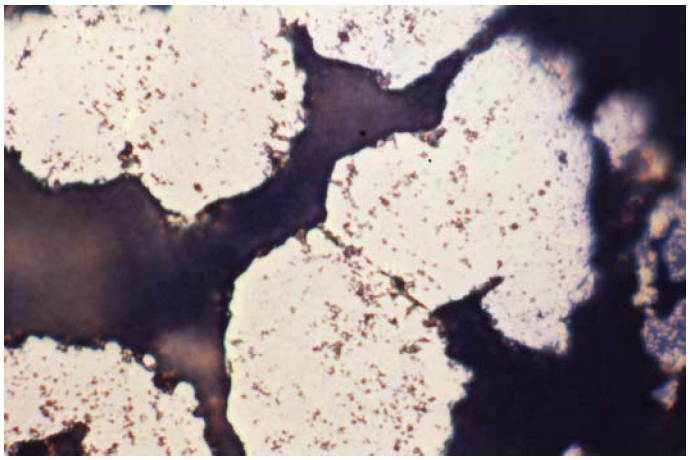

Figure {7.2.1.1} **25:** Micrograph showing densification and associated external and internal voidage for highly processed metallic phase(s) of specimen ANAT**27** (18.5 min.) which were stoichiometrically moving towards the Ti-metallic compound and away from the Ti-solid solution. [LOM, Ektachrome, fov: 0.21 mm.]

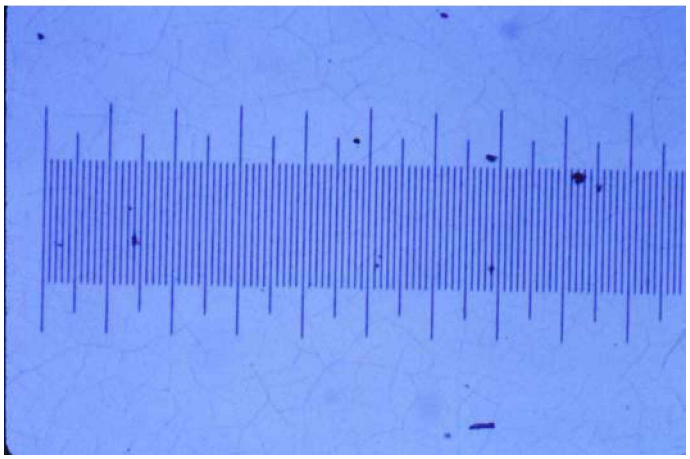

Figure {7.2.1.1} **26:** Micrograph showing most of the graticule used to affirm (by micrographic record for each magnification and for each microscope or optical system) the width of the field of view (fov); in this case for a nominal microscope eyepiece magnification of **x**100 and resulting here as field width fov: 1.05 mm, or 1050 μm. The graticule was a commercially manufactured standard mount showing a 1 mm interval precisely machine-divided into one hundred equal divisions and partitioned in groups of both 5 units and 10 units, The "blemishes" obvious in the micrograph were actually "age and usage" related markings on the mirror surface of the graticule (rather than on the film-stock). [LOM, Ektachrome, fov: 1.05 mm.]

7.2.1.2: EDS Survey of Newly Reduced Ti-Metal.

Before moving to describe EDS work and XRD work, the plain distinction must be acknowledged between the number of phases present, and how they manifest, in reduction product remnants of (*i*) laboratory mineral charges, and (*ii*) ore concentrate charges. Here, reduction product phases more specifically means "end product" or "final product" phases *at quench termination* rather than it does the more accurate "remnant balance of incompletely processed, interim and end product phases" or "reduced plus partially reduced phases" *at process interruption*. Although this distinction is simply one of process perspective reflected in terminology, it should be borne in mind when following the diagnostic deliberations of EDS and XRD presentations. Irrespective of this distinction, the number of "end product phases" present in reduction product remnants was clearly greater for the ore concentrate mineral reactants than for the essentially pure commercial or laboratory grade mineral reactants. The latter produced end-product phases with minimal elements but, nonetheless, these single metal phases exhibited convoluted arrays of metallic solid solutions and metallic compounds that, overall, were integral in a broad compositional continuum. Recurring throughout the project, this surfeit of compositional possibilities was (at least) *atypical* in comparison with the more familiar notions – the usual conventional incidence – of material analysis and classification (which might provide for a simple scatter of discrete phases). In particular, this distribution numeracy of chemically permissible final phases (as *predicted*) was physically expressed in the phase inter-relationship and complexity of reduction product morphology (as *observed*) and its corresponding analytical multiplicity – its elemental component diversity (as *assayed*).

In its simplest manifestation, the theoretical metallic reduction product for the carbothermic or metallothermic reduction of a pure metal oxide would be the single pure metal. Initially reducing to pure-Ti in the case of anatase reduction, whereafter (and more credibly), real reduction products were contained in a single-metallic continuum between the solid solution Ti-carbonitride through that metallic range (produced by "over-processing" of the alloy carbonitride) to variously approach the metallic compound possibilities $Ti(C_m,N_n)$, where $m + n = 0.5, 1, 2$, *et cetera.* Not uncommonly, these Ti-carbonitride phases retained O through the metallic range in trace proportions, O diminishing with processing time. [Other, less prevalent Ti-

oxycarbonitride phases which retained O in proportions greater than "trace" up to the point of "over-processing" tended to remain incompletely-reduced (or "under-processed") ceramic, and preferably classified as "non-metallic", or "pre-metallic".] So, inclusive of near-completely reduced phases, *metallic* Ti existed as a variable but observably single phase-identity from solid solution exhibiting a range of compositions up into the metallic compound range. Characteristically, this continuum was revealed in the metallic lustre, colour and reflectivity of the polished surface. The quench-consolidated metallic Ti-phase was physically separated (from itself) by shrinkage voids and fissures, and by a solid/solid interface from the grey "advanced" reduction remnant – an intractable "slag" remnant of un-reduced and incidental material – the negligible and only other final product (disregarding any excess reductant char). Whereas, as will be disclosed later in Section **7.4**, the minesite-derived wodginite Ta-concentrate's reduction products contained a range of metallic elements (falling into several metallic phase categories) amongst the complementary range of incompletely processed phases. Whilst, conventionally, wodginite concentrate is multiply-processed to separate target metals *before* reduction, the microwave process utilised in this programme resulted in an expanded-concept process comprised of complementary extraction process groupings in a single, intuitive reduction process-set intended to provide alternative reduction steams suitable for projection into the reality of industrial production.

As a consequence of this disparity of phase-complexities between reduction product outcomes throughout the programme of experimentation, different approaches to presentation of results are evident herein. One such distinction evident in this carbothermic section is that the presentation of experimental results of anatase reduction did not openly employ the X-ray mapping of reduction product fields because of the understandable "triviality" of such maps – maps being of an ostensibly singular phase (despite its broad light element distribution) and consequently offering little additional information to the micrographs presented. Although, comprehensive use was made of spot EDS analyses when ascertaining these single-phase fields because these yielded specific information (be it qualitative or quantitative), rather than the qualifying information of mapping exercises which were "indicative (only) of extent" of phases. Consequently, it was felt that the visual evidence of micrographical depiction with observations corroborated jointly by EDS and XRD analyses would be both analytically adequate and appropriately suited to the task of substantiating claims of real reduction

of titanium dioxide (as anatase) utilising carbothermic microwave-stimulated reduction processing. Where this procedure varied in later sections, the variations were duly noted and discussed.

Such an analytically substantive approach was applied to the range of experimental anatase reduction samples, ANAT**01** to ANAT**27**, by examining the intra-relationships within EDS results and within XRD results, and of the inter-relationship comparability between these results, and with each to micrographic characterisations. Also, where apposite (and where process-notable specifics of experimentation were recorded in supplementary documentation), results were matched with experimental observations. To this end, for all SEM studies on core specimens, all electron micrographs and X-ray maps were captured, and all EDS examinations were conducted, utilising a Leica Stereoscan 440 SEM (with integrated Oxford Link detector system) with its proprietary EDS hardware and software, and integrated with comprehensive reference standards. With specification, configuration and maintenance affording a quantitative capability, the system was well suited to adequately address the analytical requirements of this project, requirements that generally demanded only a qualitative level of adequacy to substantiate claims. [Quite obviously, for indeterminable, variable-phase specimens, whether performed at quantitative level or not, full quantitation was neither an appropriate nor achievable analytical goal. Furthermore, any tenuous claim of universal "quantitative status" would make a nonsense of analytical due diligence. These "qualitative *versus* quantitative" and "degree of quantitation" aspects of analytical competence were otherwise addressed in Section **5.3**.]

As was indicated earlier in this section, newly reduced metallic regions, particularly individual beads large enough to contain the high voltage incident beam's excitation bulb (Monte Carlo bulb), were sought and analysed by windowless EDS (unless noted otherwise). Such an exercise was conducted on specimen fields across reduction products ANAT01 to ANAT27 and the shorthand results of this quite extensive survey are presented in Table **{7.2.1.2}1**. The table represents a substantive body of evidence in this crucial experimental results section by *confirming "reduction"*. From the data of Table **{7.2.1.2}1**, the mean EDS component percentages (at%) of newly reduced metal in specimens ANAT01 to ANAT27 are shown plotted against processing time in Figure **{7.2.1.2}1**. This plot was intended simply as a graphical inventory of EDS

data (that is, as composition varied with processing time) and to illuminate any trend in the reduction status of "newly reduced" metal represented in that data. In that it is a summary of EDS results from newly reduced Ti-metal throughout the evolving process, Figure **{7.2.1.2}1** is informative, however, because it incompletely represents implications of reduction process "contiguity", Figure **{7.2.1.2}1** was not intended as *the* final format for presentation of results. Figure **{7.2.1.2}1** must be contemplated in conjunction with this commentary, and in the context of XRD results. The constituent plots which comprise Figure **{7.2.1.2}1** do, however, corroborate the consistency of both experimentation and analytical method. And further, leading into XRD studies, whilst pre-emptive of XRD databank confirmation of phases, this consistency in EDS data also conveyed a sense of "purposeful anticipation" in respect that realised phase outcomes would be forthcoming.

Most noteworthy when considering Figure **{7.2.1.2}1** is that it is *not* a graph of compositional changes in a *single unit of material* with increasing reduction and processing time. Such a presentation of changes in a single unit would see the Ti-plot approach the limit of its upper threshold before, further along the processing abscissa, subsequent regression towards (the stoichiometry of) any or several of possible Ti-carbonitride compounds represented on the percentage axis (ordinate). Similarly, the C and N plots would correspondingly approach their complementary point(s) representing the balance of Ti-compound stoichiometry(ies) from their 0at% baseline axis (abscissa). Such a plot would be representative (in part or whole) of the process path undergone by typical reduction product material – from reactant through reduced metal to over-processed compound – for each specimen of the series ANAT**01** to ANAT**27**. As it technically embodies chemical "re-oxidation", the over-processing of reduced Ti-metal into the realm of metallic compound should not (as such) be seen to represent concept failure. (As adequately discussed elsewhere) the initial *reduction to metal* for each unit of charge, and which subsequently proceeded to alloy or metallic compound, denoted "success as a reduction exercise" for this raw experimental process. The notion of "*reduction success*" was acknowledged in the compromise between systems when abandoning the practicably unattainable evacuable-reactor method for the oven set-up method – an "attainable" reduction method despite its limitations.

/Continued on page 349.

Table {7.2.1.2}1: The following table is an assemblage of provisionally quantitative elemental percentage results of the spectra of EDS acquisition counts taken on fields of newly-reduced Ti-metallic zones on carbothermically reduced anatase specimens from ANAT**01** to ANAT**27**. Spot counts were acquired from fields within single phase metallic zones whose appearance was bright silver-metallic (indicating newly reduced and not "over-processed"). Area counts were acquired at the same magnification from representative fields of nearby reduced material inclusive of the "spot-acquired" phase. Addressed elsewhere, area counts are indicative (only) of the "general bulk" and included gangue elements from grain boundary regions. The anomaly of evidently inflated values determined for the minor/ trace components is addressed in accompanying text and in the footnote* below.

Specimen.	**Field Acquisition (at%).** All EDS detection via standard Be window (BeW).					**Spot Acquisition (at%).** All windowless (NoW) detection except where denoted # which were UTW detection.				
	Ti	**Al**	**Si**	**Fe**	**bal.**	**Ti**	**O**	**C**	**N**	**balance.**
ANAT**01**	89.1	3.1	5.6	1.3	0.9 tr	90.40	7.80	0.70	0.15	0.95 (Fe,Si)#
[6 min]	91.3	1.8	5.7	0.2	0.9 tr	90.90	6.00	0.95	0.40	1.75(Fe,Si,Cr)#
	88.9	2.2	6.8	0.8	1.3 tr	89.35	6.95	1.85	0.10	1.75 (Fe,Si)#
						89.65	7.45	1.15	0.15	1.60 (Fe,Si)#
						89.55	7.50	1.05	0.25	1.65 (Fe,Si)#
					Mean:	**89.97**	**7.14**	**1.14**	**0.21**	(1.54)
ANAT**02**	88.8	3.6	3.4	1.3	2.9 tr	92.00	5.30	1.55	0.20	0.95 Si#
[8 min]	87.9	2.5	7.3	1.3	1.0 tr	91.75	5.10	1.05	0.25	1.85 (Fe,Si)#
	94.1	1.8	2.7	0.6	0.8 tr	93.50	4.35	1.15	0.15	0.85 (Si,Fe)#
						91.25	4.95	2.20	0.30	1.30(Fe,Si,Al)#
						94.10	4.30	0.95	0.15	0.50 (Si,Fe)#
					Mean:	**92.52**	**4.80**	**1.38**	**0.21**	(1.09)
ANAT**03**	89.1	1.7	7.1	0.8	1.2 tr	92.05	4.10	1.50	0.85	1.50 (Fe,Si)#
[8 min]	93.2	0.9	5.0	0.5	0.4 tr	94.80	4.15	0.70	0.20	0.15 Si#
	90.2	1.9	5.3	1.2	1.4 tr	91.75	5.20	1.25	0.20	1.60 (Fe,Si)#
						90.85	5.55	1.85	0.15	1.60 (Si,Fe)#
						90.95	5.65	2.10	0.15	1.15 (Fe,Si)#
					Mean:	**92.08**	**4.93**	**1.48**	**0.31**	(1.20)

* **NOTE:** EDS counts were acquired on a Leica Stereoscan SEM with integrated Link EDS over a number of weeks and the machine-derived component percentages were manually recorded to log. Manually recorded atomic percentage values were noted to the second decimal place, rounded to the nearest 0.05 at%. (Also as described in text) spot readings were acquired on polished surfaces of (and within the bounds of) the brightest "silver metallic" phase regions – zones deemed to be the most recently reduced metal, and not the "over processed" grey to bronze zones of metallic carbonitride phases. Area counts were acquired in the immediate vicinity of, and including, "spot acquired" phases for comparative interest. Hitherto, unavoidably, the brightest metallic phases were also the most prone to contain tramp components of incidental elements – including Si, Al and Fe, fully or partially reduced from insulation and incidental sources, and Fe as an incidental tramp impurity from mill-blending and other handling operations prior to reduction – such trace free-iron would act as a melt consolidation point for subsequent newly-reduced metals. Also, around the excitation beam, some Monte Carlo bulb interference could reasonably be expected from EDS acquisitions on such minute phase fields (resulting in extraneous counts derived from elements in adjacent phases).

Table {7.2.1.2}**1** continued/

Specimen	**Field Acquisition (at%).** All EDS detection via standard Be window (BeW).					**Spot Acquisition (at%).** All windowless NoW) detection except where denoted # which were UTW detection.				
	Ti	**Al**	**Si**	**Fe**	**bal.**	**Ti**	**O**	**C**	**N**	**balance.**
ANAT**04**	92.0	0.9	6.1	0.7	0.3 tr	91.30	5.10	1.25	0.45	1.90 (Fe,Si)#
[8 min]	89.6	1.3	6.3	1.1	1.7 tr	92.60	5.20	1.75	0.10	0.35 (Si,Fe)#
						91.75	6.15	0.90	0.15	1.05 (Fe,Si)#
						91.80	5.45	2.05	0.10	0.60 (Si,Fe)#
					[Mean:	**91.86**	**5.48**	**1.49**	**0.20**	(0.98)**]**
ANAT**05**	88.55	2.10	6.80	1.80	0.75 tr	92.10	6.00	0.90	0.20	0.80 (Si,Fe)#
[8 min]	90.80	2.00	5.75	1.15	0.30 tr	92.95	5.30	0.85	0.10	0.80 (Fe,Si)#
	91.20	0.90	5.95	1.20	0.75 tr	91.90	5.85	0.85	0.10	1.30 (Fe,Si)#
						92.15	5.90	0.95	0.15	0.85 (Fe,Si)#
						92.30	5.15	1.20	0.30	1.05 (Fe,Si)
						93.00	4.90	1.05	0.35	0.70 (Si,Fe)
	[Note here that first 4 spot acquisitions were UTW, last 2 were windowless detection but adjudged to be acceptably comparable for the purpose of this analytical assessment.]									
					Mean:	**92.40**	**5.52**	**0.97**	**0.20**	(0.92)
ANAT**06**	90.10	0.90	6.05	2.10	0.85 tr	92.15	6.05	0.75	0.10	0.95 (Fe,Si)
[8 min]	92.10	0.85	5.50	0.95	0.60 tr	93.00	4.95	0.95	0.15	0.95 (Si,Fe,Mn)
	91.45	0.85	5.80	0.60	1.30 tr	91.05	6.15	1.45	0.20	1.15 (Si,Fe)
						91.05	6.20	1.55	0.25	0.95 (Si,Fe)
						90.65	6.95	1.40	0.25	0.75 (Si,Fe)
					Mean:	**91.58**	**6.06**	**1.22**	**0.19**	(0.95)

Averaged Mean of the five 8 minute specimens ANAT**02** to ANAT**06**:

					(8 minute)Mean:	**92.09**	**5.36**	**1.31**	**0.22**	(1.02)

ANAT**07**	93.80	0.80	4.20	0.50	0.70 tr	93.75	4.30	0.85	0.25	0.85 (Si,Fe)
[10 min]	93.10	0.80	4.60	0.80	0.70 tr	93.95	4.20	0.60	0.55	0.70 (Si,Fe)
	94.00	0.75	4.10	0.75	0.40 tr	94.25	3.80	1.05	0.40	0.50 (Si,Fe)
						93.65	3.95	1.00	0.45	0.95 (Si,Fe)
						94.10	4.10	0.70	0.35	0.75 (Fe,Si)
						93.95	4.05	0.95	0.35	0.70 (Si,Fe)
					Mean:	**93.94**	**4.07**	**0.86**	**0.39**	(0.74)
ANAT**08**	93.75	0.80	4.60	0.55	0.30 tr	95.05	3.95	0.35	0.40	0.25 Si
[10 min]	92.90	0.70	4.80	1.10	0.50 tr	92.90	4.70	1.20	0.35	0.85 (Fe,Si)
	93.05	0.75	4.90	0.95	0.35 tr	93.70	4.05	0.90	0.55	0.80 (Si,Fe)
						93.25	4.05	1.10	0.50	1.10 (Fe,Si)
						93.45	4.30	0.95	0.40	0.90 (Si,Fe)
					Mean:	**93.67**	**4.21**	**0.90**	**0.44**	(0.78)

Table {7.2.1.2}**1** continued/

Specimen	**Field Acquisition (at%).** All EDS detection via standard Be window (BeW).					**Spot Acquisition (at%).** All windowless (NoW) detection except where denoted # which were UTW detection.				
	Ti	**Al**	**Si**	**Fe**	**bal.**	**Ti**	**O**	**C**	**N**	**balance.**
ANAT**09**	91.90	0.75	5.10	1.85	0.40 tr	93.70	4.05	1.10	0.80	0.35 Si
[10 min]	93.30	0.45	4.95	1.05	0.25 tr	93.85	4.60	0.55	0.45	0.55 (Si,Fe)
	92.15	0.60	5.30	0.85	1.10 tr	94.70	3.65	0.50	0.45	0.70 (Fe,Si)
						94.10	3.95	0.95	0.25	0.75 (Si,Fe)
						93.85	4.45	0.55	0.50	0.65 (Si,Fe)
					Mean:	**94.04**	**4.14**	**0.73**	**0.49**	(0.60)
ANAT**10**	88.90	0.85	6.25	2.60	1.40 tr	93.05	4.05	0.75	0.35	1.80 (Fe,Si)
[10 min]	92.15	0.65	4.95	1.40	0.85 tr	93.65	3.65	0.95	0.40	1.35 (Fe,Si)
	92.10	0.70	5.05	1.05	1.10 tr	92.90	5.05	0.80	0.40	0.85 (Si,Fe)
						94.05	4.15	0.45	0.40	0.95 (Si,Fe)
						93.10	4.55	1.15	0.45	0.75 (Si,Fe)
					Mean:	**93.35**	**4.29**	**0.82**	**0.40**	(1.14)
ANAT**11**	90.55	0.70	6.15	2.10	0.50 tr	93.65	3.90	0.85	0.65	0.95 (Si,Fe)
[10 min]	92.05	0.75	5.40	0.70	1.10 tr	95.15	4.10	0.30	0.15	0.30 Si
	92.95	0.65	4.60	1.15	0.65 tr	92.85	4.20	1.00	0.45	1.50 (Fe,Si)
						93.35	3.75	1.20	0.80	0.90 (Si,Fe)
						94.05	4.05	0.75	0.75	0.40 Si
					Mean:	**93.81**	**4.00**	**0.82**	**0.56**	(0.81)

Averaged Mean of the five 10 minute specimens ANAT**07** to ANAT**11**:

					(10 minute) Mean:	**93.76**	**4.14**	**0.83**	**0.46**	(0.81)

ANAT**12**	91.35	0.60	6.45	1.25	0.35 tr	93.85	3.40	0.70	0.90	1.15 (Fe,Si)
[12 min]	90.90	0.70	6.15	1.00	1.25 tr	94.20	3.55	0.65	0.80	0.80 (Si,Fe)
	92.25	0.55	5.85	0.75	0.60 tr	94.80	3.25	0.45	0.55	0.95 (Si,Fe)
						94.90	3.50	0.50	0.60	0.50 Si
						94.65	3.20	0.80	0.60	0.75 (Si,Fe)
						94.70	3.45	0.55	0.65	0.65 (Si,Fe)
					Mean:	**94.52**	**3.39**	**0.61**	**0.68**	(0.80)
ANAT**13**	92.05	0.75	5.80	1.05	0.35 tr	95.00	3.35	0.70	0.60	0.35 Si#
[12 min]	92.80	0.75	5.35	0.60	0.50 tr	94.15	3.50	0.65	0.75	0.95 (Fe,Si)#
	91.85	0.85	5.95	0.80	0.55 tr	94.85	2.75	0.75	0.75	0.90 (Si,Fe)#
						94.35	3.55	0.90	0.65	0.55 (Si,Fe)
						95.25	3.00	0.75	0.60	0.40 Si
						94.95	2.95	0.85	0.80	0.45 (Si,Fe)
	[Note here that first 3 spot acquisitions were UTW, last 3 were windowless detection but adjudged to be acceptably comparable for the purpose of this analytical assessment.]									
					Mean:	**94.76**	**3.18**	**0.77**	**0.69**	(0.60)

Table {7.2.1.2}**1** continued/

Specimen	**Field Acquisition (at%).** All EDS detection via standard Be window (BeW).					**Spot Acquisition (at%).** All windowless (NoW) detection except where denoted # which were UTW detection.				
	Ti	**Al**	**Si**	**Fe**	**bal.**	**Ti**	**O**	**C**	**N**	**balance.**
ANAT**14**	92.10	0.80	5.85	0.80	0.45 tr	94.70	3.25	0.80	0.70	0.55 (Si,Fe)
[12 min]	91.90	0.95	5.75	0.85	0.55 tr	95.35	2.85	0.75	0.55	0.50 Si
	91.85	0.90	5.85	0.75	0.65 tr	95.45	2.70	0.65	0.80	0.40 Si
						94.70	3.00	0.90	0.75	0.65 (Si,Fe)
						94.80	2.85	0.75	0.75	0.85 (Si,Fe)
					Mean:	**95.00**	**2.93**	**0.77**	**0.71**	(0.59)
ANAT**15**	92.25	0.80	5.80	0.70	0.45 tr	94.60	3.30	0.85	0.75	0.50 (Si,Fe)
[12 min]	91.55	0.80	6.15	0.75	0.75 tr	95.20	3.05	0.70	0.60	0.45 Si
	92.10	0,80	5.65	0.65	0.80 tr	94.90	3.30	0.70	0.70	0.40 (Si,Fe)
						94.55	3.50	0.85	0.60	0.50 (Si,Fe)
						94.95	2.60	0.95	0.85	0.70 (Si,Fe)
					Mean:	**94.84**	**3.15**	**0.81**	**0.70**	(0.51)
ANAT**16**	93.45	0.70	4.35	0.60	0.90 tr	95.80	2.40	0.75	0.80	0.25 (Si,Fe)
[12 min]	92.60	0.85	5.15	0 65	0.75 tr	94.50	3.35	0.85	0.75	0.55 (Fe,Si)
	91.85	0.80	5.65	0.80	090 tr	95.00	3.35	0.55	0.65	0.45 Si
						95.75	2.80	0.65	0.45	0.35 Si
						94.90	2.85	0.80	0.75	0.70 (Si,Fe)
						94.95	2.75	0.85	0.80	0.65 (Si,Fe)
					Mean:	**95.15**	**2.92**	**0.74**	**0.70**	(0.49)

Averaged Mean of the five 12 minute specimens ANAT**12** to ANAT**16**:

					(12 minute) Mean:	**94.85**	**3.11**	**0.74**	**0.70**	(0.60)

ANAT**17**	93.10	0.90	4.30	0.75	0.95 tr	95.15	2.30	0.90	0.85	0.80 (Fe,Si)
[14 min]	93.10	0.80	4.45	0.85	0.80 tr	95 90	2.15	0.75	0.80	0.40 (Si,Fe)
	93.25	0.75	4.70	0.70	0.60 tr	95.20	2.35	0.70	0.95	0.80 (Si,Fe)
						95.05	2.60	0.85	0.85	0.65 (Si,Fe)
						95.95	2.20	0.80	0.85	0.20 Si
					Mean:	**95.45**	**2.32**	**0.81**	**0.86**	(0.57)
ANAT**18**	94.05	0.70	4.05	0.60	0.60 tr	95.55	2.10	0.80	0.90	0.65 (Fe,Si)
[14 min]	93.25	0.80	4.65	0.65	0.65 tr	94.85	2.45	0.95	0.90	0.85 (Si,Fe) 93.75
	0.65	4.30	0.75	0.55 tr	95.80	2.10	0.70	0.80	0.60 (Si,Fe)	
						95.45	1.95	0.85	0.90	0.85 (Fe,Si)
						95.95	2.15	0.65	0.80	0.45 (Si,Fe)
					Mean:	**95.52**	**2.15**	**0.79**	**0.86**	(0.68)

Table {7.2.1.2}**1** continued/

Specimen	**Field Acquisition (at%).** All EDS detection via standard Be window (BeW).					**Spot Acquisition (at%).** All windowless (NoW) detection except where denoted # which were UTW detection.				
	Ti	**Al**	**Si**	**Fe**	**bal.**	**Ti**	**O**	**C**	**N**	**balance.**
ANAT**19**	93.30	0.70	4.45	0.95	0.60 tr	96.05	2.00	0.80	0.85	0.30 Si
[14 min]	93.35	0.60	4.55	0.90	0.60 tr	95.85	2.25	0.70	0.80	0.40 (Si,Fe)
	93.30	0.55	4.75	0.75	0.65 tr	95.15	2.45	0.75	0.90	0.75 (Fe,Si)
						95.70	2.05	0.85	1.10	0.30 Si
						95.80	1.95	0.80	0.95	0.50 (Si,Fe)
						95.85	2.20	0.80	0.75	0.40 (Si,Fe)
					Mean:	**95.73**	**2.15**	**0.78**	**0.89**	(0.44)
ANAT**20**	93.40	0.65	4.35	0.85	0.75 tr	95.80	2.00	0.90	0.90	0.40 (Si,Fe)
[14 min]	93.65	0.70	4.25	0.85	0.55 tr	95.35	2.45	0.85	0.85	0.50 (Si,Fe)
	93.60	0.70	4.45	0.75	0.50 tr	94.95	2.65	0.85	1.00	0.55 (Si,Fe)
						95.85	2.05	0.85	0.80	0.45 Si
						95.65	2.15	0.85	0.90	0.45 (Si,Fe)
					Mean:	**95.52**	**2.26**	**0.86**	**0.89**	(0.47)
ANAT**21**	93.70	0.55	4.45	0.65	0.65 tr	95.35	2.35	0.80	1.05	0.45 (Si,Fe)
[14 min]	94.10	0.50	4.10	0.65	0.65 tr	96.20	1.75	0.80	1.00	0.25 Si
	93.45	0.60	4.50	0.65	0.80 tr	95.25	2.25	0.90	0.90	0.65 (Si,Fe)
						95.65	2.15	0.80	1.00	0.40 (Si,Fe)
						95.80	2.05	0.90	1.10	0.15 Si
						95.75	2.10	0.90	0.90	0.35 (Si,Fe)
					Mean:	**95.67**	**2.11**	**0.85**	**0.99**	(0.36)

Averaged Mean of the five 14 minute specimens ANAT**17** to ANAT**21**:

					(14 minute) Mean:	**95.58**	**2.20**	**0.82**	**0.90**	(0.50)

ANAT**22**	94.05	0.55	4.50	0.55	0.35 tr	95.85	2.05	0.70	0.90	0.50 (Si,Fe)
[15 min]	93.70	0.65	4.35	0.60	0.70 tr	96.00	2.05	0.65	0.95	0.35 Si
	93.95	0.50	4.45	0.60	0.50 tr	96.25	1.90	0.80	0.85	0.20 Si
						95.90	2.20	0.70	0.90	0.30 (Si,Fe)
						96.10	2.05	0.65	0.75	0.45 (Si,Fe)
						96.45	2.20	0.55	0.70	0.10 Si
						96.30	2.20	0.60	0.70	0.20 (Si,Fe)
					Mean:	**96.12**	**2.09**	**0.66**	**0.82**	(0.30)

Table {7.2.1.2}**1** continued/

Specimen	**Field Acquisition (at%).** All EDS detection via standard Be window (BeW).					**Spot Acquisition (at%).** All windowless (NoW) detection except where denoted # which were UTW detection.				
	Ti	**Al**	**Si**	**Fe**	**bal.**	**Ti**	**O**	**C**	**N**	**balance.**
ANAT**23**	93.90	0.60	4.50	0.60	0.40 tr	96.50	1.70	0.55	0.95	0.30 (Si,Fe)
[16 min]	94.05	0.60	4.35	0.55	0.45 tr	96.40	1.75	0.65	0.90	0.30 Si
	93.45	0.65	4.70	0.65	0.55 tr	96.25	1.80	0.70	0.90	0.35 (Si,Fe)
						96.40	1.85	0.60	0.95	0.20 Si
						96.45	1.65	0.60	1.00	0.30 (Si,Fe)
						96.60	1.60	0.60	0.85	0.35 (Si,Fe)
						96.30	1.70	0.55	1.05	0.40 (Si,Fe)
					Mean:	**96.41**	**1.72**	**0.61**	**0.94**	(0.31)
ANAT**24**	94.10	0.55	4.20	0.60	0.55 tr	96.55	1.45	0.65	1.10	0.25 Si
[17 min]	94.45	0.50	4.05	0.65	0.35 tr	96.25	1.60	0.65	1.15	0.35 Si
	94.30	0.55	4.15	0.60	0.40 tr	96.30	1.70	0.70	0.85	0.45 (Si,Fe)
						96.60	1.55	0.65	1.00	0.20 Si
						96.30	1.60	0.60	1.10	0.40 (Si,Fe)
						96.35	1.75	0.65	0.95	0.30 Si
						96.60	1.60	0.70	0.95	0.15 Si
					Mean:	**96.42**	**1.61**	**0.66**	**1.01**	(0.30)
ANAT**25**	94.35	0.45	4.25	0.60	0.35 tr	97.05	1.20	0.65	0.95	0.15 Si
[18 min]	94.05	0.55	4.35	0.65	0.40 tr	96.60	1.25	0.70	1.25	0.20 Si
	94.70	0.55	3.90	0.60	0.25 tr	96.80	1.15	0.70	1.05	0.30 Si
						96.85	1.20	0.75	0.95	0.25 Si
						97.00	1.10	0.65	1.10	0.15 Si
						96 80	1.15	0.75	1.05	0.25 (Si,Fe)
					Mean:	**96.85**	**1.18**	**0.70**	**1.06**	(0.22)
ANAT**26**	93.90	0.50	4.55	0.55	0.50 tr	97.00	1.15	0.70	0.95	0.20 Si
[18 min]	94.45	0.55	4.20	0.50	0.30 tr	96.90	1.10	0.65	1.05	0.30 (Si,Fe)
	94.25	0.55	4.15	0.60	0.45 tr	96.95	1.20	0.70	1.10	0.05 Si
						96.80	1.20	0.75	1.05	0.20 Si
						96.80	1.25	0.65	1.10	0.20 Si
						96.85	1.15	0.70	1.15	0.15 Si
					Mean:	**96.88**	**1.18**	**0.69**	**1.07**	(0.18)

Averaged Mean of the two 18 minute specimens ANAT**25** and ANAT**26**:

(18 minute) Mean:	**96.87**	**1.18**	**0.70**	**1.07**	(0.18)

Table {7.2.1.2}**1** continued/

Specimen	**Field Acquisition (at%).** All EDS detection via standard Be window (BeW).					**Spot Acquisition (at%).** All windowless (NoW) detection except where denoted # which were UTW detection.				
	Ti	**Al**	**Si**	**Fe**	**bal.**	**Ti**	**O**	**C**	**N**	**balance.**
ANAT**27**	94.25	0.60	4.35	0.55	0.25 tr	96.90	1.20	0.75	1.10	0.05 Si
[18.5 min]	94.30	0.50	4.30	0.55	0.35 tr	97.00	1.15	0.70	1.10	0.05 Si
	94.10	0.65	4.40	0.50	0.35 tr	96 95	1.15	0.70	1.05	0.15 (Si,Fe)
						96.80	1.20	0.65	1.20	0.15 Si
						96.85	1.15	0.70	1.10	0.20 Si
						97.05	1.10	0.65	1.10	0.10 Si
						96 85	1.20	0.70	1.20	0.05 Si
					Mean:	**96.91**	**1.17**	**0.69**	**1.12**	(0.11)

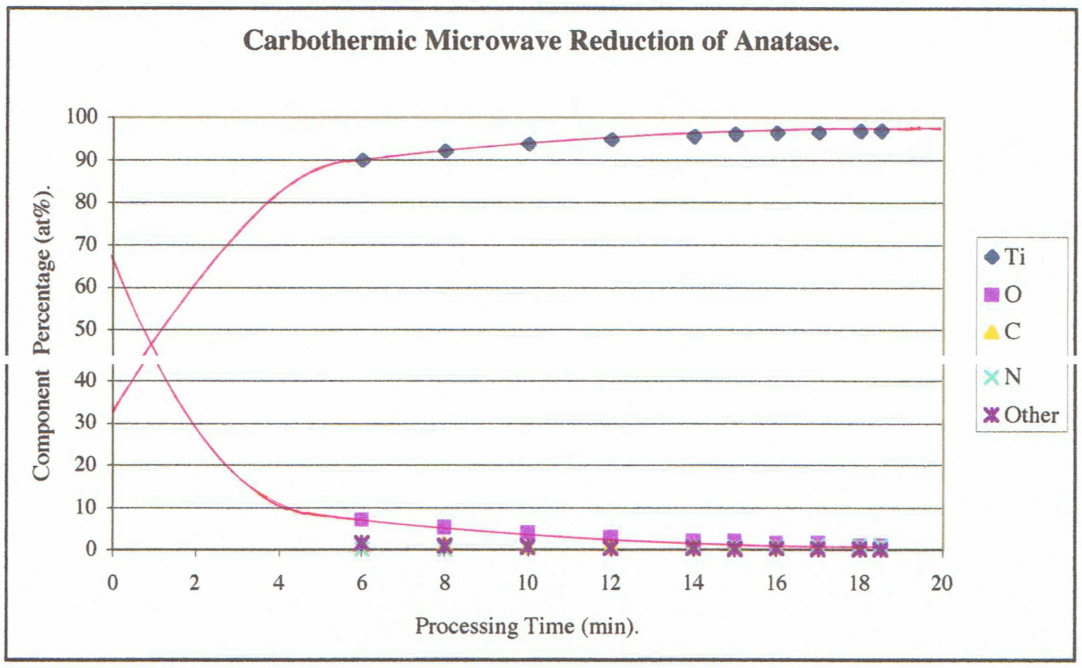

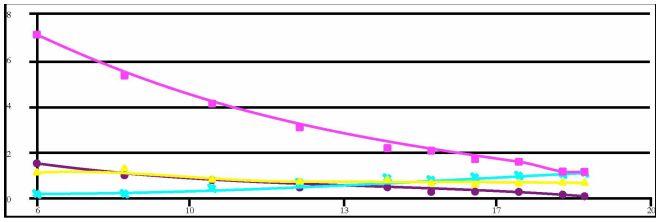

Figure {7.2.1.2}**1:** Graph of EDS analyses from Table {7.2.1.2}**1** showing component percentages in reduction product (Ti and O relevant to starting mineral, TiO_2) indicating conversion percentages of principal components in **newly** reduced Ti-metal (in the specimen) against processing time. Note that such metal, "newly reduced" at (say) 6 or 8 minutes of processing, would be "over-processed phase" metal moving towards metallic compound status as a Ti-carbonitride as processing time moved beyond (say) 10 minutes under the prevailing thermochemical conditions of the adopted microwave oven set-up method. Consequently, the variations to the minor light element (O, C and N) and gangue (other) components across the chart represent real variations in *newly reduced* Ti-metal at each quench termination point (sampling point along processing time-line). The component variations seem reasonable for such material at each point of sampling. In the case of the Ti curve, a steep increase from 33.3% Ti (at TiO_2) to ~85% Ti would occur between ~3 mins and ~5 mins (as was observed during experimentation and dependent upon system heating rate under microwave irradiation) in line with the thermodynamic requirements of reduction in each experimental case. Similarly, and inversely, the O-curve would cross the Ti-curve at TiO as the oxygen content decreases (over the same period) from the 66.7% O. From the initial TiO_2 , reduction stages pass through the transition phases of Ti_3O_5 (37.5% Ti), Ti_2O_3 (40% Ti) and TiO towards metallic Ti (which it starts to reasonably approach beyond ~5 mins processing time, as is shown in the graphical representation). Note that less-exposed oxide regions heating later (slower) will exhibit a delay in the onset of the steep section of the reduction curve.

Because *reduction to metal* (rather than *retention of metal*) was fundamental in any process deliberation, for evaluation of reduction product remnants of the microwave-stimulated reduction system and its process – and, in particular, of the microwave oven set-up – newly reduced Ti-"metal" was deemed mandatory for EDS examination for samples at each process interval. (Importantly, this "newly reduced Ti-metal" approach would permit some qualified comparison to that which could be expected of a vacuum reactor result in that reactor-reduced metal would remain in the reduced state and not "over-process" towards the metallic compound series.) Accordingly, to locate such "newly reduced" metal as processing time progressed, target reduction regions ever-deeper into those receding zones dominated in-process by N*-free CO-plasma needed to be searched to locate the requisite newly reduced bright metal fields suitable for EDS examination, such a quest was in keeping with micrographical observations (as earlier described).

Although not correspondingly represented along with "Processing Time" – and if it could be reliably gauged – some measure of ″reaction zone ′temperature′″ (the increasing thermochemical intensity in the reaction zone) could similarly be represented along the abscissa – albeit non-linearly alongside time. Within the reducing oxide charge at any commensurate point in processing time, the augmentation of local thermochemistry was accompanied by a greater degree of reduction in that unit of prior-oxide reactant. This sufficient thermodynamic stipulation largely explains the steady increase in the *degree of reduction* in the evidently "newly reduced" Ti-metallic material. Other factors which contributed to this increasing degree of reduction (in any unit of reactant with time) are (*i*) the increase with distance from possible nitrogen participation in the increasingly CO-plasma approaching the reactant charge centre (the straight CO-plasma being a more reducing medium than N_2-plasma or mixed CO/N_2 plasmas), and (*ii*) the degree of pre-reduction in the starting oxide before the onset of intensive reduction at any unit point in the charge. Ultimately, the reasons for (and consequences of) such co-incidental, peripheral phenomena were essentially immaterial to experimental outcomes, and in clear-cut terms for the experimental results as programme objectives, and for their relevance to the project overall.

Also when interpreting the plot of Figure **{7.2.1.2}1**, the necessarily interactive approach to experimentation should be acknowledged. Given the fundamentally innate

manner in which experimentation was conducted, and that the "microwave process" was never fully predictable in its affect, a methodological perspective was required which afforded legitimacy whilst being unfettered by the conformity of strict conventional experimental method. [Such conventional constraints would not openly condone the experimental undertakings (precepts) as implemented, which, on balance, *permitted* the programme of experimentation. Nor would such conventional procedure espouse the necessarily interactive nature of experimentation as adopted.] To this end, (without the benefit of any meaningful direct-measurement capability) the sensorial interposition and feedback of plasma hum*, emission intensity and colour changes were collectively interpreted to gainfully follow progress of the plasma pyro-reduction process and, indirectly, to experimentally interact or intercede as needs dictated. And, whilst only indicative initially, the state of progress as experimentation proceeded could ever more accurately be identified and documented with each quench interposition and subsequent inspection and analyses; progress by experience, experience through repeated example. A nominal sampling interval of 2 minutes was chosen as being both meaningful with respect to process-stage difference and manageable in terms of experimental ease of accomplishment – of accuracy and margin-of-error.

Having adopted the 2 minute sampling intervals, the 6 minute initial quench termination was imposed upon a "prior experience" expectation that a pervasive "majority-completion" of reduction had been attained. Beyond speculative presumption, this expectation of completed reduction was arrived-at (after said prior experimental encounter of similar charges) by observation of changes in, and the degree of, radiant intensity emanating from gaps and thin sections of crucible insulation. However, as is plainly revealed in the series of colour micrographs, and although crucially present, only a minor percentage of the starting oxide was reduced to metallic phase at 6 minutes of processing. And further, that there was a substantial divide in the degree of reduction between adjacent units of reactant oxide – this especially prominent (visually) around metallised units – so access to the means of reduction was a factor in this otherwise

* Plasma "hum" is the sonancy of the variable plasma frequency as it interacts with the applied microwave field (input energy) and under the electromagnetic load of its environment (energy output to the physical load (of the charge) via ionisation and dielectric heating). Aurally, such pulsating is akin to the sonority of the comparable *sympathetic* phenomenon of "resonance" and, albeit imprecise, for descriptive expediency the expressions "hum resonance" and "resonant hum" have (in context) been used inter-changeably with "plasma hum" as descriptors of common convenience so to accord with the "conventional understanding" in the literature, and to comply with the terminology of others.

apparently indiscriminate progress of reduction through the anatase charge. [(Not to become too mired in geometric intricacies for such a small charge) in any reduction product specimen, the evidence of "progress of reduction" revealed in the single sectioned and polished plane must always be viewed with some circumspection and "the specimen section" cautiously interpreted with reference to known or possible horizontal, vertical and radial orientations and *their* collective relationship to the reaction zone and its projections (reaction profile, break-out zones, tuyeres and imposed features, *et cetera*).]

Although it was understood that the reaction-identifying radiant intensity from the crucible compact was not a conventional means of verifying reaction-related information, no reliable conventional alternative was available. Also, correlation had been established in earlier experimentation between plasma or reaction state and the definite colour and intensity changes. These shifts in process characteristics could be followed by viewing through the oven window onto the dynamic *proscenium* of physical, chemical and plasma events as, by degrees, these events progressively transformed the insulation compact incorporating the crucible configuration. By correlating step-changes in plasma hum resonance and in plasma colour and intensity with observed physical changes such as fusing of aluminosilicate fibres from the insulation blanket material, blanket failure, *et cetera*, an overall "thermal template" was recognised. This figurative template, tantamount to "technical know-how", provided useful experimental insight *during* processing. The veracity of this "insight" could be subsequently verified by irrefutable physical evidence captured in quenched reduction remnants, evidence frozen at or near peak processing conditions for that experimental trial – and so, more broadly, corroborating pertinent system thermochemistry.

Inevitably, as can be observed in the micrographic evidence, the majority completion of metallisation for the carbothermic anatase reduction series of specimens did not occur universally through the charge specimen until quite later along the processing time-line from the predicted 6 minutes of processing. Acknowledging that visual "temperature" estimations (from those mentioned plasma shifts, radiant intensity, melting points of known materials, *et cetera*) could not be confirmed by direct, systematic "temperature" measurement, this apparent "processing under-estimation" contradiction was undoubtedly explained in part by energy disparities in processing.

This disparity factor arising from the activation energy and other energies utilised by the new Ti-metal as it "re-oxidised" into carbonitride compounds plus subsequent softening and sinter-fusing in the over-processing stages of any unit of charge, these consecutive phase-change stages in unit regions being incongruent with phases in disparate regions and, so too, the energies. However, all things considered, the collective reduction product accomplishment was self-evident across specimens representing the carbothermic microwave reduction of anatase.

Because those EDS results showing initial titania *reduction* and presented in Table **{7.2.1.2}1** represent *proof of concept*, they were accorded the relevant importance of systematic procedural treatment. Of subordinate importance, but necessary to confirm process trends, was the EDS examination of regions of reduced metallic-phase as those regions over-processed towards carbonitride metallic compounds. More truly, these "phases" were "phases under compositional transition" – that is, under continuous compositional variation. In general, such phases were not analytically determinable as exact compounds having easily recognisable stoichiometries – if indeed, in the expression of their "ultimate compound" formula, their stoichiometries were *recognised compound* stoichiometries at all. Consequently, where simpler phases were recognised, and were found in common *material reference files*, other *suspected* compounds (Ti-phases involving light elements in more complex numerical relationships) could not be found referenced in those files. This suspicion of possible unlisted compounds was based upon the observation that, across the numerous EDS output results, for some groups of EDS acquisitions there was concurrence in the "thereabout" proportion of light elements but, once generalised, such stoichiometries were not reported in reference files. Other acquisition results groups that *were* correlated with those reported in reference files (and so were assigned "recognised phase" status) also exhibited this "thereabout proportion of light elements" concurrence leading to phase/compound stoichiometries of the "recognised phases". [Later XRD studies more appositely revealed this conundrum of "suspected" complex phases/compounds being "possibly un-reported phases" in the vacuity of material reference files compiled over years from contributions reflecting the technical specialities of specific interest groups and narrowly focussed analytical laboratories under "directed research" commission.]

However problematical this recognition factor may be for phases (including the specific compounds) in that seemingly continuous range of material represented in the series of reduction products, and contained by the quarternary phase diagram Ti-O-C-N, the following Section **7.2.1.3** and Section **7.2.1.4** should establish a sufficient degree of phase classification to what, although characteristic, is otherwise a non-core aspect of the project.

7.2.1.3: The Range in Real Ti-Reduction Product Phases.

As was evident through the micrographical record, metallic densification in regions of initial reduction increased with increasing processing time; this densification manifested both as a decrease in incompletely reduced fraction of the regional field and in its increasingly uninterrupted metallic lustre. In these emergent regions, subsequent over-processing of reduced metal, including the continued reduction in such phases, was subject to a less formal set of EDS analyses. Such analyses were undertaken on metallic phases in specimen fields representing over-processed "metallic" material from inner, CO-plasma dominated regions to the most process-exposed outer rim material.

Following micrographical inspection and description, and after quite some visual evaluation of the range of phases in fields across the series of specimens, ANAT**01** to ANAT**27**, an EDS analytical option was settled-upon by which to best support the XRD studies and, separately, to materially characterise those metallic "phases beyond reduction". Intentional EDS examinations were conducted on characteristic phases present throughout the range of reduced charge material and representing the continuum from under-processed oxide-dominated ceramic, through metallic and into the over-processed metallic phases. Whilst it was held to be the case that the EDS study on "newly reduced Ti-metal" provided fundamental confirmation of *reduction*, this study of the *range of real reduction products* was mandatory in both understanding and representing the *metallic continuum* in those products of the reduction process as implemented. Also, eclipsing the vacuum reactor ideal of "reduced metal retained", and since the production of phases *beyond* plain reduction was unavoidable, examination of these products of over-processing was as inevitable as it was plainly necessary in

recording the "whole-of-process" phenomena specific to the microwave oven set-up (utilising granular char derived CO-atmosphere control). Accordingly, the routine EDS analyses were performed on a range of metallographic fields selected from depleted oxides of newly reacted material through to metallic phase(s) in those more process-advanced regions dominated by metallic phases. The selected specimen fields were purposefully discrete from those fields which provided the series of EDS results from "newly reduced Ti-metal", Also, the selected fields were complementary to, and representative of, the actual range of phases in the complex reduction products of real experimental processing. So, having postulated (in Section **7.2.1.1**) the origins of, or reasons for, the syntheses of the phases, the intention of these analyses was to show the *range* of phase compositions represented. Further, to show the distribution of phase possibilities present through the suite of reduction product specimens – that is, given prospective equivalence of process chemistry, to show the compositional variance of phases with respect to processing time and in-charge location.

As with earlier EDS work, all analyses were carried-out under windowless detector configuration (NoW) using count acquisition from a spot exposure of 100 sec live time (unless noted otherwise). During machine analytical calculations, where data acquisition or data processing foibles occurred (consequently skewing the component percentages of EDS results) and could not be acceptably bettered upon replication, acquisition data and their results were reprieved by instructing the programme to "adjust cumulatively acquired 'atomic %' to total 100 %" and recording the adjusted atomic percentages. [Noting also that identified elements needed to be "machine acknowledged" as present to be admitted into the calculation of component proportions.] Failing any preferred replication (of acquisition), and where results were adjudged permissible, such adjusted EDS results were provisionally accepted and documented; adjusted percentage cases are denoted "**å%**" in the annotation accompanying the relevant figures. Also, for each spectrum presented, because its occurrence never conflicted with authentic peaks in the low energy range, the zero loss peak (at 0 keV) was *not* routinely "stripped" from acquired spectra (for concern that more could be lost than gained by this common cosmetic manipulation of spectral data). Further, (following an amendment to machine software) it will be noted that in the suite

of spectra of Figures {7.2.1.3}**1** to {7.2.1.3}**15**, some spectra are presented with ordinate labelled "cps" (representing counts per sec) and others labelled "counts" (representing total counts beneath the curve of the spectral peaks plot) – at relevant characteristic energies, in keV. Whether labelled "cps" or "counts", the *same* quantity was measured against "time" under each acquisition regimen (that is, the same curve and contained area, irrespective of label). So, the label difference was of little consequence in all but the visual presentation of spectra and had no impact upon machine-calculated EDS compositional results. For the sake of simplifying this presentation, only the specimen spectra of Figures {7.2.1.3}**1** to {7.2.1.3}**4** are presented here, all other spectra shown in Figures {7.2.1.3}**5** to {7.2.1.3}**15** are presented in Appendix **7**, pages **C**-*iv* to **C**-*x*.

Reference is made throughout this account to the colour micrographical record presented previously as Figures {7.2.1.1}**1** to {7.2.1.1}**26** with associated supportive text. And, to reiterate, this segment contemplates the "real process" variations in reduction product phases as captured in the quench-frozen reduction remnants. Examined were real process phases either side of "newly reduced Ti-metal" whose process progression was represented in the material continuum encompassing both the devolving "oxide phases undergoing reduction" and the evolving post reduction "phases beyond reduction" including the "re-oxidation" carbide and nitride products of over-processing.

As is exhibited in the colour micrographs, close-quarter variations in adjacent phases could be quite prescient of the states of reduction existing in those adjacent material units, sometimes complementarily so (representing phase-chemistries internal to material units) and sometimes divergently so (representing the process disparities of externally imposed process variables). Demonstrative of this latter phenomenon was the clear phase-boundary distinction between dominantly Ti-carbide and dominantly Ti-nitride regions so definitively captured in the micrograph of Figure {7.2.1.1}**13**. In this micrograph the carbide region was the resultant product of reduction in CO-plasma and the nitride region a product of reduction in a predominantly N_2-plasma. The spectra essentially representative of these two phases are presented as Figure {7.2.1.3}**1** (carbide) and Figure {7.2.1.3}**2** (nitride) and, whilst these near neighbours represent the simplest phases beyond "newly reduced Ti-metal", other common complementary phases of ongoing processing were more prescient of inevitable process events. Characteristically more complex, these rather common phases where likely to be loosely categorised as

"carbonitride", or as "oxycarbonitride" in less reduction-complete regions where oxygen removal remained essentially incomplete and, in bypassing the straight metal stage, proceeded with retained oxygen towards those otherwise carbide-nitride "re-oxidation" phases common to over-processing. Before describing further the evolving syntheses of these more complex phases, Figure **{7.2.1.3}3** and Figure **{7.2.1.3}4** present spectra from Ti-metallic regions which (like Figure **{7.2.1.3}1**) had moved beyond the "newly reduced" metal into the realm of "carbide phase" whilst still retaining minor Fe from the initial metallisation phenomenon. From such examples of phases representing the *initial* stages of over-processing to spectra representing the *final* stages of over-processing. Having been openly exposed to N_2/CO plasma, the "advanced rim material" on all specimens represented material variously in final stages of over-processing and the spectra shown as Figure **{7.2.1.3}5** and Figure **{7.2.1.3}6** are of rim phases approximating the general nitride compound stoichiometry of TiN_2 [or $Ti(N(C))_2$ – where C and N are substitutionally equivalent]. [With reference to comments ending Section **7.2.1.2**, whilst the repeatedly recorded proportion could crucially have been *process*-coincidental rather than plainly *stoichiometrically*-coincident, the rim type phase with proportion $Ti_{0.33}N_{0.57}C_{0.10}$ was one "suspected compound" phase found *not* to be reported as an identified compound in materials reference files.]

Examples of the complementary type of phase differentiation occur throughout the micrographical record from earliest reduction and throughout the series as (upon quenching) the almost trivial case was exhibited in the adjacent solidification of phases of the oxide series in various stages of reduction. Whilst this was not quantitatively verified by way of EDS analysis (at best a means delivering "qualified proof" for such staged phases) the circumstantial evidence that titanium oxides representing various degrees of reduction based around the reduction series $TiO_2 \Rightarrow Ti_3O_5 \Rightarrow Ti_2O_3 \Rightarrow TiO \Rightarrow Ti$, and embracing a balance of the non-stoichiometric Ti_xO_y continuum, was quite compelling given the complementary nature of the combined evidence of EDS, XRD and microscopy. All this allowing for the usual micrographical pitfalls of internal reflection and transmission of incident light, internal reflection angles with respect to phase thicknesses, translucence and colour, entrained solids and micro-porosity, *et cetera*. [Out of interest, and in deference to machine capability, EDS analyses on enclosed oxide phases (which presumably had been merely melt-agglomerated)

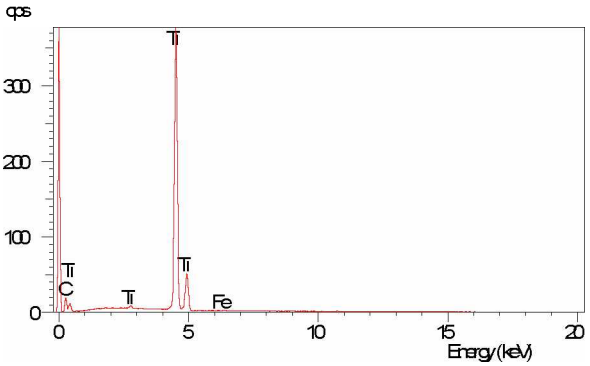

Elmt	Spect. Type	Inten. Corrn.	Std Corrn.	Element %	Sigma %	Atomic %
C K	ED	0.884	1.91	4.46	0.10	15.69
Ti K	ED	0.995	1.00	95.04	0.13	83.92
Fe K	ED	0.860	1.00	0.50	0.08	0.38
Total				100.00		100.00

Figure {7.2.1.3}**1:** EDS spectrum and analytical result of a spot acquisition from reduced material exhibiting grey "carbide-coloured" metallic lustre. The material was typical of reduced material from central in the charge where CO-plasma was dominant during processing. Such material can be seen to advantage in the colour micrograph of Figure {7.2.1.1}**13**, the "nitride or bronze coloured" material balance (right field) of that micrograph is represented in Figure {7.2.1.3}**2** below. [Both spectra are from ANAT**12** (12 min).]

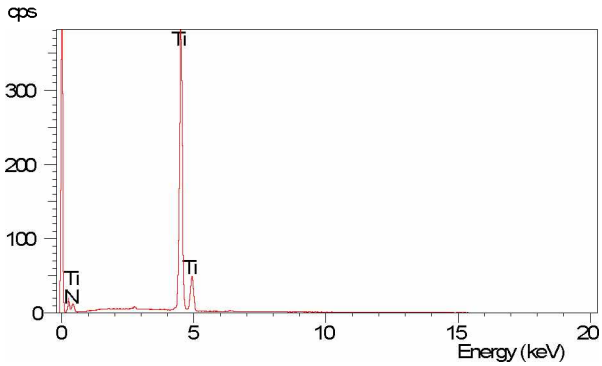

Elmt	Spect. Type	Inten. Corrn.	Std Corrn.	Element %	Sigma %	Atomic %
N K	ED	3.211	1.00	2.84	0.74	10.32
Ti K	ED	0.995	1.00	84.58	0.23	89.68
Total				87.42		100.00

Figure {7.2.1.3}**2:** EDS spectrum and result (å%) of EDS analysis of a spot acquisition from reduced material exhibiting "nitide or bronze-coloured" metallic phase as shown in the right-field of Figure {7.2.1.1}**13** and complementary to material in the above Figure {7.2.1.3}**1**.

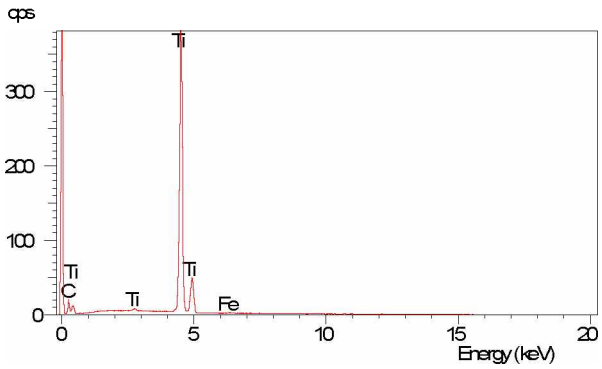

Elmt	Spect. Type	Inten. Corrn.	Std Corrn.	Element %	Sigma %	Atomic %
C K	ED	0.885	1.91	4.53	0.10	15.93
Ti K	ED	0.995	1.00	95.08	0.13	83.78
Fe K	ED	0.860	1.00	0.39	0.08	0.30
Total				100.00		100.00

Figure {7.2.1.3}**3:** EDS spectrum and result of EDS analysis of a spot acquisition from reduced material exhibiting a grey metallic lustre. This spectrum was acquired from a nearby phase in the same 12 min specimen (ANAT**12**) as that of Figure {7.2.1.3}**1**. Again, minor Fe was recorded in the specimen field.

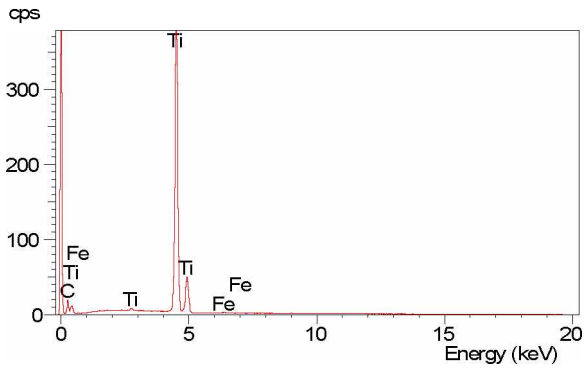

Elmt	Spect. Type	Inten. Corrn.	Std Corrn.	Element %	Sigma %	Atomic %
C K	ED	0.885	1.91	4.56	0.10	16.01
Ti K	ED	0.995	1.00	95.06	0.13	83.70
Fe K	ED	0.860	1.00	0.38	0.08	0.29
Total				100.00		100.00

Figure {7.2.1.3}**4:** EDS spectrum and result of EDS analysis of a spot acquisition from a similar mid-charge metallic phase, but from 14 min specimen ANAT**17**, again with minor Fe impurity.

recovered from under-processed regions of specimens (and similarly in pre-emptively quench-terminated cases) yielded analyses close to ~67 at% O, ~33 at% Ti for re-oxidised phases which had returned to (or otherwise had never left) the initial TiO_2 stoichiometry.]

Metallised units of material in blend regions under reduction are shown (in micrographs generally) at or near boundaries of frozen, partially reduced (translucent) prior-oxide material. This physical phase-defining phenomenon is consistent with the previously identified micro-arcing tracks describing corridors of initial reduction species and promoting adjacent reduction, thus giving definition to the early phase boundaries in shorter processed specimens (as can be seen in the micrographs of Figure {7.2.1.1}**1**, Figure {7.2.1.1}**5** and others). Circumstantial evidence indicating variations to the state of reduction in partially processed oxide phases can be seen in the micrographs of Figures {7.2.1.1}**1**, {7.2.1.1}**10,** {7.2.1.1}**11** and {7.2.1.1}**12**. Such partially processed, incompletely reduced phases yielded a range of Ti-oxycarbonitride spectra as variously represented in Figures {7.2.1.3}**7**, {7.2.1.3}**9**, {7.2.1.3}**10**, {7.2.1.3}**11**, and Figure {7.2.1.3}**12** – whose spectral analysis was pervasively typical and compositionally representative of phase fields throughout the specimen suite, characterising that range of intermediate reduction product material destined for imminent "metallic" or "post metallic" status.

In regions of relatively complete conversion of the starting oxide where metallised phases were nitride- or "bronze-coloured" Ti-carbonitride – leaning broadly toward the nitride in composition – its fractional balance of material, the remnant partially-reduced oxide phase was always a definite grey, increasingly so with decreasing volume fraction. This greying of the initially "clear-translucent", partially-processed and ever-decreasing volume fraction of reactant material was due to two phenomena; (*i*) the entrainment (entrapment) of solid (black) carbon plus possible micro-porosity during liquid-phase of processing, and (*ii*) the increasingly terminal convolution of internal reflection of incident light under LOM. Examples of this are present throughout the micrographical record, although Figure {7.2.1.1}**8** and Figure {7.2.1.1}**9** show this to good advantage, whilst analysis of a typical grey-stage phase is presented in Figure {7.2.1.3}**7**.

The final figures presenting EDS spectra show the spectrum and analysis of newly reduced Ti-metal (exhibiting minor Fe in this case) – as likely would be typical for those EDS acquisitions incorporating Table {7.2.1.2}**1** – presented in Figure {7.2.1.3}**14**, and the spectrum from a silver-grey metallic phase (adjoining this bright Ti-metal) presented in Figure {7.2.1.3}**13**. The EDS spectrum acquired from an associated, more C-saturated field (to that of Figure {7.2.1.3}**13**) is presented in full machine print-out format as Figure {7.2.1.3}**15** in Appendix 7. The spectra with analyses presented in Figures {7.2.1.3}**1** to {7.2.1.3}**15** represent common phase types typical of the process-range of reduction encountered through the specimen set ANAT**01** to ANAT**27**.

The evidence (including figures and their annotations) presented in this Section **7.2.1.3** of the "range" in real reduction product phases was *not* intended to be exhaustively comprehensive but merely *indicative* of incidental phases commonly represented in reduction product remnants. Moreover, as these "incidental" phases were representative of the stream of reduction phases around the central "newly reduced Ti-metal", the evidence was to be suggestive of the extent and continuity of phases present and the sheer scale any pretence of a "comprehensive programme" would impose upon such a task – a task (ultimately) of low end-value offering limited return in the context of this "first generation" project. And (as previously intimated), in corroboration of EDS results, a reasonable expectation was to be placed upon XRD studies in verifying the straightforward phases and identifying the remaining unresolved reduction product phases present in representative XRD powder specimens.

7.2.1.4: XRD Studies of Reduction Product Phases.

Although a more decisive method of identifying crystalline materials than EDS (given the *XRD technique* and the comprehensive reference file databases of known powder patterns), XRD studies throughout the project were particularly challenged by the range of phases in reduction product remnants. Not all remnant phases were phases in their projected final processed state; not all were product phases of reduction; not all were predicted phases given the nominal starting reactants; and some remnants were carbonaceous (char) remnants or were incidentally introduced contaminants. Although a

factor acknowledged throughout the XRD study (and especially recognised in the directed analyses (targeting) of those principal constituent phases common and increasingly prominent through the reduction series), this phase complexity conundrum was to prove a more delinquent hindrance than had been foreseen in XRD planning.

As a consequence of additional procedural and analytical rigour imposed by phase complexity, and the limited access available to the XRD facility, some XRD streams of enquiry were discontinued or were abandoned (in light of their shift from essential to sundry importance behind the sufficient analytical means of EDS-backed microscopy and mapping). Accordingly, although strands of XRD for other reduction tasks were sidelined, XRD powder patterns were used to back-up microscopy and EDS for this central, defining section of project work, the carbothermic reduction of anatase. To a lesser extent, XRD powder pattern traces were later used to analytically examine the acid-stripped remnant phases of the reduction of wodginite, that other much examined mineral at the end of this *Results* section. [Anatase being a "pure" single oxide mineral, no obvious digestion/stripping procedure was available to simplify anatase reduction product remnant phases prior to XRD powder diffraction studies. In the case of the native mineral wodginite – a complex mineral – unwanted gangue elements (Sn, Mn, Fe plus most trace impurities) could be digestion-stripped from the essential Ta/Nb/(Ti) reduction product fraction, which ultimately provided clean XRD traces in support of the central contention of "reduction".]

Nevertheless, the complexities of chemistry, phase component progressions and related transformations embodied in representative powder specimens bound for XRD exposure were taken into consideration in sampling and powder preparation. Whilst material selection was integral in sampling representative specimen material for mounting, polishing and microscopy, "sampling" for EDS analyses was effectively accomplished "down-stream" in the prudent "selection of an acquisition field or spot" on the "relatively extensive" polished specimen surface. By comparison, in the physical sampling of representative material for XRD powder specimens, care was taken to avoid granular and lump materials with foreign material intact, thus evading unwarranted proportions of such sources of contamination – "foreign material" being visibly prominent char, crucible and incidental refractory materials possessing no direct reduction "information". [Within the limits of practicable intention, some encased char

and/or refractory material plus fines from these contaminants ultimately avoided detection. On the basis of density, fine carbon could be largely eliminated from XRD powders by means of "paper to paper exchange" – to wit, denser fines appeared to remain with the powder specimen material.]

The retrieval from in-crucible reduction remnants of "representative" samples for XRD powder specimens presented problems of access and physical recovery with a view to considerations of phase-range, keeping in mind the "purpose" of analyses was to substantiate *reduction* rather than provide incontrovertible analytical accuracy or completeness – and, after all, "quantitation" was not the central tenet in XRD analyses. The existence of reduction phases and their species was to be revealed in XRD traces, so priority was given to the recovery of "metallic" phases and their immediate neighbour phases in acquiring purposeful, "representative" reduction product phase samples. And, in doing so, plasma-exposed regions of extreme hardness were included with "softer, more brittle, or friable" material from crucible inner-regions – this range of material properties needed to be accommodated in mill-preparation of powders.

Implicit in the distribution of reduction phase possibilities and the contained complexity was the relationship between the varying cell dimensions (lattice spacings) of the changing $TiO_xC_yN_z$ phase possibilities and the corresponding shift in peak positions expressed along the degrees 2θ axis of the X-ray spectrum. Whilst such shifts could be expressed either in advance or retreat along the degrees 2θ axis, the negligible and typically receding O-content of such phases dictated that the shift was generally an advance towards higher 2θ values for the case(s) of developing Ti-reduction products as TiC "nitrided" through TiC_yN_z towards TiN. This continuity relationship between cell dimension and 2θ peaks spectra for the phase possibilities and their allowable intermediates would apparently be expressed as an equivalent variability "flux" of peak-set positions in the XRD scans. However, the actual acquired XRD traces showed prominent peak intensities at TiC and TiN, rather than a generalised peak broadening between these "relatively adjacent" peak sets, a result which may reflect their "unusual" LN_2 "quench" cooling history and its attendant kinetics as, between "quench-start" and freezing, diffusion locally distributed light elements in accordance with preferred compound stoichiometry.

Any intricacy from outright convolution of peak sets which might have been expected in the output XRD traces of specimens comprised of so many phases concurrently contributing to the output spectra was not to openly eventuate in the resultant spectral scans. And, this relative absence of dominant peak sets was evident to the extent that *the few* phases were dominantly present rather than *the many* being dominant at any stage. Three main observations accompanied this revelation. Firstly, the important, basic phases Ti, TiC and TiN could, as predicted, be definitely identified, and these fluctuated with the progression of processing time. Secondly, main characteristic peaks of many of the predicted intermediate phases were unfortunately obscured within (behind) prominent peaks of the major phases, although, occasionally, a possible prominent peak from such intermediate phases was mere circumstantial evidence of its presence. Thirdly, a majority of the implied possible phases – particularly the transitory, intermediate "oxycarbonitride" phases – were not to be located in database reference files. Also, the simpler continuum of carbonitride (carbide nitride) phases was sparsely represented, and those phases that were represented could be found multiply-represented in file "nomenclature sets" of reference materials having the same stoichiometry but purportedly having different lattice dimensions and, thus, different spectra. [It is prudent here to leave aside any discussion of the implied variant possibilities of irregular powder preparation and/or machine parameters on these reference data sets as uncontested and, thus, accepted for the project.]

Unavoidably present in X-radiated powder specimens was a minor fraction of carbonaceous matter that was present as "essentially un-reacted" char plus other microwave plasma-reacted, further-carbonised and otherwise altered C-phases. These altered carbonaceous forms being partially reacted but incompletely consumed (in process reactions) or being "atmosphere control excess" char – phases caught at the point of reaction-termination by LN_2 quenching. There are *many* known C-phases in the carbonisation* product forms categorised as chars and cokes recorded in XRD databases. Nevertheless, it was expected that the exceptional and unusual

* Carbonisation is the destructive distillation of carbon-rich matter (especially plant matter and coals) in the absence of oxygen (to avoid "combustion" – a distinctly different process). In such a process the concentration of carbon solids is achieved by the chemical conversion and volatile release of non-carbon components, usually at the "cost" of some carbon in organic by-products (CH_4, tars, *et cetera*). In this microwave case, the starting reductant charcoal may be (in part) converted to pyrolytic carbon or another modified C-phase.

thermochemical conditions under which the project's experimental specimens were produced might test (extend beyond) the coverage of this database for its C-phase entries, as it did for metallic compounds. The presence of char in remnants is conceded, and whilst its presence in traces was expected, it was of no relevance in consideration of post-reduction products, so some attempt to suppress C-peak sets by removal of C-forms in XRD powders by paper-to-paper transfer was undertaken with much of the light C-fraction removed before X-irradiation. Highly altered C-forms can be notoriously difficult to match in powder diffraction file searches. [Where identified in XRD scans, and as anticipated, carbon peaks reported as "broadened" – such flattening and integral broadening of C-peaks is not uncommon in high-temperature-altered carbon forms in cokes where long coking times are reported (foundry cokes) or advanced reactivity periods were experienced (tuyere-recovered blast furnace burden cokes) resulting in texturally anomalous pyro-vitreous (amorphous) phases to be present in the otherwise crystalline coke microstructure.]

Using a commercial software programme (integral with the Philips system) to automatically analyse the computed-recorded XRD spectral output, the computer-generated solution (phase(s), file numbers, *et cetera*) to the XRD trace was verified manually by cross-checking file-provided peak positions (degrees 2θ) versus peak intensities for the auto-analyses. Additionally, some unexplained or insufficiently explained peaks were further examined by checking manually against various reference files and, usually, found to substantiate the plausibility of one or more of the panoply of intermediate phases asserted to exist in the phases record of the microwave process. Moreover, reviewing the evidence of reasonable analyses, and upon reflective overview of that evaluation with respect to elements present and available during process chemistry, it was evident that a range of intermediate phases was present in varying proportions across the suite of specimens and processing times represented.

The samples of reduction product remnants were prepared for powder diffraction analyses by minimally ring-milling the selected sample sufficiently to (*i*) break down the particle size to a uniform range, and (*ii*) to achieve a uniform size range across all specimen samples of > 95 wt%: 1.00 μm > x > 0.05 μm. In achieving this size range it

was found that a "controlled" 5 sec "burst" in the available ring mill was sufficient to reproducibly attain such size distribution. The 5 wt% falling outside this range was all fine powder, and it was largely this fraction of fines which was "lost" in three "paper-to-paper" transfer manoeuvres – much of the lost fraction being char fines, as was elsewhere noted.

X-ray diffraction patterns of the as-prepared powders were obtained using a Philips PW 1730 generator and diffractometer with Cu Kα radiation (λ = 0.15418 nm) and graphite monochromator. The generator was at operating parameters of 25 mA, 40 kV and diffractometer scans were performed at a rate of 1.0 degree/min using a step size of 0.02°. To capture adequate defining peaks – or to show their absence from the spectral trace – each trace was launched at 10° 2θ and, at 1°/min advance, took 90 min to scan to 100° 2θ, a scan arc expected to capture sufficient defining peaks (of phase possibilities) for this exercise. Acquired spectral traces were displayed in live time using Traces™ software and analyses search matches performed referencing the JCPDS powder diffraction file.

XRD powder patterns were not to be inferred as more than indicative in support of the combined micrographic plus EDS evidence of earlier sections. In that the evidence of XRD traces does support the nominal contention of "reduction achieved" for these highly stable oxide minerals, it is presented herein in as simple a form as deemed appropriate to corroborate the principal evidence of those earlier sections.

The trace record of carbothermic anatase reduction product powders indicated peak sets of a varying number of reduction product phases – with only minor indication of retained anatase-associated phases for shorter process times – and with a strong attenuation towards the duality of "principally-TiC" and "principally-TiN" phases which undoubtedly represented the progression in reduction phases towards stoichiometric compounds. Obscured behind the dominant peaks of these diffraction sets were minor peaks whose presence was suggested by the presence of other, often smaller peaks representing phases whose presence was considered possible. This conundrum was accentuated because many of the major peaks of phases "suspected to be present" were coincident with the peaks of the dominant phases assigned present (and no "peak-

stripping" or "auto-analysis" was capable of providing resolution). It was decided that in the mean traces presented in Figures {7.2.1.4}**3** to {7.2.1.4}**6**, the peak set progressions and intensities of TiC and TiN should be indicated above the traces and that additional peak presences (determined or suspected) in each mean trace should be discussed herein (only). [The TiC and TiN peak sets of Figure {7.2.1.4}**1** can be "projected" for reference comparison in Figure {7.2.1.4}**2**.]

As expected, the trace for the 6 min specimen, ANAT**01**, indicated phase complexity with some remnant anatase and/or minimally converted anatase phases adding to the peak sets that exhibited low peak heights – partly because of a problem with powder retention on the amorphous silica specimen "slip" plus from the modest counts acquired from powder of such partial conversion. The lone trace of specimen ANAT**01** is not included, however, it was quite similar to the peak set complexity evident in the trace of the mean of 8 min acquisitions for ANAT**02** – ANAT**06**, although most of the peaks originating from anatase-associated phases were absent by this 8 min stage of processing. Aside from the major TiC and lesser TiN peak sets, minor peaks were also evident in the individual traces and in the mean trace for the 8 min specimens, ANAT**02** – ANAT**06**. Identified and worthy of note were peaks for TiO, $TiO_{0.34}N_{0.74}$, Ti_2N, $TiN_{0.26}$ and metallic-Ti.

The simplest trace with the fewest peaks (and peak sets) was the mean trace for the 10 min specimens ANAT**07** – ANAT**11**. Beside the two major peak sets of TiC and TiN, minor peak sets for Ti_2N and Ti-metal were evident in all individual traces. Of all specimen sets, the minor Ti-metal peak set was most clearly defined in this series of specimen powders, although such were undoubtedly obscured by increasing phase complexity of the "over-processing" phenomenon. This "phase simplicity" at 10 min processing is equated with the peak processing time (of those times tested) in that, whilst not all reduction had taken place, the reduced metallic phases – pure Ti and close solid solution – had not significantly "over-processed" towards Ti/light element compounds of strict stoichiometry. Such stoichiometric relationships take some process time to accrete to precise proportions, there was evidence (by "possible presence" of compounds) variously through the trace output – and elsewhere, EDS evidence indicated such accretion.

As can be observed in the mean traces of specimens of processing times greater than 10 min – and especially evident in the trace comparisons presented in Figure {7.2.1.4}7 – that the onset of "over-processing" of reduced metallic phases increases with processing time. However, as was obvious in the micrographic fields of earlier Section **7.2.1.1**, this "peak" of reduction-phase simplicity should not be misinterpreted as representing the maximum of reduced phases in the reduction remnants. Once reduced to metal, such metallic phase was disposed to "re-oxidise" where thermochemistry dictated, and "re-oxidation" in the prevailing process chemistry and contacting regimen dictated that C and N each proficiently satisfied the "oxidising" role (as attentively discussed elsewhere). So, the maximum of proportion of the reactant charge reduced increased beyond this point of peak reduction, however, the already reduced phases tended towards "over-processing" for this basic system of reduction – the oven set-up method – with its fundamental system of principally effective atmospheric protection through processing and cooling. Such over-processing was a key concession to "processing integrity" that was accepted in abandoning the reactor method; *over-processing does not alter the primary fact of reduction of the refractory metal oxide*.

Whilst the base mean powder diffraction result of 10 min processed ANAT**07** to ANAT**11** exhibited a minimum of peak sets, the "over-processing" instigated peak set complexity started with the subsequent mean trace of 12 min specimens ANAT**12** to ANAT**16** and the trend continued for specimen sets of increased processing times. The determinable phases present along with the two major phases, TiC and TiN, were Ti-metal, Ti_2N $TiC_{0.3}N_{0.7}$ whilst a number of un-attributable peaks remained un-assigned. The XRD trace for the 14 min specimen set ANAT**17** to ANAT**21** was similarly dominated by the TiC and TiN peaks, however, there was an increase in background peaks as evident in Figure {7.2.1.4}7. The determinable peak sets amongst these were (in order of prominence or likelihood) $TiC_{0.3}N_{0.7}$, $TiN_{0.26}$, Ti_2N, $TiC_{0.7}N_{0.3}$ and the probable presence of Ti-metal plus one or more C-morphologies.

The final peak set – the mean of combined spectral traces of specimens ANAT**22** to ANAT**27**, representing varying processing times from 15 min to 18.5 min – was quite close to the mean trace of the 14 min specimens. Along with the dominant TiC and TiN peak sets, peaks were also identified (in order of likelihood) for Ti_2N,

$TiC_{0.3}N_{0.7}$, $TiN_{0.26}$, $TiC_{0.7}N_{0.3}$ and some C-peaks, whilst no definite peaks could be attributed to Ti-metal for this mean XRD spectral trace. The evident absence of Ti-metallic phase was not an unexpected result for specimens exposed to such over-processing times. Also, generally throughout the XRD traces record, the possibility existed for the very minor presence of phases containing the acknowledged trace elements (by process "accident") of Si, Fe or Al, or other elements such as V, Cr, Mn and Zr – incidental elements that reported at trace levels in EDS analyses. Some degree of peak broadening was exhibited in spectral traces and, after careful checking against possible peak sets of amorphous carbon forms (and found unverified), the individual cases of apparent peak broadening were attributed to cumulative effects from adjacent individual peaks of several phases.

Through a dearth of powder diffraction file information regarding Ti-oxycarbonitride phases and intermediate Ti-carbonitride phases, much was left to ponder about the presence, if not the actuality, of such phase types, and of their solid solution or compound status. Indeed, the impression formed through EDS analyses must be reviewed. The strong evidence in XRD traces of reduction product phases is that the simple TiC and TiN compounds dominate reduction phases. So the original EDS-formed interpretation of "all TiCN-phase" might be re-interpreted as "multiple TiC and TiN micro-crystalline regions in an overall TiCN-equivalent region". It is expected that peaks of the minor TiOCN phases were subsumed behind TiC and TiN peaks and therefore unresolved as a peak set. The JCPDS files were not overly helpful with such unfashionable phases.

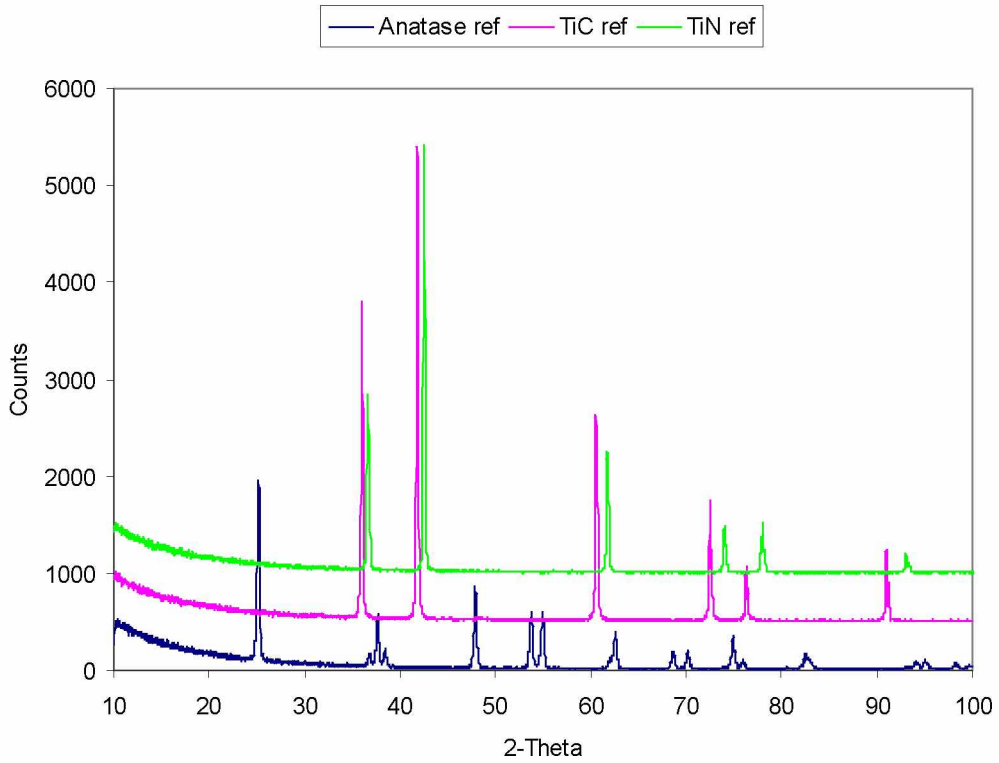

Figure {7.2.1.4}**1:** Reference traces of spectra for starting anatase (blue), pure TiC (magenta) and pure TiN (green) – all acquired on the Philips PW 1730 system under the same operational parameters employed throughout the XRD exercises. [Note the clean spectral trace and high X-ray count for these pure powders.]

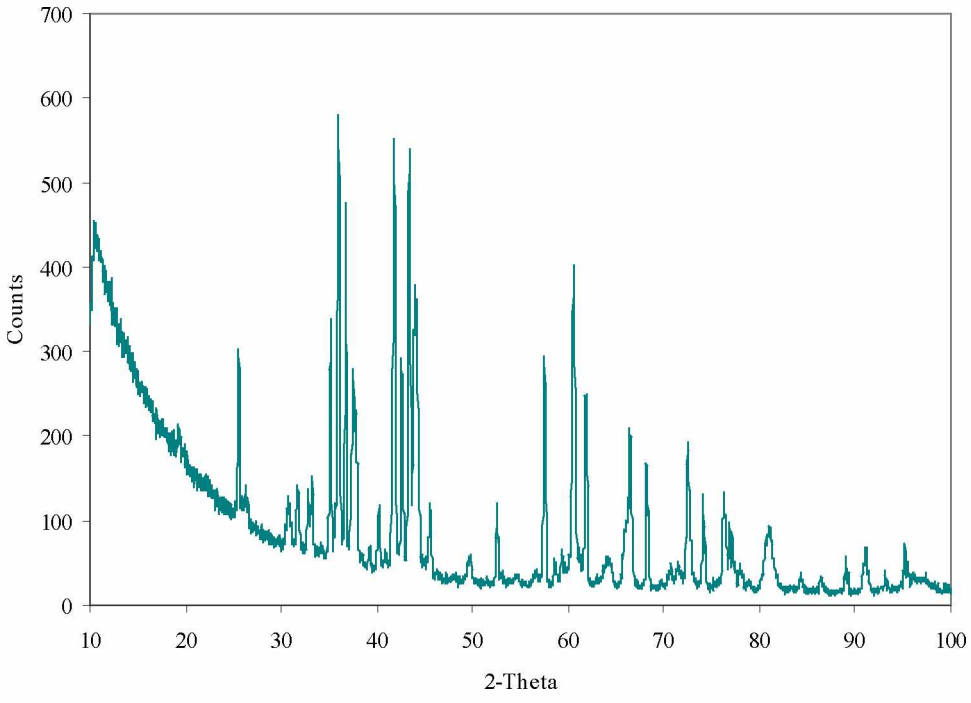

Figure {7.2.1.4}**2:** Mean XRD trace for the combined results of 8 min specimens ANAT**02** – ANAT**06**.

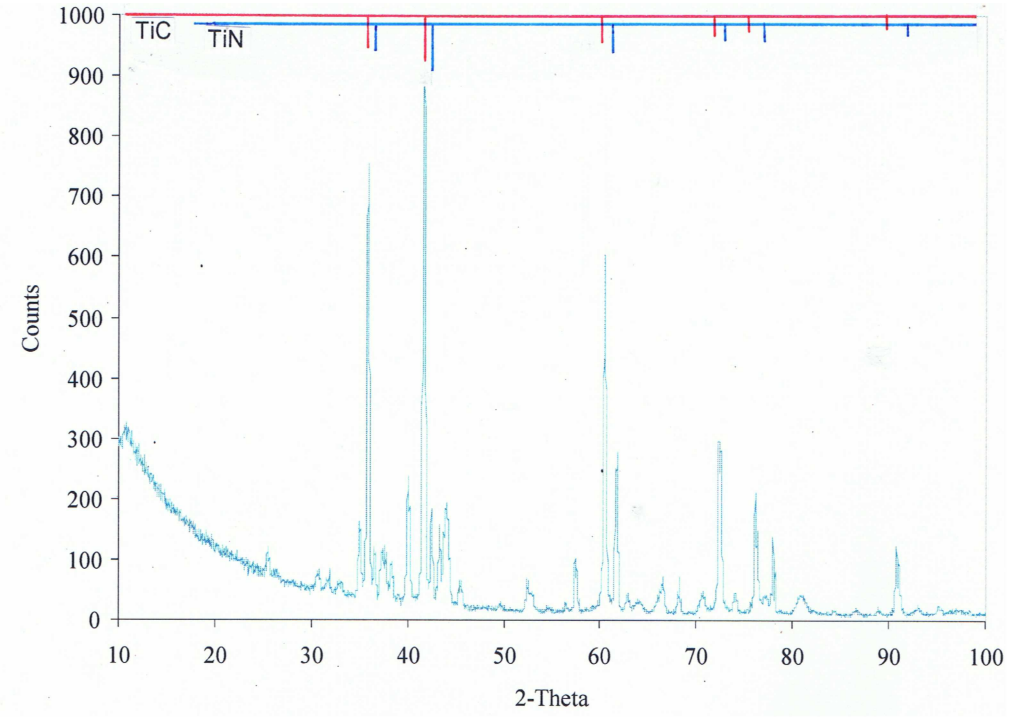

Figure {7.2.1.4}**3:** Mean XRD trace for the combined results of 10 min specimens ANAT**07** – ANAT**11**.

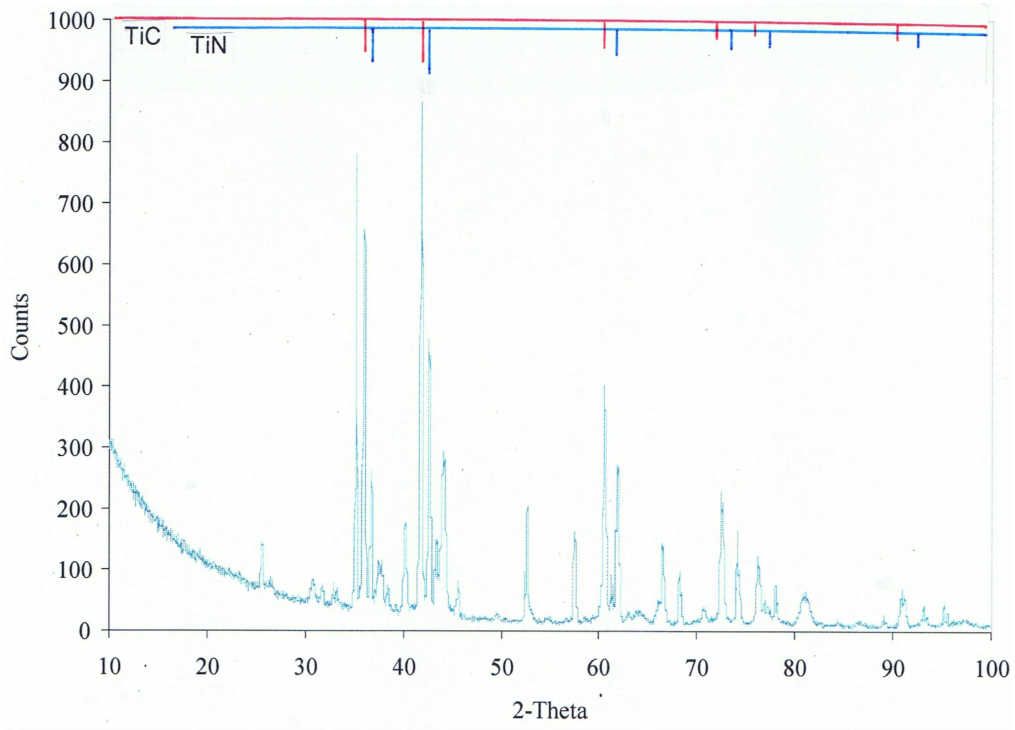

Figure {7.2.1.4}**4:** Mean XRD trace for the combined results of 12 min specimens ANAT**12** – ANAT**16**.

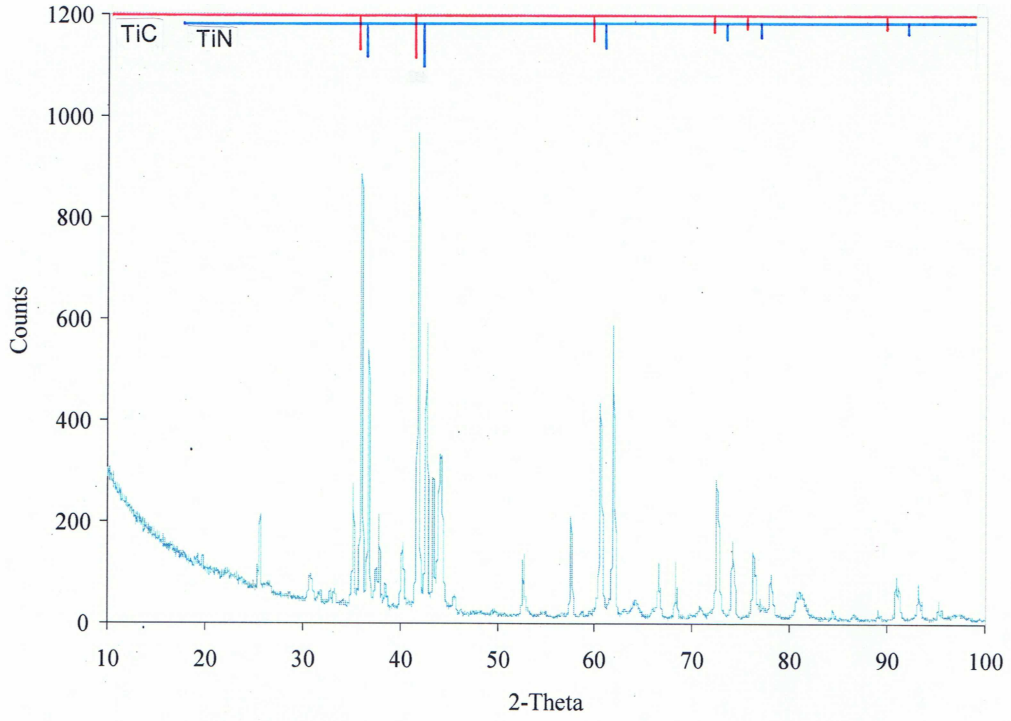

Figure {7.2.1.4}**5:** Mean XRD trace for the combined results of 14 min specimens ANAT**17** – ANAT**21**.

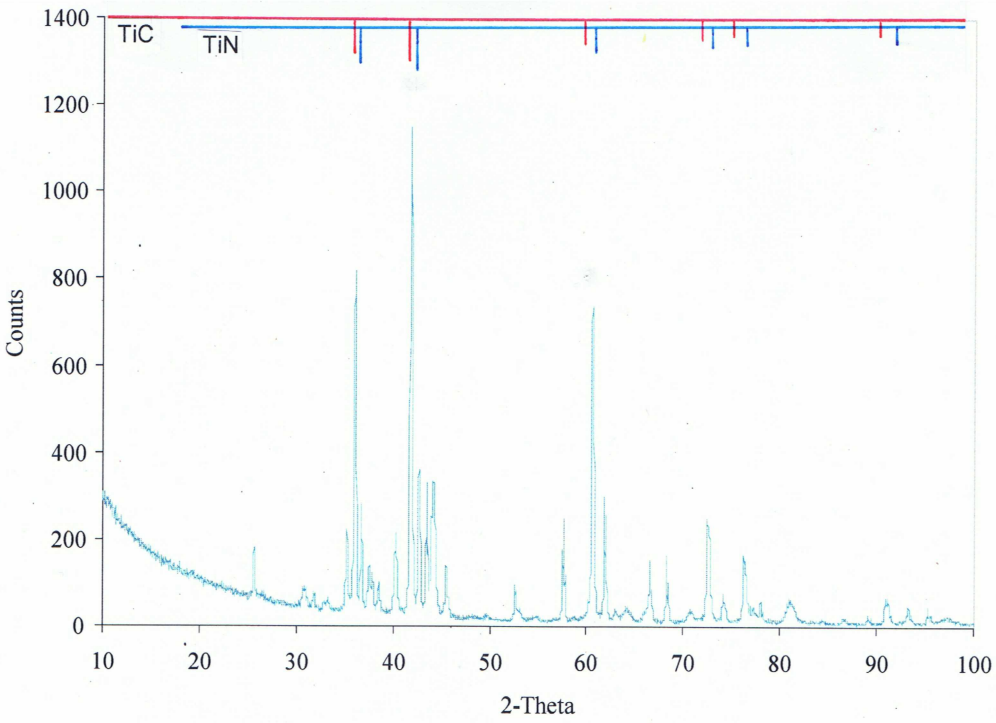

Figure {7.2.1.4}**6:** Mean XRD trace for the combined results of >14 min specimens ANAT**22** – ANAT**27**.

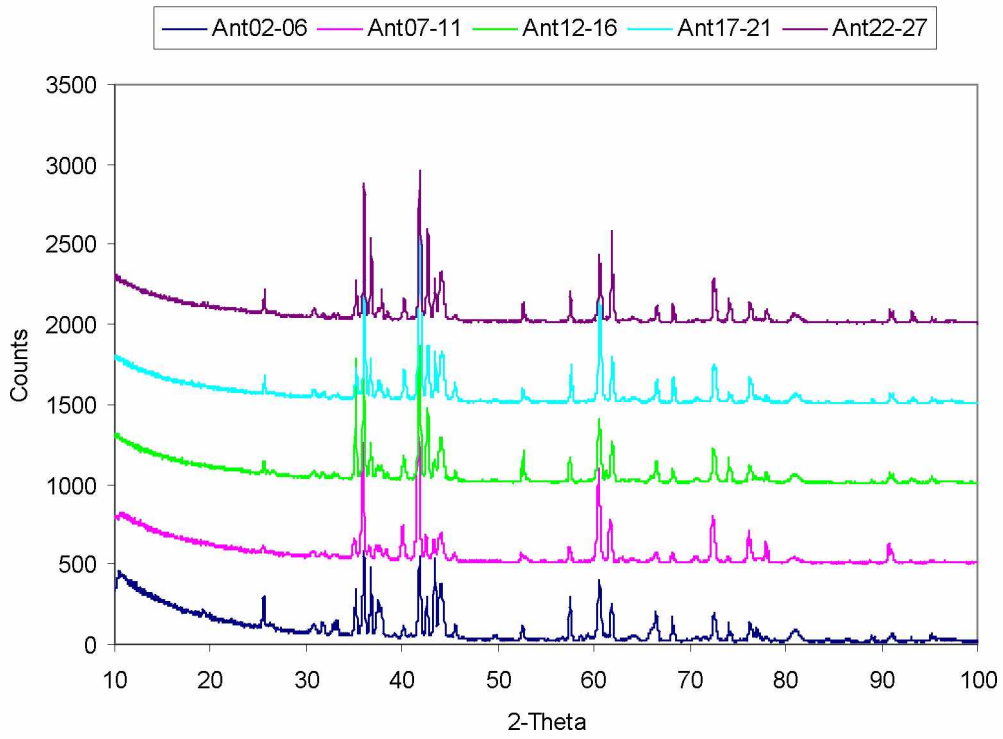

Figure {7.2.1.4}**7:** Comparison of mean XRD spectral traces of reduction product powders sampled from specimen groups varying in processing time from 8 min (bottom) up to >14 min (top) and being ANAT**02** – ANAT**06**(blue), ANAT**07** – ANAT**11** (magenta), ANAT**12** – ANAT**16** (green), ANAT**17** – ANAT**21** (aquamarine) and ANAT**22** – ANAT**27** (purple). The "drift" in species present in the specimen powders across the processing time sequence can be detected although, of course, whilst the presence of any species can be confirmed, such a drift in species present cannot be quantitatively determined by the powder method of XRD. Quantitative determination aside, this analytical method was powerful in that it confirmed the major presence of important Ti-metallic compounds and infers (by the minor presence of attributable peaks) the presence in the specimen powders of Ti-metal (if as solid solution), Ti-carbonitrides and reversion phases such as O-rich Ti-oxycarbonitrides. Considered examination of the previous traces, and as viewed in comparison here, show that the "simplest" trace is that representing the 10 min series ANAT**07** – ANAT**11** and that the series gradually become more species-complex with processing time (above 10 min). This "trace simplicity" is tantamount to "peak processing time" – beyond which, along with continued reduction in "confined" regions of charge, over-processing occurs in previously reduced metal. However, because reduction continues, the maximum of reduced phases occurs at greater process times, and whilst "over-processing" does not negate the fact of "reduction" (and indeed, substantiates reduction), the metallic retention of peak processing would be improved with increased atmospheric protection during processing and cooling.

7.2.2: Aluminothermic Reduction of TiO_2 Minerals Anatase and Rutile.

Although a more powerful reductive method than carbothermic reduction, and whilst plainly successful, the aluminothermic reduction of titania minerals presented reduction products whose description and verification could consistently be categorised as "problematical" with respect to the metallic phases represented and the facies in which those phases were contained. [This was also the case for the aluminothermic reduction of the pure single oxides of Zr and Hf, as discussed in later sections.] Further therein, over the reduction permutations possible within the ambit of this project, the Ti-mineral based aluminothermic (or metallothermic) reactions are *thermite* reactions (in that they produce spontaneous* and proportionately intense exothermic heat) and the terms are used interchangeably with respect to the sense and implication of the text in which each is contained. However, standard Ellingham diagram information suggests that Al *may* (at lower, transient operating temperatures) reduce ZrO_2 but will not reduce HfO_2, and that metallothermic reduction of these can occur under "stronger" reductant metals such as Mg and Ca. Nevertheless, (carbon-assisted) aluminothermic reduction of ZrO_2 and HfO_2 by the microwave-stimulated technique *was* realised in this experimental programme, but this marginal reduction path cannot be called *thermite*. [Also, *thermite* is equivalent to *thermit*, a spelling more associated with the commercial aluminium powder and its *Thermit process* – originally the industrial *in situ* welding process that still bears its name.]

Perhaps because of the spontaneity and vigour of true thermite reaction, and exacerbated in the loose, uncompacted reactant mixture (in the partially constrained space of the crucible) by the explosive nature of this volatile reaction, the reduction product remnants were characterised by general dispersion of reduction phases. This "general dispersion" was inclusive of the consequent dispersions of finely divided reduction product metal and reduction product alumina ("slag") plus an underlying background porosity derived from the volatility, or "explosive displacement" capacity,

---

* Reaction spontaneity is realised once an initial local reactant blend volume element (ΔV_{blend}) reaches its requisite activation energy (ΔE_A) and the exothermic energy released provides a cascade of reactions in local volume elements where $\Delta E > \Delta E_A$ and total energy ($E = \sum \Delta E$) in the reactant charge exceeds E_A required in the system for total reaction. Such a rapid cascade event (of local thermochemical conditions being "instantaneously" satisfied throughout) is tantamount to reaction spontaneity. Such phenomena are characteristic in *thermite* reactions, particularly for ilmenite, and to a lesser degree the aluminothermic reactions of single oxide Ti-minerals fall into this realm.

of the reaction. [Of course, the factual magnitude of such phenomena was commensurate with the scale of experimentation, and observations were recorded from assessments made under light optical microscopic examination – including stereoscopic techniques.]

Given this nature of reaction, the dispersion of reduced phases through reduction product remnants was to be expected, however, subsequent limited densification was evident where adequate local fluidity arose in regions of intensified heat. Unlike the un-dispersed reduction product phases of comparably passive carbothermic reaction – phases that were more often carbonitride and which eventually agglomerated – (in essence) these reaction-dispersed Al thermite-reduced phases were Ti-metal particles that locally persisted post-thermite in a softened "sub-liquid" state and that were interspersed with Al_2O_3 reduction product. These "Ti-particles" generally remained *un*-agglomerated (see following discussion also), and were quenched before either re-oxidisation "carbonitriding" or universal (pervasive) consolidation of metallic phases could markedly take effect. This proposed means of microstructural evolution also has a certain material correlation – some physical corollary – in the specimens of the single oxide aluminothermic reduction products of higher refractory metals in later sections. In searching for a sequential mechanism for this evolution, the following is proposed to explain the phase speciation in thermite reduction remnants of Ti-minerals, and the facies in which such speciation was manifest.

Although outcomes were reproducible where the thermite process proceeded as expected, some unreported aluminothermic trials (hereby acknowledged) produced only partially complete reduction outcomes – such process retardation resulted when, from region to region, local thermite ignition was erratic and chronometrically "wayward" such that broad thermochemical spontaneity was lost. The modal regularity of microwave driven heating in such cases of thermite retardation was thought to have suffered because of the realised inadequacy of sum dielectric susceptibilities in small dielectric loads (such that the reduction trial charges represented). Provision in the blend charge of a sufficient "load balance" of char – both as blend char fines and atmospheric protection char granules – was found to provide adequate sum dielectric susceptibility so to generate ignition heat, or activation energy, E_A, and initiate the thermite reaction *commonly* throughout the blend charge. Nevertheless, in successful thermite reactions,

the precise metallurgical mechanism *at* thermite reduction and immediately *post* thermite reaction remains unclear and, in that an anticipated liquid state melt-consolidation of reduced Ti-metal did not occur, is somewhat counter-intuitive in respect of the evidence contained in the reduction remnants. However, as a process model it is postulated that, at the instant of thermite reduction, the reducing titania particle was enveloped in liquid Al reductant which, at thermite conversion, was rapidly oxidised to an alumina-rich liquid (at prevailing temperatures, primarily $\mathbf{L_1}$(Al) + αAl_2O_3 – subject to gangue modification) which still enveloped the reduced phase. [Being the oxidation product of reduction, hereafter this compositionally varying liquid-come-solid phase may otherwise be referred-to as the slag phase.] At the point where this "instantaneous" reduction of the reactant titania was "complete", the titania was now converted to an enveloped Ti-entity which, (because of its evident phase separation from the Al-liquid) being either an immiscible liquid [an implausible alternative] or a solid, even if a softened solid, was isolated from like-kind Ti-entities by the still-liquid slag phase such that contacting between Ti-entities was encumbered.

This principally-alumina slag phase had sufficient fluidity to subsequently flow and coalesce, combining with other like-kind liquid slag material until burgeoning viscosity assured its rigidity and solidification. The negligible fluxing from minimal gangue components (acting as slag solidification suppressants) no longer assured slag fluidity, and with continuing oxidation in that last portion of metallic-Al in the Al/Al_2O_3 liquid slag, it quickly progressed towards a *solid* principally-Al_2O_3 slag phase. Darker "veins" of variable composition in such accumulated slag material was perceived as evidence of these "last throes of fluidity" preceding solidification in the slag phase. Possibly attributable to "discolouration" by insoluble carbon fines rather than a "genuine" second slag phase, these darker veins formed in remnant slag regions when local char-covered slag material accumulated at vanishing viscosity to become minimally blended regional slag agglomerates. Shown in the micrograph of Figure **(7.2.2}3**, these veins of lower backscatter intensity can be discerned in regions of slag phase together with the dispersion of reduced, bare Ti-phase entities which are relatively isolated in the porous structure of the reduction product remnant. Also a pertinent feature in the micrograph is the unmistakable post reduction accumulation of slag into larger, more consolidated regions by comparison with the now-isolated Ti entities, or Ti-"particles".

Prior experience of the nature, prospective "process asymmetry" and evident randomness of aluminothermic thermite reactions determined that rig configurations would be varied (from carbothermic) and that trial parameters would be less predictable than for those parallel carbothermic trials (which, of themselves, were not resolutely predictable). In particular, unlike those for carbothermic reduction trials, the setting of processing times for aluminothermic reduction experimentation trials was not a straightforward exercise. As indicated above, the "dwell period" of microwave heating time up to thermite ignition was the lengthiest period of processing, (for the purpose of this discussion) thermite reaction was "instantaneous", thence followed a provisional period of microwave heating before irradiation was terminated. This provisional post thermite period of heating was justified in that all trials could, adjudged by operator experience, be brought to a similar magnitude of crucible-top radiance before termination. It was thus anticipated (with equitable presumption of success) that a similar level of process completion might be reflected in the reduction products of the various experimental trials. It was further anticipated that such post thermite heating might produce a melt-consolidated product, however, this was not to be the case and (as mentioned elsewhere) processing beyond this third stage of irradiation was avoided to limit "over-processing" re-oxidation in the reduction product Ti-metal. Conceding the subjectivity of operator judgement, the periods of post thermite processing all fell into the range: minimum 1 min to maximum 2 min of full microwave irradiation. Such a range of times for the processing extension period was in keeping with the "known and tolerated" process foibles arising principally from dielectric heating anomalies and how such relate to charge configuration, charge constitution of char with respect to susceptible reactants, *et cetera*, and the "chance" factor of thermal runaway and its in-charge siting with respect to its thermochemical impact on the charge, on the dielectric load distribution and, ultimately, upon the merit of reduction product attributes.

The two titania minerals experimentally reduced in this aluminothermic reduction section were the laboratory grade anatase used in preceding sections and a minesite derived rutile from an east coast Australian sand-mining operation (also refer to Appendix **6.1** for general details of minerals used herein, and to Appendix **6.2** for general details of mineral blends). The refined anatase was essentially pure whilst the as-received rutile included < 1.0 wt% gangue content, principally as Fe_3O_4 and $FeCr_2O_4$

in intimate mineralogical association, plus trace miscellaneous impurity minerals remaining after the industrial sequence of mineral separation operations. As a rule, minesite derived rutile products are relatively clean (of impurities) in comparison to other minesite derived ore minerals – most conspicuously ilmenite, the titanium source mineral that is co-produced with rutile from mineral sand deposits. [Ilmenite concentrates commonly include ~ 3.0 wt% gangue content outside the base $FeTiO_3$ stoichiometry.]

Both the anatase and the rutile blend mixtures were prepared (as elsewhere described) by ring mill blending preparation – to reduce the mineral to powder (as well as the char) in the case of rutile blends – to achieve an intimate fine blend of reactant components. (The size range and distribution in blends is specified and discussed elsewhere, however, a general upper size limit of ~ 10 μm was identified as tolerable for an experimental material parameter which, it was deemed (for such powder size range and distribution), should ***not*** become an overriding consideration given the typically overwhelming intensity and exposure of each and all instances of process chemistry. The limits of blend fineness and component intimacy were ultimately determined by the necessity to avoid material modification in the milled mineral and/or unintended mechanical ignition of blend chemistry during mill attrition and blending. [This consideration always more pertinent for thermite blends.] Generally then, to negate one process variable, single milled blend "batches" for each reactant mix were prepared and subdivided by mass for use in each of the experimental trials representing relevant reduction tasks. Of the closely comparable anatase blend and rutile blend thermite reduction trials, it was noted that (on average) the rutile blend specimens required nominally longer to arrive at the point of thermite ignition and that the rutile reduction product specimens exhibited noticeably higher gangue mineral percentages. Otherwise, apart from these trends, the two titania minerals behaved comparably under microwave-stimulated thermite reduction to produce similar reduction products. It is felt that, given any reasonable "learning curve" increment to reduction processing procedure in a "next stage" of experimentation, then (with relatively minor experimental amendments, incorporating some "trial and error") thermite reduction of titania minerals would produce a melt consolidated Ti-metal reduction product of good purity.

Rather than agglomerated (consolidated) reduction product, the metallic phase particles of thermite-reduced single oxides were (as described above) always moderately scattered dispersions of fine product – this in *every* relevant experimental case – albeit with occasional species-related variation. Had the thermite-reduced remnants received the benefit of increased energy input or longer processing time so to allow general melting of Ti-metal particles, plus surfactant assistance and physical tamping, then melt-consolidation of metallic Ti-phases could have been expected. Although, with further processing exposure, the product phases of such variations might then have tended towards re-oxidation carbonitride. In support of this contention, some evidence of Ti-metallic consolidation was exhibited in specimen regions which had experienced greater energy intensity, as can be seen in micrographs of this section. (It is noted that, for those counterpart carbothermic anatase cases of the previous section, the more slowly evolving reduction centres of Ti-phases (usually TiC_xN_y), although initially *isolated*, were not physically *dispersed* by thermite volatility, and with bulk contraction throughout the remnant reduction phases, eventually coalesced into an agglomerated metallic continuum, apparently without melting.)

In general, the metallic reduction product phases of aluminothermic reduction were dispersions of minimally consolidated material, some entities showing evidence of melting or, at least, softening and sintering between neighbouring particles in contact. (Disregarding its low phase contrast) Figure **{7.2.2}1** presents the secondary electron micrograph of a thermally advanced anatase thermite reduction product field, albeit an uncommonly Ti-dense one, showing the sinter-type consolidation existing tenuously between softened metallic Ti-phase particles in a darker slag phase of "Al_2O_3 plus gangue minerals". Compared to that which might be a field more typical of aluminothermic titania reduction products, the field shown in this melt-*re*consolidated region is especially compact because, in this case, the locally gangue-fluxed-Al_2O_3 formed a molten slag that displaced the local porosity and, retaining fluid mobility, so allowed the new now-Ti particles to re-compact and come into contact (allowing minor sintering). Generally, however, the metallic dispersions were always interspersed with the thermite product Al_2O_3 which mixed post-reaction with other occasional gangue

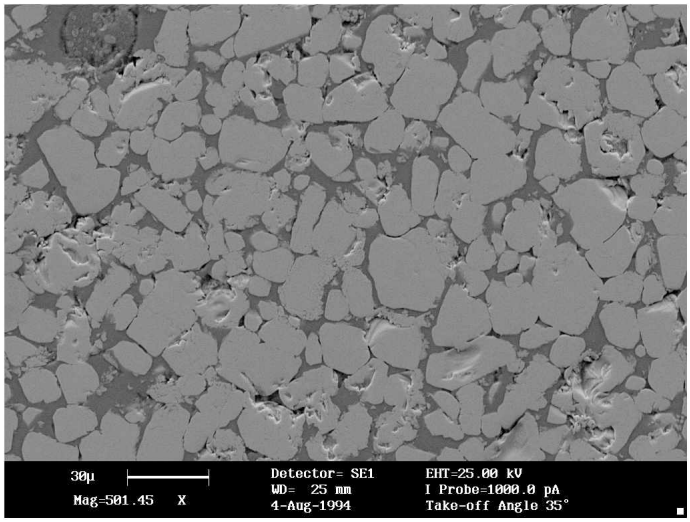

Figure {7.2.2}**1:** Secondary emission scanning electron micrograph of a locally densified region in thermite-reduced specimen ANAT**A1** showing features of the initial stages of sinter agglomeration of Ti-particles and the melt-agglomeration of slag phases. Although uncharacteristic of typical, representative fields throughout this thermite titania reduction section, the micrograph provides some insightful evidence of the potential outcome of more intensive processing. Note that the smaller (random cross-sections of) particles in the range in this field are more representative of the actual post mill-blending anatase size range and the larger particles representative of sinter-agglomerated Ti-particles, evidence of which (upon visual inspection) can be freely discerned across the field. The interstitial melt material is a principally Al_2O_3 slag, possibly locally fluxed by lower melting point gangue mineral matter, which has flowed to displace local porosity, introduce local shrinkage and thus facilitate sintering across contacting interfaces of Ti-particles. Secondary emission also highlights the "pitting" flaws in the prepared surface which were the result of both remnant porosity and where un-adhered material has been "pulled out" during polishing operations. This SE micrograph does not have the degree of phase contrast shown in the backscattered emission micrograph of Figure {7.2.2}**3** [Leica 440 SEM, SE image.]

phases – all unconsolidated components of a partially-molten, high melting point "slag" which, post reaction, had remained softened until excess $\mathbf{L_1}$(Al) liquid oxidised and solidified. After oxidation of local excess Al had forced solidification, and despite minor fluxing from gangue contamination, the newly solidified slag did not *re*-melt. That is, (in effect) liquid inter-phase mobility diminished to nil after that initial exothermal "thermite spike" from reaction had produced a short-lived melt in most phases.

The common case of reduction remnants for the microwave-stimulated aluminothermic reduction of both anatase and rutile powders is represented by a reduction product remnant mass exhibiting the abovementioned dispersion of fine Ti-particles plus Al_2O_3 (as reduction products) with minor gangue and fine remnant char in a permeable agglomerate. The infrequent occurrence of un-reacted reductant as "pockets" of Al-metal (quenched *in situ*) could be found sparsely interspersed through reduction product remnants – often around reaction zone extremities. Such metallic Al in melt-consolidated pockets was invariably of "pure" reductant Al – unadulterated by Ti or other alloying metals – or by carbon as inclusion, solid solution or compound. The reduction product Ti-particles exhibited certain definite evidence of having been at least "soft" at the quench point when submitted to process termination, and that some evidence of coalescence existed between neighbouring Ti-particles where material contact existed in the general dispersion.

As it did in other comparable straight oxide-mineral cases, and learned in preliminary trials, an anomaly occurred in reduction expectations for aluminothermic reduction of titania minerals. This anomaly was that, somewhat counter-intuitively, better metallic-Ti yields occurred in reduction product remnants of those formal trials conducted utilising Al-lean reductant powder mixes (despite the planned thermite reaction proceeding as envisaged and with less free Al metal in the reduction remnants). When reductant Al-powder was used at proportions above the stoichiometric 1:1 (with or without accompanying char excess), some of the Al reported in reduction remnants as free metal (rather than oxidised), along with reduction product phases. Of itself, this capture of Al-metal was not a problem outside the minimally increased complexity of remnant facies. In fact, considering the extreme affinity at high temperatures of liquid Al for oxygen (as gaseous O_2 or by reduction of most oxides), it may be perceived to

corroborate of the effectiveness of the combined CO-atmospheric protection/LN_2 quench method. When Al in proportions less than but approaching 1:1 stoichiometric of Al reductant in reactant mix, almost nil metallic Al reported in the reduction product remnants. It is presumed that exothermal energy (released upon oxidation) from the Al portion of reductant powder provided spontaneous activation energy for parallel carbothermic reduction of portion of the TiO_2 component of the charge. Remnant titania was not detected in reduction remnants. Whilst this explanation seems reasonable to explain the reduction outcome for the "Al-lean reactant mix", no straightforward explanation is proposed (as none is obvious) for those exploratory cases where, disregarding the char supplement and assuming Al in liquid state* to overcome the "contacting" requirement of chemical reaction, the Al proportion in the reactant mix equalled or exceeded the stoichiometric requirement of the TiO_2 reduction. Note that these comments addressed a process observation that is of interest to extensions into further experimentation, and affirming that the 1:1 stoichiometric blend option was used in experimental trials. [That 1:1 stoichiometric blend was given in Appendix **6.2** as: $TiO_2 + 4/3Al + 1/2C$.]

In further reference to the micrographic evidence presented, a general impression can be formed of reduction product remnant facies from the typical field presented as Figure **{7.2.2}2** of reduction product ANAT**A3**. The light optical colour micrograph highlights the dispersion of metallic reduction product phases (Ti and TiC_xN_y, $1 >> (x + y)$) in a representative region otherwise populated by partially reduced, still largely oxidic titania (as "non-metallic" $TiO_xC_yN_z$, $x > (y + z)$) and reduction product alumina slag (grey) plus the distribution of porosity. This general observation can be seen in more detail in the backscattered electron optical micrograph presented in Figure **{7.2.2}3** which highlights the largely thermite-derived porosity, the relationship of metallic Ti-phase particles within this porosity, and the drained slag phase which has retreated to accumulation sites prior to solidification.

* At the microscopic scale, whilst surface oxidation of Al powder particles undoubtedly took place during the initial stages of microwave heating, the subsequent development of the enveloping CO-atmosphere, with potential reduction of that newly formed oxide film, and the early melting within the film of each Al particle, the liquid Al would break the oxide film and form a liquid "pool" prior to the thermite reaction. Prior to formal reduction experimentation, general microwave-induced melting (in the presence of susceptible char) of Al-powder to Al-liquid was tested in preliminary system trials and confirmed to be an easily reproducible phenomenon.

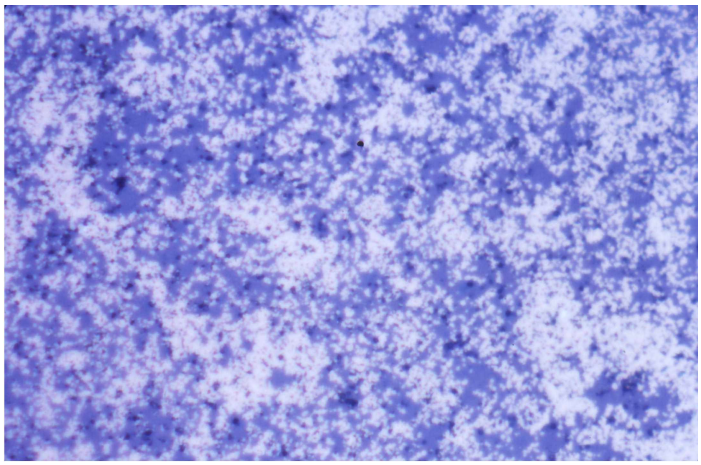

Figure {7.2.2}**2:** Light optical micrograph showing a well Ti-metallised region on the polished surface of specimen ANAT**A3** with consolidated areas of accretion and particle growth by sintering (not dissimilar to that of Figure {7.2.2}**1**) accreting from a background field of generally dispersed Ti-particles (as was more typical elsewhere on this specimen). Such regions of "greater dispersion" were typical of, and common across both the thermite reduced anatase *and* rutile specimens of this section. (Note also that polished Al_2O_3 surfaces could be quite reflective under standard micrographic illumination and in dense, agglomerated areas this tended to skew visual interpretation for LOM at this and lower magnifications.) [LOM, Ektachrome, fov: 0.21 mm.]

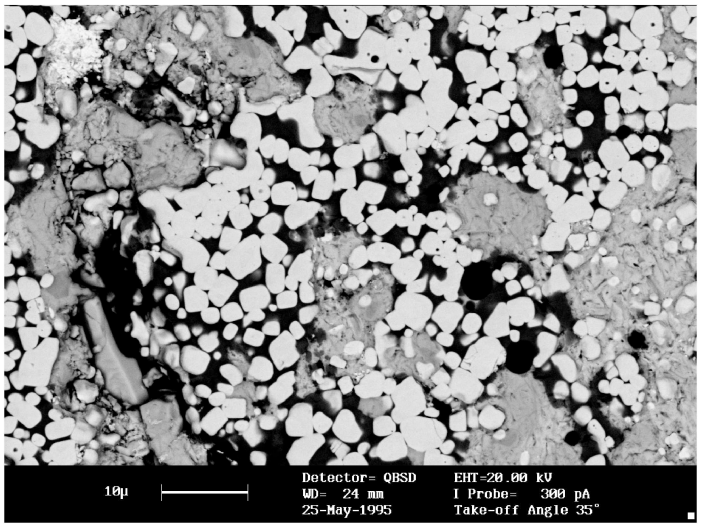

Figure {7.2.2}**3:** Backscattered scanning electron micrograph of a more typical thermite reduction product region (in specimen ANAT**A4**) showing initial particle accretion with signs of impending sinter-growth of agglomerated particles in an otherwise dispersed region of reduction product Ti-particles (bright phase) interspersed by mounting-medium-filled porosity (darkest areas) and reduction product Al_2O_3 with minor char/gangue "veins" (mid-range grey phases) which together have tended to agglomerate with like kind slag phases – some vein discolouration may be due to fine carbon (char) uptake on surfaces of small slag volumes which remain into agglomeration. [Leica 440 SEM, BS image.]

The backscattered micrograph assists in understanding the light optical images in that (with its better resolution at higher magnification) the phase contrast of the reduction product phases shows the particulate Ti-metal as the brightest phase, the seeming dual-phase slag being light grey for the principally-Al_2O_3 slag with darker "veins" likely being a char plus gangue contaminated Al_2O_3 slag phase, the plastic-filled porosity being darkest (but revealing out-of-focus sub-surface particles). A notable feature of the immediately-post thermite reduced particles – formerly TiO_2 and now Ti-metal – is that of their shape. Such a particulate shape is not the morphology expected of a liquid reduction-product, so it is assumed that the thermite-reduced Ti-metal was evolved as a soft solid product, one slightly above the solidification point of the still-oxidising, evolving and "impure" Al_2O_3 slag. Each rounded-angular "particle" must have, at reduction, initially been balanced by its associated volume element of the reduction product Al_2O_3 "slag" and this slag must, in the thermite exothermic spike, have been liquid – especially given any remnant liquid Al and the fluxing influence of the minor gangue proportion. Consequently, whilst still liquid, the slag was capable of flowing, or draining to local "points of accrual" where, due to continuing oxidation of the remaining Al in the ($\mathbf{L_1}$ + αAl_2O_3) melt, the rapidly increasing viscosity in this accumulated slag assured its *in situ* solidification at these accrual sites. [Whilst throughout the reporting of the *Results* section, mechanisms are proposed which might sensibly explain phenomenological aspects of procedural experimentation, microwave reduction processes, and the derivation and materialisation of reduction product forms, it should be reminded that the gist of project experimentation was simply to show *reduction* in stable refractory metal oxide minerals by a microwave-stimulated reduction process.]

Within the qualifying aspects as discussed in the preceding pages, the quality and consistency of the EDS acquisition results presented in Table **{7.2.2}1** support the contention that pure titania can be microwave reduced by the aluminothermic route. In the instance of this programme of experimentation, a general difference was noted in the reducibility between the anatase and rutile. This evident disparity in reducibility was attributed to the processed "commercial purity" aspect of the anatase contrasted with the

"as received" native mineral origin of the rutile plus the fact that the rutile may not have been attrited (during mill-blending) such as to afford so fine a particle size distribution

Table {7.2.2}1: The following table is an assemblage of provisionally quantitative results of EDS analyses of acquisition counts taken on polished fields on newly-reduced Ti-metal phases of aluminothermically reduced anatase specimens ANAT**A1** to ANAT**A5** and rutile specimens RUTL**A1** and RUTL**A2**. Spot counts were acquired from points clearly within titanium particles where best clearance from adjoining phases could be secured. Likewise, field counts were acquired from very small representative fields on reduction product Al_2O_3 "slag phase" material inclusive of a check on the trace to minor char and gangue element components of the slag compositions. The nature of the target Ti-particles and slag phases from which spot counts were acquired can be seen in the accompanying figures, especially Figure {7.2.2}**3**.

Specimen.	**Field Acquisition, slag (at%).** All windowless (NoW) EDS detection.					**Spot Acquisition, particles (at%).** All windowless (NoW) EDS detection.				
	Al	**O**	**C**	**Si**	**balance**	**Ti**	**O**	**C**	**Al**	**balance.**
ANAT**A1**	38.2	60.1	0.3	1.0	0.4 (Fe,Cr)	97.10	0.01	0.03	1.34	1.52 (V,Fe,Cr)
	40.2	58.2	0.3	0.8	0.5 (Fe,Ti,Cr)	98.45	0.05	0.04	1.25	0.21 (Cr,Fe)
	33.7	62.7	0.8	1.3	1.5 (Fe,Mg)	93.61	3.44	0.04	2.02	0.89 (Mg,Fe)
	38.7	58.8	0.1	1.9	0.5 (K,Fe,P)	96.53	0.35	0.08	1.44	1.60 (Cr,Fe)
	39.1	58.1	0.5	0.9	1.4 (Fe,Ti,Cr)	98.80	0.04	0.05	0.69	0.42 (Cr,N,Fe)
Slag mean:	**38.0**	**59.6**	**0.4**	**1.2**	(0.8)	98.32	0.05	0.07	0.98	0.58 (Fe,Cr)
						97.86	0.02	0.04	1.22	0.86 (N,Cr)
					Particle mean:	**97.24**	**0.57**	**0.05**	**1.28**	(0.86)
ANAT**A2**	41.3	57.8	0.2	0.5	0.2 (Fe,Mg)	98.76	0.01	0.02	0.81	0.40 (Fe)
	40.3	57.7	0.8	1.0	0.2 (Ti,Cr,Fe)	96.92	0.10	0.03	2.34	0.61 (N,Fe,V)
	41.1	57.4	0.1	0.8	0.6 (Fe,K,Cr)	98.08	0.02	0.04	0.96	0.90 (Cr,Fe,N)
	38.3	59.5	0.4	1.1	0.7 (Fe,Cr)	98.11	0.02	0.02	0.99	0.86 (N,V,Fe)
	39.6	59.0	0.1	0.9	0.4 (Ti,Fe,K)	97.86	0.01	0.02	1.20	0.91 (Fe,N,Cr)
	39.5	58.3	0.3	1.2	0.7 (Cr,Fe,Ti)	97.45	0.06	0.02	1.43	1.04 (Cr,Fe,N)
Slag mean:	**40.0**	**58.3**	**0.3**	**0.9**	(0.5)	98.78	0.01	0.03	0.88	0.30 (V,Fe)
						98.42	0.02	0.04	0.93	0.59 (Fe,Cr,N)
					Particle mean:	**98.05**	**0.03**	**0.03**	**1.19**	(0.70)
ANAT**A3**	38.0	58.3	0.4	2.5	0.8 (Fe,Ti,Cr)	97.20	0.82	0.03	1.14	0.81 (V,Cr)
	38.4	58.5	0.3	2.2	0.6 (Fe,Mg)	97.84	0.67	0.03	1.03	0.43 (Fe,Cr,V)
	38.7	57.9	0.3	2.0	1.1 (Fe,K,Cr)	98.01	0.65	0.02	0.85	0.47 (Cr,Fe)
	38.9	58.3	0.4	1.9	0.5 (Ti,Fe,K)	97.91	0.97	0.01	0.81	0.30 (Cr,N)
	38.2	58.1	0.5	2.0	1.2 (Fe,Cr,K)	98.11	0.65	0.02	0.85	0.37 (N,Fe,V)
Slag mean:	**38.4**	**58.2**	**0.4**	**2.1**	(0.9)	97.97	1.02	0.02	0.65	0.34 (N,Fe)
						98.41	0.86	0.01	0.52	0.20 (Fe,Cr,N)
					Particle mean:	**97.92**	**0.81**	**0.02**	**0.84**	(0.41)
ANAT**A4**	38.4	59.1	0.3	1.3	0.9 (K,Fe,P)	98.41	0.12	0.02	0.80	0.65 (Fe,N)
	38.1	59.8	0.2	1.2	0.7 (Fe,Cr)	98.50	0.30	0.01	0.76	0.43 (N,Cr,Fe)
	37.9	60.3	0.1	1.0	0.7 (Cr,K,Ti)	97.96	0.08	0.06	1.09	0.81 (N,Fe,Cr)
	40.3	57.6	0.2	1.3	0.6 (K,Fe,Ti)	98.60	0.09	0.05	0.78	0.48 (Cr,N,Fe)
	38.0	59.7	0.2	1.2	0.9 (Fe,Mg)	98.44	0.06	0.05	0.82	0.63 (N,Fe,V)
Slag mean:	**38.5**	**59.3**	**0.2**	**1.2**	(0.8)	98.18	0.06	0.03	0.97	0.76 (Fe,N,Cr)
					Particle mean:	**98.35**	**0.12**	**0.04**	**0.87**	(0.62)

Table {7.2.2}1 continued/

Specimen.	Field Acquisition, slag (at%). All windowless (NoW) EDS detection.					Spot Acquisition, particles (at%). All windowless (NoW) EDS detection.				
	Al	**O**	**C**	**Si**	**balance**	**Ti**	**O**	**C**	**Al**	**balance.**
ANAT**A5**	38.4	59.9	0.3	1.1	0.3 (Mg,Cr)	97.55	0.02	0.03	1.54	0.86 (V,N,Cr)
	39.7	58.5	0.3	0.9	0.6 (Fe,Cr,Ti)	98.25	0.05	0.02	1.05	0.63 (Cr,Fe)
	42.1	56.6	0.2	0.7	0.4 (K,Fe,Cr)	98.33	0.03	0.01	0.88	0.75 (N,Fe,V)
	40.1	57.7	0.2	1.2	0.8 (Fe,K,Cr)	98.43	0.03	0.02	0.86	0.66 (N,Cr,Fe)
	38.8	59.2	0.2	1.1	0.7 (Fe,Mg)	97.90	0.02	0.06	0.79	1.23 (Fe,Cr,N)
Slag mean:	**39.8**	**58.4**	**0.2**	**1.0**	(0.6)	98.46	0.01	0.02	0.80	0.71 (Fe,N,V)
						98.22	0.02	0.05	0.89	0.82 (N,Cr,Fe)
					Particle mean:	**98.16**	**0.03**	**0.03**	**0.97**	(0.81)
RUTL**A1**	36.7	61.4	0.2	0.6	1.1 (Fe,Cr)	96.68	1.70	0.01	0.87	0.74 (Cr,V)
	37.1	60.8	0.2	0.8	1.1 (Fe,Ti,P)	96.54	0.96	0.02	1.28	1.20 (Fe,Y,Cr)
	36.5	61.2	0.3	1.1	0.9 (Ti,Fe,K)	96.89	1.09	0.02	0.94	1.06 (Cr,Fe,V)
	35.9	61.5	0.1	0.7	1.8 (Fe,Ti,K)	96.44	1.12	0.04	1.16	1.24 (Cr,V,Fe)
	36.4	61.1	0.2	0.8	1.5 (Ti,Mg,K)	96.75	0.98	0.02	1.04	1.21 (Fe,Cr)
Slag mean:	**36.5**	**61.2**	**0.2**	**0.8**	(1,3)	97.01	1.09	0.03	0.96	0.91 (Cr,V,Th)
						96.73	1.17	0.02	0.85	1.23 (Cr,Fe)
					Particle mean:	**96.72**	**1.16**	**0.02**	**1.01**	(1.09)
RUTL**A2**	36.6	61.3	0.3	0.7	1.1 (Ti,Fe,Cr)	96.58	1.93	0.02	0.88	0.59 (Cr,Fe)
	36.7	61.0	0.4	0.8	1.1 (Ti,Cr,K)	96.99	1.68	0.01	0.80	0.52 (Fe,Cr,V)
	37.0	60.4	0.3	0.9	1.4 (Fe,Ti,Cr)	96.55	1.89	0.03	0.93	0.60 (Cr,V,Fe)
	36.9	59.8	0.3	1.2	1.8 (Mg,P,K)	97.04	1.77	0.02	0.78	0.39 (Cr,N,La)
	36.8	60.7	0.3	0.9	1.3 (Fe,Ti,Cr)	96.85	1.70	0.03	0.76	0.66 (Cr,Fe)
	37.6	59.9	0.2	0.9	1.4 (Ti,Fe,Cr)	97.02	1.68	0.02	0.60	0.68 (Cr,Fe,N)
Slag mean:	**36.9**	**60.5**	**0.3**	**0.9**	(1.4)	96.79	1.90	0.01	0.74	0.56 (Fe,Cr,Ce)
						96.93	1.47	0.02	0.81	0.77 (Cr,V,Fe)
					Particle mean:	**96.84**	**1.75**	**0.02**	**0.79**	(0.60)

Averaged mean of five thermite anatase specimens, ANAT**A1** to ANAT**A5**:

Particle mean: 97.94 at%Ti; 0.31 at%O; 0.03 at%C; 1.03 at%Al; ~ 0.69 % balance trace component metals (see text).
Slag mean: 38.9 at%Al; 58.8 at%O; 0.3 at%C; 1.3 at%Si; ~ 1.7 % balance of incidental trace component elements (see text).

Averaged mean of the two thermite rutile specimens, RUTL**A1** and RUTL**A2**:

Particle mean: 96.78 at%Ti; 1.46 at%O; 0.02 at%C; 0.90 at%Al; ~ 0.84 % balance trace component metals (see text).
Slag mean: 36.7 at%Al; 60.9 at%O; 0.2 at%C; 0.9 at%Si; ~ 1.3 % balance of trace component elements (see text).

as the starting anatase. However, supported by the evidence of the few micrographs presented (and the many which could not be presented for reason of the economy of opportunity), and with the declared process limitations of the experimental method, the results contained in Table {7.2.2}**1** credibly and persuasively assert the effectiveness of this microwave-stimulated technique of aluminothermic reduction of TiO_2 minerals. Development up-scaling and adaptation of such a technique to an industrial application can be seen to hold significant promise.

7.2.3: Carbothermic Reduction of Ilmenite.

Although the majority of ilmenite concentrates produced are directed to the production of pigment grade titania (by way of digestion of the ferruginous fraction), the reduction of ilmenite in this project accommodated the process co-reduction of Ti and Fe to a stable alloy product. Quite apart from the indicated processing ease and the prospect of attractive end-product value, initial impetus in pursuing this atypical reduction route was to assess the potential of *co-reduction* to assist in (*i*) reduction propensity (the relative ease of reducibility for both Fe and Ti), (*ii*) reduction efficiency (the proportional quantities of Fe and Ti won from the mineral), and (*iii*) the irreversibility of the option as a reduction exercise (the retention security of Fe and (especially) Ti to solidified reduction product metal). [Also, as a process alternative, such Ti-rich iron products could be digested to recover Ti fractions in an optional route that has the potential to be beneficial to Ti-purity and/or more process efficient than direct ilmenite digestion (although Ti in solid solution and/or carbonitride phases would need to be dealt-with, rather than the Ti-oxide of the ilmenite). This option is similarly plausible for metallothermically reduced iron products.] Reduction product irons produced in the experimental agenda of this carbothermic section were reminiscent of the iron reduction products produced in the preliminary experimentation presented in Section **7.1** and, more specifically, an ilmenite/magnetite carbothermic reduction product is micrographically represented in Figures {7.1.5}**12** and {7.1.5}**13**.

Being *iron* alloys, reduction products of this core section (as with the following Section **7.2.4**) were atypical of other core project reduction products. In respect of this

fact, these iron reduction products were treated somewhat more cursorily than reduction products of the more pivotal "single oxides" of refractory metals. Results obtained in this carbothermic reduction section were comparable to those similar, pre-core reduction exercises of the early, exploratory work – including those suitably recorded in Section **7.1**, plus others that were mentioned as "early experimentation" in Section **6**. Consequently, in part because those results of the evolving experimental method have been previously cited, and because results of the thermite reduction option addressed in the following Section **7.2.4** were plainly more commendable (as a proposed industrial process producing a commercial product of substantial value-add), the carbothermic reduction route for ilmenite was not pursued past the basic "confirmation of capability" stage as embodied in this section. (Also, to some extent, the wodginite reduction experimentation of Sections **7.4.3** and **7.4.4** produced minor quantities of base metal by-product, however, these phases generally did not include the crucial Ta(Nb) fractions which were typically contained in sintered metallic phases retained above the liquated Sn-phase alloys.)

Because of the less demanding quench requirements for iron reduction products, the reduction crucible (with its reduction product contents) was not subjected to full-term, full immersion LN_2 quench, but to initial full quench (to displace any entrapped O_2 and CO_2) thence simply to gaseous N_2 protection above the boiling LN_2 pool. Such a quench strategy provided adequate oxidation protection whilst providing efficient cooling rates – but rates sufficiently suppressed so to allow extension of melt agglomeration, thus accommodating button formation and some equilibration of microstructure. Throughout buttons, generally, realised cooling rates allowed for the development of primarily grey iron morphology in which the nucleation of Ti-carbide particles held precedence rather than the alloy Ti solid solution expected at true quench rates of cooling. White iron regions were evident to minor depths at button surfaces and universally through button appendages or extremities and in smaller iron beads. It was held that for the purpose of demonstration, Ti – as reduced thence *"retained"* in a metallic phase – could be more plainly observed as Ti-carbide particles (in the predominant grey iron regions) than could be insinuated by assessment of alloy phases in the white iron regions. Hence grey iron product was preferred for visually based micrographical evidence, also, EDS area acquisition data from either grey or white regions would equally present accurate results. Whilst grey iron microstructures – by

way of Fe-free Ti-carbides (and despite graphite flakes) – were deemed to represent more unequivocal, more definite visual displays of total Ti in metal product, white iron regions were comprised of alloy solid solutions whose Fe:Ti ratio provided less definite visual information. Nevertheless, where such could be expected in quenched wholly white iron beads and in button appendages, white iron microstructures provided closely comparable EDS area scans (for Ti %'s) to the grey iron area scans acquired centrally in the principal button. It is also a worthy observation that, where they existed at near-surface depths in beads and buttons, the white iron regions in reduction products of the carbothermic reduction of ilmenite were distinctively different from the "faux ferrotitanium" microstructures of the thermite reduction products presented in the following Section **7.2.4**.

The titaniferous mineral ilmenite ($FeO.TiO_2$) is relatively straightforward to reduce by a range of methods although, in the industrial setting, where ilmenite is mineralogically contemporaneous in magnetite concentrates then, more often, extractive processing is managed such that reduction includes only the ferruginous component, leaving the co-mineralisation fraction – the more obdurate titanium remnant (principally as TiO_2) – in a viscous but functional "foaming" slag. Once tapped, and upon post-quench recovery, such Ti-rich slag has further commercial value in being directed to titania production routes. Moreover, one such case of a lesser titaniferous mineral concentrate was the titano-magnetite (< 5 wt% ilmenite) beach sand mineral (ex-NZ Steel) that was cursorily investigated in preliminary experimentation. The New Zealand titano-magnetite is typical of numerous such resources worldwide from which iron is smelted in a pyrometallurgical iron-making operation and the (metallic complement) titanium is accumulated in the regular slag that, once tapped, frozen and granulated, is on-sold to TiO_2 production thence commercial titanium production streams.

Beyond the expediency of such pragmatic industrial metallurgical practice, in both the early project experimentation and in this brief examination, ilmenite was carbothermically reduced utilising the microwave-stimulated reduction method to yield reduction product irons exhibiting a range of Ti compositions. Such iron alloys could be grey irons suffused with Ti-carbide/carbonitride particles heavily associated (by order of solidification) with graphitic carbon, or Ti-rich iron phases (often with a sparse distribution of included Ti-carbonitride particles) in white iron reduction products. This

solidification-process-dependent "variable morphology" was revealed corresponding to cooling rate in reduction product specimens examined and was accompanied by "variable Ti-saturation" of a random nature, the degree dependent upon both intensity *and* completeness of reduction.

All five of the carbothermic ilmenite reduction trials were conducted on the mill-blended charge (as per Appendix **6.2**) employing standard crucible configuration using the standard oven set-up method with process times of 10 minutes (from cold start to "quench" introduction) for each experimental trial. As outlined above, the quench rate and quench method differed for this iron reduction product with the crucible arrangement fully immersed only initially, thence in the cold gaseous N_2 – with the boiling liquid N_2 pool maintained beneath the solidifying button, constantly replenishing the super cold gaseous N_2 blanket. Such a "sub-quench" cooling rate was sufficiently slow to allow, within a shallow white iron "shell", the development of a grey iron primary button featuring the intended Ti-carbide particle distribution so to visually establish Ti-reduction and retention. (Also as outlined above, because of the "more commendable" reduction product outcome of the alternative thermite reduction route, a minimal number of experimental trials were pursued in this "confirmation of capability" exercise for the carbothermic option.)

In a notionally interactive approach of "review and feed-back", rather than be inflexibly bound to the unwarranted rigour of a purely statistical approach to processing and specimen analyses – particularly when the exactitude of such scientific method here could experimentally "miss the point", and where process and product variability were seen as acceptable and experimentally "normal" – a reasoned, but more relaxed approach to fixing the acceptable number of experimental trials for each experimental section was required. For this section, as with previous and future sections, such an "adequate" number of reduction trials (and product specimens) was determined during the course of the experimental campaign. When, having produced (in this case) five comparable specimens, the feats of *reduction* and *reduction product reproducibility* were deemed experimentally satisfied (even with the obvious degree of compositional variability and suspected incompleteness of Ti-reduction) and the focus of the reduction

programme moved-on. It was resolved that for "real" experimentation such as this, the magnitude of compositional variability as encountered across all specimens was understandable and reasonable – and thus acceptable – and specimens from the reduction products of the five reduction trials are labelled ILME**01** to ILME**05**. Any later return to this experimental section (to augment data and reinforce evidence) was deemed un-necessary once reduction outcomes were characterised and analysed, and substantiation of reduction processes acknowledged.

In experimentally reproducing iron buttons with maximised Ti-composition, of similar size and with minimal unattached small iron beads, several simple "smelt process" procedures were repeated for all trials conducted. Discrete beads often provided both interesting microstructures and analyses, however, they were less "representative", and the properties of the consolidated iron buttons were considered more representative and thus more instructive (with respect to "mean" attributes of reduction products). Of primary concern in securing these melt agglomerated iron buttons was that, at reduction termination and before its LN_2 immersion in the quench chamber, the crucible configuration was carefully tamped on a firm surface to assist with liquid metal drainage to the crucible "hearth" where, thus consolidated, it was frozen to form the representative button. It was well understood from earlier work with reduced base metal smelt products that such physical tamping efficiently dislodged liquid metal beads that were otherwise "suspended" in structural features (comprised of char, softened crucible and slag) above the crucible hearth. For reduction products frozen from freely flowing liquid product, such suspended liquid formed isolated beads, which although interesting, being unconsolidated with a main button were effectively lost to any compositional averaging exercise, including micrographical representations. For most other sections of this project, freely flowing liquid reduction products (at reduction process termination) were not possible due to extreme melting points of phases, so high viscosity liquids were normal – often after the sintering phenomena accompanying solid state reduction. Consequently, typical reduction product remnants consisted of agglomerated metallic phases mingled with non-metallic phases – and in micrographs, typical reduction product fields-of-view showed amalgams of metallic phases within or associated with phases representing partially reduced mineral plus other gangue product phases. Such sintered or high viscosity liquid reduction product

phases were well represented in the previous studies on the microwave reduction of anatase and rutile.

Also associated with the drainage and low viscosity phenomena of liquid iron is the perennial consideration of the *contacting* of reactants and, especially, the interval of interface contact (allowing such reaction opportunity). In this ferruginous section of experiments, the final *Ti-retention* in the iron button was as pertinent as *Ti-reduction* (*per se*) – irrespective of the form of that retained Ti – and recognition of the inter-dependence of *reduction* and *retention* was requisite upon the crucial microwave-stimulated chemistry driving cross-interface diffusion and reaction. The faster the free drainage of liquid iron away from the interface sites of the lagging Ti-phase reactions, the shorter the period for cross-interface diffusion of Ti into the liquid solute. So, where the freely reducing iron liquid was "held-up" and retained against the more slowly reducing phases, the Ti-uptake was maximised as it was reduced and retained in the solute iron. At completion of microwave processing, and upon tamping of the crucible configuration and subsequent solidification, the sole consolidated iron alloy button was a fair physical representation of "average reduction product composition", or "attained composition", and with knowledge of the mean mineral concentrate composition, reduction completeness could be directly revealed.

For all five carbothermic reduction exercises completed the reduction remnants indicated that the full complement of available Ti was not recovered in the iron button products (although, this reckoned Ti-percentage was clearly approached). Also, results indicated that 10 min processing was insufficient to fully reduce and transfer the Ti to the iron solute. The key here may not have been the "Ti-reducibility" factor but may have been the "Ti-transference" factor as, without an iron diffusion interface, the reduced Ti would then have to melt (at a still higher temperature) then, before it "re-oxidised" (by any light element combination) and re-solidified, freely drain to join the liquid iron pool (and subsequently form metallic phases), or form an isolated solid Ti-carbonitride or be otherwise held-up and retained in slag phases. These latter fates, typical of batch operations, were undoubtedly the case for a minor proportion of reduced Ti that, with modest "hold-up", "circulation" or other contacting with solute iron, would have reported in the iron button. In each of the five experimental trials, little "slag" phase was produced (from molten crucible material, gangue content of

Table {7.2.3}1: The following table is an assemblage of provisionally quantitative results of EDS analyses of acquisition counts taken on polished fields on newly-reduced iron phases of carbothermically reduced ilmenite specimens ILME**01** to ILME**05**. Spot counts were acquired from points clearly within titanium carbonitride particles whose morphology corroborated their compound status. Area counts were acquired from representative fields on grey iron material inclusive of particles typical of (and including) those sustaining the spot acquisitions, as represented in Figure {7.2.3}**4**.

Specimen.	**Field Acquisition (at%).** All EDS detection via ultra-thin window (UTW).					**Spot Acquisition from particles (at%).** All windowless (NoW) detection except where denoted # which were UTW detection.			
	Fe	**Ti**	**Cr**	**Si**	**bal.**	**Ti**	**C**	**N**	**balance.**
ILME**01**	71.2	25.1	1.7	1.3	0.7 tr	69.70	17.60	12.00	0.45 (Fe)#
[10 min]	68.0	27.7	3.2	0.2	0.9 tr	68.10	20.60	9.95	1.35 (Fe,Cr)#
	65.4	29.3	3.1	1.1	1.1 tr	70.35	19.65	7.85	2.15 (Fe,Cr)#
	74.1	20.4	2.9	1.6	1.0 tr	69.60	19.95	9.90	0.55 (Fe,Cr)#
	72.6	24.9	1.7	0.5	0.3 tr	62.65	27.75	8.80	0.80 (Fe)#
Area mean:	**70.3**	**25.5**	**2.5**	**1.0**	(0.7)	67.65	24.80	6.85	0.70 (Fe,Cr)#
					Particle Mean:	**68.00**	**21.75**	**9.20**	(1.05)
ILME**02**	83.1	14.7	1.6	0.3	0.3 tr	70.80	19.00	9.70	0.50 (Cr)
[10 min]	79.8	16.2	2.2	0.9	0.9 tr	74.25	15.25	9.85	0.65 (Cr)
	85.1	13.1	0.9	0.7	0.2 tr	76.20	14.10	8.85	0.85 (Fe,Cr)
	82.3	14.4	2.1	0.5	0.7 tr	75.65	17.90	5.95	0.50 (Fe,Cr)
	81.9	16.3	1.1	0.4	0.3 tr	71.45	19.10	8.85	0.60 (Fe)
Area mean:	**82.5**	**14.9**	**1.6**	**0.6**	(0.4)	73.75	16.90	8.90	0.45 (Cr)
					Particle Mean:	**73.70**	**17.05**	**8.70**	(0.55)
ILME**03**	78.9	18.1	1.4	1.0	0.6 tr	69.90	21.50	8.05	0.55 (Fe,Cr)
[10 min]	78.0	17.2	3.1	0.8	0.9 tr	74.05	17.55	7.90	0.50(Fe,Cr)
	80.1	15.2	2.6	0.9	1.2 tr	70.65	19.50	8.85	1.00 (Cr)
	81.4	16.2	1.4	0.7	0.3 tr	75.60	15.20	8.95	0.25 (Fe,Cr)
	80.8	16.8	1.1	0.8	0.5 tr	74.15	16.35	8.90	0.60 (Fe)
Area mean:	**79.9**	**16.7**	**1.9**	**0.8**	(0.7)	73.55	18.15	7.85	0.45 (Fe,Cr)
					Particle Mean:	**73.00**	**18.05**	**8.40**	(0.55)
ILME**04**	82.2	15.2	1.4	0.5	0.7 tr	74.60	17.60	7.45	0.35 (Fe,Cr)
[10 min]	78.7	17.6	3.1	0.7	0.4 tr	74.00	16.65	8.80	0.55(Fe,Cr)
	80.4	16.6	1.2	0.9	0.9 tr	71.55	19.40	8.15	0.90 (Cr,Nb,Fe)
	81.7	16.0	1.0	0.7	0.6 tr	75.10	16.40	7.95	0.55 (Fe,Cr)
	82.8	14.8	1.4	0.6	0.4 tr	70.15	20.95	8.70	0.20 (Fe)
Area mean:	**81.2**	**16.0**	**1.6**	**0.7**	(0.5)	73.75	17.70	8.15	0.40 (Fe,Nb)
						70.35	20.75	8.25	0.65 (Cr)
					Particle Mean:	**72.80**	**18.50**	**8.20**	(0.50)

Specimen.	Field Acquisition (at%). All EDS detection via ultra-thin window (UTW).					Spot Acquisition from particles (at%). All windowless (NoW) detection except where denoted # which were UTW detection.			
	Fe	**Ti**	**Cr**	**Si**	**bal.**	**Ti**	**C**	**N**	**balance.**
ILME**05**	84.5	13.4	0.8	0.6	0.7 tr	69.95	20.65	8.75	0.65 (Cr)
[10 min]	81.6	15.5	1.6	0.8	0.5 tr	71.30	20.15	8.25	0.30(Fe,Cr)
	84.2	13.9	1.2	0.3	0.4 tr	70.80	18.95	9.85	0.40 (Cr)
	80.4	17.4	1.1	0.7	0.4 tr	71.35	20.15	7.95	0.55 (Cr)
	80.9	16.3	1.3	0.9	0.6 tr	70.95	19.80	8.65	0.60 (Fe)
Area mean:	**82.3**	**15.3**	**1.2**	**0.7**	(0.5)	72.55	18.15	8.75	0.55 (Fe,Cr)
				Particle Mean:		**71.15**	**19.65**	**8.70**	(0.50)

It should be noted that, as a raw indication, the EDS results from Ti-compound particles approximate a generalised stoichiometry of $Ti_3(C,N)$. Being of simple arithmetic ratio the result would afford certain credibility in terms of claiming compound status – except the ratio does not identify a compound in the relevant ternary phase diagram. However, the partitioning influence and major presence of Fe, and the physical circumstances of its high temperature evolution may impose conditions that allow quasi-crystalline stoichiometry between αTi (or βTi) and $Ti_x(C,N)_y$, $x \geq 2$, $y \approx 1$. One such high temperature phase field possibility which contains the above "Particle Mean" Ti:C:N ratios for the general metallic reduction product phase is the (α + β + δ) option from the Ti-C-N ternary phase diagram as calculated [264] at 1423 K.

Elmt	Spect. Type	Inten. Corrn.	Std Corrn.	Element %	Sigma %	Atomic %
C K	ED	0.823	1.91	7.43	0.16	13.92
N K	ED	0.195	1.12	18.59	0.53	26.14
Si K	ED	0.731	1.00	1.21	0.06	0.97
Ti K	ED	0.972	1.00	122.22	0.32	57.40
V K	ED	0.953	1.00	1.07	0.16	0.47
Fe K	ED	0.854	1.00	2.72	0.13	1.09
Total				153.24		100.00

Figure {7.2.3}**1:** The above EDS analysis result (although corrected to 100at%) is representative of nitride-dominated Ti-carbonitride particles which were typical of particles found close to the button surface, usually in white iron but also in near-surface grey iron regions. This spot count was acquired from a button extremity on specimen ILME**01** and shows a lower Ti % than was recorded from particles nearer the button centre (and noting the anomaly correction for Ti). The recorded trace proportions of Si, V are inconsistent with the trace component Cr which was consistently represented in the central particles – the common trace presence of Fe may be more a background "acquisition artifact" (from the Monte Carlo excitation bulb) than a real trace component in the particle. Such N-dominant carbonitride particles tended to be more salmon coloured than the generally grey C-dominant carbonitride particles from the specimen centre. Also, notably, the stoichiometry of such phases was more indicative of δ′-phase, or the simple Ti(C,N).

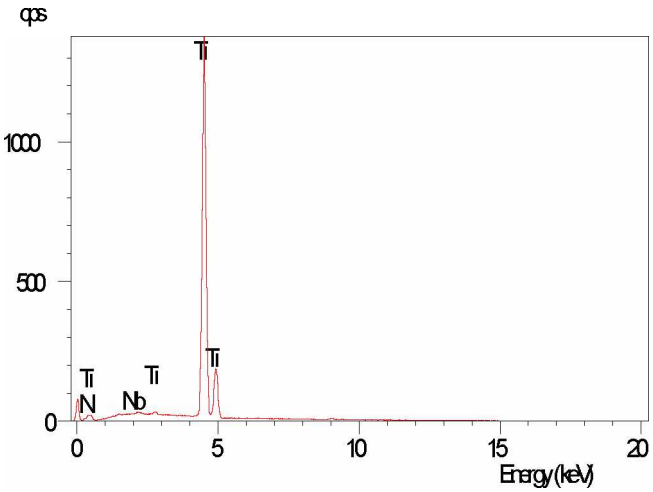

Elmt	Spect. Type	Inten. Corrn.	Std Corrn.	Element %	Sigma %	Atomic %
N K	ED	3.163	1.00	9.50	0.41	26.48
Ti K	ED	0.985	1.00	89.95	0.42	73.29
Nb L	ED	0.853	1.00	0.54	0.08	0.23
Total				100.00		100.00

Figure {7.2.3}**2:** Spectrum and analysis from a spot count acquired from an exposed nitride particle in white iron at the button surface on specimen ILME**04**. The rare absence of carbon in the particle was attributed to a possible full-period exposure to atmospheric nitrogen during reduction processing. As an example, this particle represents one end of the carbonitride spectrum. Its lack of Fe was attributed to the particle's larger size and a clear, untainted acquisition from a centrally located beam spot (resulting in no excitation overlap into the surrounding iron). The unexpected presence of Nb as a trace impurity in the particle was limited in incidence to acquisitions from ILME**04** and may represent either a trace contamination in the mineral concentrate sample or on the polished specimen at EDS examination stage. The stoichiometry of the phase approximates Ti_3N – which (again) is problematical in the same manner as was indicated for the $Ti_3(C,N)$ designation generally.

Elmt	Spect. Type	Inten. Corrn	Std Corrn.	Element %	Sigma %	Atomic %
C K	ED	0.831	1.91	5.38	0.10	17.81
Si K	ED	0.733	1.00	0.67	0.05	0.91
Ti K	ED	0.989	1.00	91.36	0.17	79.51
Fe K	ED	0.862	1.00	2.03	0.10	1.52
Nb L	ED	0.847	1.00	0.56	0.10	0.25
Total				100.00		100.00

Figure {7.2.3}**3:** Analysis from a spot count acquired from (the polished surface of) a carbide particle in grey iron which was exposed to an internal void in the principal button specimen of ILME**04** (the same button as for the acquisition of previous Figure {7.2.3}**2**). Note here that the particle was an N-free carbide and quite atypical in composition from those of the general particle distribution in the specimen. In this case, being the analysis of a metal compound particle, the apparent presence of Si could be from interface mineralisation associated with the void's solidification origin.

concentrate and, principally, incompletely reduced ilmenite phases), and this largely immobile viscous amalgam of liquid and high melting point material (itself) did not freely drain to cover the liquid iron button. Had it done so, a quite conventional large area interface would have accommodated maximum Ti transference into the iron. (The addition to mineral blends of a trace proportion of a viscosity (surface tension) suppressant such as $BaCO_3$ may have assisted in respect of such a lately realised deficiency.)

During cursory inspection of mounted specimens, preliminary EDS examination of various iron and particle phases provided initial evidence that (*i*) area-acquired counts on white iron phases provided comparable Ti-compositions to area-acquired counts on grey iron phases on the same specimen button, and (*ii*) for the range of carbonitride particles, from button surface to centre, a gradation trend of N-dominated composition to C-dominated composition was evident in all specimens. Such gradation of particle composition is represented in the EDS analyses of Figures **{7.2.3}1**, **{7.2.3}2** and **{7.2.3}3** whilst a typical particle distribution in grey iron is shown in the micrograph of Figure **{7.2.3}4** and highlighted in the etched micrograph of Figure **{7.2.3}5**.

Area acquisitions from fields on iron specimens and spot acquisitions from included Ti-carbonitride particles were analysed and are presented in outline form in Table **{7.2.3}1**, the results presented there are representative of typical acquisitions. It might be noted that, as a general observation from Table **{7.2.3}1**, the spot acquisition results derived from included particles across the specimens are suggestive of the stoichiometry $Ti_3(C,N)$ (an unrecorded compound stoichiometry nomination). However, compound possibilities may be "unconventional" given the unconventionality of experimental method and its termination technique.

Whilst Fe and Ti are present in close to equal proportions in the east coast Australian ilmenite used in the reactant blend, a relatively high Cr content is also present in the mineral by way of gangue chromite (~3 wt%) and was correspondingly present in iron phases of reduction product specimens. At the time of analyses, light elements C, N and O were not being quantitatively detected through the ultra thin Be window (UTW), so area analyses on iron fields were processed neglecting the presence of these crucial elements and allowance must be made for this fact. However, the UTW-

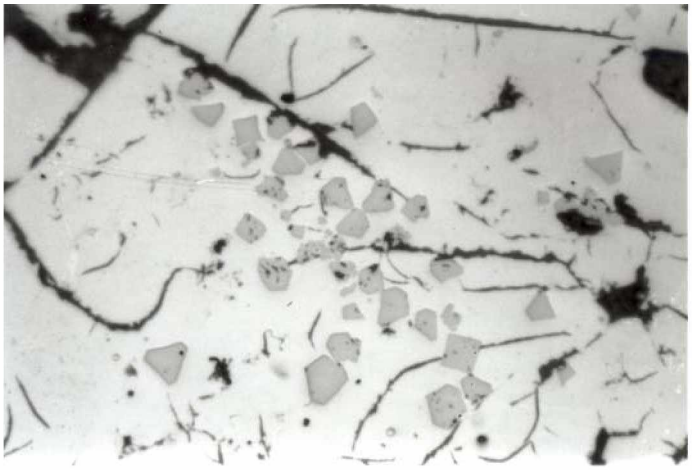

Figure {7.2.3}**4:** The micrograph presented shows the un-etched microstructure of a typical grey iron reduction product button, this field being from specimen ILME**02**. The micrograph is representative of a typical mid-button field and shows a typical scatter of primary Ti-carbonitride particles amid primary and secondary graphite flake distributions. The un-etched surface serves to illustrate the concentration of the typical carbide distribution irrespective of solid solution microstructure. Figure {7.2.3}**5** (below) shows an adjacent field in the same specimen in the etched condition. ([LOM; fov: 0.53 mm]

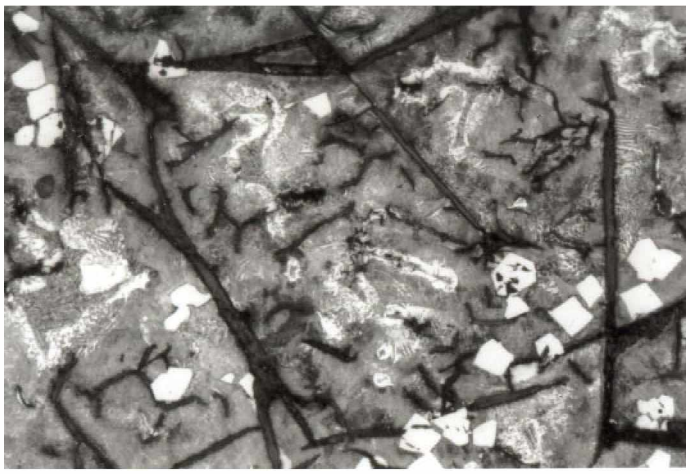

Figure {7.2.3}**5:** The micrograph presented shows the nital etched microstructure of grey iron reduction product specimen ILME**02** shown in the un-etched condition in Figure {7.2.3}**4** above. The micrograph is (again) representative of a typical mid-button field showing a scatter of Ti-carbonitride particles amid graphite flake distributions in a primarily pearlitic matrix. The proximity of the particles with the primary graphite flakes is indicative of their nucleation early in the solidification sequence – a detail of some significance in the resolution of process events. The etched surface tends to highlight the particles in the grey iron field; a grey iron which, as can be plainly seen, is largely un-remarkable of such carbon-saturated, non-quenched irons. [LOM; fov: 0. 53 mm]

-derived results were instructive because of the component proportions reported and are included because of the relevance of the Fe:Ti ratio and the instructiveness of this ratio of atomic percentages (at%'s) which is meaningful in considerations of the percentage of Ti retained in the solute iron – and, perhaps, can be projected to the degree of Ti-reduction achieved in the reduction process. Further, as a comparative observation between the typical micrographic field of Figure **{7.2.3}4** and the UTW area-acquired Ti compositions (which ranged between mean values of 14.9 at% and 25.5 at% for the five specimens, one third to one half of that theoretically possible): much of the reduced Ti captured in the iron solute must have been retained in the grey iron as alloy phases, particularly as the cementite equivalent – quite apart from that proportion of Ti precipitated as Ti-carbonitride. Again here, as with the carbonitride gradation through Ti-particles, the mechanism and limits of this partitioning of Ti between solid solution and metallic compound phases during solidification was not examined, the reduction product outcome being sufficient to fulfil project objectives.

Spot acquisitions acquired with no window (NoW) protecting the detector were not similarly compromised and the crucial light element compositions of Ti-carbonitride particles were conducted without such analytical problem. It is noted that no remnant O was detected in the spectra and analyses of particles (and, as O has greater mass and is thus easier to detect than either C or N (under normal circumstances of detection), there exists compelling evidence to accept its absence in each case). As to the variability of each C and N in the carbonitride particles, the ultimate proportion of either was interpreted to depend upon the individual particle "history" – that is, as the particle evolved in either or both the reduction environment and/or the solidification dynamic of the relevant iron. It is acknowledged that the N-dominant to C-dominant gradation in carbonitride compounds across the iron buttons is neither easily explained nor understood, however, its existence is accurately and confidently reported. Also, in respect to the "compound" status of Ti-carbonitride particles, and commensurate with earlier observations regarding "compound stoichiometry", incomplete "cooling equilibration" through particles is suspected due to the high cooling rate at "quench".

Although not rigorously investigated after proof of principle was satisfied, it is quite obvious that the microwave-stimulated reduction procedure was shown to be successful when applied to the task of carbothermic reduction of ilmenite. The EDS

acquisition results presented in Table {7.2.3}**1**, supported by the evidence presented in figures – especially the micrographs of Figures {7.2.3}**4** and {7.2.3}**5**, all combine to support the contention that microwave-stimulated reduction of ilmenite produces reduction product results of creditable worth. By way of comment on a published work, a study of similar experimental objective – and although quite different technological means was employed in pursuing their goal – (although less outcome-certain) the results of carbothermic reduction of weathered ilmenite reported by GUPTA, et al [137] had definite "outcome congruencies" with those reported here, whereas (concurrently) their products of reduction were dissimilar. Reported by COLEY, et al [265], the reduction of ilmenite using coal as reductant produced incompletely reduced products, although micrographs of their reduction product phases were reminiscent of under-processed preliminary results of the present project. Nevertheless, and whilst acknowledging other "means" of reduction, the propensity for development towards an industrial application of a system of microwave reduction for ilmenite was, for the carbothermic route, "up-staged" by the process immediacy and superior reduction product potential represented by the corresponding aluminothermic reduction route for ilmenite, a thermite process of considerable merit.

7.2.4: Aluminothermic Reduction of Ilmenite to Ferrotitanium.

Beyond the established conventional systems of reduction processing, the microwave-stimulated *carbothermic* reduction of both Fe *and* Ti fractions from ilmenite was shown to be a plausible basis for further development towards a commercial enterprise. Hereto, under microwave-stimulation the *aluminothermic* reduction of ilmenite proceeded "at temperature" (that is, when $\mathbf{E_{act}}$ was reached) by the efficient and well-documented thermite reaction. In this case, whereby, the fine Al reductant of the mill-blended reactant powder (by now liquid) spontaneously and explosively reacted with the wustite (FeO) fraction of the ilmenite, the reduction producing Al_2O_3 plus liquid Fe, (notionally) leaving the remnant titania fraction. In concert with this primary wustite reaction, the external energy supplied by the continuing microwave irradiation plus the significant and instantaneously available exothermic energy (an internal

energy) released by the wustite reduction* reciprocally supplied sufficient total energy to satisfy the energy of activation for the thermochemically more demanding parallel reduction by Al of the titania (TiO_2) fraction. Amongst the microwave-stimulated processes of this project the thermite reduction of ilmenite was distinguished by several facets, both in process and of product. Not least of these was the *process spontaneity* leading to a comparatively *"clean" reduction product* – features representing a convergence of attributes which, with minimal process refinement and up-scaling, could translate as an industrial process yielding a commercial product. Such notable general and specific characteristics ensured the aluminothermic route's conspicuous status when categorised amongst the other experimental outcomes of this project. And, in practice – by its successful realisation – the thermite reduction of ilmenite held particular appeal within the project because of its singular potential for development. It is edifying to note that the outcomes of this project generally reflect the outcome of the thermite reduction of ilmenite to ferrotitanium reported by GIESEN and DAUTZENBERG [125]. Although their work was not microwave orientated in method, the investigation was industrially based, spanning between industrial start and end points (in ilmenite and ferrotitanium respectively), and was driven by real commercial development considerations rather than by motives of pure research – motives which, when too "ideal", can distract attention from actual experimental "accomplishment" in process and product.

In comparing the aluminothermic reduction of ilmenite with other experimental tasks one fundamental fact stands out. In essence, the contribution of internal energy to the system over the brief interval of the thermite reaction far exceeded the available energy from the externally applied microwave energy (over that same time). Nonetheless, it is noted that the thermite reaction (itself) was activated by the accrual of this applied microwave energy in the reactant charge (the charge acting as the dielectric load). The pertinence here (in stating the "obvious") is that, had this inequity been so in other operations, those other microwave-stimulated processes of this project would also have proceeded in so rapid a manner. [It is feasible that, with fundamental changes to

* In blast furnace iron-making, the reduction of iron ore is characterised by the fundamental stages: haematite → magnetite → wustite → iron. Of these, the reduction of wustite is the stage requiring the greatest energy input to meet the activation energy, $\mathbf{E}_{\mathbf{act}(FeO)}$ – so allowing that reduction to proceed. By corollary, the reduction of wustite releases the greatest exothermic energy – and it is so in the thermite reduction above, the exothermic energy released plus the externally applied energy more than satisfy $\mathbf{E}_{\mathbf{act}(TiO2)}$, the activation energy for TiO_2, whilst also ensuring the melting point of reduced Ti is exceeded.

chemistry and process, a thermite-assisted alternative could be contrived and introduced into reduction routes of other minerals, including others in this project. However, because of complexities and uncertainties associated with the introduction of such metallurgical manipulation, these are *indefinite* possibilities whose further discussion must be excluded here.] Whilst it seems simplistic to acknowledge such an obvious point, it is a sound first step in understanding and exploiting the processing potential implicit in the thermochemical difference between the thermite-assisted processes and the non-thermite processes – a difference clearer in equation representation. An inference in GIESEN and DAUTZENBERG was the suggestion of imperfect thermite initiation and it should be noted that, since their solid work half a century ago, numerous reaction stimulation techniques (reference combustion synthesis techniques identified in MUNIR and HOLT [154 to 174]) have been developed which could be adopted as thermite trigger for such a process. However, the adoption of a microwave-stimulation mechanism for thermite initiation would confer synergistic benefits upon the process. Amongst these conferred benefits, and of fundamental relevance to thermite initiation and process, are the physical applications of zone targeting, the focussing and concentration of applied energy, and depth of penetration of irradiated energy, plus the specific implications of ionisation, species targeting and plasma chemistry – all could be admirably adapted into thermite processing and its industrial application.

Of course, no distinctly thermite reactions were represented amongst the single oxide reactants of the project, although some (as noted) were observably more reactive than others – specifically where greater exothermic energy (of reaction) was released resulting in greater nett system energy (with associated process benefits). The thermite reactions can be usefully represented in the following manner.

When $\mathbf{E_{apl}} \geq \mathbf{E_{act(FeO)}}$,

$$3FeO.TiO_2 + 2Al \rightarrow 3Fe + 3TiO_2 + Al_2O_3 + \delta\Delta_{Fe} \quad \ldots\ldots \quad \{7.2.4\}1$$

When $(\mathbf{E_{apl}} + \delta\Delta_{Fe}) \geq \mathbf{E_{act(TiO2)}}$,

$$^{3}/_{2}\, TiO_2 + 2Al \rightarrow Ti + Al_2O_3 + \delta\Delta_{Ti} \quad \ldots\ldots \quad \{7.2.4\}2$$

Or, generally,

$$FeO.TiO_2 + 2Al \rightarrow [Fe,Ti] + Al_2O_3 + \textit{Energy} \quad \ldots\ldots \{7.2.4\}3$$

Where; $\mathbf{E_{apl}}$ is the externally applied energy (over time) – effectively, the energy transferred into the "system" by the applied microwave field, or the microwave energy. [This is a nett positive energy.]

$\mathbf{E_{act(FeO)}}$ and $\mathbf{E_{act}}_{(TiO2)}$ are the activation energies (required for their reduction) of FeO and TiO_2 respectively. [These are nett negative energies.]

$\delta\Delta_{Fe}$ and $\delta\Delta_{Ti}$ are the exothermal energies released upon reaction in the reduction of the oxides to Fe and Ti metals respectively, they are internal (or *chemical*) energies. [These are nett positive energies.]

[Fe,Ti] is the liquid phase metal product.

And; "*Energy*" is the sum: $\sum \{(\mathbf{E_{apl}})_{total} + (\delta\Delta_{Fe} + \delta\Delta_{Ti}) - (\mathbf{E_{act(FeO)}} + \mathbf{E_{act}}_{(TiO2)})\}$, where, for this rudimentary "rule of thumb" depiction, the sum of energies is *positive* for the reduction process to have proceeded to completion yielding metallic product(s) plus "heat".

Under un-aided "real time" observation these parallel reduction reactions, in effect, take place simultaneously producing considerable exothermic heat. Such surfeit of energy (as heat) ensured that even the reduced Ti metal was produced as liquid, and that this mixed with the liquid Fe to form a FeTi liquid, [FeTi], (of process-dependent ratio approaching the mineral ratio and) of high "binary purity" at reduction – but susceptible variously to imminent re-oxidation risks. Ideally, this alloy liquid must be quickly quenched to retain as much of that "spontaneity-induced" purity as possible before oxidation impurities have the chance to be taken-up by the liquid. Specifically, these oxidation impurities may derive from blend-associated char (to carbide by C, CO and their various ionisation product particles) or the atmosphere-dominant nitrogen (to nitride by N, N_2 and their ionisation particles), or the obvious oxygen (to oxide by O_2 ,

O, CO_2 or their ionisation product possibilities). Also, it can reasonably be expected that the various metallic impurities in the mineral under reduction will report as reduced tramp impurities in the solidified metallic phases. This was particularly the case for Cr (whose affinity with both Fe and Ti ensured good liquid mixing and solid solubility across the phase field range) and for Al (as excess or otherwise remnant reductant metal caught in solution rather than reacted).

The aluminothermic reduction of ilmenite produces a significantly different reduction product to that of the carbothermic reduction. In fact, the metallic product of aluminothermic reduction is so substantively different that a case could reasonably be mounted that such reduction product could service a separate, commercial demand. The microwave-derived reduction product is, at least in composition, most closely similar to commercial ferrotitanium – that pivotal alloying addition product used for adjustment and attainment of alloy specification in the production of Ti-alloy steels destined for a range of engineering and special applications. Whilst the microwave-stimulated thermite reduction of ilmenite has certain congruence with the industrial production of ferrotitanium, the microwave-derived reduction product was a "faux" ferrotitanium in that it was microstructurally different, in part because of the nature and level of impurities and in balance because of its markedly different solidification history, including its partial exposure to an imperfect, "sometime reactive" atmospheric environment. Generally, commercial ferrotitanium is slowly cooled under either a high vacuum or a closed inert atmosphere, consequently, microstructural morphology is marked by the prominent growth of slowly cooled crystals of intermetallic phases, principally FeTi with minor Fe_2Ti (proportions being source-dependent) and relatively free of light element impurities. Beyond elementary identification (and being outside the scope of this project), a more thorough examination of reduction product phases was not pursued. Unequivocally, any further study of this microwave thermite process should include fundamental studies of reduction phases – including the product possibilities of raw material and process adjustments – as an integral component of process upgrade. (The industrial production of ferrotitanium is discussed elsewhere.)

Because of thermite reaction spontaneity, with its instantaneous release of intense heat, a minor but practical variation to the crucible arrangement was adopted. Trialled in preliminary work, this minimal but effective amendment to the crucible

arrangement was achieved by the ramming of a second crucible into the pre-charged primary crucible (so to form a friction-tight plug and leaving little "free space" above the charge) and enclosed within a similar insulation configuration to the normal (as shown in the drawings of Figures **{5}1** and **{6.2.2}1**). Apart from thermite "containment", this constraining arrangement had the further desirable effect of efficiently confining the CO-dominant reducing atmosphere within the reaction zone and, given the advantage of pressure difference from nett gas production therein, restricting the inflow of oxidising gases. Moreover, as for the cautiously ring-milled reactant blend, experience gleaned from formative thermite trials suggested that for aluminothermic reduction of minerals – especially ferruginous minerals – the reactant blends should contain only the stoichiometric composition of reductant Al, and no more. Those trials had shown that, where there was a paucity of reducible material intimate in the reactant blend charge, excess powdered Al in the charge translated partly as excess alumina slag and also directly as metallic-Al impurity in the alloy reduction product.

It was occasionally observed in processes ranging above ~ 1600°C that, where (by containment misadventure) liquid Al came into contact with aluminosilicate insulation during operational temperatures, the Al reactant reduced the silica portion leaving a powdery, eroded alumina remnant insulation leaving trace Si in reduction product metal and/or as a dark Si-oxycarbide lining on adjacent insulation. At very high temperatures (above ~ 1600°C), SiO vapour formed by the carbothermic reduction of SiO_2, this gaseous reduction product subsequently revealed itself by re-oxidisation upon cooling. The hot gas formed a white plume as it vented from the reaction environment into the cooler oxidising environment (CO_2 + remnant O_2) of the oven – the pure silica precipitate deposited on the nearest available surface. Along with some associated chemistry, this sequence of reactions may be the base mechanism of formation/deposition by which Si-oxycarbide and similar phases come to adorn insulation cavities, clefts and surfaces of experimental crucible/insulation configurations – surfaces adjacent to the principal reaction zone. [Of little direct relevance to the reduction of ilmenite, the complex reaction set outlining the gas-phase synthesis of Si-oxycarbide is avoided here. It does, however, have relevance to process development in any future research extension.]

By using a stoichiometric-only quantity of reductant-Al in aluminothermic blends (and acknowledging some loss of this directly to gaseous (O_2 and CO_2) oxidation and to metallic solid solution), in accordance with the established experimental procedure of working with an excess of reductant, that excess of available reductant was supplied by *char* in the intimate reactant blend. Also, noting that "further" stoichiometric excess was indirectly supplied by gasification of the granular char that underlaid and overlaid the charge, and whose utilisation held the dual intention in aluminothermic work (*i*) to provide initial dielectric heating, enveloping the charge and intensifying energy availability for thermite activation ($\mathbf{E_{act(FeO)}}$), and (*ii*) to provide substantial CO "atmospheric blanket" cover around the "reaction zone" of the reacting charge. Reactant blend mixes for this thermite blend and all other blends are provided in Appendix **6.2**.

Because of the tangibly metallic nature of thermite reduction products of the carbon-assisted aluminothermic reduction of the native mineral ilmenite, no attempt was made to examine the remnant products by any XRD method. It was considered that routine EDS analyses would provide clear and indisputable evidence in support of routine characterisation by light-optical and electron-optical microscopic examination. Presented together with corroborating micrographs, the combined studies would provide sufficient evidence to describe the reduction product phases and corroborate phase compositions. Also, these means of description and analyses would suitably suggest process capabilities and deficiencies, and reflect upon this reduction process and the microwave thermite route generally. In hindsight, EDS mapping of phases as they occur across the reduction product facies would have assisted in visually delineating phase distribution in the reduction product.

If the generalised Equation **{7.2.4}3** takes place as written, and there was negligible indication in the essentially alumina slag remnant (by evidence of some measured fractional presence of either ferruginous or titaniferous mineral component) that the experimental reaction did not overwhelmingly follow the equation, then (projecting from the ilmenite composition) the metal phase composition must be close to that of the intermetallic FeTi. Moreover, for the ilmenite used in trials, the Ti fraction slightly exceeded that of Fe. Even so, (and after MILLER [7]) it was assumed (if

contrarily so by a non observation-based experimental scepticism) that a minor portion of the more reactive Ti would revert to oxide before effective quenching and, so, not report in the metal. *Notwithstanding the alumina slag observation above*, such suspicion of "minimal reversion" was confirmed by subsequent analyses of metal phases – reversing the bias of the Fe:Ti ratio expected in solidified metal product to one where Fe slightly exceeded Ti. It is assumed that this "minimal reversion" of re-oxidising Ti took place in the reactive surface region of the liquid metal and the resultant Ti-oxide was "expelled" to the metallic surface upon quenching, and so reported neither in the metal nor in the bulk (alumina) slag proper. Also, realistically, the small fraction of Cr (contributed by the chromite impurity, above trace level and endemic in east coast ilmenite) plus a minor proportion of un-reacted reductant Al would report in the solidified metal as "minor" constituents. Other metallic impurities from the ilmenite concentrate reported in metallic phases at "trace" levels; representing less-common mineral constituents (carnotite, rhodonite, monazite and other rare earth minerals, *et cetera*) in "mineral sands" deposits, the elements of these otherwise unremarkable tramp impurity components are recorded in EDS output.

The tangible outcome of these aspects of reduction processing of ilmenite – that is, ilmenite as "real" industrial mineral concentrate – was that the mean composition of reduction product metal would converge close to the FeTi intermetallic in the (FeTi + Fe_2Ti) phase field of the principal *binary* diagram. Such a first approximation would be noticeably impacted by minor impurities, and the Cr, Al plus C(N) components would be reflected in the "phase field shift" into (at least) the quinary, as exposed by variation in product phases. [MASSALSKI (ed.) [266] notes the "reactivity" in solid solution of Fe_2Ti and FeTi, particularly at high temperatures in the presence of Al (an element that has its own complications in solid solution with Fe). These alloy combinations are more thermodynamically stable when C is present in solution.] Also, noting that (if merely by *thin window* EDS analyses) any ascribed light element content in the thermite reduction phases was relatively low by comparison with commercial ferrotitanium – whose C-content may vary over quite a range up to ~ 10 at% C (process- and %Ti-dependent) to stabilise the reactivity and "getter" potential of Ti [17]. The reduction phase variation is evident in Figures **{7.2.4}1** and **{7.2.4}2** and in Table **{7.2.4}1**, which (after post analysis sorting) shows EDS analyses of the two core phases separately and, in terms of

proportionality, these so-identified core phases quite closely delineate the intermetallic compounds, FeTi and Fe_2Ti (albeit with minor correction for impurity constituents).

Although commercial ferrotitanium may be helpful for purposes of discussion and illustration, it is noteworthy that clear differences exist between such products and the reduction products herein, particularly in C-content and in process and solidification history. The experimental thermite specimens presented phases that were not easily (straightforwardly) categorised given the effect upon these phases of the minor tramp metal and light element components. In concert with and compounding these alloying complications was the brief and rather awkward process history of these experimental specimens, a history represented in such alloy phases as were determined to have largely retained their compositional integrity – from liquid, through solidification to ambient temperatures – without significant reversion [17, 266]. Expected in potentially reversible reactions, this "reversion" being the predicted light element "re-oxidation" of reactive elements, especially Ti. So, frozen from the *liquid* reduction product of this thermite process, the metallic solidification products bear the following commentary, commentary based upon observation and analyses of those metallic phases, and with reflection upon the thermite reduction process including that accompanying project rarity – solidification from the liquid phase of *all* solid reduction phases.

The reduction product phases all exhibited trace to minor distributions of the central light elements (C, N and O) in compositions that require acknowledgment, if not explanation. (Of itself) the thermite reaction did not promote N-uptake; furthermore, it seems reasonable that N taken into liquid phase solution was acquired in the short post-thermite processing period (during that limited extension of microwave irradiation intended to promote "phase consolidation") before the LN_2 "quench". As a consequence of the specifics of the reaction phase(s) of processing, the overall N-content of thermite reduction products was markedly lower than that typical of other project experimental reduction products. In the various metallic phases represented in the reduction remnants it is possible that a sizeable proportion of the trace to minor fraction of N caught in solid solution may be directly linked in composition with Al (these having a particular affinity). Although there was no means of directly confirming this possibility, it is noted that in the FeTi-type core phase the 0.91 at% Al was matched by 0.08 at% N, whilst in

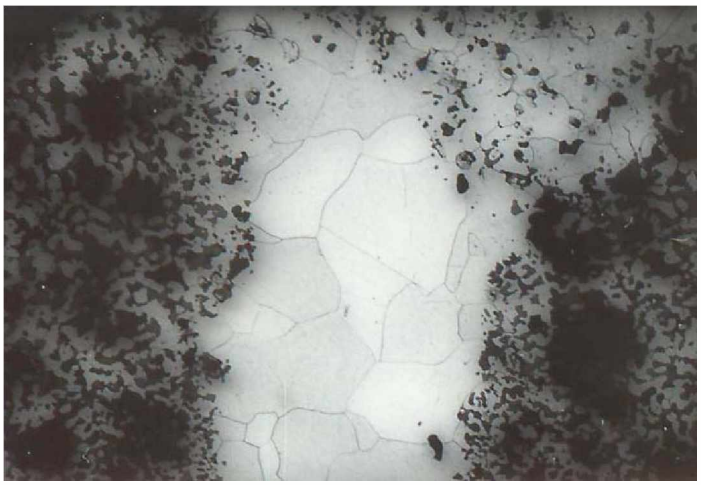

Figure {7.2.4}1: The light optical micrograph of a section through a LN_2 cooled "ferrotitanium" iron thermite reduction product of Australian east coast ilmenite. The "quench" region's "white iron equivalent" surrounds a core region of "ferrotitanium" [$Fe_wTi_x(Cr_yAl_z)C_n$], the grains appearing equiaxed in this section were otherwise elongated. Figure {7.2.4}**2** below shows further detail of the transition zone. This reduction product (specimen ILM**A06**) is representative of those latter trials that proceeded as true thermite reduction exercises to result in primarily metal reduction products. [LOM; fov: 1.06 mm]
[This field was chosen because of its "span" across a limited core region with transition into near-surface "quench" regions and is inclusive of aspects of surface region detail – particularly the "line" delineation between zones, and their transition. The quite apparent brightness difference between core grains did not correlate with phase identity, but may have been directly related to differential crystallographic pitting and/or the "angle of incidence" of the crystal lattices with the metallographic surface – although a conjecturably reasonable suggestion, no crystallographic evidence was sought to support this contention.]

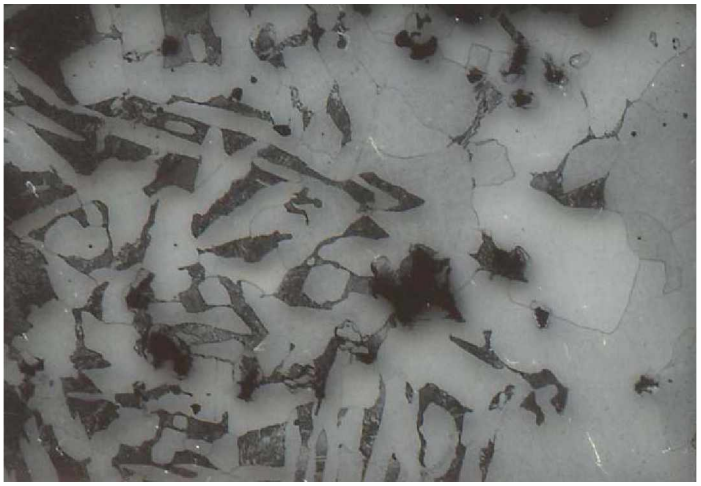

Figure {7.2.4}2: The micrograph shows detail of the transition zone (nital etched and similar to that above) between equiaxed core and beginning of lower alloy carbide phases (etched is cementite) plus associated ferrite – un-etched and, except for morphology, indistinguishable from the ferrotitanium intermetallic phases which are equiaxed and progressive into the transition zone. The darker-etched regions are cementite phase of different alloy, these varied in extent as can be seen in Figure {7.2.4}**1**. [LOM; fov: 0.21 mm]

Table {7.2.4}1: The following table is an assemblage of provisionally quantitative results of EDS analyses of acquisition counts taken on polished fields on newly-reduced metallic phases of aluminothermically reduced ilmenite specimens ILM**A01** to ILM**A12**. Spot counts were acquired from points clearly within the "core" ferrotitanium grains and reported in two distinct phase groups (see page 412), whilst area counts were acquired from "white iron type" areas between the ferrotitanium core region and the exposed outer surface of the solidified metal. The complex "white iron type" microstructure – which was subjected to initial LN_2 freezing – must have contained the highest melting point phases, although in doing so it seems that these regions captured higher light element proportions than did those more equilibrated core region phases. Typical elements of microstructure are represented in the details of Figures {7.2.3}**1** and {7.2.3}**2**. All spot and area EDS counts were acquired using the ultra-thin Be window (UTW) protecting the detector; this option *may* have minimally suppressed the EDS counts for the light elements. Note that the initial three specimens were terminated during trials at times following thermite reaction, and all specimens from ILM**A04** to ILM**A12** were set at 5 min of process time – inclusive of thermite reaction at ~ 3 min.

Specimen. **Analyses of EDS acquisitions from reduction product phases (at%).**

The following EDS counts were **spot** acquisitions by UTW detection.

	Ti	Fe	Cr	Al	C	N	balance
ILM**A01**	47.92	49.23	1.22	0.94	0.48	0.12	0.06 Mn, 0.03 O
(3 min)	48. 11	49.17	0.95	1.07	0.51	0.14	0.03 Zr, 0.02 O
	47.88	50.09	0.97	0.66	0.32	0.06	0.02 V
	48.04	49.22	1.45	0.87	0.26	0.10	0.06 Mn
	47.78	49.95	1.20	0.79	0.17	0.07	0.03 Mn, 0.01 V
Phase 1 mean:	**47.95**	**49.53**	**1.16**	**0.87**	**0.35**	**0.10**	**(0.04)**
	33.13	65.86	0.28	0.40	0.29	0.02	0.02 O
	32.85	66.18	0.21	0.51	0.16	0.05	0.03 V, 0.01 Th
	33.00	65.95	0.25	0.59	0.14	0.05	0.01 Mn, 0.01 O
Phase 2 mean:	**32.99**	**66.00**	**0.25**	**0.50**	**0.20**	**0.04**	**(0.02)**

The following EDS counts were **area** acquisitions by UTW detection.

	Ti	Fe	Cr	Al	C	N	balance
	47.52	46.98	2.43	0.77	2.11	0.10	0.08 Mn,.0.01V
	47.38	48.19	1.89	0.24	2.20	0.04	0.06 Mn
	47.67	47.60	2.36	0.29	1.98	0.05	0.05 Mn
Field mean:	**47.52**	**47.59**	**2.23**	**0.43**	**2.10**	**0.06**	**(0.07)**

The following EDS counts were **spot** acquisitions by UTW detection.

	Ti	Fe	Cr	Al	C	N	balance
ILM**A02**	48.64	49.13	0.96	0.39	0.65	0.18	0. 04 V, 0.01 Mn
(7 min)	48.28	49.88	1.13	0.33	0.28	0.07	0.03 Mn
	48.47	49.20	1.08	0.63	0.46	0.10	0.06 Mn
	47. 93	50.32	0.85	0.42	0.37	0.09	0.02 Mn
Phase 1 Mean:	**48.33**	**49.63**	**1.01**	**0.44**	**0.44**	**0.11**	**(0.04)**
	33.35	65.50	0.26	0.37	0.45	0.06	0.01 Mn
	33.09	65.92	0.14	0.18	0.48	0.14	0.04 Mn, 0.01 V
	32.94	66.01	0.19	0.41	0.37	0.04	0.02 V, 0.02 Mn
Phase 2 mean:	**33.13**	**65.81**	**0.20**	**0.32**	**0.43**	**0.08**	**(0.03)**

Table {7.2.4}1 continued over page/

Table {7.2.4}1 continued/

Specimen. **Analyses of EDS acquisitions from reduction product phases (at%).**

The following EDS counts were **area** acquisitions by UTW detection.

	Ti	Fe	Cr	Al	C	N	balance
ILM**A02** cont./	47.25	48.10	2.02	0.33	2.16	0.08	0.05 Mn, 0.01 O
	47.15	48.21	1.89	0.29	2.34	0.06	0.04 Mn, 0.02 V
	47.40	47.79	2.01	0.76	1.88	0.11	0.05 V
	46.97	47.95	2.36	0.27	2.37	0.04	0.04 Mn
Field mean:	**47.19**	**48.01**	**2.07**	**0.42**	**2.19**	**0.07**	**(0.05)**

The following EDS counts were **spot** acquisitions by UTW detection.

	Ti	Fe	Cr	Al	C	N	balance
ILM**A03**	48 56	48.85	1.34	0.71	0.36	0.15	0.02 Mn, 0.01 V
(4 min)	47.90	49.33	1.06	1.09	0.49	0.08	0.03 V, 0.02 Mn
	48.12	49.28	0.99	1.12	0.29	0.16	0.04 Mn
	47.66	50.40	0.86	0.61	0.35	0.09	0.03 Mn
Phase 1 mean:	**48.06**	**49.47**	**1.06**	**0.88**	**0.37**	**0.12**	**(0.04)**
	33.41	65.47	0.30	0.52	0.16	0.11	0.03 Mn
	31.73	67.57	0.23	0.14	0.25	0.06	0.02 V
	33.16	65.85	0.24	0.44	0.17	0.09	0.03 Mn, 0.02 V
Phase 2 mean:	**32.77**	**66. 30**	**0.26**	**0.37**	**0.19**	**0.08**	**(0.03)**

The following EDS counts were **area** acquisitions by UTW detection.

	Ti	Fe	Cr	Al	C	N	balance
	47.15	48.03	2.16	0.38	2.18	0.05	0.05 Mn
	47.24	48.22	1.89	0.51	2.03	0.06	0.04 Mn, 0.01 V
	46.94	48.26	2.15	0.45	2.13	0.02	0.04 Mn, 0.01 O
Field mean:	**47.11**	**48.17**	**2.07**	**0.45**	**2.11**	**0.04**	**(0.05)**

The following EDS counts were **spot** acquisitions by UTW detection.

	Ti	Fe	Cr	Al	C	N	balance
ILM**A04**	48.22	48.96	0.93	1.39	0.39	0.08	0.02 Mn, 0.01 Ce
(5 min)	47.63	49.41	1.35	0.89	0.58	0.11	0.3 Mn
	47.88	49.62	0.87	0.88	0.46	0.24	0.05 Mn
	47.56	50.24	0.62	1.14	0.26	0.09	0.06 Mn, 0.03 V
Phase 1 mean:	**47.82**	**49.56**	**0.94**	**0.68**	**0.42**	**0.13**	**(0.05)**
	32.89	65.66	0.32	0.72	0.37	0.02	0.02 V
	33.36	65.44	0.19	0.55	0.38	0.03	0.04 Mn, 0.01 V
	32.97	66.03	0.25	0.43	0.29	0.01	0.02 V
Phase 2 mean:	**33.07**	**65.71**	**0.25**	**0.57**	**0.35**	**0.02**	**(0.03)**

The following EDS counts were **area** acquisitions by UTW detection.

	Ti	Fe	Cr	Al	C	N	balance
	47.22	48.34	2.21	0.38	1.76.	0.04	0.04 Mn, 0.01 V
	46.86	48.38	2.28	0.50	1.88	0.04	0.04 Mn, 0.02 V
	47.28	47.92	2.22	0.46	2.01	0.06	0.05 Mn
	47.20	47.98	2.09	0.27	2.37	0.03	0.05 Mn, 0.01 V
Field mean:	**47.14**	**48.16**	**2.20**	**0.40**	**2.01**	**0.04**	**(0.05)**

Table {7.2.4}1 continued/

Only the core phases where analysed on the remaining specimens, ILM**A05** to ILM**A12. It was determined that the "white iron type" regions near the specimen "quench" surfaces would not be typical of the reduction product for an upgraded real process, and so the ferrotitanium core was solely examined in the following EDS analyses. Refer to text for further discussion of the exposed "white iron type" regions.**

Specimen.	**Analyses of EDS acquisitions from reduction product phases (at%).** The following EDS counts were **spot** acquisitions by UTW detection.						
	Ti	**Fe**	**Cr**	**Al**	**C**	**N**	**balance**
ILM**A05**	47.81	49.50	0.94	1.11	0.39	0.17	0.08 Mn
(5 min)	47.80	50.10	1.22	0.41	0.34	0.09	0.03 V, 0.01 Mn
	48.46	48.83	1.18	0.83	0.47	0.11	0.12 Mn, 0.01 La
	47.99	49.64	0.85	0.91	0.50	0.07	0.04 V
Phase 1 mean:	**48.02**	**49.52**	**1.05**	**0.82**	**0.43**	**0.11**	**(0.05)**
	33.08	65.65	0.44	0.41	0.35	0.03	0.04 V
	33.17	65.76	0.23	0.37	0.40	0.03	0.02 Zr, 0.02 Mn
	32.86	66.04	0.23	0.51	0.28	0.04	0.04 V
Phase 2 mean:	**33.04**	**65.82**	**0.30**	**0.43**	**0.34**	**0.03**	**(0.04)**
ILM**A06**	47.92	49.33	1.30	1.05	0.29	0.07	0.02 V, 0.02 Mn
(5 min)	47.59	50.06	0.85	0.94	0.42	0.09	0.05 Mn
	46.88	50.45	0.86	1.25	0.40	0.10	0.05 Mn, 0.01 Ce
	47.89	49.42	1.07	1.13	0.38	0.07	0.03 Mn, 0.01 V
Phase 1 mean:	**47.57**	**49.82**	**1.02**	**1.09**	**0.37**	**0.08**	**(0.05)**
	32.94	66.10	0.20	0.41	0.27	0.04	0.04 Mn
	33.16	66.03	0.28	0.32	0.15	0.02	0.02 V, 0.02 Mn
	33.20	65.80	0.19	0.55	0.18	0.05	0.03 V
Phase 2 mean:	**33.10**	**65.98**	**0.22**	**0.43**	**0.20**	**0.04**	**(0.03)**
ILM**A07**	47.66	50.22	0.94	0.78	0.33	0.04	0.02 V, 0.01 Mn
(5 min)	47.99	49.78	0.89	0.90	0.33	0.06	0.05 Mn
	47.75	49.63	1.13	1.01	0.40	0.03	0.04 Mn,).01Ce
	48.35	49.71	0.79	0.64	0.36	0.08	0.05 V, 0.02 Mn
Phase 1 mean:	**47.94**	**49.84**	**0.94**	**0.83**	**0.36**	**0.05**	**(0.04)**
	33.22	65.67	0.19	0.71	0.16	0.03	0.02 V
	33.08	66.02	0.22	0.38	0.22	0.04	0.04 Mn
	33.10	65.88	0.21	0.48	0.25	0.04	0.03 Mn, 0.01 V
Phase 2 mean:	**33.13**	**65.86**	**0.21**	**0.52**	**0.21**	**0.04**	**(0.03)**
ILM**A08**	47.96	49.29	1.08	1.12	0.43	0.08	0.03 V, 0.01 La
(5 min)	47.84	49.87	0.86	0.83	0.35	0.07	0.04 Mn, 0.02 V
	47.82	49.68	1.11	0.88	0.32	0.14	0.05 V
	47.91	50.18	0.96	0.43	0.37	0.10	0.04 Mn, 0.01 Zr
	47.62	49.79	1.07	1.06	0.36	0.05	0.03 V, 0.02 Mn
Phase 1 mean:	**47.84**	**49.76**	**1.02**	**0.87**	**0.37**	**0.09**	**(0.05)**

Table {7.2.4}1 continued over page/

Table {7.2.4}1 continued/

Specimen.	Analyses of EDS acquisitions from reduction product phases (at%). The following EDS counts were **spot** acquisitions by UTW detection.						
	Ti	**Fe**	**Cr**	**Al**	**C**	**N**	**balance**
ILM**A08** cont./	33.19	65.79	0.26	0.48	0.21	0.04	0.03 V
	32.95	65.94	0.24	0.64	0.16	0.03	0.03 Mn, 0.01 V
	33.10	66.05	0.18	0.43	0.19	0.02	0.03 Mn
Phase 2 mean:	**33.08**	**65.93**	**0.23**	**0.51**	**0.19**	**0.03**	**(0.03)**
ILM**A09**	47.83	50.11	0.92	0.63	0.39	0.06	0.04 Mn, 0.02 V
(5 min)	48.23	49.85	1.06	0.41	0.34	0.06	0.05 Mn
	47 66	49.84	0.88	1.17	0.37	0.04	0.02 V, 0.02 Mn
	47.91	49.97	0.75	0.83	0.40	0.06	0.07 Mn, 0.01 V
Phase 1 mean:	**47.91**	**49.94**	**0.90**	**0.76**	**0.38**	**0.06**	**(0.05)**
	32.96	66.37	0.18	0.21	0.23	0.02	0.03 V
	33.31	65.78	0.21	0.48	0.15	0.03	0.04 Mn
	32.79	65.98	0.22	0.74	0.21	0.03	0.03 Mn
Phase 2 mean:	**33.02**	**66.04**	**0.20**	**0.48**	**0.20**	**0.03**	**(0.03)**
ILM**A10**	46.82	50.34	1.26	1.05	0.44	0.05	0.04 Mn
(5 min)	47.73	49.51	0.89	1.33	0.45	0.04	0.04 Mn, 0.01 V
	46.64	50.61	0.94	1.28	0.35	0.11	0.06 Mn, 0.01 La
	47.85	49 82	1.03	0.79	0.37	0.09	0.05 V
	47.36	49.69	0.90	1.47	0.34	0.15	0.05 Mn, 0.04 V
Phase 1 mean:	**47.28**	**49.99**	**1.01**	**1.18**	**0.39**	**0.09**	**(0.06)**
	33.09	65.65	0.19	0.76	0.25	0.03	0.03 V
	33.17	65.87	0.22	0.46	0.21	0.04	0.02 Mn, 0.01 V
	32.95	66.21	0.18	0.39	0.22	0.03	0.02 V
	33.08	66.14	0.17	0.27	0.26	0.03	0.03 Mn, 0.02 V
Phase 2 mean:	**33.07**	**65.97**	**0.19**	**0.47**	**0.24**	**0.03**	**(0.03)**
ILM**A11**	47.35	49.88	1.09	1.18	0.38	0.07	0.03 V, 0.02 La
(5 min)	47.85	49.78	0.86	0.95	0.42	0.08	0.06 Mn
	47.76	50.23	0.58	0.96	0.36	0.07	0.03 Mn, 0.01 V
	47.28	50.19	1.06	0.97	0.35	0.10	0.05 Mn
	47.39	49.96	1.00	1.13	0.36	0.09	0.04 Mn, 0.03 V
Phase 1 mean:	**47.53**	**50.01**	**0.92**	**1.04**	**0.37**	**0.08**	**(0.05)**
	32.92	66.22	0.19	0.38	0.23	0.02	0.04 Mn
	33.37	65.77	0.24	0.37	0.18	0.04	0.02 V,0.01 Mn
	32 95	65.98	0.22	0.59	0.20	0.03	0.03 V
	33.14	65 66	0.26	0.66	0.21	0.03	0.03 Mn, 0.01 V
Phase 2 mean:	**33.10**	**65.91**	**0.22**	**0.50**	**0.21**	**0.03**	**(0.03)**

Table {7.2.4}1 continued over page/

Table {7.2.4}1 continued/

Specimen.	Analyses of EDS acquisitions from reduction product phases (at%). The following EDS counts were **spot** acquisitions by UTW detection.						
	Ti	**Fe**	**Cr**	**Al**	**C**	**N**	**balance**
ILM**A12**	47.35	49.99	0.88	1.30	0.37	0.06	0.04 Mn, 0.01 V
(5 min)	47.28	50.36	1.14	0.64	0.42	0.09	0.04 V, 0.03 Mn
	47.81	49.84	1.07	0.79	0.31	0.12	0.06 Mn
	47.44	50.11	0.89	1.07	0.34	0.08	0.05 Mn, 0.02 V
	48.12	49 65	0.69	1.02	0.38	0.08	0.04 Mn, 0.02 La
Phase 1 mean:	**47.60**	**49.99**	**0.93**	**0.96**	**0.36**	**0.09**	**(0.07)**
	33.17	66.04	0.21	0.34	0.19	0.03	0.02 V
	32.74	66.18	0.21	0.56	0.22	0.04	0.03 Mn, 0.01 V
	33.14	65.86	0.25	0.46	0.20	0.04	0.05 Mn
	33.06	65.79	0.22	0.69	0.19	0.02	0.02 V, 0.01 Ce
Phase 2 mean:	**33.03**	**65.97**	**0.22**	**0.51**	**0.20**	**0.03**	**(0.04)**

The average of the four area-assessed mean analyses of fields from counts acquired from near-surface "quench" regions (at%):

"Quench" region:

47.24 at% Ti; 47.98 at% Fe; 2.14 at% Cr; 0.43 at% Al; 2.10 at% C; and 0.06 at% N; with (0.05 balance).

The average of the 9 spot-assessed mean analyses of Phase 1 (from 5 min specimens ILM**A04** to ILM**A12** only:

Phase 1:

47.72 at% Ti; 49.83 at% Fe; 0.97 at% Cr; 0.91 at% Al; 0.38 at% C; and 0.08 at% N; with (0.3 balance).

This is close to the base **FeTi** intermetallic compound.

The average of the 9 spot-assessed mean Phase 2 analyses (from 5 min specimens ILM**A04** to ILM**A12** only:

Phase 2:

33.07 at% Ti; 65.91 at% Fe; 0.23 at% Cr; 0.49 at% Al; 0.24 at% C; 0.3 at% N; with (0.03 balance).

This is close to the base **Fe_2Ti** intermetallic compound.

the Al-leaner Fe_2Ti-type phase the 0.49 at% Al was matched by 0.03 at% N. In terms of such associative trends in composition, less can be inferred about C as it is preferentially favoured by each of Ti, Cr and Fe; and of these, Ti has an aggressive "getting" tendency toward N, above that of Cr and Fe. With respect to N and its possible solid solution associations in the composition and structure of the surface region, nothing ought be inferred from the multi-phase field-acquired composition. However, it can be seen in the summary of compositions in Table **{7.2.4}1** that the quench frozen surface regions of the reduction product remnants are markedly higher in C than core phases; this solidification event was not accidental. Rather, contemporaneous with entrained thermophysical events, the precedence of C-depletion was coincident between the levelling-out of the quench curve (quench rate) and requisite phase chemistries of the remnant intermetallic compounds – the cuspidal balance between the cooling rate and the core metal compositions.

A most notable general observation of the thermite reduction product phases was their relatively low light element (C, N and O) compositions in comparison to other reduction products of the project (and to commercial ferrotitanium, and ferrometals generally This suppressed C-content in thermite reduction phases was directly related to the "opportunity for C-uptake" during reduction processing. In the reaction zone, residence time at elevated heat was restricted by the alumino-centric nature of the thermite reaction, thence with a limited extension at reduction temperature before quench termination, the processing time was short compared to other experimental procedures of the project. The C-uptake was regulated by prevailing thermochemistry, and this limited "time-at-temperature" directly translated as limited reaction opportunity at reaction interfaces and/or limited solution chemistry in liquid phase metal. At the point of the LN_2 quench, the C-in-liquid was "partitioned" by phase-compositional demand-driven preferential freezing of those exposed surface-region phases. These high cooling rate phases acquired their C from the available liquid metal until either the available C was depleted, or (as in this case) the cooling rate curve flattened-out (from "quench" rates to the modest rate which allowed the solidification syntheses of those low-C core phases attained in the reduction product remnants of this experimental section). The common low-C status of the reduction product liquid was the bare pre-condition that indirectly determined this "C-partitioning", initially allowing the development of the C-abundant "white iron type" microstructure in the "quenched"

surface regions, subsequently (from C-depleted liquid) allowing crystallisation and growth of the prismatic crystals in the core regions of reduction remnants (resulting in the microstructural development exhibited in Figures {7.2.4}**1** and {7.2.4}**2**).

Moreover, the "ferrotitanium" products of microwave-stimulated thermite reduction of ilmenite were in keeping with the results either indicated by COURDURIER, *et al* [17] or reported by analyses or characterisation by JAMRACK [30] and MILLER [7], whilst considerable technical discussion regarding the plasma processes available to reduction strategies for ilmenite and comparable source minerals is provided by DEMBOVSKY [58]. DEMBOVSKY describes methods of production (from ilmenite to ferrotitanium, including to direct Ti-production) both at an industrial scale and under advanced "development stage" conditions in high energy applications. It is clear that real attention ought be paid to the potential exhibited in the results of this experimental section; the microwave-stimulation means provided a thermite initiation mechanism that, undoubtedly, proved superior to those initiation mechanisms of thermite methods of previous investigations. Also, metallurgically and compositionally, the very material characteristics of the metallic reduction product of the above experimental thermite process – whilst requiring further product analysis and system development – by merit of its evident "quality" and reproducibility, demands serious attention.

7.3: Reduction of ZrO_2 , HfO_2 and Zirconium-Bearing Mineral Zircon.

Zirconium and hafnium minerals represented the most thermochemically obdurate set of minerals confronted in the project. They have the reputation of being notoriously difficult to reduce, even given the most accommodating processing circumstances. During early microwave system development, some "nominally *un*successful" reduction trials on zirconia (as baddeleyite) and some modestly successful trials on zircon were the sum total of preliminary investigations. However, further along the "learning curve" of project development, after quite some "technique refinement" of the microwave oven set-up method of reduction, moderate success was...

surface regions, subsequently (from C-depleted liquid) allowing crystallisation and growth of the prismatic crystals in the core regions of reduction remnants (resulting in the microstructural development exhibited in Figures {7.2.4}**1** and {7.2.4}**2**).

Moreover, the "ferrotitanium" products of microwave-stimulated thermite reduction of ilmenite were in keeping with the results either indicated by COURDURIER, *et al* [17] or reported by analyses or characterisation by JAMRACK [30] and MILLER [7], whilst considerable technical discussion regarding the plasma processes available to reduction strategies for ilmenite and comparable source minerals is provided by DEMBOVSKY [58]. DEMBOVSKY describes methods of production (from ilmenite to ferrotitanium, including to direct Ti-production) both at an industrial scale and under advanced "development stage" conditions in high energy applications. It is clear that real attention ought be paid to the potential exhibited in the results of this experimental section; the microwave-stimulation means provided a thermite initiation mechanism that, undoubtedly, proved superior to those initiation mechanisms of thermite methods of previous investigations. Also, metallurgically and compositionally, the very material characteristics of the metallic reduction product of the above experimental thermite process – whilst requiring further product analysis and system development – by merit of its evident "quality" and reproducibility, demands serious attention.

7.3: Reduction of ZrO_2 , HfO_2 and Zirconium-Bearing Mineral Zircon.

Zirconium and hafnium minerals represented the most thermochemically obdurate set of minerals confronted in the project. They have the reputation of being notoriously difficult to reduce, even given the most accommodating processing circumstances. During early microwave system development, some "nominally *un*successful" reduction trials on zirconia (as baddeleyite) and some modestly successful trials on zircon were the sum total of preliminary investigations. However, further along the "learning curve" of project development, after quite some "technique refinement" of the microwave oven set-up method of reduction, moderate success was

achieved in reducing the pure oxides, and somewhat greater success in reducing the mineral-sands-derived mineral zircon ($SiO_2.ZrO_2$).

In keeping with the thermochemical obduracy of zirconia and hafnia, reduction experimentation trials on these oxides were conducted with a heightened degree of process awareness and experimental care regarding the retention of peak reduction phases and prevention of their re-oxidation.

7.3.1: Carbothermic and Aluminothermic Reduction of ZrO_2 .

Charges of mill-blended zirconia/char blend, thence charges of mill-blended zirconia/Al/char blend (each as per Appendix **6.2**) were, under granular char, reduction processed utilising the established microwave-stimulated oven set-up method. In conformity with the abovementioned thermochemical nobility of zirconia (ZrO_2), and of the heightened process awareness and care required to maximise the prospect of reduction success and product recovery, every care was taken to recover peak reduction product phases for analyses and so establish confirmation of concept. Principally, under conditions of reduction processing, the procedural sequence was supervised such as to effectively circumvent that controlling operational limitation imposed by such system atmospheric environment as allowed by the microwave oven set-up method. Of the recovery of peak reduction phases, confirmation of such achievement was contingent upon the prevention of their re-oxidation between the point of their initial reduction, through further processing and the termination of microwave reduction processing, to the effective end of quench.

Compliant with this task, a number of attentively controlled experimental trials on the microwave-stimulated *carbothermic* reduction of zirconia were attempted, and for this core sub-section of the experimental programme all reduction results failed to produce a metallic or advanced reduction product phase that could, beyond fair discussion, be meaningfully reported here as representing the analytical results from a reduction product metallic phase. In that some reduction had taken place, (and disregarding for the moment the "reversion products" aspect) it is true that such "less

than metallic" phases were reduction products. Also, it must be mentioned ahead of reporting such in Section **7.3.3** that, by contrast, the zirconia fraction of zircon in the carbothermic reduction of the ex-minesite mineral *did* reduce to yield a metallic Zr-phase. (Comment on that general result and speculation regarding a proposed mechanism is appropriately left until that section.) However, as none of these straight carbothermic trials on pure ZrO_2 produced *undeniably* metallic reduction products, it was decided not to reproduce these acquisition results here merely for the sake of doing so, but to concede that (particularly under the prevailing "marginal" system conditions) such "inconclusive" outcomes were an "equitable experimental eventuality" for such thermochemically challenging cases and to plainly report the fact as such – a result which should be viewed in cognisance of the zircon outcome.

Nevertheless, if given the benefit of atmospheric protection in a working microwave reactor (incorporating the previously described experimental configuration), it is considered that the purely carbothermic reduction of ZrO_2 would be readily attainable. This claim is made in respect of the clear evidence (in those unreported carbothermic trials) of some near-complete reduction phases prior to their re-oxidation at process end to leave reversion phases (as re-oxidation products). As they manifested in the facies of reduction remnants, the presence of "reversion phases" in microscopic fields could be readily observed as re-oxidation outwardly *around* evident prior-reduced phase material whilst the remaining "reduced" material was liable to have been partially re-oxidised by short-term diffusion (until quenching took effect). The visual appearance of the phase components in reversion facies suggested the procedural reverse of the reduction sequence, however, such reversion phases did not (as, indeed, they *can not*) return to their original fully oxide form, but remain a "light element oxide".

Including those reversion phases, the carbothermic reduction product phases which remained after quenching were Zr-oxycarbonitride ($ZrO_xC_yN_z$, $x < y + z$) phases exhibiting some visual metallic characteristics (colour and sheen) but no definite physical metallic characteristics. These carbothermic product phases were present generally as small, distinct phase entities distributed through the reduction product remnants. Further, in choosing to omit the reporting of actual *carbothermic* EDS acquisition results, it was decided that the reporting of the alternative *aluminothermic* acquisition results of the reduction of ZrO_2 (particularly as it was carbothermically

assisted) suitably presented an adequate account of reduction for this challenging section – a touchstone section of experimentation when evaluating the promise of future microwave reduction project extensions.

Accordingly, the sufficient if few results reported in this section represent microwave-stimulated *aluminothermic* reduction of zirconia. (With reference to metallothermic reduction propensities for ZrO_2 , attention is drawn to the "*thermite* observation" in the introduction to Section **7.2.2** relating the foreseen marginal reducibility of ZrO_2 by Al.) Microwave-stimulated reduction of a charge of the mill-blended, char-boosted aluminothermic ZrO_2 blend in the thermite crucible configuration (to allow for contingencies associated with possible, although unanticipated, process volatility) provided Zr-metallic reduction products in varying quantities. Although the degree of reduction was generally reproducible in reduction products of these Zr-metallic products, that *degree of reduction* in metallic phase material did not clearly exhibit an increase with increased processing time. And, although a *general* increase in quantity of reduced material was indicated with increased processing time, any *absolute* variation in quantity and form of metallic reduction product appeared to be discretely dependent upon ***no*** specific fact or discernable operational parameter. In fact, such factors of quality and quantity appeared to depend upon the procedural vagaries of microwave-driven heating in a heterogeneous load through to plasma reaction in the limited and confined volume such that the experimental configuration offered. Evidence of this prevailing "degree of reduction" plateau across all (8 min and 10 min) specimens can be seen in the EDS results of Table **{7.3.1}1** whilst, if somewhat amplified by the choice of contrasting micrographic examples, Figures **{7.3.1}1** and **{7.3.1}2** show the disparity in quantity of metallised product between 8 min and 10 min specimens.

Unlike the equivalent rutile and anatase exercises, negligible un-reacted metallic Al presented in zirconia reduction product remnants. Also, metallic reduction product phases were dispersed through the sparse, porous structural network of remnant partially-reduced zirconia plus reduction product Al_2O_3 – with little evidence of other, incidental slag components (Si- and Fe-oxides from insulation refractories) elsewhere common in the slag phases of experimental trials. Such incidental, refractory-derived oxides were common in the slags of most of the project's reduction exercises, however, they were unexpectedly uncommon in reduction trials of this zirconia section. This

Table {7.3.1}1: The table shows EDS analyses results of spot counts acquired from Zr-metallic phase fields in polished section of mounted reduction product of the microwave-stimulated aluminothermic reduction of zirconia, ZrO_2 . The campaign time for trial specimens ZRCA**A1** to ZRCA**A4** was 8 min whilst for ZIRA**A5** and ZRCA**A6** the time was 10 min from start to quench. As the analyses corroborate, the metal product of ZIRA**A2** is the least reduced specimen (that is, the specimen exhibiting the least advanced degree of reduction) whilst the most advanced reduction was evident in the most processed (10 min) specimens, ZRCA**A5** and ZRCA**A6**. Every care was taken to site the beam spot such as to only excite particles from within the volume boundaries of the intended target phase, however, some proportion of the Al and O counts could reasonably be attributed to excitation of phase material outside the volume of the target phase.

Specimen.	**EDS analyses from spot acquisitions of redn. product phase (at%).** All EDS acquisitions are spot acquisitions by windowless detection.					
	Zr	**C**	**N**	**O**	**Al**	**balance**
ZRCA**A1**	87.41	3.04	4.55	3.96	0.88	0.16 Ti
(8 min)	86.15	3.25	5.08	3.91	0.74	0.67 Hf, 0.13 Ti, 0.07Fe
	87.98	2.97	4.66	2.54	0.90	0.65 Hf, 0.30 Ti
	94.07	3.22	1.70	0.33	0.34	0.31 Hf, 0.03 Ti
	93.43	2.81	1.52	0.26	1.12	0.65 Hf, 0.21 Fe
	88.93	3.44	4.67	2.58	0.31	0.07 Hf
Spec. mean:	**89.66**	**3.12**	**3.70**	**2.26**	**0.72**	**(0.54)**
ZRCA**A2**	78.94	4.80	7.02	8.25	0.44	0.51 Hf, 0.04 Ti
(8 min)	82.87	5.11	5.67	5.82	0.27	0.24 Hf, 0.02 Ti
	81.89	4.62	6.86	4.61	1.08	0.86 Hf, 0.05 Ti, 0.03 V
	83.35	3.95	5.97	5.78	0.48	0.47 Hf
	82.88	4.62	6.18	5.54	0.37	0.39 Hf, 0.02 Ti
Spec. mean:	**81.99**	**4.62**	**6.34**	**6.00**	**0.53**	**(0.52)**
ZRCA**A3**	88.09	3.33	4.38	3.05	0.96	0.11 Hf, 0.08 Ti
(8 min)	87.41	3.38	4.39	3.80	0.76	0.26 Hf
	88.19	4.22	4.03	2.69	0.56	0.31 Hf
	89.27	3.40	3.89	2.60	0.67	0.09 Ti, 0.08 Hf
	87.88	2.95	4.22	3.31	0.92	0.70 Hf, 0.02 Ti
Spec. mean:	**88.17**	**3.46**	**4.18**	**3.09**	**0.77**	**(0.33)**
ZRCA**A4**	87.97	3.43	4.47	3.24	0.21	0.65 Hf, 0.03 Ti
(8 min)	88.18	4.11	4.06	2.90	0.49	0.26 Hf
	88.93	4.01	3.86	2.64	0.37	0.19 Hf
	87 54	3.55	4.75	3.24	0.64	0.25 Hf, 0.03 Ti
	87.77	3.92	4.14	3.27	0.56	0.23 Hf, 0.11 Ti
Spec. mean:	**88.08**	**3.80**	**4.26**	**3.06**	**0.45**	**(0.35)**
ZRCA**A5**	88.29	4.10	4.96	2.15	0.19	0.29 Hf, 0.02 Fe
(10 min)	88.90	4.07	5.13	1.65	0.17	0.08 Hf
	89.22	3.98	5.18	1.41	0.09	0.08 Hf, 0.04 Fe
	88.76	4.28	4.87	1.89	0.09	0.11 Hf
	88.58	4.57	3.85	2.60	0.26	0.09 Ti, 0.05 Hf
Spec. mean:	**88.75**	**4.20**	**4.80**	**1.94**	**0.16**	**(0.15)**

Table {7.3.1}1 continued/

Specimen.	EDS analyses from spot acquisition of redn. product phase (at%). All EDS acquisitions are spot acquisitions by windowless detection.					
	Zr	**C**	**N**	**O**	**Al**	**balance**
ZRCAA**6**	89.08	4.08	5.11	1.38	0.26	0.09 Hf
(10 min)	88.84	4.16	4.77	1.58	0.33	0.30 Hf, 0.02Fe
	88.68	3.91	5.46	1.59	0.19	0.09 Ti, 0.08 Hf
	87.89	4.45	4.76	2.30	0.32	0.25 Hf, 0.03 Ti
	88.29	4.74	5. 09	1.49	0.25	0.09 Hf, 0.05 Fe
	88.36	4.12	4.95	1.98	0.41	0.16 Hf, 0.02 Ti
Spec. mean:	**88.52**	**4.24**	**5.02**	**1.72**	**0.29**	**(0.21)**

Averaged mean composition of metallic zirconia reduction products across all six specimens: 87.52 at% Zr; 3.91 at% C; 4.72 at% N; 3.01 at% O; 0.49 at% Al, with the trace balance (0.35 %) present principally as Zr-analogue impurity Hf.

(Each unto the other, (as analogue elements) Zr and Hf are progenitor impurity elements in their primitive source mineral(s) and consequently are the primary impurity in the other's "refined" minerals.)

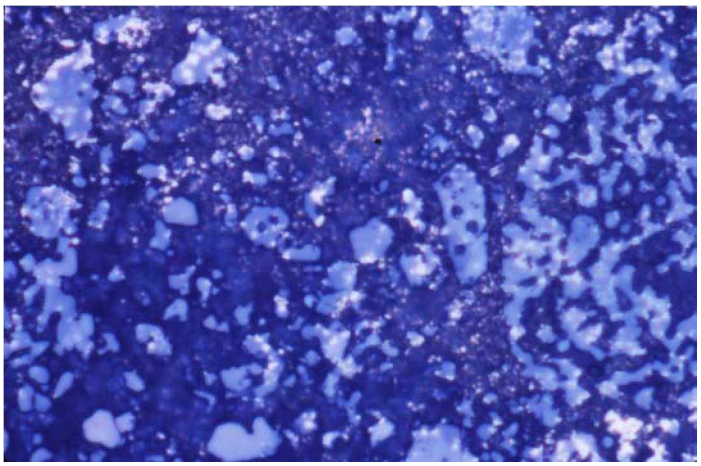

Figure {7.3.1}**1:** Light optical micrograph (under an air lens) showing Zr-metallised regions in the polished surface of specimen ZRCA**A1** highlighting the generally porous nature of the reduction remnants, with the true facies of the remnant possibly reduced by granular attrition (of reduction phase "particles") removed during polishing. Much of this field of view is that porosity, mounting-plastic-filled (deep blue), and the lighter phases are the reduction products; the small, restricted bright (white) phase being Zr-metallic and the blue-grey phases are partially reduced ZrO_2 plus reduction product Al_2O_3 – in varying degrees of mixing. The 8 min specimens ZRCA**A1** to ZRCA**A4** exhibited less metallic reduction phase material than did 10 min specimens ZRCA**A5** and ZRCA**A6** (as can be seen in Figure {7.3.1}**2** below). However, between the 8 min and 10 min specimens, the apparent degree of reduction of the metallic-Zr products is comparable – the *quantity* of product was the principal distinguishing feature. As could be expected in non-thermite aluminothermic reactions – with greater chance of oxidation – negligible metallic-Al reductant remnant was evident in reduction remnants across all specimens (and none is visible in the above field or that below). [LOM, air lens; Ektachrome; fov: 0.21 mm.]

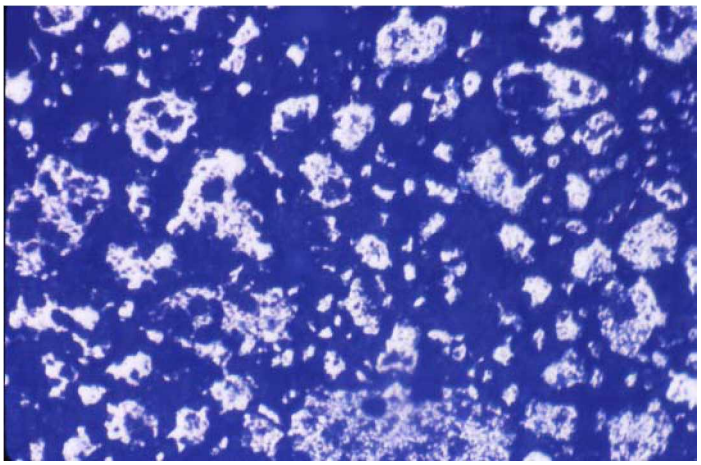

Figure {7.3.1}**2:** Light optical micrograph (under an oil immersion lens) showing Zr-metallised regions in the polished surface of 10 min specimen ZRCA**A5** highlighting the generally disparate scatter of barely interconnected and otherwise loose sections of reduction product phase in a field representative of phases in a region of advanced reduction. Whilst the field of previous Figure {7.3.1}**1** represented reduction product remnants at the "lean" end of the reduction spectrum, the above field shows phases which are generally at an advanced stage of metallisation with only sparsely distributed, limited regions still in the "ceramic" state. The deep blue matrix is mounting plastic. [LOM, oel; Ektachrome; fov: 0.53 mm.]

divergence was also true for the corresponding trace presence of components Si and Fe in Zr-metallic reduction phases. However, like those thermite titania reduction products, the aluminothermic reduction products of zirconia were disseminated particulate phases displaying only modest evidence of phase-softening beyond sintering (where such was possible). Such Zr-metallic phases were disseminated through incompletely reduced zirconia and interspersed by excess char, the negligible un-reacted Al and the Al_2O_3 oxidation product of the reductant Al-metal powder. Whilst not specified by the supplier as the common and obdurate zirconia polymorph baddeleyite, the ZrO_2 used in the experimental blends was a fine PDZ-synthesised "SF-ultra 0.5" grade Z-Tech zirconia, a commercially pure grade* of ZrO_2 (which, when considered in hindsight, was perhaps more reducible than the similarly fine laboratory grade baddeleyite used in early experimental studies). Such a size range in starting zirconia dictates that accretion of particles of either or both the ZrO_2 and/or the reduced Zr-metallic phase took place during the higher temperature stages of the microwave reduction process. Despite its lower magnification, the metallic phase material shown in the micrographic field of Figure **{7.3.1}2** presents clear evidence of sinter agglomeration, particularly in larger metallic entities, whilst there is nil-to-limited evidence of liquid phase accretion.

The EDS analyses of metallic reduction product phases of the microwave-stimulated aluminothermic reduction of intimately ring-milled zirconia/Al/char blend, as represented in Table **{7.3.1}1**, characterise that general phenomenon (which typifies the reduction exercises of this project) of joint O-reduction with concurrent C- and N-re-oxidation "uptake" in the interim reduction product – be it partially reduced oxide material or reduced metal. It should be noted that, as a "rule of thumb" observation, the last %O content vestiges are the most difficult [O] to chemically remove in any reduction operation. Correspondingly, the concurrent first %C and %N uptakes are the hardest to prevent. Consequently, the percentage levels of light element components in the range of reduction product Zr-metallic phases are considered to be acceptable. Indeed, the percentage of [C,N] in the Zr reduction product metal remained considerably lower than comparable Ti-metallic reduction product – probably a statement of the state of "over-processing" in titania specimens at equivalent times, titania arguably having been reduced to a comparable degree in less processing time

* Z-Tech zirconia:Fe_2O_3: 64 ppm; SiO_2: 27 ppm; TiO_2:137 ppm; Al_2O_3: 10 ppm; and sulphur: 73 ppm with particle size distribution: D_{90} = 1.73 μm, D_{50} = 0.52 μm, and D_{10} = 0.18 μm (by Microtrac).

than zirconia, regardless of reductant. The trace to minor impurity element component "balance" is of no particular significance in such experimentation and owes more to the idiosyncrasies of "process reality" in experimental extractive metallurgical systems than to "process purity" (an unattainable concept in such work).

Under either air or oil emersion lens examination of the phase-sparse fields on these (and comparable) mounted specimens the inescapably greater areas of transparent mounting medium – usually pressure-mounted thermosetting plastic or volume-constant cold setting resin – which, in returning (by composite internal reflection/refraction) a high proportion of the total incident illumination, accordingly, returned a significant proportion of the daylight-blue-filtered incident light to the observer, and to the camera. Consequently, the broader micrographic fields captured under such conditions of illumination are dominated by this blue hue, however, *reflected light from actual reduction phase surfaces of polished specimens are recorded as "colour true"*. (The daylight blue filter was utilised whilst capturing colour micrographs to compensate for the daylight bias of the Ektachrome film by correcting (in the system's incandescent filament illumination) for the "white light to daylight shift" in film stock chemistry – that is, correcting for *colour temperature*.) This "blueness" in micrographs is undoubtedly more conspicuous in fields of the more feature-sparse specimens such as are exhibited in specimens of this section, and in specimens of comparable reduction products. Inevitable in genuine specimen fields, such saturation "field blueness" is of micrographical "nuisance" consequence only as it singularly impacts non-opaque phases – phases that represent neither reactants nor reduction products. Typically through this project, transparent phases are representative of mounting medium, which are of no specific interest in analyses or characterisation studies. Whereas, the colour-detail reproduction in micrographs of reactant and reduction product phases is complimented by the daylight blue illumination.

The abovementioned sparsity across micrographic fields of reduction product phases is evident in the micrographs of Figures **{7.3.1}1** and **{7.3.1}2** which present fields at each end of the "successful" reduction range – the reduction continuum between initial reduction and advanced reduction (and before over-processing became a conspicuous factor). However, the contracted, fractured reduction product entities evident in the micrographs *are* representative of actual "captured" sections of reduction

remnants, despite the little evidence to substantiate the contention of a continuum of material in the "fabric" of reduction product remnants.

7.3.2: Carbothermic and Aluminothermic Reduction of HfO_2 .

Categorically, HfO_2 is more thermochemically stable than is the more common ZrO_2 , its physicochemical analogue. This greater nobility was revealed (it seems) in results of the microwave-stimulated reduction routes – both carbothermic and char-augmented aluminothermic – of hafnia (HfO_2) in intimate ring-milled blend forms (as per Appendix **6.2**) using the usual microwave oven set-up method. Whilst recognising the potential for experimental disappointment (necessitating repetition) arising from system inadequacy in light of the thermochemical challenge presented by the reduction assignments of this section, experimental economy was essential as a limited quantity only of laboratory grade HfO_2* was available for experimental reactant blends. This material scarcity together with the degree of reduction difficulty necessitated that the highest level of care be afforded in setting-up the experimental configuration, with commensurate caution being observed during actual experimental reduction processing trials. Initial trials were conducted utilising the microwave-stimulated carbothermic route, and the route that offered a greater prospect of success – the aluminothermic route – was to take-over as soon as a negative outcome for the carbothermic route became clear. (The basic inadequacy of the lesser thermochemical route was anticipated following the zirconia reduction outcomes).

Consequently, for this most thermochemically difficult of reduction tasks undertaken in the project, the few vigilantly overseen experimental trials conducted

---

* The laboratory grade of HfO_2 used in experimental blends was 98% purity (principal impurity ZrO_2); – 325 mesh (particle sizes up to 44 μm). [Note that the particles of this HfO_2 would comprise a distribution of finer sizes after the blend mixture was intimately mill-blended to a consistency where particles of all components were of comparable size range – the size ranges and distributions were somewhat captured by the physical properties of the blend-component fractions (the char being comparably brittle whilst, desirably, the Al powder tended to "smear" onto adjacent particles, and some attrition was expected in the hafnia powder, particularly of the larger particles. Blend consistencies were always visually appraised under stereomicroscope. Deemed unnecessary at the time of experimentation, quantitative size range and size distribution analyses of reactant blends were unavailable to the project. (Of this perceived non-necessity) "hindsight" may suggest otherwise.]

under the *carbothermic* route failed to produce reduction product phases that could be attributably recognisable as metallic phases. Again, as with the zirconia reduction results, the microwave-stimulated carbothermic hafnia reduction result produced only a modicum of recognisable reduction outcomes (as "oxycarbonitride" phases), even with the heightened attention during processing. Furthermore, in these predominantly ceramic phase regions, as no advanced *metallic* Hf-phase was produced, no EDS analyses are reported for carbothermic reduction product phases. (Given a modestly greater energy input capacity and a more controlled system environment, microwave-stimulated carbothermic reduction of hafnia could clearly have been achieved.)

Nevertheless, if modest, definite metallic phase results were recorded for the reduction trials of char-assisted aluminothermic reduction of HfO_2 utilising the microwave oven set-up method, and analyses of such metallic Hf-phases are reported in Table **{7.3.2}1**. The light optical micrograph of Figure **{7.3.2}1** presents a field of view on the polished surface of specimen HAFN**A2** showing both incompletely reacted hafnia phases broken by reduced Hf-metal in dispersed regions just expansive enough to allow clean EDS acquisitions. The field is typical of fields of view across all four specimens with the manifestation of the metallic phase reminiscent of the micro-arcing tracks of primitive processing stages – an observation which may explain the concentration of reduction in the metallic phases, and the relative difference in the "degree of reduction" between the metal and the next reduction stage represented by the pale grey "oxycarbonitride" phase. In the Figure **{7.3.2}1** micrograph it can be plainly seen that clear EDS acquisition sites on metal for "clean" spot counts were comparatively scarce, whilst clean sites on other phases were also sparingly distributed through reduction remnants which generally reflected the incompleteness of process reduction. Such "reduction under-processing" of specimen charges under microwave irradiation was as much a consequence of a desire not to "over-process" reduced phases beyond the solid solution stages into the metallic compound stages as it was a consequence of reduction intransigence.

Given the limited blend material available to each trial, the "imperative of success" arose at each blend charge put to reduction, and experimental caution heightened over reduction phase "legitimacy" and categorisation of reduction products and processing. A note of caution was also observed for the "absolute verification"

Table {7.3.2}1: The table shows EDS analyses results of spot counts acquired from Hf-metallic phase fields in polished section of mounted reduction product of the microwave-stimulated aluminothermic reduction of hafnia, HfO_2 . The processing time for trial specimens HAFN**A1** and HAFN**A2** was 8 min whilst for HAFN**A3** and HAFN**A4** the time was 10 min from start to quench. With only minor variation, analyses across the specimens reveal a general consistency of composition for the metallic reduction product phases. Again, because of the very small target volumes analysed, there was suggestion that a minor proportion of particle excitation originated in oxide phase material neighbouring the target metallic phase. Every care was taken to site the beam spot such as to only excite particles from within the volume boundaries of the intended target phase, however, some proportion of the Al and O counts could reasonably be attributed to excitation of material outside the volume of the target phase.

Specimen.	**EDS analyses of spot acquisitions from redn. product phase (at%).** All EDS acquisitions were spot acquisitions by windowless detection.					
	Hf	**C**	**N**	**O**	**Al**	**balance**
HAFN**A1**	85.86	4.35	5.01	2.30	1.17	1.31 Zr
(8 min)	84.66	4.74	5.85	2.63	1.11	0.94 Zr, 0.07 Fe
	84.95	5.09	4.88	3.43	0.90	0.64 Zr, 0.11 Ti
	86.22	4.35	5.19	3.14	0.67	0.43 Zr
	83.74	5.52	5.28	3.77	1.41	0.26 Zr, 0.02 Si
Spec. mean:	**85.09**	**4.81**	**5.24**	**3.05**	**1.05**	**(0.76)**
HAFN**A2**	83 81	5.42	5.30	2.95	2.06	0.45 Zr, 0.01 Fe
(8 min)	84.29	5.07	4.38	4.40	1.56	0.27 Zr, 0.03 Si
	84.16	4.98	5.44	3.73	1.42	0.27 Zr
	85.67	5.00	4.85	3.16	0.90	0.42 Zr
	84.94	4.62	5.66	3.07	1.32	0.37 Zr, 0.02 Si
Spec. mean:	**84.57**	**5.02**	**5.13**	**3.46**	**1.45**	**(0.37)**
HAFN**A3**	85.65	4.38	4.47	3.93	1.18	0.38 Zr, 0.01 Si
(10 min)	86.22	4.48	4.89	3.28	0.86	0.27 Zr
	85.61	5.03	4.23	4.28	0.67	0.18 Zr
	88.25	4.67	3.94	2.27	0.44	0.43 Zr
	84 96	5.23	4.45	4.39	0.76	0.19 Zr, 0.02 Ti
Spec. mean:	**86.14**	**4.76**	**4.40**	**3.63**	**0.78**	**(0.29)**
HAFN**A4**	84.79	4.88	5.06	4.09	0.85	0.33 Zr
(10 min)	87.14	4.31	4.68	2.95	0.67	0.24 Zr, 0.01 Si
	85.33	5.16	5.03	3.55	0.76	0.17 Zr
	84.27	4.89	5.26	4.39	1.01	0.18 Zr
	85.09	5.15	5.28	3.29	0.87	0.31 Zr, 0.01 Fe
	84.71	4.40	5.61	3.90	1.12	0.26 Zr
Spec. mean:	**85.22**	**4.80**	**5.15**	**3.70**	**0.88**	**(0.25)**

Averaged mean composition of metallic hafnia reduction products across all four specimens: 85.26 at% Hf; 4.85 at% C; 4.98 at% N; 3.46 at% O; 1.04 at% Al, with the trace balance (0.41 %) present principally as Hf-analogue impurity Zr.

(Each unto the other, (as analogue elements) Zr and Hf are progenitor impurity elements in the primitive source mineral(s) and consequently are the primary impurity in the other's "refined" minerals.)

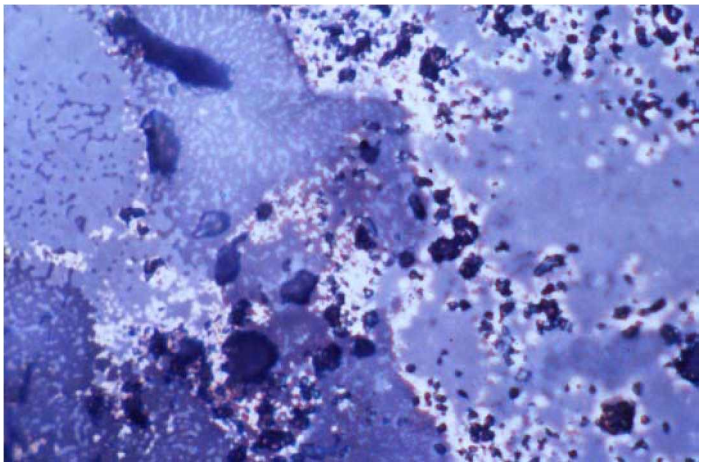

Figure {7.3.2}**1:** Light optical micrograph showing definite, if sparse metallisation in the reduction product of aluminothermic microwave-stimulated reduction of mill blended hafnia (HfO_2/Al/char) – the specimen being HAFN**A2**. Minor exposed metallic Hf-phase presents as the brightest (white) phase whilst the associated Hf-oxycarbonitride pre-metallic phase presents as bright grey. This pre-metallic material is the major phase represented in the micrograph and at top left field can be seen in intimate association with the least reduced reactant material (darker blue/grey phase – pervasive into inter-regional areas). In more expansive regions this minimally reacted phase is clear/translucent, whilst the distribution of darkest areas are porosity "features" derived either from remnant gaseous vesicularity or sites where either reduced phase entities or remnant char granules have been removed from the surface in specimen preparation/polishing operations. No un-reacted Al-metal is exhibited in this field, although minor instances were evident elsewhere in this specimen surface. As can be seen, sound metallic sites of extent adequate for EDS acquisition were limited on this, as with other Hf-reduction product specimens and some minor degree of excitation of phases outside of the metallic phase is suspected with consequent rogue contributions (especially Al and O) in EDS acquisitions recorded in Table {7.3.2}**1**. [LOM (air lens), Ektachrome; fov:0.21 mm]

requirement invested in the oxide minerals of lesser, "supplementary" refractory metals Hf and Nb. The presence in the project of minerals of these refractory metals was (*i*) because of the presence of Hf and Nb as minor native mineral components with their analogue elements Zr (in zircon) and Ta (in tantalite and wodginite) respectively, and (*ii*) to maintain the elemental continuum across the refractory metal group and thereby retain a meaningful continuity across any reduction "account of attainment". Although limited, the results obtained in this hafnia section provided direct evidence of the efficacy of the microwave reduction process – and they were sufficient to justify their inclusion with the more-central core results.

Presented in Table **{7.3.2}1** are the results of EDS acquisitions on the suite of aluminothermic derived reduction products. Whilst spot acquisition checks were made on the "Hf-oxycarbonitride" status of the partially reduced ceramic phases (to confirm such status), only spot acquisitions from Hf-metallic phases were recorded in Table **{7.3.2}1** (as these results confirm the feat of microwave-stimulated reduction of the HfO_2). Whilst separable individual specimens of metallic phase were not produced during this limited campaign of microwave-stimulated HfO_2 reduction, sufficient evidence (verified by EDS analyses) of reduction accomplishment was displayed across the reduction product specimens of all four aluminothermic reduction trials to substantiate the plain claim of *reduction attained* in this most obdurate of reduction objectives to be attempted in the project.

7.3.3: Carbothermic Reduction of Zircon.

The microwave-stimulated reduction of mine-site derived mineral zircon exhibits much in common with the plasma dissociated zircon (PDZ) process that produces PDZ zirconia. The PDZ process utilises the intense heat of thermal plasma in a confined in-flight application to rapidly heat zircon feed which, upon melting, is rapidly frozen thus isolating (as an amorphous solid) the SiO_2 fraction from the ZrO_2 fraction (which returns to (non-zircon) crystalline solid form). Such fractions are then efficiently separated by physical means, or to high purity by a combination of mechanical and solution treatments. The PDZ route is used to efficiently produce high purity zirconia

from zircon, with silica the valuable by-product. Notwithstanding, the PDZ process is in essence a plasma-stimulated thermophysical process – a process not reliant upon chemistry – and is therefore unlike the essentially thermochemical extractive metallurgical process into which category the work of this project falls. Most notably, the evident reduction product facies derived of process chemistry, frozen-in at LN_2 quench, physically reveal aspects of system stability and process order, and a reduction sequence that is (of course) absent in the thermal plasma PDZ process. At the same time, one prevalent aspect of the carbothermic zircon reduction trials was quite unexpected in that (under the prevailing circumstances) the reduction to Zr evidently preceded that of Si from the base zircon mineral. As SiO_2 is more reducible that ZrO_2, such a noteworthy phenomenon was not foreseen – even when entertaining the possibility of re-oxidation of reduced Si-phase (a panacea whose implausible supposition would require reduced-Si to be preferentially re-oxidised before reduced-Zr) – and although the visual evidence suggests such an unlikely prospect. A plausible explanation could be inherent in the event of early melting and liquation of SiO_2 (integral with PDZ-type separation). Such a phase transformation in SiO_2 would result in its microwave susceptibility being abruptly and significantly lowered leaving the residual solid phase ZrO_2 to preferentially attract the applied microwave energy, to heat, to react and consequently lead to preferred reduction in that "PDZ-isolated" ZrO_2 phase.

Such a reduction order phenomenon can be observed in evidence offered in Figures **{7.3.3}1** to **{7.3.3}4** which present light optical micrographs and WDS scan output* of reduction product from a preliminary carbothermic microwave reduction trial conducted on as-received zircon† mineral. The zircon was mixed with char (not mill blended) and microwave processed in an exploratory exercise to ascertain reduction propensity and campaign or trial time required. Whilst appreciable reduction success was achieved on that occasion, the outcome was "at the expense of achievable process" because the reduction process was terminated at the thermal failure of crucible and

* Work undertaken on Cameca scanning electron microscope (microprobe) with wavelength dispersive X-ray spectrometry (WDS) capability – analyses principally carried-out with the assistance of Mr Les Moore at Central Laboratories, BHP steelworks, Port Kembla, and also at the University of New South Wales electron microscope unit, Faculty of Engineering, Kensington, Sydney.

† The zircon ($ZrSiO_4$) used in this core experimental section was the east coast Australian mineral sands derived mineral of Zr:Si ~ 53 %:47 % by stoichiometry *and* incorporating ~ 2 at% Hf substitution for Zr in $(Zr,Hf)O_2$ fraction, plus trace Cr, Ti, Fe and various REE's in either direct mineralogical impurity, or by intimate mineralogical association or loose mineral impurity component.

containment insulation – the reduction products saved by immediate LN_2 quenching. (Subsequent mill-blended trials led to superior reduction outcomes, and such within the ultimate life of crucible and associated containment.) The "exploratory" example is included here because the distinctive zircon grains are distinguishable and with the "corroboration accessibility" of visual plus scan evidence (of Figures **{7.3.3}1** to **{7.3.3}4**) helps to introduce both the potential of process possibilities and the reduction of thermochemically obdurate ZrO_2 under microwave-stimulated carbothermic reduction processing. The example also serves to illustrate the propensity inherent in microwave reduction (as against conventional methods) for processing idiosyncrasy – and the recognition of irregular traits in processing which (hitherto) could lead to new extraction routes. The evidence contained in the figures can perhaps be best evaluated when contemplated against the thermal-only zirconia separation processing of the PDZ process – whilst (in rough comparison) the reduction process was imposed for a longer time it used much lower applied energy and, on balance, can be advantageously compared "outcome for outcome". Moreover, the phenomena in evidence in Figures **{7.3.3}1** to **{7.3.3}4** may fairly be construed to be representative of the prevailing process mechanism for the following reported carbothermic reduction trials on mill-blended zircon/char charges.

The experimental trials conducted on the carbothermic microwave reduction of mill-blended zircon/char blends was quite restricted on the dual basis that (*i*) the interpretation from Ellingham diagrams of carbon reduction of ZrO_2 places the temperature at which reduction occurs (> 2000°C at atmospheric pressure) is within the "temperature" capability of the microwave reduction process but above the thermal tolerance (melting point) of the containment refractory materials, and (*ii*) that the same reference diagrams indicate better reduction prospects for the aluminothermic route. Nevertheless, although indicating rather ambivalent prospects for the carbothermic route, the experience of trials conducted was that this microwave reduction route *did* reduce ZrO_2 to Zr-metal. Consequently, and without "pushing limitations" regarding the "thermal tolerance dictated" utility of containment materials, the few *carbothermic* trials conducted provided specimens that were considered sufficient for "proof of principal" substantiation (and these core trials, it is worth noting, were conducted without containment failure incident).

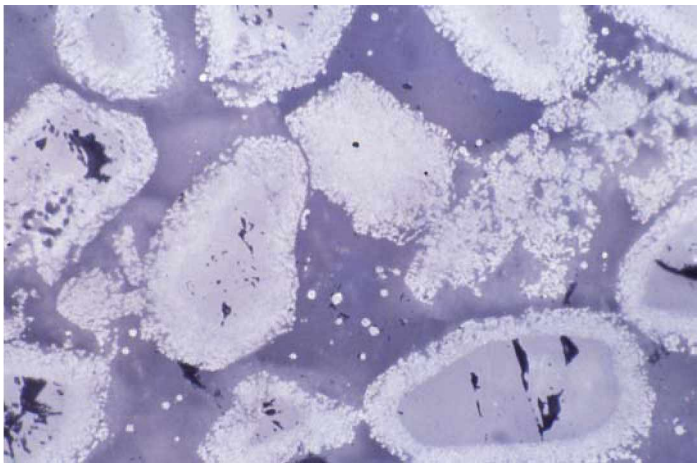

Figure {7.3.3} **1:** Light optical micrograph of the polished surface of a reduction product of the straight *carbothermic* reduction of zircon – the trial was on "as received" zircon mineral. The field is comparable in magnification and (being of the same specimen) is at the same reduction stage to that shown in the WDS scans of Figures {7.3.3} **3a** to {7.3.3} **3d** and so is worthy of consideration along with those following WDS-based figures. The bright phase is highly metallised Zr-phase, the grain cores are un-reacted zircon and the interstitial material is primarily silica slag. [LOM, Ektachrome; fov: 0.53 mm]

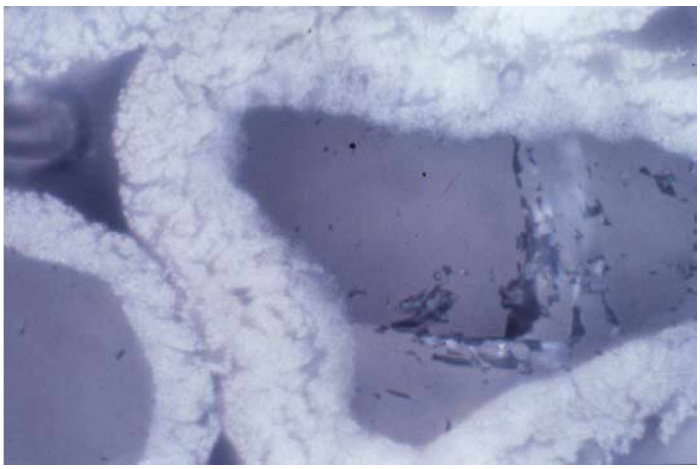

Figure {7.3.3} **2:** Light optical micrograph on the polished surface of the carbothermic zircon reduction product shown in Figure {7.3.3} **1** above showing greater detail of the metallised Zr-phase retained in the reaction zone surrounding the core zircon grains. The un-reacted zircon material in (as shown here) the principal zircon grain displays evidence of physical attrition due to the effects of prior mineral processing on crystal imperfections. [LOM, Ektachrome; fov: 0.21 mm]

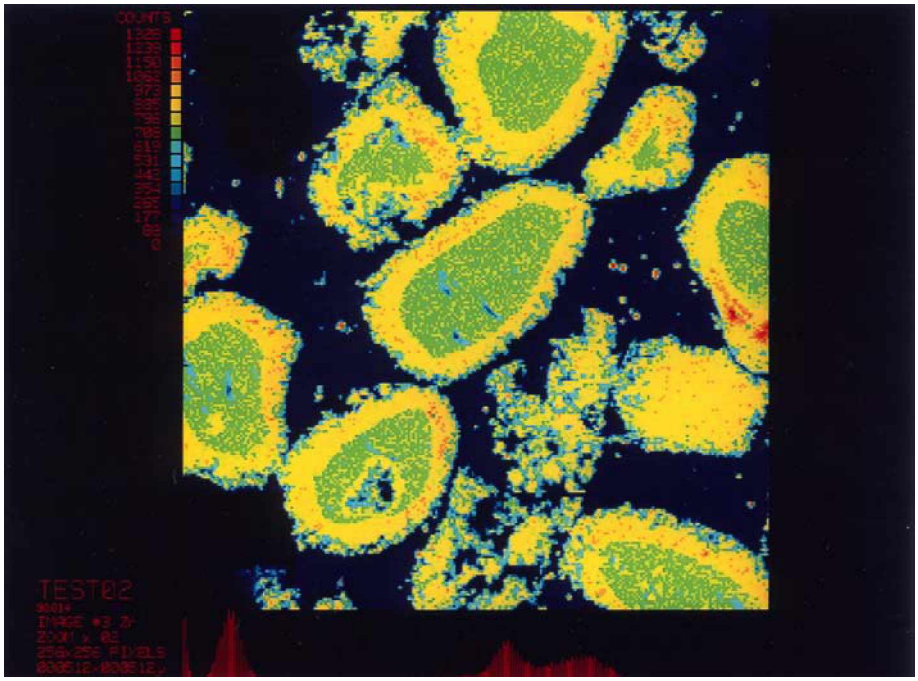

Figure {7.3.3} **3a:** WDS area scan on a polished surface of a reduction product of straight *carbothermic* reduction of zircon. The trial reduction was on "as received" zircon mineral, the field scans conveniently reveal reduction process sequence under the microwave-stimulated method of reduction. This figure represents the scan count intensity for the element Zr, and micrographs at similar magnification are presented in previous Figures {7.3.3} **1** and {7.3.3} **2**. Complementary scans representing the fundamental elements Si, O and C are presented in accompanying Figures {7.3.3} **3b**, {7.3.3} **3c** and {7.3.3} **3d** respectively.

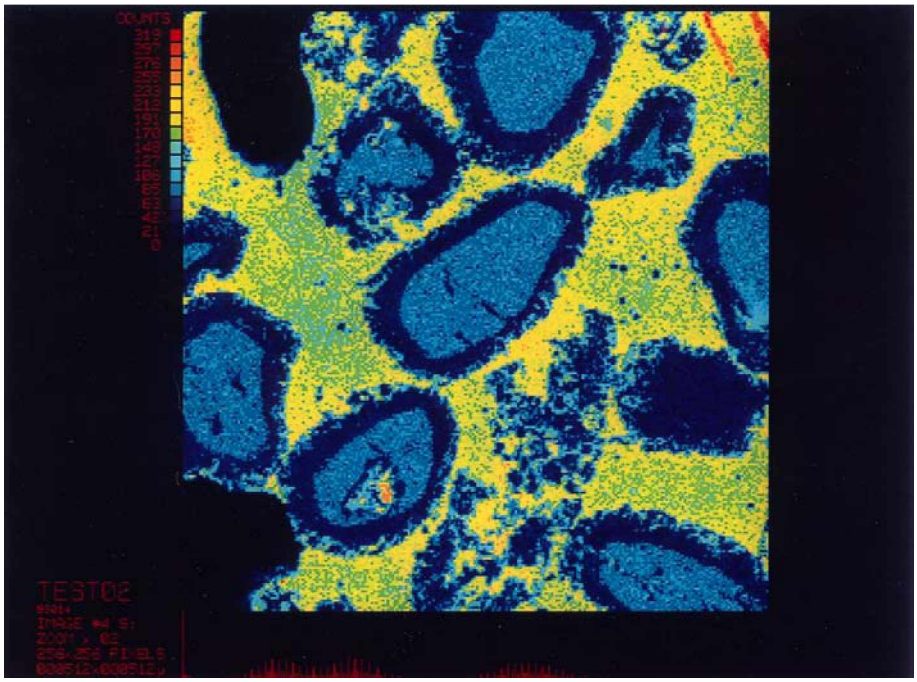

Figure {7.3.3} **3b:** WDS area scan being complement to Figure {7.3.3} **3a** showing count intensity for the element Si. Note that the slag has higher count intensity for Si than does the un-reacted mineral zircon – which is in agreement with the line scans of Figure {7.3.3} **4**.

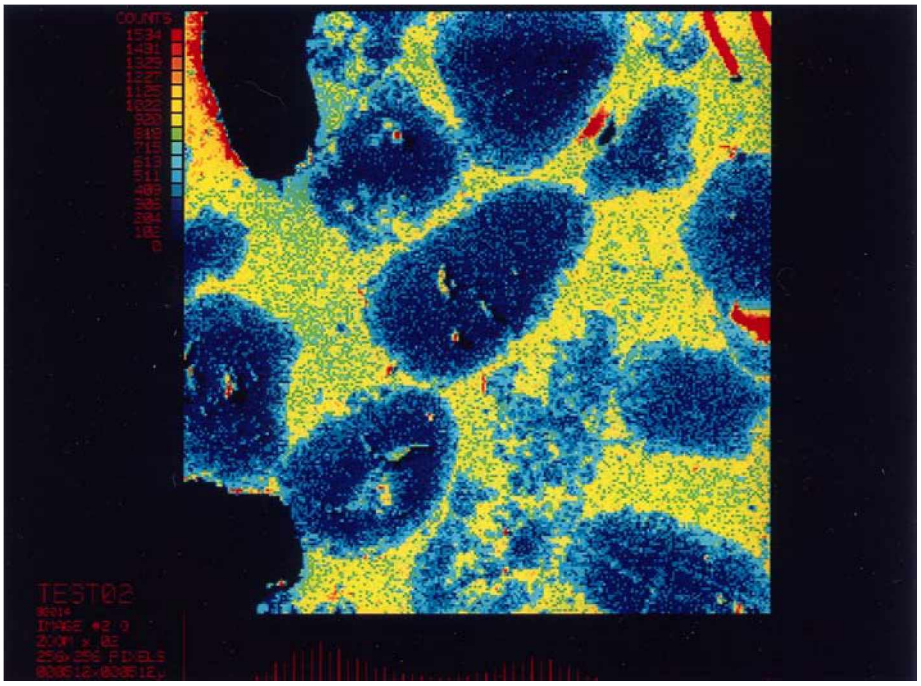

Figure {7.3.3} **3c:** WDS area scan being complement to Figure {7.3.3} **3a** showing count intensity for the element O. The area *scan count intensity* for each of the area scans is indicated beside the upper left border in each of the four scan images by the colour scale, with deep blue representing the lowest count intensity and the red representing the highest count intensity. Of note is the low O-count registering in oxygen-depleted ex-zircon core regions indicating mass transport to the reaction interface, where a hight O-count is indicated by the paler blue. The image width is ~ 0.5 mm for the scan images of this set.

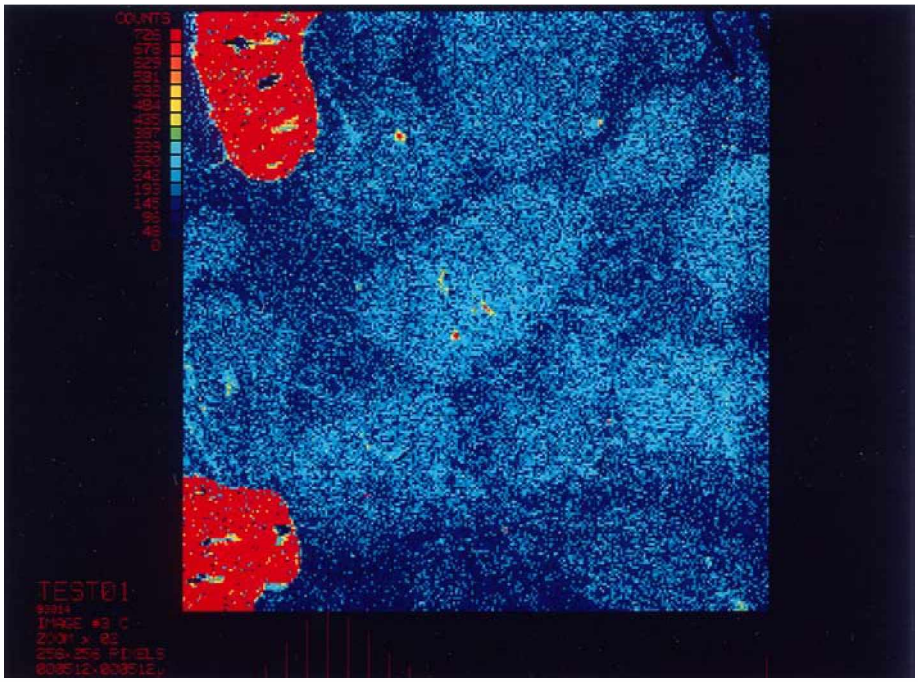

Figure {7.3.3} **3d:** WDS area scan being complement to Figure {7.3.3} **3a** showing count intensity for the element C. Note that the red, highest count intensity areas delineate char granules, not porosity as could be interpreted from the previous scan images.

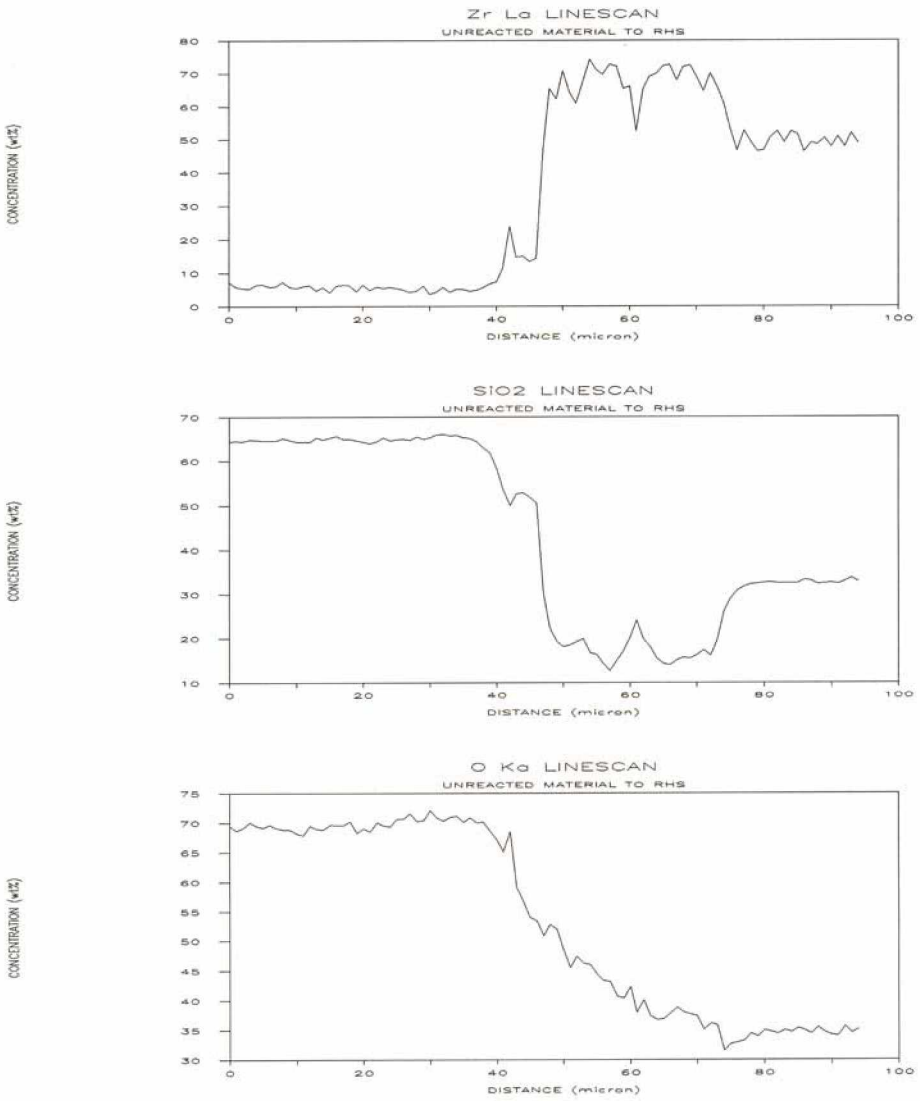

Figure {7.3.3} **4:** WDS line scan set through the reaction interface of a carbothermic reduced zircon grain (as in previous Figures {7.3.3} **3a** to {7.3.3} **3d**). Note that, for the three scans represented, the un-reacted zircon material is represented on the right, the inter-face reaction material is in the central section, and the reacted slag material is represented on the left. Also, crucially, the machine-entitled "SiO LINESCAN" – a geologically orientated, software-imposed anomaly – should read: "Si LINESCAN" as only the single element Si was scanned-for in this acquisition. Upon interpretation, consequently, the slag phase is predominantly SiO_2 material, the zircon can be seen to be outside the usual stoichiometric range of $ZrSiO_4$ with suppressed Si-count and an even more-depleted O-count, verifying the WDS maps. The reaction zone material is dominantly represented by metallic-Zr – metallic phase which can be discerned in the light optical colour micrographs of Figures {7.3.3} **1** and {7.3.3} **2**.

The Zr-metallic phase material analysed in the five reduction product specimens ZRCN**01** to ZRCN**05** was equivalent to that silver/white metallic phase seen in the micrographs of Figures {7.3.3}**1** and {7.3.3}**2** whilst, for the mill-blended origin specimens of Figures {7.3.3}**5** and {7.3.3}**6** this initial silver/white metal of less processed regions shifts to the more-coloured metal of the agglomerated regions of more processed Zr-metallic phase, a phase characteristic of solid state reduction and sinter agglomeration. The results of EDS analyses of these more advanced Zr-metallic phases are presented in Table {7.3.3}**1**, spot analyses of various silver/white phase sites (identified in electron microscope by cross-reference to light optical micrographs) yielded metallic-Zr with lower C and negligible N contents. The accumulation and agglomeration of solid like-kind Zr-phase material seems to have taken place in the "buoyancy" of liquid state silica (after that phase's separation from the "zirconia" phase) – and this advent of metallic-Zr agglomerate "islands" in a matrix of silica has been frozen-in at quench (see Figures {7.3.3}**5** and {7.3.3}**6**). Note that the mechanisms that continued to deliver reductant-C to the reaction interface (of solid prior-zircon grains) were the liquid-state diffusion of C through the silica plus the entrained presence of CO in a "foaming" slag-like medium of that same silica liquid at high temperatures enhanced by the exothermic reduction processes.

Such separation and configuration of phases across the specimen field was quite foreign in specimens of the previous single oxide reduction exercises. Whilst the metallic-Zr phases varied across each specimen, and from specimen to specimen, and whilst some EDS excitation from material external to the target phase was undoubtedly the case (as evident by the occasional raised Si- and O-components of the analyses), the typical metallic reduction product phase was representative of a solid solution Zr-carbonitride, a metal with greater C and lesser N. Notable in the reduction product Zr-metal was the revealing presence of a significant proportion of the mineral's Hf content, apparently in solid solution with the Zr-metal (analogues having mutual solubility across the range) and implying "mutual" reduction under the process conditions. Also, although not reported in the table, the silica-rich ceramic (slag) regions (accompanying the metallic-Zr) were compositionally indicative (by EDS) of SiO_2 stoichiometry, and no metallic regions were encountered which indicated the presence of metallic-Si or partially reduced Si-oxycarbonitride – or any significant mullite type alumino-silicate

Table {7.3.3}1: The table shows EDS analyses results of spot counts acquired from Zr-metallic phase fields in polished section of mounted reduction product of the microwave-stimulated carbothermic reduction of minesite-derived zircon, $ZrSiO_4$. The results are the analyses of EDS spot counts acquired from restricted sites on Zr-metallic phase material on the polished surfaces of 10 min specimens ZRCN**01** and ZRCN**02** and the 12 min specimens ZRCN**03** to ZRCN**05**. The metallic phase extent was not always easily defined, so care was taken to site the beam spot such as to minimise excitation from external phases. However, some proportion of the O counts may plausibly have originated in phase material outside the target volume.

Specimen.	**EDS analyses of spot acquisitions from redn. product phase (at%).** All EDS acquisitions were spot acquisitions by windowless detection.						
	Zr	**Hf**	**C**	**N**	**O**	**Si**	**balance**
ZRCN**01**	95.84	0.18	2.66	1.01	0.09	0.22	-
(10 min)	96.09	0.51	2.43	0.81	0.05	0.10	0.01 Ti
	94.96	2.22	2.21	0.27	0.14	0.17	0.03 Fe
	96.11	0.05	2.58	0.47	0.41	0.38	-
	96.34	0.09	2.40	1.12	0.02	0.03	-
Spec. mean:	**95.87**	**0.61**	**2.46**	**0.74**	**0.14**	**0.18**	**(0.01)**
ZRCN**02**	96.07	0.14	2.54	0.98	0.08	0.10	0.05 Cr, 0.04 Fe
(10 min)	96.38	0.09	2.33	0.86	0.06	0.25	0.03 Ti
	95.59	1.45	1.99	0.83	0.07	0.07	-
	96.16	1.03	2.19	0.55	0.02	0.04	0.01 Cr
	95.90	0.67	2.25	1.02	0.04	0.10	0.02 Ti
Spec. mean:	**96.02**	**0.68**	**2.26**	**0.85**	**0.05**	**0.11**	**(0.03)**
ZRCN**03**	96.65	0.18	2.44	0.62	0.04	0.07	-
(12 min)	96.31	0.88	2.03	0.68	0.03	0.06	0.01 Fe
	95.29	2.06	1.87	0.65	0.08	0.04	0.01 Ce
	96.27	0.91	2.42	0.33	0.06	0.01	-
	96.18	0.46	2.28	0.92	0.05	0.08	0.02 Ti, 0.01 Cr
Spec. mean:	96.14	0.90	2.21	0.64	0.05	0.05	(0.01)
ZRCN**04**	96.08	0.32	2.78	0.58	0.17	0.06	0.01 Ti
(12 min)	96.00	1.20	2.21	0.38	0.11	0.08	0.02 Fe
	96.11	0.85	2.04	0.79	0.06	0.14	0.01 Ti
	96.44	0.28	2.55	0.60	0.06	0.06	0.01 Ti
	96.12	0.81	2.17	0.59	0.08	0.20	0.02 Ce, 0.01 Cr
Spec. mean:	96.15	0.69	2.35	0.59	0.10	0.11	(0.01)
ZRCN**05**	96.23	0.30	2.35	0.71	0.20	0.17	0.03 Ti, 0.01 Fe
(12 min)	95.89	1.22	2.18	0.55	0.09	0.07	-
	96.42	0.77	2.17	0.51	0.05	0.07	0.01 Mn
	96.20	0.81	2.29	0.52	0.11	0.05	0.02 Ti
	96.12	0.63	2.33	0.72	0.04	0.14	0.02 Cr
Spec. mean:	96.17	0.75	2.26	0.60	0.10	0.10	(0.02)

Averaged mean composition across all five carbothermic zircon reduction specimens for Zr-metallic reduction products: 96.07 at% Zr; 0.73 at% Hf; 2.31 at% C; 0.68 at% N; 0.09 at% O; 0.11 at% Si; with trace impurities (0.01 %).

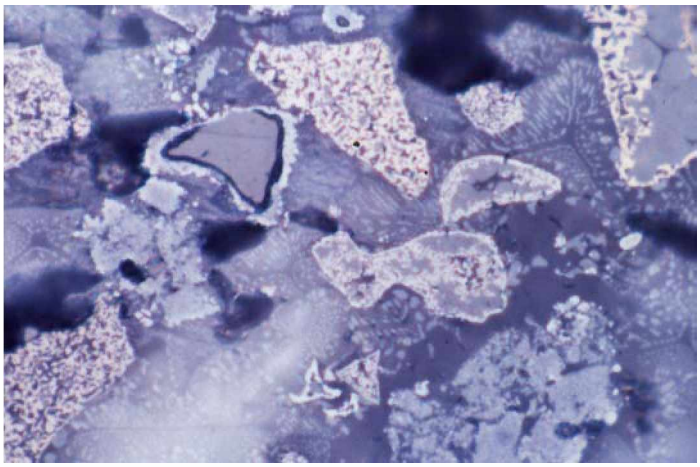

Figure {7.3.3} **5:** Light optical micrograph of the polished surface of a reduction product of the straight *carbothermic* reduction of mill-blended zircon/char and being a field in 10 min specimen ZRCN**01**. This field is in contrast to the 12 min specimen shown in Figure {7.3.3} **6** below in that it exhibits more of the minimally processed silver/white Zr-metal phase (lower C and negligible N), a phase that is barely in evidence in the 12 min specimen field. Also, the field is nearly devoid of mounting medium, the matrix is essentially "silica including reducing phases", the dark-rimmed grey grain is remnant zircon, and the "milky" area is a region of internal refraction/reflection interference. [LOM, Ektachrome; fov: 0.21 mm]

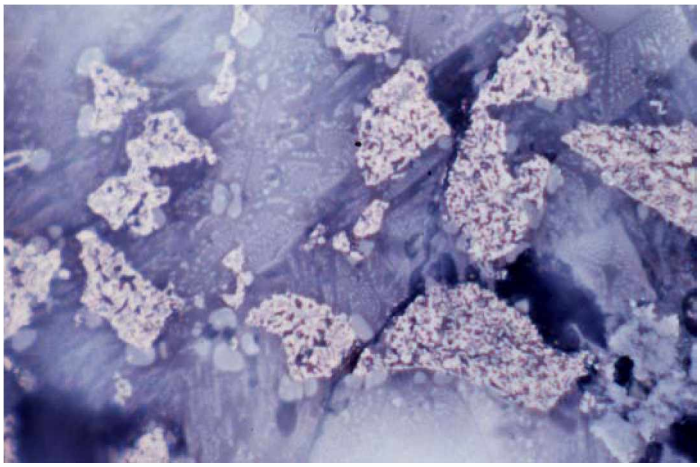

Figure {7.3.3} **6:** Light optical micrograph of the polished surface of a reduction product of the straight *carbothermic* reduction of mill-blended zircon/char and being a field in 12 min specimen ZRCN**04**. In contrast to the 10 min specimen shown in Figure {7.3.3} **5** above, this field is dominated by the more processed, coloured Zr-metallic phase which was the subject of EDS acquisitions whose analyses comprise Table {7.3.3} **1**. Some evidence of Zr-metallic phase agglomeration can be discerned in those agglomerates, whilst the silica phase shows evidence of further processing. [LOM, Ektachrome; fov: 0.21 mm]

(discussed elsewhere, a separate, divergent outcome in its own right). Minor remnant features still containing Zr in plainly ceramic form occurred in lesser-reduced regions,

these revealed (by EDS-indicated stoichiometry) the presence of incompletely reduced, scattered remnant zircon material – a process flaw rather than a process incapacity.

However, in general summary on the microwave-stimulated carbothermic reduction of zircon, it was noted that (except for minor regions of reactant material at the extremities of the reaction zone) Si-phase material had at least seen SiO_2-ZrO_2 oxide separation, and most Zr material was characterised by metallic conversion. Although some variation existed in the degree of that Zr-metallic conversion, the overall standard of Zr-metallisation represented by that conversion was high. Consequently, and somewhat unexpectedly (given the limitations of scale and resources available to the project), it was shown that zircon could be carbothermically reduced utilising the microwave-stimulated oven set-up method to yield sound Zr-metallic product.

7.3.4: Aluminothermic Reduction of Zircon.

Earlier aluminothermic reduction conducted on the less thermochemically noble ferruginous mineral ilmenite was conducted as a thermite reaction, however, as discussed in preceding zirconia and hafnia sections, the carbo-aluminothermic reactions involved in the microwave-stimulated reduction of zircon would not have that thermite intensity status. This being said, and keeping in mind the PDZ-type separation propensity in zircon, if the SiO_2 portion of the zircon remained solid long enough to drive its temperature up to activation energy, then the reactant Al would energetically reduce the silica. Exothermal energy so released should prove sufficient (on top of the applied microwave energy input) to allow the reduction of ZrO_2 by Al. However, such a propensity for reduction of zirconia by Al is, at best, only marginal and (by rough estimation from Ellingham diagram) is only applicable up to ~ 750°C (± 100C°)* beyond which, at more elevated temperatures, Al_2O_3 is reduced by Zr-metal. So, reduction product expectations rested with ongoing appraisals of experimental output

* The Ellingham diagram "curve" approximations for the reactions $Zr + O_2 \rightarrow ZrO_2$ and $^4/_3\ Al + O_2 \rightarrow {}^2/_3Al_2O_3$ are mutually shallow in their inclinations across the pressure/temperature field of the standard Ellingham diagram and the straight line "curves" intersect at (as a rough approximation) ~ 750°C. Such "curves" vary with system partial pressures and with the impact on process parameters of applied *microwave* energy. (Refer to Figure {3.1}1 for the Ellingham diagram for oxides.)

and outright "predicted" outcomes were avoided. This "reduction outcome ambivalence" was borne-out in experimental outcomes and the following discussion should be contemplated in this tenor.

Being more conditional than for pure single oxides, the exploratory trials on the minesite-derived mineral zircon were carried-out largely as a strategy of experimental enquiry into the reduction outcome possibilities contained in pre-refinement reduction of a native mineral – a highly valuable mineral in the case of zircon. This reduction strategy generated a reduction product metal *ahead* of separation processes or, perhaps, instead of separation processes leading to pure single oxide minerals. Such pure oxide minerals are the starting material in conventional refractory metal extraction routes (the Kroll process, *et cetera*). Implicit in the experimental assignment was that the usual industrial approach of *mineral beneficiation* – an approach yielding some intermediate upgrading of the starting mineral concentrate to another more "saleable", value-enhanced mineral form which still required refinement – was replaced by an approach yielding (at worst) an impure metal which may require less nett processing to commercial or functional purity. (That is, that the commercial minesite standpoint promoting "mineral commodification" be reversed to a metallurgical standpoint favouring "preferred raw material". To achieve this, "Metallurgy" must both determine the extractive process (route) and set the preferred feed mineral price according to its production merit in that process, rather than the "Miner" off-loading its preferred product into an ambivalent market, a market wider than just metallurgy. The cause of zircon in the zirconium (and silicon) production stream is seen as a possible case at point for this processing revisionism featuring a new class of raw material – impure metal rather than beneficiated mineral.)

In this programme of reduction experimentation involving a mineral concentrate (albeit of a dual mineral) – a "real" product of mining operations – two categories of reduction outcomes were inadvertently produced. These categories, delineated by reduction product remnants, were the result of the varying of one basic process parameter. That varied parameter being process time, and in particular, that proportion of the process time *beyond* that point of peak reduction reaction – a point experimentally evident only (but plainly) by the plasma intensity visible at insulation gaps around the crucible top. The first reduction outcome category was attained by

inadvertent over-processing, the second by subsequent rectification to processing time. Where (in initial trials) prolonged processing time was intended to secure a melt-consolidated reduction product metallic Zr-phase, in these zircon trials prolonged time actually had the effect (under the prevailing "non-failsafe" system atmosphere) of over-processing reduced metals such that these "re-oxidised" to carbonitride and intermetallic compound forms. This predisposition to relatively rapid-onset over-processing in reduction product phases seemed particularly to have been a processing characteristic of the metallurgical chemistry of this reactant/reductant combination.

Such an "over-processed" reduction product agglomerate of phases in 10 min specimen ZRCN**A1** is shown to advantage in the WDS scan output summary presented in Figure **{7.3.4}1** whilst, by way of illustrative reference, the comparative light optical micrograph featured in the scanned phases is presented in Figure **{7.3.4}2**. Other fields representative of the facies (distribution of phases) in this reduction product and those of the other "over-processed" specimens (ZRCN**A2** and ZRCN**A3**) are presented in Figures **{7.3.4}3, {7.3.4}4** and **{7.3.4}5**. Although these over-processed specimens each essentially represent a "success shortfall", their necessary inclusion as genuine results beside the latter four more successful results (featuring conventional metal phases) serves to show (*i*) the magnitude of difference which (apparently) minimal processing variations can make, (*ii*) the concurrent effect on reduction product phases due to operational deficiencies in atmosphere control and the reduction environment *per se*, and (*iii*) different means (by resultant phases) by which fulfilled reduction can be physically expressed. The accumulated excess of un-reacted reductant-Al that remained (to report in isolated pockets upon quenching as (Al + AlN)) was exacerbated by the total system char being too low to drive (under microwave irradiation) the charge "temperature" high enough, quickly enough such that the purely *aluminothermic component* of the proposed reaction could efficiently take place producing Zr-metal plus Al_2O_3 – separate to any carbothermic component reduction products. From specimen ZRCN**A4** on the total atmospheric control granular char – above and below the charge – was increased by 25% for the purpose of attracting a higher microwave energy density (from the applied field) to the reactant charge, thus increasing the heating rate and leading to earlier reaction spontaneity. Reduction product phases of such reaction

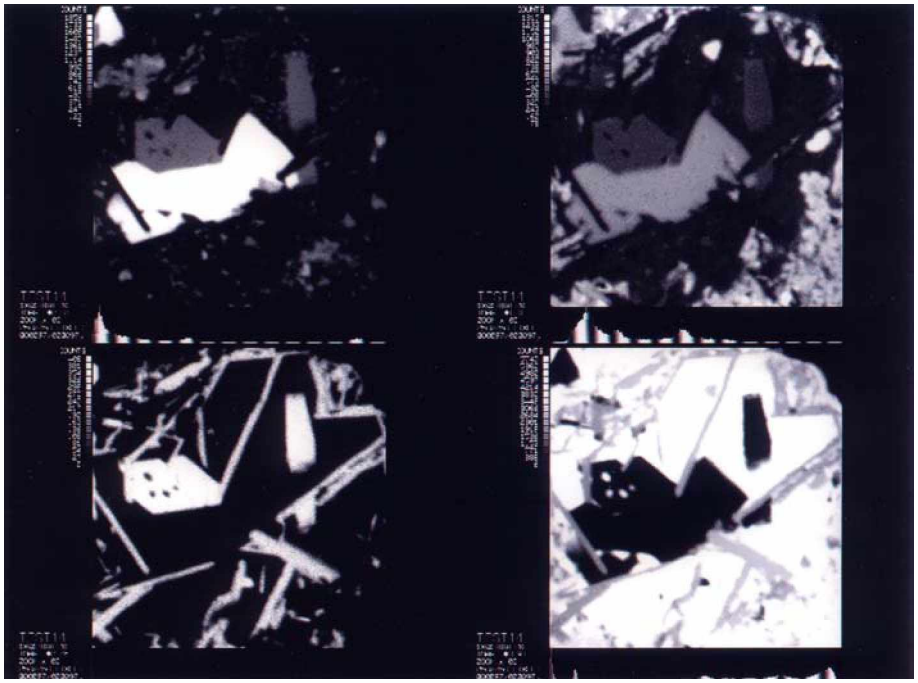

Figure {7.3.4}**1:** The above WDS scan image compilation shows, in summary form, the area scan intensity maps for the elements (clockwise from top left) Si, O, Al and Zr acquired from the reduction product of aluminothermic reduction of zircon, specimen ZRCN**A1**, an "over-processed" reduction product (see discussion). The acquired images are of the region shown in the following Figure {7.3.4}**2**. Note that the large angular Si-phase still has a considerable O content. Sharing an angular interface with the [Si,O]-phase is a [Zr,Si]-phase which (almost O-free) proved to be an oxycarbonitride. The fine prismatic phase is an O-free [Zr,Al] intermetallic phase with a minor carbonitride component (also by EDS). Finally, the balance is Si-free, Al-rich *non-alumina* material that, crucially, is comprised of "un-reacted" metal, frozen as (Al + AlN) in confined regions (as evident below).

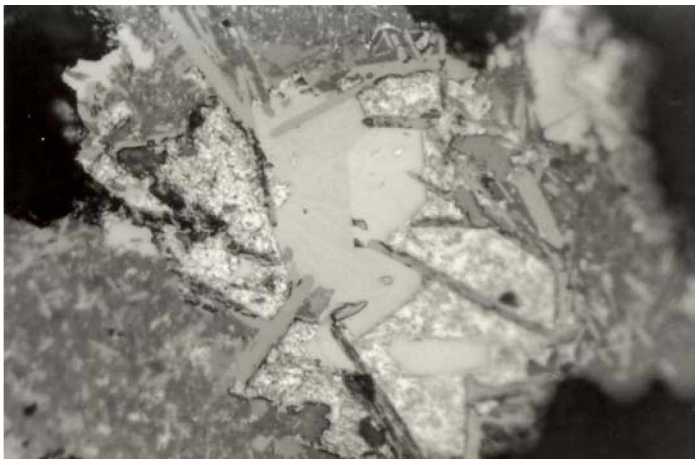

Figure {7.3.4}**2:** The WDS scan images in the above figure, as can be recognised, are advanced ~ 90° of clockwise rotation in this light optical micrograph of a complex region featuring reduction product phases as identified in the annotation for Figure {7.3.4}**1**. This reduction product (specimen ZRCN**A1**) represents the over-processing into "re-oxidisation" which characterised the first three reported zircon reduction experimental trials, ZRCN**A1** to ZRCN**A3**, the following reduction product specimens from ZRCN**A4** to ZRCN**A7** reported with minimal phases exhibiting angular morphologies and the principal metallic Zr-phase presenting in less-angular metallic forms (comparable to Ti-phases of anatase products). Supporting EDS analyses are provided in Table {7.3.4}**1**. [LOM; fov: 0.17 mm]

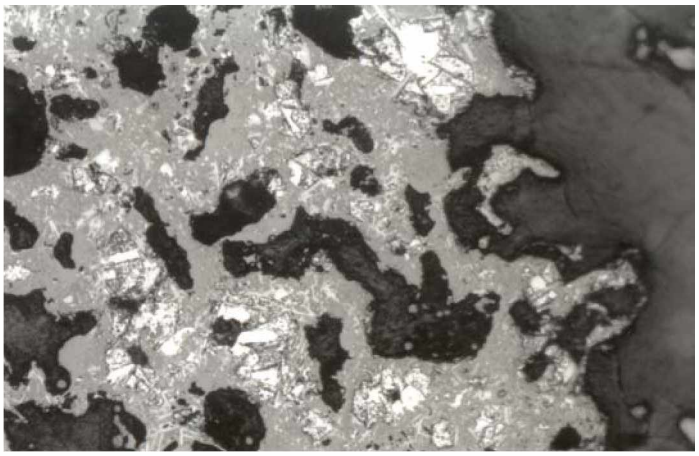

Figure {7.3.4}3: Light optical micrograph (LOM) showing a typical field of view on 10 min reduction product of the microwave aluminothermic reduction of zircon specimen ZRCN**A1**. The dark grey regions are mounting medium whilst the pervasive light grey material is essentially an alumina slag – note this phase (outside WDS field) in Figure {7.3.4}**2**. The larger bright phases distinguishable at this magnification are the various Zr and Si compound phases contained within the general alumina matrix (and whose finer detail emerges in the following higher magnification of Figures {7.3.4}**4** and {7.3.4}**5**), also, identifiable in top-central field is that of Figure {7.3.4}**2**. It seems to have been the case that early-separation SiO_2 liquated to separate (lower) regions of the remnants otherwise such would have freely formed an aluminosilicate liquid. Such an aluminosilicate "slag" phase was not to be located throughout the remnants, however, minor regions of isolated silica phase (material including trace Cr and Fe components) was found in remnant extremities as were minor regions retaining fine, incompletely reduced zircon grains from which WDS line scans (including that following in Figure {7.3.4}**6**) were acquired for confirmation and comparison with the carbothermic line scan (Figure {7.3.3}**4**). [LOM; fov: 0.68 mm.]

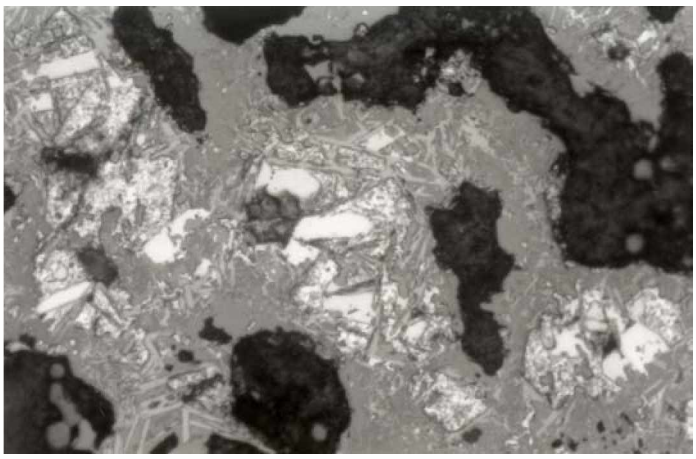

Figure {7.3.4}4: Light optical micrograph (LOM) showing a typical field of view (in Figure {7.3.4}**3** above) on 10 min aluminothermic reduction product ZRCN**A1** The field shows the typical reduction facies with dispersion of reduction product phases in this over-processed specimen. The darker regions are mounting medium whilst the grey phase matrix is primarily alumina and details of the distributed phases within this are identified and best observed at higher magnification in the micrographs of Figure {7.3.4}**2** and Figure {7.3.4}**5** with cross-reference to the WDS area scans of Figure {7.3.4}**1** and "verification" analyses for minor metallic compounds in Table {7.3.4}**1** [LOM; fov: 0.34 mm.]

Figure {7.3.4}5: Light optical micrograph (LOM) showing detail of a central region the two preceding micrographs of 10 min specimen ZRCN**A1**. The following should be viewed with cross-reference to the WDS area scans of Figure {7.3.4}**1** and "verification" analyses for minor metallic compounds in Table {7.3.4}**1** whilst, being of similar magnification, the micrographic detail in Figure {7.3.4}**2** can be equivalently described by the following non-definitive summary of phases. In a background Al_2O_3 matrix, the larger area, light grey phases with angular morphology are (see WDS scans with respect to Figure {7.3.4}**2**) either Zr_4SiO or crystalline $SiO_{2-x}C_yN_z$, x = (y + z) (as distinct from the initially separated liquid which, at remnant extremities, tended to freeze to a "splintery" amorphous solid). The almost reticulated, fine prismatic to possibly lath-like mid grey network-phase is mainly Zr_2Al_3 with some ZrAl (by EDS). Bounded by these fine elongated forms are areas of re-solidified "liquid reductant" as (Al + AlN) – the bright (whitest) phase being Al metal inter-woven by grey AlN– such volumes of reductant Al were generally isolated from O_2 upon quenching and have solidified independently of the predominant Al_2O_3 slag regions. No true Zr-metal phase was found in reduction product remnants of the three over-processed 10 min specimens. [LOM; fov: 0.17 mm]

needed to be fixed by efficient quenching before oxidation or reversion reactions had the chemical impetus or inter-species opportunity to intercede.

Once this processing shortcoming was amended such that processing time was considerably shortened, the remaining reduction output results returned reduction products featuring undeniably metallic Zr-phase products. Such Zr-metallic phases were comparable to their counterpart carbothermic output, although their light element contents were markedly higher (by proportion). Being of solid solution metallic form – the form considered most acceptable for all experimental programmes – the metal phase reduction product of specimens ZRCN**A4** to ZRCN**A7** best represented the reduction product Zr-metal required, and was clearly comparable to the metallic output of the carbothermic route. In straight comparison to the carbothermic output, the aluminothermic produced metal was modestly lower in Zr, modestly higher in Hf and, by proportion, notably higher in C, N, O and Si (a factor of processing which could be changed with experimental experience). Although the Zr-metallic phase, "internal" in agglomerate reduction product regions, were selected for EDS acquisition, analyses and reporting, a minor percentage of reduced metal was exposed to "over-processing" and therefore classified as un-representative of a peak reduction product phase. Such phases were predictably high in C and N and were on-track to form stoichiometric Zr-carbonitride compounds. The provisional EDS evidence presented as Figure **{7.3.4}9** is indicative of the development of such a metallic Zr-compound.

The broader results of this section show that native zircon can be reduced under the microwave-stimulated aluminothermic route using the oven set-up method given sufficient char assistance for co-reduction, atmosphere control and to ensure adequate heating rate (rate of energy input). This route and the carbothermic route require much greater exploratory experimentation before any future experimental development course could be contemplated, however, in-principle substantiation that zircon can be reduced under a microwave regime has been established. Generally, it was considered that the aluminothermic reduction route for zircon imposed both process and product complexities which the carbothermic route did not impose and, for this reason, further experimentation should (in the first instance) favour the carbothermic processing option – particularly where a system is envisaged which incorporates provision of superior atmospheric control, as it must.

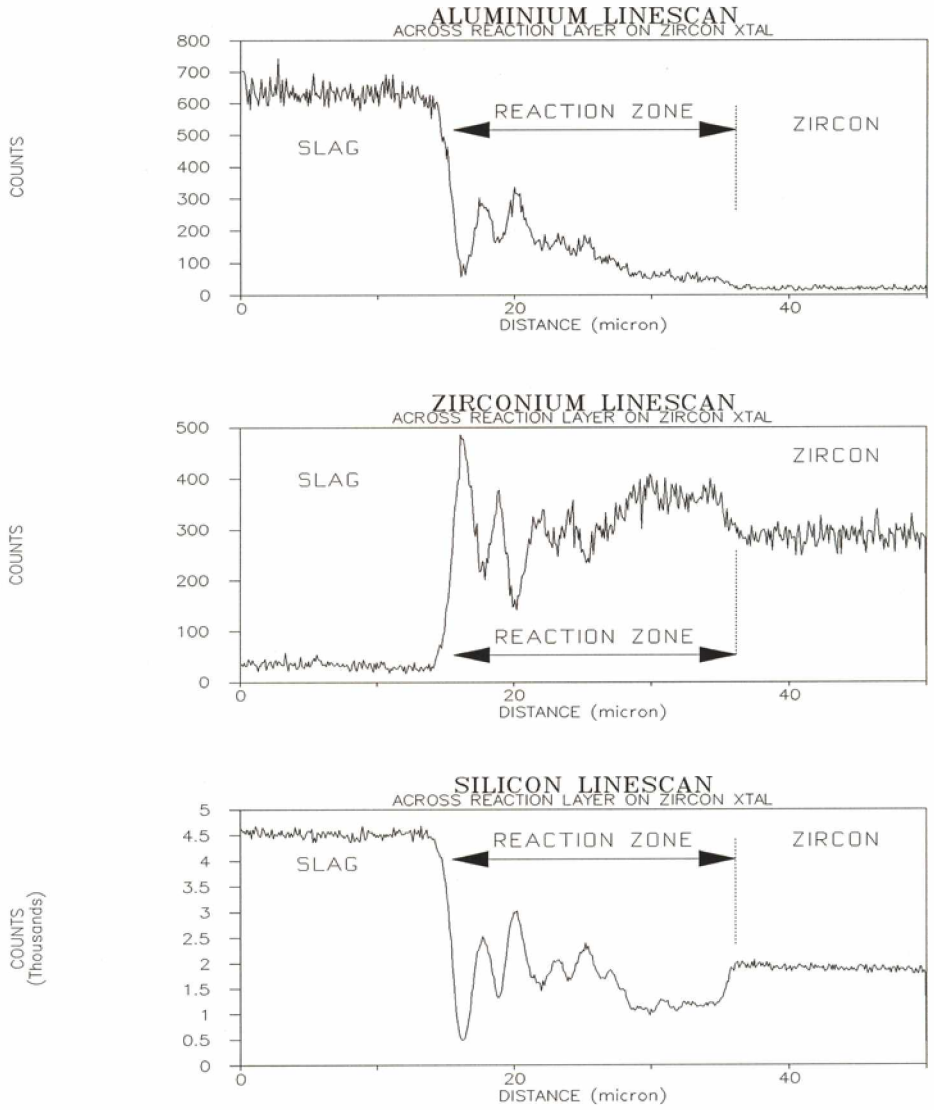

Figure {7.3.4}**6:** These WDS line scans were acquired in a traverse across the reaction zone (interface) between the "slag" phase(s) and the un-reacted interior of a fine zircon grain (a remnant reactant component from the initial mill-blended reactant charge). The fine zircon grain existed in an extremity "region of incomplete reduction" in the reduction remnants of 10 min aluminothermic reduction product ZRCN**A1**, the feature is of reduction process significance but was located in a region atypical of other more advanced reduction remnants which made-up the majority of reduced material. As can be discerned from the three line scans that Si (as SiO_2) and Al (possibly as Al_2O_3 in an aluminosilicate phase – uncommon in the broader specimen) are present in the "slag" phase (left); the "reaction zone" (centre) shows increased levels of Zr (metallised by other determination) with decreased levels of Si (possibly as SiO_2) whilst the Al level decreases through this zone to negligible at the reaction/zircon interface; the line scan traces for SiO_2 and ZrO_2 remain unaltered in the un-reacted zircon grain proper. These aluminothermic line scans compare favourably with the carbothermic line scan set of Figure {7.3.3}**4**. (Note that limited access to the WDS facility prevented a more complete set of elemental line scans being acquired for this aluminothermic case *and* for the earlier, carbothermic case. However, the line scans presented provide compelling evidence in respect of declared claims.)

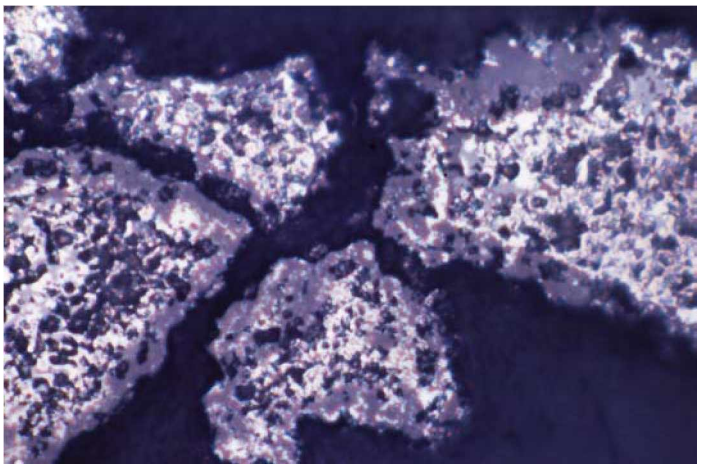

Figure {7.3.4}**7:** Light optical colour micrograph showing a typical field in specimen ZRCN**A4**, aluminothermic reduction product after LN_2 quench at 7 min of microwave processing. Plastic-mounted and polished, these reduction product agglomerate pieces reveal Zr-metallic phase (white) with some varied angular Zr-Al intermetallic (light grey, accompanying Zr-metal and more easily distinguished in the following Figure {7.3.4}**8**). These reduction phases are generally encased in an Al-dominated aluminosilicate "slag" phase (darker grey, possibly darkened by char fines subsumed when in liquid state). The facies of the reduction remnants of the four "abbreviated process" specimens, ZRCN**A4** to ZRCN**A7**, are markedly different from the "over-processed" facies shown (to finer detail) in the nonochromatic micrographs of Figures {7.3.4}**2** to {7.3.4}**5**. [LOM, Ektachrome; fov: 0.21 mm.]

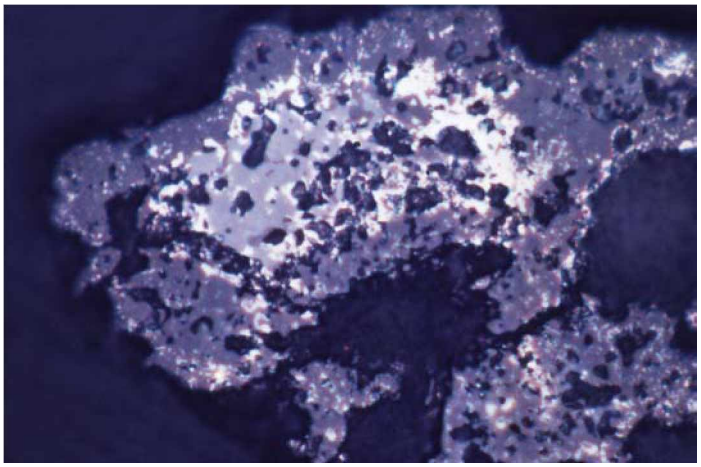

Figure {7.3.4}**8:** Light optical colour micrograph showing a typical fields in specimen ZRCN**A6**, reduction product after LN_2 quench at 6 min of microwave processing. The mounted and polished specimen revealed (in this and other fields) a greater proportion of slag phase accompanying bright metal of good metallic conversion and showing more clearly the light grey Zr-Al intermetallic phase [~ Zr_3Al_2 with ~ 6 at% C(N)] heavily associated with the white "solid solution" Zr-metallic phase. Only minor occurrences (at "exposed" external sites) of Zr-metallic compound phases were evident in all four specimens; and **no** metallic Al was detected in any of the "abbreviated process" specimens – perhaps a statement of the greater Ellingham nobility of Al at lower temperatures prevailing late in the cooling curve of the quench. [LOM, Ektachrome; fov: 0.21 mm.]

Table {7.3.4}1: The table shows EDS analyses results of spot counts acquired from (*i*) in account of specimens ZRCN**A1** to ZRCN**A3**, from phase fields of prominent crystalline compounds, and (*ii*) in account of specimens ZRCN**A4** to ZRCN**A7**, from Zr-metallic phase fields (only). All EDS acquisitions are from polished surfaces (refer to accompanying figures) of mounted reduction product of the microwave-stimulated carbo-aluminothermic reduction of minesite-derived zircon, $ZrSiO_4$. The initial reported results are from "over-processed" 10 min specimens; results from the latter four specimens are more pertinently indicative of the actual reduction propensity of the aluminothermic process. [Such an over-processing distinction did not manifest similarly in comparable reduction exercises, and this may be due to convoluted processing stages necessitated by the thermochemical obduracy of ZrO_2 following initial thermal "separation processing" resolving the dual mineralogy of zircon.] The extent of each metallic phase was not always easily defined, so care was taken to site the beam spot such as to minimise excitation from without the examined phase, however, for the various phases examined, some proportion of the Al, Si or O counts may plausibly have originated in phase material outside the target volume.

Specimen.	**EDS analyses of spot acquisitions from redn. product phase (at%).** All EDS acquisitions were spot acquisitions by windowless detection.							
	Zr	**Hf**	**C**	**N**	**O**	**Si**	**Al**	**balance**
ZRCN**A1**	**Zirconium aluminide phase 1** (fine prismatic phase).							
(10 min)	41.03	0.12	0.85	0.69	0.04	0.07	57.11	0.09 Ti
	39.88	0.35	0.67	0.77	0.00	0.09	58.18	0.06 Ti,
	39.18	0.27	0.88	0.89	0.02	0.43*	58.28	0.03 Ti, 0.02 Y
	41.75	0.11	0.71	0.49	0.07	0.04	56.77	0.04 Ti, 0.02 Cr
	40.78	0.26	0.94	0.66	0.01	0.04	57.24	0.7 Ti
Mean:	**40.52**	**0.22**	**0.81**	**0.70**	**0.03**	**0.13***	**57.52**	**(0.07)**
	Zirconium aluminide phase 2 (fine prismatic phase – indistinguishable from phase 1).							
	50.48	0.22	0.65	0.76	0.00	0.03	47.81	0.04 Ti, 0.01 Cr
	48.45	0.49	0.58	0.81	0.02	0.03	49.60	0.02 Ti
Mean:	**49.47**	**0.36**	**0.62**	**0.79**	**0.01**	**0.03**	**48.70**	**(0.02)**
	Zirconium silicide phase (granular, angular morphology).							
	80.63	0.07	0.99	0.88	1.08	16.33	0.01	0.01 Fe
	80.01	0.04	0.79	0.63	0.62	18.52	0.00	0.01 La
	80.48	0.11	0.58	0.65	1.15	17.02	0.01	-
	79.92	0.06	0.89	0.34	0.95	17.80	0.02	0.02 Ti
Mean:	**80.26**	**0.07**	**0.81**	**0.63**	**0.95**	**17.42**	**0.01**	**(0.01)**
	Silicon oxide (carbide nitride) phase (granular, angular morphology).							
	0.00	0.00	2.38	0.21	58.62	38.77	0.02	-
	0.04	0.00	1.66	0.27	58.77	39.22	0.04	-
	0.01	0.00	2.45	0.51	55.31	41.67	0.02	0.03 Fe
	0.02	0.00	1.98	0.28	56.82	40.83	0.07	-
Mean:	**0.02**	**–**	**2.12**	**0.32**	**57.38**	**40.12**	**0.04**	**(–)**
ZRCN**A2**	**Zirconium aluminide phase 1** (fine prismatic phase).							
(10 min)	41.38	0.18	0.82	0.43	0.04	0.12	57.00	0.03 Ti
	42.03	0.07	0.97	0.53	0.03	0.06	56.27	0.02 Ti, 0.02 Cr
	40.78	0.09	1.11	0.62	0.01	0.04	57.35	-
	41.26	023	0.88	0.87	0.04	0.08	56.61	0.02 La, 0.01 Ti
Mean:	41.36	0.14	0.95	0.61	0.03	0.08	56.81	(0.02)

[Table continued over page.]

Table {7.3.4}1 (Specimen ZRCNA2) continued/

Specimen. **EDS analyses of spot acquisitions from redn. product phase (at%).**

All EDS acquisitions were spot acquisitions by windowless detection.

	Zr	Hf	C	N	O	Si	Al	balance
	Zirconium aluminide phase 2 (fine prismatic phase – indeterminable from phase 1).							
	49.76	0.20	0.75	0.81	0.02	0.03	48.42	0.01 Ti
	48.71	0.17	0.69	0.86	0.01	0.07	49.47	0.02 Ti
	50.08	0.31	0.66	0.75	0.01	0.04	48.15	-
Mean:	**49.52**	**0.23**	**0.70**	**0.81**	**0.01**	**0.05**	**48.68**	**(0.01)**
	Zirconium silicide phase (granular, angular morphology).							
	79.53	0.08	1.17	0.68	0.97	17.56	0.00	0.01 Ti
	79.84	0.11	0.89	0.78	1.02	17.34	0.02	-
	80.44	0.08	0.87	0.78	1.22	16.58	0.02	0.01 Fe
	80.07	0.06	0.84	0.65	1.00	17.37	0.01	-
Mean:	**79.97**	**0.08**	**0.94**	**0.72**	**1.05**	**17.21**	**0.01**	**(0.01)**
	Silicon oxide (carbide nitride) phase (granular, angular morphology).							
	0.03	0.00	2.07	0.31	58.30	39.27	0.01	0.01 Fe
	0.01	0.00	1.79	0.36	57.65	40.18	0.01	-
	0.05	0.01	2.37	0.44	56.88	40.22	0.03	-
	0.01	0.00	2.02	0.28	57.58	40.09	0.02	-
Mean:	**0.03**	**0.00**	**2.06**	**0.35**	**57.60**	**39.94**	**0.02**	**(–)**
ZRCNA3	**Zirconium aluminide phase 1** (fine prismatic phase).							
(10 min)	39.95	0.15	0.64	0.70	0.02	0.09	58.42	0.03 Ti
	40.19	0.09	0.98	0.68	0.04	0.11	57.86	0.05 Ti
	40.32	0.28	0.94	0.81	0.01	0.06	57.56	0.02 Ti
	39.91	0.17	0.88	0.59	0.03	0.07	58.33	0.02 Ti
Mean:	40.09	0.17	0.86	0.70	0.03	0.08	58.04	(0.03)
	Zirconium aluminide phase 2 (fine prismatic phase – indeterminable from phase 1).							
	50.42	0.30	0.59	0.93	0.01	0.02	47.71	0.02 Ti
	50.49	0.26	0.68	0.77	0.01	0.03	47.74	0.01, Ti, 0.01 Cr
	49.55	0.19	0.71	0.87	0.01	0.03	48.60	0.04 Ti
Mean:	50.15	0.25	0.66	0.86	0.01	0.03	48.02	(0.02)
	Zirconium silicide phase (granular, angular morphology).							
	81.14	0.04	0.88	0.75	1.01	16.16	0.01	0.01 Fe
	79.99	0.05	0.76	0.74	0.97	17.47	0.02	-
	79.83	0.08	0.91	0.70	1.13	17.32	0.01	0.02 Fe
	80.18	0.07	1.03	0.60	1.02	17.09	0.01	-
Mean:	**80.29**	**0.06**	**0.90**	**0.69**	**1.03**	**17.01**	**0.01**	**(0.01)**
	Silicon oxide (carbide nitride) phase (granular, angular morphology).							
	0.01	0.00	1.56	0.73	61.77	35.89	0.04	-
	0.02	0.00	2.42	0.36	59.22	37.95	0.02	0.01 Fe
	0.01	0.00	2.26	0.29	58.64	38.78	0.02	-
	0.01	0.00	2.22	0.23	61.34	36.17	0.03	-
Mean:	**0.01**	**– 2.12**	**0.40**	**60.24**	**37.20**	**0.03**	**(–)**	

[Table continued over page.]

Table {7.3.4}**1** continued/

Spot EDS analyses of the above phases in each of the specimens ZRCN**A1** to ZRCN**A3** provide the following overall mean compositions with the accompanying implied general formulae.

Spot EDS analyses of the **zirconium aluminide phase 1**, as present in each of the specimens ZRCNA1 to ZRCNA3, provide the overall mean composition:

40.66 at%**Zr**; 0.18 at%**Hf**; 57.46 at%**Al**; 0.87 at%**C**; 0.67 at%**N**; [0.03 at%**O**; 0.10 at%**Si**; 0.03 %balance).
This zirconium aluminide (phase 1) can be approximated to *binary* compound Zr_2Al_3 but with a carbonitride *quarternary* compound component.

Spot EDS analyses of the **zirconium aluminide phase 2**, as present in each of the specimens ZRCNA1 to ZRCNA3, provide the overall mean composition:

49.71 at%**Zr**; 0.28 at%**Hf**; 48.47 at%**Al**; 0.66 at%**C**; 0.82 at%**N**; [0.01 at%**O**; 0.03 at%**Si**; 0.02 %balance).
This zirconium aluminide (phase 2) can be approximated to *binary* compound ZrAl but with a carbonitride *quarternary* compound component. Several small but proportionally significant compositional differences exist between the two "aluminide" phases. (Compared to phase 1) in phase 2 the Hf content is greater, the C and N proportions are reversed and, although it may not be statistically significant, the O-content is less. It is thought that the presence of Si and trace components is plainly circumstantial and of no significance to phase morphology.
This phase 2 was considerably less prevalent than phase 1 and, if considered as a binary compound pair, a general composition of the single melt (from which these two solidified) would suggest a binary proportion of ~ 58 at%**Zr**, 42 at%**Al**.

Spot EDS analyses of the **zirconium silicide phase** present in each of the specimens ZRCNA1 to ZRCNA3 provide the overall mean composition:

80.16 at%**Zr**; 0.07 at%**Hf**; 17.20 at%**Si**; 0.87 at%**C**; 0.68 at%**N**; 1.01 at%**O**; [0.01 at%**Al**; 0.01 %balance].
The zirconium silicide phase can be comparatively aligned with the *binary* compound Zr_4Si, however, (including C, N and O) the phase is a re-oxidation *quinary* compound.

Spot EDS analyses of the **silicon oxide (carbide nitride)** phase present in each of the specimens ZRCNA1 to ZRCNA3 provide the overall mean composition:

39.09 at%**Si**; 58.41 at%**O**; 2.10 at%**C**; 0.36 at%**N**; [0.02 at%**Zr**(**Hf**); 0.02 %balance]
This silicon oxide (carbide nitride) phase can be approximated to $SiO_{2-x}C_yN_z$, $x \geq (y + z)$, a "generalised" oxygen-depleted, partially reduced SiO_2 phase.

[Table continued over page.]

Table {7.3.4}1 continued/

The remaining specimens, ZRCN**A4** to ZRCN**A7**, are products of the microwave-stimulated carbo-aluminothermic reduction method. They were processed for the indicated processing times, times being short of the "over-processing" pitfall. The spot EDS counts were acquired from Zr-metallic phase (refer to Figures {7.3.4}7 and {7.3.4}8). The times were progressively shortened to identify any region of process optimisation. Keeping in mind that much of the "processing time" was dedicated to raising the charge temperature into the nominal "process temperature range", processing times shorter than 5.5 min would have resulted in the proportion of "under-processed" reduction product reporting in the processed remnants to be unacceptably high. The following results record only the metal quality (composition), no measure is implied regarding the *quantity* of conversion – which fell-away with decreasing process time.

Specimen. **EDS analyses of spot acquisitions from redn. product phase (at%).**
All EDS acquisitions were spot acquisitions by windowless detection.

	Zr	**Hf**	**C**	**N**	**O**	**Si**	**Al**	**balance**
ZRCN**A4**	94.45	1.32	2.25	1.23	0.17	0.09	0.44	0.04 Cr, 0.01 Ti
(7 min)	94 63	1.09	2.30	1.04	0.20	0.31	0.38	0.05 Ti
	95.14	0.67	2.21	1.00	0.13	0.26	0.52	0.04 Ti, 0.03 Ce
	94.76	0.71	2.65	0.98	0.08	0.17	0.54	0.06 Ti, 0.05 Fe
	93.85	1.46	2.56	1.48	0.11	0.19	0.30	0.05 Cr
	94.87	0.82	2.26	1.38	0.08	0.12	0.41	0.05 Ti, 0.01 Fe
Mean:	**94.62**	**1.01**	**2.37**	**1.19**	**0.13**	**0.19**	**0.43**	**(0.06)**
ZRCN**A5**	93.94	1.03	2.59	1.51	0.20	0.08	0.61	0.04 Ti
(6.5 min)	94.22	0.89	2.48	1.72	0.21	0.11	0.31	0.03 Ti, 0.03 Ce
	95.18	0.78	2.28	1.36	0.07	0.06	0.22	0.05 Cr
	93.84	1.27	3.02	1.26	0.15	0.15	0.29	0.02 Ti
	94.35	1.35	2.57	1.31	0.09	0.06	0.20	0.04 Cr. 0.03 Ti
Mean:	**94.31**	**1.06**	**2.59**	**1.43**	**0.14**	**0.09**	**0.33**	**(0.05)**
ZRCN**A6**	93.97	1.07	2.55	1.47	0.28	0.20	0.42	0.02 Cr, 0.02 Ti
(6 min)	94.38	0.88	2.65	1.09	0.25	0.34	0.38	0.03 Ce
	94.30	1.01	2.89	0.78	0.17	0.35	0.47	0.03 Ti
	94.88	0.46	30.4	0.73	0.20	0.26	0.37	0.04 Ti, 0.02 Fe
	93.92	1.37	2.79	1.11	0.18	0.51	0.11	0.01 Cr
	95.25	0.44	2.76	0.75	0.10	0.33	0.32	0.05 Ti
Mean:	**94.45**	**0.87**	**2.78**	**0.99**	**0.20**	**0.33**	**0.35**	**(0.03)**
ZRCN**A7**	93.75	0.96	3.09	0.98	0.41	0.43	0.36	0.02 Ti
(5.5 min)	94.19	1.15	2.85	0.86	0.21	0.39	0.34	0.01 Ti
	94.22	0.79	3.27	0.67	0.26	0.45	0.28	0.05 Ti, 0.01 Fe
	93.83	0.94	2.89	1.10	0.25	0.36	0.58	0.05 Cr
	94.43	0.84	3.12	0.69	0.37	0.26	0.23	0.04 Fe, 0.2 Ti
	93.77	1.16	3.16	0.79	0.33	0.48	0.29	0.02 Fe
	93.99	0.91	3.08	0.80	0.38	0.35	0.45	0.02 Ti, 0.02 La
Mean:	**94.03**	**0.96**	**3.07**	**0.84**	**0.32**	**0.39**	**0.36**	**(0.03)**

The averaged mean composition of reduction product Zr-metallic phase for the above four specimens is:
94.35 at%**Zr**; 0.98 at%**Hf**; 2.70 at%**C**; 1.11 at%**N**; 0.20 at%**O**; 0.25 at%**Si**; 0.37 at%**Al**; with 0.04 %balance.

[Table continued over page.]

Table {7.3.4}**1** continued/

Note here that such an "averaged mean" composition is intended only as an indication of metal composition for a reduction process that approximates "optimal" (for the method employed). As a casual summary with regard to "results for process times" the following comments are worthy of note. Firstly, the persistent presence in metal compositions of Si and Al may in large part be due to EDS excitation of phases adjoining the metallic phase under examination. Similarly, whilst know to be dominant before reduction, the apparent presence of remnant O in the Zr-metallic phase may also owe some of its proportion to being associated with the Si and Al "external-phase" components. As an observation of reduction product remnants, the quantity of metal phase present in remnants decreased with decreasing processing time, however, the composition of the metal did not vary to such a marked degree. Nevertheless, the least processed specimen ZRCN**A7** does present with lowest Zr(Hf) and N and highest C and O, facts which imply incomplete process metallurgy, and which indicate that process optimisation has not been reached at 5.5 min.

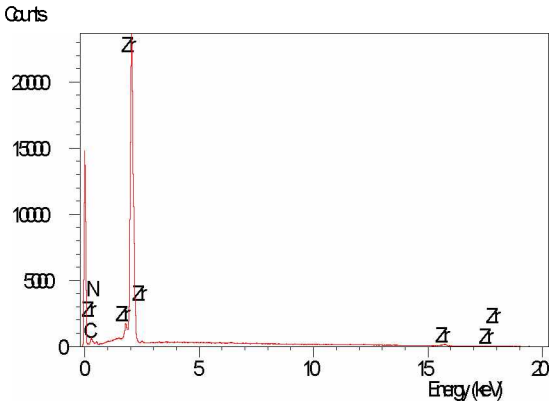

Elmt	Spect. Type	Inten. Corrn.	Std Corrn.	Element %	Sigma %	Atomic %
C K	ED	0.200	1.91	5.59	0.47	28.20
N K	ED	0.107	1.31	2.48	0.32	10.73
Zr L	ED	0.980	1.11	91.93	0.55	61.07
Total:				100.00		100.00

Figure {7.3.4}**9:** In presenting this EDS spectrum and analysis it must be emphasised that the count was acquired from an *atypical* metallic phase, one highly exposed to gas-phase processing at a reaction interface at the charge surface of ZRCN**A4**. (Similar to earlier Ti reduction product equivalents) this O-free metallic phase has progressed much further towards metal compound stoichiometry than did the Zr-metal sought for EDS acquisitions from the internal regions of specimen agglomerates. In selecting a "typical" EDS target phase it was recognised that the "internally sourced" Zr-metallic phase provided sound acquisition sites, was compositionally consistent, was prevalent throughout the specimens; it was therefore ideally suited to best represent Zr-metallic reduction product material. However, occasional phases such as the one captured above were found "externally" on specimen agglomerates – these compositionally atypical phases were sparse in occurrence and were of N-rich carbonitride composition varying widely up to the range of that in this Figure. Also, the pre-emptory spectrum shown here was acquired during a purely exploratory exercise and, on that pre-cursor basis, the "trace" component elements were not tested. Nevertheless, intended as supplementary evidence only, this EDS output of a lesser "real" phase is presented because it is indicative of the degree of processing variation inherent in both the method and at this small scale of experimentation.

7.4: Reduction of Nb_2O_5 , Ta_2O_5 and Tantalum/Niobium-Bearing Mineral Wodginite.

Relative to the Group **4** metals, the metals of Group **5** reveal some concession in their reduction obduracy, however, slower rates of dielectric heating in blends and the melting points of reduction products introduced new challenges. Being easier to reduce than the common oxidic minerals of the Group **4** elements (Ti, Zr and Hf), minerals of the Group **5** elements of interest, Nb and Ta, did not require the thermochemical intensity of the aluminothermic reduction route to produce metallic products, although the aluminothermic reduction option was trialled on the minesite-derived wodginite concentrate. The pure minerals Nb_2O_5 (niobia) and Ta_2O_5 (tantala) are the familiar stable metal oxides in their Nb^V and Ta^V oxidation states, such pure oxides are the eventual refinement products of metalliferous minerals. As is comprehensively discussed by GUPTA and SURI[29] and MOLLER, et al[78], these source minerals range in crystallographic and speciation complexity from columbite (Nb>Ta) or tantalite (Ta>Nb) $[(Fe,Mn)(Ta,Nb)_2O_6]$ up to related resource minerals such as wodginite $[((Mn,Fe)Sn(Ta,Nb))_{16}O_{32}]$. Of the initial, root mineral, columbite is the more common variation in ores worldwide, nonetheless, in Australia the common outcrops are as tantalite and its Sn-rich variant, wodginite, whose concentrates are mineral products of manifold ore deposits and, as such, in the Australian mineral processing experience, tantalite is commonly a "digestion processing stage" mineral in the refining route from minesite-derived concentrate to commercially pure Ta_2O_5 (plus Nb_2O_5 as the minor co-product). The investigation of these pure oxides assumed particular importance in acknowledgment of the singular place that wodginite (through its export-bound mineral derivatives) occupied in Australian resource commerce. More so than for ilmenite, wodginite occupied a significant place in the conception of the project; particularly when acknowledging export trade's nett "value-add imbalance" which could be "tipped" back towards Australia's favour, and because of the proposed process route options suggested by this microwave-stimulated alternative overview.

The pure single oxides and wodginite were each carbothermically reduced utilising the microwave-stimulated method to yield metallic reduction products; although slow to initiate, the reduction operations were accomplished with an efficacy of process not experienced in the reduction operations on the Group **4** minerals. These reduction product phases, whilst not metallic products of high nominal purity, provided sufficient proof of principle in that the prime oxide minerals Nb_2O_5 and Ta_2O_5 can be reduced to metal, and that wodginite can be reduced to useful categories of metallic phases, under the "moderately" rigorous conditions of the microwave-stimulated oven set-up method successfully used through the project.

In this section devoted to Nb and Ta minerals, the pure oxides afforded "clean", uncomplicated metallic reduction product outcomes yielding relatively straightforward analytical results; it should further be noted that these pure oxides are the "starting point" minerals in the commercial production of commercial niobium and tantalum metals. More notably, the minesite-derived mineral wodginite – a far more complex mineral than would normally comprise a starting-point option for refractory metal (or any other) extraction routes – yielded good metallic products (under both carbothermic and aluminothermic regimes). These metallic products presented processing stream options not normally considered, options which could pre-empt new processing routes and future application strategies. Because it represented this most complex processing option-set, the mineralogically complex wodginite was chosen as an indicator of processing potential – a predictor of process options and possibilities for this commercially important mineral class.

Accordingly, to support the later crucial results of wodginite reduction, it was considered that rudimentary experimental trials on pure oxides would both (*i*) provide single-mineral "reduction yardsticks" for direct comparison with the reduction results of the mine-derived wodginite concentrate, and (ii) afford a link in the conceptual continuum between the Group **4** metals (minerals) and major Group **5** metal Ta (wodginite) by its Group **5** analogue, Nb – the minor wodginite constituent.

7.4.1: Carbothermic Reduction of Nb_2O_5 .

In keeping with the need for a plain outcome to support the later wodginite sections, bare process-representative reduction experimentation was undertaken on laboratory grade Nb_2O_5* (and on Ta_2O_5 in the following Section **7.4.2**). Restricting experimentation in this niobia section – more so than for most other of the pure oxides used in the project – the outright number of experimental trials that could be undertaken was limited by the availability of Nb_2O_5 for the reactant blend. Along with the normal consignment of granular char for atmosphere protection, equal quantities of mill-blended Nb_2O_5/char mixture (as per Appendix **6.2**) were charged into the standard crucible configuration (of Figures **{5}1** and **{6.2.2}1**) and processed under microwave-stimulation in the manner of previous carbothermic experimental trials. In light of (the experience of) earlier trials, processing time was started at 10 min with processing of later specimens extending to 12 and 14 mins. In exhausting the available blend material, 6 reduction trials were gainfully conducted producing specimens NIOB**01** to NIOB**06**.

Generally, the initial thermal rate of progress (the preparatory heating towards reaction stimulation) for the reactant charge of each experimental trial was slower than for previous experimental trials and this, it was assumed, was because the microwave susceptibility of the overall charge (mineral plus char plus configuration) was lower than for earlier experimental examples. [Microwave susceptibilities in dielectric loads vary from mineral to mineral and from blend to blend, and not necessarily in a predictable behavioural manner.] Whilst this slower rate of heating was impartially recorded, and although no specific reason could be proposed to equitably explain such dielectric retardation, the "lower susceptibility" assumption was not tested by augmentative experimentation. Also, remaining mindful that, under processing conditions, Nb_2O_5 is reduced by CO at a lower temperature than for earlier oxides. Although, for more conventional extractive systems, MILLER [8] discusses the chemical kinetic and thermodynamic challenges of Nb-reduction from the oxide, including the obduracy of the mineral and the slow reaction rate in reduction. ("Reduction" here may have been equated with "smelting" – reduction with melting – dismissing solid state reduction for the operational pragmatism of being able to "cast"

---

* As Appendix **6.1**; Nb_2O_5 > 99.0 %, – 325 mesh (particle size: $0 < \phi \leq 44\mu m$).

the smelt product into a more tangible, identifiable product form.) Moreover, as it seems clear that the introduction of microwave energy as the primary applied energy brings to extractive reduction processing a new, amplified element of thermochemical stimulation, an element which produces reduction product phases with different characteristics to those experienced by MILLER and others working in conventional fields. Although his descriptions of experimental and development initiatives related to more expansive works, the over-riding kinetic or thermochemical obduracy connection between the present experimentation and the MILLER recount is undeniable.

Nevertheless, this unforeseen low rate of heating was inconsequential in that, as predicted, carbothermic reduction ultimately proceeded "at temperature" (and below melting point, phase dependent), and with relatively insignificant processing extension being primarily aimed at melting. (The slower heating rate in the charge being balanced by lower reduction temperature.) The typically sound reduction product metal was broadly distributed tending towards regional agglomeration – perhaps distinguishing remnant regions of micro-arc intensity – although, (by visual estimation) with lower "total percentage reduced" at any given processing time ("lower" than for previous minerals). On grounds (verified by EDS checks) of negligible observable intermediate reduction phase(s) present (as *non-metallic* "oxycarbonitride" phases), this apparently leaner account of reduced phase may have been underestimated. No straight thermodynamic account could be mounted to explain this apparent discrepancy of less "intermediate" reduction phases (between untainted oxide and metal), however, the "capacity" effect of chemical kinetics is likely to have played some role as the reduction rate was noted to have been low. (Measurement and analyses of these fundamental factors was outside the scope of this foundation project.) Moreover, beyond reaction rate, the typical reduction outcome yielded Nb-metallic phase of good quality, whether discernible as the smallest metallised entities (individual reduced components) or exhibiting as concentrated metallic regions of sintered agglomeration. Of analytical consequence, the agglomerated regions of reduction product metal were sufficiently expansive and volumetrically accommodating to permit clean EDS acquisitions; it was presumed that inter-phase contamination of EDS counts was effectively eliminated for Nb reduction product metal.

Microscopic examination of metallographically prepared reduction product specimens revealed general conformity across all specimens with the materialisation of reduced particulate entities in agglomerated metallic regions. These metallic regions were distributed through reduction product remnants and, not unlike specimens of earlier comparable single minerals, the agglomerated regions appeared to reflect pre-cursor high-thermal conditions of micro-arc activity. It is noted (in YNTEMA and PERCY [128] and elsewhere [4, 5, 79]) that pure Nb has a melting point of ~ 2470°C and related carbide/nitride phases and compounds melt over an inclusive temperature range of very high temperatures. Under light optical examination, the expression of the reduced Nb-metal particles suggests solid state reduction (by intra-particle diffusion through a particle/gas phase interface) with accompanying solid state sintering to accommodate the concentrating agglomeration of metallised regions. These reduction phenomena are in accord with those of previous pure single oxides.

The EDS analyses of Table {7.4.1}1 present typical analyses of reduction product metal exhibiting 8 at% to 10 at% light elements – principally C and N – and (contamination possibilities excluded) with enough O to imply that reduction is incomplete rather than re-oxidation (by O_2 or CO_2) has taken place. [After subjective "statistical editing" (of statistically small sample numbers), the tendency in EDS results was that O-compositions varied more so between specimens than within specimens, and (compared to C and N) that "at% O" was the "largest % variable" in deliberations of light elements in metal composition.] The relatively high C and N in the product metal may indicate re-oxidation by these environment-dominant elements rather than their direct replacement of O (at lattice sites during diffusion) in the reducing remnant oxide. (As there is no true precedence of similar "pig" alloy in an "unrefined state", real material comparisons are generally unavailable for alloys of such uncommon composition. Furthermore, there is some suggestion [8, 181] that these compositions are unstable, and under conventional routes are not synthesised.)

This being said, in assessing the trends in EDS analysis results regarding the fluctuations of component elements (percentages) it can readily be seen that straight "processing time" has not been the *clear* primary factor in predicting the "degree of reduction" evident in individual phase volumes (sintered particle agglomerations) for

any reduction specimen. In fact, the results in Table **{7.4.1}1** of EDS analyses show a compositional scatter which is generally unrelated to processing time and may be more related to other processing factors. Such factors could include charge configuration, the reduction environment, or the variable environment during quench termination. Disregarding processing time, the compositional variation across the specimens was marginal (considering any reasonable "statistical variability" which could be imposed for such experimental operations), and some lesser trends seem more indicative of "specimen specific" process and reduction events. Such "trends" include the C:N ratio across and between reduction product specimens. Indeed, although marginal, a shift towards greater metallisation with increased processing time is evident in the compositional results – if genuine, this trend is contrary to all previous reduction cases and quite counter-intuitive given that greater exposure to re-oxidation factors should yield greater C and N compositions (as metal carbonitride phases); like other refractory metals, Nb has great affinity for the light elements, readily forming metallic compounds under the prevailing energy and ongoing thermochemical regimes.

Regarding the melting point progression through the metals of this project*, and although not the largest difference, the substantial disparity in outright melting points of the pure metals Hf to Nb is ~ 240C°. The magnitude of this temperature range probably extends the melting point of product metallic phases just beyond the system's "applied thermal energy" capability to effectively concede a liquid phase metal. This "melt marginality" being a consequence of the slower "thermal flywheel" effect (of dielectric heating) within the fixed limitations of processing time, applied microwave energy and the dielectric load (varying within the reacting charge). Correspondingly, the thermal input must be matched by the thermal resistance of system insulation – this thermal resistance capability of "containment" components was tested during these later stages of project experimentation, however, the experimental set-up and containment configuration were "nursed" through reduction trials by an experimental discretion learned by way of experience in earlier experimentation. (Discussed elsewhere) the

---

* The progression of melting points for the refractory metals of the project is: **Ti**: 1670°C; **Zr**: 1855°C; **Hf** 2231°C; **Nb**: 2469°C; and **Ta**: 3020°C. Whereof, as alloy content increases, melting points of metals vary greatly (and not necessarily predictably) under the influence of, and with increasing light element and other components in the alloy composition. Also, pure metal melting points do not necessarily indicate propensities for solid state reduction in minerals of the refractory metals. (This under any regime of reduction, and for any processing system – although, being a chemical kinetics driver, microwave-stimulation will enhance diffusion and reaction rates; mass transfer and conversion are fundamental.)

Table {7.4.1}1: The table shows EDS analyses results of spot counts acquired from Nb-metallic phase fields in polished section of mounted reduction product of the microwave-stimulated carbothermic reduction of niobia, Nb_2O_5 . The scarcity of supply (to this project) of pure niobia limited the number of experimental trials that could be undertaken. In good agreement, the analyses recorded here are the set of results for this niobia reduction strand (which was not undertaken by a metallothermic route). The processing time for trial specimens NIOB**01** to NIOB**06** ranged from 10 to 14 minutes. As with other pure oxide reduction cases the reduction product metallic phase entities were quite limited in individual volume, so care was taken to site the beam spot such as to minimise external excitation. However, some proportion of the O counts may plausibly be due to excitation of phase material outside the target volume.

Specimen.	**EDS analyses of spot acquisitions from redn. product phase (at%).** All EDS acquisitions were spot acquisitions by windowless detection.				
	Nb	**C**	**N**	**O**	**balance**
NIOB**01**	91.43	4.01	3.36	0.19	0.93 Fe, 0.06 Si, 0.02 Ta
(10 min)	92.08	3.37	3.17	1.04	0.18 Fe, 0.09 Cr, 0.05 Ta, 0.02 Si
	90.35	4.65	3.95	0.93	0.09 Ta, 0.02 Si, 0.01 Fe
	91.86	4.11	3.27	0.28	0.38 Fe, 0.05 Mo, 0.05 Si
	91.49	3.79	4.53	0.16	0.03 Ta
	90. 72	4.26	4,15	0.66	0.16 Fe, 0.05 W
Spec. mean:	**91.32**	**4.03**	**3.74**	**0.53**	**(0.38)**
NIOB**02**	89.46	5.23	3.97	1.15	0.18 Ta, 0.01 Fe
(10 min)	90.38	5.14	4.04	0.39	0.05 Ta
	88.79	4.92	4.76	1.46	0.05 Fe, 0.02 Ta
	89.53	4.99	4.67	0.68	0.12 Ce, 0.01 Si
	89.06	5.22	4.65	0.90	0.09 Ta, 0.07 Fe, 0.01 Si
Spec. mean:	**89.44**	**5.10**	**4.41**	**0.92**	**(0.13)**
NIOB**03**	86.18	6.87	5.46	1.29	0.16 Fe, 0.04 Ta
(10 min)	88.48	5.34	4.88	1.19	0.09 Ta, 0.02 Mo
	87.98	6.15	4.75	1.00	0.12 Ta
	88.11	5.81	4.69	1.28	0.05 Ta, 0.04.Al, 0.02 Si
	87.27	6.44	4.82	1.38	0.06 Fe, 0.03 Ta
Spec. mean:	**87.60**	**6.12**	**4.92**	**1.23**	**(0.13)**
NIOB**04**	89.35	5.16	4.59	0.81	0.08 Ta, 0.01 Ce
(12 min)	89.90	4.91	4.61	0.51	0.04 Fe, 0.03 Ta
	90.43	4.77	3.74	0.99	0.07 Ta
	89.06	5.54	4.10	1.20	0.09 Ta, 0.01 Si
	91.01	4.55	3.76	0.61	0.07 Ta
Spec. mean:	**89.95**	**4.99**	**4.16**	**0.82**	**(0.08)**
NIOB**05**	92.76	4.08	2.71	0.40	0.05 Fe
(12 min)	91.44	4.83	3.01	0.64	0.04 Ta, 0.04 Al
	91.47	4.92	2.91	0.66	0.02 Ta, 0.02 Fe
	90.78	5.11	3.10	0.85	0.11 Ta, 0.05 W
	92.21	4.16	3.11	0.46	0.04 Ta, 0.02 Al
	91.34	4.44	3.42	0.57	0.17 Ta, 0.04 Fe, 0.02 Si
Spec. mean:	**91.67**	**4.59**	**3.04**	**0.60**	**(0.10)**

Table {7.4.1}1 continued/

Specimen.	EDS analyses of spot acquisitions from redn. product phase (at%). All EDS acquisitions were spot acquisitions by windowless detection.				
	Nb	**C**	**N**	**O**	**balance**
NIOB**06**	92.18	4.20	3.16	0.40	0.04 Ta, 0.02 Si
(14 min)	93.54	3.88	2.16	0.38	0.04 Ta
	92.33	4.02	2.93	0.69	0.03 Fe
	93.20	3.55	2.58	0.57	0.08 Ta, 0.02 Al
	91.80	4.31	2.71	1.08	0.09 Ta, 0.01 Fe
Spec. mean:	**92.61**	**3.99**	**2.71**	**0.62**	**(0.07)**

Averaged mean composition of metallic niobia reduction products across all six specimens: 90.43 at% Nb; 4.80 at% C; 3.83 at% N; 0.79 at% O; with the trace balance (0.15 %) present principally as Nb-analogue impurity Ta.

(Each unto the other, (as analogue elements) Nb and Ta are progenitor impurity elements in their primitive source mineral(s) and consequently are the primary impurity in the other's "refined" minerals. The presence of trace to minor quantities of Fe, Si (and possibly Al) can be attributed to incidental reduction products of refractory materials.)

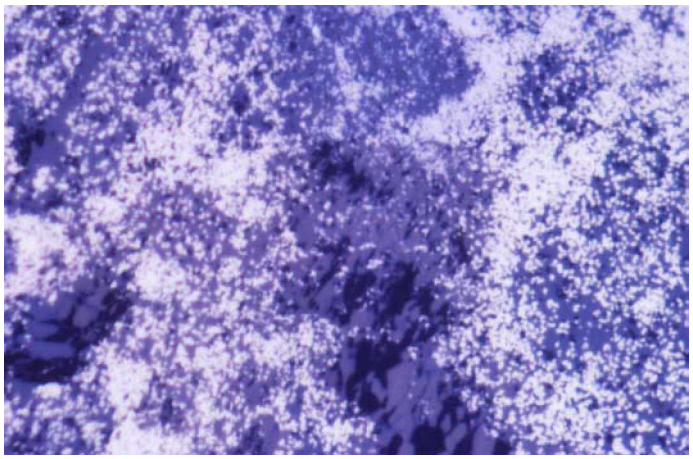

Figure {7.4.1}**1:** Light optical micrograph showing a typical field of view of reduction product remnants of 10 min specimen NIOB**02**, the field is representative of all specimens from 10 min NIOB**01** to 14 min NIOB**06**. Whilst "%-reduction" increased modestly, the extra "time at temperature" had no perceptible impact on melt-agglomeration of this high melting point alloy. Also, no definite trend could be determined regarding the level of light element components in the alloy (with increasing processing time). Such a lack of trend for alloy components was not usual amongst the experimental results of other sections. The metallic regions provided clear acquisition sites and the EDS analyses of Table {7.4.1}**1** are provided with good confidence that contamination of EDS acquisitions by inter-phase excitation (across phase boundaries) was inconsequential. The niobia reduction products are an integral link in the continuum of microwave reduction potentialities across oxides of the refractory metal oxides. [LOM (oel), Ektachrome; fov: 0.21 mm.]

point of thermal failure in containment components was exemplified in the "zirconia" crucibles by the crucial thermal resistance capacity of cementitious agent alumina (nominal melting point 2045°C); this property ultimately determined crucible softening leading to failure.

By interpretation of the binary alloy phase diagrams of Nb-C and Nb-N, and by reasoned projection into the ternary phase field for Nb-C-N – and disregarding the imposition of any minimal phase modifications conferred by O- and trace components – **if frozen from the liquid**, the expected solid solution would be **(**Nb + $Nb_2(C,N)$**)**, where Nb would represent ~ 80 vol%, with the $Nb_2(C,N)$ balance being β phase (or β' if phase transformation (at ~ 1200°C) had taken place during quench cooling). However, and fundamental in any metallic phase characterisation, it must be reported that no visual distinction defining these individual phases was determined during microscopic examination – although, the individual metallised particles were "miniscule", and their amassed sintered regions of metallic agglomeration would still have reflected restraint of phase growth (had they been present) due to the same phase distribution dynamic as the initial isolated metallic entities. (Any phase present being "pinned" within the magnitude of the initial particle, phase growth would be contained – and so may not be detected.) However, from the evidence of microscopic examination and EDS analyses, and regarding the physical properties of niobium metal, it seems unlikely that enough energy (as "heat") was generated during the reduction trials to *melt* the solid state reduced Nb-alloy. (The melting point of pure Nb is ~ 2470°C, whilst the eutectic governing quenched alloy phase of Nb(C,N) composition (contained in reduction metal as analysed) is ~ 2340°C.)

Despite the nominal difficulties discussed above, the experimental work of this section showed that the single oxide Nb_2O_5 could be carbothermically reduced using the established procedure of the microwave-stimulated microwave oven set-up method to produce metallic Nb. Being products of solid state reduction, the metallic particulate entities aggregated and, without specific evidence of individual particle (grain) growth, were sinter-agglomerated during the thermal processing of on-going irradiation, but remained un-melted at quench termination. Of fundamental importance was that reduction of the oxide was demonstrated, and in relative terms, that this reduction was

comprehensive – the metallic reduction product was reproducible, and was consistent across and between specimens.

7.4.2: Carbothermic Reduction of Ta_2O_5 .

After the Nb_2O_5 reduction experience of the previous section, the reduction of Ta_2O_5 – the equivalent "standard" oxide of its analogue refractory metal – proved to be contemporaneous in both procedure and outcome. Again, carbothermic reduction of the high melting point oxide (of a high melting point metal) revealed process characteristics that may be attributed to those thermal and related physical properties. Under the stimulation of microwave irradiation, the reactant blend (mill-blended Ta_2O_5*/char as per Appendix **6.2**) behaved analogously under equivalent thermochemical conditions to its counterpart niobia blend. In particular, tantala charges progressed similarly (in terms of heating rate of the reactant blend) towards a reduction stage yielding clean Ta-metallic product of composition comparable with that of the parallel Nb-product.

In line with established experimental procedure, equal quantities of blend were charged into crucibles with granular char (for atmospheric protection) and arranged in the standard experimental containment configuration and in the manner of the usual microwave oven set-up method (of Figures **{5}** and **{6.2.2}1**). In all, 6 experimental charges were carbothermically reduction-processed under microwave stimulation and these 6 experimental trials were of 2 each distributed over 10 min, 12 min and 14 min processing times, the reduction trials and product specimens were allocated labels TANT**01** to TANT**06**. Despite their slow initial heating rate, the longer-term processed specimens reached extremely high temperatures that tested the thermal capacities of crucible and insulation, and whilst resilience was "tested" during reduction trials, the sole indication of this borderline thermal performance was the "incidental" presence of minor quantities of aluminosilicate slag – at thermal failure, quite fluid melt phase in

---

* As Appendix **6.1**; Ta_2O_5 > 99.0 %, – 325 mesh (particle size: $0 < \phi \leq 44\mu m$). [Melting point of pure Ta metal ~ 3020°C.]

comparison to other, reducing phases – and more common in "permeation pockets" around the crucible base region.

As indicated, much of what was reported in the previous (Nb_2O_5) Section **7.4.1** is relevant to this section of experimental work. As with niobia, the tantala was solid state reduced with only a hint of particle (grain) growth before larger scale agglomeration of reduced particles in regions of "metallisation prevalence" – as with Nb and earlier metals, congregating in regions of "formerly high thermal concentration" along remnant micro-arc activity. Although their thermochemical system was not directly comparable, the observation of liquid-state intransigence of reduced product and the actual Ta-products of pyro-extraction outlined by BORCHERS and KORINEK [31] bear clear comparison to the experimental Ta-metal of this section, albeit with lower N-content. This post reduction melt-intransigence in also affirmed in the account by MILLER [8] whose early authoritative work has been re-affirmed in more recent accounts by others including MOLLER, et al [78] and GUPTA and SURI [29].

In terms of thermal impact upon reduced metallic phase, the typical facies of reduction product remnants of the three processing time groups generally varied in a manner as might be predicted, with rounding and apparent phase-softening of individual particles and nett agglomeration of metallic phase increasing with time. Products of solid state reduction, the least thermally altered reduction product particles were to be found in the least processed 10 min specimens TANT**01** and TANT**02**, of which a typical micrographic field is presented as Figure **{7.4.2}1**. The micrograph shows retention of pre-reduction particle angularity with little apparent particle softening or agglomeration of solid state reduced Ta_2O_5 particles [now essentially > 90 at% Ta, < 10 at% (C,N)] which, by their angularity, have undergone some impact-attrition during mill-blending as the size distribution may represent smaller sizes than expected in a true distribution passing 325 mesh (mesh passing $\phi \leq 44$ μm).

As processing time of specimens increased above 10 min, (and disregarding minimal compositional shift in reduced metal) the already reduced particles were beset by two principal changes to product expression, these being the rounding and apparent softening of individual metallised particles and the regional agglomeration of particles

to affect metallic concentration zones (from which EDS counts were acquired). Microscopic examination over the range of specimens indicated that this apparent partial melting with assimilation and growth between adjacent Ta-grains was facilitated locally by incidental "immersion" in liquid slag (from failed insulation). Evidence of the "rounding" of formerly angular particles and its clear enhancement by "in-slag softening" is shown to advantage in the back-scattered electron optical micrograph of Figure **{7.4.2}2**. The field is representative of dispersed, localised regions – occurring especially in the crucible base – where the invasive and quite fluid aluminosilicate slag accumulated, enveloping Ta-particles which, beyond plain sintering, showed signs of growth by mutual incorporation. As Ta-particles softened and protrusions rounded, they adopted curved surfaces (by way of minimising surface area to volume ratio) – thus promoting larger mutual interfaces between phases, conditions geometrically and thermally conducive of assimilation. Whilst the contamination slag was evident in discrete volumes (inclusive of the dense Ta-metal) there was increasing incidence of aluminosilicate "artifact" slag from insulation failure with increasing time at high temperature.

Like the Nb agglomeration regions of the last section, Ta-metallic phase presented in agglomeration regions through the range of specimens with visual evidence of agglomeration increasing with time, and (again) these zones of metal concentration appeared to reflect remnant micro-arc activity. (As was the case for most reduction product regions) where *no* contaminant slag existed (or had existed in liquid transit), the agglomerated array of reduction product Ta-metal, save for a minor quantity of incompletely reacted tantala material, was slag-free. Consequently, the Ta-particles in specimens of advanced processing exhibited a morphology of "rounded angularity" with sinter-type incorporation increasing with increasing proportion of agglomeration. [As a comment preceding the subject's introduction, the particle/slag "microstructure" typical of the particulate regions impregnated by aluminosilicate slag and as exhibited in the micrograph of Figure **{7.4.2}2** bear good likeness to comparable Ta-metallic regions of wodginite reduction product presented in the following sections. This relatively innocuous observation is seen as encouraging given the similar thermal regimes of both sets of reduction trials, and knowing the Ta(Nb) metallic group separation which was evident throughout the wodginite trials.]

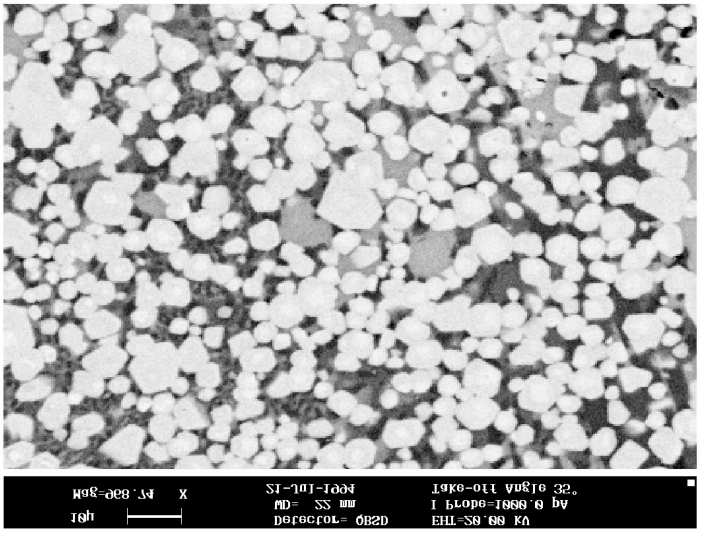

Figure {7.4.2}**1:** Electron optical micrograph showing a typical field of view of reduction product remnants of 10 min specimen TANT**02**, the field is generally representative of specimens from 10 min to 14 min, although some particle growth and slag supplementation was evident in more processed specimens (see Figure {7.4.2}**2** below). The SEM back-scattered micrograph shows the bright metallic Ta-phase in contrast to remnant incompletely reduced phase (mid grey), alumina-based contamination phase (darker grey) dispersed with voids (black). The solid state reduced particles are typically angular and show minimal signs of growth or sinter agglomeration at 10 min processing time. [Leica 440 SEM, BE image.]

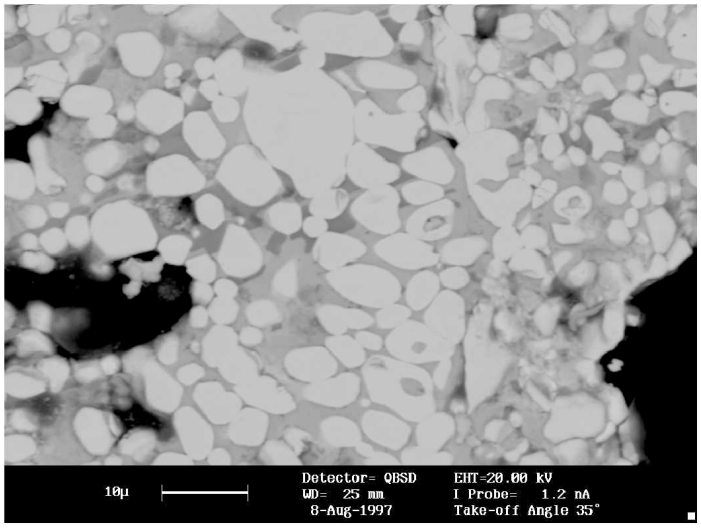

Figure {7.4.2}**2:** Electron optical micrograph showing a more thermally affected region (from crucible base) in 14 min specimen TANT**05**. The bright Ta-metallic phase here shows some evidence of grain growth and softening resulting in rounded particle entities. The presence of a slag phase may have inhibited sintering between these metallic particles. The oxidic slag phase was found (by EDS) to be primarily aluminosilicate with minor Ta, material derived from contamination by thermal failure of insulation. Whilst the lighter grey phase contained minor Ta, differentiation in the slag-phase was not analytically determined, so analysis of the lesser, darker grey phase may have yielded Ta-free aluminosilicate. [Leica 440 SEM, BE image.]

Table {7.4.2}1: The table shows EDS analyses results of spot counts acquired from Ta-metallic phase fields in polished section of mounted reduction product of the microwave-stimulated carbothermic reduction of tantala, Ta_2O_5 . The scarcity of supply (to this project) of pure niobia limited the number of experimental trials that could be undertaken. In good agreement, the analyses recorded here are the set of results for this tantala reduction strand (which was not undertaken by a metallothermic route). The processing time for trial specimens TANT**01** to TANT**06** ranged from 10 to 14 minutes. As with other pure oxide reduction cases the reduction product metallic phase entities were quite limited in individual volume, so care was taken to site the beam spot such as to minimise external excitation. However, some proportion of the O counts may plausibly be due to excitation of phase material outside the target volume.

Specimen.	**EDS analyses of spot acquisitions from redn. product phase (at%).** All EDS acquisitions were spot acquisitions by windowless detection.				
	Ta	**C**	**N**	**O**	**balance**
TANT**01**	90.21	4.37	4.40	0.97	0.03 Fe, 0.02 Nb
(10 min)	91.30	4.26	3.90	0.44	0.07 Nb, 0.03 Si
	91.62	3.95	4.13	0.26	0.04 Nb
	91.45	3.74	4.42	0.33	0.04 Fe, 0.02 Nb
	91.06	4.55	4.11	0.25	0.03 Nb.
	90.84	4.14	4.53	0.40	0.08 Nb, 0.01 La
Spec. mean:	**91.08**	**4.17**	**4.25**	**0.44**	**(0.06)**
TANT**02**	91.07	3.99	4.42	0.44	0.05 Nb, 0.03 Fe
(10 min)	90.58	4.35	4.52	0.50	0.04 Nb, 0.01 Al
	91.46	3.71	4.51	0.29	0.03 Fe
	90.94	4.20	4.49	0.33	0.02 Nb, 0.02 Si
	91.86	3.61	4.08	0.39	0.04 Fe, 0.02 Nb
Spec. mean:	**91.18**	**3.97**	**4.40**	**0.39**	**(0.06)**
TANT**03**	92.13	3.76	3.67	0.37	0.04 Mn, 0.03 Nb
(12 min)	91.39	4.10	4.19	0.26	0.06 Nb
	92.22	4.03	3.56	0.17	0.02 Nb
	92.31	3.58	3.80	0.25	0.05 Nb, 0.01 Mn
	91.88	3.67	4.23	0.18	0.02 Nb, 0.02 Fe
Spec. mean:	**91.99**	**3.83**	**3.89**	**0.25**	**(0.04)**
TANT**04**	91.36	4.02	4.12	0.43	0.04 Si, 0.03 Nb
(12 min)	92.35	3.86	3.63	0.13	0.03 Nb
	92.38	3.61	3.76	0.20	0.04 Nb, 0.01 Si
	91.62	3.66	4.41	0.28	0.02 Nb, 0.01 Fe
	92.90	3.59	3.24	0.24	0.02 Nb, 0.01 La
Spec. mean:	**92.12**	**3.75**	**3.83**	**0.26**	**(0.04)**
TANT**05**	92.63	3.57	3.46	0.29	0.05 Nb
(14 min)	91.58	3.85	4.35	0.19	0.03 Nb
	93.04	3.46	3.25	0.20	0.03 Fe, 0.02 Nb
	92.15	3.57	3.89	0.28	0.07 Nb, 0.02 Fe, 0.02 Si
	91.94	3.61	4.11	0.26	0.04 Nb, 0.03 Al, 0.01 Fe
Spec. mean:	**92.27**	**3.61**	**3.81**	**0.24**	**(0.07)**

Table {7.4.2}1 continued/

Specimen.	EDS analyses of spot acquisitions from redn. product phase (at%). All EDS acquisitions were spot acquisitions by windowless detection.				
	Ta	**C**	**N**	**O**	**balance**
TANT**06**	92.05	4.03	3.46	0.42	0.03 Nb, 0.01 Al
(14 min)	91.17	4.09	4.45	0.26	0.03 Nb
	91.79	3.64	4.25	0.22	0.09 Nb, 0.01 Si
	92.44	3.35	3.99	0.19	0.03 Nb
	91.89	3.77	3.72	0.56	0.04 Nb, 0.02 Fe
Spec. mean:	**91.87**	**3.78**	**3.97**	**0.33**	**(0.05)**

Averaged mean composition of metallic niobia reduction products across all six specimens: 91.75 at% Ta; 3.85 at% C; 4.03 at% N; 0.32 at% O; with the trace balance (0.05 %) present principally as Ta-analogue impurity Nb.

(Each unto the other, (as analogue elements) Nb and Ta are progenitor impurity elements in their primitive source mineral(s) and consequently are the primary impurity in the other's "refined" minerals. The presence of trace to minor quantities of Fe, Si (and possibly Al) can be attributed to incidental reduction products of refractory materials.)

The apparent "lower percentage reduced at time" observed for all the Nb_2O_5 reduction specimens was generally not observed for the Ta_2O_5 reduction specimens, the reduction rate – the progress of the reaction – did not seem to be retarded (compared to Group 4 oxide minerals). Further, as with niobia, the tantala reduction phases between the full oxide and the final metallic Ta-phase did not feature prominently (in terms of presence in reduction phases) – and it is assumed that the process of reduction was effectively complete before the minimum 10 min processing time. As this was the case, then dielectric heating to reduction temperature must have been reasonably effective; it should be noted that the expected temperature at which reduction by CO took place (~ 1450°C) to yield a solid state reduction product. This reduction metal, if pure Ta, would melt at ~ 3020°C, although for the Ta-alloy produced, the melting point range begins above ~ 2800°C for Ta-carbonitrides in the specimens' compositional range. (The melting point range for compositions up to 10 at% C in the Ta-C binary phase diagram range from the (Ta + Ta_2C) eutectic at ~ 2825°C up to ~ 3825°C for the compound TaC, if relevant.) Fourth and higher trace to minor impurities in this basic Ta(C,N) metallic phase would not significantly lower the melting point of the phase.

The results of EDS analyses over the 6 specimens, TANT**01** to TANT**06**, were quite consistent both from phase to phase in each specimen and from specimen to specimen – with the minor proviso (as discussed above) of reduction completeness increasing with processing time. To "eliminate" inter-phase contamination during acquisitions, EDS counts were acquired through windowless detection option from spot excitations sited centrally in larger Ta-particles innermost in metallic agglomerate regions. Typically, the analyses revealed a very consistent Ta composition across the specimen range, the compositional means varying over 1.19 at% between 91.08 at% and 92.27 at% – generally increasing with processing time. There can be no obvious explanation for the general but small *decrease* in C and N over the same specimens, except by comment to affirm that the values were candidly recorded and are truly reported here. However, despite the un-nervingly constant downward trend for the C and N compositions, the variations are within acceptable experimental and statistical limits. More gratifying was the downward trend in "at% O" with increasing time, with low trace metal contaminants throughout. It can fittingly be observed that such compositional consistency in reduction product metal reflected positively upon the

degree of experimental consistency that had come to be marked by reproducible reduction product results from the reduction output of experimentation using the oven set-up method in conjunction with the LN_2 quench termination procedure to secure sound metallic product(s).

Not least to report that, like the analogous Nb_2O_5 before it, the commercially important Ta-oxide Ta_2O_5 was carbothermically reduced under microwave-stimulation using the oven set-up method of reduction to yield metallic-Ta phase in a reproducible manner, and that this operation was realised at a successful, productive level of accomplishment.

7.4.3: Carbothermic Reduction of Wodginite.

It was found in the experimental work of the previous two sections that both oxides Nb_2O_5 and Ta_2O_5 could be efficiently reduced by the rudimentary carbothermic microwave-stimulated route to yield metallic products. By extension, it was anticipated that the complex native mineral wodginite $[((Mn,Fe)Sn(Ta,Nb))_{16}O_{32}]$ would behave in a comparable fashion when subjected to the same reduction conditions to yield (what was expected to be) a creditable and instructive set of reduction product phases, including a crucial metallic Ta(Nb)-phase. One reasonable assumption made of the accomplishments of reduction for previous pure oxides is that, given practicable but "modest" system upgrades, greater metal purities could realistically have been attained; and although species and system variables assumed greater complexity, it was reasonably supposed that wodginite reduction products might also similarly benefit from a "tightening" of system environment and process procedure. Under microwave-stimulated reduction, both the carbothermic route and the carbo-aluminothermic route (with its augmented chemical energy profile) produced creditable reduction product ranges. The aluminothermic option provided an extra element of compositional complexity and, although prominent, this compositional complexity did not necessarily produce a greater "convolution of species". Of the two reduction routes, the micro-textural difference in reduction products was distinct and the demarcation between phases evidently more defined in remnants of aluminothermic reduction – the phase

boundaries being more readily delineated by any of the various modes of visual inspection. Whilst the two routes provided both common and individual process benefits (which as attributes were correspondingly conferred upon reduction products), there were real possibilities for plausible subsequent processing stages presented by each reduction route – possibilities that could revise (even reverse) the sequence of extractive operations in real production streams. Accordingly, the results of these carbothermic and the later aluminothermic reduction options for minesite-derived wodginite* should be evaluated in this light.

In both carbothermic and carbon monoxide assisted aluminothermic reduction products of wodginite blends similar reduction trends seem apparent in that similar reduction product phases exist in the reduction remnants. Remnant phases representing different degrees of reduction – that is, phases of different species at different stages of reduction – are evident in all reduction product remnants. This reduction heterogeneity is dependent upon the locally varying degree of reduction with respect to processing time, contacting and reactant interface, species and reaction counterpart, and crucible position relative to processing energy profiles. And, over-riding these aspects of reduction is the plain fact that, in systems of reduction processing featuring such high melting point phases, an all liquid-state system (contained or otherwise) was never reached – melt liquid(s) from which a simplifying *minimum* number of product phases are the result of equilibrated solidification.

For all wodginite reduction products, the phase groups representing the primary reduction phase distributions, and common across all specimens, always fell into two broad species-specific metallic phase groups plus slag phases, and each group into several principal compositional types based upon local reduction degree and route. Each phase group intimately co-existed in varying, physically different type-morphologies within the same region of reduction product and representing their origin in gas-phase reduction or from liquid phase (by nucleation in a molten remnant-oxides phase). The phase groups of principal interest were the Ta/Nb/(Ti) solid solutions and the Sn/Mn/Fe

* The wodginite $[((Mn,Fe)Sn(Ta,Nb))0_{16}O_{32}]$ mineral concentrate was sourced from the Fortescue Metals Group Wodgina mine, (Pilbara) W.A.; at% Ta:at% Nb ~ 33:1; ~ 0.5 at% Ti, Mn ≥ Fe, trace Al, Si and Ca.

solid solutions (including free-Sn), both groups being reduction products from direct plasma-exposure, and the range of melt-borne metallic phases plus various combinations of oxygen-depleted metal oxides representing stages of mineral reduction and genuine, gangue-derived slags of varying composition. [Slags were Ca/Si/Al-based oxidic for the carbothermic route, then "manifestly Al-dominated"/Ca/Si-based oxidic for the aluminothermic route.]

The phase type of principal interest was the tantalum metallic phase whilst phases of other commercial metals were to be taken into account as important by-products – particularly where these by-products may be delivered in metallic form to a "next stage" of production. The primary Ta/Nb-phase being the impure end product ("pig") phase – which nominally, at the process end-point, contained all of the Ta and Nb* and retained trace to minor percentages of Ti, these varying "locally" within the specimens (with "incidental-mineralisation" determining local composition in the charge). All three metals are light element "getters" contributing to the eventual "sub-compound" CN-solid solution leading to metallic compounds – along with other "incidental component" metals at trace levels as tramp elements derived from the gangue fraction of the concentrate. Microscopic observations indicate that this reduction product phase-type begins (at least) its chemical conversion as solid-state reduction. Windowless and ultra-thin window EDS light element analyses revealed varying but retarded C and N uptake and (depending upon the phase) nil to negligible remaining O in this metallic phase type – affirming the relative completeness of the reduction process. The generally lower total light element content of these phases typically precluded their classification as *metallic compound* but suggested that metallic solid solution was the common metallic type. This sub-compound compositional distinction was corroborated by EDS analyses and the contention supported by observation of morphological forms under light-optical and/or electron-optical microscopy. However,

---

* Niobium displays full solid solubility across the range with tantalum on the binary equilibrium phase diagram. Being intimately related Group 5 elements - the metals share similar chemical and physical characteristics (other than mass) and, thus, are difficult to separate by any extractive means [78]. (The common separation strategy for such a primary "pig" metal reduction product (of a primary extraction route) would involve halidation of the pig metal plus fractional distillation of the halide. This would be followed by refining of the pure halide – undertaken as a tertiary or quarternary stage of the production route. The conventional commercial extractive routes for refractory group metals involve the halidation of the metal oxides plus fractional distillation of the product metal halides before any metal has been produced, the pure distilled metal halides are then reduced to their metals at high purity - so *reduction* is delayed until the final processing stage and refining is promoted to the primary processing stage.)

this "contention" regarding solid solution status is not overtly supported by the evidence of XRD investigations on Ta/Nb/(Ti)-phase retrieved as the acid-digestion product of reduction remnants from regions of extensive plasma exposure – the digestion method and XRD output are discussed in the last paragraphs of this section.

This "phase classification conundrum" being articulated, the light element content of some, *"plasma-exposed"* tantalum metallic phases placed their phase composition in the higher compositional realm of the metallic compound (as was more commonly the case for typical reduction product phases in earlier experimental work). Another prime compositional trend evident in wodginite reduction products – both carbothermic and aluminothermic – was that, whilst C-levels tended lower (than for most earlier refractory metals) across the range of specimens, and except for the few occurrences of metallic compound in high-N plasma-exposed sites, the N-levels in reduction product Ta/Nb-phases were considerably lower than C-levels. Also, N-contents for Ta/Nb phases were typically lower than for comparable phases produced in preceding refractory metal experimentation. No explanation for this evident disparity (of lower light element composition) is proposed here given the considerable mineralogical complexity (and therefore process complexity) confronted in this wodginite reduction programme, nor was light element content especially central to the overall purpose of the wodginite exercise. It should further be acknowledged that such a fact of *lower* light element content in reduction phases must be regarded as a *positive* attribute in any primary reduction product, whilst the *disparity* here is the inability to reconcile this with the typically higher light-element component of metallic products comparable pure single oxides (when the same experimental light-element outcome was expected). Perhaps the physico-chemical "proclivities" imposed by the periodic difference between Group **4** and Group **5** metals may hold part of the answer to this conundrum-come-distraction – and *distraction* only – of minor-element distributions within the overall compositional consistency of experimental results, within each section and across all sections of experimentation.

The general development and distribution of the Ta/Nb/(Ti)-phase in the reduction product facies and through the specimen sequence is represented in the micrographs and EDS map sets of Figures **{7.4.3}1** to **{7.4.3}9**, plus Figures **{7.4.3}11** to **{7.4.3}13** in Appendix **7.4.3**, where accompanying annotations provide relevant

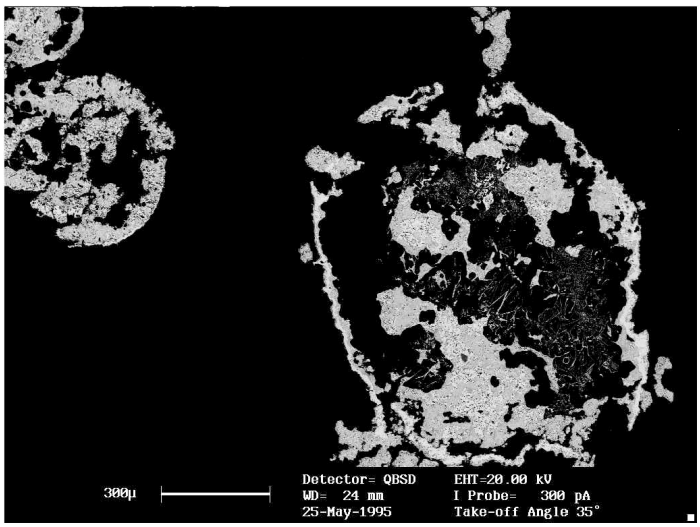

Figure {7.4.3}**1**: Electron micrograph showing the aspect of typical reduction product remnants, this case from 16 min specimen WODG**09**. The remnant features heavily reduced "shell structures" approximating the profile of its initial charge segment at exposure to plasma reduction. The larger "hulk" internally contains the two other principal common features – the Sn-phase regions containing the primary, "plasma exposed" Ta/Nb reduction product (of the shell-structure) and a region of slag (from the concentrate's gangue minerals) containing Ta/Nb morphs (such as are far more common in aluminothermic reduction products.

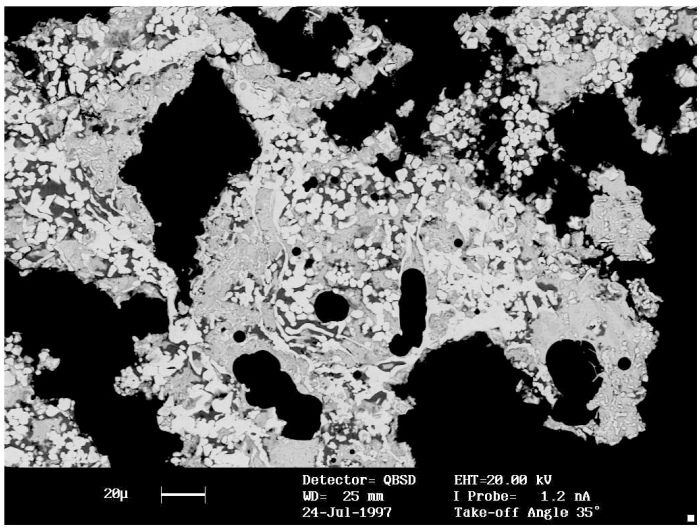

Figure {7.4.3}**2**: Electron micrograph showing the typical facies of an "internal" Sn-phase-dominated region in which are enveloped Ta/Nb-phase particles (both individual and sinter-agglomerated formations). The "Sn-phases" regions (as can be seen by the shade variations of grey) are an "phase amalgamation in process" and these distributed Sn-phases vary from "pure" Sn to Mn/Fe hardhead variations with both Mn and Fe varying upwards from 0 % in Sn. For reasons of drainage and pooling, hardhead-type phases were more prominent in carbothermic products. For aluminothermic reduction products the comparative excess of free slag (oxidised reductant Al on top of gangue) determined that the "fluidity" of liquid-state phases imposed somewhat different chemical dynamics upon the overall reduction processes and which ultimately determined the solidified structure. [Field in WODG**04**.] [*Note that QBSD designates backscattered electron detection.*]

descriptions. The presentation of the broader Ta-phase material, represented in these carbothermic remnants almost entirely by the solid-state reduced "particulate" form and its sinter-agglomerated extension, is shown in varying stages of development through this range of micrographs, and these can be gainfully compared with the micrographs and maps of the following aluminothermic section. General reduction remnant facies are shown in the micrographic set of Figures **{7.4.3}3** to **{7.4.3}6** which illustrate facies development in a typical reduction product in a field at low magnification through to close detail within that field; the series shows the inter-relationship of reduction phases. Of the highly processed Ta/Nb-phase in sinter-agglomerated particulate form, the advanced agglomeration of Ta/Nb-phase presented in the colour micrograph of Figure **{7.4.3}8**, plus those of Figures **{7.4.3}11** and **{7.4.3}12** in Appendix **7.4.3**, show the textured structure of a typical sponge metal – a true sponge irrespective of the polished-section alignment (with respect to agglomerate thickness) of the planes represented in these micrographic fields. Such sponge metal is a common and distinguishing feature in high temperature metallic reduction products (including the reduction products of Kroll and Hunter processes).

It can be seen in Table **{7.4.3}1** that the central Ta/Nb/(Ti)-phase exhibited consistent EDS analyses across the range of processing times, with minor downward divergence of total metal composition to correct for the increasing carbonitride content as this increased with increasing processing time. Otherwise unremarkable, the EDS results show a good total refractory metal yield in this central reduction product of wodginite reduction. Whilst perhaps for this section it should be regarded as a "ring-in" component, Ti is a refractory metal and so reports with its fellow refractory metals in their high temperature reduction product metallic phase(s), it is here included with Ta and Nb in "total metal". The (Ta,Nb,Ti) total metal mean value over the combined nine specimens across all processing times reveals 94.41 at% (Ta,Nb,Ti) and 5.43 at% (C,N) with (Ta,Nb,Ti):(C,N) being (17.4):1 [and (Ta,Nb):(C,N) being (16.9):1] – the total metal composition in the reduction phases (at 94.41 at%) is comparatively high against previous refractory metal reduction products. Further, as elsewhere mentioned, the important O-component retained in this reduction product is very low (at ~ 0.10 at%) in comparison to previous reduction products and the trace element metals may largely be an inter-phase impurity aberration of EDS acquisition.

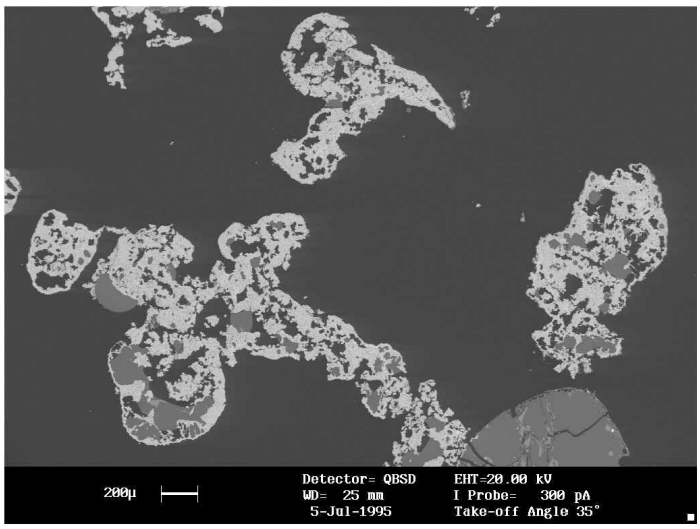

Figure {7.4.3}**3**: Low magnification electron micrograph showing agglomerated product of advanced reduction in mounted and polished reduction, remnant features of 14 min specimen WODG**07**. Note the relatively fused nature of the reduction product remnants after extended processing time under plasma exposure has consolidated reduced phases. This field is the first of four consecutive fields "zooming-in" on detail of reduction product phases, thereby providing some understanding of the evolution of facies and the specimen phases therein.

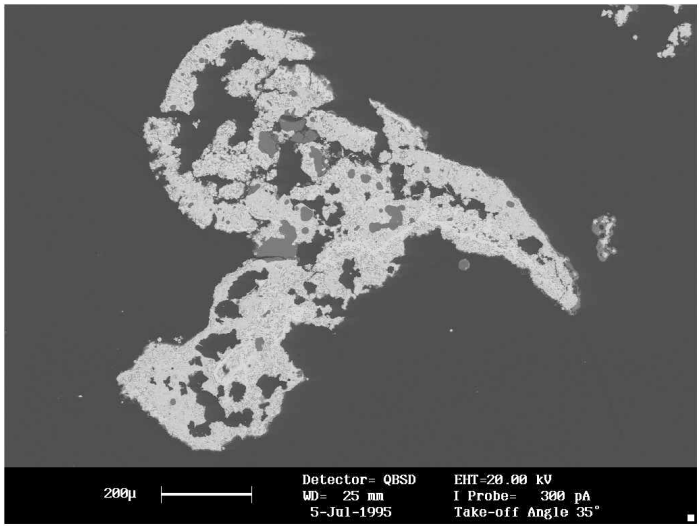

Figure {7.4.3}**4**: Incremental magnification increase showing one reduction product feature presented in Figure {7.4.3}**3** above. The reduction remnant "feature" is quite highly metallised (given the achievable limit which the reactant blend could theoretically yield upon reduction).

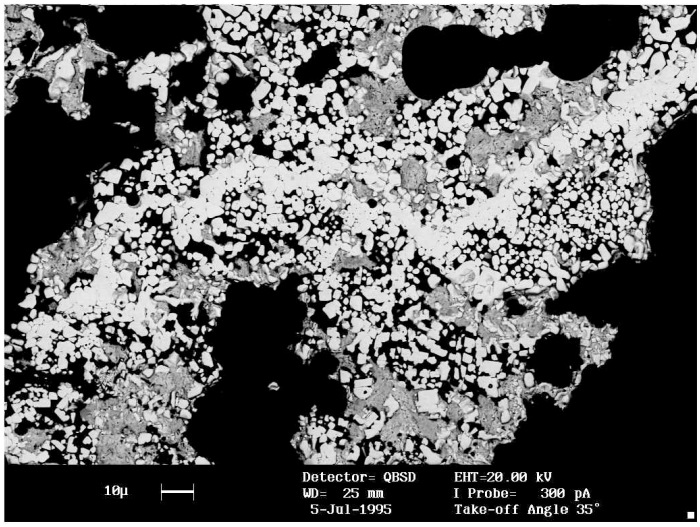

Figure {7.4.3}**5**: At this magnification the field best exhibits visual information regarding both distribution (pattern) of reduction phases through the reduction product remnants (in polished section) and, with the benefit of attuned "contrast", the inter-relationship of the various phases (or phase groups) to one-another. The central "spine" of Ta/Nb-phase (the brightest phase) most likely represents a remnant artefact of a past high thermal intensity zone of either a relic plasma-exposed surface or (preceding such volumetric gaseous plasma) the relic of a micro-arc track through the charge's "primal" blend. Such a field with its irregular distribution of phases was quite representative of carbothermic reduction products.

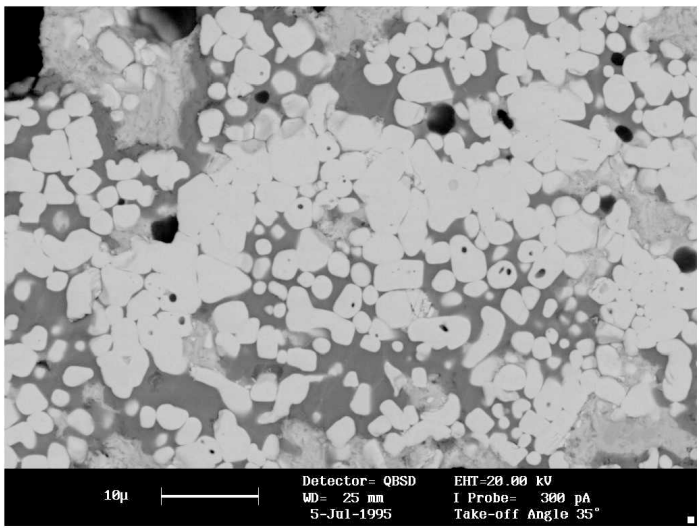

Figure {7.4.3}**6**: Contained centrally in Figure {7.4.3}**5** above, this sequence-final backscattered electron micrograph sheds light upon finer detail (not obvious at lower magnification). The mill-blended Ta/Nb-particles (brightest phase) show evidence of sinter agglomeration and/or growth in zones of obvious thermal intensity; the darkest grey phase is Ca/Si/Al/(Mn,Fe) oxide slag; whilst the light-to-mid grey phase(s) are regions of Sn-phase varying in (Mn,Fe); black features are voids.

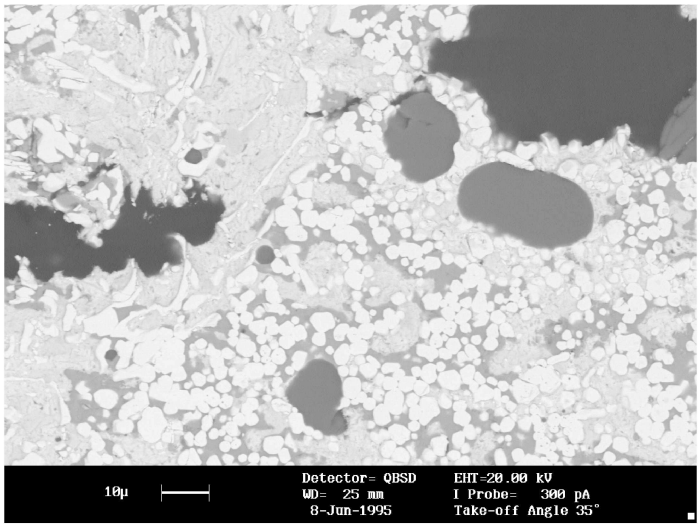

Figure {7.4.3}**7**: Electron micrograph showing detail in 12 min specimen WODG**05**. The sampled material was recovered from a region low in the crucible and was typical of remnants recovered from "puddled" zones throughout the specimen range. The field delineates the minutiae of phase variation in Sn-phase material (the mid-grey phases, esp. upper left field) that, with minor slag presence (darker grey), enfold the Ta/Nb-phase particles. Because slag was gangue-derived (only) in carbothermic reduction remnants, the minor volumes present were not sufficient to ensure overall confluence of slag into larger phase volumes, as was the case for slag in the aluminothermic remnants.

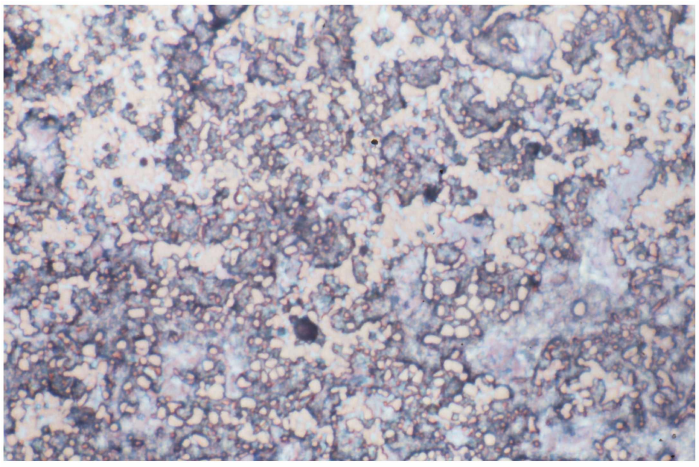

Figure {7.4.3}**8**: Light optical colour micrograph showing a typical metallised field in the above specimen WODG**05**. The field shows Ta/Nb/(Ti)-phase "sponge" (cream-pink) with some Sn-phase (silver-grey) in voidage, smeared during specimen preparation. Resolution of particulate agglomerates is indefinite in light optical micrographs because of limited focal length at magnification. (Also see LO micrographs in Appendix **7.4.3**.)s [LOM (air); Ekta.; 208 µm]

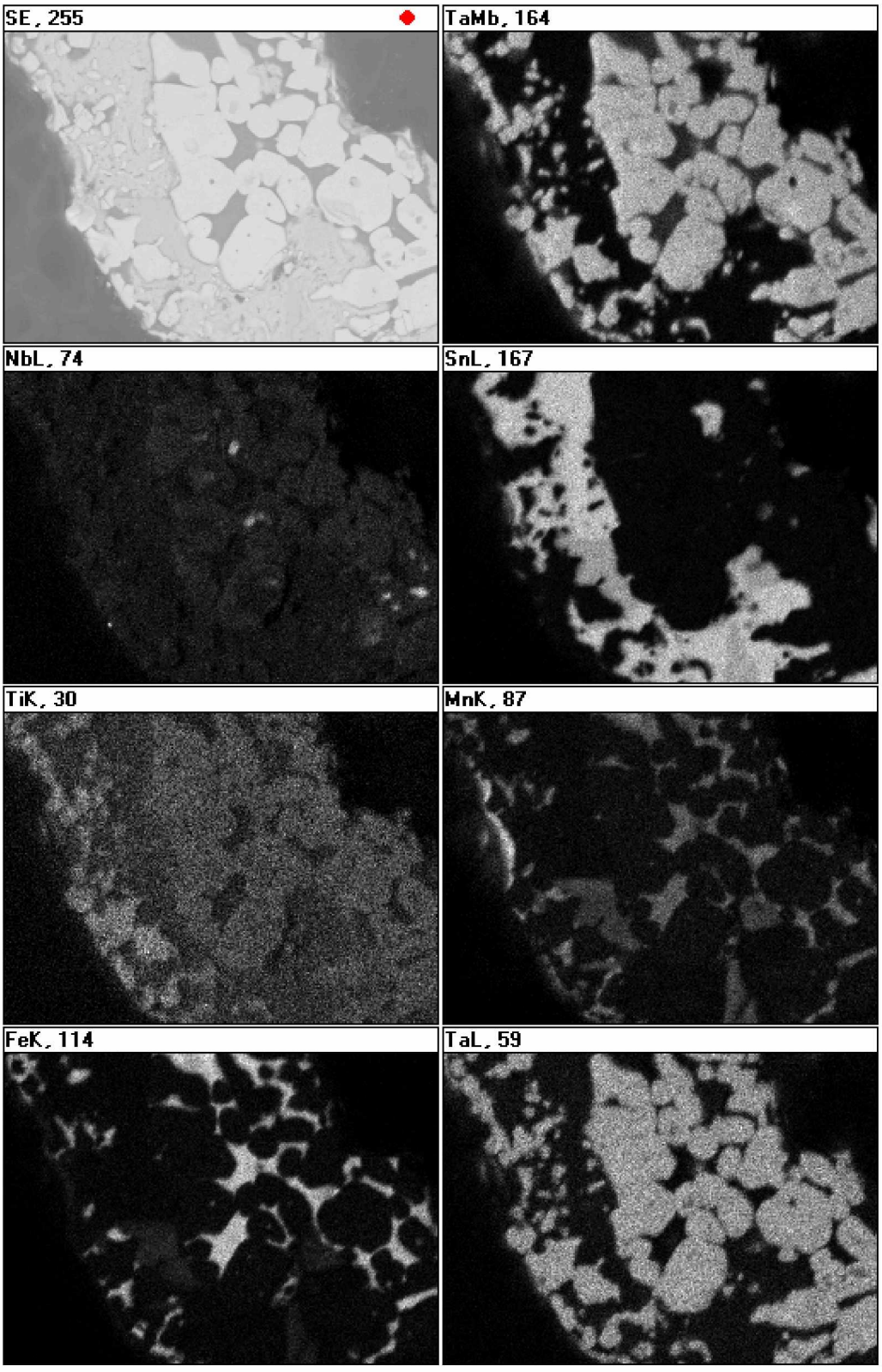

Figure {7.4.3}**9:** Map set showing detail of typical reduction remnant facies in carbothermic wodginite reduction product (12 min WODG**06**). Apart from the dominant presence of untainted Ta/Nb/Ti-phase, the separate distributions of Mn and Fe in both "hardhead" and slag phases are of relevance. Also, as minor impurities in wodginite, the "slag-forming" elements Ca and Al were "indiscernible" in carbothermic slag remnants. [The numbers accompanying each map-acquisition indicate detected "counts/sec".] [fov: ~ 30 μm]

Table {7.4.3}1: The table shows results of EDS analyses of spot counts acquired from Ta/Nb-metallic phase in fields in mounted and polished reduction product of the microwave-stimulated carbothermic reduction of wodginite as the minesite-derived mineral concentrate [(Ta,Nb)Sn(Mn,Fe)$_{16}$O$_{32}$]. The processing times for trial specimens WODG**O1** to WODG**O9** ranged from 8 min to 16 min in keeping with the processing requirements in delivering a suitable range of metallisation in reduction products, the modest and unreactive slag volume was generated from the gangue content of the concentrate (plus any "incidental" quantity from insulation failure). Of significance for these reported EDS analyses is that, because of the otherwise wide range of metallic phases, only the Ta/Nb-phase metal was addressed. In carbothermic reduction products the only significant Ta/Nb-phase material was the particulate form (including its sinter-agglomerated progression), and this solid-state-reduced phase expression provided clear EDS acquisition sites. The fellow refractory metal Ti, a minor impurity in the mineral concentrate, typically reported in the reduced Ta/Nb-phase – which is alternatively written as "Ta/Nb/Ti-phase" (context dependent) and, on average, the Ti-content was of similar proportion to the Nb-content in the principal metallic "phase of interest".

Specimen.	**EDS analyses of spot acquisitions from redn. product phase (at%).** All EDS acquisitions were spot acquisitions by windowless detection.						
	Ta	**Nb**	**Ti**	**C**	**N**	**O**	**balance**
WODG**01**	90.47	3.51	2.22	2.90	0.79	0.06	0.03 Fe, 0.02 Al
(8 min)	91.28	2.95	2.60	2.37	0.61	0.11	0.06 Fe, 0.02 Si
	89.78	2.90	3.04	3.49	0.66	0.08	0.05 Si
	88.96	3.08	2.88	3.91	1.07	0.03	0.04 Fe, 0.03 Al
	89.65	4.11	2.75	2.74	0.56	0.12	0.05 Al, 0.02 Fe
Spec. mean:	**90.03**	**3.31**	**2.70**	**3.08**	**0.74**	**0.08**	**(0.06)**
WODG**02**	90.25	3.05	2.35	3.46	0.56	0.27	0.04 Al, 0.02 Si
(8 min)	89.19	3.94	2.53	3.47	0.75	0.08	0.03 Fe, 0.01 Al
	89.33	4.42	2.12	3.65	0.28	0.13	0.04 Si, 0.03 Fe
	88.97	3.86	4.23	2.30	0.48	0.07	0.09 Al
	89.77	2.97	2.25	4.62	0.29	0.05	0.05 Fe
Spec. mean:	**89.50**	**3.65**	**2.70**	**3.50**	**0.47**	**0.12**	**(0.06)**
WODG**03**	88.79	3.07	3.01	4.56	0.37	0.11	0.09 Fe
(10 min)	90.14	2.88	2.78	3.42	0.67	0.06	0.03 Si, 0.02 Al
	89.44	3.15	2.66	4.06	0.59	0.05	0.05 Fe
	89.34	1.94	2.17	5.75	0.52	0.16	0.09 Fe, 0.03 Al
	88.76	3.31	3.00	4.43	0.37	0.09	0.04 Si
Spec. mean:	**89.29**	**2.87**	**2.72**	**4.44**	**0.51**	**0.09**	**(0.08)**
WODG**04**	88.72	3.49	1.77	4.99	0.78	0.18	0.07 Fe
(10 min)	89.02	2.76	2.88	4.80	0.34	0.12	0.04 Fe, 0.04 Si
	89.93	3.10	1.98	4.38	0.46	0.11	0.04 Si
	88.49	3.87	2.08	5.03	0.38	0.08	0.06 Fe, 0.01 Al
	88.68	4.14	2.23	4.30	0.43	0.14	0.05 Al, 0.03 Fe
Spec. mean:	**88.97**	**3.47**	**2.19**	**4.70**	**0.49**	**0.13**	**(0.05)**

[Table continued over page.]

Table {7.4.3}1 continued/

Specimen.	EDS analyses of spot acquisitions from redn. product phase (at%). All EDS acquisitions were spot acquisitions by windowless detection.						
	Ta	**Nb**	**Ti**	**C**	**N**	**O**	**balance**
WODG**05**	88.82	2.95	2.96	4.30	0.86	0.04	0.05 Fe, 0.02 Al
(12 min)	88.76	3.15	1.84	5.60	0.56	0.07	0.02 Si
	89.37	1.69	3.19	5.07	0.58	0.04	0.04 Fe, 0.02 Si
	87.79	4.42	2.77	3.91	0.89	0.16	0.06 Fe
	88.65	2.54	1.86	6.06	0.70	0.10	0.06 Fe, 0.03 Al
	84.64	6.03	3.05	5.50	0.53	0.11	0.10 Al, 0.04 Fe
Spec. mean:	**88.01**	**3.46**	**2.61**	**5.07**	**0.69**	**0.09**	**(0.07)**
WODG**06**	88.71	3.10	3.04	4.70	0.29	0.09	0.05 Si, 0.02 Al
(12 min)	87.68	2.45	2.18	6.86	0.60	0.17	0.06 Fe
	87.90	2.82	3.17	5.49	0.48	0.06	0.06 Fe, 0.02 Si
	86.04	5.32	2.44	5.77	0.33	0.05	0.05 Al
	88.41	3.67	2.14	4.71	0.85	0.16	0.04 Fe, 0.02 Al
Spec. mean:	**87.75**	**3.47**	**2.59**	**5.51**	**0.51**	**0.11**	**(0.06)**
WODG**07**	86.87	3.55	2.70	6.04	0.78	0.02	0.04 Fe
(14 min)	87.44	3.10	3.18	5.56	0.59	0.08	0.03 Fe, 0.02 Al
	87.09	3.88	1.95	6.18	0.70	0.15	0.05 Fe
	88.38	2.91	1.89	6.28	0.43	0.05	0.06 Al
	85.96	5.41	2.85	5.17	0.48	0.08	0.05 Si
Spec. mean:	**87.15**	**3.77**	**2.51**	**5.85**	**0.60**	**0.08**	**(0.04)**
WODG**08**	85.72	3.82	4.25	5.41	0.55	0.17	0.05 Fe, 0.03 Si
(14 min)	88.08	2.45	2.00	6.70	0.61	0.10	0.06 Fe
	87.52	3.66	2.25	5.57	0.82	0.07	0.07 Si, 0.04 Fe
	87.48	4.80	1.88	5.28	0.34	0.14	0.08 Fe
	88.92	3.63	2.26	4.61	0.46	0.06	0.04 Si, 0.02 Al
	86.56	5.80	1.75	5.02	0.73	0.09	0.05 Fe
Spec. mean:	**87.38**	**4.03**	**2.40**	**5.43**	**0.59**	**0.11**	**(0.06)**
WODG**09**	86.77	3.50	2.78	6.31	0.45	0.13	0.04 Si, 0.02 Fe
(16 min)	87.10	3.44	2.49	6.31	0.51	0.09	0.06 Fe
	86.46	4.09	3.03	5.39	0.76	0.17	0.08 Al, 0.02 Fe
	88.43	2.98	2.17	5.65	0.69	0.04	0.04 Fe
	84.59	7.36	1.68	5.70	0.49	0.09	0.05 Al, 0.04 Si
	85.50	4.06	2.53	7.17	0.55	0.14	0.05Fe
Spec. mean:	**86.48**	**4.24**	**2.45**	**6.09**	**0.58**	**0.11**	**(0.05)**

Averaged mean composition of metallic wodginite reduction product Ta/Nb/(Ti)-phase across all nine specimens: 88.28 at% Ta; 3.59 at% Nb; 2.54 at% Ti; 4.85 at% C and 0.58 at% N, with the balance of O plus trace metals. Notably, C-content increased with processing time and the principal metals consequently decreased.

(Each unto the other, (as analogue elements) Ta and Nb are progenitor impurity elements in the primitive source mineral(s) and consequently are the primary impurity in the other's "refined" minerals.)

Although the pyro-reduction of the "whole" mineral concentrate is not envisaged in conventional industrial practice, and this is reflected in publications over the many years since Ta and Nb were first produced at an industrial level, some reference to *pyrometallurgical* reduction products of single oxides (or "pure" oxides) was found in the more comprehensive texts which have generally seen fit to follow and professionally up-date the industrial extractive metallurgy of these Group **5** refractory metals. Notwithstanding, the conventional concept of refinement then halide reduction is well entrenched in the mindset of Industry. MILLER [8] described Ta-reduction phases of " reduction of the oxide" as being less than metallic and with a remnant-O content high enough as to render the "intermediate product" an "unlikely" product for any further process stream. CHASTON [13] discussed an apparently similar outcome without citing any specific results. In a personal communication, WORNER [181] suggested that, contemporary with these authors, these early industrial research programmes were particularly influenced by the lack of technological refinement and system development (including automated control) in processing, refractory and vacuum technologies. Such unavailability dictated the likelihood of success for much of the "crucial thermochemistry" experimentation up to late last century; developments in materials and process technologies are so quickly "taken for granted".

In descriptions of the various metallic and slag phases of reduction products of this wodginite reduction work, the repeated use of "plural" descriptors was emblematic of the clear fact that *heterogeneity* (rather than homogeneity) was universal throughout reduction remnants. Essentially, this heterogeneity arose because extensive liquid-phase mixing could not occur to metallurgically homogenise each phase group before solidification. Moreover, of all microwave reduction experimental sections, even more so than for other minesite-derived minerals, wodginite produced complex reduction products, even within each phase group – having extremely high melting points, some phases were "softened solids" throughout process temperatures. The absence of desirable liquid-state mixing – incorporating melt chemistry – a feature in orthodox pyrometallurgical systems, was a "price paid" in adopting the experimental method employed. However, despite the more complex metallurgical chemistry of the wodginite system, the "volume percentage" (in the reacting charge) of slagging phases available to the later stage liquid-phase reduction process(es) was greater than for other

mineral trials (disregarding accidents of slag augmentation by inadvertent thermal failure of containment insulation).

The second significant general phase occurring in wodginite reduction products was the range of Sn-based metallic phases, these metallic phases were widely represented as Sn-based compounds in "pure"-Sn to low-alloy-Sn – the solid solution range being solidified in the last throes of cooling. Sn-rich "hardhead-type" metallic phases, typically as impurity compounds of composition "incidental" with the root minerals and location of their reduction, were contained in matrix material of low alloy Sn to "pure" Sn. Whilst the Sn/Mn/Fe-phase was of unquestionable reduction process importance, its precise constitution was not considered a *core* project concern. Consequently, only subjective EDS analyses were carried-out "incidentally or as encountered" on the often very restricted, if not visually indistinct Mn-"hardhead" regions (from which only "inter-phase contaminated" EDS counts could be acquired from spot excitations and only anecdotal observations noted in visual studies). Such incidental compositions were expected to have fallen into the phase/compound series: $\alpha Fe \Rightarrow Fe_3Sn \Rightarrow Fe_3Sn_2 \Rightarrow FeSn \Rightarrow FeSn_2$ and $\alpha Mn \Rightarrow Mn_9Sn \Rightarrow Mn_3Sn \Rightarrow Mn_2Sn \Rightarrow MnSn_2$ plus the Mn-Fe phase-continuum, higher permutations of these ($Sn_xMn_yFe_z$), and any other incidental inclusions to this range (Ca, Si, Ta, *et cetera* – in occasional, minor composition). These phase continua and compound series are related (*i*) by the mineralogical association of their antecedent species, and (*ii*) by the modest "temperature" range of the reduction of such species and of subsequent syntheses of their metallic forms.

With respect to the experimental intent of this compounded reduction process and of its overall "systematisation" as an optional process, it is of considerable significance that this Sn-based "continuum of phases" served to concentrate the mineral's major tramp elements in metallic phase(s) separate to the principle metallic objective. If not for the Sn-phase group the metallic tramp elements might otherwise have then gravitated to the Ta/Nb/(Ti)-phases. However, presenting as they did in the reduction product remnants, the Sn-alloy-agglomerate could be physically or chemically separated from the tantalum phase(s). [Also, other tramp metals present as gangue in the

mineral concentrate – "metals" such as Ca, Si and Al – (*if* reduced will have re-oxidised and) reported in slag phase(s) rather than in a metallic phase.] Sn is the first element reduced to metallic form from wodginite and, being highly fluid at process temperatures, would freely "flow and pool" *if not for* the over-riding restraint of high surface tension on liquid Sn beads – (relative to other metals in the liquid state) high surface tension a characteristic of liquid-Sn. [(As was realised by use of $BaCO_3$ in the cassiterite reduction of pre-core experimentation) this surface tension could have been overcome by the use of a surfactant agent, but such an approach was not employed in this case so entrained liquid Sn could "mop-up" the subsequently reduced Mn and Fe.] So, remaining generally distributed throughout the reducing charge, the liquid Sn-beads were *locally present* to coalesce and combine (as alloy or compound) with Mn and Fe, the next-stage products of the wodginite reduction sequence.

A common conundrum in the "traditional" smelt-reduction of cassiterite to Sn-metal is its great affinity to form the brittle tin-iron intermetallic amalgam of Sn-Fe metallic compounds known as "hardhead" (by co-reduction of the cassiterite's Fe-impurity). This mixture of intermetallic phases was unavoidably replicated in wodginite reduction by extension of the "hardhead" grouping of "alloys and metallic compounds" into the ternary Sn-Fe-Mn phase field. Briefly, (in its phase field inter-relatedness) Mn exhibits good compatibility with Sn and Fe in the evolving phase(s), and such compatibility was advantageous to the purpose of the "mopping-up" and containment of these three metals in a metallic composite that (importantly) remained physically separate from the Ta/Nb-based phases. Unlike the ductile "pure"-Sn metal (liquid Sn down to ~ 232°C), ductility decreases and melting point increases with increasing "impurity" such that, once enough Mn/Fe-"alloying" took place in solidifying remnants, a range of brittle new "Mn-hardhead" metallic compounds solidified within a matrix of the balance of Sn-alloy – a composite "amalgam" having an overall brittle nature. The greater the up-take of Mn and Fe in the available Sn, the more brittle and more infusible the Mn-hardhead residue became, leaving it amenable to physical separation strategies (alone, if commercially desirable, without the adaptation of solution-digestion).

By at% in the wodginite concentrate, Sn≥ (Mn + Fe), so "matrix -Sn" alloy was present in reduction products of *limited* processing; and it should be noted that, with ongoing processing, this "free" solid solution Sn would be taken-up in conversion to

$Sn_xMn_yFe_z$ intermetallic compounds of higher Sn stoichiometry ($Fe_3Sn_2 \Rightarrow FeSn$, $Mn_9Sn \Rightarrow Mn_3Sn$, *et cetera*), ultimately exhausting the "free"-Sn of solid solution phases. It seems plausible that, in the development of this secondary metallic product, such a trend towards compound synthesis may be evident in specimens for Sn-phase material in regional remnants of higher thermal intensity and/or in specimens of longer processing times. And further, that such a trend was not easily identified because XRD studies would have been required to confirm the actual phase or compound (and thereby its presence) of such miniscule volume entities, entities interlocked with compounds of like kind in a composite phase of only slightly larger magnitude. [A relevant and *otherwise* important strand of enquiry, but being outside the "refractory metal" scope, a task that was not a project objective.]

Of reduction product regions representing various stages of process reduction, the recorded evidence of observations plus EDS analyses showed quite clearly the various stages of Mn-hardhead evolution, from regions of "pure"-Sn through to amalgamated regions of varying Sn/Mn/Fe-intermetallic compounds in minimal Sn-alloy matrix. Although Sn/Mn/Fe-phases feature in all micrographs, that of Figure **{7.4.3}2** shows a typical dispersal of "Mn-hardhead" through particulate structures of Ta/Nb-phase and "anchored" to the high melting point structure – initially by virtue of surface tension in the liquid-Sn, thence by intermetallic phase "stiffening" of the amalgam. Figures **{7.4.3}6**, **{7.4.3}7** and **{7.4.3}8** reveal aspects of distribution of the broad Sn/Mn/Fe-phase with its variations and inter-relationship with other phases. The colour micrographs of Figures **{7.4.3}11** and **{7.4.3}12** show the elusive nature of primary Sn-phase material – as the soft metal (in this instance) was distributed in Ta-phase voidage from which it showed a propensity to be removed and/or smeared during specimen preparation and polishing. The EDS maps of Figures **{7.4.3}9** and **{7.4.3}13** corroborate element distributions in regions of good Ta/Nb-phase development, in particular the former map set shows a near-surface band of Sn including intervening Sn-Mn-phase sections. Of note in this Figure **{7.4.3}9** map set is that, whilst some Mn exists in the Sn-phase, the balance of the Mn and "all" of the Fe exist in slag phase. In conjunction with other mapping exercises, such an exposé of element distribution was used to interpret processing sequences. Further, and common between the reduction systems, distinctive Sn/Mn/Fe-phase detail can be seen in micrographs of the aluminothermic reduction product remnants of Section **7.4.4** where this second metallic phase group was less

"different" from its carbothermic equivalent than were the Ta-group phase(s) and the slag phase from their equivalents.

Whilst almost all Mn and Fe ultimately reported in Mn-hardhead metallic form, the evidence of analyses of carbothermic reduction products confirm that minor proportions of both Fe and the more abundant Mn persist, to greater or lesser degrees, in isolated oxide phases that may be either un-reduced or re-oxidised phases and which were ultimately classified as oxide slag phases. Where unconstrained by physical isolation, such Mn and Fe slag phases plus those oxidic regions of the gangue elements (principally Si, Al and Ca) plus rare regional portions of un-reduced Ta, Nb and Ti oxides were generally combined in blended oxide slag phases – phases whose compositions were evidently as complex as they were varied (by their root minerals). The carbothermic reduction route produced a volumetric minimum of slag(s) integral with reduction product remnants, and being identified with regional mineralogy from "reactant charge" to "reduction remnant", the different volumetric elements of slag exhibited compositional variation from remnant to remnant through the specimen, each tending to stay with the regional reduction remnant from which it was generated. Locally in carbothermic remnants, where slag volumes were supplemented by thermally failed insulation, then a commensurate degree of liquid phase mixing could occur in slag material. In aluminothermic reduction remnants of the following section the Al-dominant "aluminothermic" slag was more compositionally universal and, because of its volumetric prevalence after the aluminothermic reaction, was found to be more pervasive through reduction remnant regions.

Typically for final carbothermic slags, the minor Mn and Fe that remained in oxide form, or reverted to oxide form, was often captured in "sponge" porosity of metallic reduction product Ta/Nb-phases, and was tied-up with Ca, Al, Si and other trace gangue elements that constituted the final slag composition, which was *generally* devoid of Ta and Nb (and Ti). In cases of greater processing time (and intensity) slag pockets ran together, or were augmented from molten insulation, and in these larger, more "thermally subjected" slag volumes certain further "process events" could occur (and were captured upon freezing) which did not occur in less thermally subjected remnants. Some more accumulated pockets of slag in carbothermic remnants exhibited features common in aluminothermic slags. One such altered slag remnant is in evidence

in the broad-field micrograph of Figure {7.4.3}1 in which the "extensive" slag region exhibits Ta/Nb-phase features reminiscent of the distinctive faceted plate features so prevalent in aluminothermic slags – *and against which those aluminothermic slag features should be contemplated.* As there was no aluminothermic reaction to which these "plate" phase features can be attributed, this rather uncommon feature is suggestive of a possibility of the dissolution or melting into super-heated slag of adjacent particulate Ta/Nb-phase material with subsequent plate solidification upon quenching. Plate synthesis/formation is discussed further in Section **7.4.4**.

With respect to the processing potential represented by material outcomes and the extractive simplicity of this extraction alternative, the significance of this experimental accomplishment should not be overlooked! Unlike the industrial processes, in this pyrometallurgical solution the Sn confines the two other prominent unwanted metallic elements (Mn and Fe) which occur in quantity in the ore and which (*i*) could otherwise be a major impediment if taken-up by metallic Ta/Nb-phase, and (*ii*) impose a processing burden in the commercial chemical digestion routes undertaken in industrial extraction practice [8, 29, 78]. It should be noted that, in the ore, Mn and Fe are not associated with Sn in a simple manner but have a more complex mineralogical association (which includes the Ta and Nb). The "mopping-up" capability peculiarly characteristic to this microwave reduction process was found to be quite complete, a fact confirmed by analyses of intermediate and advanced reduction products. Also, being cleanly separable by initial physical means, this Mn-hardhead intermetallic residue has the commercial potential to be a valuable by-product (as a solution-process-ready feedstock). So the inherent process capability contained in the microwave-stimulated reduction of raw mineral concentrate must be seen as having real potential for possible industrial implementation.

With the third major reduction phase group, the slag phases, are included those oxides which fall into the range between the primary oxides present in the ore concentrate and the process end-point slag. Because they are products of a reduction process, these reducible-metal oxides represent a continuous range of O-deficient

phases in varying stages of C- and N-uptake, the oxycarbonitride range, into which several loosely defined sub-group categories or types fall depending upon their remaining-metals composition. The least converted remnant oxides retained some Sn, the next in the reduction sequence retained some Mn and Fe as oxycarbonitrides, thence Ta, Nb and Ti oxides, being last to reduce, moved through the gradations of "oxycarbonitride" towards the "carbonitride", either solid solution or compound – all phases being subject to compositional permutations derived from the idiosyncrasies of both small-scale processing and microwave processing. The oxides (ranging through the oxycarbonitrides and into the carbonitrides) display a wide range of internal morphological variation dependent not only upon the metal composition and oxygen-deficiency, but also upon whether solid-state reduced or liquid-state reduced and upon solidification dynamics of the phase during quench-cooling. Although, in wodginite reduction programmes the presence in final reduction product remnants of metal-*oxy*carbonitrides was uncommon, and the extent of C plus N in metallic carbonitrides was generally less prevalent in Ta/Nb-phase remnants of wodginite reduction than for equivalent reduction phases derived from the pure metal oxides of earlier experimental assignments. A convenient attribute of the experimental reduction process for wodginite was that, irrespective of the precise reduction route (in any regional-element) or the phase distinction of intermediate phases, the end product phases of this microwave reduction system were consistent and commendable.

Commercially, wodginite is regarded as a Sn-rich tantalite, a submission that is incorrect in the strict mineralogical sense. Moreover, the presence of Sn in the mineral is properly regarded as a "down-stream" processing impediment and is therefore detrimental to its commercial value. Sn is valuable in its own right, and following mineral concentration of the wodginite from the ore by mechanical mineral processing, the Sn fraction may be chemically leached from the wodginite concentrate as a further minesite mineral beneficiation process. None of the various minesite leaching processes employed worldwide is totally effective in removal of the Sn, and few are necessarily targeted at either manganese or iron (which must also be removed in consecutive or subsequent leaching). Environmentally undesirable aspects, including by-products for which disposal and pollution problems are perpetuated, accompany these leaching processes – so, indisputably, each industrial stage must be clearly necessitated to justify its inclusion in the process route. Essentially, leaching of Sn-rich tantalite/(columbite)

type ores is pursued simply to produce a pseudo-tantalite/(columbite) concentrate that is acceptable (and therefore saleable) to downstream processors (who evidently have always held such "marketplace" power – in its effect, a power which has historically determined the established reduction route for tantalite/(columbite) and its more complex variants). So, in the industrial production stream, the opportunity to vary the reduction route for wodginite (or similar) is greatly constrained by "downstream command". Consistent with this concession to "commercial reality" – and of industrial significance in Australia [1] – wodginite is acid leached to produce a synthetic tantalite concentrate that is (*i*) then acceptable for trade in a quite limited world market, or (*ii*) is converted to pure Ta_2O_5 (plus Nb_2O_5) for export. Neither Ta nor Nb leave Australia in the far more valuable metallic form.

Microwave reduced wodginite reduction products produced in this project clearly show that the metallic components Sn, Mn and Fe can be reduced and thereafter contained in one metallic composite phase. This phase can be discretely and efficiently separated from the metallic phase(s) containing the principal elements, Ta and Nb (and from the slag phases) by various methods (leaching, liquation, mechanical or a combination of these) to leave separated Ta/Nb/(Ti)-phase. Clearly, also, the Ta/Nb/(Ti) metallic phases resulting from microwave-stimulated reduction techniques are produced by solid-state reduction processes with integral sinter-agglomeration susceptibility between the softened, still diffusively-active metallic-particulate entities (before quench), these agglomerated sponge-like metallic phases ranging in composition from solid solution up to stoichiometric metallic compounds. The solid-state processes proceed by transmission of a reactant particle (radical) through a plasma/solid reaction interface, thence [*the reductant particle*] to, and [*the oxidised product particle*] from the crystallographic reaction inter-change/deposition site by solid diffusion mechanisms. (Such reaction and mass transport mechanisms are comprehensively discussed in the broad literature of process metallurgy, and specifically in CORDURIER, et al [17], DEMBOVSKY [58], ALCOCK [60], GASKELL [65] and LEVENSPIEL [67], as cited.)

The solid-state reduction metals produced were of good purity, particularly in view of the lack of experimental sophistication, this good conversion was apparently accompanied by highly acceptable recovery rates. However, with further processing

time and/or intensity, Ta(Nb)-*metallic compounds* would undoubtedly be more pervasive through the reduction remnants, as evidenced by those samples from exposed regions selected for XRD examination and which were found to have mean composition approaching (Ta,(Nb))(C,N) (with some minor unidentified peaks of nuisance consequence only). It has to be said that, in respect of industrial extractive production routes for Nb and Ta, where authors routinely report as to *why* pyrometallurgical reduction is not conducted on either pure single oxides or raw mineral concentrates, they generally have no pyrometallurgical experimental or pilot trial results to report or discuss. In this vein, BORCHERS and KORINEK [31] provide good discussion as to why pyrometallurgy is by-passed for the regular halide routes, as do GUPTA and SURI [29] and MOLLER, et al [78] in informative and comprehensive works (with a view to metal utilisation in the latter) that are tantamount to "industry overviews"; so no pyrometallurgical studies which could be considered "comparative" for this project – and certainly no microwave reduction studies.

An efficient if modest technique was devised to isolate the pivotal Ta/Nb-phase so that XRD analyses could be conducted on this metallic phase, the metal in a state "uncontaminated" by other remnant phases; such results would be used to assist with the interpretation of EDS analyses and, accordingly, corroborate the overall results of the wodginite reduction programme. The straightforward method involved (*i*) initial sampling from reduction remnants of adjudged "suitably converted" metallic Ta/Nb/(Ti)-phase material from regions of evident advanced reduction (to ensure conversion), (*ii*) light manual crushing of the sampled material to release most of the brittle reduction product fractions and to "open" all volumetric regions (voids and vesicles) to the subsequent leach procedure, (*iii*) simple "gravity-concentration" of the heavy Ta/Nb/(Ti)-phase fraction which was then subjected to immersion in dilute HCl (pH ~ 4) for 24 hrs with regular agitation, the final solids thoroughly rinsed and dried, and (*iv*) the dry Ta/Nb/(Ti)-phase solids were ring-milled to the finest powder (-325 mesh) which would practicably avoid significant mill-loss of the limited material *and* be suitable for XRD powder diffraction. In this manner, samples from specimens representing the processing times 10 min (WODG**04**), 12 min (WODG**06**), 14 min (WODG**08**) and 16 min (WODG**09**) were prepared, thence powder samples were

routinely diffracted* through 10° to 100° (degrees **2θ** on the abscissae) and the traces of these exercises are presented in Figure **{7.4.3}10** beneath the reference trace of the "as-received" wodginite concentrate source material, suitably "mill-prepared" (only). [Also indistinct in the trace format of Figure **{7.4.3}10**, the "XRD Counts" on the ordinates are in 1000 X-ray count divisions for the wodginite trace **(a)**, 400 X-ray count divisions for reduction phase traces **(b)**, **(c)** and **(e)**, and 1000 X-ray count divisions for the trace **(d)**.]

Of particular significance in the reduction phase spectra of traces **(a)** to **(e)** is the consistency of the Ta/Nb-phase peak sets. The spectral agreement is enhanced because of the inherent narrowness of the peak spreading (enveloping the ((Ta,Nb)(C,N))-phase permutations), both within each peak and along the degrees **2θ** ordinate(s). (Whilst checked only manually against PDF references) the carbonitride peaks for Ta and Nb remain close along this **2θ** range, and likewise, the shift between the pure carbide and the pure nitride is very narrow for these two refractory metals along the **2θ** range. Essentially, in taking into consideration the parameters of this minimal peak-spreading the following peak shifts were accounted-for: TaC with respect to NbC and TaN with respect to NbN, and for TaC with respect to TaN and NbC with respect to NbN. With reference to EDS results for this Ta/Nb-phase, various underlying matters need to be considered. The XRD-identified "clean" peaks are best thought-of as representing a "composite compound", (Ta,(Nb))(C,(N)), Ta and Nb having continuous solid solubility across their binary phase range, and C and N being similarly interchangeable across their metal-carbonitride ranges. Noting total confidence in the EDS-confirmed presence of Ti in all Ta/Nb-phases analysed, and that this Ti-presence was not accounted-for in XRD analyses, this XRD-unaccounted Ti-fraction must be considered as being represented in the phase(s) whose XRD presence is contained in the minor peaks left un-attributed. And, with respect to those un-attributed peaks in Figure **{7.4.3}10** traces, the peaks were likely a *peak set* for an obscure Ti/(Ta/Nb)-phase, one un-encountered in

* All XRD powder diffraction was carried out in an automated Philips 1730 generator and diffractometer using Cukα radiation with graphite monochromator at 1° **2θ**/min over 90° **2θ** from 10° to 100°. In this case of wodginite spectra, the JCPDS – ICDD PDF reference files were consulted manually in an attempt to bypass the failure of the automated system to suitably identify the minor peak (set) left unidentified on the traces of Figure **{7.4.3}10** and notionally ascribed to a consanguineous Ti-rich phase (of no PDF entry).

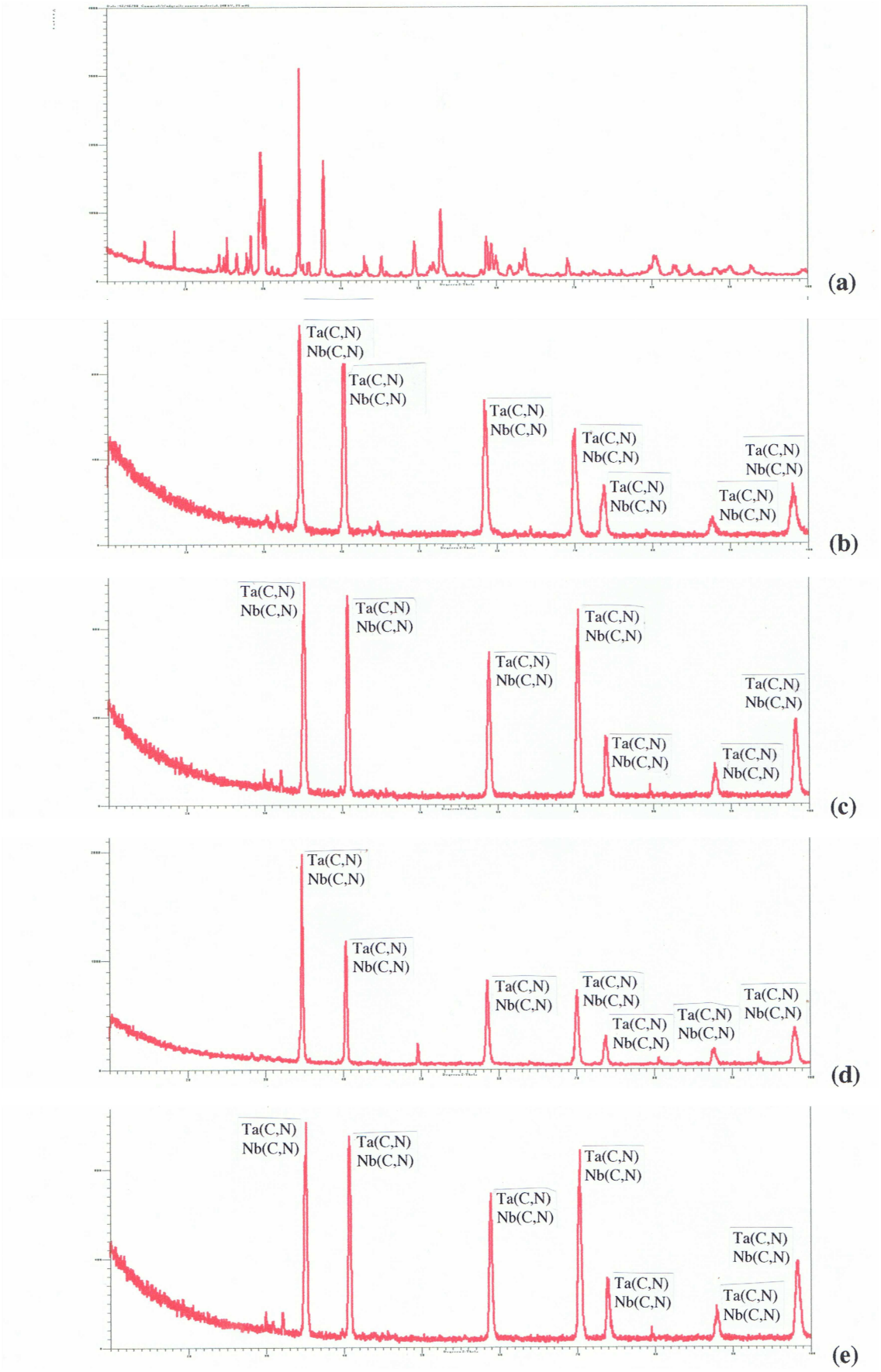
(a)
Ta(C,N) Nb(C,N)
(b)
Ta(C,N) Nb(C,N)
(c)
Ta(C,N) Nb(C,N)
(d)
Ta(C,N) Nb(C,N)
(e)

Figure {7.4.3}**10**: XRD traces for (**a**) "as-received" wodginite concentrate, remaining traces representing specimens: (**b**) WODG**04** (10 min), (**c**) WODG**06** (12 min), (**d**) WODG**08** (14 min) and (e) WODG**09** (16 min). Diffracted were ***residue*** specimens – essentially Ta/(Nb/Ti)-phase(s) – after attrition plus acid digestion of reduction product samples. [Diffn. arc: 90° from 10° to 100° **2θ**, max. counts: ~ 3000 (**a**), ~ 1000 (**b**), (**c**) and (**e**), ~ 2000 (**d**).]

PDF searches, or one with no PDF entry. This identification shortcoming of the peak set balance and the "metallic compound" status of phase material sampled for XRD studies (but contra-indicated by EDS) require further discussion.

The XRD system's auto-analysis capability failed to provide a component-element correct, phase-suitable alternative in "identifying" the minor peaks (or peak set) – no Ti-based or Ti/Ta/Nb-based phase. Thereafter, working by manual referencing, the JCPDS – ICDD powder diffraction files (PDF) reference was searched to match any Ti/(Ta/Nb)-phase as to satisfy such a reasoned assumption (of a Ti(Ta,Nb) presence). Despite exhaustive manual PDF reference file-searches, no reasonable match (partial or total) for this peak set could be found for *any* possible Ti-based phase considered – and noting that the phase satisfying such a peak set would need to be a Ti-compound with compatibility enabling its integration as a composite phase within the identified major phase (compound) – probably as a compound of higher, (Ti,(Ta,Nb))(C,N)-composition – perhaps a phase "unlikely" to be on PDF record. Consequently, the search was sidelined as representing an un-necessary enterprise – a "distraction" – the over-riding outcome of phase identity being already confirmed (broadly if not concisely) as a complex metallic compound.

The microwave-stimulated carbothermic reduction processing method presented benefits not conventionally considered in application to this otherwise un-processed concentrate of a complex native mineral, wodginite; the microwave process potentially represents substantial value-add as a process route alternative. Such a compatible series of reduction process events was, of itself, validation that a case for the "direct reduction of the mineral concentrate" route was substantiated – of course, a new final refining stage would be required to complement such change – and perhaps this refining stage might represent a further value-add. And, if the route and process examined represented only portion of a process route, the option represented a viable alternative to the sequence of "mineral separation, chlorination, distillation-purification thence reduction" option-set currently followed.

7.4.4: Aluminothermic Reduction of Wodginite.

The successful carbothermic reduction results for both wodginite and the earlier single oxides suggested that the step up to the aluminothermic reduction route was not a processing necessity for successful reduction of the wodginite concentrate. However, pursuing the comparative alternatives of "carbon-assisted aluminothermic versus carbothermic" would throw light on the thermochemical essence of these reductant options and inform of the difference between reduction routes. Also, because of the "chemical energy" spontaneity of any thermite component to aluminothermic reduction, it was thought possible that comparison of the two systems might obliquely suggest a "base value" worth to the reduction process of *microwave-stimulation and its associated plasma chemistry*. [Noting here that no reduction trial conducted under "energy-equivalent" conventional pyrometallurgical conditions was pursued so to provide a comparative "control" result, although, a carbothermic wodginite charge *was* heated in an oven and held at the 1500°C oven limit for 1 hr before liquid N_2-quenching. The crucible contents contained reduced Sn with regions of "Sn/Mn/Fe-phase", some minor slag pockets, and nil-to-indeterminable reduction product phases associated with Ta, Nb and Ti, which evidently remained in the un-reduced form akin to that of the concentrate mineral.]

What must be emphasised is that, in a non-intuitive sequential twist, initial reduction under this carbon-assisted aluminothermic route evidently occurred by indirect reduction by plasma-activated CO-particles to the reaction interface thence solid-state diffusion of energetic C-particles to the reduction site and the reduction of MO $\{CO^*_{[If]} \rightarrow O^*_{[If]} + C^* \rightarrow [C^*] + MO \rightarrow M + [CO^+]\}$; then the return of CO to the interface, and the release of CO $\{[CO^+] \rightarrow CO^+_{[If]} + O^*_{[If]} \rightarrow CO_2 (+ C \rightarrow 2CO)\}$ into the plasma – precise states of ionisation or excitement aside. So, the evolving Ta/Nb-phase could be quite advanced by the point that – *reactant contacting* and $\mathbf{E}_{act}$ being satisfied – the aluminothermic reaction was activated, and such solid Ta/Nb-phase material physically held its particulate form into the aluminothermic stage of reduction and facies development. Beyond this, by and large, the aluminothermic process presented aspects of processing and material results that saw those of the carbothermic route eclipsed in certain important respects. As they were experimentally conducted, the

fundamental difference between the two reduction systems resided with the *relative "surfeit"* of slag present in the reacting charge of the aluminothermic system. [In terms of phase-proportionality, this relative "surfeit" would be regarded as a relative "deficiency" in typical systems of conventional pyrometallurgy where liquid reduced metal is protected by a regulating slag "blanket"; and noting again that, because of the "experimental design" stipulation limiting reactant/process variables and their "first generation experimentation" status, no explicit addition of a "slag-forming" mineral was made to experimental blends (so to limit (minimise) experimental variables in already complex systems).]

The relative excess of slag was provided by the aluminothermic reaction (itself) as, "at temperature", liquid-Al spontaneously reduced the remaining oxidic wodginite phases producing alumina slag at intense temperature (derived from the exothermic heat of reaction), a slag that readily combined with the disparate pockets of gangue-derived slag phases. At the root of the "desirable difference" in the step up from carbothermic to the aluminothermic system of reduction, and conferring process advantages upon the aluminothermic route, was this relative "excess" of very hot slag that provided enhanced thermochemistry (including kinetics). This elevated system energy both promoted reaction dynamics and provided adequate thermal energy to partially melt-strip existing particulate Ta/Nb-phase metal – which, along with direct Al-reduction of the oxide, was the likely auxiliary reason leading to Ta/Nb-phase faceted plate evolution. So, the aluminothermic reduction route was as *process-beneficial* as it was *product-dynamic* in its delivery of desirable reduction outcomes.

There are several distinctive physical morphologies (from two sub-groups) in which the predominantly tantalum metallic phase presents itself in the range of reduction products. In EDS analyses, these morphological forms register "indiscernible" through to "minor" compositional variation from form to form. Such variation often presents in the same reduction product region as is in evidence in the representative micrographs of Figure **{7.4.4}2** and Figure **{7.4.4}7** (and other micrographs) which show varying forms of Ta/Nb-phase in the same microscopic fields-of-view. Whilst this variation may simply represent solidification sequence in certain cases, the state of the originating phase within which reduction and phase nucleation took place, and within

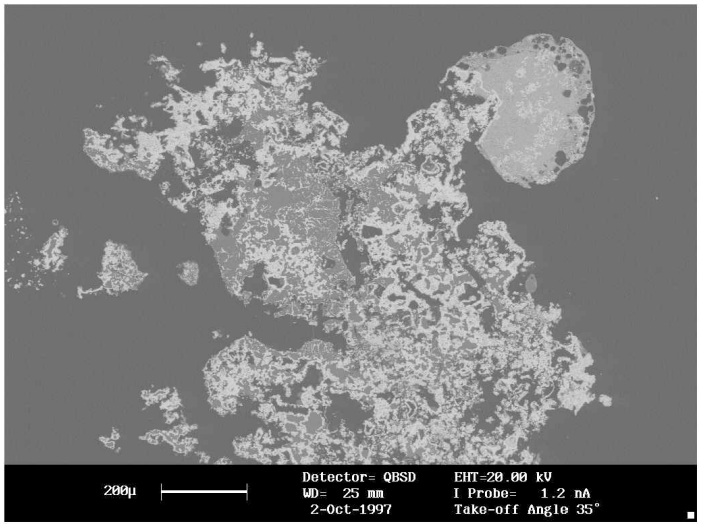

Figure {7.4.4}**1**: Electron micrograph capturing a typical field (in polished section) of an aluminothermic reduction product remnant (in 10 min specimen WODG**A5**) showing the development of reduction phase metallisation of the Ta/Nb-phase and Sn-phase groups and the associated Al-dominated oxidic slag – the slag phases being extensive by comparison to those of the reduction remnants of carbothermic trials. The extent and coalescence of aluminothermic slag was a common feature that gave rise to the reducing Ta/Nb-phase evolving a more elongated morphology in liquid slag than was the case in initial plasma-phase exposure.

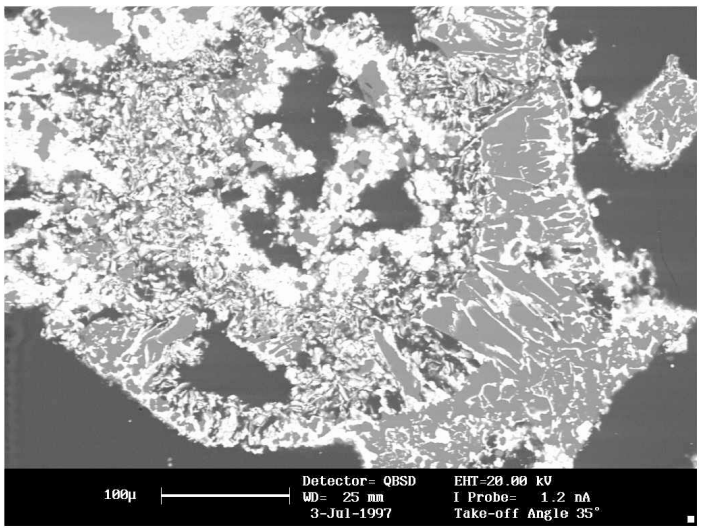

Figure {7.4.4}**2**: Electron micrograph from WODG**A4** exhibiting widespread metallic reduction product phases permeated by slag phases. This field is shown in Figure {7.4.4}**3** as an EDS map set in which various features of phase and slag development can be resolved – features which are not overtly obvious in the above micrograph. This representative field was captured using the backscattered electron facility to configure the image, the same field presented with the EDS maps of Figure {7.4.4}**3** is a secondary electron image. Where appropriate, such detection alternative of image capture is repeated elsewhere in this section.

[Note that, in electron images, black regions are voids (vesicles) in the specimen structure, and/or are areas of mounting medium. Accordingly, these black regions should be taken into account when appraising accompanying EDS map images. Also, in the recorded images, the evident "brightness" of detected elements increases not only with proportional quantity, but also with increasing atomic mass.]

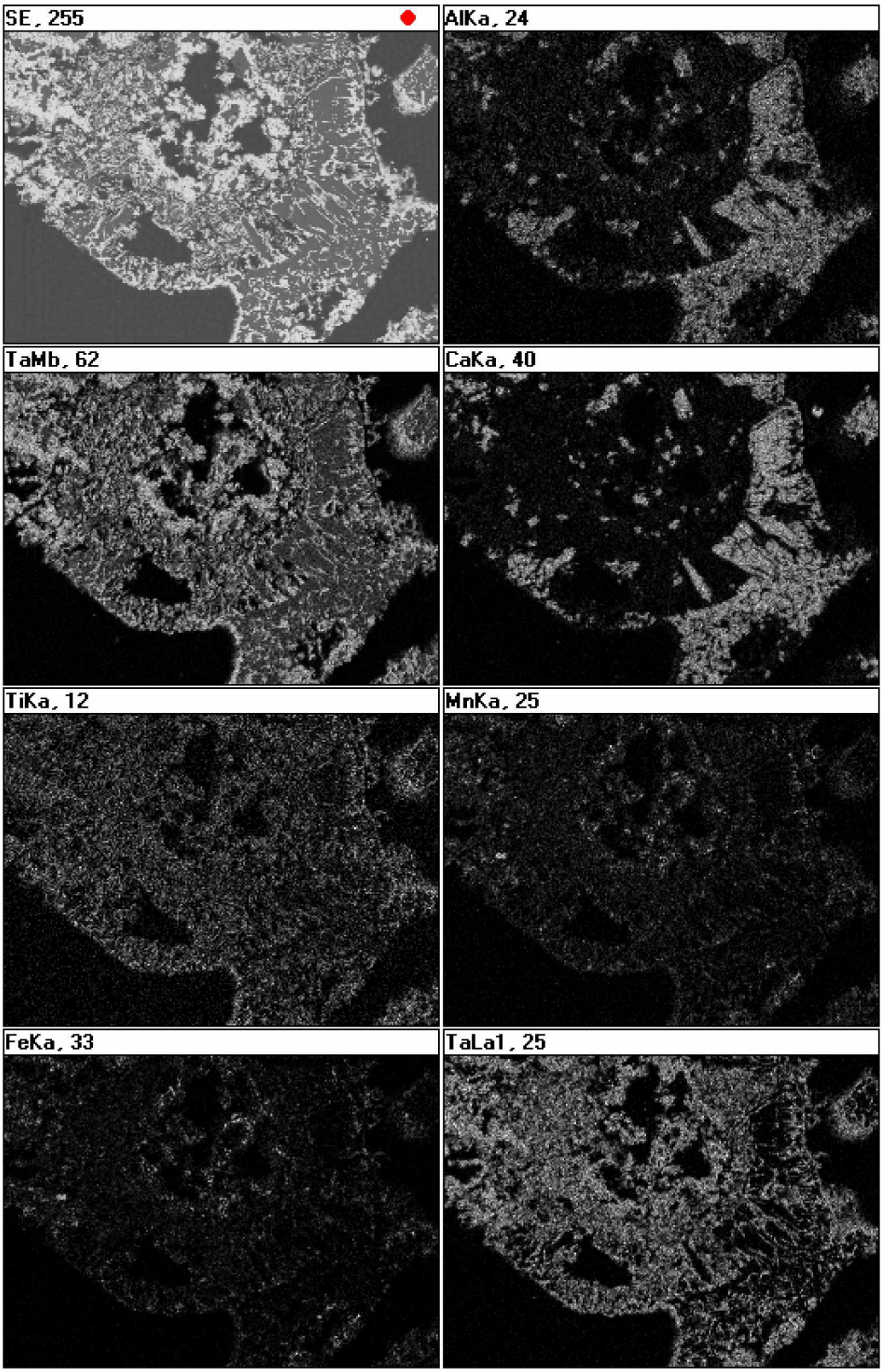

Figure {7.4.4}**3**: (With reference to the previous figure) this EDS map set presents a series of metallic components in the reduction remnant of WODG**A4**, a 10 min product of microwave-stimulated aluminothermic reduction of wodginite mineral concentrate. Of note is the distribution of Al/Ca-slag through the remnant structure of metallic phases, and the apparent absence of such slag phase in regions of initial plasma reduction featuring "closed" vesicles in-filled by "primal" slag (gangue plus Mn/Fe) and Sn (by inference).

which phase-growth took place, is of fundamental importance. The C-initiated solid-state reduced particulate-come-agglomerate form originated in the plasma environment, whilst the faceted plate forms originated in liquid-state slag – and their morphologies (or forms) at solidification reflect those evolutionary roots. These metallic Ta/Nb-phases may be essentially equiaxed (at least initially) in particulate form – or in the cases of slag-borne plates, derived from cellular growth, this lamellar-like phase sometimes showing angular disposition, the laths and curved sheet-like foliates or shells (possibly representing remnant reduction or solidification fronts which replicate microwave pulsations (at $n\lambda$)), and folded parallel plates which resemble common eutectic structures. [These variations are represented in Figures **{7.4.4}14** to **{7.4.4}18**.] In this complexity (and not infrequently), across a microstructure one of these forms can be observed to transform into another morphology – a fact more likely representing the solidification dynamics prevailing during quenching of the reduction product rather than solid-state growth during processing. These phase forms are provisionally related, as is confirmed by microscopical observation of reduction products and the evidence and order of excavation of remnants, to their in-crucible siting with respect to the deduced plasma exposure and thermal profile, the material state of the reduction environment, reaction interfaces and the plasma's chemical activity. Their compositional relationship was confirmed by EDS analyses with light element content providing the principal compositional variation with higher N-content for plasma-exposed phases and low N-content in phases from regions not immediately exposed to plasma intensity (such as those phases chosen for "characteristic phase" EDS analyses).

Touched-upon as a thermal peculiarity in carbothermic Section **7.4.3**, the presentation and morphology of the second-stage Ta/Nb-phase plates (above), captured when frozen in the slag phase, was perhaps the most defining general process-feature associated with the aluminothermic route. This varied collection of ideomorhs evidently represented a range of process and solidification events, and for simplicity of "group identity", these faceted particles in the form of plates were categorised as the "plate" phase of the principal Ta/Nb/(Ti)-phase reduction product, the latter-stage equivalent of the initial granular or equiaxed "particulate" form of Ta/Nb/(Ti)-phase metal, or its more process-advanced, compounded sinter-agglomerate form. The presence of this general idiomorphic range seemed to represent the overlapping outcomes of two

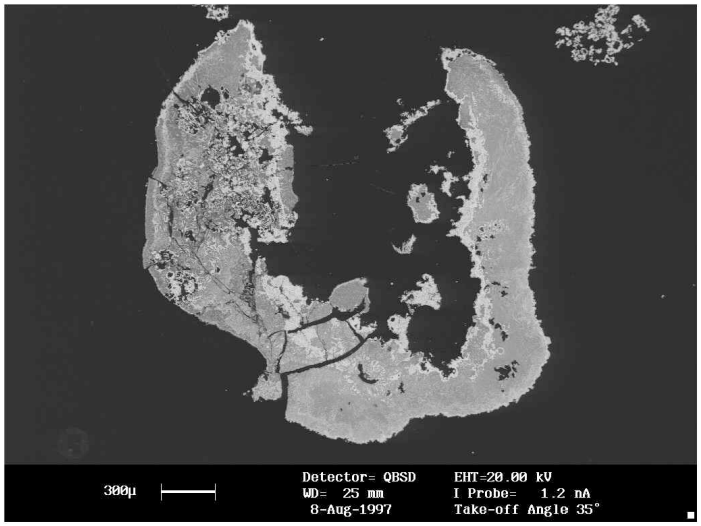

Figure {7.4.4}**4**: Electron micrograph of a slag-dominated remnant feature in 7 min specimen WODG**A1**, a minimally processed reduction product exhibiting a wide range of microwave-stimulated reduction phenomena (as captured in physical form by way of phases representing varying degrees of reduction). Note that the original reactant surface representing greatest exposure to gaseous plasma-phase reduction is on the inside of this "horse-shoe" remnant, and that the remnant region was "flooded" with aluminothermic Al/Ca-slag which suspended gas-phase for a liquid-state diffusion function as reduction proceeded by a new nucleation mechanism deriving Ta/Nb-phase plates. The following Figures {7.4.4}**5** to {7.4.4}**9**, all captured within the above low magnification field, present micrographic details plus mapped elements – all of which illustrate various fundamental characteristics of process and product, and which exemplify reduction products throughout the range of process times.

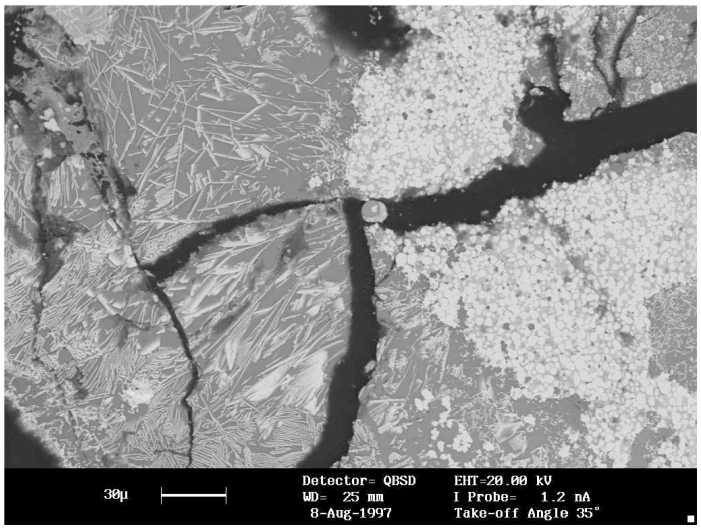

Figure {7.4.4}**5**: Electron micrograph of detail in WODG**A1** showing plasma-phase derived Ta/Nb particulate phase region in an Al/Ca-slag featuring the nucleated plates of equivalent Ta/Nb-phase. The likely distinction in phase evolution (apart from the environmental state-of-matter from which this evolution takes place) is that particulate reduction product formed in CO-plasma through reduction inter-change by solid state diffusion of reactants, [C] for [O], whilst the in-slag faceted plate forms are principally the product of direct aluminothermic reduction, the reaction proceeding once thermochemical requirements are met in un-oxidised molten Al – whereafter Al_2O_3 supplemented slag volumes.

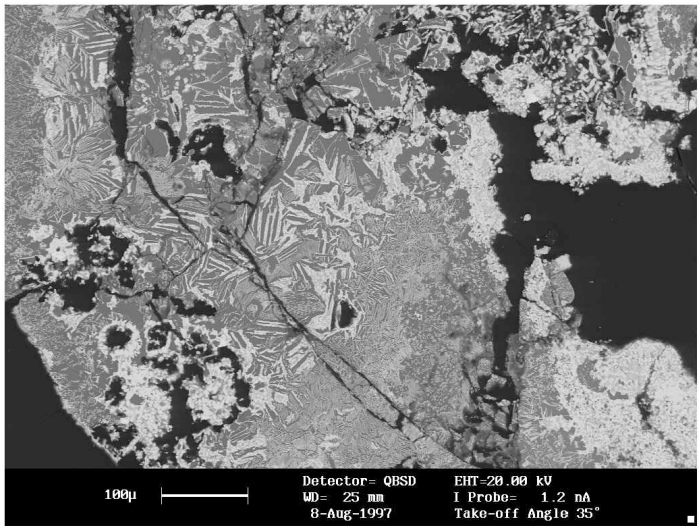

Figure {7.4.4}**6**: Electron micrograph of a reduction product field in WODG**A1** indicating typical distribution of metallic Ta/Nb-phases (bright) in a background combination, principally of slag with metallic Sn-phases, both having mid-range reflectance (mid-greys) at low magnification and in monochromatic capture (that is, the grey tone of Sn-phases ≈ that of the Al/Ca-slag phases); colour capture of these phase groups would distinguish the phases and their claim to metallic status. The hardhead and slag phases can be visually resolved (with refined contrast) at higher magnification, as is verified in following micrographs.

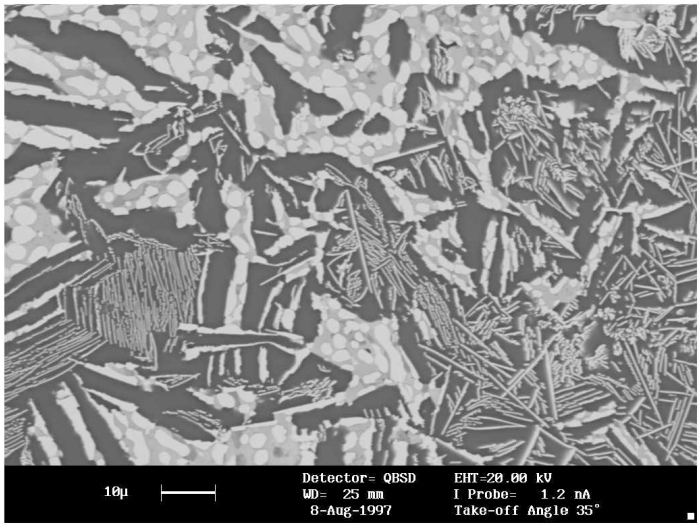

Figure {7.4.4}**7**: Electron micrograph presenting a field which exists centrally in the micrograph of Figure {7.4.4}**6** above and Figure {7.4.4}**8** following. This most important "microstructural" link shows elements of reduction remnant facies prominent in aluminothermic reduction specimens and which reflect reduction and process history and the sequence of extractive metallurgical "events" which are captured at solidification. The field exhibits the inter-relationships of reduction phases that are characteristic of all aluminothermic reduction specimens. The essential aspects of detail are the Sn-phase (lighter grey) engulfing the primary particulate Ta/Nb-phase surrounded by slag (darker grey) containing secondary Ta/Nb-phase faceted plates – recurring features of aluminothermic reduction and facies development. These plates can be observed (here and more prominently in later, more processed specimens) to be occasionally integral with the particulate form of the Ta/Nb-phase. This region (in a "young" specimen) did not generally exhibit the particle-stripping phenomena attributed to longer processing and evident in later specimens.

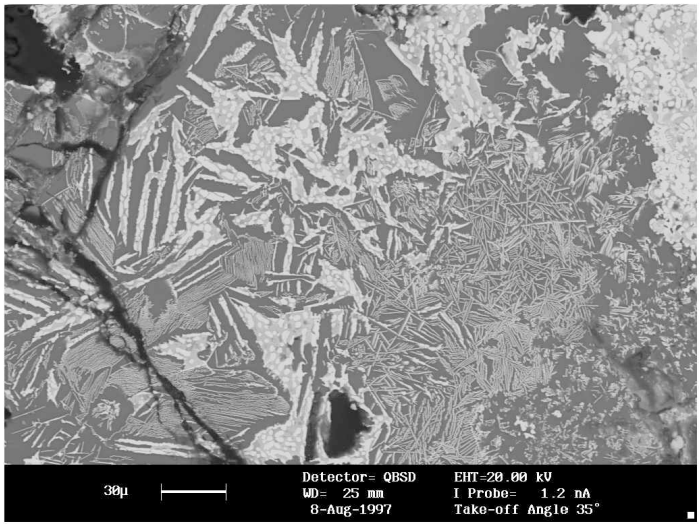

Figure {7.4.4}**8**: (Associated with preceding figures) this backscattered electron micrograph presents a field representative of typical aluminothermic reduction remnants; it is the subject of the following EDS map set. [Note that, whilst this field was in the least-processed specimen, WODG**A1**, in more-processed specimens the less-alloyed Sn-phases drained to lowest regions of the crucible containment and so, with increased processing time, Sn-phases were less prominent in remnants retrieved from higher crucible regions.]

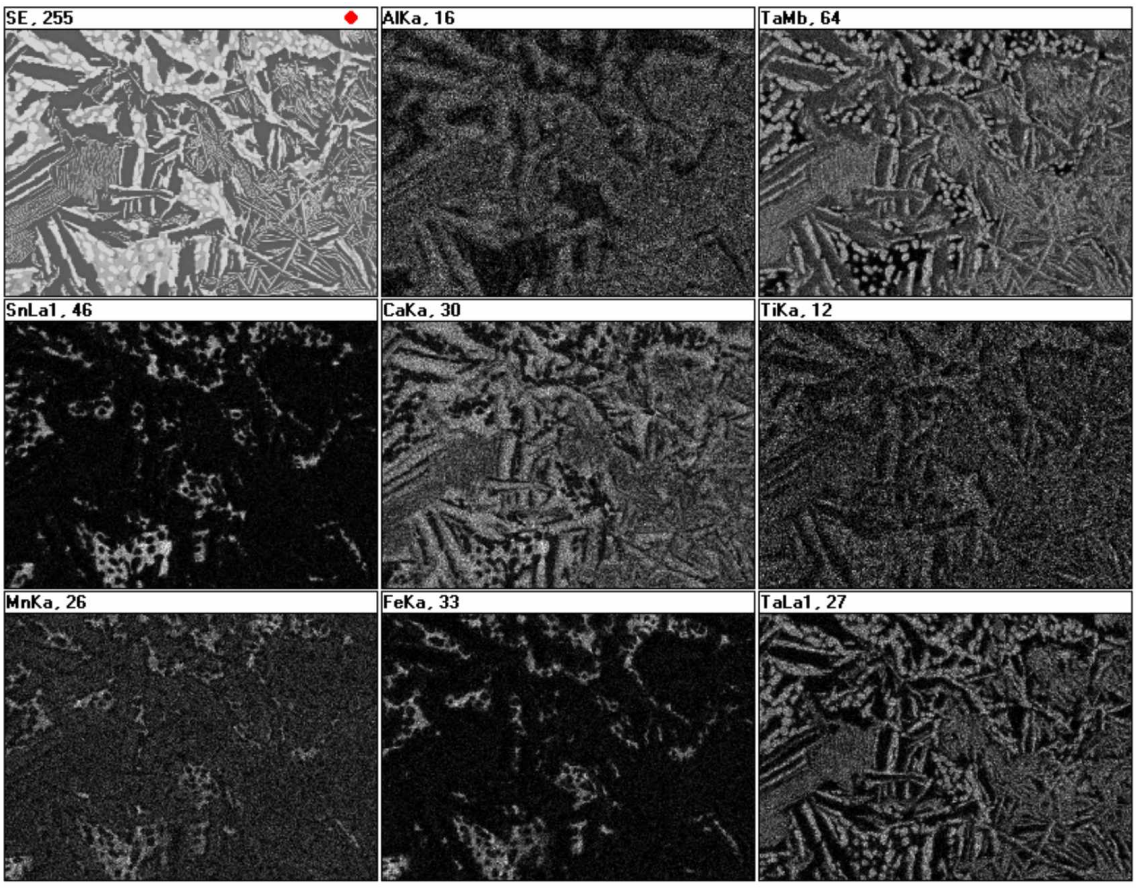

Figure {7.4.4}**9**: EDS map set of a field in 7 min WODG**A1** showing the distribution(s) of Sn/Mn/Fe-phase (MN-hardhead) around particulate Ta/(Nb)/Ti-phase, with the "same" Ta/(Nb)/Ti-phase as elongated plates distributed through the Al/Ca-phase "aluminothermic" slag. (Note that the "SE" image is a secondary electron micrograph.)

entwined process events – the more straightforward being the direct aluminothermic reduction of the metal oxide to produce the metal plus alumina-based slag and, derived from the resulting super-heated melt of Ta/Nb-metal/slag. The second "event" being the phenomenon of partial "phase-stripping" of the pre-existing particulate form (either by the dissolution into the slag or by melting into an immiscible liquid mixture). This "stripping" of the initial particulate/agglomerate Ta/Nb-phase resulting (at quench) in *increased* faceted plate evolution in the slag (above that attributable to the aluminothermic reaction alone) – with accompanying characteristic slag/particulate interface modification or particulate/plate integration (both in evidence in various micrographs). This latter "phase-stripping phenomenon" may not have been acknowledged had it not been recognised in reduction product remnants in which it was not expected – that is, in carbothermic reduction remnants. In such there being no aluminothermic reaction to provide the "direct reduction" explanation for their existence, the incidence of Ta/Nb-plates in carbothermic slag could only have eventuated by the latter, "phase-stripping" option in which super-heated slag "retrieved" TaNb-metal from the initial, particulate phase. Such option was believed reasonable for both reductant systems, although conceded to be more prescient in the thermally greater aluminothermic route. Specifically, the secondary "event" option was thought credible for cases of thermal "runaway" in reaction zones of charges under purely carbothermic reduction. In cases of its occurrence in remnants it was only "incidentally" recorded – a rarity of occurrence in line with what might be expected in the lesser thermal conditions of that system. In aluminothermic reduction remnants of this Section **7.4.4**, the "faceted plate" phenomenon was as pervasive as the occurrence of the slag. And, irrespective of the evolutionary source of the Ta/Nb-plate phase – and although the more intricate secondary "stripping" process increased with processing "energy/time" – evidence of *both* processes of plate-evolution was common throughout the specimen suite.

In terms of process, and whilst initial carbothermic reduction was in progress in the reductive evolution of the particulate phase, the first Ta/Nb/(Ti)-phase taken into slag "solution" occurred in the "instantaneous" heat derived from the thermite element of aluminothermic reduction as liquid-Al reduced the contact-available metal-oxides of the mineral concentrate of the charge. Much of this metal in liquid solution was deposited from the liquid in the familiar lamellar-like "faceted plate" form of microstructure that was commonly recorded and is well represented in the images of

figures presented. These lamellar-like plates presented in arrangements whose forms were recurrent and, in certain instances, were observed to have conformed to rounded "loops" or, more likely, into cupped sheets, as can be seen in the micrographs of Figures **{7.4.4}14** to **{7.4.4}18**, such features can also be seen in the finer detail of some other micrographs.

The heat generated by the release of exothermic energy from the aluminothermic reaction was, evidently, sufficient to strip into solution, or (at least) into "liquid", some of the pre-existing, partially reduced Ta/Nb-phase particles, or agglomerated particulate clusters (if reduction was advanced), such as to both "modify" the slag/particulate interface and allow intimate crystallographic connection between the particle and plate phase materials, such that (in micrographs) incorporated plates can be observed "jutting out" from particles into the slag phase. Whilst these phenomenological events were of little material importance to the final reduction outcome, the fact of their *existence* and their *varietal presentation* were sure signs of *process*, and of the *sequence and development* of that process.

Given that much of the description of process and product provided in the previous carbothermic Section **7.4.3** remains relevant to this aluminothermic reduction section, and that a great proportion of description accompanies (in annotation) the extensive micrographic and EDS map-set coverage of Figures **{7.4.4}1** to **{7.4.4}21**, plus Figures **{7.4.4}22** to **{7.4.4}32** in Appendix **7.4.4**, only the essential minimum of descriptive coverage is provided in this text. Whilst the particulate Ta/Nb-phase and the Sn/Mn/Fe-phase(s) were the predominant phase groups in carbothermic reduction remnants, their proportional predominance was matched by the slag-borne plate group in aluminothermic reduction remnants. What is immediately evident in perusing the range of images presented is the general pervasiveness that accompanies the visual prominence of the slag phase throughout the remnants of aluminothermic specimens. Of the slag-dominated remnant feature from 7 min specimen WODG**A1** presented in Figure **{7.4.4}4**, the various Figures **{7.4.4}5** to **{7.4.4}8** show details of various fields which show to advantage the developing Sn-borne particles and slag-borne plates of the primary Ta/Nb-phase in an "*immature* reduction product" remnant – of all figures, these micrographs present to best advantage the truly only-aluminothermic-derived plate distribution of newly generated slag phase. The component-element distribution is

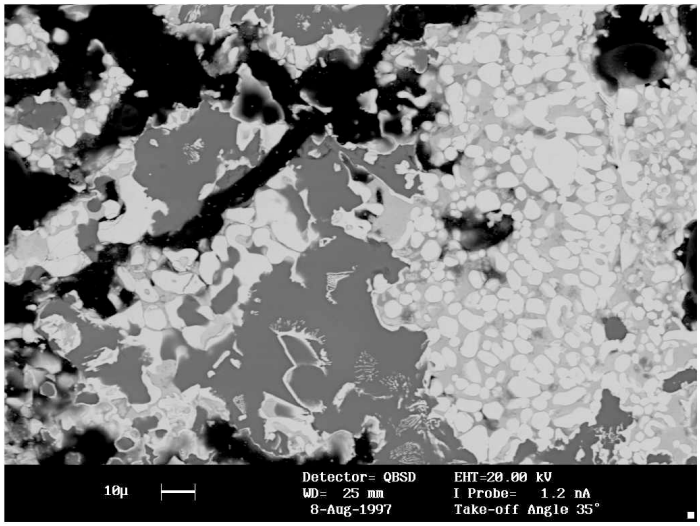

Figure {7.4.4}**10**: Electron micrograph showing the backscattered electron image of detail in more highly processed specimen (12 min WODG**A6**). Of note in this field is the tendency of Ta/Nb-phase particles towards sinter-agglomeration with a possible deficit of engulfing Sn-phase material, whilst in the slag regions there is less of the "interim" Ta/Nb-phase evident as the initially nucleated plates. The elongated plates appear to have migrated in their liquid slag to attach to adjacent solid phase features whilst, atypically, some Sn-phase appearing to have acquired a fine Ta/Nb-phase interface with the slag. Significantly, also, the elongated Ta/Nb-metal remnant plates remaining wholly within slag has transformed by curving (in two dimensions) and cupping (in the third dimension) – a characteristic which is more apparent in following micrographs, but the stages of evolution of such phenomena can be variously identified in this field.

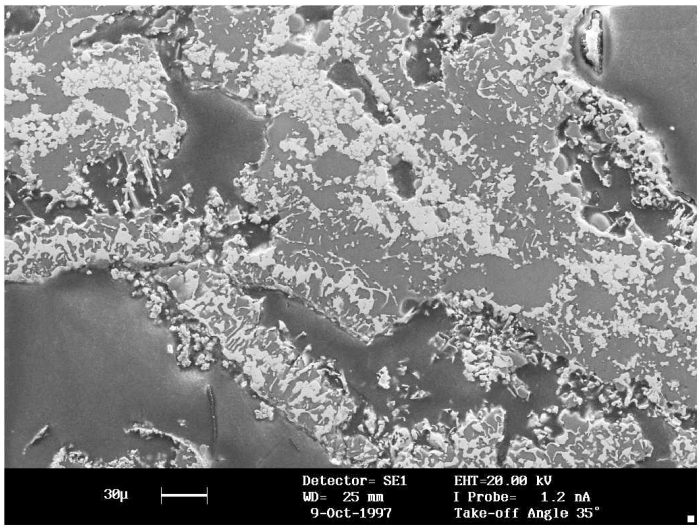

Figure {7.4.4}**11**: Low magnification electron micrograph presenting a secondary electron image (SE1) of a broader field in specimen WODG**A6**. The varied articulation of Ta/Nb-reduction phases across the reduction remnant is seen to advantage, including the general "retreat" of Ta/Nb-phase plates from the slag to adjacent solid metallic regions. [Because of the discontinuous and non-conductive nature of specimen phases, with or without carbon- or metal-sputter coating, conductive-mounted reduction product specimens tended to "charge-up" under the HT-beam of the electron microscope, particularly under SE-acquisition (as can be seen here).]

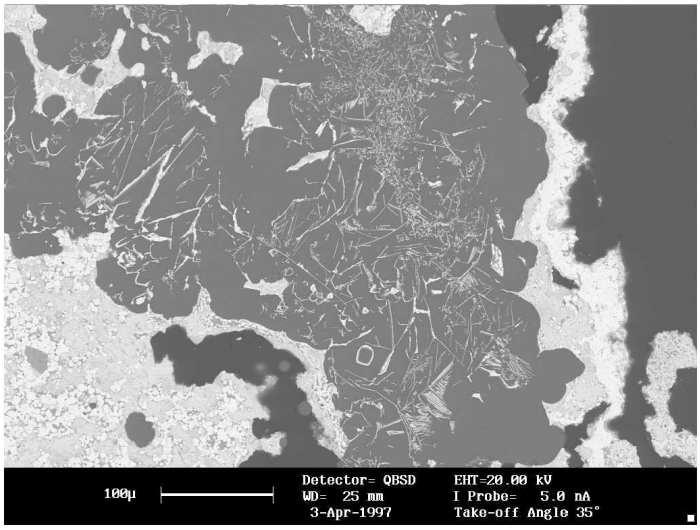

Figure {7.4.4}**12**: Electron micrograph acquired from 10 min specimen WODG**A4** showing a field with significant regions of Sn-phase containing distributions of agglomerated particles of Ta/Nb-phase. The substantial in-filled region of slag that bonds the remnant contains a distribution of faceted Ta/Nb- phase plates at varying stages of development. The Sn-phase regions here are reminiscent of carbothermic products.

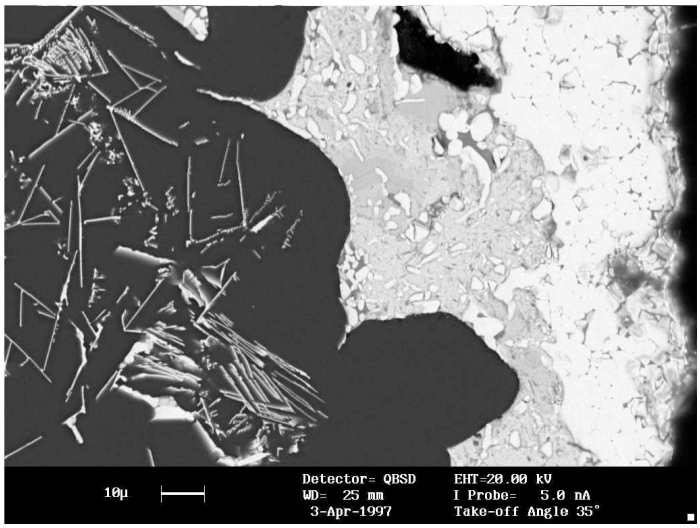

Figure {7.4.4}**13**: Electron micrograph presenting a field which exists in Figure {7.4.4}**12** above and shows in more detail certain of the pertinent characteristics of this degree of reduction. Firstly, different grey tones identify the variation existing through the Sn-phases with the lighter areas representing lower-alloy Sn-phases, phases which (should they not mix or increase in alloy content) may be free to drain with increased time and temperature. The darker regions through the Sn-phase are higher alloy Sn-Mn-Fe phases that approach compound composition, if not already at one of the metallic compound compositions. The particulate Ta/Nb-phase (right field) is quite sinter-agglomerated, whilst in the aluminothermic slag the primary Ta/Nb-phase plates are still quite thin and straight (verifying shorter processing time). All up, the agglomerated Ta/Nb-phase particles have been sufficiently plasma-exposed during initial processing to have sintered whilst the remainder of the phases in this field look to have been only moderately processed – arguably more in keeping with the processing (time) status.

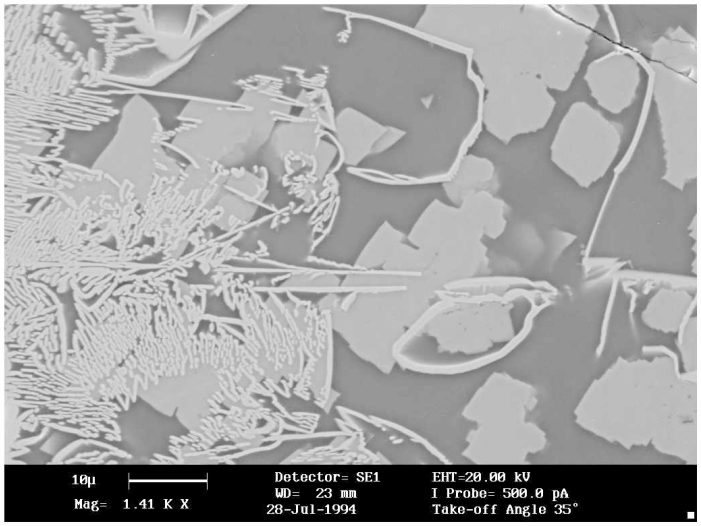

Figure {7.4.4}**14**: This and the following four micrographs are included to illustrate some of the common variations encountered in the nucleation and ongoing development of the Ta/Nb-phase faceted plates which are so prevalent in aluminothermic slag phases, and keeping in mind that these are the reduction product of the reduction of the metal oxide(s) by liquid Al-reductant. Consequently, the slag in which the lamellar and similar plates are borne is the reduction product of that reaction – the presence of the bright granular Ta/Ca-oxide crystals indicates that the reaction is incomplete (see map set of Figure {7.4.4}**28** in Appendix **7.4.4**). In the above and following micrographs the brightest phase (the metallic plates) have solidified from the melt – possibly before quench cooling – then the next brightest, the granular phase is partially reduced Ta/Ca/(Nb)/Ti-oxide ("oxide" verified by spot EDS examination) which has solidified later from the melt (during the quench), the dark phase is primary slag – still developing in composition towards its eventual composition (which will include the Ca still tied-up here in oxide with the refractory metals).

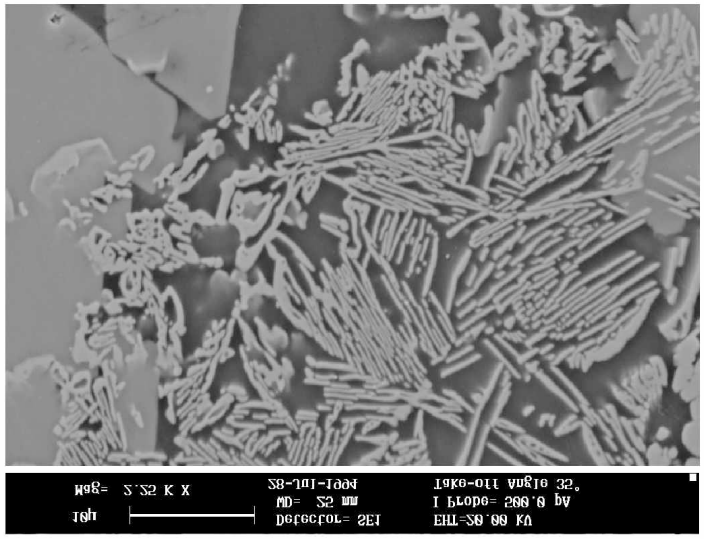

Figure {7.4.4}**15**: Electron micrograph showing phase solidification and appearance similar to that in Figure {7.4.4}**14** above; the micrograph is also from minimally processed specimen WODG**A1**. Note the presence in the aluminothermic deposition of Ta/Nb-phase the configured expressions of the lamellar, "tuning fork" and "cuneiform" type forms and their recurrence and "variation with processing" in fields across the suite of specimens.

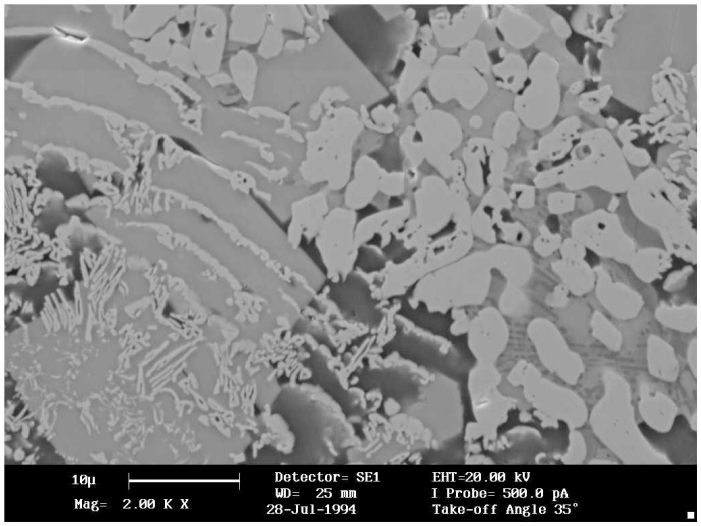

Figure {7.4.4}**16**: Electron micrograph (in WODG**A2**) showing Sn/Mn/Fe-phase binding Ta/Nb-phase particles (in right-field) and plates in oxide phases (in left-field). The initial stages of chemo-physical interaction (as mutual attraction and sintering) between the two forms of Ta/Nb-phase can be made-out along the ill-defined interface between metallic and slag regions. Note the regular "wave front" forms of the faceted-phase plates deposited from the liquid – these the author believes to be directly inter-related with a liquid-state "pulsation response" to the applied microwave irradiation. Such pulsation response-features were also a recurrent phenomenon through the range of specimens (although, almost exclusively restricted to aluminothermic reduction remnants because of the relative surfeit of slag in which such liquid state phenomena could manifest, and because the aluminothermic route provided a deposition product to make possible the physical evidence of such phenomenon.

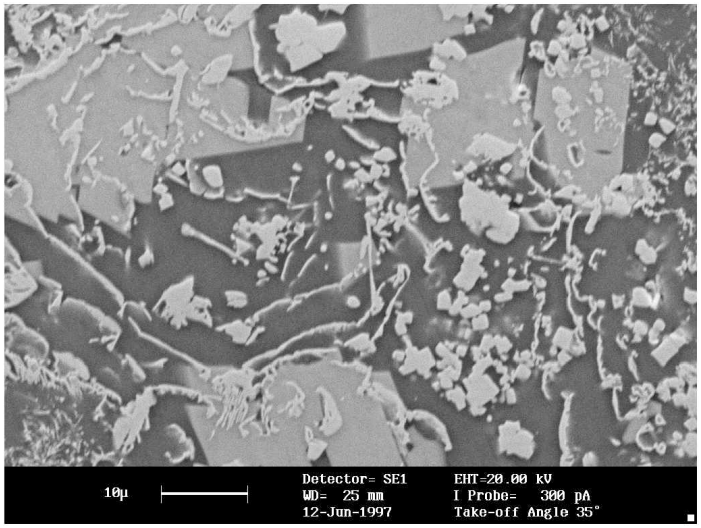

Figure {7.4.4}**17**: Electron micrograph (of WODG**A4**)) showing possible "pulsation front" type features associated with the dispersing Ta/Nb-phase plates in a background slag (dark phase) still harbouring (at this 10 min stage of processing) enough refractory metal in oxide phase liquid at quench to nucleate incompletely reduced (bright) granular crystals.

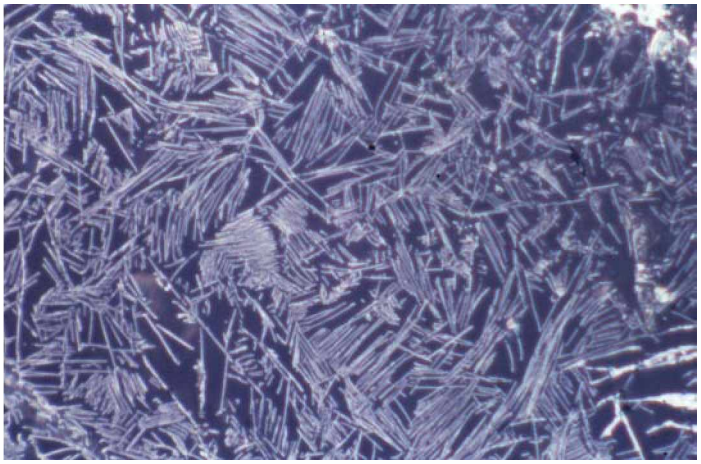

Figure {7.4.4}**18**: Light optical colour micrograph in specimen WODG**A5** showing an expansive region of Al/Ca-phase slag, the aluminothermic slag exhibits a heavy distribution of faceted Ta/Nb plate-shaped particles which can be distinguished here by their metallic cream Ta/Nb colour in the green-grey slag. The arrangement of the metallic plate phase here is random, has not reached the mobile stage of accretion and/or dispersal to particulate metallic regions, and is comparable to the primary plate regions in electron optical micrographs of earlier figures. [LOM, (air lens); Ektachrome; fov: 208 μm (0.21 mm)]

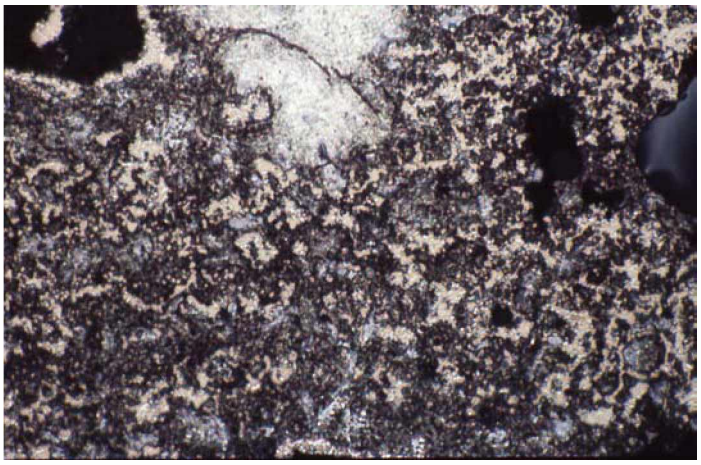

Figure {7.4.4}**19**: Light optical colour micrograph showing (at low magnification) the distribution of Ta/Nb-metallic phases (cream) through crucible-base remnants which were subjected to maximum processing (in WODG**A6**), the various silver-grey regions are Sn/Mn/Fe-phases incorporated in and around the sintered-particulate regions of Ta/Nb-phase, the extensive silver-white region in upper field is a freely-drained pool of low-alloy Sn-metal (incorporating some smearing due to specimen preparation). [LOM, (air lens); Ektachrome; fov: 530 μm (0.53 mm)]

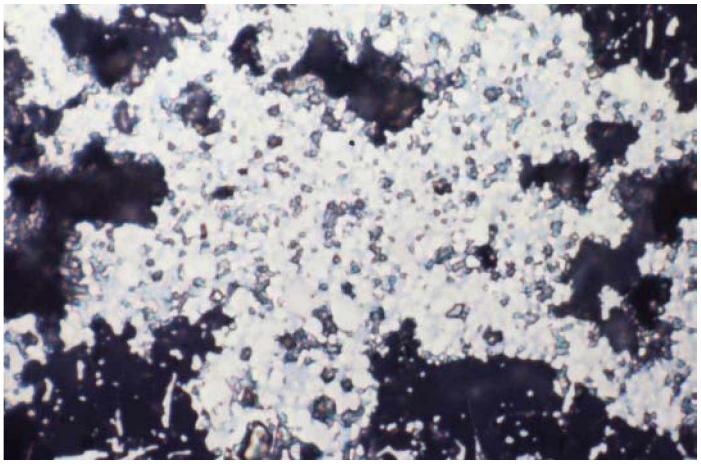

Figure {7.4.4}**20**: Light optical colour micrograph showing "detail" of a region of amassed, sintered Ta/Nb-phase (cream) in-filled by Sn/Mn/Fe-"hardhead" phase (silver-grey) standing prominent beside void (once slag-filled) in which some physical evidence of attached Ta/Nb-plates can be detected. This field, just outside the previous field (above), was evidently parallel to the plasma-exposed surface (rather than representing a section through it, as were previous micrographic fields). The brittle slag here was lost in specimen preparation and polishing. [LOM, (air lens); Ektachrome; fov: 208 μm (0.21 mm)]

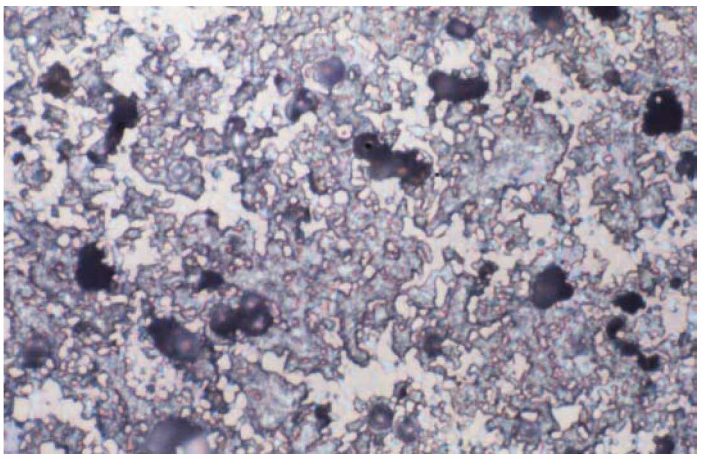

Figure {7.4.4}**21**: Light optical colour micrograph in specimen WODG**A4** showing an amassed Ta/Nb-phase region (cream) representing moderate processing time. The in-fill silver-grey phase is nominal Sn/Mn/Fe-phase, black areas are voids in the metallic agglomerate. [LOM, (air lens); Ektachrome; fov: 208 μm (0.21 mm)]

presented in accompanying EDS map-set of Figure {7.4.4}**9**. The degree of "under-development" of the "secondary phase-stripping into solution" stage is plainly evident (by the "clean" slag/metal interfaces) in this "shortest processing time" specimen – a development that had quite observably progressed with processing time in later specimens. Such a development of the secondary, Ta/Nb-stripping with resultant interface modification is evident in a number of micrographs including those of Figures {7.4.4}**10**, {7.4.4}**11** and {7.4.4}**31** which show both detail and variation of interface modification and particle/plate interconnectedness.

The peculiarities of facies development in more-processed reduction remnants – particularly as represented in the development of plate features in the progression of slag "microstructure" – are represented in the micrographs and map-set of Figures {7.4.4}**10**, {7.4.4}**11** and {7.4.4}**22** to {7.4.4}**24**. Where profuse plate distribution in slag phases was the "norm" for typical remnant fields, the fields of these micrographs show a "departure" from that norm. Indeed, there is some visual evidence of liquid-state migration of faceted plate features to adjacent particulate agglomerate features, correspondingly, these may be regions in which only minor materialisation of plate-phase initially occurred. The slag can generally be attributed as original "aluminothermic" slag, and so must have contained or been associated (by co-deposition) with an apportioned fraction of plate phase, moreover, those advanced and highly-faceted plate features remaining in the slag phase, and still identifiable as such, can be seen to be amalgamated with like-kind features, or to be drawn to the interregnum region (the "interfacial zone" between slag and agglomerate). This evident disposition of the slag-borne plate phase to aggregate with the particulate Ta/Nb/(Ti)-phase suggested a likely eventual agglomerate outcome if processing had been continued.

Conversely, where a principally Sn-group phase was found to have an interface with slag phase, then such intimate boundary did not present the same attraction to the slag-borne plates as did the comparable Ta/Nb-phase at particulate/slag interfaces (where phase compatibility presumably produced mutual attraction). There may have been a simple "electronic charge" reason to explain such anomalous behaviour in liquid phase adjacent to Sn/(Mn/Fe)-phase/slag interfaces, however, no specific reason is required to validate mere mention of the observation. Such primarily Sn-phase/slag

Table {7.4.4}1: The table shows results of EDS analyses from spot counts acquired from Ta/Nb-metallic phase in fields in mounted and polished reduction product of the microwave-stimulated aluminothermic reduction of wodginite as the mine-site-derived mineral concentrate [(Ta,Nb)Sn(Mn,Fe)$_{16}$O$_{32}$]. The processing times for trial specimens WODG**A1** to WODG**A6** ranged from 7 min to 12 min in keeping with the processing requirements in delivering a suitable range of metallisation in reduction products. Of significance for these reported EDS analyses is that, because of the otherwise wide range of metallic phases, only the Ta/Nb-phase metal was addressed. In this, because the slag-borne "morph" phase was too narrow to generally acquire a representative, non-contaminated count, the Ta/Nb-phase metal was assessed from spot EDS counts on larger particles or agglomerates of solid-state reduced metal representing intense plasma exposure. The lamellar-like Ta/Nb-phase that was deposited in aluminothermic slag was found (by individual EDS checks) to be close in composition to the particulate equivalent for all specimens. The fellow refractory metal Ti, a minor impurity in the mineral concentrate, typically reported in the Ta/Nb-phase – which is alternatively written as "Ta/Nb/Ti-phase" (context dependent) and, on average, the Ti-content was of similar proportion to the Nb-content in the metallic "phase of interest".

Specimen.	**EDS analyses of spot acquisitions from redn. product phase (at%).** All EDS acquisitions were spot acquisitions by windowless detection.							
	Ta	**Nb**	**Ti**	**Al**	**C**	**N**	**O**	**balance**
WODGA**1**	89.68	3.16	2.88	0.10	2.75	0.91	0.45	0.04 Fe, 0.03 Zr
(7 min)	90.12	2.17	3.14	0.09	2.81	1.38	0.27	0.02 Si
	87.31	4.62	1.89	0.73	3.44	1.60	0.34	0.05 Fe, 0.02 Si
	90.87	1.95	1.99	0.18	4.07	0.45	0.41	0.08 Cr
	88.92	2.55	3.45	0.08	3.96	0.38	0.61	0.04 Fe, 0.01 V
Spec. mean:	**89.38**	**2.89**	**2.67**	**0.24**	**3.41**	**0.94**	**0.42**	**(0.05)**
WODGA**2**	90.11	2.77	1.89	0.15	4.19	0.48	0.37	0.04 Fe
(8 min)	88.76	2.59	2.75	0.23	5.00	0.17	0.43	0.05 Fe, 0.02 Mn
	86.69	6.32	1.98	0.15	4.28	0.29	0.22	0.07 Ca
	88.93	2.17	1.78	0.08	5.89	0.60	0.49	0.03 Fe, 0.03 Si
	88.65	3.56	3.31	0.09	3.75	0.39	0.19	0.04 Si, 0.02 Mn
Spec. mean:	**88.63**	**3.48**	**2.34**	**0.14**	**4.62**	**0.39**	**0.34**	**(0.06)**
WODGA**3**	87.48	3.57	4.02	0.05	4.09	0.58	0.18	0.03 Si
(8 min)	88.17	2.05	3.43	0.21	4.90	0.95	0.26	0.03 Fe
	88.74	2.81	2.61	0.08	5.36	0.25	0.09	0.05 Fe, 0.01 Zr
	88.55	3.76	3.07	0.08	3.92	0.45	0.13	0.04 Fe
	87.38	4.00	2.29	0.11	5.19	0.88	0.11	0.02 Fe, 0.02 Si
Spec. mean:	**88.06**	**3.24**	**3.08**	**0.11**	**4.69**	**0.62**	**0.15**	**(0.05)**
WODGA**4**	87.75	4.22	3.99	0.16	3.33	0.44	0.09	0.02 Si
(10 min)	88.54	2.66	2.92	0.12	4.73	0.78	0.17	0.08 Fe
	85.97	7.34	1.93	0.07	4.23	0.36	0.05	0.03 Fe, 0.02 Si
	86.86	2.47	3.76	0.30	5.46	1.03	0.06	0.05 Fe, 0.01 Si
	89.18	3.55	2.04	0.09	4.48	0.46	0.13	0.07 Fe
Spec. mean:	**87.66**	**4.05**	**2.93**	**0.15**	**4.45**	**0.61**	**0.10**	**(0.05)**

[Table continued over page.]

Table {7.4.4}1 continued/

Specimen.	EDS analyses of spot acquisitions from redn. product phase (at%). All EDS acquisitions were spot acquisitions by windowless detection.							
	Ta	**Nb**	**Ti**	**Al**	**C**	**N**	**O**	**balance**
WODGA5	87.93	3.56	1.88	0.22	5.01	1.27	0.08	0.03 Fe, 0.02 Si
(10 min)	88.14	3.23	2.36	0.16	5.10	0.72	0.24	0.05 Si
	88.03	4.32	1. 85	0.20	4.99	0.38	0.16	0.07 Fe
	86 18	2.67	2.35	0.30	7.65	0.65	0.11	0.6 Mn, 0.03 Si
	86.75	3.39	2.88	0.09	6.46	0.28	0.09	0.06 Fe
Spec. mean:	**87.41**	**3.43**	**2.26**	**0.20**	**5.84**	**0.66**	**0.14**	**(0.06)**
WODGA6	86.54	3.06	4.12	0.08	5.52	0.43	0.17	0.06 Fe 0.02 Si
(12 min)	88.28	2.78	4.18	0.16	3.88	0.61	0.08	0.03 Si
	85 89	5.16	3.26	0.09	4.79	0.48	0.24	0.09 Fe
	86.58	2.99	2.76	0.25	6.72	0.59	0.04	0.05 Fe, 0.02 Si
	85.83	1.95	4.38	0.15	6.61	0.87	0.09	0.12 Fe
Spec. mean:	**86.62**	**3.19**	**3.74**	**0.15**	**5.50**	**0.60**	**0.12**	**(0.08)**

Averaged mean composition of metallic Ta/Nb-phase reduction products of wodginite across all six specimens: 87.96 at% Ta; 3.38 at% Nb; 2.84 at% Ti; 4.75 at% C; 0.64 at% N, with the minor balance of Al, O and trace metals. Note the general increase in C-content with increasing processing time, and the consequent minor decline in principal metals to accommodate such C-increase. The N-content in Ta/Nb-metallic phases was (again) not as prominent as in the reduction products of previous refractory metals.

(Each unto the other, (as analogue elements) Ta and Nb are progenitor impurity elements in the primitive source mineral(s) and consequently are the primary impurity in the other's "refined" minerals.)

interfaces possessing adjacent plate-free zones can be seen in the micrographs of Figures {7.4.4}**12** and {7.4.4}**13**. In general, descriptions and discussion are well served in annotations accompanying the micrographs and EDS map-sets of the figures of this Section **7.4.4** (including those in Appendix **7.4.4**). Again, the sheer concentration of metallurgical "events" occurring in any microwave reduction process – represented in reduction remnants – was greater for this aluminothermic wodginite reduction assignment than for any previous reduction assignment in the project. EDS analyses of Ta/Nb/(Ti)-phase is presented in Table {7.4.4}**1** along with some relevant discussion. Consequently, more metallurgical detail was available to record and, significantly, this "assignment" **7.4.4** presented more visual confirmation of the propensity of microwave-stimulated plasma reduction processing than did any other refractory metal reduction assignment. Its fuller coverage is representative of this observation, and provides a fair indication of possibilities for microwave plasma processing of real minerals.

7.5: Halidation, and Decomposition of Halides.

As elsewhere, although its use is more "conspicuous" here, the nomenclature of this section is not the standard usage in that it reflects the ***resultant product*** *rather than the* ***derivative processing route****; it is generally the product that has relevance to this project. The adopted nomenclature is set out specifically in Section* ***3.2.1****. As a consequence of this re-assignment of emphases, "halidation" supplants "halination", "chloridation" "chlorination",* et cetera, *such as to emphasise the material product. Also, "chlorination" (the process) does not necessarily lead to a "chloride" (product), whereas, "chloridation" assumes the product irrespective of route. This moot distinction was seen as pertinent in the context of the project.*

Consequent upon the importance of halides and halidation – or chlorides and chloridation, specifically to commercial production – in the commercial production of refractory metals, this author felt bound to report upon some associated process phenomena that arose from enquiry into investigational observations of certain "intriguing" *microwave capabilities*, capabilities which have considerable bearing upon both the synthesis and disproportionation of metal halides. [Here the term…

/interfaces possessing adjacent plate-free zones can be seen in the micrographs of Figures {7.4.4}**12** and {7.4.4}**13**. In general, descriptions and discussion are well served in annotations accompanying the micrographs and EDS map-sets of the figures of this Section **7.4.4** (including those in Appendix **7.4.4**). Again, the sheer concentration of metallurgical "events" occurring in any microwave reduction process – represented in reduction remnants – was greater for this aluminothermic wodginite reduction assignment than for any previous reduction assignment in the project. EDS analyses of Ta/Nb/(Ti)-phase is presented in Table {7.4.4}**1** along with some relevant discussion. Consequently, more metallurgical detail was available to record and, significantly, this "assignment" **7.4.4** presented more visual confirmation of the propensity of microwave-stimulated plasma reduction processing than did any other refractory metal reduction assignment. Its fuller coverage is representative of this observation, and provides a fair indication of possibilities for microwave plasma processing of real minerals.

7.5: Halidation, and Decomposition of Halides.

As elsewhere, although its use is more "conspicuous" here, the nomenclature of this section is not the standard usage in that it reflects the ***resultant product*** *rather than the* ***derivative processing route****; it is generally the product that has relevance to this project. The adopted nomenclature is set out specifically in Section* ***3.2.1****. As a consequence of this re-assignment of emphases, "halidation" supplants "halination", "chloridation" "chlorination",* et cetera, *such as to emphasise the material product. Also, "chlorination" (the process) does not necessarily lead to a "chloride" (product), whereas, "chloridation" assumes the product irrespective of route. This moot distinction was seen as pertinent in the context of the project.*

Consequent upon the importance of halides and halidation – or chlorides and chloridation, specifically to commercial production – in the commercial production of refractory metals, this author felt bound to report upon some associated process phenomena that arose from enquiry into investigational observations of certain "intriguing" *microwave capabilities*, capabilities which have considerable bearing upon both the synthesis and disproportionation of metal halides. [Here the term

"disproportionation" is the more positive industry jargon whose meaning is tantamount to "intentional decomposition". It is the pretence to "design" in processes that confers upon "disproportionation" the *intent* not allocated to "decomposition"; otherwise these operations are chemically and procedurally equivalent.] Fundamental in this section is that descriptions and discussion *give an* ***account*** *only* of experimental observations of "exploratory" investigations that, in line with their compositions, produced a non-refractory metal (in the initial case) and no plain physical remnants (in the latter). The observations of these provisional tests are relevant because the experimentation dealt with significant ideas – ideas whose application could define new process initiatives or shape specifications for new process and plant design. The primary concepts presented in the narrative are not necessarily new, however, their process configuration and/or process outcome is sufficiently facilitated by the implementation of applied microwave energy to warrant re-assessment or, indeed, new assessment of process routes and strategies relating to the processing of metal halides.

In the conventional reduction routes for the refractory metals (and some other metals), the well-entrenched Kroll process and the comparable Hunter process are established methods of extractive reduction that are used worldwide. (Magnesothermic and sodothermic respectively) these intensive metallothermic reactions are conducted on the relevant refractory metal chloride. Carried-out in rudimentary plain steel batch reactors, the aggressive reaction yields the refractory metal as the reduction product – a sponge metal permeated by liquid $MgCl_2$ or NaCl, (at elevated temperature) the volatile by-product is subsequently removed by a vapour-evacuation process to leave clean, chloride-free sponge. (Despite its capacity to pollute, the inexorable efficiency of this process-type has ensured that the quite antiquated industrial practice has persisted into the "modern" age of production where it has survived almost unchanged, an enduring *niche* industry. Because of their sometime *strategic metals* status, refractory metals extraction industries have not been shunted into the Third World along with so much other "dirty or dubious" industrialisation.)

Regarding halidation processes, an initial consideration relates to fundamental electronic structure in that the halides of the alkaline (Group **1**) metals and alkaline

earth (Group **2**) metals exhibit largely ionic bonding, whereas the halides of transition metals (including the refractory metals) exhibit substantial covalent bonding, and this distinction renders the refractory metal halides with lower melting and vaporisation points than exhibited by the halides of Groups **1** and **2** metals. The distinction also facilitates the metallothermic reduction of refractory metal halides by metals of Groups **1** and **2**. Of the metal halides, the chlorides are the most abundant in both terrestrial ore and seawater-derived deposits, as they are also the most common halide in industrial exploitation.

There are separate, process-dependent routes employing different chlorination agents (Cl_2 , HCl and MCl_2 commonly) which satisfy various thermochemical criteria, whereof, the familiar gaseous route presented in Equation **{7.5}1** is only possible when the chloride is more thermodynamically stable than the oxide.

$$MO_{(s)} + Cl_{2(g)} \rightarrow MCl_{2(l)} + {}^{1}/_{2}O_{2(g)} \quad \ldots\ldots \quad \textbf{\{7.5\}1}$$

Where this is not the case, intermediate carbothermic assisted reduction is employed and the following reactions are relevant, energy and contact dependent.

$$MO_{(s\})} + C_{(s)} \rightarrow M^{*}_{(v)} + CO_{(g)} \quad \ldots\ldots \quad \textbf{\{7.5\}2}$$

$$MO_{(s)} + CO_{(g)} \rightarrow M^{*}_{(v)} + CO_{2(g)} \quad \ldots\ldots \quad \textbf{\{7.5\}2a}$$

$$M^{*}_{(v)} + Cl_{2(g)} \rightarrow MCl_{2(l)} \quad \ldots\ldots\ldots \quad \textbf{\{7.5\}3}$$

For its part, in a chlorination stream, chloridation of a metal oxide always proceeds more rapidly when the Cl is in the plasma state (rather than the gaseous state) because the activated particles supplement the Gibbs energy ($-\Delta\mathbf{G}$). Furthermore, Hess' law assumes the shift of $\Delta\mathbf{G}^{0}_{T}$ towards more negative values will be proportional to the dissociation and ionisation energies of the halogen [58]. However, this identity ($\Delta\mathbf{G}^{0}$) assumes species in their standard state and, with increasing ionisation, the system is leaving that realm and moving into an increasingly favourable thermochemical realm (of plasma). This shift provides the thermochemical impetus for the plasma conversion to metal halide of fine metal oxides in a halogen plasma environment. [This may be

assisted by the presence of fine C-reductant (to remove the O) when, otherwise, as a reduction product, the metal oxide would be more thermodynamically stable than the metal halide, and the reaction would not proceed.]

Refining of metal halides may rely on the capability of the distillation system to separate mixed metal halide liquids based upon difference in boiling points. However, in the project-relevant case of distilling $TaCl_5$ from $NbCl_5$ after their chloridation from the mixed pure oxides, these chlorides have nearly identical boiling points, a fact which obviates an immediate difficulty for distillation. However, selective condensation procedures make use of differing concentrations that can result in chlorides exhibiting different dew points, thus allowing a strategy for separation. Further to this, whilst it is not necessary to provide a plasma environment in order to drive halidation reactions, reaction rates may be increased by several orders of magnitude [34, 58] when conducted under such environments of highly activated species.

Of further note with respect to relevant refractory metals processing, if Cl_2 gas is used in the chloridation of ilmenite, $FeO.TiO_2$, to produce $FeCl_3$ plus $TiCl_4$ – a mixture which can be fractionally distilled quite readily to produce a valuable product plus the invaluable $FeCl_3$ (a product which may be seen as a combined chlorination cost, distillation cost and disposal problem cost rather than as a product of value). It is both cost effective and procedurally preferable to selectively chlorinate the ilmenite with HCl to yield $FeCl_2$ plus H_2O whilst for the titania component, formation of its chloride having a positive free energy, the parallel chloridation of the TiO_2 component does not take place [17]. This selective chloridation method represents the process route for the extractive production of synthetic rutile (TiO_2), a valuable mineral product, from the more abundant and comparably less valuable ilmenite.

The second fundamental halide process of interest in this microwave-stimulated plasma study is the inverse process to halidation, that is, the dissociation process of decomposition, or disproportionation. Many compounds are liable to decompose upon heating, this decomposition proceeds by the dissociation of chemical bonds in the

compound, whether solid, liquid or gas. Such dissociation is accompanied by particle excitation and ionisation where the compound is promoted into the plasma state. Also, by rote, a compound's propensity to decompose decreases with its increasing thermochemical stability. Consequently, although decomposition processes may vary manifestly, they are best represented by the following simple generalised equation.

$$AB_{(s\ or\ l)} \rightarrow A_{(s\ or\ l)} + B_{(g)} \quad \ldots\ldots\ldots \quad \{7.5\}4$$

By definition, thermal decomposition reactions are always endothermic (that is, they *require* energy to proceed) and consequently proceed more readily as applied energy increases – most commonly, such applied energy is thermal energy, or "temperature". Moreover, in the common identity $\Delta\mathbf{G} = \Delta\mathbf{H} - T.\Delta\mathbf{S}$, the entropy term is especially temperature dependent. Moreover, in many reactions the temperature-dependent changes for $\Delta\mathbf{H}$ and $\Delta\mathbf{S}$ are minimal, and at high "temperatures" $T.\Delta\mathbf{S}$ and $\Delta\mathbf{G}$ are near linear functions of T [58, 80, 87]. So it follows that the high "temperatures" and constant system pressures (of ~ 1 atm) of the simple oven set-up method of this project favour dissociation and disproportionation processes, with the increasing entropy factor increasingly benefiting process efficiency; and this before the benefits of plasma thermochemistry are superimposed upon the straightforward plasma-free thermodynamic factors.

Under the non-equilibrium conditions of microwave-stimulated plasma, and depending upon the applied energy, system pressure and species available in the system environment, "thermal" decomposition takes place for the refractory metal halides in a compliant manner with iodides and bromides generally more susceptible to decomposition than the chlorides and fluorides, species dependent [17]. Surprisingly because of their acknowledged stability, and as alluded-to in a previous section in respect of O-deficiency and reductant-free oxide "reduction", even metal *oxides* can be decomposed. Under the intensive, activated conditions of plasma thermochemistry, highly stable oxides – including refractory metal oxides – can be decomposed when their *dissociation tension* exceeds the *partial pressure* of oxygen (O_2, O^*, O^-, *et cetera*) in the system. DEMBOVSKY [58] reports further that common minerals of high refractoriness Al_2O_3, MgO, SiO_2 and the similarly stable and important resource

mineral molybdenite, MoS_2 , have been successfully disproportionated in a reductant-free plasma environment to yield the metals at high purity. [Some measure of this reported result was observed (and previously reported) in experimental outcomes of this project.]

The conversion of oxide raw-materials – normally pure oxides, often pure mixed oxides, sometimes run-of-mine ore minerals – into their metal halide is a standard industry procedure in the conventional extractive process route for refractory metals production. Typically these are chloridation processes, and whilst the important reactions are thermodynamically feasible in a chlorination stream, for practicable reasons are carried-out in the presence of the co-reactant carbon (C or CO) which promotes both the reaction rate and the conversion rate by converting the metal oxide to CO and CO_2 (as Equations **{7.5}1** to **{7.5}3**). **An experimental microwave-stimulated prototype of this gaseous chloridation process was planned but, for reasons of "laboratory safety", actual halidation of a metal oxide in a halogen stream was deemed "dangerous" to nearby personnel, consequently, no material *halidation* investigation was undertaken.** However, microwave-stimulated decomposition trials for (each of) two quite different chlorides were successfully undertaken, and discussion of these experimental trials follows.

Available time, materials and experimental facilities only allowed a cursory examination of this "fringe core" subject, the thermal decomposition of halides. Of note is that the halides chosen – both chlorides – were each relevant within project objectives and, importantly, each was solid and not volatile at ambient temperatures. Hydrated cobaltous chloride ($CoCl_2.6H_2O$, laboratory grade) and mineral halite (NaCl, as a geological sample from Lake Frome deposit, S.A.) – each a *salt* by definition – were the chosen halides for the microwave disproportionation investigation trials. Each chloride was charged loosely and alone into a clean new "microwave-transparent" "zirconia" crucible (to about 3/4-full, ~ 12 g each charge) with a lid and double layers of insulation blanket all around in the same manner as previous experimental configurations. No char or other material was added to the crucible, nor around the crucible to augment heating – so (beyond air and its ionised species) no reductant, catalyst or other agent (solid,

liquid or gas) was available to directly influence chemistry, and total "heating" was left to the microwave-susceptibilities of the materials under irradiation – this dielectric heating supplied the total system "heating" – and inevitably, the "mineral" halite salt heated more slowly than the hydrated cobalt salt.

7.5.1: Dehydration and Disproportionation of Cobaltous Chloride Hydride.

In the standard oven set-up and crucible configuration described above, a charge of hydrated cobaltous chloride, $CoCl_2.6H_2O$, was microwave irradiated. Whilst it did not become a tangible problem, particular attention was paid to the possibility of arcing at the magnetrons *if* the charge did not present sufficient dielectric load to the applied field. After minimal irradiation, blue cobaltous chloride, $CoCl_2$, was produced quickly as the highly susceptible water of hydration was driven off the dark $CoCl_2.6H_2O$ crystals. After a short period during which the temperature rose past the melting point of the chloride, decomposition was noted as the distinctive sharp odour and yellow-green colour of evolved Cl_2 gas was detected. Given the small charge, the evolution of Cl_2 became profuse, thence tapered away for some minutes to apparent cessation. [Despite only occasional exposure to the odour of Cl-gas, its familiar and pungent presence was identified by the author and verified by Professor Worner.]

Microwave processing was terminated once the yellow-green chlorine was no longer visibly detectable and the crucible arrangement slightly opened enough to place ~ 5 g of granular char onto the liquid metal such as to assist in atmospheric protection against oxidation of the Co-metal, the lid closed and a nominal 30 sec of microwave irradiation applied to generate CO without appreciable further heating. The arrangement was allowed to cool under the nominal protection of a CO-blanket plus char. This strategy did not contravene the above principle of reductant-free decomposition as decomposition was adjudged to be complete by the stage of intervention. Also, as the Co-metal was presumed to already be in the fully reduced state, further "reduction" (by carbonaceous means) was not possible. Also, it was known that the atmospheric protection afforded by the char addition would be limited under the thermal regime of

cooling, however, as it happened, this rudimentary method proved satisfactory upon its introduction and the initial method was not altered thereafter.

Once cold, the slowly cooled crucible configuration containing the disproportionated metallic product was opened to reveal a metal button of mass approximate to that expected from stoichiometry. The disproportionation-remnant button of metallic cobalt which (given only brief exposure to char) was found to be relatively carbon saturated with a microstructure just delineable to the unaided eye, and under microscopic examination reminiscent to a grey cast iron. The cobalt metal was otherwise "pure" and no detritus of incompletely decomposed chloride was found in the decomposition crucible. This experiment was repeated on various occasions as a demonstration "vehicle" to exhibit microwave propensities in extractive processing of materials. In all, seven metallic-Co disproportionation products were produced and recorded, these seven "demonstration events" were conducted at intervals over a number of years. Sometimes more than the one metal button was produced (dependent upon in-crucible dynamics after char addition) if "consolidation tamping" was not conducted. But windowless EDS examination always yielded the same, reproducible high-C Co-metal result with no remaining Cl or any other detected component element (and whilst none were "quantitatively" determined, C was "qualitatively" verified to be "present" and other light elements N and O "absent"); microscopical inspection revealed the same C-saturated microstructure [αCo + graphite] in all specimens. [A desirable experimental improvement to that employed may be to conduct the disproportionation in an Ar-atmosphere thence, more importantly, cool the product entirely in an Ar-atmosphere, possibly aided by an Ar-stream into the crucible. However, this possibly costly improvement would not alter nor improve the *fact* of disproportionation, just the purity of the product.]

What was essential in determining (for this chloride) the completeness of microwave-stimulated disproportionation as a successful process was that the Cl had been totally dissociated and removed from the Co in the instance of each experimental trial. This was achieved in a convincing if non-quantitative fashion, and reported faithfully if only by written account, the outcome was clear that hydrated cobaltous chloride, $CoCl_2.6H_2O$, could be dehydrated thence, under ongoing stimulation, the neat chloride disproportionated into its elemental components. Further, it was likely that

some amount of in-crucible ionisation occurred in the newly evolved Cl-gas, and that this "heightened activation" of particles played a part in driving the decomposition. However, the relatively modest thermochemical potential inside the crucible environment evidently constrained the "temperatures" attained during the process, and that this would have confirmed the ionisation level reached should only warrant the status of a low level partial plasma. Physically, under microwave irradiation, the vibrational resonance of the component atoms through and about their chemical bonds would have initiated much of the dissociation, a phenomenon well documented in the literature [71, 76, 80, 83, 87, 105, 206] and one which would have benefited both from the low dissociation energy required by the chloride and from the thermal activation continuously driven by the applied microwave energy.

7.5.2: Disproportionation of Halite (Sodium Chloride).

A charge of NaCl (as the "mineral" salt halite from Lake Frome deposit) in the standard oven set-up and crucible configuration described above was microwave irradiated so to initiate and drive disproportionation of this most common chloride. Being less microwave-susceptible than the previous hydrated salt, care was exercised in the initial stage of irradiation when arcing phenomena at the magnetrons was a real possibility, this threat was alleviated by augmentation of the dielectric load. Such augmentation simply involved the positioning of solid blocks of chemically inert mid-range-dielectric ceramic around the crucible configuration in the oven chamber to draw an adequate portion of initial irradiated energy, so to avoid arcing at the magnetrons. Upon concurrent heating of all load-elements in the oven, then once the configured charge increased its susceptibility (capacity) as a dielectric load past that of the combined dielectrically-suppressed "dummy" loads thence, increasingly, it would attract "all" applied microwave energy (until process-end).

In a more anecdotal account than that of the cobaltous chloride – there being *no* recovered remnant or product (as such) from this trial orientated more around "process capability" – the following process events were recorded. In line with the initial

microwave irradiation outlined above, the NaCl charge heated progressively until, at a dull red glow in the inner-crucible zone, the initially evolved Cl-gas was detected issuing from the crucible top. The initiation of decomposition was corroborated by the evolution of this acrid and visible yellow-green gas. The initially modest evolution of Cl-gas rapidly became profuse and the crucible glow increased to red-yellow whereupon, quite rapidly, the intensity of light emitted from the crucible top increased several-fold, its colour shifting to white-blue. The thermal intensity accompanying this shift resulted in melting and contraction of crucible containment and insulation around the crucible top. (Here noting that, consistent with this mode of "containment failure", the applied microwave plus exothermic heat was generated from inside – dissipating outwards, rather than from the outside – conducted inwards).

The relatively "sudden" thermal escalation was the result of the newly reduced liquid Na-metal exothermically re-oxidising (this time to the more stable *oxide*, so releasing greater heat) at the ingress of O_2-gas to the crucible. After a minute or so from the initial dissociation the whole "disproportionation-of-NaCl plus re-oxidation-of-Na" was complete and the crucible arrangement – particularly the inner-crucible zone – was unrecognisable with respect to its former configuration. Any attempt to meaningfully sample re-oxidation-product powder was frustrated at recovery by the state and distribution of the crucible-content remnants and with the inter-mixing of white "ash" materials (largely the decomposition powder of "thermally failed" insulation materials). Inter-mixing of oxidation product with decomposition ash aside, no matter the *chemistry* of the Na-oxide product, any analyses of the product could only have shown it to be the combustion product of Na-metal (assumed to have exclusively been the white Na_2O, although a $Na_xSi_yO_z$ compound (like sodium silicate, $mNa_2O.nSiO_2$) was thought plausible – the peroxide Na_2O_2 is pale yellow, and was thermochemically unlikely). The witnessed intensity and white-blue colour of the Na-combustion "flame" was identified (by the author and Professor Worner) as being characteristic of such combustion, whether or not the combustion flame was augmented by microwave-initiated ionisation species. By way of verification, this perfunctory experimental trial was repeated three (more) times and each outcome was identical to that (rather sketchily) reported above, no specific attempt was made, beyond the cause of

verification, to recover either of the decomposition products – the oxide too impure, and the Cl_2 gas toxic, unpleasant to handle and too corrosive to process or store for testing.

Under "ideal" processing conditions of a purpose-built system, oxidation of the Na-metal disproportionation product could have been circumvented, wherein, for such a system both Na and Cl_2 could be collected for alternative processing purposes. As previously declared, this exercise was conducted with the Hunter process in mind – acknowledging that both Na and Cl are imperative elemental components in the Hunter route – and, no less relevant, that Australia has an extraordinary abundance of accessible terrestrial salt deposits. Further, the fact that relevant disproportionation of chlorides can be attained solely by an efficient technique of microwave-stimulated decomposition – entirely free of intervention, by design or impediment, from any "third party" chemistry – is of fundamental importance. This alone should emphasise the potential, and provide necessary and sufficient recommendation for further research towards the development of a pilot plant and beyond to a combination NaCl-disproportionation/Hunter process refractory metals extractive production scheme. Given the ongoing brace of "value-add export deficits", such a panacea is not over-stretching the bounds of plausibility given Australian resource adequacy, availability and ingenuity; Australian disposition may proclaim otherwise. Not (yet) free of its colonial comportment, Australia may not recognise the magnitude of its exported value-add until it is all gone.

The decomposition of halide minerals by thermal dissociation is an established method of high-purity metal production – the van Arkel-de Boer iodide decomposition process being the prime example. Along with other metal halides, refractory metal halides have relatively low energies of formation that allow the relative ease of their thermally stimulated decomposition [17, 29, 58, 242]. This low energy barrier is easily and conveniently surmounted by the application of microwave energy, which selectively engages the susceptibility of the targeted halide that is to be decomposed. Also, by way of relevant comment, being the halide of a Group **1** metal, NaCl exhibited a "higher energy barrier" than do the refractory metal halides, and so experimentally represented a

legitimately affirmative decomposition accomplishment. Again, only a modest amount of experimental work was devoted to this section of the project but evident and indisputable success was indicated by the results (as observed and reported) for this specific subject, a complementary topic that has resonant, reciprocal affinities with any and all refractory metal extraction studies.

Despite the absence of "results" and the qualitative nature of the reporting of this work, the work itself would have been no more successful if compiled "results" *had* accompanied the report narrative. Fittingly, however, it was deemed that the broaching of such a topic of consequence to refractory metals production could only enhance the "confluence of relevance" between core segments: refractory metals oxides, halidation (accompanying refining and reduction) and microwave processing. These confluent core divisions may be seen to represent the industry sectors of minerals processing, metallurgical processing and scientific application – extractive production sectors often "out of step" in crucial co-operation that, fittingly, should define Industry – the "divisions" brought together in the contextual framework of this project. And whilst this halidation/decomposition section does not introduce into processing any utterly "new" route, it does suggest the desirability of an inclusive "review" – and introduces the real possibility of an evolutionary advancement in processing strategy and procedure for this essential metallurgical industry.

AN INVESTIGATION OF

THE MICROWAVE - STIMULATED REDUCTION OF

OXIDES OF REFRACTORY METALS.

VOLUME III

[Section 8 to Appendices.]

8

DISCUSSION.

"Where it is a duty to worship the sun it is pretty sure to be a crime to examine the laws of heat."

John Morley - *Voltaire,* 1872.

"Vision is the art of seeing things invisible."

Swift - *Thoughts on Various Subjects*, 1711.

8; DISCUSSION.

Although matters of immediate relevance were appropriately highlighted and discussed throughout the course of descriptions in Section 7, "*Results*", a broader, more cohesive appraisal of the overall experimental results is presented in the following Section **8.1**. Whereas, Section **8.2** re-visits certain of the more recurrent concerns which governed experimentation because of their bearing on the means and determination of procedure, the execution and the evaluation of experimental programmes for the various minerals. Overall, the review brings together "elements of experimentation" common throughout the experimental trials and, in consolidating discussion, connects those characteristics of "process" and "product" made evident by microscopical and analytical evaluation – characteristics universal across the various reduction assignments of the experimental programme.

In corroboration of its relevance to project experimentation, acknowledgement must be made of that fore-borne precursor section of pre-core experimentation reported in Section **7.1** of the co-reduction of industry-relevant refractory metal minerals into their more reducible ferruginous co-mineralogical fraction, or ferruginous co-reactant in other cases. Such ferruginous fractions were always the proportionally dominant fraction and, as in the cases of V-bearing magnetite and the Ti-bearing magnetite ("titano-magnetite"), some of these minerals are furnace-reduced to iron in commercial extractive operations, leaving the V- or Ti-content in the accompanying slag in these examples. Section **7.1** also presented the potential of parallel reduction exercises representing non-ferruginous minerals including non-refractory metal and sulphide examples such as cassiterite and Kambalda nickel/cobalt concentrate, which were shown to be readily reducible. **However, this instructive suite of experimental results was fundamental in substantiating the *reducibility of refractory metal mineral species* by the "capturing" of reduced refractory metals in ferrous solid solution and suppressing their re-oxidation (so forestalling the "over-processing" prevalent in core experimental trials). The results verify the microwave-stimulated reducibility of stable refractory metal oxide minerals relevant to the core project experimentation, albeit for co-mineralised and variant mineral species.**

The experimental programme was devised such as to show the potential of microwave-stimulated reduction as applied across a representative range of thermochemically stable oxide minerals of refractory metals, the minerals selected as previously discussed. The oxide minerals were chosen from both (*i*) "laboratory grade" or "commercially pure" minerals of good purity, and (*ii*) Australian minesite-derived mineral concentrates as commercially traded. Such ore concentrates are traded on the cost-adjusted basis of their pure single oxide equivalence – that is, wodginite on the basis of its equivalent Ta_2O_5 plus Nb_2O_5 content (neglecting its Sn, *et cetera* contents) and ilmenite on the basis of its TiO_2 equivalence, *et cetera*. Consequently, there is a duality in the inclusion of the pure oxide minerals in the experimental programme, firstly to provide a continuity of refractory metals represented across the suite of reactant minerals, including a "pure oxide" corresponding to each included concentrate mineral. And secondly, the typical penultimate reactant at the refining stage of refractory metals production is the pure oxide – converted into the process-defined halide form that is refined by fractional distillation, thence reduced to a commercial grade metal of prescribed specification, or "purity".

Also, the inclusion of the pure oxides of the five project refractory metals, particularly those of hafnium and niobium – the minor "analogue" metals represented in minerals of the chosen minesite concentrates – allowed continuity in the experimental programme. Such an approach, it was felt, would allow comparison of microwave reduction results with those of conventional thermochemistry, establishing experimental data point "dots" on the "broad and empty canvas" of microwave reduction processing. Along with the clearer results of the more experimentally investigated exercises, these experimental "dots" could, figuratively, be connected to present a more complete "picture", a more substantive overview of microwave-stimulated reduction. And whilst such reduction outcomes might be expected, such results provided confirmation of the capability of the microwave reduction process as applied to the obdurate refractory metal oxide minerals. Ultimately, in including the more sparsely examined oxides, a more comprehensive overview was realised.

8.1: Discussion of Results.

In planning and performing the microwave reduction work throughout the experimental programme, in essence, the author had effective control over the carriage and conduct of procedural experimentation but, with respect to analytical facilities, a greatly reduced level of control over the availability and execution of analytical operations (as might be expected for facilities of common-use). Because of the necessarily "pooled" availability of such common-use facilities – and despite considerable involvement with some analytical equipment – the timely access to, and use of analytical facilities was an ongoing management balance integrated with the more predictable routine of experimentally producing sound microwave reduction specimens – heterogeneous specimens which crucially included a proportion of transient phases.

Where necessary, reduction trials were deferred until analytical availability was assured, such to minimise the impact of time and exposure upon the likely instability or meta-stability of various intermediate reduction phases – despite dry storage under N_2. Although these intermediate phases were crucial in determining the process route, when (later in experimentation) it was better understood that the relevance of these intermediate phases did not directly impact upon the ***fact of reduction***, a less rigorous application of protection was afforded to "phase preservation". However, where an unacceptable period had elapsed, some experimental trials were repeated such to secure "at-quench integrity" of unstable and meta-stable phases in specimens *at the time of analyses*. Reduced control over certain dynamics of analytical procedure was a "price paid" for the unavoidable combination of heterogeneity with partial phase instability in specimens.

The heterogeneity and varying distribution of phases provided a wealth of information regarding reduction route and process mechanism, and the microwave plasma environment and thermochemical capacity. Although the degree of reduction at process termination was represented in reduction product heterogeneity, of itself, such reduction phase complexity was not a statement on the reduction potential of the system, nor of the state of reduction, nor of the crucial *fact of reduction*.

The phase complexity characterising this typical heterogeneity was exhibited generally throughout reduction product phases of different processing times and for all refractory metal minerals reduced, although, this was expressed differently in the case of ilmenite. The range and distribution of phases visually evident in microscopic studies was corroborated by EDS results and (where pursued) further substantiated in the range of phases either confirmed or "suspected" to be present by XRD studies. The XRD option of analysis was intended to be supportive of the more available SEM-generated options. However, although XRD option was partially carried-out (in anticipation of "analytical necessity" for other mineral reduction exercises, XRD was utilised and reported only for the carbothermic reduction exercises for commercially-pure anatase and the minesite-derived wodginite concentrate. These routine exercises proved to be time- and resource-consuming and did not necessarily reveal exhaustively complete analyses, although the acid-digestion alternative applied to the wodginite reduction product remnants did simplify the powder destined for diffraction, and thus simplify the XRD trace. The difficulties encountered in identifying minerals, or the presence of indeterminate phases, in XRD traces either by software-generated identification or by identification by manual database searches of JCPDS-ICDD powder diffraction files were addressed in relevant *Results* sections.

All in all, project experimentation did generate multi-faceted reduction product remnants that, to approach analytical "completeness", required an uncommon measure of analytical attention, each phase complex and varied rather than straightforward. Accordingly, as best could be, the programme of EDS and XRD analyses was managed in an accommodating but appropriate manner, analytical exactitude giving way to outcome-driven pragmatism with a view to providing meaningful "adequacy" in the reporting of results. This "pragmatism" recognising the ultimate importance of the "overall picture" of reduction outcomes rather than "insistence" upon the absolute detail and identity of minor and trace phases whose presence did not affect the *fact of reduction*. Also, along with identified phases, such "indeterminate compound types" were represented in all reduction products – particularly where some amorphous material may have been present along with micro-crystalline phases frozen from "melt" phase material of stoichiometry between solid solution and metallic compound. Alternatively, such "melt" phase may have been a mixture of solid-state-reduction

product (pre-existing the "quench") in a liquid of lower melting point phase(s). [Phase complexity at the micro-level is suggested in clearer, highest resolution micrographs and discussed in earlier sections.]

Condensed from the broad scope of this ambitious topic – and as a most suitable means of concluding this results discussion – the following generalised summary presents the essential facts supported where necessary by a minimum of relevant information. Further, it is apposite to separate the *specific* from the *general* in endeavouring to fairly represent the solid achievements of this project in the silhouette form of summarised observations drawn from those achievements. Accordingly, the general concluding observations of ***(II)*** to ***(VI)*** relate universal experimental observations; they link microwave-stimulated processing, refractory metal reduction and the conduct of project experimentation overall. Specific concluding observations recounted in ***(I)*** [as ***(I(i))*** to ***(I(viii))***] directly outline the experimental outcomes of the project's microwave-stimulated reduction goals; consequently, the following represent a summary-in-conclusion of those specific objectives (as provisionally put forward in Section **6.4**).

(I) **Under both carbothermic and metallothermic reduction options, the evolved microwave-stimulated reduction system was capable of the reduction to metal of those oxide minerals that comprise the suite of obdurate refractory metal minerals represented in the project.**

(I(i)) It was shown in early, formative experimentation that a wide range of commercially pure minerals and industrially important ore-derived concentrate minerals could be reduced under (the then developing technique of) microwave-stimulated carbothermic reduction, and that aluminothermic reduction could be gainfully substituted in particular cases where thermodynamic requirements commended such increased intensity of reductant capacity.

(I(ii)) Of the commercially prominent titania (TiO_2) minerals, commercially pure anatase could be reduced to metallic form using the microwave-stimulated carbothermic reduction method*. The corresponding aluminothermic reduction evidently rapidly reduced the refined anatase, however, the titanium thermite reduction product (with its excess liquid aluminium and access to a necessary minimum of oxygen from various sources) spontaneously re-oxidised in the newly acquired intensity of exothermal heat (energy) and the exercise appeared inconclusive. Aluminothermic reduction was modestly successful in reducing the un-refined, minesite-derived rutile and, ironically, reduction products were more metallic (than for the anatase) due to process spontaneity, excess aluminium aside. Whether as-received or mill-blended fine, native rutile did not respond favourably under carbothermic reduction. (Perhaps some thermal process of soaking or annealing of the native phase could alleviate this "nobility" in ex-mine rutile – otherwise, it does possess the dielectric dopant benefit derived from trace impurities.)

(I(iii)) Whilst carbothermic reduction was possible, under aluminothermic reduction the commercially important titano-ferruginous mineral ilmenite ($FeTiO_3$) was spontaneously reduced by the thermite reaction to yield a ferrotitanium alloy (including minor chromium by mineral impurity plus excess reductant aluminium). This highly successful result represents considerable possibilities for further study and development.

(I(iv)) The pure laboratory minerals ZrO_2 (zirconia, as baddeleyite) and HfO_2 (hafnia) were carbothermically reduced with modest success to yield inconclusive reduction products (non-oxide, metallic carbonitride phases or compounds). However, these oxides were each more successfully

* The "microwave-stimulated carbothermic reduction method" refers particularly to such carbonaceous reduction utilising the "microwave oven set-up method" as described in earlier sections. Where reduction was achieved using this method, then it might quite reasonably be presumed to also be possible using the microwave-stimulated vacuum reactor method, further comment of which appears noted in the *general* conclusion items. Also, in the context of the post reactor method, "aluminothermic" generally means "carbo-aluminothermic" as char was added to the aluminium reductant in the reactant blend to control re-oxidation (as elsewhere discussed).

reduced to metallic form[#] under microwave-stimulated aluminothermic reduction.

(I(v)) The commercially important minesite-derived mineral zircon ($SiZrO_4$) was carbothermically reduced with modest success to non-oxide phases, however, zircon was successfully reduced under microwave-stimulated aluminothermic reduction to minor "pure" metal plus metallic phases and compounds.

(I(vi)) The pure laboratory minerals Nb_2O_5 (niobia) and Ta_2O_5 (tantala) were carbothermically reduced under microwave-stimulation with substantial success yielding products in the range from metal through metallic carbonitride phases and compounds. [Because of this degree of reduction success, verification of aluminothermic route was not deemed necessary.]

(I(vii)) The commercially important minesite-derived mineral wodginite [$\{(Mn,Fe)Sn(Ta,Nb)\}_{16}O_{32}$] – a major mineral from which the two pure oxides Nb_2O_5 and Ta_2O_5 [above in *(I(vi))*] are won preceding their Kroll reduction to metal – was successfully reduced to complex metallic agglomerates of free tin metal, hardhead phases [$Sn_x(Mn,Fe)_y$] and tantalum(niobium) metal, carbonitride phases and compounds. The agglomerated reduction product held considerable propensity to be upgraded by process separation thence refined to desired pure forms. The aluminothermic route was also successfully employed to microwave reduce wodginite to yield a similar agglomerated metallic product (but for the minimal addition of extra slag phase bearing a separate Ta/Nb-morphology) – it was decided that this route presented separate "on-processing" benefits.

[#] "Metallic form" here implies a metallic range including the "pure" metal, through solid solution phases into the metallic compounds, specifically the metal carbides, nitrides and carbonitrides – the full range regarded as metallic in this project. For metallic phases, this compositional range was an unavoidable experimental outcome once the reactor option was sidelined for the more manageable microwave oven set-up method.

(I(viii)) As an obvious and complementary augmentation to the reduction programme, a brief exercise exposing the processing potential of the disproportionation (decomposition) of metal halides utilising an applied microwave field as energetic stimulus to break bonds between chemical species under irradiation. The revealing exercise suggested potential re-processing and co-processing strategies in refractory metal production and, importantly, could lead towards reductant-free reduction applications. This supplementary section of project work should be enthusiastically pursued either in its own right or in any future research extension.

In the experimental pursuit of these specific project goals, a residual category of general observations emerged as being representative of the broader experimental experience, inclusive especially of particular aspects of the microwave-stimulated thermochemical process. Being derived from "process" rather than "product", these supplementary observations, as and where appropriate, were common across the range of processing exercises and ought be examined at a more sophisticated level in future work. However, at this point in the present work, the observations spawned the following set of general conclusions.

(II) **Employing microwave irradiation as the sole externally imposed input energy source and reaction initiator/stimulant, a specifically designed and purpose-built, evacuable, atmosphere controlled reactor with quench-capability and having interactive and monitored control was established as an "ideal" reaction apparatus in application to the reduction of refractory metal and comparable minerals.**

Although observed over only a brief campaign, the limited evidence of preliminary trials using the evacuable microwave reactor established that such a system was eminently capable of the carbothermic reduction of target oxide minerals to yield metal products of good purity.

Despite the physico-chemical and procedural system difficulties inherent in developing and operating such a reactor, a microwave-stimulated evacuable reactor system remained a legitimate approach to the reduction tasks of this project – including those contemplated systems based upon other energy forms and alternative energy-delivery procedures. [Also, of the various system options considered when devising the experimental programme, an enclosed, system-controlled microwave reactor was adjudged the most appropriate research option in pursuing a new reduction process for thermodynamically stable minerals, including the refractory metal minerals of interest. Further, the microwave-stimulated non-equilibrium plasma process could best be contained and controlled within such a reactor chamber environment. Accordingly, those reactor operational problems encountered in this project ought be overcome such that a contained microwave reactor cant be pursued in any research extension.]

(III) **Given suitable reaction-environmental conditions in any system, the microwave-stimulate reduction method will produce metal of good purity.**

Pursuant to *(II)* above, it is reasonable to presume that those recovered metallic reduction products of the adopted "microwave oven set-up" method – whose "metallic" categorisation ranged from the pure metal, through the solid solution phases and into the ambit of metallic compounds – would have been retained as pure metal (or dilute solid solution) had the reduction been carried-out in an operational controlled-atmosphere microwave reactor system.

(IV) **Where thermodynamically necessary or metallurgically desirable, obdurate refractory metal minerals can be reduced to metal by a microwave-stimulated metallothermic method.**

Adjunct to the essential carbothermic reduction processes, where the metallothermic reduction option was employed throughout this project, then, out of experimental expediency, the aluminothermic route was engaged to demonstrate a stronger alternative-reductant route to that of the carbothermic. And further, *a priori*, it was presumed that other metallothermic alternatives could sufficiently replicate the aluminothermic route. Along with aluminium, and in particular here, the Kroll process' magnesium and the Hunter process' sodium were of automatic interest whilst potassium, calcium and manganese were of possible interest for reduction of chloride and other halide systems, whereas calcium, magnesium, sodium and silicon were of possible interest to replace aluminium in the direct metallothermic reduction of oxide systems.

It was evident from the last section of experimentation, Section **7.5**, that a looped continuous extractive system was operationally plausible. This system arising from the disproportionation of common halite (NaCl) and leading to both Hunter process sodothermic reduction of a target metal chloride ($TiCl_4$, $ZrCl_4$, *et cetera*) plus the chlorination of a target metal oxide (TiO_2 , ZrO_2 , *et cetera*) to yield anew the metal chloride ($TiCl_4$, $ZrCl_4$, *et cetera*). Also, other comparable integrated looped systems are conceivable – including a similar operation utilising (as a starting resource) the geological mineral carnallite ($KMgCl_3.6H_2O$).

(V) **The non-equilibrium plasma environment created within systems under microwave-stimulation – with its attendant distinctive high populations of energetic, activated and reaction-compatible particle species – proved to be amply capable of the reduction of refractory metal minerals – minerals which, in general, are physically and chemically obdurate and, wherein, exhibit commensurately high thermal stability.**

Irrespective of process design, reaction system configuration or reductant choice (including reaction route), the fundamental process described herein as a microwave-stimulated plasma reduction process, and

being a non-equilibrium thermochemical process, was shown to be capable of the reduction of thermodynamically stable refractory metal (and other) oxides. In the prevailing plasma chemistry of such systems, the high populations of energetic, chemically activated particles provided a reduction environment quite atypical of the chemistry exhibited in a "reactant equivalent" conventional system (being typically "at or near" equilibrium and exhibiting negligible excitation/ionisation). Also, such plasma environment ensuring elevated "bulk temperature" in the reactant-mass-come-reduction-product so allowing melt-consolidation of high melting point metals. In the absence of a reductant, microwave irradiation could be employed as activation stimulation to break chemical bonds in matter. Such was comprehensively shown in the microwave-stimulated decomposition of metal halides to yield the metal plus the halogen (as ion, gas or vapour).

In supplement to the microwave process, it is hypothesised that a "delayed" energetic extension of the prevailing non-equilibrium thermochemistry towards or into the equilibrium realm of thermal plasma could provide a plausible post metallurgical-chemistry extension to thermally augment or physically complete some material processing applications. As has been noted elsewhere in this work, some facets of materials processing – such as melt consolidation in specimens – benefited from prolonged exposure to the intensity of the plasma environment. Perversely, however, this decided physical benefit proved contrary to the central tenet of reductive processing as it was accompanied by such joint chemical deficits as "re-oxidation" and the retreat from purity in reduction product metal – and this anomaly manifested generally across ventured processing applications.

(VI) **It was evident from experimentation generally that both anticipated and realised techniques of microwave-stimulated materials processing could be advantageously employed across a range of thermophysical and thermochemical applications.**

Although not of core consequence to this project, concurrent with their description, some aspects of microwave-stimulated processing were variously discussed in the course of presenting this document. And whilst not directly related to mineral reduction or extractive applications, some postulated applications in the broader fields of materials processing and synthesis, beneficiation, combustion synthesis, sintering and melt processing were identified – and discussion is left with their original mention. These applications are essentially not new, but it is suggested that significant benefits reside with the adaptation to their process route of systems delivering microwave energy to stimulate processing, and to impart inherent benefits of microwave processing (as widely reported in the literature). Whilst such applications may fall outside the purview of this project, being of related metallurgical interest or otherwise being unavoidably compelling in their promise, they need not necessarily be excluded from future research extensions of an "extractive and related processing" nature.

In a project whose objectives were straightforward but whose experimental outcomes were not so clearly "cut and dried", the above summary is an endeavour to best provide a broad presentation of all reduction-related matters pertinent to the project. Although of necessity abbreviated, the overview ranges across those procedural and product items requiring mention, between process variations, process metallurgy and associated matters to reduction product idiosyncrasies and further possibilities for microwave processes.

8.2: Discussion of Supplementary Matters Relevant to Microwave Processing and Refractory Metal Production.

From the outset of the programme of experimentation it was determined that a *sufficient* level of experimental application and analytical deliberation would be paid in addressing project tasks. However, because of the novel, almost "open-ended" nature of the subject of microwave reduction, this "sufficiency" would ultimately be determined

by what was experimentally possible and the constraints of material and analytical resources and allocated time. For the experimentation of this project, neither was the experimental process as predictable nor its reduction product specimens and their analyses as routine as for most metallurgical investigations. Also, as discussed elsewhere, the constraints of time plus concept and development extensiveness ruled-out any pursuit of *process optimisation* – that key tenet of investigation bridging research and development stages of endeavour, and one ultimately delineating output efficiency, or productivity. Broached in Section **7**, process optimisation was juxtaposed with the constraints of procedural involvedness, allocated time and the limitation of resources commitment to experimental equipment and system development. Ultimately, process optimisation succumbed to the demands imposed by the broadening of scope of "included" refractory metals and the shift in project rationale to "reasonable and achievable reduction accomplishment" for such stable minerals. Such "shift in rationale" coincided with the re-assessment that accompanied the necessary abandonment of the microwave reactor (with its promise of reduction potential with system development) for the simple but practicable oven set-up method – an un-sophisticated system, but one that generated reproducible results of appropriate quality. In practical terms, this shift to the oven set-up method provided predictability to the experimental process and continuity across reduction product specimens, despite the tendency towards over-processing of reduced metallic phases.

Although process optimisation was not pursued as such, some sense of optimal processing time was achieved under the experimental method used. However, the relevance of such "optimal" processing time was compromised between "clean" reduction to metal and over-processing of this metal into re-oxidisation "carbonitride" phases. Some attempt to subvert this tendency was made in the carbothermic reduction of anatase series of Section **7.2.1.2** where sites on "newly-reduced metal" were sought for EDS spot acquisitions. The "purity" of reduced metal for the carbothermic anatase series is plotted in Figure **{7.2.1.2}1** and the trend shows Ti-metal purity increasing with increasing processing time, tantamount to increasing process "temperature". Nonetheless, neither "optimal" nor "optimisation" ought be conceded too much recognition for a batch process of such small scale, and further up-scaling development of process parameters is required before such a notion becomes openly sensible.

Acknowledging that this "search for newly-reduced metal sites for EDS acquisitions" approach was not adopted for subsequent reduction exercises (**7.2.2** to **7.4.4**), in hindsight, the anatase results of Section **7.2.1** do verify that good purity metal can be attained by microwave-stimulated reduction under desirable processing conditions. Purity in newly reduced Ti-metal increased with ongoing processing (time and temperature) and this trend suggested that, under the conditions at which a pilot or small commercial operation might proceed (and in more controlled atmosphere), quite good metal purity should be expected for microwave reduction of anatase. Also, consideration of the overall reduction results of microwave processing suggest that a "next stage" of experimentation using an oven set-up equivalent method might adopt a magnitude shift up into the 100g to 200g range of reactant charge size (a nominal five-fold to eight-fold increase on the present experimental charges). Such an increase in charge size would produce reduction product specimens large enough to approach phase homogeneity, or at least provide adequate material for parallel arc-melt specimen studies, and avert the need of "consolidation" by over-processing. This magnitude step-up would suitably precede a later move to "pilot scale" output, one which might only require an up-sizing of similar magnitude. Of course, similar up-scale stages might be considered for any future development of the microwave reactor concept. Once a workable configuration can be proven, ancillary equipment servicing such a "next generation" microwave reactor could be sufficient to service the various up-scale versions to pilot plant stage. Operationally, the reactor versions should be "process-flexible" to accommodate a range of experimental contingencies, thereby preserving interim experimental outcomes along with reactor integrity at times of equipment failure or other procedural misadventure.

The inclusion in the refractory metal minerals examined in this project of impure, or un-refined, minesite-derived mineral concentrates, minerals of prominence in Australian exports, was a decision predicated upon prospects that might emerge from such a venture, an option taken with "real" minerals. Historically, the Group **4** element minerals rutile, ilmenite and zircon of are recovered from mineral sands deposits and separated in the same mineral processing stream along with other important minerals (such as xenotime and monazite). Representing the Group **5** elements, the complex

tantalite-type mineral wodginite is mined in a surface-mining operation and, like the other three native minerals, is only minimally value-add up-graded before export. Nominally, Australia is the largest nett producer and exporter of the "equivalent" oxides TiO_2 , ZrO_2 , HfO_2 and Ta_2O_5 and an important exporter of Nb_2O_5 – a rather dubious honour given the total value-add conceded. Nevertheless, these five single oxide minerals (in "pure" forms) were added to the four root minerals to convene the experimental suite of minerals investigated in the experimental programme. And, further expanding the experimental range investigated, importantly, the reduction trials were conducted by the carbothermic route for all minerals, and by the carbo-aluminothermic route for most minerals, in investigating the potential of microwave-stimulated non-equilibrium plasma environments in pursuit of these reduction goals; and particularly, the general confirmation of the *fact of reduction* of such stable oxides. Despite the unusual breadth of experimental scope represented in this complementary range of resource minerals, the outcomes of experimentation delivered a definite and confluent spread of reduction results that was neither fully comprehended nor earnestly anticipated at the outset of the project. Once the fundamental over-processing re-oxidation of the "carbonitride categories" is figuratively "stripped" from reduction product phases, the essential *fact of reduction* reveals plainly successful reduction outcomes across the experimental suite.

By volume and by kind, most extractively processed ore minerals are oxidic minerals; the notable exceptions (which are significant in Australia) are the sulphide ores of zinc, lead, copper and nickel. Generating "customarily" more-innocuous by-products, oxide minerals are preferred for extraction processing routes; despite being energy intensive, these routes are direct and uncomplicated by reduction stage interruptions; (unlike the intermediate products (matte, speiss, *et cetera*) of sulphides and similar) their carbothermic by-products, principally CO_2 and CO, have historically been disposed-of by toll-free discharge into the atmosphere – but this abandon is no longer cost free. As with the operations of the broad metallurgical industry producing the common metals, the relatively much smaller operations producing the refractory metals all depend upon a refined grade of the refractory metal oxide as starting material for extractive reduction operations (and recalling that refining precedes extraction for

refractory metal production). These operations producing today's commercial grades of refractory metals typically proceed through carbon-assisted halidation of the pure oxide – or refining distillation of the complex halide if the oxide was not pure – thence metallothermic reduction of the pure metal halide. Consequently, in producing near-pure commercial grades of refractory metal, the industry is indirectly dependent upon refined oxides of good to high purity.

These rudiments are more evident when production is considered in the historical context. Moreover, the "historical" is irrevocably interwoven with the "profitable". Consequently, because of operational marginalities throughout the extractive metallurgy industry – and where such alternative was available – a high dependence has ultimately been placed upon extractive routes utilising carbothermic reduction of oxide minerals to profitably produce the target metal. Those more process-intensive operations directly reducing sulphides, arsenides, *et cetera* have always faced a heavy cost burden (above that of oxide reduction). This pronounced preference has arisen out of industry's need to comply with both the obligations of environmental restrictions (including statutory laws) and the realities of total processing cost – again, where optionally available, the oxide route has tended to minimise these factors. This is as true for hydrometallurgical or chemical means as it is for pyrometallurgical means. The straight reduction of metal sulphides, phosphides and phosphates, the halides, and especially the arsenides, stibnides, selenides, tellurides, and certain others – plus the salts (RSO_3, RSO_4, *et cetera*) corresponding to these minerals – all produce cost-intensive by-products. Such by-products may be highly corrosive (such as acids), highly toxic or otherwise noxious and, in general, as liquids or gases are costly and difficult to dispose-of, isolate and monitor, re-process or other treatment, conversion or management option. [Note that, in refractory metal production, the reduction of the metal halide will ultimately lead to re-cycling of the halogen, thus circumventing the contamination problem.]

However, recent worldwide public concern regarding global warming and its causes has placed new and urgent demands upon consumers (at all economic levels and production stages, direct and indirect) of all forms of carbon to conform to overdue compliance structures involving costs imposed for "*projected* pollution". Such "compliance" equates carbon consumption with a level of generation of the alleged

greenhouse gases. Representing a large proportion of these greenhouse gases, CO and CO_2 are becoming increasingly prominent in the atmosphere – particularly when the rate of annual world "volume produced" is taken into consideration alongside their accumulating attributed effects. (Once CO has escaped the environment of the smoke stack it overwhelmingly oxidises to CO_2 under the prevailing atmospheric equilibrium.)

Also, because of this "overdue" nature of the imposition of compliance costs, the actual "carbon cost" structure through from producer to consumer is still rather uncertain (although, under the certainty of "death and taxes" lore, the end consumer will ultimately pay the accumulated carbon tax from each stage of economic activity – as assessed and passed-on). Assessment and oversight of carbon consumption, carbon-based pollution and compliance concerns have become issues of acute political sensitivity and, currently, governments worldwide are devising suitable means of regulation – it seems that a befitting formulation may be by carbon tax, cap-in-trade or by other emissions trading scheme. Consequently, in terms of carbon cost resolution and implementation into public policy, the evolving carbon cost structure for carbothermic and other carbon-intensive operations has some policy-expanse to negotiate before industry can settle into commercial stability. Until then, the costing of carbon intensive operations will remain ambiguous and the future of such operations quite uncertain; alternative production routes will be diligently re-assessed. It is generally acknowledged that the two world industry sectors which will consequently be most affected by this "pricing carbon pollution into production costs structure" are the electricity production sector (nominally, fossil fuel fired power generation) and the broad metallurgical industries, particularly with respect to the extractive metallurgy sector of those individual industries.

Increasingly, because oxide minerals are reduced primarily using carbon as sole reductant, it must be acknowledged that extractive routes to metal by means of those non-oxide options that *might* minimise either carbon usage or carbonaceous by-products have to be re-visited. Auspiciously – and acknowledging observations in early project work regarding the "reducing" behaviour of sulphides under microwave irradiation – the pertinent and revealing late experimental work conducted on halide decomposition showed every prospect of representing a pioneering technique in an alternative processing route. Although this initiative was not experimentally pursued beyond a

preliminary stage of enquiry (initially intended to substantiate certain erstwhile observations regarding the breaking of otherwise tightly-held chemical bonds), the phenomenon of disproportionation embodied in the experimental outcomes represents an effective alternative route to the conventional processing routes. *Per se*, the use of high-energy methods across a range of decomposition processes is not new, however, it would be industrially novel to utilise microwave energy through the very efficient means of an applied microwave field to break the chemical bonds in metal halides. Of course, such applications assume that nett energy increase sourced from coal-fired "power" generation is more than matched by the nett energy savings of adopting the application.

Indeed, from the perspective of the metal, disproportionation of metal halides is analogous to their reduction by the usual chemical means of a reductant as co-reactant. (Here the "charges" providing the activation energy to break chemical bonds is provided by an applied field rather than applied heat: the energy (quanta) required is equivalent, the source is different.) Consequently, the carbothermic and carbo-aluminothermic reduction pyro-chemistry employed for the earlier microwave-stimulated plasma routes of this project might well be reviewed and/or revised in light of this observation. Also, as was previously observed for very-high energy systems[58], oxides can be effectively decomposed and, *system permitting* in an intensive process, the product metal quickly frozen to avoid re-oxidation. [A *thermal* plasma process may be more applicable to such a system.] It is also feasible that a hybrid system between metallurgical routes could be contemplated (pyrometallurgical leading to hydrometallurgical, for example) or, very likely, that the energetic gaseous halogen by-product of disproportionation could be returned directly to a halidation processing stage of the next batch of raw oxide mineral, and so on.

Furthermore, and whilst *neither* qualitatively *nor* quantitatively estimated, it is quite apparent to this author that for systems under carbothermic reduction – all consumed carbon included – the all-in nominal quantity of carbon required for the experimental microwave-stimulated reduction systems utilised throughout this project in reducing mineral to refractory metal, and those proposed in this project, would be an order of magnitude less than for the long established conventional routes. But, being

deemed of only indirect relevance to the applied science of this project, and consequently outside project scope, no specific claim is made regarding carbon consumption comparisons.

9

TECHNOLOGICAL OVERVIEW and RECOMMENDATIONS.

"A powerful idea communicates some of its power to the man who contradicts it."

Marcel Proust -
Remembrance of Things Past, 1919.

"Look for the ridiculous in everything and you will find it."

Jules Renard - *Journal*, 1890.

9: TECHNOLOGICAL OVERVIEW AND RECOMMENDATIONS.

Any concise outline of the technology that both defined and limited this project should not be too plainly portrayed for fear of misrepresentation of essential aspects of detail or fact of microwave processes; and similar caution should be borne-out for recommendations that might flow from such endeavours. A fundamental review of the overall technology and its function plus the relevance of microwave-stimulated thermochemistry as applied to the extractive metallurgical processes central in this project is presented in overview as Section **9.1**. The overview presents core reasons why non-equilibrium plasmas generated in systems under microwave irradiation impart processing advantages not available in comparable plasma systems and in those systems being processed under conditions of conventional thermochemistry. [The conventional thermochemistry of regular pyrometallurgy is characterised by its dependence upon combustion processes* for both energy delivery and requisite chemistry – in effect, combustion sustaining species excitation without species ionisation or with negligible incidental ionisation.] The overview proffers how and where microwave-derived processes present distinct process advantages and deliver different and/or better outcomes over other plasma processes and over the corresponding or comparable conventional system process. These aspects of process advantage are then marshalled in support of a limited range of recommendations proposed and discussed in the later Section **9.2**. This selected range of recommended applications largely follows the theme of process-metallurgical applications and has been limited because so much is presented in the broad literature regarding each microwave processing and plasma processing, and the extension of microwave processes into non-equilibrium plasma applications.

---

* A combustion flame implies chemical reaction and change (such as $A + B \rightarrow AB$, or $AB + C \rightarrow AC + B$, *et cetera*). Whilst such reactions can and do occur in plasma, conversely, such chemical change is not an automatic pre-requisite of plasma processing. Consider the ionisation possibility $A \rightarrow A^+ + e^-$ and the complementary re-combination possibility $A^+ + e^- \rightarrow A$. Here, despite the presence of ionised species, no nominal chemical *change* has taken place at any stage, although (for the microwave case), energy has been transmitted from an external source via the applied field into the system. Such ionisation events are a defining characteristic of plasma environments – or "plasma flames" in the instance of plasma torch devices. Of course, conducted within the ionised environment, the *intended* process chemistry is a separate matter – in effect, this plasma chemistry occurs independently to the *sustenance* of the plasma flame, although it will visibly affect its nature.

Section 9

9.1: Technological Overview: Advantages of the Microwave-Stimulated System.

As "pure scientific procedure", project experimentation may have conveyed the general sense of being unrefined in concept, conduct and outcome. Although, despite any reserve in the interpretation of such, the undeniable broader success of experimental outcomes plainly vindicated the simplicity of experimental practice as implemented throughout the project. Whereat, key to process outcomes, the *microwave-stimulated thermochemistry* of reduction processes – which proved to be so essential to experimental viability – was necessarily contained within experimental procedure and was integral to experimental process completion. In conjunction with known (published) advantages of plasma processing, the processes of microwave-stimulated thermochemistry here require such address and review as to consign the accomplishments of these realised experimental successes to record, so to recommend for future applications a projected range of microwave processing possibilities.

Established throughout the diverse literature of plasmas and their extensive applications in processing, and in the publicly declared domain of the more restricted "commercial know-how", the process advantages are embraced relevant to the experimental work herein and in context of their integrated, configured parts and the disciplines governing these. Controlling various aspects of processing, these "governing disciplines" include the ionisation physics and chemistry of plasmas, non-equilibrium thermochemistry in microwave-stimulated systems, and the encompassing principles of extractive process metallurgy. This process metallurgy incorporates the reduction of minerals, process reactions and mass transfer within phases and across interfaces of multi-phase environments, insulation and thermal protection in systems under processing, plasma-chemical environments, atmospheric protection and system evacuation, plus quenching and product phase possibilities.

To varying degrees of detail, the essence of the following material has been presented in earlier sections, however, *facets are selectively re-compiled here to more succinctly emphasise those salient aspects and their impact upon promising elements of the project.* Also, what benefits these aspects might convey to prospective applications of a related nature as identified elsewhere and for future development in the recommendations of Section **9.2**. [Other more speculative development possibilities

from indirectly related fields may be mentioned, but are not explicitly promoted because of the surfeit of project possibilities (over a wide range of fields) available to be advanced and exploited.] The following is presented with a view towards providing understanding of the benefits of the microwave-stimulated plasma system as it was applied to metallurgical processing in this project. In particular, as microwave-stimulated plasma processing was applied to the reduction of physico-chemically obdurate oxide resource minerals – be they ore minerals or refined minerals – with a view to extending and adapting the technology to industrial-scale extractive production operations.

In revisiting the core plasma fundamentals, it is necessary to re-establish the crucial processing essentials in a manner most meaningful within this overview. Consequently, the following limited but sufficient discussion unavoidably ranges *across and between* aspects of the various defining characteristics prevailing in microwave-stimulated plasma environments and which are central to the reduction processes as identified.

In process-metallurgy and comparable processes, whether operating in mixed, plug or counter current flow regime and at any degree of configurational complexity, process chemistry proceeds on a basis governed by the prevailing driving force. Whilst (promptly enough) the applied energy plus evolved exothermal energy will cumulatively assume that governing role, in conventional processes the initial driving force for chemical (and physical) change is provided by the energy represented by the temperature difference (ΔT) between feed components upon initial contact – the feed components mixing from the point the reactant streams enter the reactor or furnace system. The heat transfer supplied by this initial contacting and temperature difference may be an intentional if not necessary element of process design. [When applied to the maintenance of "system energy", energy conservation measures are mandatory in operations of high energy consumption.] Whereat, however significant the operational temperature range both in terms of outright process temperatures and as temperature difference, chemical processes take place in such systems of conventional extractive pyrometallurgy in which the outright temperature difference between reacting

components is magnitudinally insubstantial in comparison with the corresponding "temperature" difference between reacting components (or species) for corresponding extractive systems of *plasma* pyrometallurgy.

For low temperature or "cold" plasmas – plasmas operating under thermal non-equilibrium – the temperature difference at the reaction interface between chemically active "heavy" plasma particles and the reactant solid may attain one or more orders of magnitude. Such activated particle species deliver their own activation energy to the reaction site, or at a converted interface, this energy driving their own diffusion to a reaction site. By comparison, the very light activated particles, such as free electrons (e^-), may attain several magnitudes more in outright particle "temperature". Their high rates of extinction and re-generation deliver energy into the system but, at any instant, their collective impact upon the detectable "bulk" temperature of the system is negligible. In high temperature or "thermal" (equilibrium) plasmas the temperature of reaction components is of a nominally higher order of magnitude with activated plasma particles reaching into the millions of kelvin. However, the impact of such activated particles in equilibrium plasma is magnitudes lower than those in non-equilibrium plasmas, their rate of extinction and re-generation is higher – their mean free path shorter in the typically higher pressure. To attempt (in the name of comparative completeness) to address the numerous plasma types derived under the very many possible *system conditions* (thermal range and profile, sheath thickness, evacuation rate, contamination sources, stability of plasma, *et cetera*) and *environments* (species present and possible, system pressure and stability, *et cetera*) and *generation methods* so to compare and contrast with the microwave-stimulated plasma of this project would be incomprehensibly complex. Also, perversely, such a hollow exercise would perhaps be pointless because the different established plasma forms have long been recognised and utilised for specialised, niche applications – but their characteristics do not necessarily recommend their utility for reduction metallurgy. For the sake of clarity-of-purpose in this overview, it is best that descriptions here remain with the plasma type, system conditions and environment(s) encountered through the project's programme of experimentation. Consequently, discussion here will remain with the atmospheric pressure non-equilibrium plasma processes such as typified the microwave-stimulated

reduction pyrometallurgy of this project and, presumably, to any derived extension which might come from the work.

The high "temperature" difference prevailing in plasma systems (above those of conventional systems) has the attendant effect of exhibiting correspondingly higher thermodynamic driving force between the ionised or otherwise activated particle species and the targeted reactant solids of blend-components. It is apposite to reiterate that it is *chemical* thermodynamics – rather more than the physical (or mechanical) thermodynamics – which is pertinent in any consideration of the microwave-stimulated thermochemistry of this project. We may safely assume that the chemical kinetics is also accentuated by the greater available system energy, typified in the higher particle "temperatures" at the reaction site. The presence of both free radicals and ionised particles in the reaction environment dictate that more than one reaction mechanism will control the kinetic model, and the relative rate(s) will vary with conditions. Also important is that, because of accentuated rates of diffusion in both liquid and solid phases, and the already high rates of creation and extinction of excited, ionised and recombined species plus free electron, photons, *et cetera*, in the plasma volume, there is a beneficial predominance of process reactions at or near the plasma-solid or plasma-liquid interface of the reducing (oxide) mineral. [It should briefly be noted that the plasmas employed in the project were partial plasmas, with the degree of ionisation (activation) increasing with increasing system energy. Such partial plasmas are at the lowest, furthest extremity of the ionisation band to that of fully ionised plasma, that almost theoretical entity for which all particles in the matter are in the highest ionised state; in reality, such "matter" does not exist above helium – as in the thermonuclear core of our Sun.]

Non-equilibrium plasmas are commonly divided into groups distinguished by containment geometry, system pressure and plasma sheath characteristics, and the mechanism of their generation. The five discharge types most commonly associated with non-equilibrium plasma are (*i*) glow discharge, (*ii*) corona discharge, (*iii*) silent discharge, (*iv*) RF discharge, and (*v*) microwave discharge. [The temporal behaviour, pressure range of operation, appearance and trends within and between these is shown in Figure **{4.4}2**.] However, it is the microwave discharge and, specifically, the range of

conditions within which it is generated that set it apart as most suitable for application to pyrometallurgical reduction processing.

In plasma pyrometallurgy, even for exothermic applications where there may exist sufficient available energy, it is the electrical discharge which supplies the initiating activation energy for reactions in plasma chemistry, and in non-equilibrium plasmas the prevalent free electrons very largely supply this energy. As initial activated particles, free electrons are present at the initiation of plasma chemistry. Driven by the electrical component of the applied field, the energy of each free electron is augmented until an inelastic encounter with another particle whereby (*i*) the electron is "extinguished" and becomes bound to the recipient particle (ion, atom or molecule), and (*ii*) the recipient's excitation threshold is met (producing an excited particle) or its ionisation threshold is met (producing an ionised particle, a recombined particle or fragment species, recipient dependent). (In raising the energy state of the recipient particle, the total *kinetic* energy in the system is lowered.) Intermittently along the free electron's mean free path it may experience an elastic encounter with another particle, a deflection, in which the electron merely transfers *some* kinetic energy to the recipient particle without that particle reaching its excitation (or ionisation) threshold, the deflected free electron continuing on its free path, resuming its energetic amplification from the applied field. Hitherto, microwave plasmas are far from thermodynamic equilibrium as, under microwave irradiation – across the range of microwave wavelengths – only the lightest particles, free electrons (predominantly), follow the oscillations of the applied electromagnetic field[80]. This initial energy inequity between particle species drives the notional quasi-equilibrium of the system rapidly into system non-equilibrium and the inequity between species manifests throughout the particle population. The fundamental concepts of elastic and inelastic particle collisions, and the expressions of state of excitation/relaxation and ionisation/recombination – including the associated range of possible particle species and their physico-chemical proclivities – are the essence of microwave-stimulated environments and associated processing.

Microwave-stimulated plasmas can be operated over a wide pressure range up to one atmosphere in large-volume non-equilibrium discharges of consistent homogeneity[80] rendering this means suitable for a wider range of processing

applications than are addressed in this project. The processing effectiveness of non-equilibrium plasmas arrises from the high population and reactivity of the chemically active species existing in the discharge *rather than* the total energy of the plasma made available to the process application [80, 90]. Under constant stimulation, such populations of activated species remain relatively constant as re-combined particles are replaced by newly re-generated particles in an ongoing process of replenishment – the population varied only by variations in system energy, especially applied energy. [Because of their high energy densities, thermal (or equilibrium) plasmas are typically employed for thermally orientated applications (such as heating and melting), less frequently are they employed because of the reactivity at extremely high temperatures attained by their smaller population of activated particles.] It should be noted that, whilst non-equilibrium plasmas are also known as cold plasmas, or low temperature plasmas, the plasma "temperatures" reached in the experimental pyrometallurgical trials of this project ranged well up toward the lower end of the recognised thermal plasma range. This included both the mean bulk temperature in the charge (which, it was acknowledged, commonly exceeded 2,000°C) and the presumed "temperatures" of ion particles, which may have been double the nominal bulk temperature (and for free electrons would have soared into the tens of thousands of kelvin (K) – or several electron volts (eV).

An essential condition in plasmas is the uncertain notion of "temperature". In conventional thermodynamics – and accordingly being in equilibrium – temperature is very closely equivalent to the thermal energy in the system ($T \equiv E_{thermal} \cong E_{total}$). However, in plasmas where particle energies, or "temperatures", vary and have components of energy related to electron spin, or to translational energy, plus rotational and vibrational energies which exist whilst the particle remains above ground state; these energies revert, or decompose, to thermal energy when relevant relaxation takes place. These energies are characteristic of system *non*-equilibrium, and differences increase with increasing non-equilibrium – a fact self-consistent within definition, that is, energy non-equivalence between particles being tantamount to system non-equilibrium. So, discrete from the internal energy of chemical processes, for systems in non-equilibrium, the "temperature" equivalent of any particle is represented by the sum of its energies:

$$\text{"T"} \cong E_{thermal} \neq E_{total} = \{E_{thermal} + E_{translational} + E_{rotational} + E_{vibrational} + \ldots\ldots\}$$

{9.1}1

And the system energy – the sum of particle energies (including the substantial majority at an elevated ground state which do not possess the ionisation quotients):

$$\sum E_{system} \equiv \sum E_{total} = \{\sum E_{thermal} + \sum E_{translational} + \sum E_{rotational} + \sum E_{vibrational} + \ldots\ldots\}$$

{9.1}2

Whereas these minimal expressions are intended to be plainly symbolic of a system for which, under ongoing stimulation and with increasing thermodynamic non-equilibrium, the populations of particles inevitably exhibit increasing energy non-equivalence between both similar species and disparate species; the equations are inadequate in any definitive or quantitative sense. The point made evident by their inclusion above being that, at any instant along the processing time line, if "temperature" is a measure of the expressed thermal energy (heat), then it is not a sufficient measure of total available energy for systems in states of advanced non-equilibrium, as is typical for systems under microwave-stimulated thermochemistry. However, if irradiation is *terminated* in a system under the stimulation of applied microwave energy then the lesser intra-particle "energies of state" transmute and report as thermal energy (heat), and this thermal energy can then be conventionally measured as temperature. Should temperature measurement be imposed, then such process interruptions would be inconvenient in real operations, and impractical in the context of reaction continuity for ongoing processes.

In everyday terms, moreover, the hearsay contention amongst early experimentalists working in microwave processing that predictable physical and chemical events (such as melting points and the activation of specific reactions) "seemed to happen at lower temperatures than expected when processing under microwave irradiation" may inadvertently have been founded upon an unrecognised experimental "actuality". Also, building upon this "anecdotal keystone", and although solely a subjective observation, evidence witnessed in his work by the author suggested that microwave heated materials seemed to hold their temperature (that is, from a given

temperature, had a flatter, slower cooling curve) more so than conventionally heated materials. The rather problematical proviso here was that both equal specimens were heated to apparently equivalent temperatures – this equivalence allowing for latent heat phenomena (in liquids), the microwave field interference step-off, *et cetera*. [Having little impact upon reduction, *per se*, the temperature anomaly was variously explored on opportune occasions determined by the providence of procedural obligation rather than intentional experimental trial. As a controlled, scientifically conducted procedure, experimental confirmation of such an apparently simple task proved always to be quite a complex undertaking. Investigation of (*i*) the temperature anomaly, (*ii*) a routine method for measurement of "true temperature" (or energy-equivalence) in microwave processes, and (*iii*) a practicable definition of "temperature in respect of total system energy and available system energy" were not rigorously pursued as such exercises were *not* core aims of project experimentation. Nevertheless, in future work the confluence of plasma theory and its pure science for such basic phenomena should be examined as an adjunction to the central applied strands of research pre-empting industrial processing applications.]

Outside "the conventional wisdom" regarding species stabilities, a relevant aspect during processing throughout the project was the evident stability-into-higher-temperatures of CO-based diatomic particles such as ions, re-combined and excited molecules (CO^{-}, CO^{+}, CO^{*}, *et cetera)*, species that played such a crucial reduction role in processing. The accumulated experimental evidence suggests that diatomic [CO] particles were stable up into the *very* high temperature stages of reduction processing where, nominally, it is understood that most diatomic particles break down into monatomic particles to remain stable in the plasma. According to the literature, molecular nitrogen (N_2-based) particle species broke-down into two monatomic N-based particle species (N, N^{+}, N^{2+}, N^{-}, *et cetera*) remaining functionally active, and the CO-based diatomic ions (although, in this study, their immediate destiny remained uncertain) either re-combined to CO (preceding further ionisation) or degenerated reversibly into short-lived monatomic particles, which played no immediate part in process chemistry [58, 90]. This inferred decline in active CO-based particles in the *extremely* high thermal conditions of the latter-stages of processing could account for the apparent increasing dominance in exposed and latter regions of bronze "nitride"

phases. This trend was observed universally* across the relevant ranges of specimens for regions in the advanced stages of processing. Such bronze phases being more dominated by "nitride" than "carbide" in the compound range of carbonitride products (for the refractory metals investigated). Significantly, the monatomic nitrogen ions remain both chemically and re-generatively active – this despite [CO] species being of greater nominal reactivity than [N_2] or [N] species sets when present in a conducive, reducing environment.

When conducting any chemical processing operation in a plasma environment, be it non-equilibrium plasma or otherwise, two fundamental and sufficient operational elements must be satisfied. Firstly, there must exist the requisite *energy* necessary for initiating and sustaining a stable and process-sufficient plasma (in a purpose-configured system providing containment). And, secondly, in sufficient fulfilment of ongoing *process* requirements, there must exist the constituent capacity to generate the required activated reactant species so to satisfy the essential process chemistry. Conditional in this process component is the presumption that inter-species contacting of reactant species is facilitated and sufficient to sustain the chemical reaction processes in the plasma chemistry.

Further, it is fitting to re-affirm that each of the relevant non-equilibrium plasmas of the project was partial plasma – a gaseous mixture [upon processing, air $\rightarrow$ an O_2-depleted, (CO + CO_2)-enriched mixture] supporting populations of excited atoms and molecules, ionised atoms and molecules, re-combined atoms and molecules, miscellaneous fragments, free electrons and photons – all of which could exist at different discrete energies over imperceptibly short periods before returning to ground state (or an otherwise re-combined state with new, non-ground-state energy). In terms of reaction chemistry, these "activated" particles are the "stuff" of the plasma, they provide the chemically reactive species to each reaction and they provide the requisite activation energy to the plasma chemistry environment to facilitate reactions in proceeding to completion. [Of course, the other available internal energy source is the

* This "universality" of observed "late synthesis of predominantly-bronze phases" was experimentally contained in reduction product phases of sufficient processing exposure and limited to the refractory metals titanium, niobium and tantalum. Due to their reduction "nobility", the consequently minor proportions of truly metallic reduction product phases derived from zirconium and hafnium minerals did not allow sufficient certainty in committing these products to this "nitride dominated phase" generality – irrespective of *their* nitride colour.

sum of activated chemical energies: the exothermic energies released minus endothermic energies absorbed for included reactions.] In atomic and molecular based particles, electrons will have adopted new orbitals in agreement with new higher particle energies and so will consequently behave more energetically than they did in their prior ground states.

Figure **{4.4}1** and (preferably) Figure **{4.5.4}2** show that, as system pressures decrease, the thermal energy ("temperature") levels of the light free electrons diverge above the thermal energy levels of the heavy particles, and this deviation represents the elevation of free electrons to "temperatures" higher by some orders of magnitude. Also, at still lower system pressures, that principal set of heavy particles, the ions, follow this trend by energetically deviating above their ground state molecular equivalents, albeit to a lesser magnitude than free electrons. Although these particle traces are not represented in the figures (being absent in the sourced diagrams), "temperature" traces of other energised particle sets will likewise diverge above their ground state equivalents – the "ions temperature" curve can be taken to approximately represent these (collectively). [It should be emphasised here that source authors equated thermal energy with total energy. Under the indicated non-equilibrium conditions, the total energies of the various particles could reasonably exhibit more accentuated divergence curves than their thermal energies.] Figure **{4.5.4}2** represents that essential characteristic of non-equilibrium plasmas – the divergence of particle "temperatures" – which is fundamental in understanding the dynamic determining chemical thermodynamics and kinetics in systems of microwave-stimulated thermochemistry. The sourced figures were illustrative of typical *non-microwave* systems in characteristic low pressure non-equilibrium. The general effect on such a representation by a shift in system thermodynamics to *microwave-stimulated non-equilibrium* is indicated in the latter Figure **{4.5.4}2**. In this latter representation the "particle(s) temperature" curve is shown shifting to the right (with increasing system pressure) to represent the trend under microwave-stimulation of non-equilibrium conditions into higher system pressures (nominally to around one atmosphere – as was the case for project experimentation).

In their substantially higher energetic states, the physical and chemical behaviour of atom-based and molecule-based excited, ionised or re-combined "heavy" particles is appreciably different to that behaviour exhibited by these entities in their

(initial) ground state. Observing also that (as previously disclosed), at very high plasma energies, ionised molecular particles will break down into monatomic ions. So, these heavy particles are not only likely to play a reaction-driving role in plasma chemistry, in terms of speciation they may be freed to play a role for which there is no equivalent in conventional processes (as they are not present in such)[87]. (Given the presence of requisite species) this superior capacity of activated particle species is a characteristic of plasma chemistry (or ionisation chemistry) and allows for process possibilities not available in conventional, combustion-driven pyro-chemical processes.

At some variance of function are those complementary particles, the lighter sub-atomic particles, which are essentially energy "providers" to reactions occurring in microwave plasmas. Although, as a commensurate function aligned with this "provision" of energy, free electrons also provide the key re-combination link in returning ion particles to their root species, normally the re-combined derivative. Overlooking the particle products of certain limited phenomena (which occur infrequently in partial plasma but proliferate with advancing ionisation) such re-combined particles will be the root atom or molecule with internal energy elevated above the initial ground state. Similarly, photons contribute energy in quanta that contribute to and determine the degree of excitation – the energy state – to which such recombined particles return. This excited state in recombined particles is normally at a level above ground state (for the prevailing nominal "temperature") but below ionisaton energy. This elevated energy is why such re-combined particles can contribute to the physico-chemical phenomena in plasma environments.

Further to the chemical potential imbued in plasma particles, the absolute number of these particles at any instant is governed ultimately by *collision theory* – in particular, the *mean free path* experienced by activated particles before they are "extinguished" by re-combination. In microwave plasmas this fundamental phenomenon is determined by the action of the applied microwave field as it stimulates particle energies – particularly the free electrons – and promotes the number of excited and ionised activated particles. The microwave energy imparted to the ionised particles, particularly that individually acquired by each free electron during its unique mean free path, is recovered (with its surfeit of transposed microwave energy) as "system energy"

upon particle re-combination. As previously addressed, such method of stimulation facilitates in the plasma environment under irradiation a greater number of activated particles than for any other comparable method of ionising stimulation [58, 80]. This concept becomes less surprising where, under microwave-stimulation, non-equilibrium occurs at high relative pressures. Herein, under collision theory, with the greater population of activated particles for non-equilibrium systems generated under microwave-stimulation, collision frequency is increased, mean free path of particles is decreased, the mean acquired energy of particles is less so the discrete energies imparted to the system are less, and particle "temperatures"* are lower but their incidence is more numerous. This outline is self-consistent with theory for *microwave-stimulated* non-equilibrium "low temperature" plasmas such as typify the experimental conditions in this project. This desirable capability in microwave-generated plasma allows the continued initiation of non-equilibrium plasma in system pressures up to atmospheric pressure [80, 261]. (Hereto not expected to be noticeable for such systems "open" to the atmosphere, any contribution to the effect upon ionisation of system pressure by variations to component partial pressures was not determined in the course of experimentation for this project.) Such non-equilibrium plasmas generated and sustained at atmospheric pressure operate at considerably greater system pressure (typically by orders of magnitude) than is possible for non-equilibrium plasma generated by any other comparable means – a fact of great providence to this project and to any realised adaptation for the potentially many plausible industrial applications.

So, now the basics of microwave-stimulated plasma environments and the consequent thermochemical characteristics of metallurgical processes conducted within such environments have been re-visited, how these collectively conspire to distinguish the method in application is of central importance. This "performance in application" was crucial to the project as it provided that discriminate "edge" to processing which so marked project experimentation in both process and outcome. This processing edge was crucial in the development of processing configurations throughout the experimental

* Whilst often converted to kelvin (or °C) for purposes of comparison in working systems and although such was generally favoured throughout the project, particle "temperatures" are commonly expressed in electron volts, eV (a unit of *energy*, it might be noted).

programme and has similar bearing for future applications in processes of extractive pyrometallurgy conducted in purpose-built, operationally configured reactor systems, and for further applications necessitating comparable process parameters. For any process of extractive pyrometallurgy being conducted in a microwave-stimulated reactor under the non-equilibrium thermochemistry described above, the following discussion canvasses issues around process initiation, its activated chemistry and environment, system stability and ongoing phenomena associated with the continuing process.

For low temperature plasma generated in a microwave discharge at or close to atmospheric pressure, the "push" to higher particle "temperatures" takes longer as the important free electrons have curtailed mean free paths (relative to much lower system pressures) and electron temperatures are suppressed. The "temperature" range across the various activated particles is also at a minimum in this initial stage. As the applied microwave field stimulates (or "captures") a far greater number of active particles there is generated an "energy flywheel" effect that propels the thermodynamic status past the quasi-equilibrium and rapidly into the non-equilibrium.

Metallurgical reactions taking place in plasma under non-equilibrium thermochemistry proceed under circumstances where the translational, rotational and vibrational energies of participating activated particles differ markedly from particle to particle and from particle type to particle type [58]; "participating" particles being those capable of accruing these discrete energies. In the circumstances of such a plasma, the various activated particles may be considered as having their own explicit "temperatures" – if fleetingly so – and these transient "temperatures" may be divided between rotational, vibrational and translational temperature "components". Such a spread of temperature possibilities is in some part due to the receipt (or liberation) of energy quanta, including photons and the transferred energies from collisions. Consequently, this departure from the Maxwell-Boltzmann energy distribution amongst particles dictates that the fundamentals of equilibrium thermodynamics and statistical mechanics can no longer be applied. Further, for the system initially in thermal "quasi-equilibrium", the activation energy (E_{act}) exceeds the mean energy kT for the translational motion of particles. Moving into non-equilibrium this mean energy

increases such that, once kT closely approaches E_{act} , the Arrhenius equation (equation **{3.4}2**) can no longer be employed to resolve the reaction kinetics of the process, nor other reaction rate characteristics in the process thermochemistry [58, 80].

The extremes of high temperature in the plasma environment of a reactor (or furnace, oven, kiln, *et cetera*) designed for metallurgical reduction or comparable processing would ensure that the overwhelming proportion of gases in the reactor atmosphere would be present in the monatomic state – quite apart from excitation and ionisation phenomena. No matter what extractive metallurgical configuration is adopted in which to plasma-process the mineral input, the atmosphere and the thermochemistry it supports, and the required and possible reactions are of the most acute consequence in determining process chemistry. Consequent upon this shift from molecular to atomic, the associated increases in Gibbs energy plus the reduced activation energies (E_{act}) (required for reactions to proceed) would enable process results utterly unlike the chemistry of conventional processes [58]. In this temperature range where molecules are no longer stable entities, (from species to species) their prospective molecular ions are also no longer thermally feasible, and (generally) only monatomic ions and their associated particles are present in the plasmas arising from the base of such higher background temperature environments. Of course, these articulation shifts in plasma manifestation could impose unpredictability upon processing conditions in applications where "process certainty" would be expected as more than an "operational luxury". Consequently, knowledge of both process requirements (including thermal limitations of state of contributing components) and the background bulk "temperature" of the atmosphere, the system pressure, the range and chemistry of particle species and the energy they contribute once the operating plasma is induced, and lastly, the general "ground state" of the environment in which processing is to be conducted are requisite mandatory knowledge in a system for which reproducible processes are expected, as would be the case in industrial application. However, for such range of variables, "pure" knowledge of conditions may neither be so straightforward nor so easily determined.

In a plasma reactor operating under non-equilibrium conditions the reactions taking place may do so at or near the plasma/reactant-body interface, at the plasma/slag interface, at a crystallographic site (when accompanied by diffusion in solid minerals),

at a plasma/liquid interface (or universally in liquid-phase following convection), and most fundamentally with respect to activated species transfer, in the environment of the ionised atmosphere of the plasma. Plainly, as has been made clear in preceding paragraphs, we need to know the projected/expected outcomes of the plausible reactions possible under the activation of the plasma. Further, other factors which must be known are the operating conditions under which reduction can be expected given the target mineral reactant, its form and physico-chemical stability, bed permeability and reactant contacting, the reactant atmosphere, the plasma's regeneration propensity and stability, particle species produced and their chemistries. (And, of course, in systems of reduction we need to secure process *irreversibility* to secure process productivity.) In an industrial setting, to begin to predictively understand or assess the full process thermochemistry and its resultant chemistry would occupy the talents and facilities of a patient corporate master. Initially, aided by available resources, a trial and error approach would be well suited to beginning any search for knowledge of such complex systems – with review and re-trial of learned facts.

Once the generalised overall process has been tested and identified by such rudimentary procedure, and individual processes within this overall whole qualified in their contribution and extent, then process objectives can be meaningfully described and process routes specified. Whilst, being prescriptively known, the mineral being reductively processed and the end-product metal are plainly evident as "process book-ends" in the design of any process, it is the selection of the intervening process parameters, the "reductant" species plus the operational confluence of "reactants, intermediates and products" with applied energy and process control, including the management of these factors, which distinguish the merit of process implementation and categorise the accomplishment of the overall operation – and its commercial viability, book-end to book-end.

In all this, some semblance of development reality must be held in reserve – some comprehensible sense of the scale of any proposed application, and of outright thermal limitations imposed by the sensible process temperatures, thermal rating and campaign life expectancy of insulation, and pragmatic containment and quench strategies. During the course of early, exploratory experimentation in this project, it was found that commercial (iron ore) blast furnace pellets could be efficiently and

reproducibly reduced in a controlled atmosphere under microwave processing to a virtually carbon-free steel "reduction product". With this first-hand knowledge taken as provisional fact, even in wide-eyed optimism, this author could never suggest the industrial obsolescence of the modern, highly efficient and productive blast furnace in its role as the pre-eminent means of world iron and steel production.

However, there is a legitimate role for a system of microwave-stimulated reduction in modern extractive metallurgy. Such a role ought be quite firmly concentrated around those reduction applications which represent either or both (*i*) the highest economic value-add and/or (*ii*) the most difficult thermochemical challenge in producing high end-value products. In the bare reality of conventional production routes, such applications are frequently small-scale operations or operations conducted in collective small-batch stages. Such staged routes may or may not need to be continuous processes to represent an optimised profitable operation, particularly where batch processes have been the established or "traditional" mode of production – such as for the production routes of the refractory metals. Minimal reflection on the production route circumstances of refractory metal production suggests that these production routes are obvious candidates for adaptation to a microwave-stimulated reduction solution, their commercial value at end-product refractory metal – that is, their value-add from mineral to commercial grade metal – ensures their candidature on the rationale of profitability. The "reduction nobility" aspect of the obdurate refractory metal minerals renders them as appropriate target mineral reactants for a microwave-stimulated reduction route solution – a solution well suited to the "thermochemical challenge", with the value-add margin to justify the investment.

In reviewing the significant benefits of microwave-stimulated pyrometallurgical processing, and in acknowledging the fundamental principles that dictate conditions for such high energy processing, it is not necessarily so straightforward an enterprise to envisage and expediently develop the principles of microwave processes into working pyrometallurgical systems. Such systems should be unfettered by constraints of scale and technology up to real commercial applications, applications distinguished by industrial productivity (as realised in quality, quantity and profitability). Nevertheless,

the following discussion seeks to provide some redress to this impasse between qualifying research stage and initial development stage. Or, in the author's experience, between the "experimental proof of principle" and a realised "scale-up to working pilot plant" of a microwave-stimulated, fluidised-bed metallurgical reactor amongst other contemplated systems.

9.2: Recommendations: Development of Commercial Microwave Applications.

Recommendations are limited here to those aspects of microwave-stimulated pyrometallurgy that have been embraced in the conduct of this project, and to those related fields in applications of process chemistry and metallurgy to which the implementation of microwave-stimulated processing has particular synergy. It has to be emphasised that since the earliest microwave applications were introduced, enthusiastic "recommendations for development towards commercialisation" have periodically been disseminated in the broader literature and, more commonly, outlined in presentations tendered in industry-focussed conferences and symposia on microwave applications. Such dissemination exists for microwave applications in diverse disciplines from the electrical engineering of circuit design, power and applicator systems, through the process engineering of specialised applications for clean "laboratory" production systems (such as etching, ozone production, medical syntheses, *et cetera*) to basic commercial applications (such as bulk heating and drying, thawing and industrial "cooking" and curing, synthesis of chemicals, regenerative remediation of spent catalysts and other agents of industrial processing, process chemistry in both aqueous and gaseous environments, *et cetera*). It is noteworthy that a great many of the commercial applications are representative of *low* value-add operations; whilst this observation seems remarkable in what it conveys of commercial foresight, it is undisputable evidence of the economy of microwave operations in "real world" commercial applications.

"Industry overview" surveys and general industrial applications – both developing and established – have been cited throughout this thesis **[71, 73, 80, 89, 90, 105,**

113, 152, 178-180, 244, 262, *et* cetera], whilst surveys and applications pertaining to the microwave processing of minerals have been acknowledged and similarly documented **[74, 86, 99, 117, 121, 247, *et cetera*]** where their more process-specific citation was warranted. Also addressing microwave processing potential in industrial applications, other such microwave application overviews (not specifically cited herein, that is) are to be found published in periodical volume proceedings of professional journals and magazines, in text volumes, and in the contents of the many microwave orientated conference and symposia proceedings of professional bodies (such as IEEE, ACS, TMS and MRS) and industry associations (such as IMPI)*.

Microwave processes addressing diverse extractive metallurgical applications have been proposed by numerous authors since the introduction of the first rudimentary waveguide "applicators" to the current armoury of applicators, ovens, evacuable chambers, and reactors. All of these configurations are designed, aided and operated through the surfeit of available system management options including diagnostic devices to interactively control system variables, devices to monitor and auto-correct microwave-to-applicator tuning, power-to-feed devices to regulate system-to-process interaction and other process-enabling devices; all of which have advanced microwave system capabilities and developments in applications and processes. Ultimately, of course, the clearly advanced state of understanding that now exists for microwave field behaviour has allowed design and fabrication professionals to predict system trends (given particular conditions) for proposed system configurations, calculate requirements and provide design for the variety of system peculiarities that might be encountered in the operation of the proposed microwave system.

Generally, microwave applicator systems have been greatly improved towards the goal of predictable performance, and both process conception and the design and

* IEEE is The Institute of Electrical and Electronic Engineers (which publishes many journals (including the influential *Trans. On Plasma Science*) over the wide range of the collective professional disciplines which they serve); ACS is The American Ceramic Society; TMS is The Minerals, Metals and Materials Society of The American Institute of Mining, Metallurgical, and Petroleum Engineers, Inc. (AIME); MRS is The Materials Research Society; IMPI is The International Microwave Power Institute. These bodies are prominent in promoting microwave applications and have been active in both the facilitating of conferences and the extensive publication of technical literature relating to microwave technology.

specification of components and systems alike are today as "optimised" as they are likely to become into the foreseeable future, major theoretical advances aside. New fronts in the technological development of microwave generation and energy delivery are mooted to occupy the attention of system designers whilst actual applications catch-up with the current standing of microwave applications technology. [Mention ought be made of the supplementary use of microwave energy in various applications at the "very high technology" end of the utilisation spectrum. Such applications include the deployment of microwave fields to generate and sustain the magnetically confined plasma at the energetic core in the toroidal chamber of tokamaks (sustaining the process-control in fusion-based thermonuclear power generation) and in components of comparable infrastructure. Other than to indicate the level of systems sophistication existing in some levels of microwave application, however, such impressive applications have little direct relevance to the substance of this project.]

The broader metallurgical areas of note that recommend themselves to the enterprise of real experimental research utilising a method of microwave-stimulated energy application are noted as follows and are either extractive process-metallurgical or are secondary process-metallurgical or chemical engineering. Those areas of potential pyrometallurgical research, and more typical of the work of this project, include feasibility studies into microwave reduction routes for (*i*) cassiterite (to recover tin metal avoiding the economically detrimental intermediate by-product, hardhead), (*ii*) the concentration and recovery of indium from indium-bearing tin ores, (*iii*) nickel and nickel/cobalt sulphide ores (to recover metal products avoiding intermediate matte by-products), (*iv*) molybdenum metal (from the common sulphide molybdenite avoiding the intermediate by-products), (*v*) chromium and tungsten metals (from chromite and tungstate oxidic ore minerals (respectively)), and (*vi*) vanadium metal from its pentoxide, and similar for the other refractory metals (reduced directly from their pure oxides by metallothermic routes). The secondary process-metallurgy microwave studies which recommend themselves are (*a*) the disproportionation of refractory metal and alkali metal halides – incorporating reductant-free reduction processes, (*b*) the microwave-stimulated combustion synthesis of pure compacts to produce pure alloys of high density and advanced physical properties, (*c*) the microwave sintering of metal matrix composites and inter-metallic materials, and (*d*) the chemical synthesis of ammonia and derived compounds including fertilisers. Further to this list is that broad,

self-evident topic of waste and waste disposal, incorporating the remediation of wastes and recovery of contaminants and resource metals from wastes so allowing un-monitored storage or disposal – options representing a general surfeit of economic opportunities for microwave and comparable processes.

Reported over recent decades have been many lower-end value-add studies of microwave "treatment" of ore and waste mineral trials that have not been carried through to full-scale operations although, in this author's estimation, the studies indicated that such was warranted. Perhaps dictated by their origins in bureau of mines and geological survey offices, the thrust of these microwave treatment studies was directed towards the upgrading or beneficiation of ores and mineral concentrates or the basic *stabilisation* of waste minerals enabling their indefinite disposal-to-fill with long-term monitoring. A high proportion of these papers were devoted to the *physical* beneficiation of ores and ore minerals – tantamount to mineral processing operations – and concentrating upon the augmentative application of microwave heating to induce thermally-derived inter-phase stresses, thus facilitating attrition and minimising the ore dressing stages leading to mineral processing. Such stresses result from dielectrically-derived volumetric expansion differences between co-mineralised components contained in complex, metalliferous ore facies and so resulting in grain-boundary cleavage of minerals so to facilitate cleaner cut-off limits and higher recovery for mineral/gangue separation operations.

Those studies reviewing the *chemical* beneficiation of ores and mineral concentrates invariably found that "melting" or "mineral modification" or "apparent reduction" took place under continued microwave irradiation, not to mention those phenomena ("forbidden" in the "lore" of microwave applications) of arcing, thermal runaway, and volumetric (plasma) discharging in and around the specimen under examination [100, 101, 200]. It seems rather quaint that such respectable teams of geophysical and minerallogical geologists (principally) viewed the outcomes of such transformative phenomena as negative – or perhaps, "detrimental" to the commercial value of the minerals. These scientists were evidently dismissive of the possibilities these thermochemical precursors presented, irrespective of any contemplation of the minerals' eventual extraction route prospects. However, some took a more metallurgical

view [74, 75, 76, 86, 99, 117, 121, 122, 133] and followed elementary reduction paths for the ranges of minerals they investigated – with reasonable success, it might be added – although (possibly constrained by funding) not all pursued their results towards development of microwave-stimulated systems of extractive metallurgy. And yet, so many feasible possibilities exist across the broad scope of mining and associated metallurgy to identify and develop systems of (both) mineral beneficiation processing, to up-grade both the value and the extractive reducibility of ex-mine mineral concentrates, and extractive reduction processing – pyrometallurgical or otherwise. As was earlier identified, microwave-stimulated reduction processing (and comparable) operations are well suited to smaller operations (possibly output-limited to batch processes) distinguished by a high value-add component and/or to minerals having a high degree of reduction "nobility" due to their obduracy – the thermochemical stability of the mineral(s) in question. Further, it is plausible that such microwave processing operations could be accommodated within the bounds of extension into a *continuous* production process.

Beyond that self-evident priority that should accompany the metallurgical recovery from waste of valuable resources (metallic or other), other considerable financial rewards are to be accrued from remediation operations on mining and metallurgical wastes. Once remediated, tailings or gangue waste material no longer attracts the considerable and on-going cost burdens accumulated by the same material in its un-remediated state, such by-products of mining and metallurgical operations usually require chemical and/or physical stabilisation with on-going management. Such wastes are often intractable (radioactive or toxic) wastes requiring long-term or indefinite management at considerable site preparation, maintenance, monitoring and guardianship costs. (To avoid or minimise such responsibilities and associated costs, intractable waste materials may be "returned" to geologically and hydrologically stable strata deep in exhausted shafts and pit sectors of the mine of origin.) As appropriate, the predominant cost burdens for un-remediated wastes are composed of management elements from the transport and handling (including accounting) of such waste materials to environmentally safe storage where it attracts on-going maintenance and monitoring *in perpetuity*. If it is to be returned deep underground in closed mine sectors where, in

stopes and undisturbed fill, it may *not* require ongoing security and chemical monitoring, at a saving of considerable cost over time for the indeterminable alternative.

Where it is stored or buried above ground, *remediated* waste is less vulnerable to aqueous seepage and does not leach undesirable components into inaccessible watertables, it does not have to be invulnerably protected from wind drift and bulk erosion, and its oversight is no longer a financial albatross around the corporate neck at asset sale or take-over, or worse. Also, once intractable waste material has been remediated by the removal (and recovery) of that which rendered it "intractable", and whilst it may still be waste material, it is also now a "clean waste" material and may have value as such. Also, that which rendered the waste "intractable" may, upon its removal, have its own value ("heavy" metals and radioactive elements are a case at point). Remediated waste materials become resources and as such have their own value for utilisation from the mundane "clean fill" (no longer attracting the costs of monitoring, *et cetera*) to the possibility of being further processed into (perhaps) approved construction aggregate, a foundry product, a component for specific ceramics manufacture, a landscaping aggregate, or numerous other marketplace possibilities.

In short, the value elements of remediation processing which may be commercially realised are (*i*) the market value of the recovered metal(s) and/or other commodity (methane, sulphur, phosphorous, *et cetera*), (*ii*) the value of the as-produced bulk material to "clean fill"-type applications, (*iii*) the value-add to "as-produced bulk material" if up-graded to a higher-value product such as a lightweight aggregate for construction, *et cetera*, (*iv*) the cost saving of **not** needing to dispose-of, transport, store, manage, monitor and maintain security over un-remediated waste materials, or part thereof, and (*v*) the "greener", "responsible" corporate image facilitated by the absence of noxious or problematical by-products of corporate activities – an image to which a dollar value can always be allocated. It is plausible that, as "income" streams, any of these five factors could be the major "income" generator, or loss averter. Of course, once remediation has been implemented, the avoidance of any attributable longer-term personal and public health risk is an un-ascribed cost saving of some magnitude, to whatever corporate arm or authority, and quite apart from the equitable imperative of "ethical obligation".

Utilising straightforward techniques of microwave processing – in one, or in multiple processing stages – industrial by-product waste can be effectively remediation-processed to produce an environmentally acceptable bulk output plus one or more fractions incorporating pure or concentrated toxic fractions which can be further processed or managed as the new, greatly volume-reduced waste. Whilst there are numerous smaller-volume metallurgical, petrochemical and comparable industrial waste examples (which are often wastes of high toxicity) – the truly high-volume cases of industrial waste disposal are those of mining and smelting which are stored under managed oversight and exist as monitored tailings dams and slag heaps, typically in the vicinity or their mine, plant or furnace of origin. These by-product wastes are frequently deposited in vast quantities which often-enough dominate local landscapes, the problem is centuries old, and old deposits may need remedial re-working where their load is environmentally unsafe or chemically unstable. If such deposits are viewed as "resource deposits" in their own right and, as economic deposits, many are currently identified as "marginal or better" commercial prospects, then for the resource worth of recoverable commodities (typically metals), remediation processing – or "recovery" processing – will be a growth industry in the foreseeable future. And again, value of the recovered commodity will not be the only value retrieved from such ventures (as other remediation factors will ultimately become important elements of such enterprise). Because microwave-stimulated methods of processing can be configured to target specific minerals or specific reaction zones, the overall process requirements can be arranged to best address an optimised convergence of results with regard to the above-mentioned remediation factors.

In a commercial project convened by this author, and independent of this thesis project, a pilot programme of experimentation was undertaken to recover zinc and lead from lead blast furnace slag supplied by an Australian operation in Queensland. The slag was classified as "intractable" waste because of its potential, if stored in exposed conditions, to leach zinc (and to a lesser extent, lead) into surrounding groundwater, consequently contaminating artesian watertables – notably, the zinc component being notionally "soluble" for the purposes of the relevant authority's determination. [Trace zinc is essential in biological systems (life forms), however, such levels in groundwater

at "trace" concentration could not be guaranteed following ongoing contamination, and its widespread artesian range would be largely unpredictable.] Both zinc (Zn ~ 15 at%) and lead (Pb ~ 2 at%) were incorporated in the mineralogy of the principally oxidic slag phases and therefore required metallurgical reduction to free these from the mineralogical fabric of the slag, and do so without smelt reduction of other metallic components.

The "proof of principle" stage justification was established in a microwave oven configuration similar to that used throughout this project. Once the general reduction dynamics were revealed, a proposed system of microwave reduction was established incorporating a fluidised bed (FB) shaft as a working microwave reactor – the FB shaft doubling in function as the (microwave) waveguide applicator. The fluidising gas being hot air passed through heated char to yield ~ 20% CO/N_2 reducing gas mixture with the fluidised bed being a static, batch load, whilst hot escaping gases carried reduced metal vapour(s) through to a water-cooled condensation chamber where condensate as pure metal or as pure oxide (upon air addition) could be concentrated for recovery thence analyses (see Figures **{9.2}4** and **{9.2}5**).

The design concept was refined and a final design completed by microwave systems and applications expert Dr Hugo Huey of Micramics, Inc., Santa Clara, California, with other professional input from Mr Des White (metallurgical consultant, of Sydney), Mr Stan Morrow (microwave consultant, of Oak Ridge, Tennessee) and Professor Nguyen Tran (microwave consultant, of Melbourne), who supplied the microwave generator and infrastructure. Once the applicator dynamics were specified, final design was agreed between the commissioning company Tesla Technologies Pty. Limited (Tanner-Jones), Dr Huey and CSIRO Minerals, Clayton, Victoria, who were commissioned to integrate the microwave design into an optimised fluidised bed design, construct and "fit-out" the system with necessary scrubbing, quenching, safety and associated augmentation, and carry-out the experimental programme at their Clayton Laboratories in Melbourne. CSIRO Minerals fluidised bed group leader, Mr Paul Peeler, Dr Seng Lim and their team were ultimately responsible for the conduct and successful outcome (including independent analyses) of the experimental programme that was carried-out over some months in 2001 – 2002. The general pilot set-up at Clayton is shown in Figures **{9.2}1** to **{9.2}3**. It should also be indicated that the

microwave FB pilot programme at CSIRO Minerals was part of a funded programme under the Industry Research and Development Board as AusIndustry R&D Start Programme Grant No. GRA02013: "Microwave extraction of metals from slag". Also pertinent, the programme was carried-out under the commercial and legal sanction of this author's (then) provisional patent "Plasma Reduction Processing of Materials" (whose granted patent details – current in Australian, U.S. American, European and World jurisdictions – are provided in Appendix **9.2**), then owned by Tesla Group Holdings Pty. Limited and now owned by Plasma Technologies Pty. Limited. [The said patent was avowed by the University of Wollongong as being contained outside the purview of the intellectual property contained in the subject matter of this thesis. Refer to the relevant University of Wollongong document reproduced in Appendix **9.2**.]

As conducted, the metal recovery from the lead blast furnace slag was a relatively straightforward reduction/remediation operation. The oxidic lead and zinc minerals were reduced "insitu" from the mineral "fabric" of the fluidised slag granules. Crushed and sieved to provide a standardised size distribution, provide experimental continuity, and remove the bottom size range to avoid excessive elutriation of solids from the fluidised bed which would un-necessarily contaminate the condensed recovered metal, the slag used in experimental trials fell into the size range: – 833, + 100 μm. The 2 kg charge of slag contained ~ 3 wt% char granules (~ 2 mm size) such as to ensure that the FB atmosphere remained a reducing environment by returning the oxidising reduction product CO_2 to CO.

To anticipate the reality of industrial application, the intake air was pre-heated and passed through heated char to produce the fluidising reductant gas mixture before further heating and plasma initiation in the system being provided by the applied microwave energy (variable up to ~ 6 kW, 2450 MHz). As might be expected, the Pb-mineral was reduced initially and condensed on the water-cooled coil first (as verified by visual inspection at recovery) before the greater quantity of Zn-mineral was reduced and subsequently condensed and deposited as finely-divided metal powder, albeit in a somewhat "sinter compacted" deposition (with a moderate proportion of attrited slag fines). It was established that, although their reduction occurred at lower temperatures, the reduced metals needed to be raised to points of elevated vapour pressure to allow phase-separation from the slag and entrainment from the FB shaft into the condenser.

The boiling point $T_B \approx$ 907°C for Zn evidently determined a marked increase in Zn recovery at the condenser by process temperatures ~ 950°C, consequently, the process was conducted at 1000°C to ensure good recovery; and whilst $T_B \approx$ 1740°C for Pb, it has high vaporisation potential which ensured "complete" Pb recovery.

Noting that, because *treated* slag was essentially free of Zn and Pb phases, some loss in recovery was experienced in the quantities of Zn and Pb in the metallic condensate – this loss was particularly evident for Zn. (By order of magnitude) the losses were attributed to (*i*) metal vapour by-passing the condenser and being carried-through in the spent fluidising (carrier) gas to scrubbing and exit-gas handling stages of process, (*ii*) some plating-out in the pre-condenser sections of the reactor, and (*iii*) to metal un-recovered or lost during manual metal recovery from the condenser apparatus. With condenser deposition of Pb-phases being more definite, these possibilities for loss were more particularly represented for Zn-metal and Zn-oxide products. However, these criteria of loss being acknowledged, recovery in condensate of target metals was 98 % of Pb recovered and 90 % of Zn recovered from that reported in the *starting* slag. Conversely, the typical condensate was ~ 13 wt% Pb, ~ 70 wt% Zn, a percentage of O where these metals were present in oxide forms ZnO and PbO, and the balance (~ 10 wt%) as Fe_2O_3 , SiO_2 , Al_2O_3 , CaO, MgO and S – "fractions" of more complex mineralogies (and present as elutriated slag fines).

The experimental apparatus was designed such that it could be operated without microwave irradiation and over a temperature regime consistent with that known for the microwave process option. To this end, a number of trials were conducted following this conventionally heated FB reactor process, a process that ensured the high temperatures employed to vaporise the metals, where results were directly comparable to microwave-stimulated output. The reaction times were evidently more retarded (by monitor feedback) and total removal of each Pb and Zn was clearly lower than the equivalent microwave trials, leaving them close to the minimum allowable "intractable" level of classification (regarding disposal options). In keeping with the original process concept, an alternative procedure would have been to microwave process the slag at much lower "temperatures" with a following "solution-recovery of metals" procedure. Such an operation would utilise the lower-temperature reaction chemistry typical of

microwave processes, with lower input energy, although a further process stage would be required (in the solution recovery and plating-out of pure metals).

Nonetheless, the results of such a novel, foundation pilot programme were illuminating of the potential of microwave processes, and were significant against the parallel conventional process. It must be remarked-upon that microwave systems offer better relative prospects when applied to higher thermochemical challenges (for which conventional means are impotent) than was the case for lead and zinc, although (separately), the specific slag remediation problem is of worldwide significance. The independently run CSIRO pilot programme established the "production plant" feasibility of microwave applications, including the durability of the microwave system-components – even through some unexpected episodes of *ancillary* equipment malfunction – the bane of every experimentalist. Photographs of the CSIRO pilot plant set-up plus metal recovery output are presented in Figures **{9.2}1** to **{9.2}5** accompanied by inclusive annotations, whilst a real industrial microwave reactor is presented in Figure **{9.2}6**.

Figure {9.2}1: Photograph showing the overall experimental set-up of pilot plant instigated by the author and carried-out by the Fluidised Bed Group of CSIRO Minerals at Clayton, Victoria, over some months in 2001 – 2002. In the foreground is the microwave generator that delivered microwave energy of up to 3 kW, 2450 MHz via the round (cross-section) water-cooled waveguide into the base of the fluidised bed reactor shaft. Present in photograph with the author are the then head of CSIRO's Fluidised Bed Group, Mr Paul Peeler (right, now retired), and the subsequent head of CSIRO's Fluidised Bed Group, Dr Seng Lim (left).

Figure {9.2}2: Photograph (taken during re-charging down-time) of experimental fluidised bed microwave reactor in which a successful set of pilot trials was carried-out at CSIRO Minerals' Clayton Laboratories, Victoria. The reactor was designed to recover zinc and lead from otherwise intractable lead blast furnace slag of industrial origin. The open heat jacket exposes the central fluidised bed (FB) shaft, lagging offered protection against excessive heat loss. Entering the lower shaft at inclination (lower left) is the waveguide inclusive of water jacket introducing 2450 MHz microwave input from the variable power (nominal) 10 kW microwave generator source (out of frame).

Figure {9.2}3: View of the above fluidised bed reactor showing some of the ancillary service input points including pre-heat burner feeding the windbox for FB air intake (bottom), pipes for offtake gases to remote scrubber (top right) plus numerous lines and cables fmonitoring of essential system functions.

Figure {9.2}4: Photograph of water cooling coil mechanism taken immediately upon its removal from the newly opened cooling chamber atop the FB shaft of the microwave reactor of the previous Figures **{9.2}1** and **{9.2}2**. The fume condensate is the Zn(~ 13.0 wt% Pb, ~ 10 at% other) powder product of the microwave-stimulated carbothermic reduction of lead blast furnace slag containing up to 15 at% Zn and up to 2 at% Pb as mineralised inclusion in the tapped slag. The blue tinge to the encrusted condensate is indicative that the Zn metal is only newly exposed to oxidising air, opening the condenser when still hot resulted in spontaneous combustion of Zn. A process alternative was to allow O_2 (as air) into the condensation chamber (only) during reactor operation to produce the white zincite (ZnO) powder; pure ZnO is comparable in value to pure Zn metal, and much high purity Zn is consumed in the manufacture of pure, pharmaceutical grade ZnO. However, until a possible "next stage" operation concentrating upon refining, this was a resource recovery operation and purity was not of immediate concern.

Figure {9.2}5: This photograph is purposefully instructive in that it visually shows the Zn metallic powder yield (finely divided powder loosely heaped on paper, on left) and the quantity and granular size distribution (bagged, on right) of an actual trial charge (2 kg) quantity of the slag – equivalent in every way to that from which the powder yield on left was recovered. Indicated by the balance of post-treatment slag, the reduced proportion was, by weight, close to the theoretical yield of recoverable Zn and Pb in the slag (based on assays of both the CSIRO laboratory and smelter laboratory).

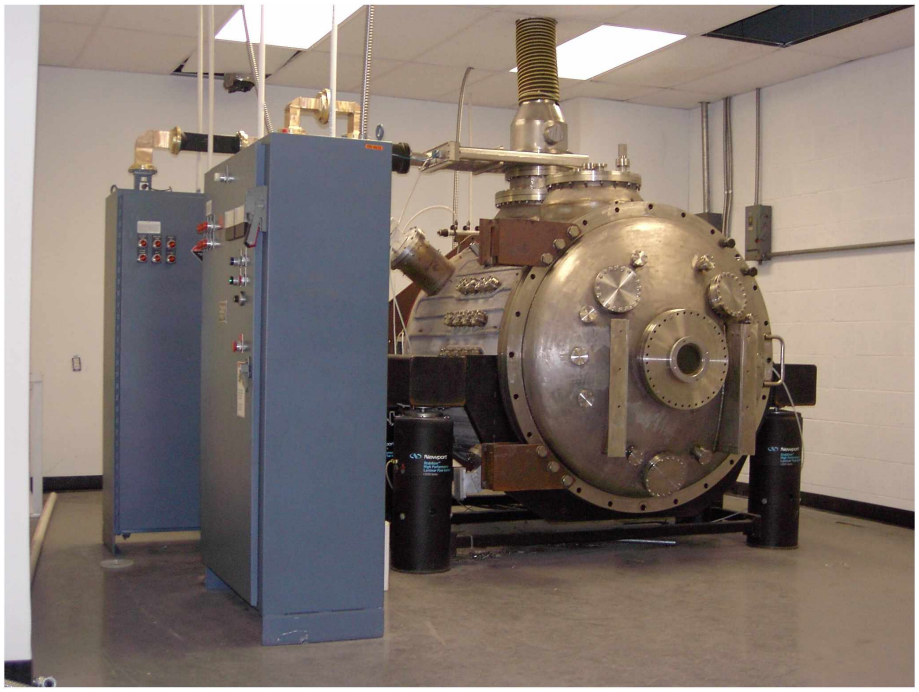

Figure {9.2}6: This photograph shows, installed and commissioned, a stainless steel microwave furnace (after previous successful models) designed specifically for high vacuum heating/melting tasks, particularly the melting of high purity metals and the melt-blending to specification of clean alloys for use in the aerospace and defence industries of select contractors to the Government of the U.S.A. The power supply generates up to 10 kW power with (for this particular chamber) microwave input of 2450 MHz. The microwave energy is "interfaced" with the solid metal load via purpose-designed crucibles of application-specific ceramic which (*i*) shield the metal load from the applied field, (*ii*) being especially susceptible (or dielectrically "lossy") to microwave irradiation, heat rapidly to very high temperatures, (*iii*) have a very high melting point, and (*iv*) are not wetted by the liquid metals being heated and therefore are not contaminated within their ceramic microstructure nor cause contamination in the alloy melt. (Image reproduced with the permission of designer/owner, Mr Stan Morrow, president, Microwave Synergy, Inc.)

10

CONCLUDING DISCUSSION.

"Irrationally held truths may be more harmful than reasoned errors."

T.H. Huxley -
The Comming of Age of the 'Origin of Species', 1880.

"The irrational is not necessarily unreasonable."

Sir Lewis Namier -
Personalities and Powers, 1955.

10: CONCLUDING DISCUSSION.

In the relatively recent history* of modern industrial science and engineering, systems of extractive metallurgical processing have inevitably moved towards processes and system configurations which utilise the capability, the power and the capacity resulting from that "convergence of benefits" inherent in the marrying of compatible technologies. For the processing objectives central to modern extractive operations – as they were duly central in this project – such convergence is facilitated by the incorporation of elementary components from three fundamental sets of processing factors. The initial of these sets embraces the adoption of novel or contemporary techniques (including plasma systems, microwave technologies, *et cetera*) – techniques that carry the substantial expectation of the *new and evolving technology*. By and large, the two remaining factor sets represent the latest state in *established technology and procedure*, and these promise the acknowledged means and system capabilities so to enable plausible development and exploitation of such new technologies. The second set comprises the adoption of greatly improved existent technologies (such as vacuum systems, electrical circuitry and systems, new materials, fabrication techniques, component quality and availability, *et cetera*). The third set encompasses oversight initiatives and integrates in the former sets the co-ordination and implementation of crucial management options including system monitoring and regulation, process assessment and analyses, reporting and output capabilities – these by computer-aided control of systems, process intervention plus materials and process inventory.

Through provisional stages of development, system refinement thence pragmatic adaptation to specific applications, numerous technological advances have been laboratory or "pilot" proven and incorporated accordingly into real industrial applications. Whereupon, the literature of industry-orientated publications and commercial conference proceedings bear testament to the considerable benefits that

---

* In the years following the conflagrations of World War I and World War II, much emphasis was placed by nations upon the modernisation and advancement of such technologies that sustained their national security and geo-political ambitions. The elevation of the barely existent aluminium industry into a commercial production giant and the development of specialised steels to suit increasingly specialised applications are two metallurgical cases at point. The post World War II era also witnessed the expansion to commercial level of the refractory metals industries, not only to enable those special steel and aluminium alloy developments, but for high technology applications in their own right. It is this "modern metallurgy" era onwards that bears specific relevance to the refractory metals and is nominated "relatively recent history".

have accrued from such advances in process technologies – some advances, indeed, made possible only by the introduction of contemporaneous techniques and technologies. Regarding the investigations of this project, the convergence of a number of these technologies* has resulted in the simple, operationally modest microwave-stimulated process being developed and successfully employed to generate refractory metal reduction products – the results of plasma-pyrometallurgical reduction of their thermochemically stable oxide minerals.

Of experimental outcomes produced in the experimental "microwave oven set-up" configuration, the reduction success so immediately apparent by virtue of visual assessment was always confirmed by subsequent microscopic and spectrographic analyses. Each reduction "success" – each reduction product specimen – was the product of the project's objective programme of experimentation, whereof, one realised out of the serendipitous confluence of cautious management, controlled procedure and experimental persistence. Also, although presupposed expansive, the usual "trial and error" aspect expected in such experimentation was, fortuitously, rather more *orderly* than might otherwise have been expected for such a fundamental project, an original project arisen from a conceptual and abstract base.

Although not systematically addressed here (as sufficient discussion was presented in previous sections), the necessary shift in experimental procedure from the discarded, operationally deficient microwave reactor system to the microwave oven set-up method presented few conceptual difficulties, few experimental drawbacks and no problems of experimental reproducibility. In embracing this experimental "leap of faith" – placing experimentation and its products outside an experimental "comfort zone" with respect to atmospheric protection for both reaction chemistry and solidification recovery of products to stable temperatures – the simple oven set-up method yielded reproducible reduction products through reproducible process "campaigns". Whilst the reduction products were "notably successful", this assessment comes with the caveat that a substantial level of non-oxide re-oxidation of reduction product metal was conceded and

* Although recent advances in the relevant "technologies" individually present at a low key and minimal level in experimentation, when viewed in relation to project applications, the latest product developments in microwave equipment and applicator-device design, ceramics technology, vacuum technology, and various computer aided monitoring and analytical systems were presumed to have collectively benefited the programme of experimentation and assessment.

diagnostically "forgiven" where "outright metallic purity" was not experimentally possible in quenched reduction remnants. Significantly, because of this aspirational shortfall of experimental method, and whilst the reduction products were not pure metals but a continuum of metallic phases exhibiting a range of solid solution and metallic compound compositions, these phases represented the requisite and sufficient feat of ***reduction of the oxide mineral***. Consequently, in generating acceptable experimental reduction products the simple microwave oven set-up system represented a "realistic" experimental alternative (to the controlled atmosphere reactor) thus providing a workable solution for the practicable conduct of experimentation. By comparison, this "lesser" microwave oven set-up system offered reliability with acceptable reproducibility of both process and product. Fitting descriptions and analyses of experimental reduction products are presented in the comprehensive Section **7**, *Results*, with further discussion provided in Section **8.1**, *Discussion of Results*.

Whilst the primary goal of reduction experimentation was to establish *reduction* – particularly *reduction to metal* – from oxide minerals of the five refractory metals, a secondary objective was to establish the capability and apparent efficiency of the microwave-stimulated process employed. An adjunct goal was to evaluate the suitability of the microwave process when applied to the allied procedure of disproportionation of metal halides, a concept one might presume to include important implications for refractory metals production. Throughout the range of experimental objectives, certain of the reduction exercises revealed a greater "willingness" to proceed to completion than did others. Furthermore, observed across the range of experimental trials, this varied propensity for a "thermochemical inclination towards process completion" was evident in the fact that, at a minimum, an *acceptable* degree of "experimental success" was recorded for each and all tasks of the project's experimental programme.

The evident "ease of reduction" revealed early on in preliminary reduction exercises was to be confirmed in later "core" experimental trials where it was shown how "process-compliant" such reduction exercises could be under the technique of microwave-stimulated plasma processing. Nonetheless, process compliance aside, some core experimental trials proved to provide outcomes of greater process consequence, and/or indicated greater commercial potential, and these cases were given more-prominent experimental emphasis. Such cases were initially identified in Section **6.4**

and were given greater prominence through *Results* Section **7** and into the following discussion of Section **8.1** where an expanded summary is presented of both reduction achievements and general process characteristics – including a generalised *précis* of the potential of microwave reduction processes and reduction products.

10.1: Discussion of Process and Procedure.

The plasma initiated in a closed environment by an applied microwave field quickly sets-up the non-equilibrium conditions in a microwave-susceptible dielectric load (charge volume) to sustain and promote a non-equilibrium plasma suitable for reaction thermochemistry over a range of chemical and metallurgical applications. In environments exhibiting expansive temperature-difference amongst activated particles such as those typical of this project, and for plasma pyrometallurgical systems generally, an exceptional range of energised particles is present (and generally, "activated" particles incorporates reactant species and energetic particles as "reactive" particle species). This exceptional range of elevated energy levels amongst excited and ionised particles bestows upon the process thermochemistry of systems under microwave-stimulation such physical and chemical behaviour as to differ widely from "ground state" behaviour in conventional thermal systems. From this divergence above ground state of the plasma's particle population it can be inferred that such difference is apportioned relative to the degree of ionisation in the system. And such divergence will be represented in process behaviour and in the range of physical and chemical attributes of reduction products, solidification path dependent. The nature of non-equilibrium plasma environments is addressed in relevant sections through the thesis, with the work of ELIASSON and KOGELSCHATZ[80] being particularly relevant to non-equilibrium plasmas, including microwave-induced plasmas. The *kinetic* energy non-equilibrium between activated particles in microwave plasma (up to 1 atm system pressure) is induced by the individual interactions between the applied electromagnetic field and the various particles under its direct influence. Initially drawing free electrons and small "fragment" particles, this particle/field interaction indirectly ensures the decisively non-equilibrium thermochemistry in evidence in system process chemistry. Generally, under

microwave-stimulation it is this system non-equilibrium that characterises microwave processes, and which enables (by way of high populations of activated reactant species) the varied chemical capabilities of non-equilibrium microwave reduction processing. This processing effectiveness by way of population and reactivity of chemically active species rather than by outright thermal energy of the plasma (as for equilibrium plasmas) is well covered by BOULOS[90] and by other authors cited through this thesis.

Further to the distribution of reactive particles, and somewhat counter-posed in terms of operational desirability, is the uncertainty introduced by the "temperature" dependence of the rate constant, k, in the Arrhenius equation ($k = Ae^{-Eact/RT}$), the identity that determines the chemical kinetics in the system (see Sections **4.3** and **4.4**). The work of DEMBOVSKY[58] is particularly comprehensive for metallurgical applications where plasma systems proceed under conditions devoid of thermal equilibrium. In such systems there not only exist particles whose energies differ between species and from one to the next within species, but also where larger, molecular particles and fragments exhibit "rotational" and "vibrational" energies (or "temperatures") that are both individual and additional to the former. These deviations from equilibrium (where the Arrhenius equation holds true) increase towards the non-equilibrium as the value of k.T approaches that of the activation energy, $\mathbf{E}_{act}$ – moreover, such deviations increases with reaction rate. Once k.T approximates $\mathbf{E}_{act}$, the Arrhenius equation can no longer reveal the kinetic characteristics of chemical reaction processes. Furthermore, to proceed with any theoretical approach we would need to descend into the convoluted realm of statistical thermochemistry.

In their application to real processes, these operational factors of non-equilibrium plasmas bear immensely significant implications; and just how these non-equilibrium characteristics affect the course of their introduction to industrial applications, and what outcomes might be expected from their introduction to extractive metallurgy, is attentively addressed by STANDISH and WORNER[133] and by others variously cited through the thesis. Acknowledgement of ionisation processes and the ramifications of non-equilibrium thermochemistry has only been pursued at the *conceptual* level in this project, any *rigorous* pursuit would have been out of place in the overview format of this investigational, survey-type project, a project which pursued

a practical industry-based topic. However, also acknowledged for the success in meeting project objectives is the key role in microwave reduction played by *the broad whole* of the phenomena of ionisation thermochemistry, whose necessarily non-equilibrium elements of (*i*) vastly increased particle "temperatures" with attendant "temperature" range (against a lower background "bulk" temperature), (*ii*) associated high relative populations of activated reactive species, and (*iii*) amplified process kinetics collectively afforded prospectively "new" reaction route and reduction product possibilities at enhanced reaction rates. Such a superlative trinity of thermochemical positives assured the ease of experimental execution and was the fundamental strength in implementation of this microwave-stimulated reduction project.

How these thermochemical factors were revealed in the conduct of microwave reduction processing afforded process conditions of reduction thermochemistry that were highly conducive of the reduction objective. In this process-metallurgical environment – one created within the constraints of experimental scale – certain simple parameters contributed to the success of experimental outcomes and thus validating the worth of the microwave-stimulated reduction process and recommending its adaptation in future up-scale applications. A most noteworthy condition here was that experimental procedures were carried-out at atmospheric pressure, as are many common extractive and process metallurgy operations, and whilst this may seem inconsequential, for the plasma process, it represented a very high operational limit under which *non-equilibrium* thermochemistry could be conducted. Typically generating a high concentration of highly reactive particle species, this high pressure non-equilibrium plasma represented an uncontaminated, thermochemically desirable environment in which the stable minerals could be efficiently reduced.

Also, an incidental process of crucial convenience was that the volume-discharge plasma was generated out of the inter-mineral dielectrically promoted micro-arcing environment created *within* the reactant blend charge, such a phenomenon ensuring that the non-equilibrium processing plasma was initiated and sustained from within the reaction zone. This essential fact of applied microwave energy manifesting centrally in the reactant charge imposed an energy profile, or "temperature" profile within the increasingly susceptible charge – at the intended seat of reaction chemistry. Maximising the efficiency of energy delivery, such temperature profile is accentuated

and prolonged by the ongoing application of the microwave field, with heat *outflow* from the charge by conventional means of conduction, radiation and convection; required applied energy is minimised and the in-service life of containment refractories is extended. **A significant measure of the experimental success represented in this project is embodied in aspects of the *experimental process* of microwave-stimulated reduction, particularly in the *convergence* of *mutually complimentary* factors of processing in non-equilibrium plasma reduction.**

Out of this convergence of processing advantages, **the core experimental microwave reduction programme yielded a fortunate and unbroken range of successful results; these represent the *experimental products* of microwave-stimulated reduction operations.** The more favourable of these deserve mention here, favoured not only by the evident statement of success which they represented, but also because of the feasibility of each to be gainfully developed into real commercial ventures. The initial target mineral was anatase (TiO_2) which was methodically reduced by the carbothermic route with good success, despite the penalties of over-processing, to yield a metal of consistently good purity at initial reduction (given experimental conditions). By any standards, this overall result was a notable achievement, and broadly, it compares favourably with the progress standing of other large-budget government- and industry-sponsored anatase reduction projects of which this author has knowledge. In an operation that was as momentous as it was brief, the thermite reduction of ilmenite to yield a faux-ferrotitanium metallic reduction product was a result that could profitably be converted into industrial application, whether the ferrotitanium was used as an alloying component in steelmaking or as a feedstock for acid dissolution and titanium recovery.

Of special interest to this author was the PDZ-type microwave processing of zircon sand to separate the vitreous SiO_2 fraction from the crystalline ZrO_2 fraction, allowing further processing of each product stream. Also, the reduction results of the obdurate pure oxides ZrO_2 and HfO_2 exhibited encouraging, if minor, conversions to their pure metals. As realised objectives, these two reduction achievements represented the thermochemical pinnacle of project experimentation. Benefiting manifoldly from the microwave process, the convergence of several contemporaneous factors during wodginite reduction determined that the otherwise complex heterogeneity in reduction

remnants was conveniently simplified as metallic Ta/Nb/Ti-carbonitride phase could be digestion-separated from the other metallic phase, Mn-hardhead ($Sn_xMn_yFe_z$), and mechanically separated the slag phase, allowing next stage processing of each phase-group (as dictated by economic recovery factors). The options identified in the experimental work on wodginite present some viable development options that would complement the existing processing route for this complex but valuable mineral of export significance. Across the suite of minerals investigated, both carbothermic and aluminothermic reduction routes were found (collectively) to present a desirable range of process options, and it is considered desirable that other metallothermic routes – particularly those of the industrially relevant Kroll (magnesothermic) route and Hunter (sodothermic) route – should be investigated with respect to the microwave reduction option. In fact, these options may be more "palatable" to Industry than the carbothermic or aluminothermic routes.

Finally, the very simple but instructive disproportionation exercises conducted on common halides represent an allied area of investigation which is wholly complimentary to the subject of this thesis project, and which has ramifications extending widely outside this refractory metals production topic. In a concept that is not new (refer the van Arkel-de Boer process), the short exercises showed the potential of microwave-stimulation to initiate and sustain reductant-free reduction of weakly-bound compounds to yield the pure components. Further noting that it was previously reported in Section **7.5** (after DEMBOVSKY [58], amongst others) that such strongly-bound compounds as transition-metal oxides could be decomposed by microwave or comparably ionised plasma systems. In a world of rapidly changing social and environmental expectations, and of legal obligations, this brief diversion into the related topic of microwave disproportionation holds legitimate, if not significant, promise for future processing in chemical and metallurgical engineering applications.

As yet the Rosetta Stone of plasma physics has not been decoded to the point where full decipherment of plasma thermodynamics and kinetics has allowed a universal understanding of crucial ionisation characteristics within such complex,

intricately balanced and intra-related thermochemical environments. This is particularly the case for the ionisation physics and chemistry initiated in environments under the stimulation of microwave irradiation. A full understanding of the theory and practice of such could be some decades away and it is possible that, like the principles of thermodynamics, the *practice* may be wholly understood before the *theory*, or proof of the theory. Nonetheless, as for other engineering applications, the process implications and resulting reaction products of plasma operations may be learned by rote through application and repetition.

In this work, given the general premise of a desired reaction-route outcome, repeated trials were undertaken to confirm process plausibility and reduction product, thence determine processing potential. Therein, of necessity, experimental trials were undertaken understanding the process outcome and the material consequences of reduction in each case but, inevitably, proceeding *without* a full understanding of contemporaneous process phenomena in the incompletely described thermochemistry of the microwave-stimulated plasma environment. Against broader experimental objectives and within the project outline, such a deficit of process detail was not to be regarded as an experimental millstone; the acquired results were generally in "good agreement" and the experimental programme positively regarded as "gratifyingly" successful. After all, in line with the intent of those objectives, reduction was demonstrated on some of the most highly thermochemically stable minerals known; reduction in light of such mineralogical obduracy was a mark of the considerable processing "power" of the microwave-stimulated reduction set-up and process – an untainted and honest indicator of system potential. Outside of the inevitable proclivity to "over-process", and free of experimental contrivance, metallic reduction product phases were undeniable proof of reduction, and therefore representing *proof of principle* for the microwave reduction system.

Accordingly, the many meaningful experimental results attained were generated across the scope of the experimental programme without expansive knowledge of the theory of the plasma environment, and with incomplete knowledge of all "standard" thermo-physical conditions and variables. The broader legitimacy of such results notwithstanding, and although advancing into the metallurgical "unknown", an over-riding goal of project work was to investigate the *potential* of microwave-stimulated

processing rather than its *limitations*. ["Limitations" here being represented by the encumbered deficiencies in documented *knowledge* of theoretical procedure and process.] Moreover, *apropos* of project merit, it was neither a project objective to investigate the specifics of the thermochemistry of microwave-stimulated plasma systems, nor to define the scientific characteristics and underlying theory of such.

Nonetheless, in reconciling the experimental reduction results with the attributes of microwave-stimulated reduction processing, and in evaluating simple "pros versus cons" validity across the programme, the successful nature of experimental outcomes as demonstrated across the breadth of the experimental programme is deserving of recognition. Indeed, acknowledging the precursory status of the present work's origins, there exists a clear path for an expanded follow-up programme of experimentation seeking further process and product verification, investigating system theory and leading towards an industrially orientated pilot scale programme. A reactor with vacuum, atmosphere control and quench capabilities should be central to such development – current vacuum and gas scrubbing difficulties must be solved or circumvented to achieve this goal. To ensure greatest benefit, the projected pilot plant would be of such output as to be comparatively significant (within 1 to 2 orders of magnitude) against the typical industrial batch output of the magnesothermic Kroll process for any of the relevant refractory metals. Thus, with moderate up-scaling, such a pilot programme would lead seamlessly towards suitable industrial application. Also, consideration of experimental process variables employed in the present work, plus reflection upon in-process behaviour and reduction outcomes for the various reduction routes investigated, leads the author to contemplate a more propitious alternative proposal. Such proposal would address the real possibility of procedurally elevating the present *batch* status of experimental microwave reduction trials towards *continuous batch* or *fully continuous* processes – either advance would represent a noteworthy breakthrough in such a batch-process-based industry, and either alternative route would substantially amplify the output capability for any future extractive metallurgical setting of refractory metal production.

10.2: Concluding Summary.

In the context of the overwhelming worth of Australia's refractory metal mineral exports – and with specific reference to the known value-add and its deplorable "value-add conceded" to "value-add recouped" ratio reflecting irretrievable loss to export – the technological and economic implications arising out of this work are exceptional, and in abiding this exploitation, the societal implications quite remarkable. Moreover, much is to be learned in pursuing the neglected extractive metallurgy of such minerals. The substance of this thesis contains the broad detail of experimental experience of this expansive topic – a topic whose "overview profile" was, across the range, intended to delineate system and process possibilities – keystone engagements for future, more directed research endeavours.

Whilst employing modest experimental techniques throughout the project, the experimental programme provided results that incontestably substantiate the claim that obdurate "oxide" refractory metal minerals can be effectively reduced to metallic form under reaction in a microwave-stimulated, non-equilibrium plasma reduction environment. And further, that such reduction environment can be amply maintained for sufficient processing time; and that such environment can be "contained" within a crucible or other refractory-lined system. Under microwave irradiation, containment of such high temperature environments is facilitated by *susceptibility centring* of the temperature profile *within* the reactants charge (and clear of refractory containment). [Indeed, given this "reversed" temperature profile, the microwave environment would be an ideal candidate in contemplating *containerless processing* initiatives.] In this way, centred within reactants and clear of containment refractories, the "targeting" of applied energy conveys concurrent processing advantages largely characteristic of methods utilising electromagnetic forms of energy input for metallurgical "heating". Such centrally concentrated energy profiles are plainly demonstrable for systems under microwave-irradiated energy input, as in the experimental output of this project where local thermal intensities were self-evident in product phases recovered throughout reduction remnants.

Despite the basic "over-processed" light element impurity of metallic reduction phases, *proof of principle* for the reduction programme of this project is contained most

simply in the confirmed ***fact*** *of reduction* of each *oxide*. Indeed, as a thermochemical accomplishment, the microwave-stimulated reduction of refractory metal oxide minerals to yield metallic products at *any* purity ought not be underestimated. [Such reduction feats are generally not realised under conventional regimes of thermochemistry.] And ultimately, the post-reduction purity of end-product metals is a function of post-reduction process sophistication (including reactor refinement) – purity is not reflected in process exposure beyond the primary reduction interval. Obliquely, the demanding reduction environment created under microwave-stimulation, with its non-equilibrium plasma thermochemistry and "thermal extremes", provided its own "proof of process capability" in that refractory metal oxide minerals of very high thermochemical stability can be pyrometallurgically reduced. The feats of reduction for the suite of oxide minerals of the five nominated refractory metals – titanium, zirconium, hafnium, niobium and tantalum – represent a set of thermochemical statements that ought be fittingly regarded as outstanding indicators of system potential. The bare microwave-stimulated non-equilibrium system devised should similarly be applauded, its propensity recognised, and this merit pursued through meaningful system development toward a refined, operational reduction route.

REFERENCES

and Author Index

REFERENCES .

"A great deal of learning can be packed into an empty head."

Karl Kraus, 1909.

1 Department of the Prime Minister and Cabinet; *Value-Adding in the Australian Minerals Industry.* - Papers presented at the third meeting of the Prime Minister's Science Council. Parliament House, Canberra, 29 October, 1990 - Australian Government Publishing Service, Canberra, 1990.

2 Department of Resources and Energy: *Mineral Sands.* - Department of resources and Energy, Australian government Publishing Service, Canberra, 1986.

3 J. EMSLEY; *The Elements.* - Clarendon Press, Oxford, 1989.

4 R.L. FLEISCHER; *Review: High-strength, high-temperature intermetallic compounds.* - J. Mats. Sci., Vol. **22** , 1987, (pp.2281-2288).

5 R.C. WEAST, D.R. LIDE, M.J. ASTLE and W.H. BEYER (Eds.); *CRC Handbook of Chemistry and Physics. 70th Edition.* - CRC Press, Boca Raton, Florida, 1989.

6 G.L.MILLER; *Metallurgy of the Rarer Metals. 2- - Zirconium. 2nd. Edition.* - Butterworths Scientific Publications, London, 1957.

7 G.L.MILLER; *Metallurgy of the Rarer Metals. 4 - Titanium.* - Butterworths Scientific Publications, London, 1958.

8 G.L.MILLER; *Metallurgy of the Rarer Metals. 6 - Tantalum and Niobium.* - Butterworths Scientific Publications, London, 1959.

9 W.A. KRIVSKY (Ed.); *High Temperature Refractory Metals.* - Gordon and Breach Science Publishers, New York, 1965.

10 E.N. SIMONS; *Guide to Uncommon Metals.* - Frederic Muller Ltd., London, 1967

11 W. KOCK and P. PASCHEN; *Tantalum - Processing, Properties and Applications.* - JOM, October, 1989.

12 J.W. RODGERS; *The Metallurgy of Titanium and Zirconium.,* in *The Metallurgy of the Rarer Metals.* - The Institution of Metallurgists, London, 1952.

13 J.C. CHASTON; *The Metallurgy of Tantalum and Niobium.* - **ibid**.

14 F. RUTLEY (Revised by C.D. GRIBBLE); *Rutley's Elements of Mineralogy. 27th Edition.* - Unwin Hyman, London, 1988.

15 W.J. HOWELL, C.A. ECKERT and R.N. ANDERSON; *Carbothermic Reduction Using Liquid Metal Solvents.* - JOM, July, 1988. pp. 21-23.

16 H.S. RAY and A. GHOSH; *Principles of Extracive Metallurgy. 2nd. Edition.* - John Wiley and Sons (Wiley Eastern Ltd.), New Delhi, 1991.

References

17 L. COUDURIER, D.W. HOPKINS and I. WILKOMIRSKY; *Fundamentals of Metallurgical Processes. 2nd .Edition.* - Pergomon Press, London, 1985.

18 Bureau of Resource Economics; *Mineral Processing in Australia: Potential for Growth in the Mineral Sands, Manganese and Silica Processing Industries.* - Bureau of Resource Economics, Australian Government Publishing Service, Canberra, 1987.

19 I.W. MORLEY; *A History of the Mineral Sand Mining Industry in Eastern Australia.* - University of Queensland Press, St Lucia, 1982.

20 A.F. REID; *Value Adding in the Australian Minerals Industry: the Role of R and D.* - in V.I. LAKSHMANAN, R.G. BAUTISTA and P. SOMASUNDARAN (Eds.); *Emerging Separation Technologies for Metals and Fuels.* - The Minerals, Metals and Materials Society, Warrendale, PA., 1993.

21 A.N. WINCHELL; *Elements of Optical Mineralogy. Part II: Descriptions of Minerals.* - John Wiley and Sons, New York, 1964.

22 W.R. SCHOELLER and A.R. POWELL; *The Analysis of Minerals and Ores of the Rarer Elements.* - Charles Griffin and Co. Ltd., London, 1955.

23 P.G. EMBREY and J.P. FULLER (Eds.); *A Manual of New Mineral Names 1892 - 1978.* - British Museum (Natural History), Oxford University Press, London, 1980.

24 O.C. RALSTON; *Zirconium Ores.* - in American Society for Metals; *Zirconium and Zirconium Alloys.* - A.S.M., Cleveland, Ohio, 1953.

25 H.S. KALISH; *The Preparation of Zirconium Powder.* - **ibid**.

26 M.A. STEINBERG, M.E. SIBERT and E. WAINER; *The Extractive Metallurgy of Zirconium by the Electrolysis of Fused Salts.* - **ibid**.

27 S.M. SHELTON and E.D. DILLON; *The Manufacture of Zirconium Sponge.* - **ibid**.

28 R.T. PRIDER; *Mining in Western Australia.* - University of Western Australia Press, Perth, 1979.

29 C.K. GUPTA and A.K. SURI; *Extractive Metallurgy of Niobium.* - CRC Press, Boca Raton (Florida), 1994.

30 W.D. JAMRACK; *Rare Metal Extraction by Chemical Engineering Techniques.* - Pergamon Press, Oxford, 1963.

31 P. BORCHERS and G.J. KORINEK; *Extractive Metallurgy of Tantalum..* in H.Y. SOHN, O.N. CARLSON and J.T. SMITH (Eds.); *Extractive Metallurgy of Refractory Metals.* - TMS-AIME, Warrendale, Pa., 1980.

32 R.A. GUSTISON; *Process for Recovery of Columbium Values for use in Preparing Columbium Alloy Products.* - **ibid.**

33 D.R. SPINK and K.A. JONASSON; *Separation of $HfCl_4$ and $ZrCl_4$ by Fractional Distillation.* - **ibid.**

34 C.A. PICKLES and S.N. FLENGAS; *The Separation of $HfCl_4$ from $ZrCl_4$ by the Selective Reactivity of $HfCl_4$ vapour with Solid or Molten Alkali Chlorides and Their Mixtures.* - **ibid.**

35 E. FOLEY; *The production of Reactor Grade ZrO_2 and HfO_2.* - **ibid.**

36 T.F. COOK and Y.J. KWON; *Fabrication of Zirconium Alloys.* - **ibid**.

37 J.K. TYLKO, J.J. MOORE and K.J. REID; *Reduction of Lean Chromite Ore Using a New Type Plasma Reactor.* - **ibid**.

38 D.R. SADOWAY and S.N. FLENGAS; *The Thermodynamics of Tantalum/Niobium Separation by Gas-Solid Reaction in Chloride Systems.* - **ibid**.

39 P. HAYES; *Process Principles in Minerals and Materials Production.* - Hayes Publishing Co., Brisbane, 1993.

40 R.H. NIELSEN; *Preparation of Refractory Metals.* - in H.H. HAUSNER and M.G. BOWMAN (Eds.); *Fundamentals of Refractory Compounds.* - Plenum Press, New York, 1968.

41 T. ROSENQVIST; *Principles of Extractive Metallurgy.* - McGraw-Hill Kogakusha, Tokyo, 1974.

42 T.A. HENRIE; *Extractive Metallurgy of Titanium.* - in W.A. KRIVSKY (Ed.); *High Temperature Refractory Metals.* - Gordon and Breach Science Publishers, New York, 1965.

43 A.W. SCHLECHTEN; *Extractive Metallurgy of Zirconium and Hafnium.* - **ibid**.

44 G.W. ELGER and L.H. BANNING; *Producing High-Hafnium Material from Zircon.* - **ibid**.

45 D.R. SPINK, J.W. COOKSTON and J.E. HANWAY,Jr.; *The Fluidised-bed Chlorination of Zirconium-bearing Materials.* - **ibid**.

46 A.C. GOODRICH and D.R. SPINK; *Hafnium Electrorefining.* - **ibid**.

47 T. NODA: *Titanium from Slags in Japan.* - **ibid**.

48 C.F. RERAT; *High-Temperature Inert-Gas Purification of Refractory Metals Compacts.* - **ibid**.

49 KN.C. LIDDELL, D.R. SADOWAY and R.G. BAUTISTA (Eds.); *Refractory Metals Extraction, Processing and Applications.* Proc. symposium of Reactive Metals Committee of TMS, New Orleans, Feb., 1991. - The Minerals, Metals and Materials Society, Warrendale, Pa., 1991.

50 P. PASCHEN, A. ANZINGER and H. FEICHTNER; *Titanium - A Techno-Commercial Evaluation of the Reduction Process.* - in KN.C. LIDDELL, D.R. SADOWAY and R.G. BAUTISTA (Eds.); *Refractory Metals Extraction, Processing and Applications.* Proc. symposium of Reactive Metals Committee of TMS, New Orleans, Feb., 1991. - The Minerals, Metals and Materials Society, Warrendale, Pa., 1991.

51 F.K. OJEBUOBOH and G.P. MARTINS; *Thermal Plasma Technology in the Extractive Metallurgy of Titanium.* - **ibid**.

52 P. PASCHEN and W KOECK; *Fused Salt Electrolysis of Tantalum.* - **ibid**.

53 A.P. LAMAZE and D. CHARQUET; *Development of Hafnium Chloride Electrolysis.* - **ibid**.

54 I. GABALLAH, E. ALLAIN and M.CH. MEYER-JOLY; *Leaching of Tin Slags and Subsequent Chlorination of the Tantalum and Niobium Concentrate.* - **ibid**.

55 C.K. GUPTA and T.S. KRISHNAN; *Production Technology of Zirconium and Aluminium - Zirconium Master Alloy - Development Work at the Bhabha Atomic Research Centre.* - **ibid**.

56 M.V. KLEIN and R.G. REDDY; *Kinetics of Reduction of Chromite with Carbon.* - **ibid**.

57 J.K.R. WEBER, S. KRISHNAN and P.C.NORDINE; *Containerless Processing of Refractory Metals.* - **ibid**.

58 V. DEMBOVSKY; *Plasma Metallurgy: The Principles.* (Translated by J. Freundlich) - Elsevier, Amsterdam, 1985.

References

59 R. M^{C}PHERSON and B.V. SHAFER; *Spherulites and Phase Separation in Plasma-Dissociated Zircon.* - J. Mats. Sci., Vol. **19**, 1984 (pp. 2696-2704).

60 C.B. ALCOCK; *Principles of Pyrometallurgy.* - Academic Press, London, 1976.

61 J.D. GILCHRIST; *Extraction Metallurgy: 2nd. Edition.* - Pergamon Press, Oxford, 1980.

62 - G.S. UPADHYAYA and R.K. DUBE; *Problems in Metallurgical thermodynamics and Kinetics.* Pergamon Press, Oxford, 1982.

63 H.J.T. ELLINGHAM; - J. Soc. Chemistry Industry, London, Vol. **63**, No. 125, 1944.

64 F.D. RICHARDSON and J.H.E. JEFFES; *The Thermodynamics of Substances of Interest in Iron and Steel Making from 0°C to 2400°C: I - Oxides.* - J. Iron and Steel Inst., British Iron and Steel Research Assn., Vol. **160**, November, 1948.

65 D.R. GASKELL; *Introduction to Metallurgical Thermodynamics.* - McGraw-Hill Kogakusha, Tokyo,1973.

66 P.M. MORSE; *Thermal Physics. 2nd.Edition.* - W.A. Benjamin, New York, 1969.

67 O. LEVENSPIEL; *Chemical Reaction Engineering. 2nd. Edition.* - John Wiley and Sons, New York, 1972.

68 T.A. ENGH; *Principles of Metal Refining.* - Oxford University Press, Oxford, 1992.

69 F. HELFFERICH; *Ion Exchange.* - M^{c}Graw-Hill, New York, 1962.

70 S. GLASSTONE, K.J. LAIDLER and H. EYRING; *The Theory of Rate Processes.* - McGraw-Hill Book Company, New York, 1941.

71 J. SZEKELY; *An Overview of Plasma Processing.* - in J. SZEKELY and D. APELIAN (Eds.); *Plasma Processing and Synthesis of Materials.* - Materials Research Society symposia procs., North-Holland (Elsevier Science Publishing Co.), New York, 1984.

72 E. PFENDER; *Plasma Generation.* - **ibid**.

73 W.C. ROMAN; *Thermal Plasma Melting/Remelting Technology.* - **ibid**.

74 W.H. GAUVIN and H.K. CHOI; *Plasmas in Extractive Metallurgy.* - **ibid**.

75 K.J. REID, J.J. MOORE and J.K. TYLKO; *In-Flight Metal Extraction in a Novel Plasma Reactor.* - **ibid**.

76 Yu.L. KHAIT; *Non-Equilibrium Modelling and Dissipative Structures in Solid Material Plasma Interactions.* - **ibid**.

77 B. LUSTMAN and F. KERZE (Eds.): *The Metallurgy of Zirconium.* (1st Edn.) - McGraw-Hill Book Co., Inc., New York, 1955.

78 P. MOLLER, P. CERNY and F. SAUPE (Eds.); *Lanthanides, Tantalum and Niobium.. - Proceedings of a workshop in Berlin, November 1986.* - Springer-Verlag, Berlin, 1989.

79 J.R. DAVIS (Ed.): *ASM Specialty Handbook: Heat-Resistant Materials.* - The Materials Information Society (ASM International), Materials Park, OH., 1997.

80 - B. ELIASSON and U. KOGELSCHATZ; *Nonequilibrium Volume Plasma Chemical Processing.* IEEE Transactions on Plasma Science, Vol. **19**, No. 6, Dec., 1991 (pp. 1063-1077).

References

81 J.H. INGOLD; *Anatomy of the Discharge*. - in M.N. HIRSH and H.J. OSKAM; *Gaseous Electronics, Vol. 1.* - Academic Press, New York, 1978.

82 A. GARSCARDDEN; *Ionization Waves in Glow Discharges.* - **ibid**.

83 A.D. MacDONALD and S.J. TETENBAUM; *High Frequency and Microwave Discharges.* - **ibid**.

84 M. GOLDMAN and A. GOLDMAN; *Corona Discharges.* - **ibid**.

85 E. PFENDER; *Electric Arcs and Arc Gas Heaters.* - **ibid**.

86 D.M.P. MINGOS and D.R. BAGHURST; *The Application of Microwaves to the Processing of Inorganic Materials.* - British Ceramic, Vol. **91**, No. 4, 1992, (pp.124 - 127).

87 F.K. M^{c}TAGGART; *Plasma Chemistry in Electrical Discharges.* - Elsevier, London, 1967.

88 L.S. POLAK; *Kinetics and Thermodynamics of Chemical Reactions in Low-Temperature Plasma.* - Nauka, Moscow, 1965.

89 R.F. BADDOUR and R.S. TIMMINS; *The Application of Plasma to Chemical Processing.* - MIT Press, Cambridge, Mass., 1967.

90 M.I. BOULOS; *Thermal Plasma Processing.* - IEEE Transactions on Plasma Science, Vol. **19**, No. 6, Dec., 1991 (pp.1078 - 1089).

91 W.A.G. VOSS and H.K. KUA: *Model-Informed Microwave Processing of Materials.* - in W.B. SNYDER, Jr., W.H. SUTTON, M.F. ISKANDER and D.L. JOHNSON (Eds.); *Microwave Processing of Materials II.* - M.R.S. Symposium Procs. Vol.189, Materials Research Society, Pittsburgh, 1990.

92 G.E. FANSLOW; *Microwave Enhancement of Chemical and Physical Reactions.* - **ibid**.

93 J.B. SALSMAN and S.P. HOLDERFIELD; *A Unique Application of a Microwave Plasma for Material Synthesis.* - **ibid**.

94 M.F. ISKANDER: *Computer Modelling and Numerical Techniques for Quantifying Microwave Interactions with Materials.* - **ibid**.

95 F. HELIODORE, D. COTTEVIEILLE and A. LE MEHAUTE; *Anomolous Behaviour of Heterogeneous Materials at Microwave Frequencies: Introduction to Fractional Derivatives in Electromagnetism.* - **ibid**.

96 V.M. KENKRE, L. SKALA, M.W. WEISER and J.D. KATZ; *Theory of Microwave Effects on Atomic Diffusion in Sintering: Basic Considerations of the Phenomenon of Thermal Runaway.* - **ibid**.

97 E.E. EVES and R.L. SNIDER; *Preliminary Thermal Model for High Temperature Processing Using Microwave Energy.* - **ibid**.

98 J.B. SALSMAN; *Technique for Measuring the Dielectric Properties of Minerals as a Function of Temperature and Density at Microwave Heating Frequencies.* - **ibid**.

99 D.E. BULLARD and D.C. LYNCH; *Processing of Refractory Ores in a Microwave Induced "Cold" Plasma.* - in R.L. BEATTY, W.H. SUTTON and M.F. ISKANDER (Eds.); *Microwave Processing of Materials III.* - M.R.S. Symposium Proceedings Vol. 269, Materials Research Society, Pittsburgh, 1992.

100 J.H. BOOSKE, R.F. COOPER, L. McCAUGHAN, S. FREEMAN and B. MENG; *Studies of Nonthermal Effects During Intense Microwave Heating of Crystalline Solids.* - **ibid**.

References

101 M.A. JANNEY, H.D. KIMREY and J.O. KIGGANS; *Microwave Processing of Ceramics: Guidelines Used at the Oak Ridge National Laboratory.* - **ibid**.

102 M. MITCHNER and C.H. KRUGER; *Partially Ionized Gases.* - John Wiley and Sons, New York, 1973.

103 T.H. STIX; *The Theory of Plasma Waves.* - McGraw-Hill Book Co., New York, 1962.

104 D.C. MONTGOMERY and D.A. TIDMAN; *Plasma Kinetic Theory.* - McGraw-Hill Book Co., New York, 1964.

105 A.C. METAXIS and R.J. MEREDITH; *Industrial Microwave Heating.* - Peter Peregrinus Ltd., London, 1983.

106 W.R. TINGA; *Design Principles for Microwave Heating and Sintering.* - in Y. CHEN (Ed.); *Defect Properties and Processing of High-Technology Non-Metallic Materials.* - Materials Research Society, Pittsburgh, 1986.

107 F. PAOLONI, personal communication with, February, 1989 - associate professor, Department of Electrical and Computer Engineering, University of Wollongong, N.S.W., Australia.

108 J.A. BELK; *Vacuum Techniques in Metallurgy.* - Pergamon Press Ltd., Oxford, 1963.

109 D.S. PYUN and E.W. COLLINGS; *Self-Rectifying Electron Beam Melting Technique.* - in W.H. HOFMEISTER and R. SCHIFFMANN (Eds.); *Containerless Processing.* - The Minerals, Metals and Materials Society, Warrendale, PA., 1993.

110 A.D. HELMS and C.M. O'BRIEN: *Advances in Melting Technology for High-Temperature Alloys.* - JOM, Vol. **50**, No. 3, March, 1998, The Minerals, Metals and Materials Society, Warrendale, Pa., (p. 12).

111 T. YAHATA, T. IKEDA and M. MAEDA; *Deoxidation of Molten Titanium by Electron-Beam Remelting Technique.* - Metallurgical Tranactions B, (TMS), Vol. **24B**, Aug., 1993 (pp. 599-604).

112 I. DRANGEL and G.T. MURRAY; *Parameters Pertinent to Purification by Electron Beam Zone Refinement.* - in R.W. FOUNTAIN, J. MALT and L.S. RICHARDSON (Eds.); *High Temperature Refractory Metals.* - Met. Soc. Conf. Vol. **34**, Gordon and Breach Science Pub., New York, 1966.

113 D. APELIAN; *Materials Synthesis: A New Horizon for Plasma Processing.* - in N. EL-KADDAH (Ed.); *Thermal Plasma Applications in Materials and Metallurgical Processing.* - The Minerals, Metals and Materials Society, Warrendale, Pa.,1992.

114 J.R. FINCKE, T.E. REPETTI, S.C. SNYDER, G.D. LASSAHN and B.A. DETERING; *Departure From Equilibrium in Atmospheric Pressure Thermal Plasmas.* - **ibid**.

115 R.A. ORTEGA, D.E. BULLARD, D.C. LYNCH and W.G DAVENPORT; *Emissivity Determinations for Non-Contact Temperature Measurements in Non-Equilibrium Plasma Processing.* - **ibid**.

116 S.L. COMACHO; *Plasma Melting/Smelting and Refining.* - **ibid**.

117 D.E. BULLARD, D.C. LYNCH and W.G. DAVENPORT; *Non-Equilibrium Plasma Processing of Ores.* - **ibid**.

118 P.R. TAYLOR, M. ABDEL-LATIF, S.A. PIRZADA and X. HOU; A Non-Transferred Arc, Thermal Plasma Cyclone Reactor. - **ibid**.

119 T. KITAMURA, K. SHIBATA and K. TAKEDA; *In-Flight Reduction of Fe_2O_3, Cr_2O_3, TiO_2 and Al_2O_3 by Ar-H_2 Plasma.* - **ibid**.

References

120 J.K.S. WAN, N.J. COWLEY, M.S. IOFFE and S.D. POLLINGTON; *High-Power Pulsed RF Decomposition of Ore Samples with a Carbon Source.* - J. Microwave Power and Electromagnetic Energy (Int. Microwave Power Inst.),Vol. **31**, No. 1, 1996, (pp.54-58).

121 S.L. McGILL and J.W. WALKIEWICZ; *Applications of Microwave Energy in Extractive Metallurgy.* - J. Microwave Power and Electromagnetic Energy (Int. Microwave Power Inst.), Symposium Summaries, 1987.

122 T. KITAMURA, K. SHIBATA and K. TAKEDA; *In-Flight Reduction of Fe_2O_3 , Cr_2O_3 and Al_2O_3 by Ar-H_2 and Ar-CH_4 Plasma.* - ISIJ International, Vol. **33**, No. 11, 1993 (pp.1150 - 1158).

123 C.A. PICKLES; *In-Flight plasma Reduction of Metal Oxides.* - Journal of Metals (TMS), December, 1988 (pp. 31 - 35).

124 R.K. RAINS and R.H. KADLEC; *The Reduction of Al_2O_3 to Aluminium in a Plasma.* - Metallurgical Transactions (TMS), Vol. **1**, June, 1970 (pp. 1501 - 1506).

125 K. GIESEN and W. DAUTZENBERG; *Untersuchungen zur Aluminothermischen Gewinnung von Ferrotitan. (Investigations of the Thermite Process for the Production of Ferrotitanium.)* - Stahl und Eisen, Vol. **68**, April 22, 1948.

126 P. GROSS; *Extraction of Pure Titanium from Ferro-Titanium.* - in J.H.E. JEFFES and R.J. TAIT (Eds.); *Physical Chemistry of Process Metallurgy: The Richardson Conference.* - The Inst. of Mining and Metallurgy, london, 1974.

127 D.R. MARTIN and P.J. PIZZOLATO; *Hafnium.* - in C.A. HAMPEL (Ed.); *Rare Metals Handbook.* - Reinhold Publishing Corpn., New York, 1954.

128 L.F. YNTEMA and A.L. PERCY; *Tantalum and Columbium.* - **ibid**.

129 H.R. OGDEN and B.W. GONSER; *Titanium.* - **ibid**.

130 A.W. SCHLECHTEN; Zirconium. - **ibid**.

131 C.A. HAMPEL; Physical Properties of Metals. - **ibid**.

132 M. HOCH: *Winning and Refining.* - in R.I. JAFFEE and H.M. BURTE (Eds.): *Titanium Science and Technology. -Volume 1* - The Metallurgical Society of AIME, Plenum Press, New York, 1973.

133 N. STANDISH and H.K. WORNER; *Microwave Application in the Reduction of metal Oxides with Carbon.* - J. Microwave Power and Electromagnetic Energy (Int. Microwave Power Inst.), Vol. **25**, No. 3, 1990 (pp. 177 - 180).

134 S.W. EL-TAWIL, I.M. MORSI and A.A. FRANCIS; *Kinetics of Solid-State Reduction of Ilmenite Ore.* - Canadian Metallurgical Quarterly (Pergamon Press), Vol. **12**, No. 4, 1993 (pp. 181 - 188).

135 M.E. EL-GUINDY and W.G. DAVENPORT; *Kinetics and Mechanism of Ilmenite Reduction with Graphite.* -Metallurgical Transactions (TMS), Vol. **1**, June, 1970 (pp. 1729 - 1734).

136 M. PAJUNEN and J. KIVILAHTI; *Thermodynamic Analysis of theTitanium - Oxygen System.* - Z. Metallkd., (CarlHanser Verlag, Munchen), **83** (1992)1 (pp. 17-20).

137 S.K. GUPTA, V. RAJAKUMAR and P. GRIEVESON; *The Influence of Weathering on the Reduction of Ilmenite with Carbon.* - Metallurgical Tranactions B, (TMS), Vol. **20B**, Oct., 1989 (pp. 735-745).

138 J.P. BONSACK; *Entrained-Flow Chlorination of Ilmenite to Produce Titanium Tetrachloride and Metallic Iron.* - Metallurgical Tranactions B, (TMS), Vol. **23B**, June, 1992 (pp. 261-266).

References

139 W.K. TOLLEY, R.M. IZATT and J.L. OSCARSON; *Titanium Tetrachloride-Supercritical Carbon Dioxide: A Solvent Extraction and Thermodynamic Study.* - Metallurgical Transactions B, (TMS), Vol. **23B**, Feb., 1992 (pp. 65-71).

140 S.K. JAIN, P.M. PRASAD and P.K. JENA; *Preparation of Titania from Ilmenite by Selective H_2S Sulfidization.* - Metallurgical Transactions (TMS), Vol. **1**, June, 1970 (pp. 1527 - 1530).

141 R.A. HALL and G.V. GLAUM; *Simultaneous Solubilizing and Pelletizing - U.S. Patent 4,247,523 (1981)* - from M.J.COLLIE (Ed.); *Extractive Metallurgy: Developments Since 1980.* - Noyes Data Corp., Park Ridge, N.J., 1984.

142 J.A. RAHM and D.G. COLE; *Manufacturing Titanium Compounds Using a Reducing Agent. - U.S. Patent 4,288,415 (1981)* - **ibid**.

143 G. MAGALHAES; *Obtaining Anathase Concentrates. - U.S. Patent 4,256,266 (1981)* - **ibid**

144 J.P. BONSACK; *Low Temperature, Fluid Bed Process. - U.S. Patent 4,310,495 (1982)* - **ibid**.

145 W.K. TOLLEY and W.C. LAUGHLIN; *Extraction with Organophosphoric Acid. - U.S. Patent 4,269,809 (1981)* - **ibid**.

146 R.A.HARD and M.A. PRIETO; *Conversion to Fluorides. - U.S. Patent 4,390,365 (1983)* - **ibid**.

147 H. MEYER; *Recovery of Hydrofluoric Acid. - U.S.Patent 4,309,389 (1982)* - **ibid**.

148 A. TAMARU and M. KITSUNAI; *Use of Sulphuric Acid in Producing Tantalum Concetrates. - U.S. Patent 4, 302,243 (1981)* - **ibid**.

149 M. QUABDESSELAM and Z.A. MUNIR; *The Sintering of Combustion-Synthesized Titanium Diboride.* - J. Materials Science (Chapman and Hall), Vol. **22**, 1987 (pp. 1799 - 1807).

150 P.R. TAYLOR and S.A. PIRZADA; *An Investigation of Silicon Carbide Synthesis in a Nontransferred Arc Thermal Plasma Reactor.* - Metallurgical Transactions B (TMS), Vol. **23B**, Aug., 1992 (pp. 443 - 448).

151 K. TANAKA, K. ISHIZAKI, S. YUMOTO and T. EGASHIRA; *Production of Ultra-Fine Silicon Powder by the Arc Plasma Method.* - J. Mats. Sci., Vol. **22**, 1987 (pp. 2192- 2198).

152 R. CLAUDE, M. MOISAN and M.R. WERTHEIMER; *RF and Microwave Plasma Deposition of Polymer Films: Effect of Frequency.* - in J.W. COBURN, R.A. GOTTSCHO and D.W. HESS (Eds.); *Plasma Processing.* - Materials Research Society, Pittsburgh, 1986.

153 Y. TESSIER, J.E. KLEMBERG-SAPIEHA, S. POULIN-DANDURAND and M.R. WERTHEIMER; - *Silicon Nitride from Microwave Plasma: Fabrication and Characterization.* - **ibid**.

154 S.B. MARGOLIS, B.J. MATKOWSKY and M.R. BOOTY; *New Modes of Quasiperiodic Burning in Combustion Synthesis.* - in Z.F MUNIR and J.B. HOLT (Eds.); *Combustion and Plasma Synthesis of High-Temperature Materials.* - VCH Publishers Inc., New York, 1990.

155 V. HLAVACEK, P. DIMITRIOU, J. DEGREVE and J. SCHOLTZ; *Modelling of SHS Operations.* - **ibid**.

156 R. ARMSTRONG and M. KOSZYKOWSKI; *Combustion Theory for Sandwiches of Alloyable Materials.* - **ibid**.

157 Y. KAIEDA, M. OTAGUCHI and N. OGURO; *Combustion Synthesis of Intermetallic Compounds.* - **ibid**.

158 B.H. RABIN, A.BOSE and R.M. GERMAN; *Combustion Synthesis of Nickel Aluminides.* - **ibid**.

References

159 H.C. YI and J.J. MOORE; Self-Propagating High-Temperature Synthesis of NiTi Intermetallics. - **ibid**.

160 S.J. WORK, L.H. YU, N.N. THADHANI, M.A. MEYERS, R.A. GRAHAM and W.F. HAMMETTER; *Shock-Induced Chemical Synthesis of Intermetallic Compounds.* - **ibid**.

161 L.L. WANG, Z.A. MUNIR and J.B. HOLT; *Combustion Synthesis of Oxide-Carbide Composites.* - **ibid**.

162 R. WARD, N. THADHANI and P.-A. PERSSON; *Shock-Induced Reaction Synthesis-Assisted Processing of Ceramics.* - **ibid**.

163 S. OTANI, T. TANAKA and Y. ISHIZAWA; *Preparation of a Single Crystal by the Floating-Zone Method from a Self-Combustion Rod.* - **ibid**.

164 T. YOSHIDA; *Thermal Plasma Synthesis of Ceramic Powders and Coatings.* - **ibid**.

165 J.W. McKELLIGET and N. EL-KADDAH; *A Theoretical Comparison of Conventional and Hybrid RF-Plasma Reactors.* - **ibid**.

166 S.L. GIRSHICK and C.-P. CHIU; *Homogeneous Nucleation and Growth in Thermal Plasma Synthesis.* - **ibid**.

167 M. YOSHIMURA, M. NISHIOKA and S. SOMIYA; *Rapid Preparation of Titanium and Other Transition-Metal Nitride and Carbide Powders by a Carbo-Reduction Method Using Arc-Image Heating.* - **ibid**.

168 S.M. KNITTEL and S.H. RISBUD; *Microwave Plasma Densification of Aluminium Nitride.* - **ibid**.

169 P.C. KONG and E. PFENDER; *Plasma Synthesis of Fine Powders by Counter-Flow Liquid Injection.* - **ibid**.

170 J.S. McFEATERS and J.J. MOORE; *Application of Nonequilibrium Gas-Dynamic Techniques to the Plasma Synthesis of Ceramic Powders.* - **ibid**.

171 J.J. MOORE; *Plasma Synthesis of Iron and Chromium Carbides by Carbothermic Reduction of Their Mineral Oxides.* - **ibid**.

172 W.C. ROMAN, J.H. STUFFLEBEAM, A.C. ECKBRETH and C.J. ULTEE; *Laser Diagnostics of Plasma Species in PACVD Deposition of Hard-face Coatings.* - **ibid**.

173 J.S. HAGGERTY and FLINT; *Synthesis of Si, SiC and Si_3N_4 Powders under High Number Density Conditions.* - **ibid**.

174 M. COSTANTINO and J.B. HOLT; *High-Pressure Burning Rate of Silicon in Nitrogen.* - **ibid**.

175 P.V. ANANTHAPADMANABHAN, K.P.SREEKUMAR, K. IYER and N. VENKATRAMANI; *Plasma Thermal Dissociation of Indian Zircon.* - J. Alloys and Compounds (Elsevier Sequoia), Vol. **196**, (JALCOM 620), 1993 (pp. 251 - 254).

176 G.M. MARTINEZ and D.E. COUCH; *Electrowinning of Zirconium from Zirconium Tetrachloride.* - Metallurgical Transactions (TMS), Vol. **3**, February, 1972 (pp. 571 - 574).

177 A. LANDSBERG, C.L. HOATSON and F.E. BLOCK; *The Chlorination Kinetics of Zirconium Dioxide in the Presence of Carbon and Carbon Monoxide.* - Metallurgical Transactions (TMS), Vol. **3**, February, 1972 (pp. 517 - 523).

178 M.A. LIEBERMAN, G.S. SELWYN and M. TUSZEWSKI; *Plasma Generation for Materials Processing.* - MRS Bulletin, Materials Research Society, Vol.**21**, No.8, August, 1996 (pp.32 - 37).

References

179 G. COLLINS and D.J. REJ; *Plasma Processing of Advanced Materials.* - **ibid**, (pp. 26 - 27).

180 M. BOULOS and E. PFENDER; *Materials Processing With Thermal Plasmas.* - **ibid**.

181 H.K. WORNER, personal communication with, January, 1997 - honorary professor, Department of Materials Engineering, University of Wollongong, N.S.W., Australia.

182 D.D. BOESIGER and F.D. STEVENSON; *Kinetics of the Vapor Phase Chlorination of Niobium Oxychloride by Phosgene.* - Metallurgical Transactions (TMS), Vol. **1**, July, 1970 (pp. 1859 - 1861).

183 Y.V. BYKOV and V.E.SEMENOV: *Processing of Material Using Microwave Radiation.* - in A.V. GAPONOV-GREKHOV and V.L. GRANATSTEIN (Eds.): *Applications of High-Power Microwaves.* - Artech House, Boston, 1994.

184 J.D. FAST; *Entropy. 2nd. Edition.* - Macmillan and Co., London, 1970.

185 R.O. DAVIES; *Irreversible changes: New Thermodynamics from Old.* - Science News 28,1954, (pp.41-45).

186 L. VAN HOVE; *Lectures on Statistical Mechanics of Non Equilibrium Phenomena.* in C. DE WITT and J.F. DETOEUF; *La Theorie des Gas Neutres et Ionisés.* - Hermann, Paris, 1960.

187 D.A. FRANK-KAMENETSKII; *Plasma: the Fourth State of Matter.* (trans. J. Norwood) - Plenum Press, New York, 1972.

188 B.M. SMIRNOV; *Introduction to Plasma Physics.* - Translated by O. Glebov, Mir Publishers, Moscow, 1977.

189 B. CHAPMAN; *Glow Discharge Processes - Sputtering and Plasma Etching.* - John Wiley and Sons, New York, 1980.

190 P.M. PLATZMAN and P.A. WOLFF; *Waves and Interactions in Solid State Plasmas.* - Academic Press, New York, 1973.

191 M.F. HOYAUX; *Solid State Plasmas.* - Pion Limited, London, 1970.

192 A.A. GALEEV and R.N. SUDAN (Eds.); *Handbook of Plasma Physics; Vol. 1: Basic Plasma Physics I.* - North-Holland Publishing Company, New York, 1983.

193 F.F. CHEN; *Introduction to Plasma Physics.* - Plenum Press, New York.

194 G. BEKEFI; *Radiation Processes in Plasmas.* - John Wiley and Sons Inc., New York, 1966.

195 M.F. HOYAUX; *Arc Physics.* - Springer-Verlag, New York, 1968.

196 G.J. SCHULZ; *Vibrational Excitation of Molecules via Shape Resonances.* - in J.W. McGOWAN and P.K. JOHN (Eds.); *Gaseous Electronics: Some Applications.* - North-holland Puplishing Company, Amsterdam, 1974.

197 J. UHLENBUSCH; Non-Equilibrium Effects in Arc Discharges. - **ibid**.

198 E. NASSER; *Fundamentals of Gaseous Ionization and Plasma Electronics.* - Wiley-Interscience, New York, 1971.

199 M.L. PASSOW, M.L. BRAKE, P. LOPEZ, W.B. Mc COLL and T.E. REPETTI; *Microwave Resonant-Cavity-Produced Air Discharges.* - IEEE Transactions. on Plasma Science, Vol. **19**, No. 2, April,1991 (pp. 219 - 228).

References

200 R.H. CHURCH, W.E. WEBB and J.B. SALSMAN: *Dielectric Properties of Low Loss Minerals.* - United States Department of the Interior / Bureau of Mines and University of Alabama, Tuscaloosa, 1987.

201 F.E. GARDIOL: *Introduction to Microwaves.* - Artec House, 1984.

202 I. BUNGET and M. POPESCU; *Physics of Solid Dielectrics.* Materials Science Monographs, 19 - Elsevier, Amsterdam, 1984.

203 J.F. LEE, F.W. SEARS and D.L. TURCOTTE; *Statistical Thermodynamics.* 2nd. Edn. - Addison-Wesley Publishing Company, Inc., Reading, Ma. , 1973.

204 I.R. CHABINSKY nnd E.E. EVES: *The Application of Microwave Energy in Drying, Calcining and firing of Ceramics.* - Interceram, No 6, 1986 (pp. 30 - 35).

205 M. GASGNIER, L. ALBERT, J.DEROUET, L. BEAURY, A. LOUPY, A. PETIT and P. JACQUAULT; *Chemical Synthesis by Means of Microwave Digestion as a Focused Open-Vessel System: Structural Properties of Oxides and Hydroxides as Powders.* - J. Alloys and Compounds (Elsevier-Sequoia), Vol. **198**, (JALCOM 649),1993 (pp. 73 - 83).

206 R.F. SCHIFFMAN: *Principles of Industrial Microwave and RF Heating.* – in D.E. CLARK, W.H. SUTTON and D.A. LEWIS (Eds.) - *Microwaves: Theory and Application in Materials Processing IV. [First World Congress on Microwave Processing.]* – The American Ceramic Society, Westerville, Ohio, 1997.

207 D.E. CLARK, W.H. SUTTON and D.A. LEWIS: *Microwave Processing of Materials.* – **ibid**.

208 M. WILLERT-PORADA: *A Microstructural approach to the origin of "Microwave Effects" in Sintering of Ceramics and Composites.* – **ibid**.

209 R.N.GEDYE: *The Question of Non-Thermal Effects in the Rate Enhancement of Organic Reactions by Microwaves.* – ***ibid.***

210 W.V. CORSO and J. M IJOVIC: *Comparison of Microwave and Thermal Reaction Kinetics Via In-Situ FTIR Spectroscopy.* – **ibid**.

211 D. ATONG and D.E. CLARK: *The Effect of Reaction Parameters on Microwave-Induced Combustion Synthesis of AlO2O3-TiC Composite Powders.* in D.C. FOLZ, J.H. BOOSKE, D.E. CLARK and J.F. GERLING: *Proceedings of the Third World Congress on Microwave and Applications, 2002, Sydney, Australia.]* – The American Ceramics Society, Westerville, Ohio, 2003.

212 N. TRAN: *Successful Microwave Processing Applications in Industry.* - **ibid**.

213 S.A. FREEMAN, J.H. BOOSKE and R.F. COOPER: *Novel Method for Measuring Intense Microwave Radiation Effects on Ionic Transport in Ceramic Materials.* – American Inst. Phys., Rev. Sci. Instrum. 66 (**6**), June, 1995.

214 B.S. TERRY and P. GRIEVESON; *Some Anecdotes about the Production of Carbides and Nitrides.* - in B.C.H. STEELE(Ed.); *High Temperature Materials Chemistry: The Charles Benjamin Alcock Symposium.* - The Institute of Materials, (Bourne Press Ltd.), London, 1995.

215 A. CHRYSANTHOU; *Self-Propagating High Temperature Synthesis of Al_2O_3 - TiC and Al_2O_3 - TiB_2 Composites.* - **ibid**.

216 I.D. SOMMERVILLE and A. McLEAN; *Plasma Enhanced Reactions.* - **ibid**.

217 F.P. TULLY; *The Study of Gas-Phase Chemical Reactions.* - in H.S.W. MASSEY, E.W. McDANIEL and B. BEDERSON (Eds.); *Applied Atomic Collision Physics. Volume 5: Special Topics.* - Academic Press, New York, 1982.

References

218 A. FRONTIJN; *Combustion and Flames.* - **ibid**.

219 C. EMILIANI; *Dictionary of the Physical Sciences.* Oxford University Press, New York, 1987.

220 R.C. BISHOP and H. ATMANSPACHER; - *Contextural Emergence in the Description of Properties* in *Foundations of Physics.* Vol. **36**, No. **12**, December, 2006.

221 L.B. LOEB; *Basic Processes of Gaseous Electronics. 2nd. Edition.* - University of California Press, Berkeley, 1961.

222 R.N. FRANKLIN; *Plasma Phenomena in Gas Discharges.* - Clarendon Press, Oxford, 1976.

223 R. MARX; *Energetics and Dynamics of Ion-Molecule Reactions at Thermal Energies.* - in M.A. ALMOSTER-FERREIRA (Ed.); *Ionic Processes in the Gas Phase.* - D. Reidel Publishing Co., Dordrecht, 1984.

224 T. BAER; *Dissociation Dynamics of Energy Selected Ions Studied by One and Multiphoton Ionization.* - **ibid**.

225 B.J. GREEN; *Overview and Survey of Plasma Physics.* - in R.D. GILL; *Plasma Physics and Nuclear Fusion Research.* - Academic Press, London, 1981.

226 R.J. HASTIE; *Introduction to Plasma Physics.* - **ibid**.

227 R.W.P. M^{c}WHIRTER; Plasma Radiation. - **ibid**.

228 G. HÖRZ; *Mechanisms and Kinetics of Absorption and Desorption Reactions in Systems of Refractory Metals with Nitrogen, Oxygen or Carbon.* - Metallurgical Transactions, (TMS),Vol. **3,** December, 1972, (pp. 3069 - 3076).

229 W.C. GARDINER and J. TROE; *Ch.4: Rate Coefficients of Thermal Dissociation, Isomerization, and Recombination Reactions.* - in W.C. GARDINER, Jr. (Ed.); *Combustion Chemistry.* - Springer-Verlag, new York, 1984.

230 N.J. THEMELIS; *Techniques of Process Analysis in Extractive Metallurgy.* - Metallurgical Transactions, (TMS),Vol. **3,** August, 1972, (pp. 2021 - 2029).

231 M.W. BLADES, P. BANKS, C. GILL, D. HUANG, C. Le BLANC and D. LIANG; *Applications of Weakly Ionised Plasmas for Materials Sampling and Analysis.* - IEEE Trans. on Plasma Science, IEEE, Vol. **19**, No. 6, Dec., 1991.

232 F.D. RICHARDSON; *Physical Chemistry of Melts in Metallurgy.* Vols. 1 and 2 - Academic Press, London, 1974.

233 I.H. LOH, R.E. COHEN and R.F. BADDOUR; *Modification of Carbon Surfaces in Cold Plasmas.* - J. Materials Science (Chapman and Hall), Vol. **22**, 1987 (pp. 2937 - 2947).

234 E. FROMM and H. JEHN; *Thermodynamics and Phase Relations in Refractory Metal Solid Solutions Containing Carbon, Nitrogen, and Oxygen.* - Metallurgical Transactions, (TMS),Vol. **3,** July, 1972, (pp. 1685 - 1692).

235 F. HABASHI; *Principles of Extractive Metallurgy. Vol. 3: Pyrometallurgy.* - Gordon and Breach, New York, 1969.

236 C.M.B. WALKER, A.H. HUIZINGA, W.A. VOSS and W.R. TINGA; *A System for Controlled Microwave Heating of Small Samples.* - J. Microwave Power (Int. Microwave Power Inst.), Vol. **11**, No. 1, March, 1976 (pp.29-32).

237 E. KARMAZSIN, R. BARHOUMI and P. SATRE; *Thermal Analysis with Microwaves: Temperature and Power Control.* - J. Thermal Analysis, Vol. 29, 1984 (pp.1269-1277).

References

238 J.R. FINKE, W.D. SWANK and C.L. JEFFERY; *Simultaneous Measurement of particle Size, Velocity, and Temperature in Thermal Plasmas.* - IEEE Transactions. on Plasma Science, Vol. **18**, No. 6, Dec.,1990 (pp. 948 - 957).

239 T.C. ROZZEL, C.C. JOHNSON, C.H. DURNEY, J.L. LORDS and R.G. OLSEN; *A Nonperturbing Temperature Sensor for Measurements in Electromagnetic Fields.* - J. Microwave Power (Int. Microwave Power Inst.), Vol. **9**, No. 3, Sept., 1994 (pp. 241 - 249).

240 M.A. HEALD and C.B.WHARTON; *Plasma Diagnostics with Microwaves.* - John Wiley and Sons, Inc., New York, 1965.

241 A.D. MERRIMAN; *A Dictionary of Metallurgy.* – MacDonald and Evans, Ltd., London, 1958.

242 G.V. SAMSONOV and I.M. VINITSKII; *Handbook of Refractory Compounds.* - Translated by K. Shaw, IFI/Plenum, New York,

243 A. TAYLOR; *An Introduction to X-Ray Metallography.* – Chapman and Hall Ltd., London, 1949.

244 J.M. OSEPCHUK; *Microwave Power Applications.* – IEEE Transactions on Microwave Theory and Techniques, Vol. **50** No. 3, March, 2002 (pp.975 – 985).

245 Unidentified; *97/02249: Reduction of Iron Ore with Coal by Microwave Heating.* - Fuel and Energy Abstracts, Vol. **38**, No. 3, July, 1997 (p.180).

246 Unidentified; *98/03242: Reduction of Iron Ore with Coal by Microwave Heating.* – Fuel and Energy Abstracts, Vol. **39**, No. 4, July, 1998 (p.300).

247 K.E. HAQUE; *Microwave Energy for Mineral Treatment Processes – a Brief Review.* – Int. J. of Mineral Processing, Vol. **57**, No. 1, July, 1999 (pp. 1 – 24).

248 D.A. JONES, S.W. KINGMAN, D.N. WHITTLES and I.S. LOWNDES; *The Influence of Microwave Energy Delivery Method on Strength Reduction in Ore Samples.* – Chemical Engineering and Processing, Vol. **46**, No. 4, April, 2007 (pp. 291 – 299).

249 W. VORSTER, N.A. ROWSON and S.W. KINGMAN; *The Effect of Microwave Radiation upon the Processing of Neves Corvo Copper Ore.* – Int. J. of Mineral Processing, Vol. **63**, No. 1, June, 2001 (pp. 29 – 44).

250 P.A. OLUBAMBI, J.H. POTGIETER, J.Y HWANG and S. NDLOVU; *Influence of Microwave Heating on the Processing and Dissolution Behaviour of Low-Grade Complex Sulphide Ores.* – Hydrometallurgy, Vol. **89**, Nos. 1 - 2, September, 2007 (127 – 135).

251 S.W. KINGMAN, K. JACKSON, A. CUMBANE, S.M. BRADSHAW, N.A. ROWSON and R. GREENWOOD; *Recent Developments in Microwave-Assisted Comminution.* – Int. J. of Mineral Processing, Vol. **74**, Nos. 1 – 4, November, 2004 (pp. 71 – 83).

252 S.W. KINGMAN, K. JACKSON, S.M. BRADSHAW, N.A. ROWSON and R. GREENWOOD; *An Investigation into the Influence of Microwave Treatment on Mineral Ore Comminution.* – Powder Technology, Vol. **146**, No. 3, September, 2004 (pp. 176 184).

253 Anon. for CSIRO; *Improved Method for Titanium Production.* – Mag. of Engineers Australia, Vol. **79**, No. 11, November, 2007 (pp.62 – 63).

254 D. WEXLER; personal communication with, October, 2007 - senior research associate, Faculty of Engineering, Discipline of Materials Engineering, University of Wollongong, N.S.W., Australia.

255 C. NOCKOLDS; *X-Ray Physics.* – from *Training School: Microanalysis in Electron Microscopy*, eds., C. Nockolds and D. Cockayne – Electron Microscope Unit, University of Sydney, 1990.

256 N. WARE; *Energy Dispersive Spectrometers.* – **ibid**.

257 C. NOCKOLDS; *Electron-Specimen Interactions.* – **ibid**.

258 G. CLIFF; *Qualitative Analysis in Bulk and Thin Films.* – **ibid**.

259 C. NOCKOLDS; *Quantitative Analysis – Bulk.* – **ibid**.

260 P.J. GOODHEW and F.J. HUMPHREYS; *Electron Microscopy and Analysis.* – Taylor and Francis, London,1988.

261 C.H. KRUGER, T.G. OWANO and C.O. LAUX; *Experimental Investigation of Atmospheric Pressure Nonequilibrium Plasma Chemistry.* – IEEE Trans. on Plasma Science, Vol. 25, No. 5, October, 1997.

262 R.F. SCHIFFMANN; *Microwave Power Applications in the World: Present and Future.* – J. Microwave Power, Vol. **14**, No. 3, 1979.

263 W.H. RAY and J. SZEKELY; *Process Optimization – with Applications in Metallurgy and Chemical Engineering.* – John Wiley and Sons, New York, 1973.

264 D.A. ANDERSSON, P.A. KORZHAVYI and B. JOHANSSON; *First-principles based calculation of binary and multicomponent phase diagrams for titanium carbonitride.* – Computer Coupling of Phase Diagrams and Thermochemistry, Vol. **32**, Elsevier, 2008, pp. 543–565.

265 K.S. COLEY, B.S. TERRY and P. GRIEVESON; *Simultaneous Reduction and Carburization of Ilmenite.* – Metallurgical and Materials Transactions B, Vol.**26B**, June, 1995, pp. 485 – 494.

266 T.B. MASSALSKI (Ed-in-chief); *Binary Alloy Phase Diagrams, Vols. 1 and 2.* – American Soc. for Metals, Metals Park, Ohio, 1983.

267 D.A. PORTER and K.E. EASTERLING; *Phase Transformations in Metals and Alloys.* – 2nd edition, Chapman and Hall, London, 1992.

268 H.K. WORNER, J.J. JONES and L. REILLY; *"Microwaves in Pyrometallurgy"* – from "First Australian Symposium on Microwave Power Applications, Wollongong, 1989", University of Wollongong, 1989, pp 179 – 188.

"Where do I find all the time for not reading so many books?"

Karl Kraus -1909.

AUTHOR INDEX to REFERENCES.

AUTHOR; Reference No.

HABASHI, F.; **235**
HAGERTY, J.S.; **173**
HALL, R.A.; **141**
HAMMETTER, W.F.; **160**
HAMPEL, C.A.; **127**, **131**
HANWAY, J.E.(Jr); **45**
HAQUE, K.E.; **247**
HARD, R.A.; **146**
HASTIE, R.J.; **226**
HAYES, P.; **39**
HEALD, M.A.; **240**
HELFFERICH, F.; **69**
HELIODORE, F.; **95**
HELMS, A.D.; **110**
HENKRE, V.M.; **96**
HENRIE, T.A.; **42**
HESS, D.W.; **152**
HIRSH, M.N.; **81**
HLAVACEK, V.; **155**
HOATSON, C.L.; **177**
HOCH, M.; **132**
HOFMEISTER, W.H.; **109**
HOLDERFIELD, S.P.; **93**
HOLT, J.B.; **154**, **161**, **174**
HOPKINS, D.W.; **17**
HÖRZ, G.; **228**
HOU, X.; **118**
HOWELL, W.J.; **15**
HOYAUX, M.F.; **191**, **195**
HUANG, D.; **231**
HUIZINGA, A.H.; **236**
HUMPHREYS, F.J.; **260**
HWANG, J.Y.; **250**

IJOVIC, J.M.; **210**
IKEDA, T.; **111**
INGOLD, J.H.; **81**
IOFFE, M.S.; **120**
ISHIZAKI, K.; **151**
ISHIZAWA, Y.; **163**
ISKANDER, M.F.; **91**, **94**, **99**
IYER, K.; **175**
IZATT, R.M.; **139**

JACKSON, K.; **251**, **252**
JACQUAULT, P.; **205**
JAMRACK, W.D.; **30**
JANNEY, M.A.; **101**
JAFFEE, R.I.; **132**
JAIN, S.K.; **140**
JEFFES, J.H.E.; **64**, **126**
JEFFERY, C.L.; **238**
JEHN, H.; **234**
JENA, P.K.; **140**
JOHANSSON, B.; **264**
JOHN, P.K.; **196**
JOHNSON, C.C.; **239**
JOHNSON, D.L.; **91**
JONASSON, K.A.; **33**
JONES, D.A.; **248**
JONES, J.J.; **268**

KADLEC, R.H.; **124**
KAIEDA, Y.; **157**
KALISH, H.S.; **25**
KARMAZSIN, E.; **237**
KATZ, J.D.; **96**
KERZE, F.; **77**
KHAIT, Yu. L.; **76**
KIGGANS, J.O.; **101**
KIMREY, H.D.; **101**
KINGMAN, S.W.; **248**, **249**, **251**, **252**
KITAMURA, T.; **119**, **122**
KITSUNAI, M.; **148**
KIVILAHTI, J.; **136**
KLEIN, M.V.; **56**
KLEMBERG-SAPIEHA, J.E; **153**
KNITTEL, S.M.; **168**
KOCK, W.; **11**
KOECK, W.; **52**
KOGELSCHATZ, U.; **80**
KONG, P.C.; **169**
KORINEK, G.J.; **31**
KORZHAVYI, P.A.; **264**
KOSZYKOWSKI, M.; **156**
KRUGER, C.H.; **102**
KUA, H.K.; **91**
KRISHNAN, S.; **57**
KRISHNAN, T.S.; **55**
KRIVSKY, W.A.; **9**, **42**
KRUGER, C.H.; **261**
KWON, Y.J.; **36**

LAIDLER, K.L.; **70**
LAKSHMANAN, V.I.; **20**
LAMAZE, A.P.; **53**
LANDSBERG, A.; **177**
LASSAHN, G.D.; **114**
LAUGHLIN, W.C.; **145**
LAUX, C.O.; **261**
LE BLANC, C.; **231**
LEE, J.F.; **203**
LE MEHAUTE, A.; **95**
LEVENSPIEL, O.; **67**
LEWIS, D.A.; **206**, **207**
LIANG, D.; **231**
LIDDELL, KN.C.; **49**, **50**
LIDE, D.R.; **5**
LIEBERMAN, M.A.; **178**
LOEB, L.B.; **221**
LOH, I.H.; **233**
LOPEZ, P.; **199**
LORDS, J.L.; **239**
LOUPY, A.; **205**
LOWNDES, I.S.; **248**
LUSTMAN, B.; **77**
LYNCH, D.C.; **99**, **115**, **117**

MacDONALD, A.D.; **83**
MAEDA, M.; **111**
MAGALHAES, G.; **143**
MARGOLIS, S.B.; **154**
MASSALSKI, M.; **266**
MASSEY, H.S.W.; **217**
M^{C}CAUGHAN, L.; **100**
M^{C}COLL, W.B.; **199**
M^{C}DANIEL, E.W.; **217**
M^{C}FEATERS, J.S.; **170**
M^{C}GILL, S.L.; **121**
M^{C}GOWAN, J.W.; **196**
M^{C}KELLIGET, J.W.; **165**
M^{C}LEAN, A.; **216**
M^{C}PHERSON, R.; **59**
M^{C}TAGGART, F.K.; **87**
M^{C}WHIRTER, R.W.P.; **227**
MALT, J.; **112**
MARTIN, D.R.; **127**
MARTINEZ, G.M.; **176**
MARTINS, G.P.; **51**
MARX, R.; **223**
MATKOWSKY, B.J.; **154**
MENG, B.; **100**
MEREDITH, R.J.; **105**
MERRIMAN, A.D.; **241**
METAXIS, A.C,; **105**
MEYER, H.; **147**
MEYER-JOLY, M,CH.; **54**
MEYERS, M.A.; **160**
MILLER, G.L.; **6**, **7**, **8**
MINGOS, D.M.P.; **86**
MITCHNER, M.; **102**
MOISAN, M.; **152**
MOLLER, P.; **78**
MONTGOMERY, D.C.; **104**
MOORE, J.J.; **37**, **75**, **159**, **170**, **171**
MORLEY, I.W.; **19**
MORSE, P.M.; **66**
MORSI, I.M.; **134**
MUNIR, Z.A.; **149**, **161**
MUNIR, Z.F.; **154**
MURRAY, G.T.; **112**

NASSER, E.; **198**
NDLOVU, S.; **250**
NIELSEN, R.H.; **40**
NISHIOKA, M.; **167**
NOCKOLDS, C.; **255**, **257**, **259**
NODA, T.; **47**
NORDINE, P.C.; **57**

O'BRIEN, C.M.; **110**
OGDEN, H.R.; **129**
OGURO, N.; **157**
OJEBUOBOH, F.K.; **51**
OLSEN, R.G.; **239**
OLUMBAMBI, P.A.; **250**
ORTEGA, R.A.; **115**

OSCARSON, J.L.; **139**
OSEPCHUK, J.M.; **244**
OSKAM, H.J.; **81**
OTAGUCHI, M.; **157**
OTANI, S.; **163**
OWANO, T.G.; **261**

PAJUNEN, M.; **136**
PAOLONI, F.; **107**
PASCHEN, P.; **11**, **50**, **52**
PASSOW, M.L.; **199**
PERCY, A.L.; **128**
PERSSON, P.-A.; **162**
PETIT, A.; **205**
PICKLES, C.A.; **34**, **123**
PFENDER, E.; **72**, **85**, **169**, **180**
PIRZADA, S.A.; **118**, **150**
PIZZOLATO, P.J.; **127**
PLATZMAN, P.M.; **190**
POLAK, L.S.; **88**
POLLINGTON, S.D.; **120**
POPESCU, M.; **202**
PORTER, D.A.; **267**
POTGIETER, J.H.; **250**
POULIN-DANDURAND, S.; **153**
POWELL, A.R.; **22**
PRASAD, P.M.; **140**
PRIDER, R.T.; **28**
PRIETO, M.A.; **146**
PYUN, D.S.; **109**

QUABDESSELAM, M.; **149**

RABIN, B.H.; **158**
RAHM, J.A.; **142**
RAINS, R.K.; **124**
RAJAKUMAR, V.; **137**
RALSTON, O.C.; **24**
RAY, H.S.; **16**
RAY, W.H.; **263**
REDDY, R.G.; **56**
REID, K.J.; **37**, **75**
REID, A.F.; **20**
REILLY, L.; **268**
REJ, D.J.; **179**
REPETTI, T.E.; **114**, **199**
RERAT, C.F.; **48**
RICHARDSON, F.D.; **64**, **232**
RICHARDSON, L.S.; **112**
RISBUD, S.H.; **168**
RODGERS, J.W.; **12**
ROMAN, W.C.; **73**, **172**
ROSENQVIST, T.; **41**
ROWSON, N.A.; **249**, **251**, **252**
ROZZEL, T.C.; **239**
RUTLEY, F.; **14**

SADOWAY, D.R.; **38**, **49**, **50**
SALSMAN, J.B.; **93**, **98**, **200**
SAMSONOV, G.V.; **242**
SATRE, P.; **237**
SAUPE. F.; **78**
SCHIFFMAN, R.; **109**
SCHIFFMAN, R.F.; **206**, **262**
SCHLECHTEN, A.W.; **43**, **130**
SCHOELLER, W.R.; **22**
SCHOLTZ, J.; **155**
SCHULZ, G.J.; **196**
SEARS, F.W.; **203**
SELWYN, G.S.; **178**
SEMENOV, V.E.; **183**
SHAFER, B.V.; **59**
SHELTON, S.M.; **27**
SHIBATA, K. **119**, **122**
SIBERT, M.E.; **26**
SIMONS, E.N.; **10**
SKALA, L.; **96**
SMIRNOV, B.M.; **188**
SMITH, J.T.; **31**
SNIDER, R.L.; **97**
SNYDER, S.C.; **114**
SNYDER, W.B.(Jr); **91**
SOHN, H.Y.; **31**
SOMASUNDARAN, P.; **20**
SOMIYA, S.; **167**
SOMMERVILLE, I.D.; **216**
SPINK, D.R.; **33**, **45**, **46**
SREEKUMAR, K.P.; **175**
STANDISH, N.; **133**
STEELE, B.C.H.; **214**
STEINBERG, M.A.; **26**
STEVENSON, F.D.; **182**
STIX, T.H.; **103**
STUFFLEBEAM, J.H.; **172**
SUDAN, R.N.; **192**
SURI, A.K.; **29**
SUTTON, W.H.; **91**, **99**, **206**, **207**
SWANK, W.D.; **238**
SZEKELY, J.; **71**, **263**

TAIT, R.J.; **126**
TAKEDA, K.; **119**, **122**
TAMARU, A.; **148**
TANAKA, K.; **151**
TANAKA, T.; **163**
{Tanner-Jones, J.J.; see Jones, J.J.}
TAYLOR, A.; **243**
TAYLOR, P.R.; **118**, **150**
TERRY, B.S.; **214**, **265**
TESSIER, Y.; **153**
TETENBAUM, S.J.; **83**
THADHANI, N.N.; **160**, **162**
THEMELIS, N.J.; **230**
TIDMAN, D.A.; **104**
TIMMINS, R.S.; **89**
TINGA, W.R.; **106**, **236**
TOLLEY, W.K.; **139**, **145**
TRAN, N.; **212**
TROE, J.; **229**
TULLY, F.P.; **217**
TURCOTTE, D.L.; **203**
TUSZEWSKI, M.; **178**
TYLKO, J.K.; **37**, **75**

UHLENBUSCH, J.; **197**
ULTEE, C.J.; **172**
UPADHYAYA, G.S.; **62**

VAN HOVE, L. **186**
VENKATRAMANI, N.; **175**
VINITSKII, I.M.; **242**
VORSTER, W.; **249**
VOSS, W.A.G.; **91**, **236**

WAINER, E.; **26**
WALKER, C.M.B.; **236**
WALKIEWICZ, J.W.; **121**
WAN, J.K.S.; **120**
WANG, L.L.; **161**
WARD, R.; **162**
WARE, N.; **256**
WEAST, R.C.; **5**
WEBB, W.E.; **200**
WEBER, J.K.R.; **57**
WEISER, M.W.; **96**
WERTHEIMER, M.R.; **152**, **153**
WEXLER, D.; **254**
WHARTON, C.B.; **240**
WHITTLES, D.N.; **248**
WILKOMIRSKY, I.; **17**
WILLERT-PORADA, M.; **208**
WINCHELL, A.N.; **21**
WOLFF, P.A.; **190**
WORK, S.J.; **160**
WORNER, H.K.; **133**, **181**, **268**

YAHATA, T.; **111**
YI, H.C.; **159**
YOSHIDA, T.; **164**
YOSHIMURA, M.; **167**
YNTEMA, L.F.; **128**
YU, L.H.; **160**
YUMOTO, S.; **151**

Acknowledgements.

Throughout the somewhat protracted course of this project I was blessed with the kind assistance of numerous people. To these friends and colleagues I earnestly owe a debt of gratitude and I wish herein to acknowledge their contributions.

Principal among these persons were my three academic supervisors. Firstly, Emeritus Professor the late Howard Knox Worner by warrant of his inquisitive spontaneity, his ardent analytical competence, and his broad knowledge in both laboratory and foundry. Professor Worner possessed uncanny presence-of-mind throughout experimentation, and the composure under apparent "failure" to turn procedural disappointment into "alternative success" – a lesson well learnt for this unconventional field. Out of this prescience, and especially his foresight for microwave applications, it was Professor Worner with whom I devised the experimental programme after a period of profound experimental accomplishment early in the life of the Microwave Applications Research Centre at the University of Wollongong. In his espousal of "intuitive" methods of experimental investigation, Professor Worner's enthusiasm, technical knowledge and vast experience of the history and workings of Australian and world mining and extractive metallurgy were repeatedly a source of inspiration in matters technical and aspirational. At this time he is sorely missed.

Secondly, I wish to thank Professor Noel F. Kennon whose attentiveness and perceptiveness guided me through the maze of "core" experimentation, and who judiciously advised upon matters of material characterisation and analyses, their reporting, and writing generally. Lastly, it is with heartfelt thanks that I acknowledge the patience of Emeritus Professor Druce P. Dunne who provided that essential nurturing role as I "waded" through my thesis write-up; accommodating and supportive, his amiable persistence and understanding saw me to this culmination. As a completed manuscript, this thesis is largely his success.

I wish to acknowledge the generous assistance of Geology colleagues and the (now) School of Earth Sciences for access to essential facilities. Especially, thanks are due to Mr Aivars Depers for coal petrological and geological discussions and assistance with light-optical microscopy – his high technical standards an inspiration. Earnest

thanks also to Dr Bryan Chenhall for mineralogical discussions and access to XRD and XRF facilities. Acknowledgement is due to (the former) BHP Central Laboratories, Port Kembla, and specifically to Mr Les Moore for kind and ready assistance with WDS mapping and microanalyses.

In my discipline of Materials Engineering – in the various guises under which it has masqueraded since the honest title of *Department of Metallurgy* became unfashionable – a number of worthy technical colleagues provided crucial assistance in technical matters or everyday assistance in material support. Most notable was the continuing and principal support of Mr Nick Mackie and Dr David Wexler (variously) for their assistance with SEM/EDS, XRD (and TEM) and ongoing interpretation throughout acquisition, analyses and data output. Thanks also to Mr Ron Kinnell for fabrication and repair of experimental apparatus and facilities, to Mr Greg Tillman for advice regarding specimen and photomicrogaph preparation, and to Mr Bob deJong, Albert Bult and Mr Graham Hamilton for continuity of support across various technical matters. Special mention also should be made of the contribution rendered each by Mr Mark Reid for much assistance with computer presentation for thesis documentation and by Mrs Joy deMaistre for kindly advice on numerous word-processing matters.

No less so, student colleagues deserve mention for many and varied formative technical discussions and for the genuine fondness with which they proffered their support and sense of collegial community over many years. Central to my student survival were the devoted friendship of Ms Lena Plambeck, and later, that of Dr Samsiah Sulaiman and Dr David Nolan. Of memorable significance, both socially and technically, were the friendships of Dr Yu Dake, Dr Huijun Li, Ms Destini Rosawinati, Mr Djoko Muljono, Dr Jonathan LLoyd and Mr Hammid Yasbandha.

I also acknowledge my indebtedness to long-term friend and colleague Dr Neil Sherwood of CSIRO Petroleum for discussions and inspiration; and for their motivational and technical contributions, Dr Hugo Huey of California, Dr Seng Lim of CSIRO Minerals, and Mr Stan Morrow of Tennessee. I am in debt to Professor Raghu Singh and Dr Joe Shonhardt from Mining Engineering for assistance with mineral processing, mining and mining industry matters generally – and especially to Professor Singh, my sometime mentor and "collegial sponsor", for recurrent *inexorable*

"motivational" discussions and profound personal support – he elicited (from me) a sense of self-belief.

Not least in this gallery of friends, for their patience, my children, Lynnette, Brys and Evan; my brother, Bruce; Wendy and Maralyn; and my mother, Margaret, who now will never comprehend my achievement – my eternal thanks.

Jeffrey Tanner-Jones.

PUBLICATIONS, PATENTS and CONTRIBUTED REPORTS.

Published articles and reports by Jeffrey J. JONES/Jeffrey J. TANNER-JONES*.

1 N. Standish and **J.J. Jones**; *"A Tracer Study of Discharge Segregation from a Paul Wurth Hopper."* – from "Extractive Metallurgy Symposium", AusIMM, Melbourne, 1984, pp 279 – 285.

2 A.M. Depers, **J. Jones** and A.C. Cook; *"Third Generation Petrographic Studies in Coal Carbonisation."* – final project report for the Department of National Development and Energy (NERDD Programme project 79/9013), Department of Geology, University of Wollongong, 1982.

3 A.M. Depers, **J. Jones** and A.C. Cook; *"Petrology and Microstructure of a Swedish Coke Before and After Reactivity with Carbon Dioxide."* – confidential report commissioned by Kembla Coal and Coke Pty. Limited, Wollongong, by Department of Geology, University of Wollongong, 1982.

4 A.M. Depers, **J. Jones** and A.C. Cook; *"Petrology and Microstructure of Beehive Oven Cokes Produced from Bulli Seam Coal at the Illawarra Coke Works, Coalcliff, N.S.W., Australia."* – confidential report commissioned by Kembla Coal and Coke Pty. Limited, Wollongong, by Department of Geology, University of Wollongong, 1982.

5 A.M. Depers, **J. Jones** and A.C. Cook; *"Petrography and Microstructure of Cokes Produced from Freshly Washed Coalcliff Coal."* – confidential report commissioned by Kembla Coal and Coke Pty. Limited, Wollongong, by Department of Geology, University of Wollongong, 1983.

6 A.M. Depers, **J. Jones** and A.C. Cook; *"Petrography and Microstructure of a Formcoke and a Japanese Foundry Coke."* – confidential report commissioned by Kembla Coal and Coke Pty. Limited, Wollongong, by Department of Geology, University of Wollongong, 1984.

7 N. Standish, H.K. Worner, **J. Jones** and G. Gupta; *"Properties of Blends of Brown Coal and Bituminous Coals – second project report for the Department of National Development and Energy."* – Department of Metallurgy and Materials Engineering, University of Wollongong, September, 1987. [20 pages.]s

8 D.H. Bradhurst and **J.J. Jones**; *"Microwave Applications Research Centre of Wollongong Uniadvice Limited: Progress Report to Muswellbrook Energy and Minerals Limited, 22 June to 22 September, 1988."* – confidential report to Muswellbrook Energy and Minerals Limited, Microwave Applications Research Centre, University of Wollongong, 1988. [17 pages.]

9 H.K. Worner, D.H. Bradhurst and **J.J. Jones**; *"Microwave Applications Research Centre of Wollongong Uniadvice Limited: First Annual Report."* – confidential report to Muswellbrook Energy and Minerals Limited, Microwave Applications Research Centre, University of Wollongong, 1988. [19 pages.]

10 H.K. Worner, **J. Jones** and L.Reilly; *"Microwaves in Pyrometallurgy"* – from "First Australian Symposium on Microwave Power Applications, Wollongong, 1989", University of Wollongong, 1989, pp 179 – 188.

11 B.P. Barnsley, L. Reilly, **J. Jones** and J. Eshman; *"Iron and Steelmaking with Microwaves."* – **ibid**. pp 189 – 195.

12 H.K. Worner, D.H. Bradhurst, **J. Jones**, J. Eshman and A. Dominis; *"Progress Report to Muswellbrook Energy and Minerals Limited, 1st January to 31st March, 1989."* – Microwave Applications Research Centre, University of Wollongong, 1989. [19 pages.]

---

* The candidate formally changed his surname in 2000 (during the period of PhD enrolment) from *JONES* to *TANNER-JONES* to incorporate his surname-at-birth and as an initial measure to (in future) revert solely to his birth-surname, *TANNER*. Consequently, the candidate's authorship attributions prior to May. 2000 appear as *J.JONES or J.J. JONES.*

13 H.K. Worner, D.H. Bradhurst, **J. Jones**, J. Eshman and A. Dominis; *"Progress Report to Muswellbrook Energy and Minerals Limited, 1st Aprily to 30th June, 1989."* – Microwave Applications Research Centre, University of Wollongong, 1989. [17 pages.]

14 H.K. Worner, D.H. Bradhurst, **J. Jones**, L. Reilly, J. Eshman and A. Dominis; *"Second Annual Report to Muswellbrook Energy and Minerals Limited, November 30, 1989."* – Microwave Applications Research Centre, University of Wollongong, 1989. [39 pages.]

15 H.K. Worner, D.H. Bradhurst, **J. Jones**, L. Reilly, J. Eshman and A. Dominis; *"Quarterly Progress Report to Muswellbrook Energy and Minerals Limited, 1st January to 30th March, 1990."* – Microwave Applications Research Centre, University of Wollongong, 1990. [13 pages.]

16 H.K. Worner, D.H. Bradhurst, **J. Jones**, G. Young, A. Dominis and L. Reilly; *"Progress Report to Muswellbrook Energy and Minerals Limited, 1st April to 30th June, 1990."* – Microwave Applications Research Centre, University of Wollongong, 1990. [22 pages.]

17 H.K. Worner, D.H. Bradhurst, **J. Jones**, L. Reilly, J. Eshman, A. Dominis and G.Young; *"Final Report to Muswellbrook Energy and Minerals Limited, December 31, 1990."* – Microwave Applications Research Centre, University of Wollongong, 1989. [87 pages.]

18 **Jeffrey Jones**; *"Short Microstructural Report Including EDX Analyses of Phases Produced in Smelt Product of Microwave Stimulated Carbothermic Reduction of Neodymium Oxide Plus Iron Oxide."* – ANSTO/Microwave Applications Research Centre, University of Wollongong, 1989. [18 pages.]

[Note: Upon the commercial imperative of insistent legal advice, publication activity from late 1996 until late 2002 ceased whilst patent authorship and registration was finalised, and intellectual property protection was enforced.]

19 **J.J. Tanner-Jones** and C. Clare; *"First Interim Report for R&D START Grant GRA02013: Microwave Extraction of Metals from Slag."* Tesla Technologies Pty. Limited, Burrawang, 2000.

20 C. Clare and **J.J. Tanner-Jones**; *"Second Interim Report for R&D START Grant GRA02013: Microwave Extraction of Metals from Slag."* Tesla Technologies Pty. Limited, Burrawang, 2000.

21 C. Clare and **J.J. Tanner-Jones**; *"Third Interim Report for R&D START Grant GRA02013: Microwave Extraction of Metals from Slag."* Tesla Technologies Pty. Limited, Burrawang, 2001.

22 **J.J. Tanner-Jones** and C. Clare; *"Final Report for R&D START Grant GRA02013: Microwave Extraction of Metals from Slag."* Tesla Technologies Pty. Limited, Burrawang, 2001.

23 **Jeffrey Tanner-Jones** (sole inventor); international patent *"Plasma Reduction Processing of Materials."* Present owner: Plasma Technologies Pty. Limited, Victoria. The patent jurisdictions and patent numbers of current patent registrations are as listed below, some lapsed jurisdictions (South Africa, Japan, plus others) are omitted:

1. Australian patent **AU 2002220358 B2**.
2. US American patent **US 2004/0060387 A1**.
3. German patent **DE 601 31 365 T2 2008.10.23**.
4. European patent **EP 1 348 038 B1**.
5. World patent **WO 02/46482 A1**.

APPENDIX A

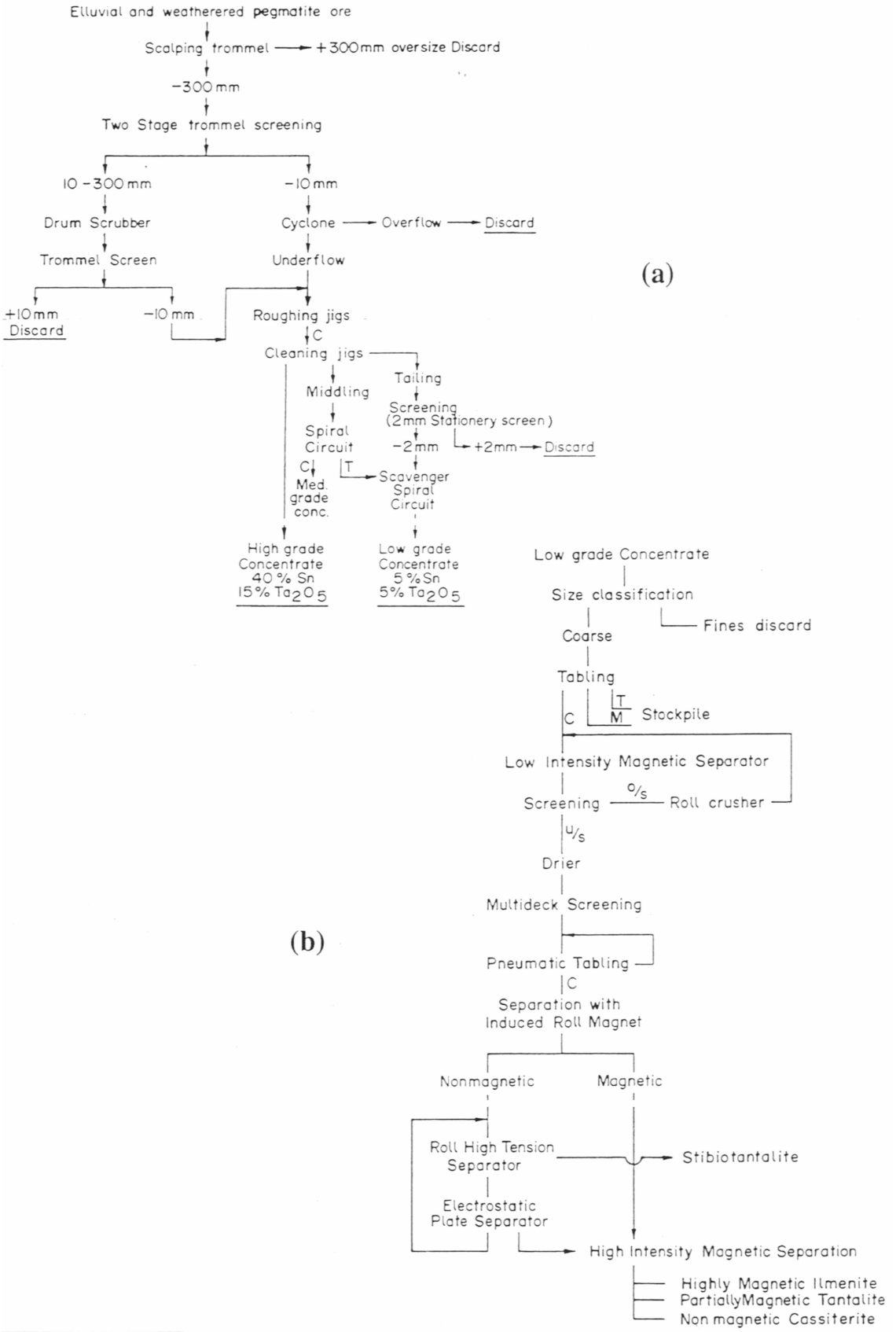

Figure {3.1.3}1: Flowsheet of the tin and tantalum (stibiotantalite) ore processing plant (**a**) and mineral dressing (for further mineral separation of low grade cuts) plant (**b**) at Greenbushes, Western Australia [29].

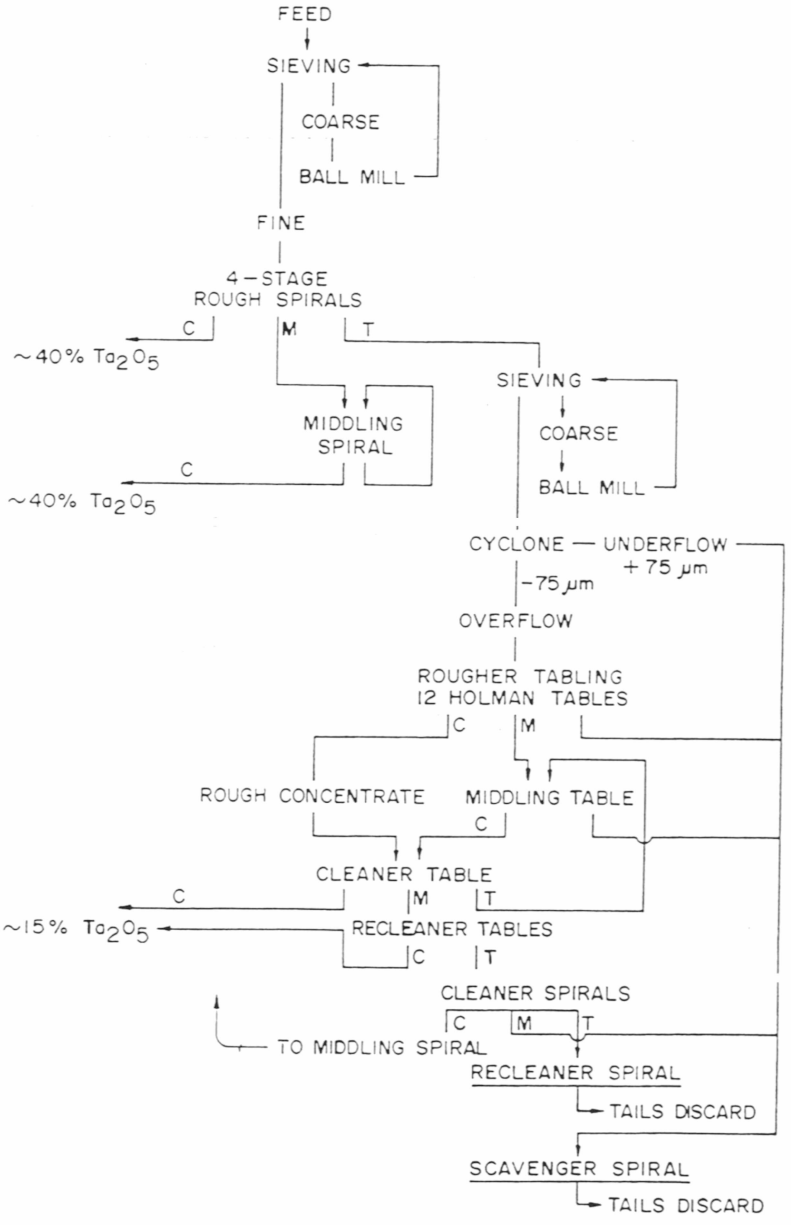

Figure {3.1.3}2: Flowsheet of the tantalum (wodginite) ore processing plant at Wodgina, Western Australia [29].

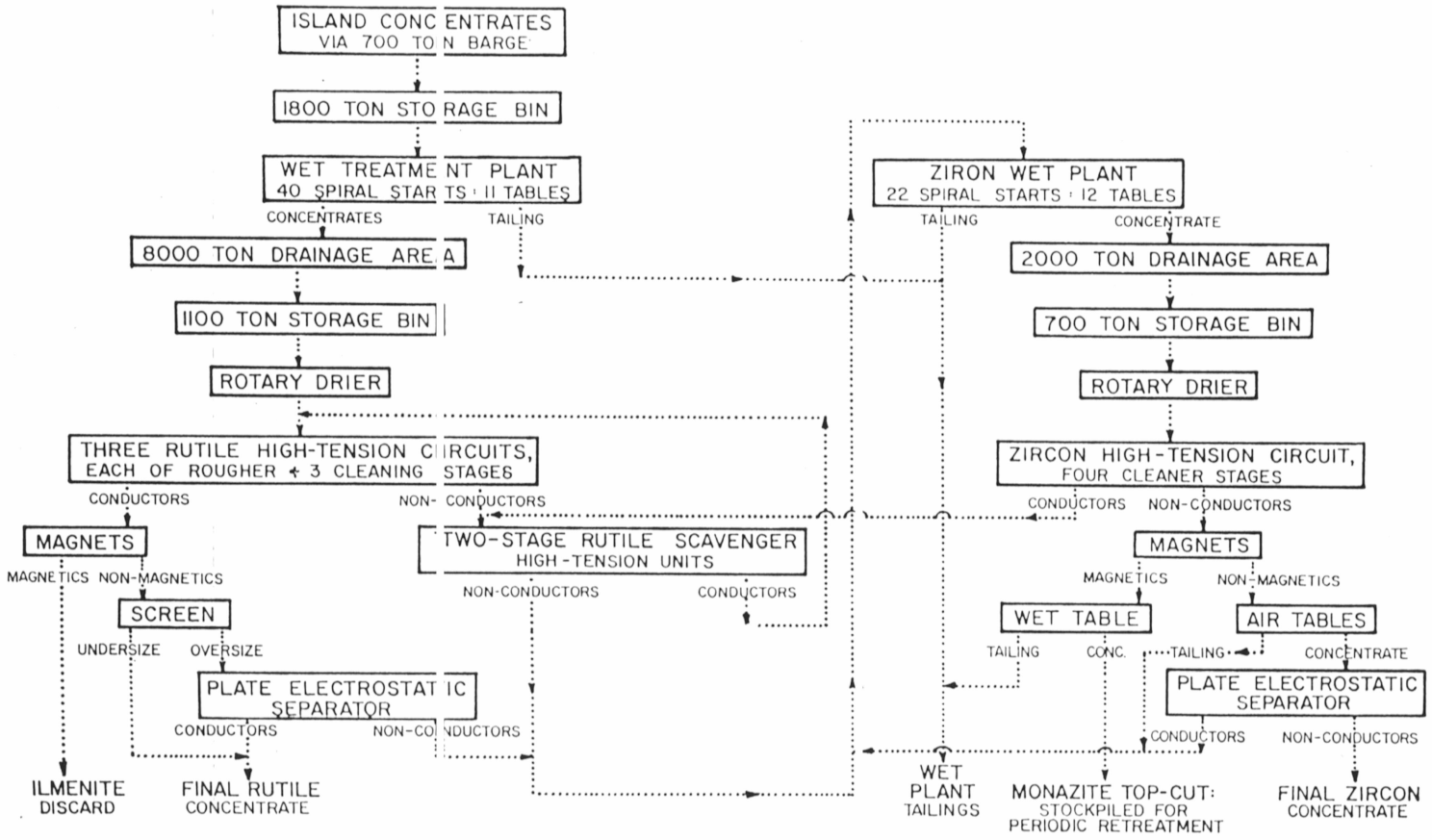

Figure {3.1.3}3: Flow sheet showing a typical sequence of processing stages employed in a mineral sand mining operation (in this case by Australian east coast miner Consolidated Rutile Limited) [19]. The full range of separation equipment is not necessarily indicated nor, out of necessity, is the full implications of wet and dry stage options.

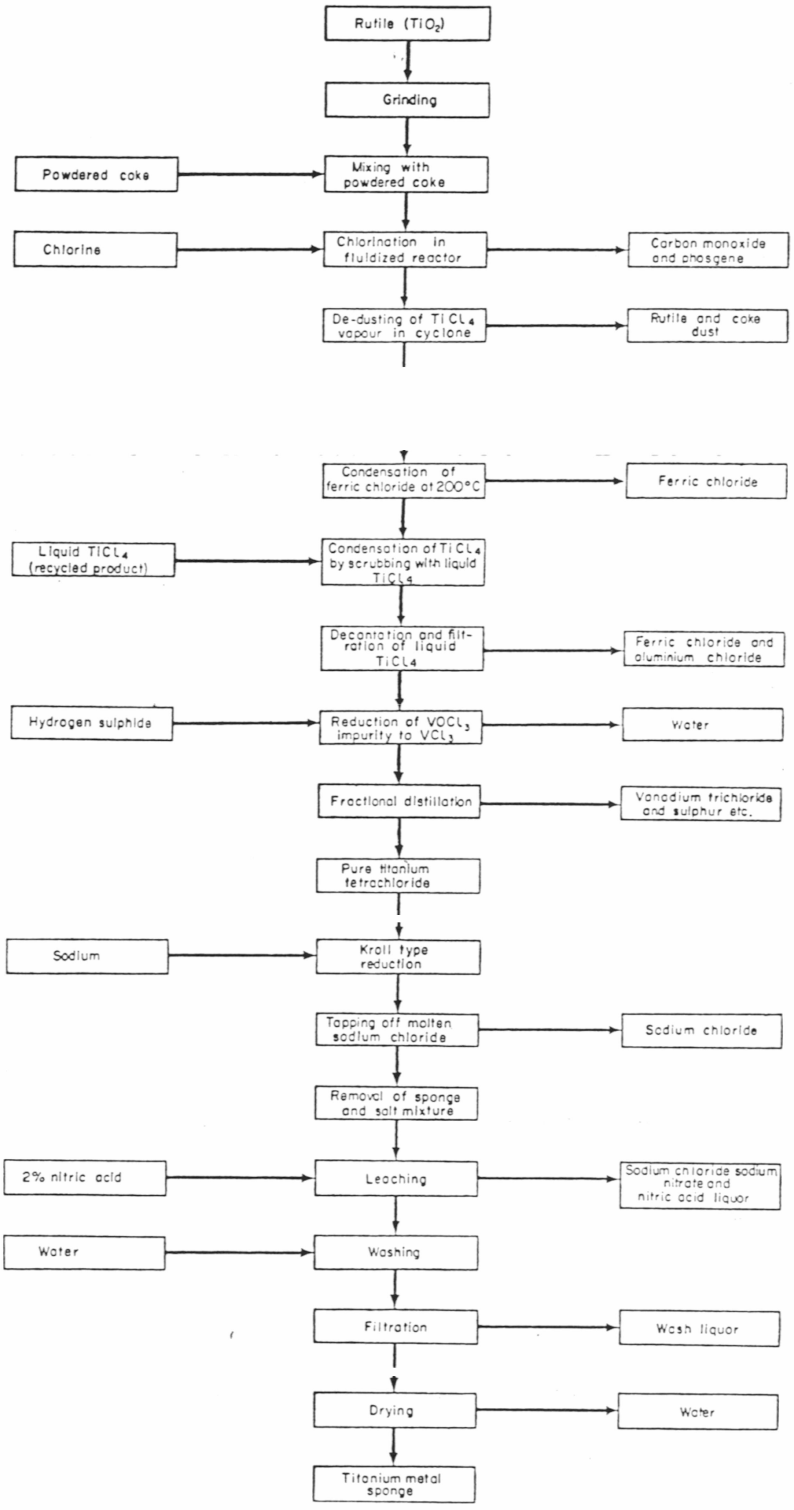

Figure {3.1}6: Flow sheet showing the production route to titanium metal from the tetrachloride via the Hunter (sodium) reduction method [30]. This route has largely been replaced by the Kroll (magnesium) alternative where metallothermic reduction is incorporated in the industrial process.

Figure {3.1}7: Flow shee t showing a long established extra ction route employing chlorination, hexone pu rification and electrolysis stages o f production [30]. This extraction route has largely been superseded by the route sh own in the following Figure **{3.1}8.**

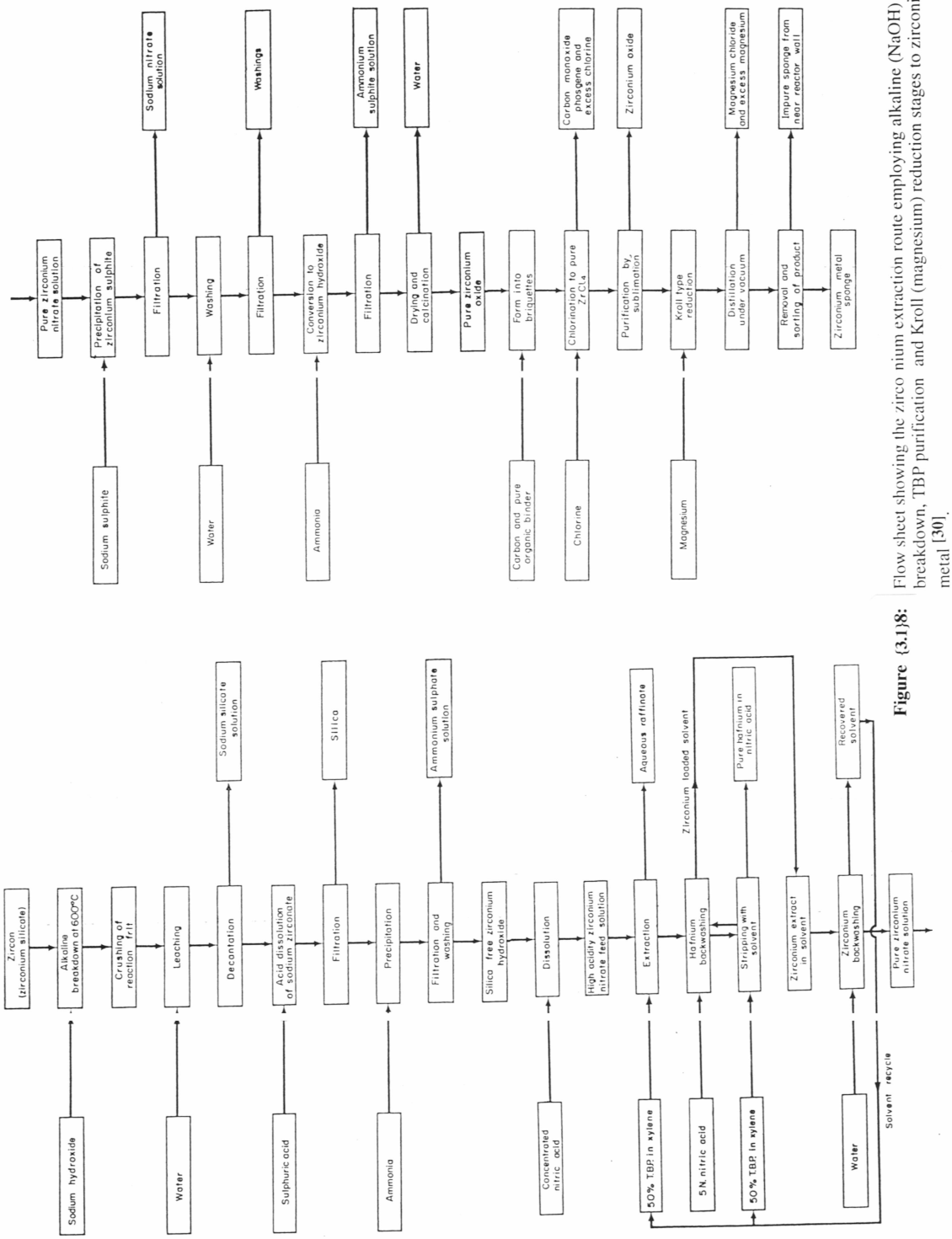

Figure (3.1)8: Flow sheet showing the zirco nium extraction route employing alkaline (NaOH) breakdown, TBP purification and Kroll (magnesium) reduction stages to zirconium metal [30].

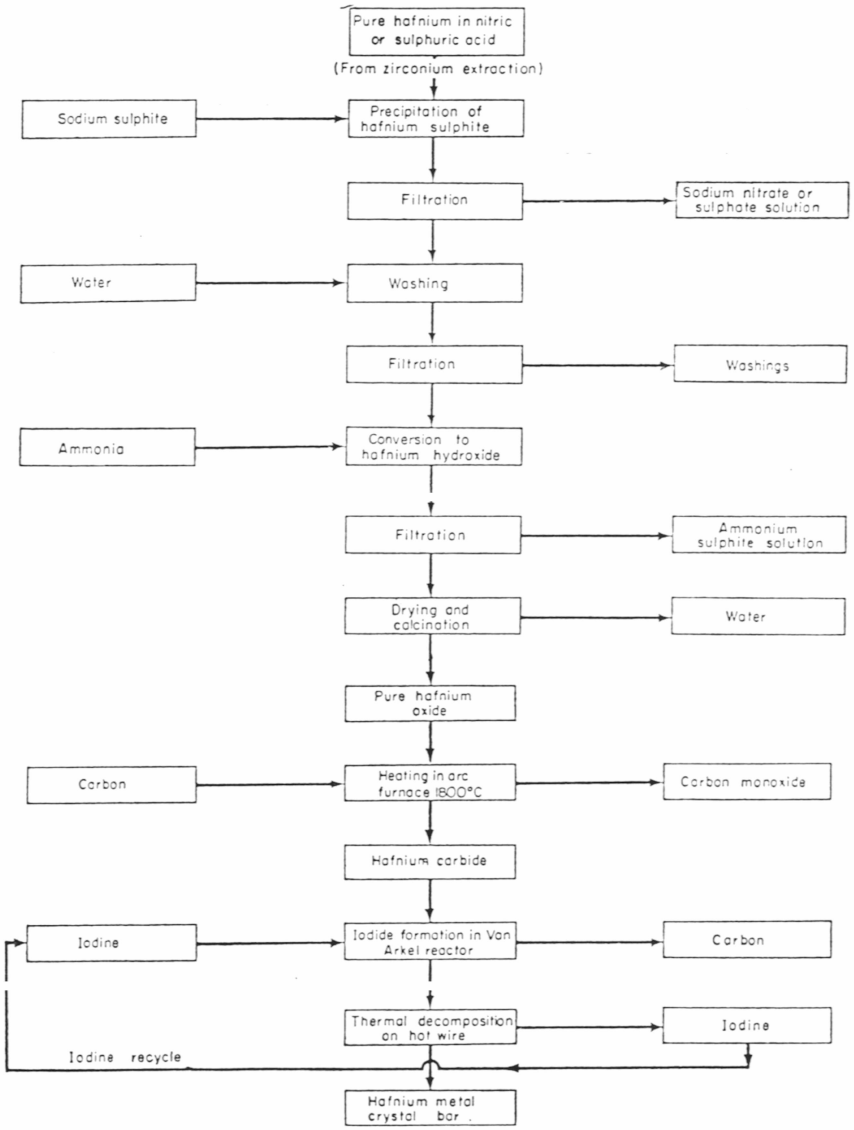

Figure {3.1}9: Flow sheet showing the conventional hafnium extraction route from the zirconium by-product liquor (see previous Figures {3.1}7 and {3.1}8) via oxide, carbide thence iodide decomposition to hafnium metal [30].

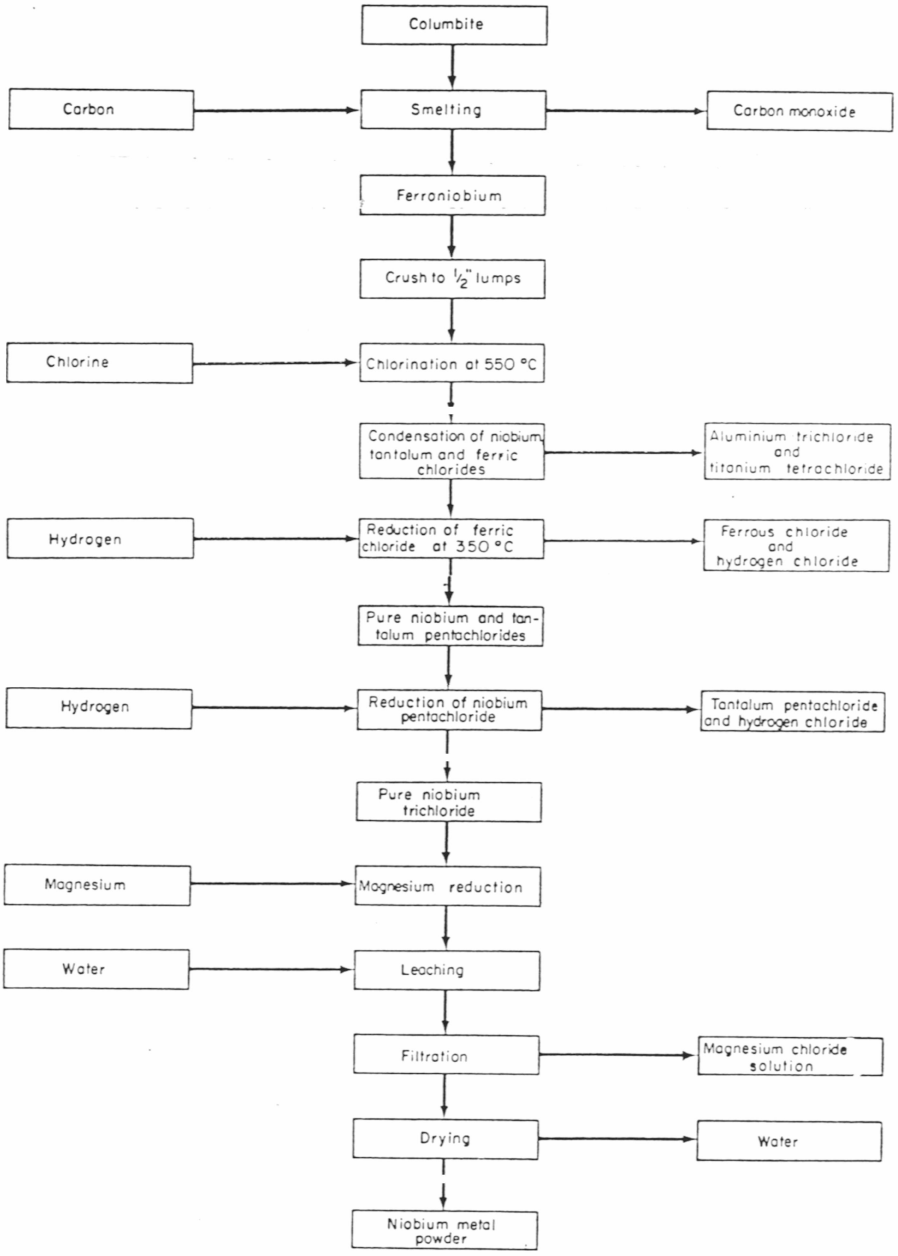

Figure {3.1}10: Flow sheet showing the conventional niobium extraction route via chlorination of ferroniobium, hydrogen purification and Kroll (magnesium) reduction to niobium metal [30].

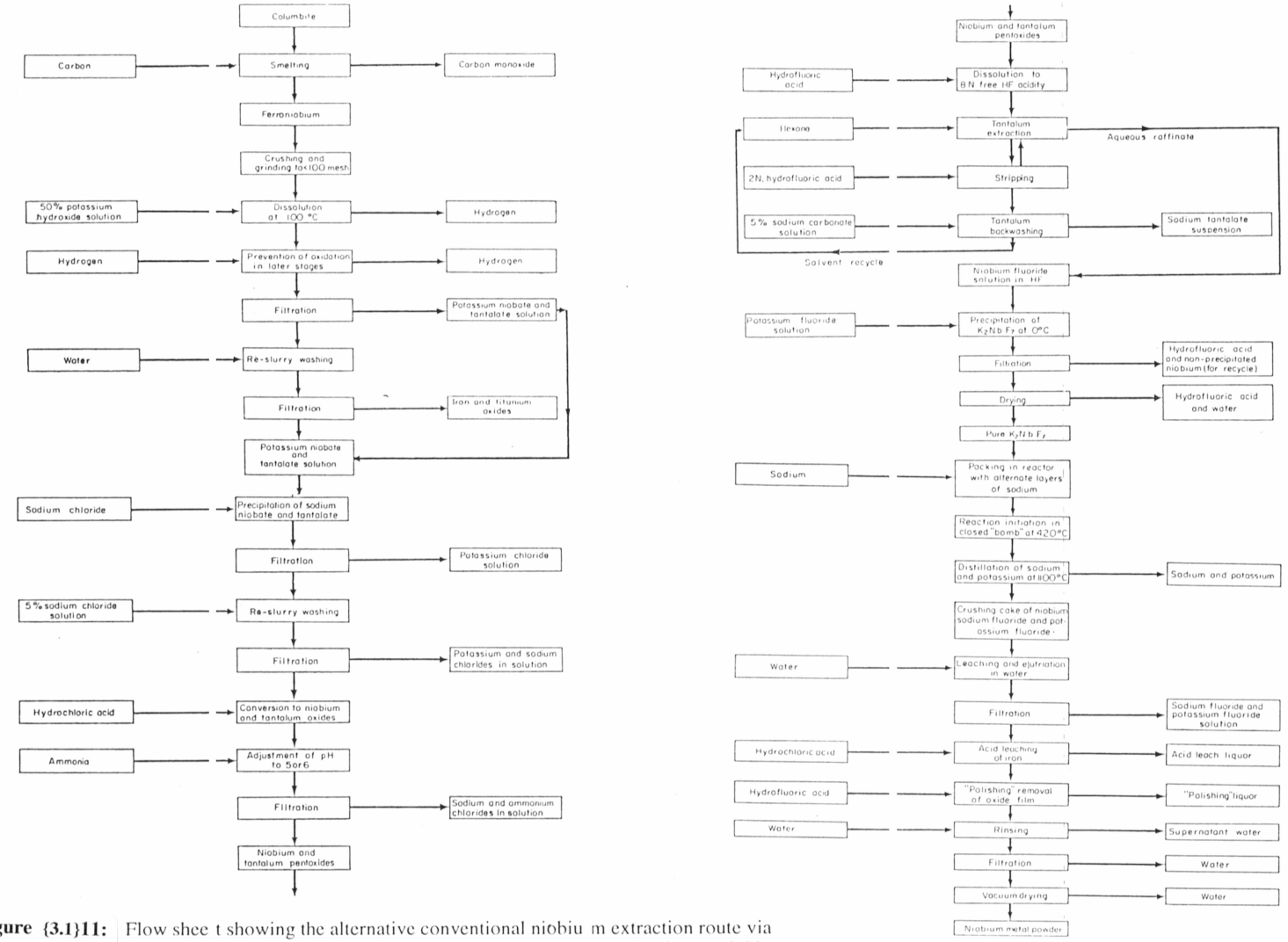

Figure {3.1}11: Flow shee t showing the alternative conventional niobiu m extraction route via alkali diss olution, solvent extraction and Hunter (sodiur n) reduction to niobium metal [30] .

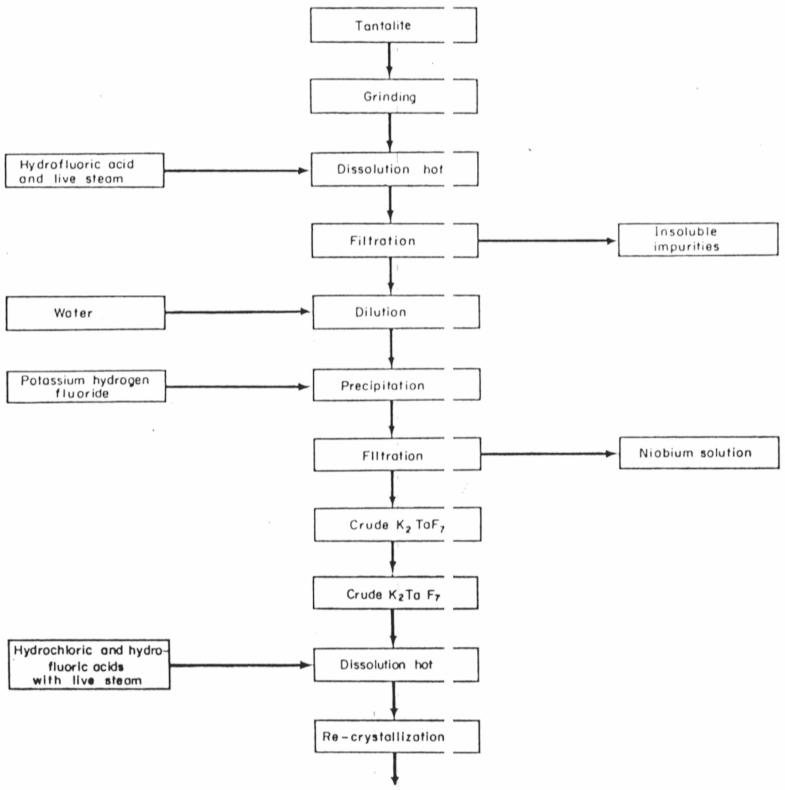

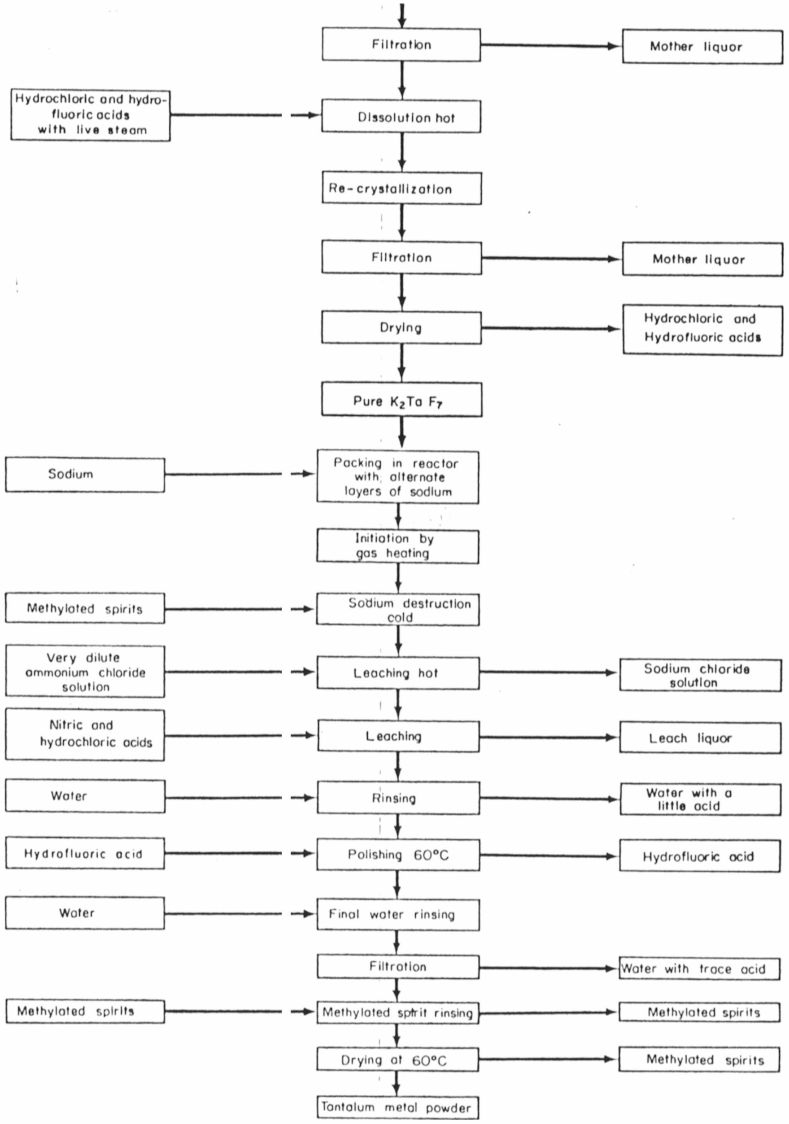

Figure {3.1}12: Flow sheet showing the long established conventional tantalum extraction route via fluoride c lissolution, re-crystallisation of the double fluoride and Hunter (s odium) reduction to tantalum metal [30]

(a)

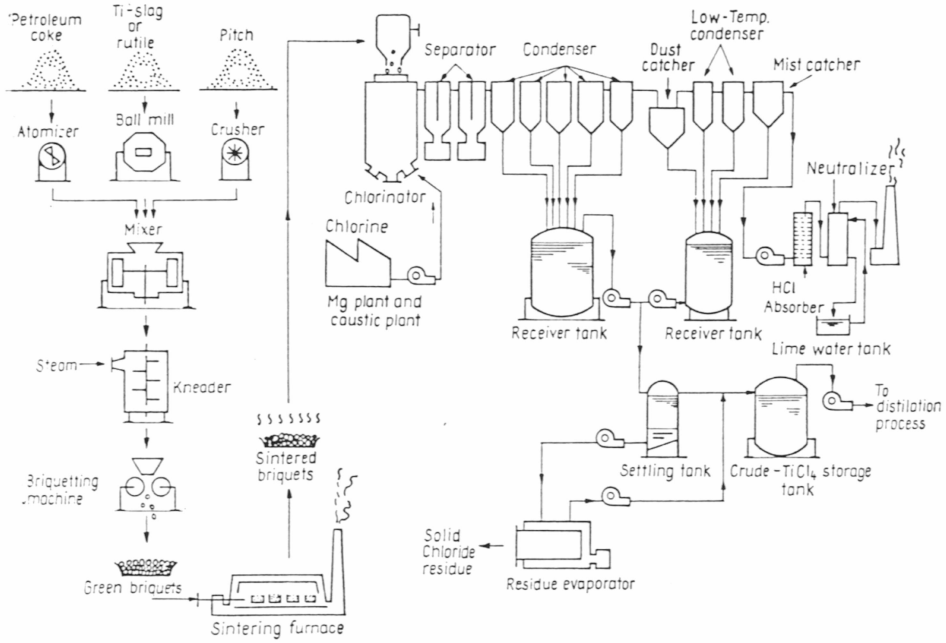

(b)

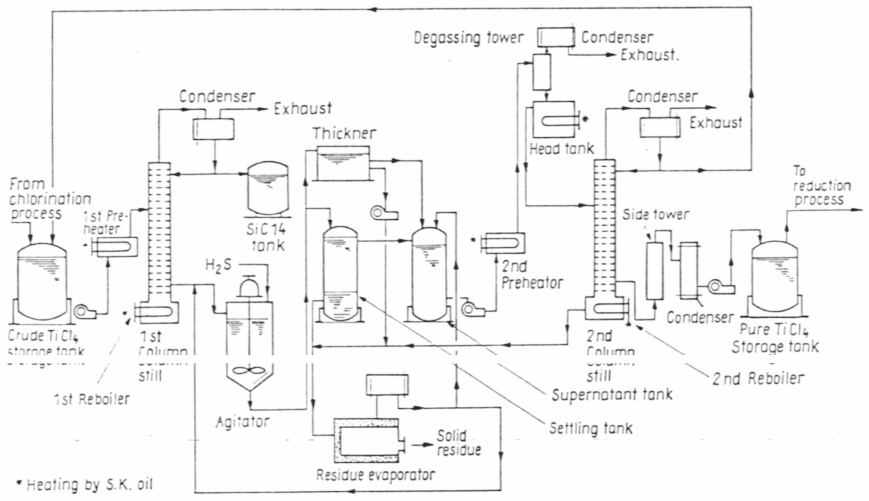

Figure {3.1}13: Schematic flow sheet showing the principal steps in the continuous chlorination of oxide titaniferous source material to produce a pure titanium tetrachloride final product. Stage (**a**) shows the initial processes which produce a crude titanium tetrachloride - the source material for stage (**b**), the distillation stage [47]. This system is similar to chlorination processes for ores of other refractory metals and of comparably reactive metals.

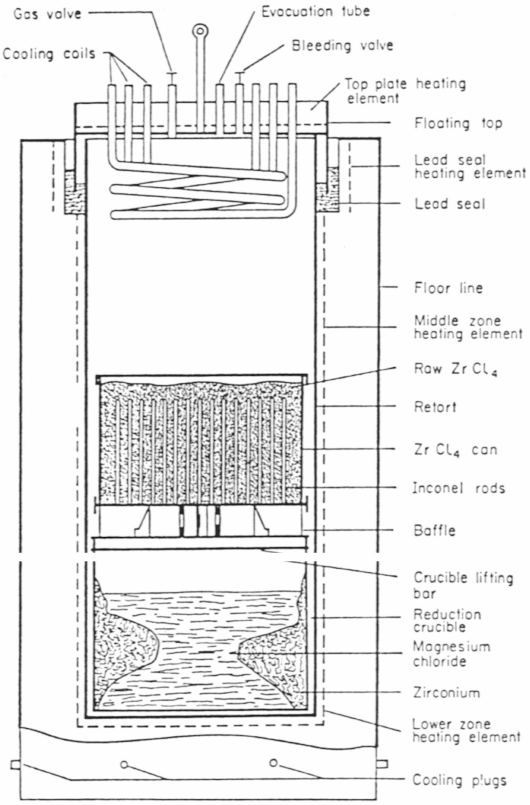

Figure {3.1}14: Sketch of a typical Kroll type reduction furnace showing the pre-reduction chloride charge (zirconium tetrachloride in this case) prior to immersion in molten magnesium. Shown below the charge is the final reaction products (zirconium sponge at the wall with liquid magnesium chloride) which go to reclamation and distillation [30].

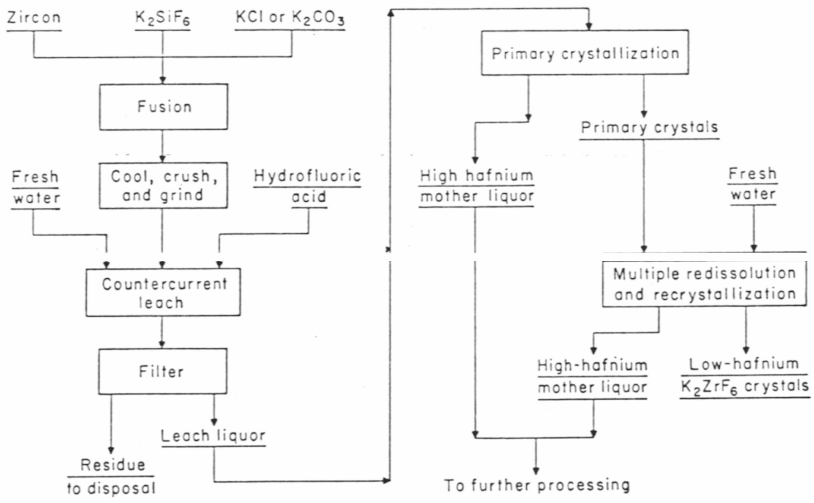

Figure {3.1}15: Flow sheet showing the production from zircon (with ensuing separation) of zirconium and hafnium with production emphasis on the optimisation of a high hafnium mother liquor [44].

The following Figures {3.1}16 to {3.1}26 represent a more rigorous treatment of the production route possibilities for one of the five relevant refractory metals: niobium - with some consideration to tantalum separation and production. The procedures presented (shown mainly as flow sheets) are analogous to, or can be easily extrapolated to, the production of other refractory metals.

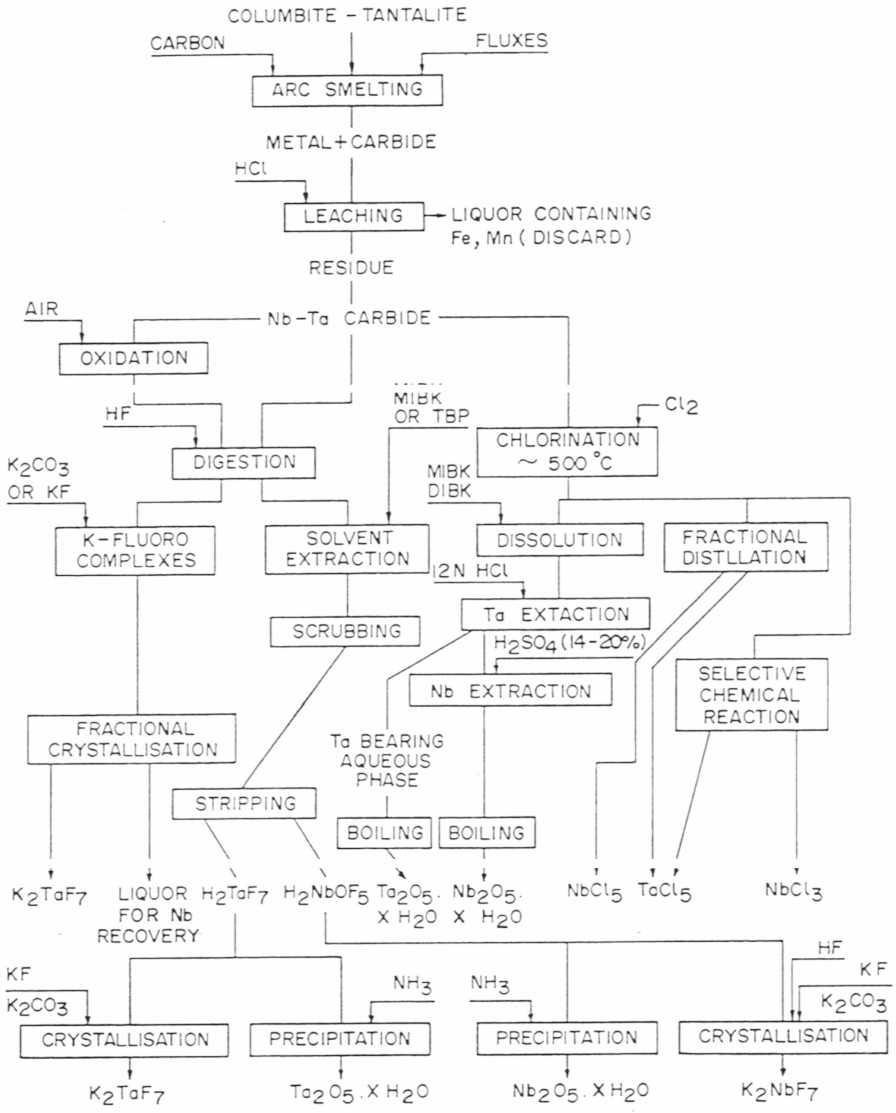

Figure {3.1}16: Schematic flow diagram showing treatment options for the processing of columbite/ tantalite ore concentrate via the direct carbothermic reduction of arc smelting [29]

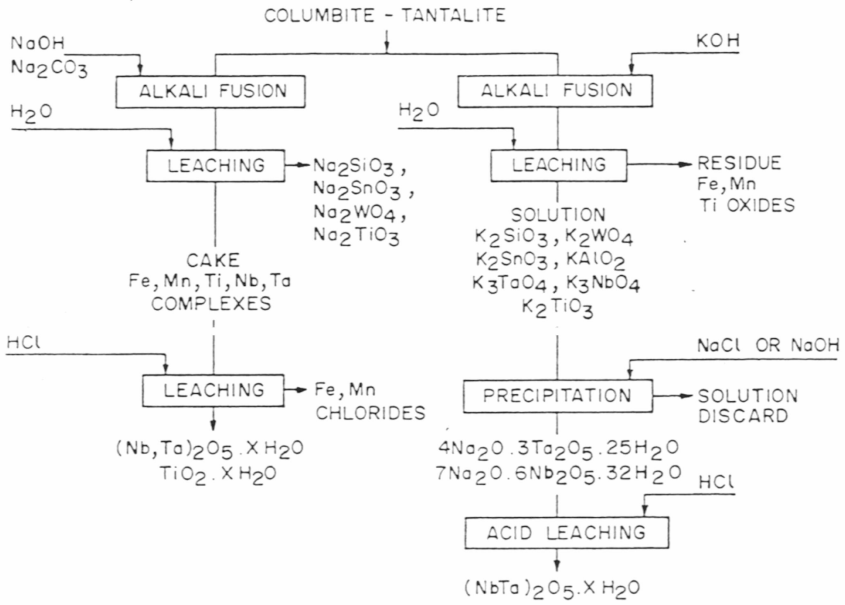

Figure {3.1}17: Simplified flow sheet showing the alkali fusion treatment of columbite/tantalite ore concentrate to a crude, pre-separationoxide intermediate product [29].

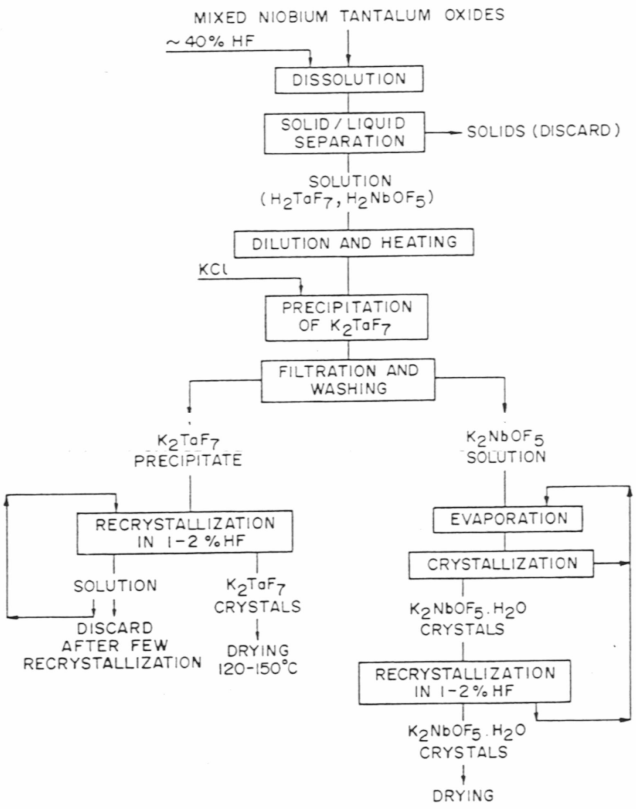

Figure {3.1}18: Flow sheet showing an alternative (to figure {**3.2.4**} **1**) method of separation of niobium from tantalum by fractional crystallisation [29].

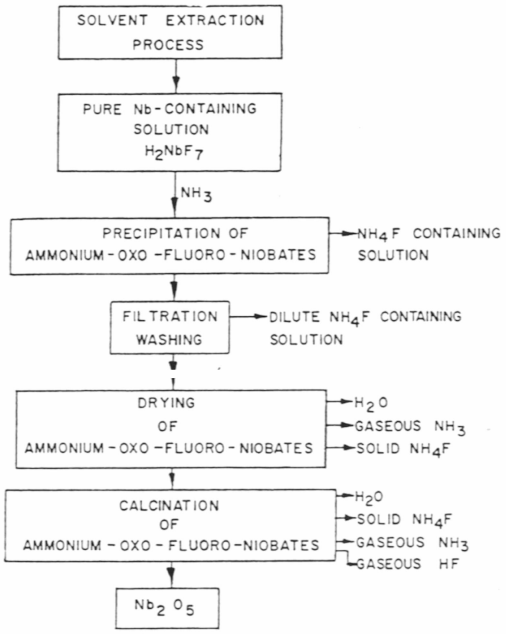

Figure {3.1}19: Flow sheet showing the preparation of niobium pentoxide via the ammonia route [29].

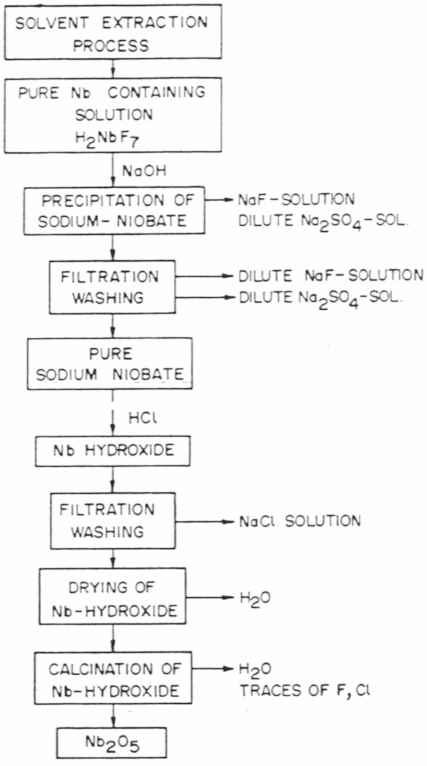

Figure {3.1}20: Flow sheet showing the preparation of niobium pentoxide via the sodium hydroxide route [29].

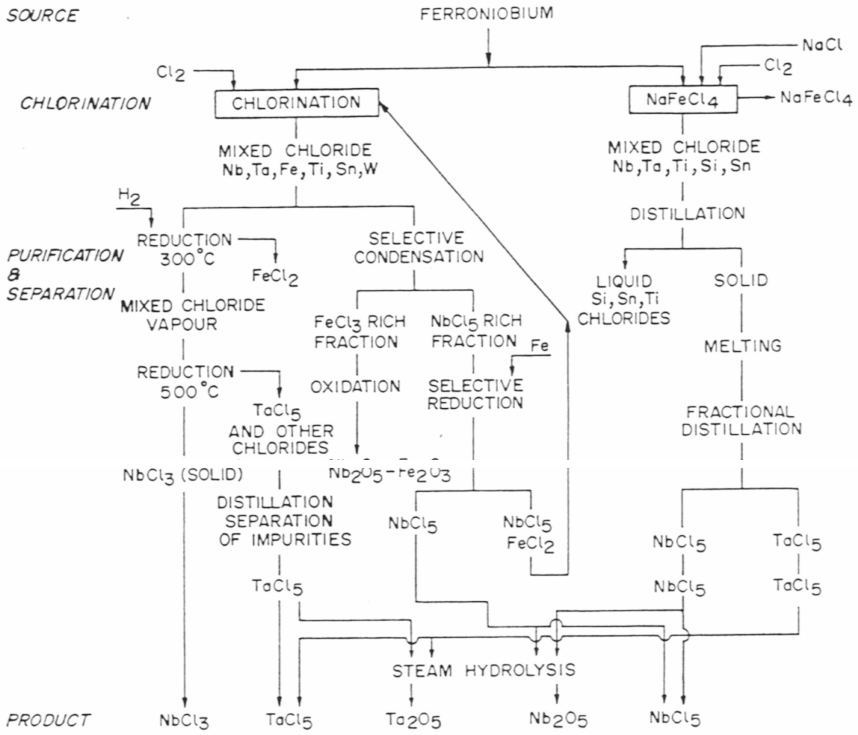

Figure {3.1}21: Schematic flow diagram showing the chlorination route options from ferroniobium to pure niobium and tantalum chlorides and to pure oxides by steam hydrolysis [29]

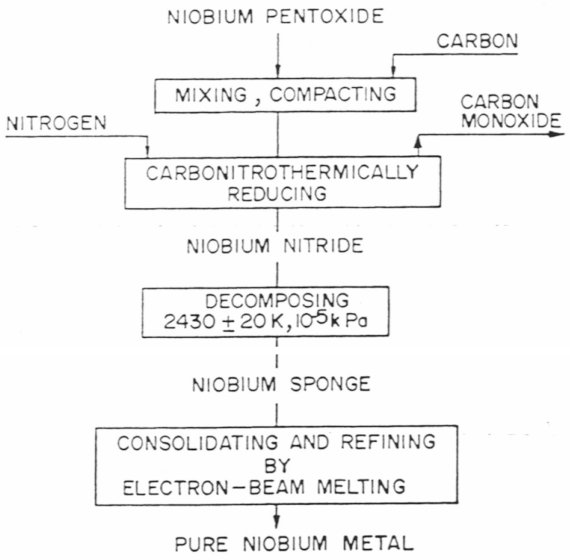

Figure {3.1}22: Flow sheet showing the extraction route for niobium metal from the pentoxide via carbonitrothermically reduced niobium nitride intermediate [29].

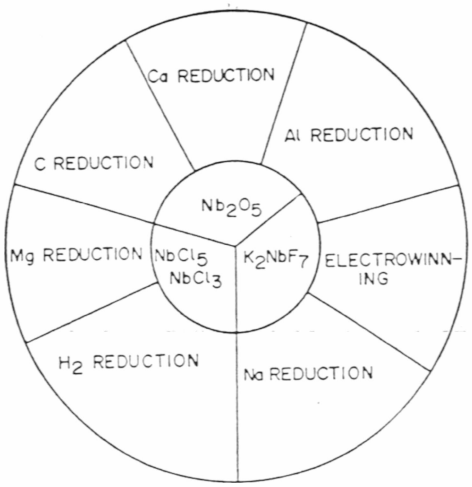

Figure {3.1}23: Representation of reduction process alternatives in the production of niobium metal [29]

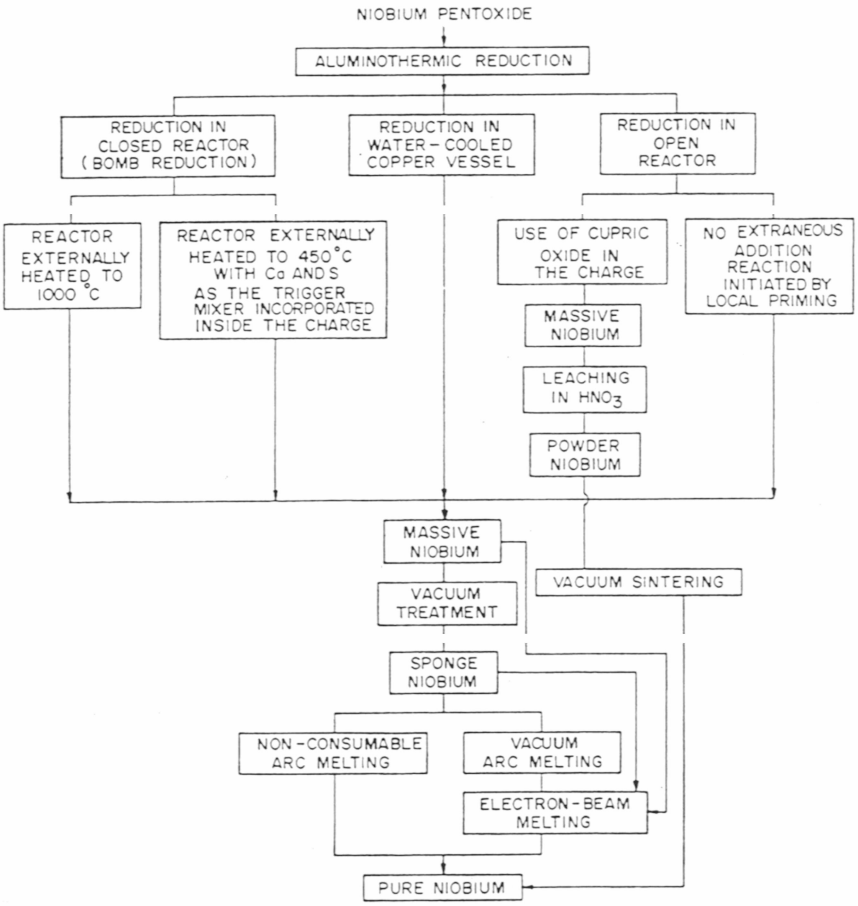

Figure {3.1}24: Flow sheet showing the aluminothermic reduction route alternatives from the pentoxide to niobium metal and refining alternatives to pure niobium [29].

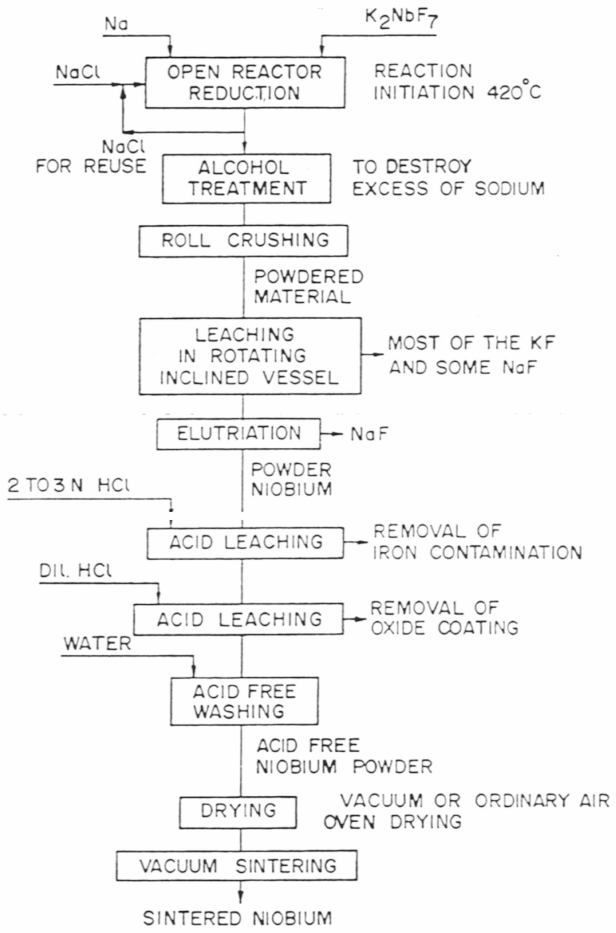

Figure {3.1}25: Flow sheet showing the sodiothermic reduction route from the double fluoride to niobium metal [29].

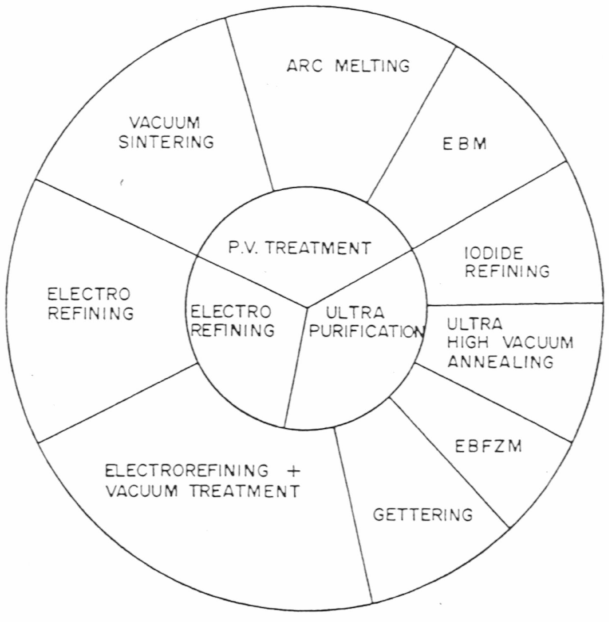

Figure {3.1}26: Representation of process alternatives in the refining of crude (sintered or sponge type) metal to pure niobium [29].

APPENDIX B

Appendix 6.1.

Where and to the limits that they are known (as provided to the project), the following are the source derivations and analyses of minerals used throughout this project. Unless otherwise noted, the listed minerals were the sole sample of that mineral to be used in the project.

1. Refractory metal minerals core to this project.

Titanium source minerals.

Rutile: TiO_2 > 99%, with trace Fe and Cr, origin unknown but sourced from northern N.S.W.

Ilmenite: $FeTiO_3$ with minor ($\leq$ 3%) $FeCr_2O_4$ and trace Mn, Si and Al, origin unknown but sourced from northern N.S.W.

Anatase: comm. pure TiO_2 (TiONIA®), > 99.9% TiO_2

Zirconium/hafnium source minerals.

Zircon: $Si(Zr,Hf)O_4$ with Hf $\approx$ 2at%, with trace impurities Cr, Ti, Fe and REE's (rare earth elements), source and origin unknown but from N.S.W.

Zirconia: as commercial grade ZrO_2 > 99.96% with tr. Fe, Si, Ti, Al and S, source Z-TECH® Pty. Ltd., Melbourne.

Baddeleyite: as lab. grade zirconia, ZrO_2 > 99% (Hopkin and Williams) – used principally in early work.

Hafnia: lab. grade, HfO_2 > 99.5%.

Tantalum/niobium source minerals.

Wodginite: $((Mn,Fe)Sn(Ta,Nb))_{16}O_{32}$ as mineral concentrate sourced from the Fortescue Metals Group Wodgina mine, at%Ta:at%Nb $\approx$ 33:1, Ti $\approx$ 0.5at%, Mn $\geq$ Fe, tr.Al,Si and Ca.

Tantala: lab. grade, Ta_2O_5 , 99.0% (Aldrich).

Tantalum chloride, $TaCl_5$, 99.8% (Aldrich).

Niobia: lab. grade, Nb_2O_5 > 99.0%.

Halide decomposition, source minerals.

Cobaltous chloride hydride [or cobalt (II) chloride hexahydrate], $CoCl_2.6H_2O$, as laboratory grade reagent (98%).

Mineral halite, NaCl, as a geological sample from Lake Frome deposit, S. Aust.

2. Supplementary (extraneous) non-core minerals used in this project.

Haematite: Fe_2O_3 sourced from Mt Newman as ore, ~ 98% pure.

Magnetite: Fe_3O_4 source unknown, trace to minor Mn, Si and Al.

Magnetite: (Ti-rich) Fe_3O_4 (titano-magnetite) < 5% Ti as ilmenite, source New Zealand Steel Ltd., origin (beach sand mining in) New Zealand.

Magnetite: (V-rich) Fe_3O_4 , < 1.5% V, tr. Mn, Si, Al; source: Savage River, Tas.

Iron carbide: Fe_3C > 99%, product of Wundowie pilot plant, W.A.

Stannic Oxide: as lab. grade SnO_2 >99% (Hopkin and Williams).

Cassiterite: SnO_2 as high grade min. concentrate sourced from Ardlethan mine, N.S.W.,

Chromite: $FeCr_2O_4$ as high grade min. concentrate, > 85% $FeCr_2O_4$ sourced from

Muswellbrook Energy and Minerals Ltd. (MEM), origin N.S.W.

Chromite: $FeCr_2O_4$ as low grade min. concentrate, > 70% $FeCr_2O_4$ sourced from Minpro N.L., origin Philippines.

Chromium oxide: Cr_2O_3 as lab. grade mineral > 98%

Vanadium pentoxide: V_2O_5 as lab. grade mineral, V_2O_5 > 99.8%.

Tenorite: cupric oxide as lab. grade mineral, CuO > 97.5%, tr. Fe, As, S, N, Cl (Analar).

Uraninite (pitchblende): UO_2 as massive mineralisation, milled, UO_2 > 96%, source unknown but from N.T.

Xenotime: $(REE,Y)PO_4$ with major La and Ce, tr. Sm, Nd. Origin W.A. and sourced from Muswellbrook Energy and Minerals Ltd. (MEM).

Monazite: $(REE,Th)PO_4$ with major Ce, minor Th, tr Zr, Ti, Y, sourced from Cable Sands (W.A.) Pty. Ltd., origin W.A. [Mine assay: min. concentrate

23.4% CeO_2 , 1.06% Y_2O_3 , 0.88% TiO_2 , 0.77% Al_2O_3 , 1.89% SiO_2 , 20.53% P_2O_5 , 1.49% ZrO_2 and 6.02% ThO_2 in gangue with 5.1% acid insolubles.]

Bastaesite: $(Ca,La)CO_3(OH,F)$ with minor $CaCO_3$ and tr.Ce, Nd and Pr, source Dept. Metallurgy and Materials Eng., UoW, origin unknown.

Neodymium oxide: Nd_2O_3 as Meteor® brand commercial grade mineral > 99.9% Nd_2O_3 sourced from SX Holdings Ltd., origin W.A.

Cerium Oxide: CeO as lab. grade mineral > 99%.

Yttria: Y_2O_3 as commercial. grade mineral, 99.99%, source SX Holdings Ltd.

Barium oxide: BaO_2 as lab. grade mineral > 99.5%.

Barium carbonate: $BaCO_3$ as lab. grade mineral > 98%.

Molybdenum Trioxide: MoO_3 as lab. grade mineral > 99.5% MoO_3 , tr. Pb, S, N (Anivar).

Molybdenite: MoS_2 as massive mineralisation, ore > 99% MoS_2 , source source unknown but origin Tas.

Wolframite: $(Fe,Mn)WO_4$ as crude min. concentrate with minor Fe_3O_4 and tr Si, Ti and Al, source Denehurst Ltd., Mount Carbine, Qld.

Wolframite: (Nb-bearing) $(Fe,Mn)WO_4$ (> 97%) as min. concentrate, with minor

Nb ~1.5% and tr. Si, Al and Cr, source Dr B. Chenhall, UoW, orign Tas.

Scheelite: $CaWO_4$ as min. concentrate with minor CaF_2 and tr. Fe, Mn and Na, source unknown but origin Tas.

Calcite: $CaCO_3$ as high purity mineral, milled, sourced from Dept. Geology, UoW, origin unknown.

Fluorite: CaF_2 as high purity mineral, milled, sourced from Dept. Geology, UoW, origin unknown.

Dolomite: $CaMg(CO_3)_2$ as good purity mineral lump, milled, sourced from BHP Central Laboratory, origin N.S.W.

Gypsum: $CaSO_4 . 2H_2O$ as good purity mineral, milled, source from Dept. Geology, UoW, origin N.S.W.

Magnesia: MgO as lab. grade mineral >98%.

Magnesite: $MgCO_3$ as high purity commercial mineral, milled, source MM Metals, origin southern N.S.W.

Alumina: Al_2O_3 as lab. grade mineral > 99.9%.

Boehmite: AlO(OH) as mineral of good purity, sourced from Dept. Geology, UoW, origin north Qld.

Goethite: FeO(OH) as mineral of high purity, sourced from Dept. Geology, UoW, origin Qld.

Zincite: ZnO as lab. grade mineral > 99.95%

Franklinite: $\{(Fe^{3+},Zn,Mn^{2+})(Fe^{2+},Mn^{3+})\}_2O_4$ as good purity mineral, milled, sourced from Dept. Geology (Dr B. Chenhall), UoW, origin U.S.A.

Bauxite: [boehmite/diaspore (AlO(OH)) + goethite (FeO(OH))] sourced from Alcoa, origin Weipa, north Qld.

Minium: Pb_3O_4 as lab. grade mineral > 99%.

Cerussite: $PbCO_3$ as good purity mineral, milled, sourced from Dept. Metallurgy and Materials Eng., UoW, origin unknown.

Chalcopyrite: $CuFeS_2$ as min. concentrate ~97% $CuFeS_2$,source unknown but origin Cobar, N.S.W.

Chalcocite: Cu_2S as min. concentrate ~99% Cu_2S, source and origin unknown.

Pyrite: FeS_2 min. concentrate ~ 97% FeS_2 , source unknown but origin Broken Hill, N.S.W.

Pyrrhotite: $Fe_{1-n}S$ as min. concentrate ~98%, sourced from Dept. Geology UoW, origin N.S.W.

Stannite: Cu_2SnFeS_4 as good purity mineral lump > 96%, milled, sourced from Dept. Geology, UoW, origin northern N.S.W.

Galena: PbS min. concentrate ~ 98% PbS, source BHAS Port Pirie, origin Broken Hill, N.S.W.

Sphalerite: ZnS min. concentrate > 96% ZnS, source North Broken Hill mine, N.S.W.

Arsenopyrite: FeAsS min. concentrate > 95% FeAsS, source unknown but origin Kambalda, W.A.

Stibnite: Sb_2S_3 min. concentrate > 97% Sb_2S_3 , source WMC, origin W.A.

Hydrated nickel nitrate: $NiNO_3 \cdot 6H_2O$ as lab. grade chemical > 99.9%.

Millerite: NiS as high purity mineral ~99.5%, milled, sourced from Dept. Geology, UoW, origin S.A.

Pentlandite: $(Fe,Ni)_9S_8$ min. concentrate > 96%, source WMC, origin W.A.

Cobaltite/Pentlandite: (Co,Fe)AsS/$(Fe,Ni)_9S_8$ min. concentrate ~ 95% as 1:1 (Co,Fe)AsS/$(Fe,Ni)_9S_8$, source WMC, Kambalda, W.A.

Hamersley blast furnace pellets (indurated iron ore), sourced via BHP, origin north-west W.A.

Robe River blast furnace pellets (indurated iron ore), sourced from Cliffs Robe River operation, origin north-west W.A.

Savage River blast furnace pellets (indurated iron ore), sourced from Savage River Mine, origin north-western Tas.

Whyalla blast furnace pellets (indurated iron ore), sourced from BHP Whyalla, Whyalla, S.A.

Titanium carbide: TiC as lab. grade mineral > 99%.

Titanium nitride: TiN as lab.grade mineral > 99%, source HCST.

Titanium diboride: TiB_2 as commercial grade mineral > 99%, source HCST, Berlin, Germany.

Boron carbide: B_4C as commercial grade > 99%, source HCST, Berlin, Germany.

3. Carbonaceous reductant forms used in this project.

Morwell brown coal slurry, used in earliest experimentation only.

Brown coal char, Auschar®, used in early experimentation only.

Dupont™ activated charcoal, in granular and milled forms, > 99.9% C, used in all Ta/Nb, Zr/Hf plus rutile and ilmenite Ti core experimental work plus non-core work.

Norit® RO 0.8 activated charcoal, in pellet and milled forms, > 99.9% C, used in all anatase Ti core experimental work.

4. Aluminium powder used in aluminothermic reduction experimentation.

Finely divided Al > 99.9% as fresh, un-oxidised powder, 212 – 300 μm as lab. grade chemical.

Appendix 6.2.

This appendix contains **(*i*)** the very basic calculations to facilitate the apportionment of reactants prior to ring mill blending, plus **(*ii*)** the actual charge masses for all core reactant charges as charged into the chosen (16 ml) crucible type used through the core experimentation.

1. Proportion calculations to address stoichiometry for blending of minerals.

For the purposes of this project, given that a deliberate excess of reductant was intended, stoichiometric precision was not an issue, hence, (in calculations) the relative atomic mass for each element was rounded down and is a close approximation of values listed in Emsley's "The Elements"[3]. For carbothermic blends an intentional **20% excess of carbon** was used in the actual intimate, milled blend to allow for CO gasification locally within the blend as charged and independent of the general CO gasification in the adjacent granular char layers. [Early experimentation was indicative that such gasification indeed occurred within the fine char blend, and that reduction exercises were "more complete" when excess char was included in the actual intimate reactant blend. This minor gasification was distinct from that generated in the supplementary granular char destined to provide the reducing CO atmosphere "blanket" intended to envelope the reactants from initial heating, through reaction to completion and quench.]

It was found (by early trial and error) that a small amount of accompanying carbon in the aluminothermic blends neither impeded nor replaced the aluminothermic reaction but provided discernible process benefit. This benefit was dually derived as the charcoal provided an intimate, local source of heating within the blend (through its own high microwave susceptibility plus the accompanying dielectric dopant effect) thus to initiate the thermite reaction plus, through local gasification, it rapidly provided an insitu O_2-reducing environment *within* the blend.

Whilst a 20% stoichiometric excess of char was assigned to all carbothermic blends, when combining the aluminothermic components for mill blending, carbon additions were determined by a nominal mass ratio of 6:1 (Al:C), irrespective of the target mineral. It was deemed that, given the intimacy of the milled blend, the thermite type aluminothermic reactions did not require any nominal excess of Al and that the char-generated CO was sufficient protection against oxidation of the fine Al particles and, indeed, may reduce any oxidation layer present. Process heating generated in the char also provided the requisite exothermic energy to initiate the near instantaneous thermite reaction in the reactants.

Whereby, as the abovementioned was based moreso upon reasoned suppositions and observations than upon hard and fast rules and, although rudimentary, the method provided predictability to reduction process routine and accomplishment which (as adjudged against early experimentation) was reflected as consistency in core experimental results – that is to say, reproducibility.

(a) Blend calculation for both rutile and anatase with carbon.

TiO_2	+	2.4 C	→	Ti	+	2 CO ↑ (nominal)
[**1**(47.9) + **2**(16.0)]		**2.4**(12.0)				
79.9		28.8				

That is, 79.9 g of TiO_2 for each 28.8 g of charcoal in each milled blend for carbothermic reduction blend.

(b) Blend calculation for both rutile and anatase with aluminium.

TiO_2	+	(2/3)2Al	+	(1/2) C	→	Ti	+	Al_2O_3
[**1**(47.9) + **2**(16.0)]		[(**4/3**)(27.0)]		**1/2**(12.0)				
79.9		36.0		6.0				

That is, 79.9 g of TiO_2 for each 36.0 g of aluminium powder plus 6.0 g of char in milled blend for aluminothermic reduction blend. (Refer also to comments in Section **7.2.2** regarding minor variations to mass of Al powder provisionally employed in some experimental trials.)

(c) Blend calculation for ilmenite with carbon.

$$\underset{[(55.8)+(47.9)+\mathbf{3}(16.0)]}{FeTiO_3} + \underset{\mathbf{3.6}(12.0)}{3.6\ C} \rightarrow FeTi + 3\ CO\uparrow \text{(nom.)}$$

$$151.7 \qquad 43.2$$

That is, 151.7 g of ilmenite for each 43.2 g of charcoal in each milled blend for carbothermic reduction.

(d) Blend calculation for ilmenite with aluminium.

$$\underset{[(55.8)+(47.9)+\mathbf{3}(16.0)]}{FeTiO_3} + \underset{\mathbf{2}(27.0)}{2\ Al} + \underset{\mathbf{3/4}(12.0)}{3/4\ C} \rightarrow FeTi + Al_2O_3 \text{ (nom.)}$$

$$151.7 \qquad 54.0 \qquad 9.0$$

That is, 151.7 g of ilmenite for each 54.0 g of aluminium powder plus 9.0 g of char in milled blend for aluminothermic reduction.

(e) Blend calculation for zircon with carbon.

$$\underset{[(91.2)+(28.1)+\mathbf{4}(16.0)]}{ZrSiO_4} + \underset{\mathbf{4.8}(12.0)}{4.8\ C} \rightarrow Zr + Si + 4\ CO\ (nom)$$

$$183.3 \qquad 57.6$$

That is, 183.3 g of zircon for each 57.6 g of char in each milled blend for carbothermic reduction.

(f) Blend calculation for zircon with aluminium.

$$ZrSiO_4 + 8/3\ Al + C \rightarrow Zr + Si + 4/3\ Al_2O_3\ (nom.)$$

$$[(91.2) + (28.1) + \mathbf{4}(16.0)] \quad \mathbf{8/3}(27.0) \quad 12.0$$

$$183.3 \quad 72.0 \quad 12.0$$

That is, 183.3 g of zircon for each 72.0 g of aluminium powder plus 12.0 g of char in each milled blend for aluminothermic reduction.

(g) Blend calculation for zirconia with carbon.

$$ZrO_2 + 2.4\ C \rightarrow Zr + 2\ CO \uparrow\ (nom.)$$

$$[(91.2) + \mathbf{2}(16.0)] \quad \mathbf{2.4}\ (12.0)$$

$$123.2 \quad 28.8$$

That is, 123.3 g of zirconia (baddeleyite) [ZrO_2] for each 28.8 g of char in each milled blend for carbothermic reduction.

(h) Blend calculation for zirconia with aluminium.

$$ZrO_2 + 4/3\ Al + 1/2\ C \rightarrow Zr + 2/3\ Al_2O_3\ (nom.)$$

$$[(91.2) + \mathbf{2}(16.0)] \quad \mathbf{4/3}\ (27.0) \quad \mathbf{1/2}(12.0)$$

$$123.2 \quad 36.0 \quad 6.0$$

That is, 123.3 g of zirconia (baddeleyite) [ZrO_2] for each 36.0 g of aluminium powder plus 6.0 g of char in each milled blend for aluminothermic reduction.

(i) Blend calculation for hafnia with carbon.

$$HfO_2 + 2.4\ C \rightarrow Hf + 2\ CO \uparrow\ (nom.)$$

$$[(178.5) + \mathbf{2}(16.0)] \quad \mathbf{2.4}(12.0)$$

$$210.5 \quad 28.8$$

That is, 210.5 g of hafnia for each 28.8 g of char in each milled blend for carbothermic reduction.

(j) Blend calculation for hafnia with aluminium.

$$HfO_2 + 4/3\ Al + 1/2\ C \rightarrow Hf + 2/3\ Al_2O_3\ (nom.)$$

$$[(178.5) + \mathbf{2}(16.0)] \quad \mathbf{4/3}(27.0) \quad \mathbf{1/2}(12.0)$$

$$210.5 \quad 36.0 \quad 6.0$$

That is, 210.5 g of hafnia for each 36.0 g of aluminium powder plus 6.0 g of char in each milled blend for aluminothermic reduction.

(k) Blend calculation for wodginite with carbon.

It was known from verbal advice provided by the miner through Professor Worner and subsequently substantiated in EDS analyses of early trial reduction products that the proportions to be used in wodginite mineral conversions were: 55:45 (Mn:Fe), 97:3 (Ta:Nb), and that Sn was ~ 30wt% of reduced metal.

$$((Mn,Fe)Sn(Ta,Nb))_{16}O_{32} + (1.2)32\ C \rightarrow (Fe,Mn)Sn + (Ta,Nb) + 32\ CO\uparrow$$

$$\mathbf{16.0}\{[\mathbf{0.55}(54.9) + \mathbf{0.45}(55.8)] + \mathbf{1.0}(118.7) + [\mathbf{0.97}(180.9) + \mathbf{0.03}(92.9)] + \mathbf{32.0}(16.0)\}$$

$$\mathbf{16.0}\{30.2 + 25.1 + 118.7 + 175.5 + 2.8 + 512\} \qquad \mathbf{(1.2)32.0}(12.0)$$

$$6{,}148.8(/50) \qquad 460.8(/50)$$

That is, 123.0 g of wodginite for each 9.2 g of charcoal in each milled blend for carbothermic reduction.

(l) Blend calculation for Ta_2O_5 (tantala) with carbon.

$$Ta_2O_5 + 6\ C \rightarrow 2\ Ta + 5\ CO\uparrow\ (nominal)$$

$$[\mathbf{2}(180.95) + \mathbf{5}(16.0)] \quad \mathbf{6}(12.0)$$

441.9 72.0

That is, 221.0 g Ta_2O_5 for each 36.0 g charcoal in each milled blend for carbothermic reduction.

(m) Blend calculation for Nb_2O_5 (niobia) with carbon.

Nb_2O_5	+	6 C	→	2 Nb	+	5 CO ↑ (nominal)
[**2**(92.9) + **5**(16.0)]		**6**(12.0)				
265.8		72.0				

That is, 132.9 g Nb_2O_5 for each 36.0 g charcoal in each milled blend for carbothermic reduction.

---

2. Actual charge masses used through each core mineral reduction sequence.

In all cases, the chosen standard crucible [alumina/zirconia of high temperature rating, designated as 50 mm × 18 mm × 32 mm having a nominal maximum capacity of 16 ml] was filled to volumetric capacity by the simple three-layered charge which was resolved as standard for all core experimentation. In all reduction cases the bottom layer was of 1.0 g of granular char charged evenly and without compaction, thence the appropriate mineral blend quantity (as below) was charged evenly and without compaction; thence 6.0 g of char was evenly charged to fill the crucible to a nominal level. Because the aluminothermic reactions were modestly explosive, a simple but successful solution to retaining reduction product through aluminothermic operations was devised. A fresh second crucible was forced into the first crucible containing the reactants charge, forming a neat, void-free fit. This "aluminothermic" configuration was then wrapped and secured in the regular insulation blanket binding similar to the carbothermic configuration (as per Figure **{6.2.2}1**).

The following charge quantities neither reflected any bias nor represented any specific quality or quantity other that that each (quantity) sufficiently filled the crucible accompanied by (and allowing for) the loose granular char.

Mineral/reductant:charge mass (for the noted mill-blended charge).

Anatase and rutile; TiO_2/char blend: 8.0 g.

Anatase and rutile; TiO_2/aluminium(char) blend: 11.0 g.

Ilmenite; $FeTiO_3$/char blend: 8.0 g.

Ilmenite; $FeTiO_3$/aluminium(char) blend: 10.0 g.

Zircon; $ZrSiO_4$/char blend: 18.0 g.

Zircon; $ZrSiO_4$/aluminium(char) blend: 21.0 g

Zirconia; ZrO_2/char blend: 20.0 g

Zirconia; ZrO_2/aluminium(char) blend: 23.0 g.

Hafnia; HfO_2/char blend: 27.0 g.

Hafnia; HfO_2/aluminium(char) blend: 30 0 g.

Wodginite; $[(Mn,Fe)Sn(Ta,Nb)]_{16}O_{32}$/char blend: 27.0 g.

Tantala; Ta_2O_5/char blend: 27.0 g.

Niobia; Nb_2O_5/char blend: 18.0 g.

APPENDIX C

Figure {7.1} **3:** Detail (from Figure {7.1} **2**) of exposed dendrites from the surface of an air cooled high carbon iron smelt product of microwave reduction. Process detritus materials fused to dendrites were verified as remnant slag and char particles and insulation blanket fibres. [EOM stereomicrograph.]

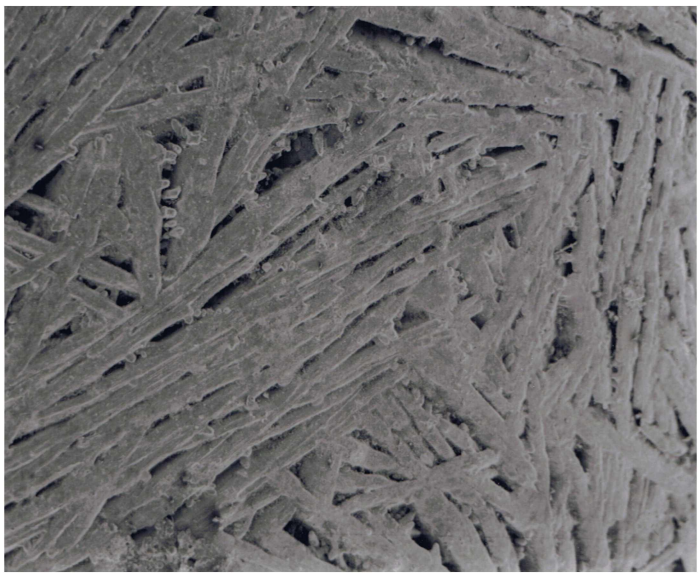

Figure {7.1} **4:** Acicular morphology of exposed primary carbide in an *internal* void of an air cooled carbon-saturated, low (~3 at% W) tungsten alloy iron button, product of microwave-stimulated carbothermic reduction of an intimate wolframite/magnetite/char blend. [EOM stereomicrograph, fov: ~1 mm

Figure {7.1} **5:** This stereo-macrograph shows zincite (ZnO) deposited adjacent to fume vents in the charged body of carbothermically reduced franklinite ($ZnFe_2O_4$) where metallic Zn was released at reduction of the franklinite. The crystal trunks were prismatic crystals of zincite, ZnO, laid-down during application of the microwave field and the tabular hexagonal plates deposited after extinguishing of the microwave field, but all crystals deposited from the product metallic Zn fume as it re-oxidised at the crystallographic site during cooling. Such deposition of crystals from a fume environment is not common, and the integral oxidation-at-deposition from that fume even moreso. [Sec EO stereo-macrograph, fov: ~3.5 mm]

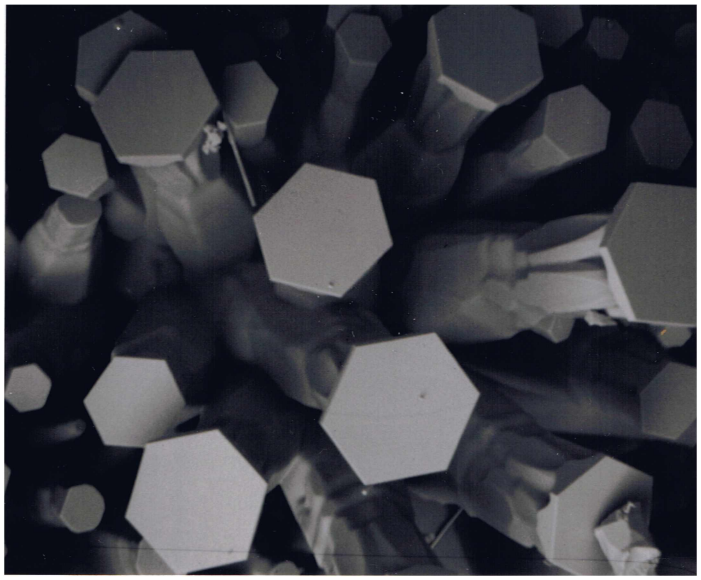

Figure {7.1} **6:** Detail of the above phenomenological crystal growth by deposition at oxidation from metallic zinc fume of hexagonal zincite caps on prismatic trunks. [Sec EO stereo-macrograph, fov: ~0.33 mm]

Figure {7.1} **7:** Photograph showing the sectioned product of a microwave precursor treated carbothermic smelt of Kambalda Ni-concentrate, a sulphide mineral concentrate (being principally pentlandite). The impure FeNi base being ~4 at% S, the Fe largely from a "heel" addition to instigate the post-microwave bath smelt. The upper, dark matte phase being Ni(Fe) ~9 at% S with regions of increased C content. The precursor microwave smelt work was on a larger scale of processing and pre-empted this wholly microwave-stimulated reduction project. [LO photograph, specimen diameter ~100 mm]

Figure {7.1} **8:** The photograph shows one whole and one sectioned cast iron ingots (or "pigs") being the collective smelt product of a microwave precursor treated, carbothermically reduced haematite/brown coal slurry composite, extruded as cylinders, dried then bath smelted after microwave pre-treatment (to instigate reduction). Each ingot weighed ~2 kg and multiple ingots were produced at each microwave precursor treated bath smelt campaign in work that pre-empted this project with its programme of reduction at magnitudes smaller-scale. [LO photograph.]

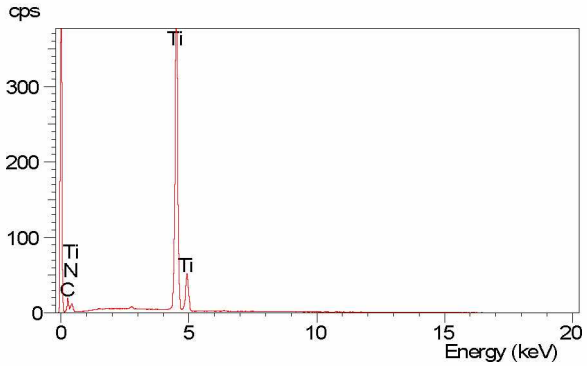

Elmt	Spect. Type	Inten. Corrn.	Std Corrn.	Element %	Sigma %	Atomic %
C K	ED	0.937	1.91	6.69	0.12	9.92
N K	ED	2.692	1.00	44.98	1.14	57.20
Ti K	ED	0.952	1.00	88.43	0.24	32.88
Total				140.11		100.00

Figure {7.2.1.3}**5:** EDS spectrum and result of EDS analysis of a spot acquisition from exposed rim material on the same 14 min specimen ANAT**17** as the previous, centrally acquired spectrum. The spectrum was acquired from a hard nitride metallic rim similar to that shown in Figure {7.2.1.1}**17**. (å%)

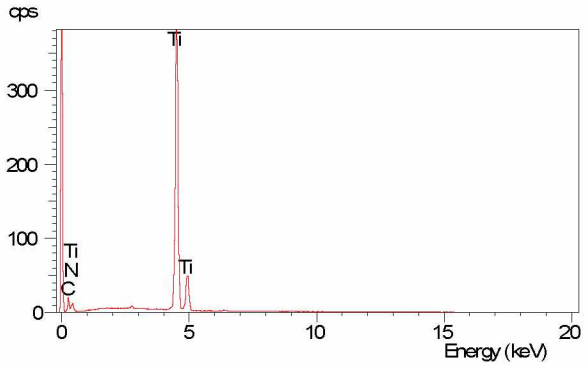

Elmt	Spect. Type	Inten. Corrn.	Std Corrn.	Element %	Sigma %	Atomic %
C K	ED	0.938	1.91	6.77	0.12	10.01
N K	ED	2.686	1.00	45.05	1.15	57.16
Ti K	ED	0.952	1.00	88.48	0.24	32.83
Total				140.30		100.00

Figure {7.2.1.3}**6:** EDS spectrum and result of EDS analysis of a spot acquisition from exposed inner material of 14 min specimen ANAT**20** as shown in the micrograph of Figure {7.2.1.1}**20**. The composition of this (and the example above) is near that of TiN_2 – conceding some substitution of C for N [that is, $Ti(C,N)_2$]. (å%) [In addition, see spectrum of adjacent C-free nitride phase presented as Figure {7.2.1.3}**8**, also ANAT**20** in Figure {7.2.1.1}**20**.]

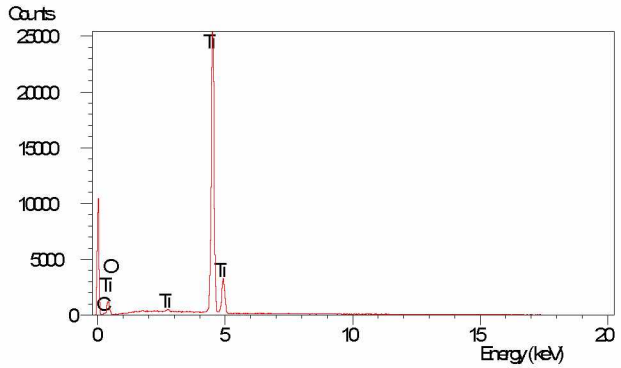

Elmt	Spect. Type	Inten. Corrn.	Std Corrn.	Element %	Sigma %	Atomic %
C K	ED	0.873	1.91	2.95	0.14	9.77
O K	ED	0.181	1.12	5.92	0.43	14.70
Ti K	ED	0.991	1.00	91.12	0.44	75.54
Total				100.00		100.00

Figure {7.2.1.3}**7:** EDS spectrum and result of EDS analysis of a spot acquisition from partially reduced oxide material typical of the grey-stage remnant oxide phase found in median processed specimens between bronze metallic clusters as seen in Figure {7.2.1.1}**8** [ANAT**07** (10 min)], Figure {7.2.1.1}**9** [ANAT**11** (10 min)] and Figure {7.2.1.1}**15** [ANAT**15** (12 min)] – equivalent material in longer-processed specimens exhibited some N and less O.

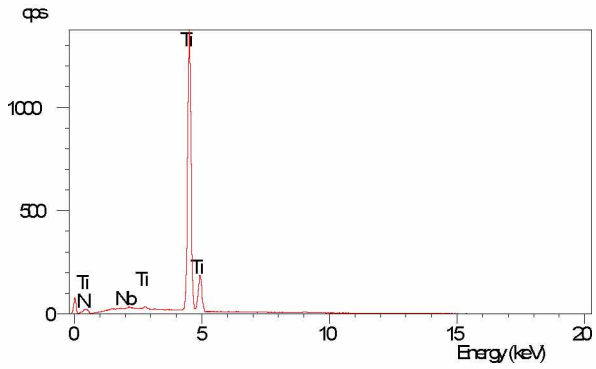

Elmt Type	Spect. Corrn.	Inten. Corrn.	Std %	Element %	Sigma %	Atomic %
N K	ED	3.163	1.00	9.50	0.41	26.48
Ti K	ED	0.985	1.00	89.95	0.42	73.29
Nb L	ED	0.853	1.00	0.54	0.08	0.23
Total				100.00		100.00

Figure {7.2.1.3}**8:** EDS spectrum and result of EDS analysis of a spot acquisition from heavily nitrided, densified phase typical of the upper-central regions of quenched product, in this case ANAT**20** (14 min) and shown in Figure {7.2.1.1}**20**. The Nb impurity was localised.

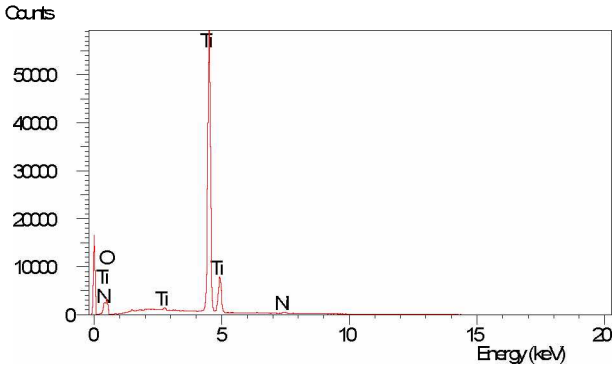

Elmt	Spect. Type	Inten. Corrn.	Std Corrn.	Element %	Sigma %	Atomic %
N K	ED	0.607	1.31	1.01	0.05	2.16
O K	ED	0.212	1.12	22.37	0.22	46.52
Ti K	ED	0.965	1.00	77.62	0.23	51.32
Total				100.00		100.00

Figure {7.2.1.3} **9:** EDS spectrum and result of EDS analysis of a spot acquisition from a partially reduced oxide phase (approximating TiO) from an under-processed region exposed to N_2-plasma. Such regions are seen in the micrograph of Figure {7.2.1.1}**1**, discernible as deeper blue regions (under oil-immersion lens LOM) and delineated by metallic flecks at grain boundaries.

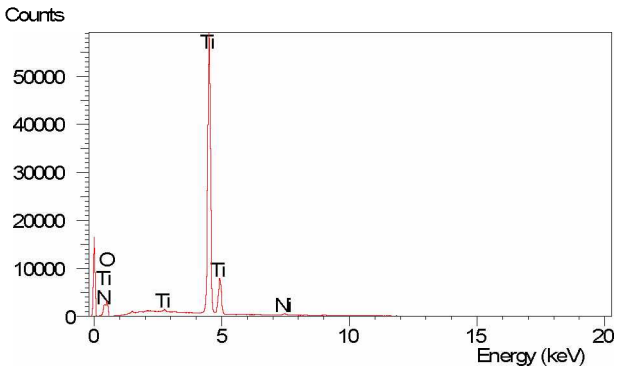

Elmt	Spect. Type	Inten. Corrn.	Std Corrn.	Element %	Sigma %	Atomic %
N K	ED	0.611	1.27	7.57	0.05	16.15
O K	ED	0.213	1.10	3.25	0.21	6.55
Ti K	ED	0.966	1.00	89.18	0.24	77.30
Total				100.00		100.00

Figure {7.2.1.3}**10:** EDS spectrum and result of EDS analysis of a spot acquisition from a section of advanced nitride rim material in specimen ANAT**11** (10 min) comparable to that "nitride" material shown in the micrograph of Figure {7.2.1.1} **9**.

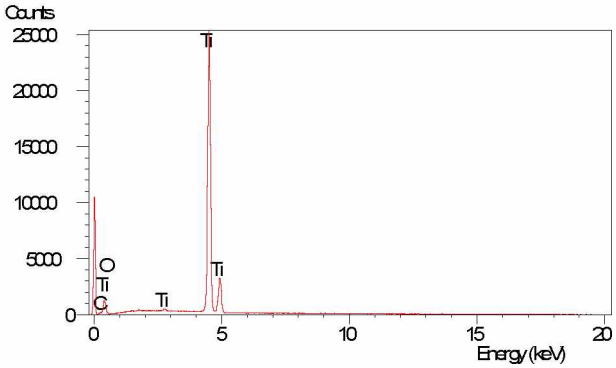

Elmt Type	Spect. Corrn.	Inten. Corrn.	Std %	Element %	Sigma %	Atomic
C K	ED	0.842	1.91	2.94	0.07	7.42
O K	ED	0.216	1.12	24.78	0.21	46.90
Ti K	ED	0.960	1.00	72.27	0.21	45.68
Total				100.00		100.00

Figure {7.2.1.3}**11:** EDS spectrum and result of EDS analysis of a spot acquisition from an enclosed region of partially reduced oxide phase exposed to CO-plasma processing. The phase, from an 8 min specimen, was similar to those (blue) oxide fields located centrally in the charge, adjacent to more-reduced phases and metallised flecks, and around remnant char particles in the micrographs of Figures {7.2.1.1}**3**, {7.2.1.1}**4** and {7.2.1.1}**5**.

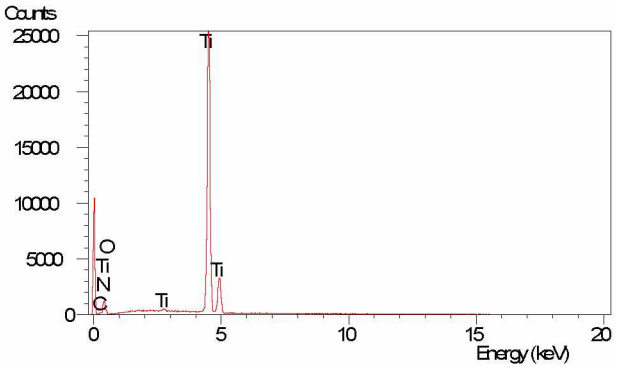

Elmt Type	Spect. Corrn	Inten. Corrn.	Std %	Element %	Sigma %	Atomic
C K	ED	0.873	1.91	2.90	0.15	9.64
N K	ED	0.533	1.29	2.76	0.13	9.81
O K	ED	0.181	1.12	1.96	0.44	6.74
Ti K	ED	0.991	1.00	92.38	0.46	73.81
Total				100.00		100.00

Figure {7.2.1.3}**12:** EDS spectrum and result of EDS analysis of a spot acquisition from bronze coloured phase in ANAT**14** – as shown in Figure {7.2.1.1}**12** accompanying oxide reduction phases – and being compositionally representative of "carbonitride-destined" phases throughout the processing range where exposed to a CO/N_2-plasma environment.

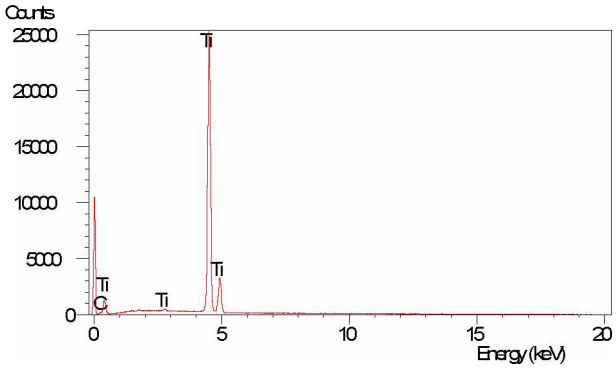

Elmt	Spect. Type	Inten. Corrn.	Std Corrn.	Element %	Sigma %	Atomic %
C K	ED	0.885	1.91	1.29	0.09	4.96
Ti K	ED	1.004	1.00	98.71	0.09	95.04
Total			100.00		100.00	

Figure {7.2.1.3}**13:** EDS spectrum and result of EDS analysis of a spot acquisition from silver-grey coloured phase in ANAT**07** – as shown accompanying "bright" newly reduced metal in of Figure {7.2.1.1}**6**. The phase represents the Ti-phase-band category, transitional between *solid solution* and *metallic compound*. [Also, see the similar but more advanced C-phase from ANAT**07**, shown in full print-out format and presented as Figure {7.2.1.3}**15** in Appendix 7.]

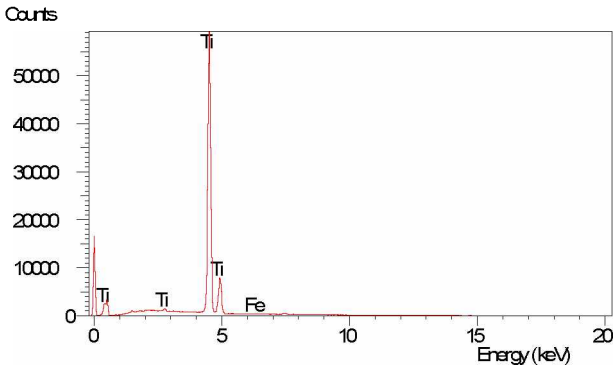

Elmt	Spect. Type	Inten. Corrn.	Std Corrn.	Element %	Sigma %	Atomic %
Ti K	ED	1.005	1.00	99.75	0.07	99.79
Fe K	ED	0.861	1.00	0.25	0.07	0.21
Total				100.00		100.00

Figure {7.2.1.3}**14:** EDS spectrum and result of EDS analysis of a spot acquisition from a region of "newly reduced" Ti-metal such as those counts (manually) recorded and used in the fundamental survey of Table {7.2.1.2}**1**. This spectrum was acquired from bright metal near the core of 18 min specimen ANAT**26** and, despite minor Fe, is noteworthy for the absence of light elements.

Appendix 7

Figure {7.2.1.3}15: Example of the SEM systems format of a full print-out of the EDS spectrum and result of consequent EDS analysis of a spot acquisition from grey metallic phase in ANAT**07** (10 min) from the broad metallised region in Figure {7.2.1.1}**6**. The acquisition was unremarkable other than it represented a modest "Total spectrum counts" of 305,241 (for 100 sec live time at 65 eV under 20 kV accelerating voltage). This count was acceptable, however, although typical acquired counts were in the range: 600,000 to 900,000 – dependent upon machine variables and the overall conductivity of the specimen coating and sampled region. Note also that, in this case, the spectrum ordinate is depicted in total "counts" beneath the spectrum curve rather than counts per second, or "cps", as in spectrum representations of some figures. Also, whilst this print-out was in full format, it was considerably abbreviated by virtue that it represented an analysis of only two machine-acknowledged component elements.

Operator : Jeff J.

Client : JJ

Job : Thesis work

Spectrum 87 (4/12/99 11:19) (ANAT07)

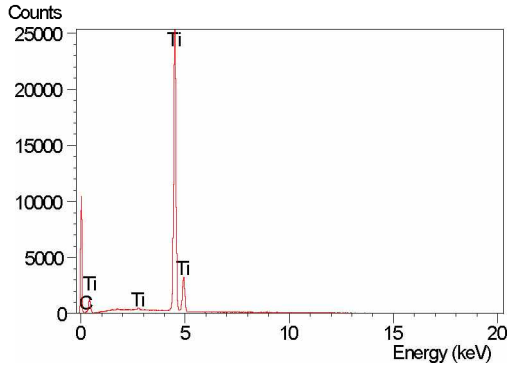

SEMQuant results. Listed at 5:31:39 PM on 15/12/99
Operator: Jeff J.
Client: JJ
Job: Thesis work
Spectrum label: Spectrum 87 (ANAT07)

Calibration data: Energy Resn. Area
Strobe: -7.6 59.54 364223
Calib. element: 6918.7 143.44 97558
Gain factor = 50.006
Livetime = 100.0 seconds

Sample data: Energy Resn. Area
Strobe: -7.6 59.35 361179
Total spectrum counts = 305241
Livetime = 100.0 seconds

Appendix 7

System resolution = 65 eV

Geometry (degrees):
Tilt = 0.00

ED geometry (degrees):
Elevation = 35.00
Azimuth = 0.00
Entry angle = 0.00

Accelerating voltage = 20.00 kV

Quantitative method: ZAF (2 iterations).
Analysed all elements and normalised results.

2 peaks possibly omitted: 1.48, 1.76 keV

Standards :
C K CaCO3 01/12/93
Ti K Titanium a 5/09/97

Elmt	Spect. Type	Fit Index	Apparent Conc.	Stat. Sigma	k Ratio	k Ratio Sigma
C K	ED		2.550	0.136	0.21250	0.01133
Ti K	ED	0.6	102.483	0.338	1.04255	0.00344

Elmt	Spect. Type	Inten. Corrn.	Std Corrn.	Element %	Sigma %	Atomic %
C K	ED	0.886	1.91	2.74	0.14	10.09
Ti K	ED	1.002	1.00	97.26	0.14	89.91
Total			100.00	100.00		

- = <2 Sigma

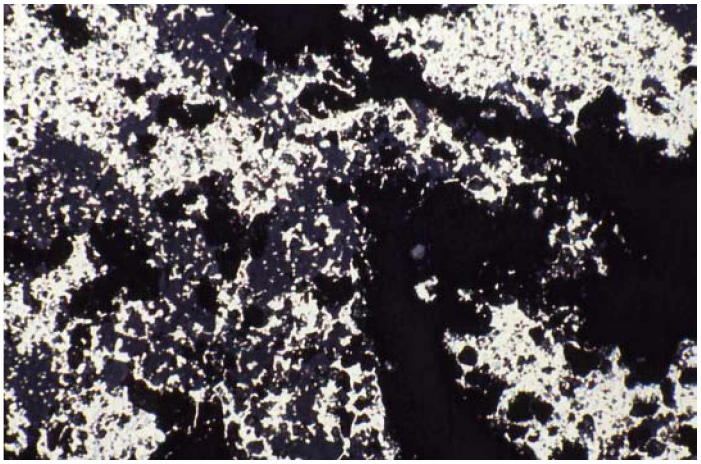

Figure {7.4.3}**11**: Low magnification light optical colour micrograph of heavily sintered Ta/Nb-phase metal retrieved from high in crucible remnants of 16 min processed specimen WODG**09**. The grey and black regions in this field are voidage from fissures and where material of other phases has been removed from the metallic sponge during specimen preparation, the polishing relief (because of Ta/Nb-phase hardness) caused LO focussing difficulty on polished specimens. [LOM (air lens); Ektachrome; fov: 530 μm (0.53 mm)).]

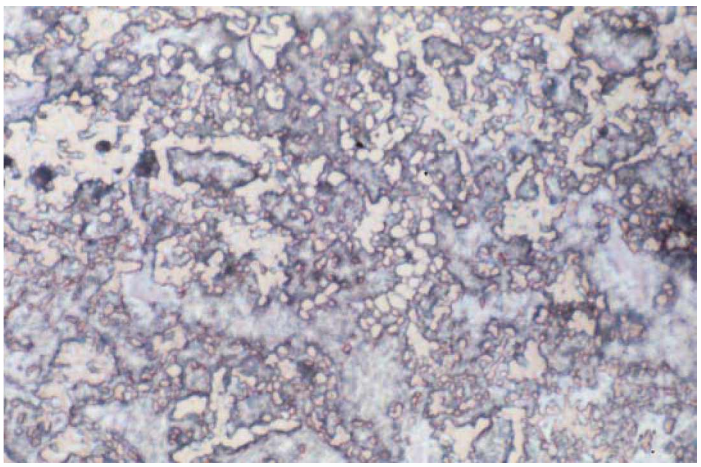

Figure {7.4.3}**12**: LO colour micrograph of a typical Ta/Nb-phase-dense region in a 12 min processed specimen WODG**05**. The field shows silver Sn-phase in the "interstitial voidage" of the cream-pink Ta/Nb-phase metal (some smearing (during polishing) of ductile Sn is evident). [LOM (air lens); Ektachrome; fov: 208 μm (0.21 mm)).]

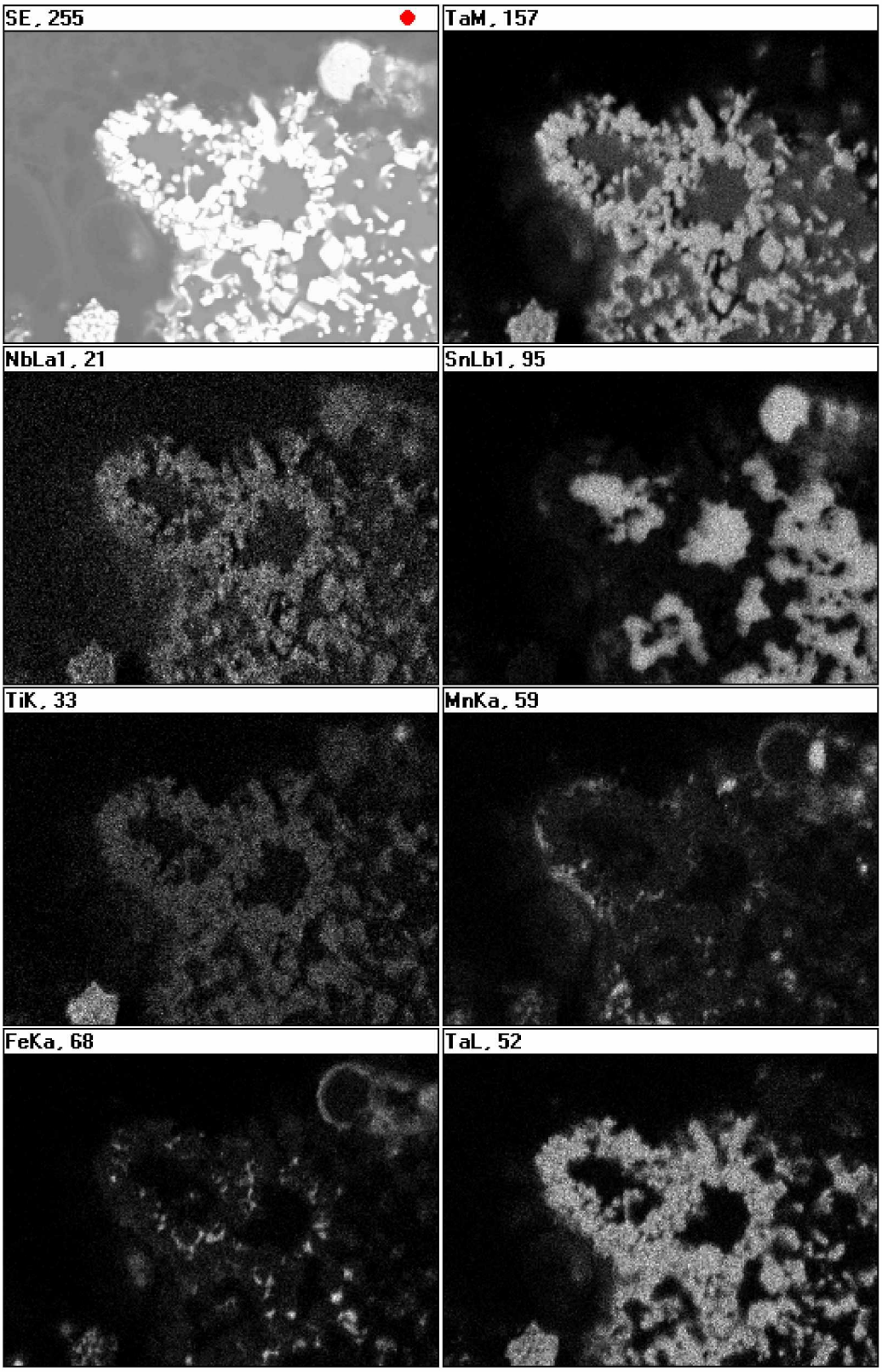

Figure {7.4.3}**13**: Map set showing detail of typical reduction remnant facies in a carbothermic wodginite reduction product (10 min WODG**04**). Because of a detector window problem, (except for late aluminothermic maps) no light element acquisition was available to map-acquisition exercises on wodginite specimens. However, elements mapped are metals of central relevance in any analyses of wodginite reduction products. [fov: ~ 100 μm]

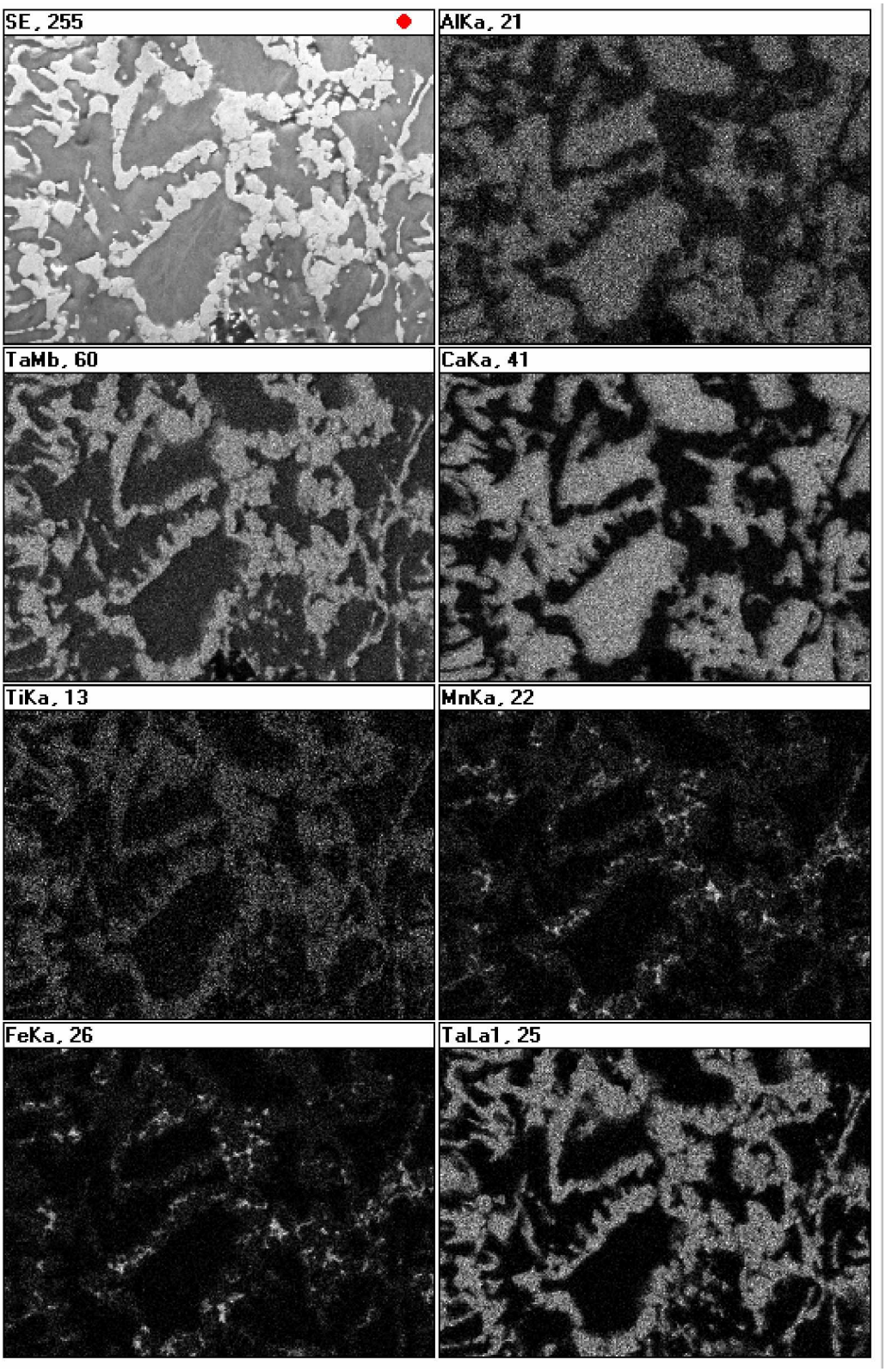

Figure {7.4.4}**22**: EDS map set of a region of intense processing in specimen WODG**A5** showing the advanced development of Ta/(Nb)/Ti-phase features engulfed by aluminothermic Al/Ca-slag. The minor infill features of Mn/Fe are likely (Sn)/Mn/Fe-phase (Mn-hardhead) which has persisted whilst less-alloyed Sn-phase has drained away to lower regions. The field is shown also in the backscattered micrograph of following Figure {7.4.4}**23**.

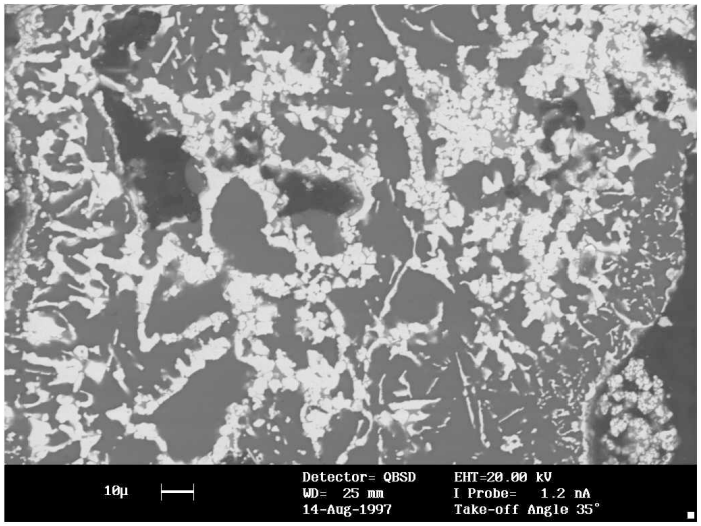

Figure {7.4.4}**23**: Electron micrograph showing the general region of the mapped field presented in the previous figure. Some minor areas of Sn/Mn/Fe-phases (lightest grey) can be delineated "internally" with the agglomerated Ta/Nb/Ti-phase features (brightest phase), whilst Al/Ca-slag (mid grey, extensive) encloses these. The darkest grey-to-black regions are external to the remnant or are voids in-filled by mounting medium. The region indicates that it has a history of high (relative) thermal intensity and the lack of Sn-phases implies that this remnant was recovered from high in the crucible contents.

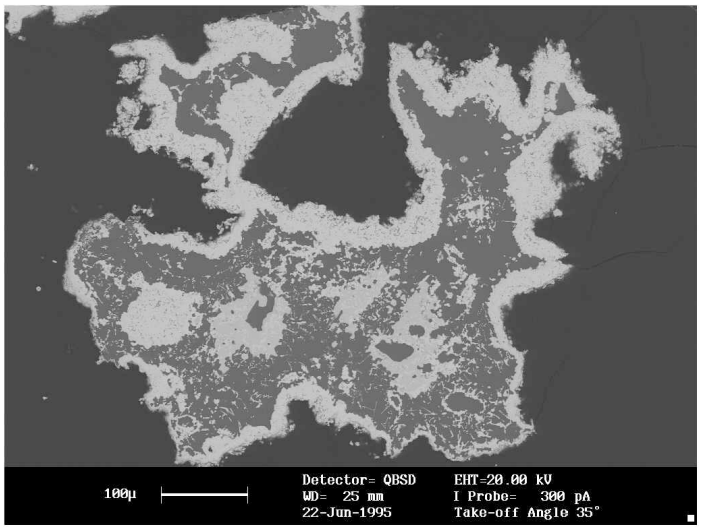

Figure{7.4.4}**24**: Electron micrograph showing the span of a typical extensively-reduced remnant from specimen WODG**A5**. Whilst the solid-state reduced Ta/Nb-phase material tends to remain rigid, resisting the volume shrinkage that accompanies the chemical and physical processes of reduction. In this case the skeletal shell has retained the associated liquid phase(s), most of the mid-grey regions seen here are slag phase.

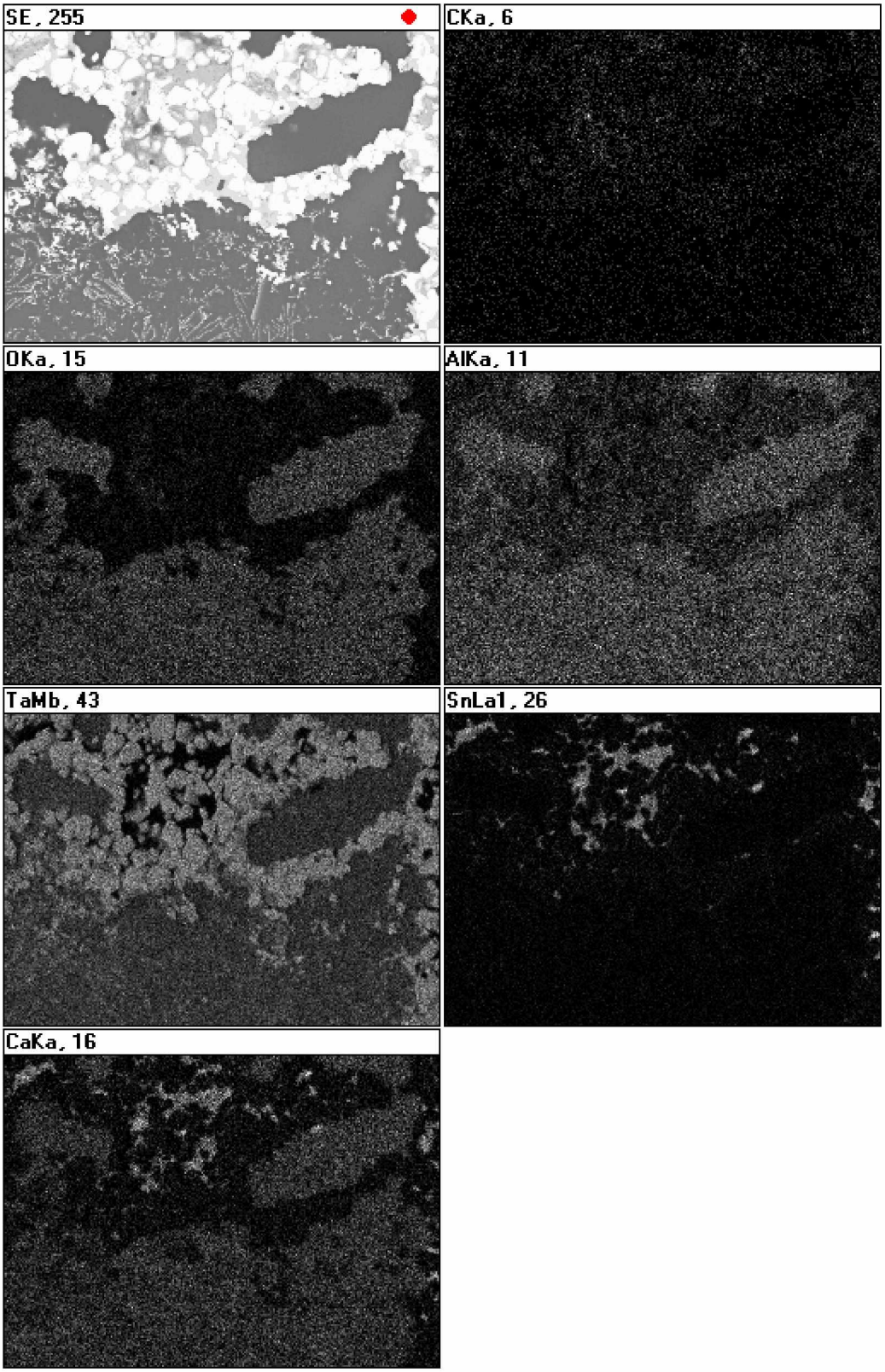

Figure {7.4.4}**25**: EDS map set utilising thin window detection (which allowed light elements to be acquired – although counts were weak because of the combination of window plus field (area) acquisition). This field shows the smattering count of C to be associated with the metallised regions whilst the O composition is weighed heavily with the slag regions (delineated by counts in the Al and Ca maps). Small as they are for usual count acquisitions, the numbers accompanying each image represent "counts per second".

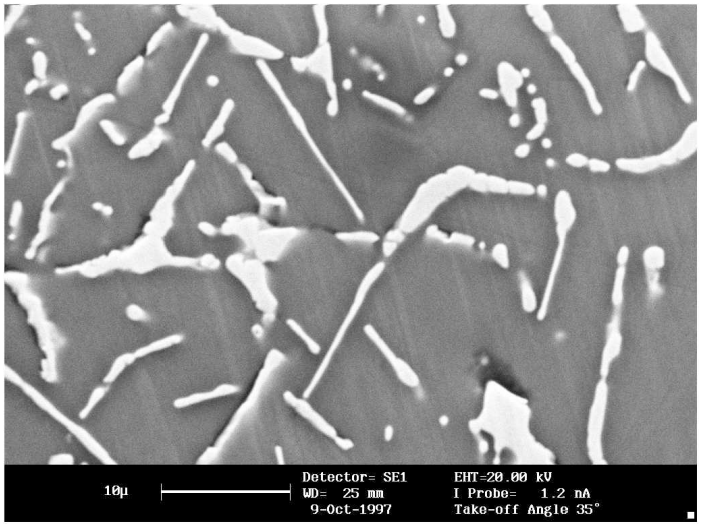

Figure {7.4.4}**26**: SE micrograph of Ta/(Nb)/Ti-phase plate particles in aluminothermic Al/Ca-slag from 8 min specimen WODG**A3**, the field presented in EDS map set in Figure {7.4.4}**27** below.

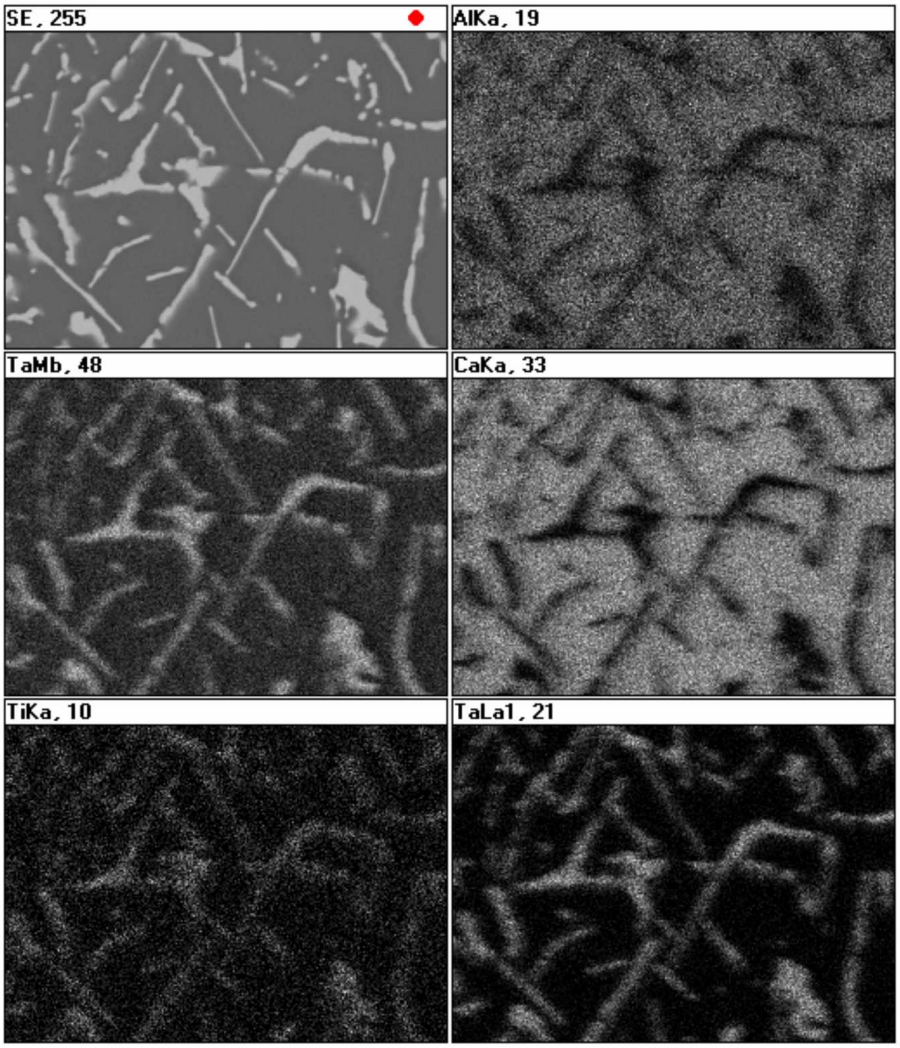

Figure {7.4.4}**27**: Map set corroborating the identities of metallic Ta/(Nb)/Ti-phase plates and Ca/Al-slag shown in the above Figure {7.4.4}**26**. [Light element detection was unavailable.]

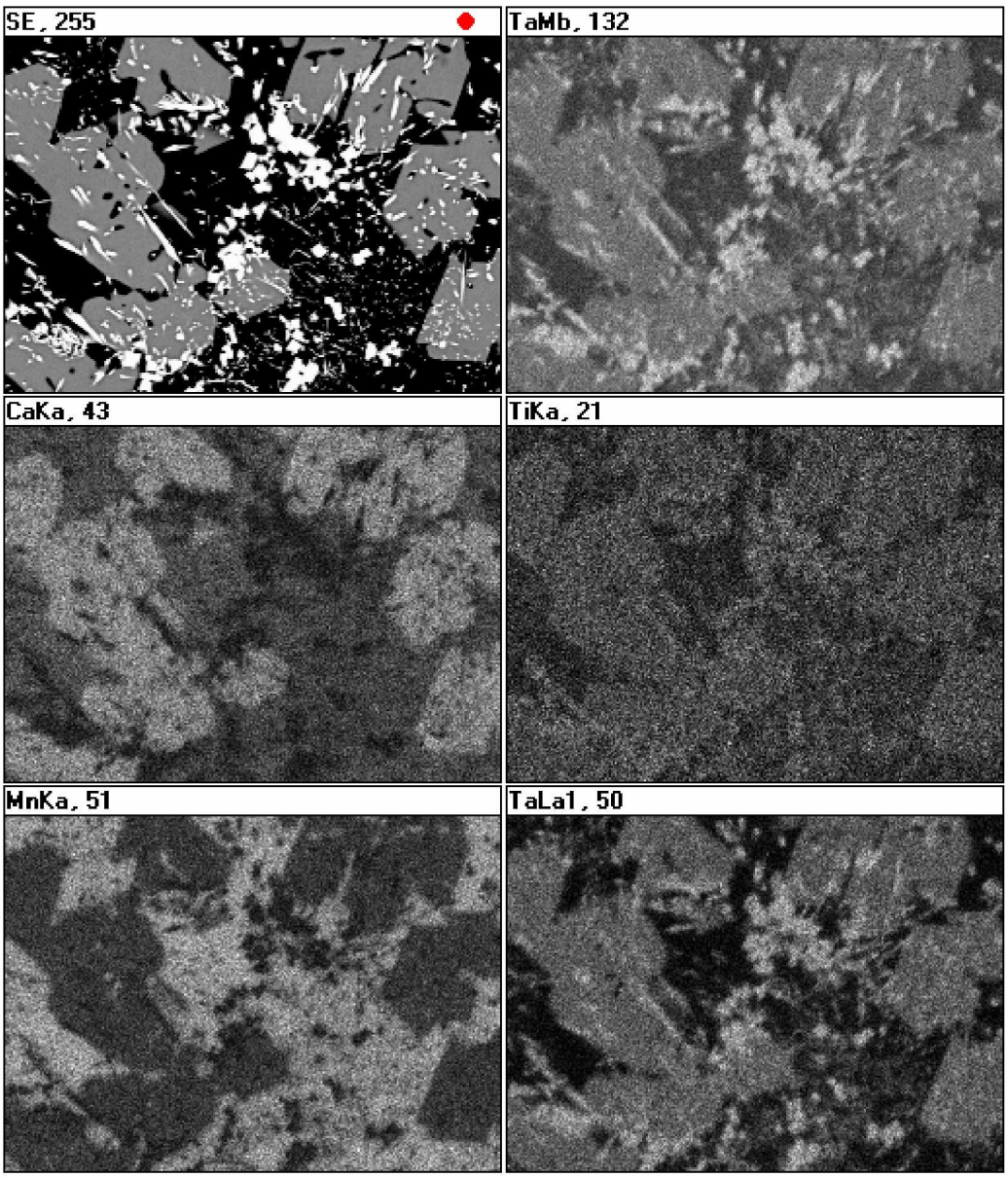

Figure {7.4.4}**28**: The inclusion of this inelegant, rather "streaky" map set is justified because it identifies the compositional development of phases and their distributional relationship in a slag region of a reduction remnant in 8 min WODG**A2** at a stage of processing representing incomplete reduction, the mapped field is representative of the facies and phases present in the micrographic fields of Figures {7.4.4}**14** to {7.4.4}**17**. With reference to the SE image, the scattering of brightest metallic phase represents Ta/(Nb)/Ti-phase plates; the angular crystals of mid brightness are the Ta/(Nb)/Ti/Ca-oxide phase, solidified from the melt; so leaving the dark slag phase of (Al)/Ca/Mn/(Fe)-oxide. Note that the "oxide" standing of phases was separately confirmed by spot EDS acquisitions; the Ca-map indicates that proportionally more Ca exists in the composition of the refractory metals oxide crystals than in that of the slag phase; and that Sn-phase plus associated Ta/Nb-phase particulate/agglomerate (presumably) exists outside the field of this map set

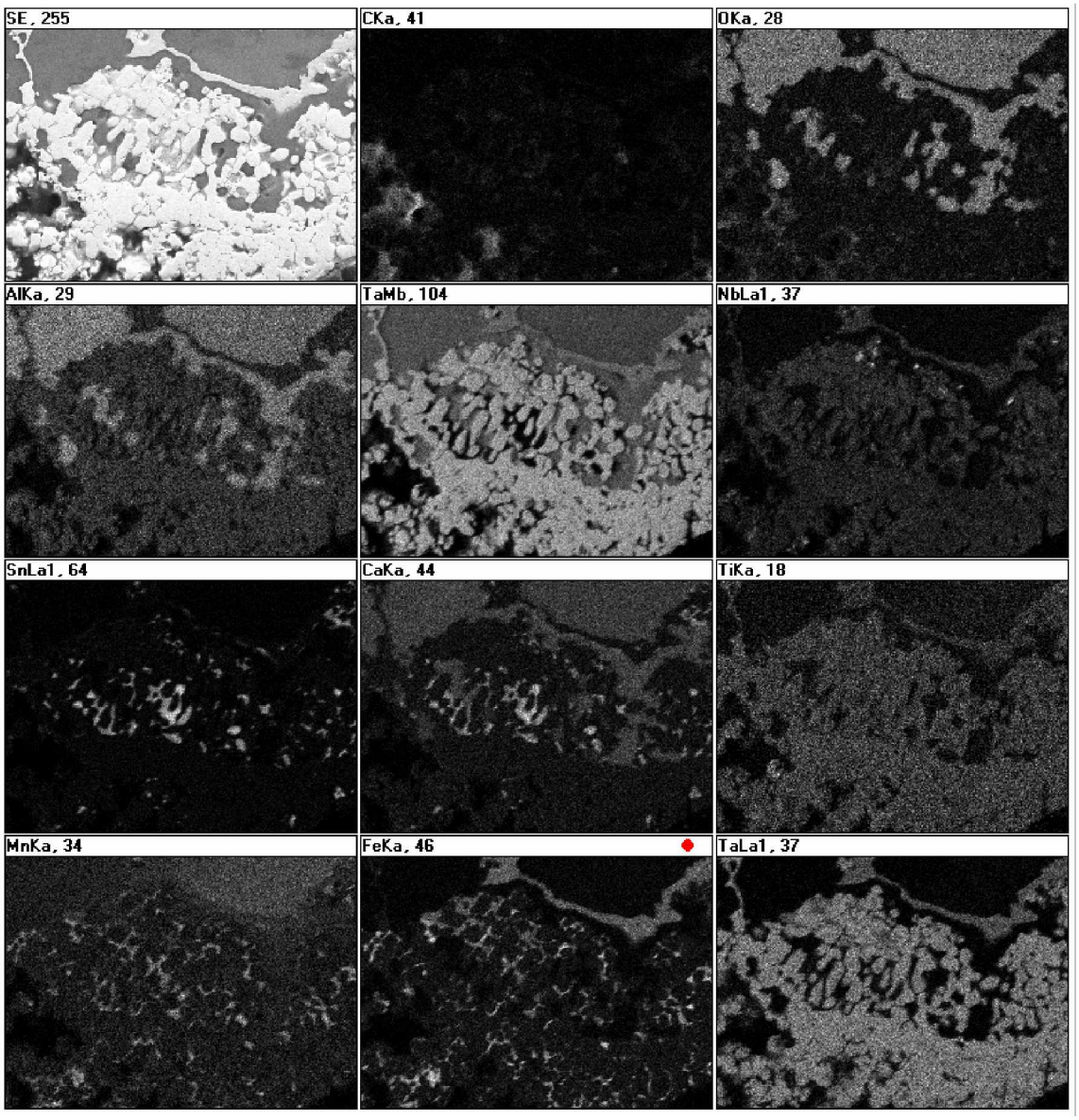

Figure {7.4.4}**29**: EDS map set showing a field in 10 min specimen WODG**A5** and noting the presence here of light element area acquisitions for C and O. The micrographic field is also presented as a backscattered image in following Figure {7.4.4}**30**. The field captures detail of phases just behind outer, plasma exposed Ta/Nb-phase "rim material" showing a degree of sinter agglomeration between the particulate entities. Some variable Sn/Mn/Fe-phase remains trapped in interstices of the particulate structure – including a minor Sn/Ca-phase that is likely to be an oxidic remnant. The limited visible region of Al/Ca-oxide slag phase is free of Ta/Nb-plates (in this field of view), however, a singularly rare Ta/Nb/Fe-metallic phase is represented in the feature surrounded by slag but adjacent to the particulate phase. Of note is the apparent absence of C in reduction product phases, including the slag and hardhead phases, the few regions registering C-content are most likely remnant char pieces caught in the solidified mass. The O-content also seems restricted to the slag phase. Ostensibly, having light element availability for area acquisition here, this EDS map set is significant EDS evidence as it delivers *confirmation of reduction* and *extent and degree of reduction* over phase bodies which otherwise could only be left to conjecture with regard to their metallic appearance, lustre, reflectance intensity, shape and habit, or other property.

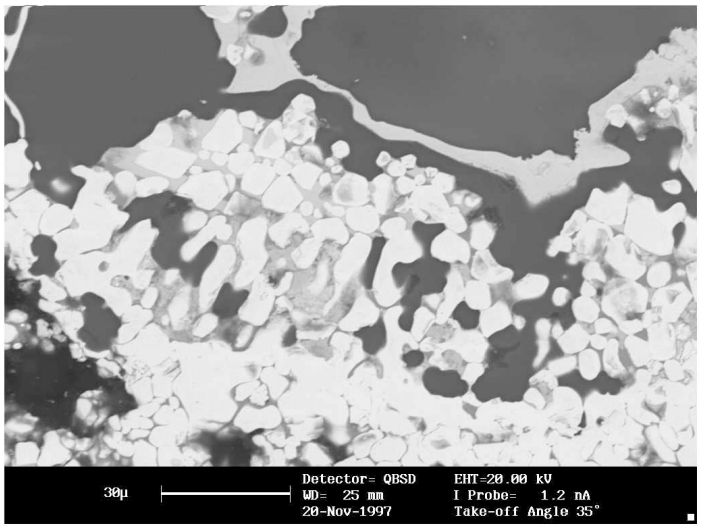

Figure {7.4.4}**30**: Electron micrograph showing the backscattered electron image as presented as an EDS map set in preceding Figure {7.4.4}**29**.

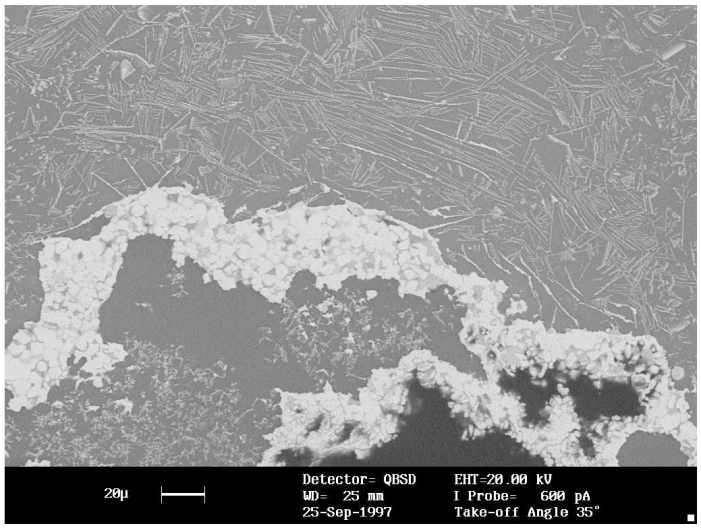

Figure {7.4.4}**31**: Electron micrograph of a field in 10 min specimen WODG**A4** showing extensive distribution of faceted Ta/Nb-phase plates in slag surrounding characteristic Ta/Nb-phase particulate agglomerate in Sn-based phases. Detail in the field is the subject of the EDS map set of following Figure {7.4.4}**32**, Darkest regions (bottom field) are voids infilled with mounting medium.

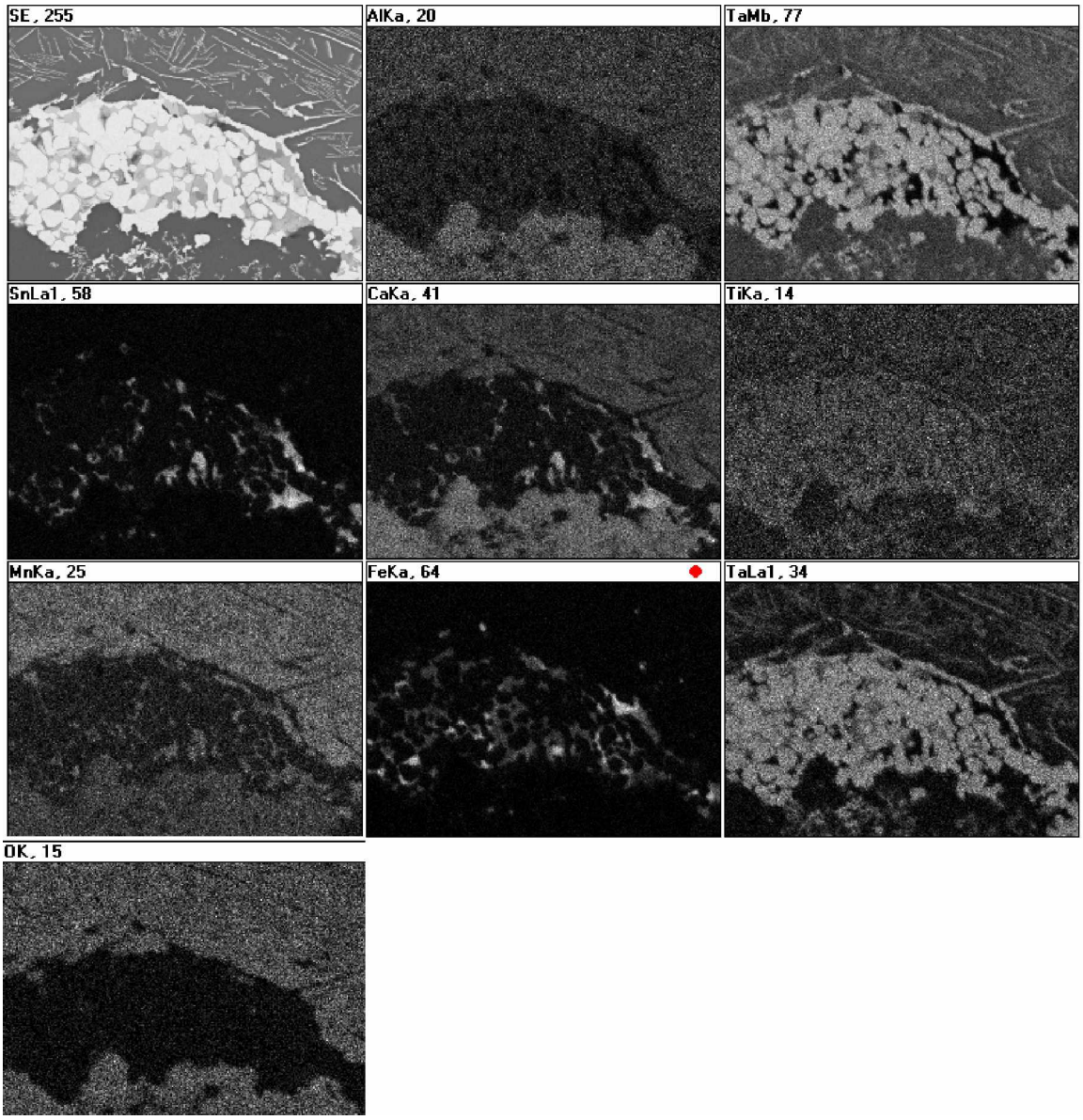

Figure {7.4.4}**32**: EDS map set (including O-acquisition) of the field presented in Figure {7.4.4}**31** of a rim region in specimen WODG**A4**. Most notable is the evident Ta/Nb-phase reciprocity between particulate and plate forms, this mutual phase tolerance – perhaps complete compositional tolerance – between the phase-forms is exhibited around the interface zone of the metallised particulate/hardhead region where mobile slag-borne faceted plate-features have rotated into alignment with the amassed particulate region. The aluminothermic slag region contains Ta/Nb-plates that were precipitated prior to quenching (thus allowing mobility and morphological evolution during ongoing processing), whilst the Sn-phase remnant cementing the Ta/Nb-particles is quite "lean", possibly by drainage to lower regions.

APPENDIX D

University of Wollongong

Good Universities Guides
AUSTRALIA'S UNIVERSITY OF THE YEAR
Preparing Graduates for the e-World — Joint Winner 2000-2001
Outstanding R&D Partnerships — Joint Winner 1999-2000

9 May, 2001

Tesla Technologies Pty Ltd
"Fern Court"
Dale Street
BURRAWANG NSW 2577

Dear Jeff,

RE: MICROWAVE EXTRACTION OF METALS FROM SLAG
R&D START GRANT: GRA02013

Further to your discussions with myself and Mr Aapo Skorulis of our Office of Research, I've had an opportunity to read the documentation which was provided including the copy of the application for the AusIndustry R&D Start grant.

I can confirm that the University of Wollongong will not make a claim on any technology developed under the proposed project, *Microwave Extraction of Metals from Slag* as detailed in the application for the R&D Start Grant GRA02013. Should there be an infringement of any University of Wollongong background intellectual property rights relating specifically to the research proposed in this project, the University of Wollongong will waive its rights with respect to this intellectual property.

I would like to take this opportunity to wish you every success with this project and should you feel that the University of Wollongong could be of any assistance, please do not hesitate to contact me.

Yours sincerely,

P M Robinson
Deputy Vice-Chancellor

Deputy Vice-Chancellor University of Wollongong NSW 2522 Australia
Telephone: (61 2) 4221 3940 **Facsimile:** (61 2) 4227 1771
peter_robinson@uow.edu.au www.uow.edu.au

Australia's University of the Year 50 celebrating 50 years

Letter from the University of Wollongong releasing any claim to intellectual property contained in the Tesla Group Holdings Pty. Limited patent from that contained in the intellectual property of this thesis.

Appendix D

The following pages **D**-*iii* to **D**-*vii* present facing page details of the patent "Plasma Reduction Processing of Materials" – sole listed inventor Jeffrey Tanner-Jones – as it remains current in five jurisdictions. The patent owner was Tesla Group Holdings Pty. Limited but is presently Plasma Technologies Pty. Limited, Victoria.

D-*iii*: Australian patent **AU 2002220358 B2**.

D-*iv*: United States of America patent **US 2004/0060387 A1**.

D-*v*: German patent **DE 601 31 365 T2 2008.10.23**.

D-*vi*: European patent **EP 1 348 038 B1**.

D-*vii*: World patent **WO 02/46482 A1**.

(11) Application No. **AU 2002220358 B2**

(19) AUSTRALIAN PATENT OFFICE

(54) Title
Plasma reduction processing of materials

(51)* International Patent Classification(s)
C22B 1/00 (2006.01) C22B 5/02
C22B 5/02 (2006.01) 2006010IAFI20051
C22B 1/00 2006010IAL120051
2006010IAF120051 C22B 5/02 (2006.01) WO2002046482 PCT/AU01/01569

(21) Application No: 2002220358 (22) Application Date: 2001.12.04

(87) WIPO No: WO02/46482

(30) Priority Data

(31) Number (32) Date (33) Country
PR1962 2000.12.04 AU

(43) Publication Date: 2002.06.18
(43) Publication Journal Date: 2002.08.22

(71) Applicant(s)
Plasma Technologies Pty Ltd

(72) Inventor(s)
Tanner Jones, Jeffrey

(74) Agent/Attorney
Spruson & Ferguson, Level 35 St Martins Tower 31 Market Street, Sydney, NSW, 2000

(56) Related Art
WO 99/04379
US 6409051
JP 55-149642
US 4753675
BILLARD D.E., LYNCH D.C. AND DAVENPORT, W.G. : "Non Equilibrium Plasma Processing of Ores" In Thermal Plasma Applications in Materials and Metallurgical Processing" 1992, TMS, WARRENDALE, PA, XP000954927
* page: 175 page: 191 *
US 43 11520
US 6277168

US 20040060387A1

(19) **United States**

(12) **Patent Application Publication** (10) **Pub. No.: US 2004/0060387 A1**

Tanner-Jones (43) **Pub. Date: Apr. 1, 2004**

(54) **PLASMA REDUCTION PROCESSING OF MATERIALS**

(76) Inventor: **Jeffrey Tanner-Jones**, Gwynneville (AU)

Correspondence Address:
Clifford W Browning
Bank One Center Tower
111 Monument Circle Suite 3700
Indianapolis, IN 46204-5137 (US)

(21) Appl. No.: **10/433,356**

(22) PCT Filed: **Dec. 4, 2001**

(86) PCT No.: **PCT/AU01/01569**

(30) **Foreign Application Priority Data**

Dec. 4, 2000 (AU) PR1862

Publication Classification

(51) **Int. Cl.**[7] **C22B 4/00**

(52) **U.S. Cl.** **75/10.2**

(57) **ABSTRACT**

In a process for the reduction of a metalliferous ore or concentrate the ore or concentrate is first prepared into a particulate form. A reaction chamber (**3, 103, 203, 301, 401, 503, 603, 702**) is then charged with ore or concentrate, a reductant and an input gas. The reaction chamber (**3, 103, 203, 301, 401, 503, 603, 702**) is irradiated with electromagnetic radiation within a frequency range of **30** MHz to **300** GHz until a non-equilibrium plasma is initiated. The plasma is sustained and controlled with the radiation until the ore or concentrate is reduced to form reduction product.

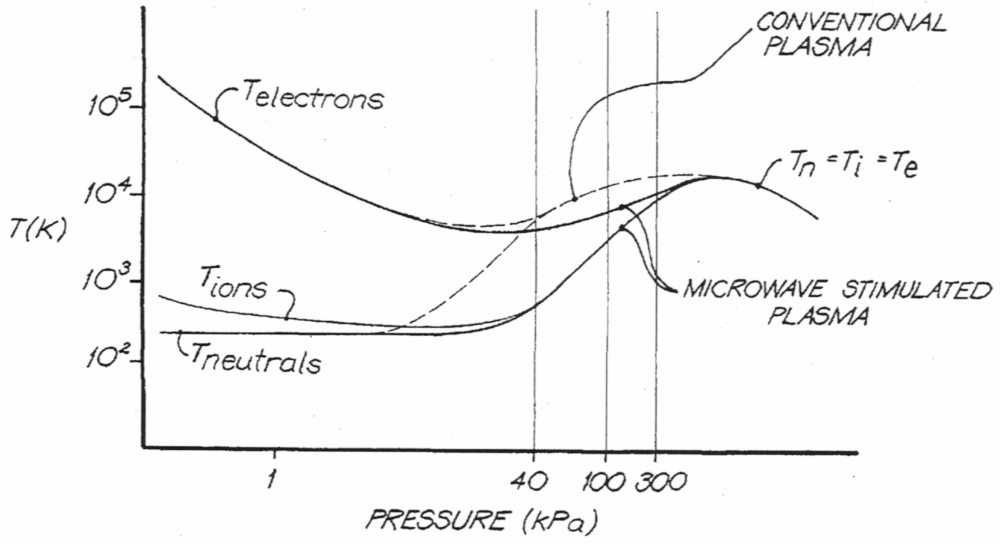

(19) Bundesrepublik Deutschland
Deutsches Patent- und Markenamt

(10) DE 601 31 565 T2 2008.10.23

(12) # Übersetzung der europäischen Patentschrift

(97) EP 1 348 038 B1
(21) Deutsches Aktenzeichen: 601 31 565.0
(86) PCT-Aktenzeichen: PCT/AU01/01569
(96) Europäisches Aktenzeichen: 01 999 678.4
(87) PCT-Veröffentlichungs-Nr.: WO 2002/046482
(86) PCT-Anmeldetag: 04.12.2001
(87) Veröffentlichungstag der PCT-Anmeldung: 13.06.2002
(97) Erstveröffentlichung durch das EPA: 01.10.2003
(97) Veröffentlichungstag der Patenterteilung beim EPA: 21.11.2007
(47) Veröffentlichungstag im Patentblatt: 23.10.2008

(51) Int Cl.[8]: *C22B 5/00* (2006.01)
C22B 4/00 (2006.01)
C22B 5/02 (2006.01)

(30) Unionspriorität:
PR136200 04.12.2000 AU

(84) Benannte Vertragsstaaten:
AT, BE, CH, CY, DE, DK, ES, FI, FR, GB, GR, IE, IT, LI, LU, MC, NL, PT, SE, TR

(73) Patentinhaber:
Plasma Technologies Pty Ltd., Newport, AU

(74) Vertreter:
derzeit kein Vertreter bestellt

(72) Erfinder:
TANNER-JONES, Jeffrey, Gwynneville, NSW 2500, AU

(54) Bezeichnung: **PLASMAREDUKTIONSVERARBEITUNG VON MATERIALIEN**

(19) Europäisches Patentamt
European Patent Office
Office européen des brevets

(11) EP 1 348 038 B1

(12) **EUROPEAN PATENT SPECIFICATION**

(45) Date of publication and mention of the grant of the patent:
21.11.2007 Bulletin 2007/47

(21) Application number: **01999678.4**

(22) Date of filing: **04.12.2001**

(51) Int Cl.:
C22B 5/00 *(2006.01)* ***C22B 4/00*** *(2006.01)*
C22B 5/02 *(2006.01)*

(86) International application number:
PCT/AU2001/001569

(87) International publication number:
WO 2002/046482 (13.06.2002 Gazette 2002/24)

(54) **PLASMA REDUCTION PROCESSING OF MATERIALS**

PLASMAREDUKTIONSVERARBEITUNG VON MATERIALIEN

REDUCTION PLASMATIQUE DE MATERIAUX

(84) Designated Contracting States:
AT BE CH CY DE DK ES FI FR GB GR IE IT LI LU MC NL PT SE TR
Designated Extension States:
SI

(30) Priority: **04.12.2000 AU PR186200**

(43) Date of publication of application:
01.10.2003 Bulletin 2003/40

(73) Proprietor: **Plasma Technologies Pty Limited**
Newport VIC 3015 (AU)

(72) Inventor: **TANNER-JONES, Jeffrey**
Gwynneville, NSW 2500 (AU)

(74) Representative: **Bates, Philip Ian**
Reddie & Grose
16 Theobalds Road
London WC1X 8PL (GB)

(56) References cited:
WO-A-89/04379
US-A- 4 311 520
US-A- 4 361 441
US-A- 4 501 717
US-A- 5 282 880
US-B- 6 277 168

- **BULLARD D.E., LYNCH D.C. AND DAVENPORT W.G.: ""Non-Equilibrium Plasma Processing of Ores" in Thermal Plasma Applications in Materials and Metallurgical Processing" 1992, TMS , WARRENDALE, PA , XP009053927 * page 175 - page 191 ***
- **WAN J K S ET AL: "HIGH-POWER PULSED RF DECOMPOSITION OF ORE SAMPLES WITH A CARBON SOURCE" JOURNAL OF MICROWAVE POWER AND ELECTROMAGNETIC ENERGY, THE INSTITUTE, VIENNA, VA, US, vol. 31, no. 1, 1996, pages 54-58, XP009007396 ISSN: 0832-7823**
- **YOUNG R M ET AL: "Generation and behavior of fine particles in thermal plasmas-a review" PLASMA CHEMISTRY AND PLASMA PROCESSING, PLENUM PRESS. NEW YORK, US, vol. 5, no. 1, March 1985 (1985-03), pages 1-37, XP002123724 ISSN: 0272-4324**
- **PATENT ABSTRACTS OF JAPAN & JP 55 149 642 A (RIKAGAKU KENKYUSHO) 21 November 1980**

EP 1 348 038 B1

Printed by Jouve, 75001 PARIS (FR)

(12) INTERNATIONAL APPLICATION PUBLISHED UNDER THE PATENT COOPERATION TREATY (PCT)

(19) World Intellectual Property Organization
International Bureau

(43) International Publication Date
13 June 2002 (13.06.2002)

PCT

(10) International Publication Number
WO 02/46482 A1

(51) International Patent Classification[7]: C22B 5/00

(21) International Application Number: PCT/AU01/01569

(22) International Filing Date: 4 December 2001 (04.12.2001)

(25) Filing Language: English

(26) Publication Language: English

(30) Priority Data:
PR 1862 4 December 2000 (04.12.2000) AU

(71) Applicant *(for all designated States except US)*: **TESLA GROUP HOLDINGS PTY LIMITED** [AU/AU]; "Fern Court", Dale Street, Burrawang, NSW 2577 (AU).

(72) Inventor; and

(75) Inventor/Applicant *(for US only)*: **TANNER-JONES, Jeffrey** [AU/AU]; 3/9 Eastern Street, Gwynneville, NSW 2500 (AU).

(74) Agent: **SPRUSON & FERGUSON**; GPO Box 3898, Sydney, NSW 2001 (AU).

(81) Designated States *(national)*: AE, AG, AL, AM, AT, AU, AZ, BA, BB, BG, BR, BY, BZ, CA, CH, CN, CO, CR, CU, CZ, DE, DK, DM, DZ, EC, EE, ES, FI, GB, GD, GE, GH, GM, HR, HU, ID, IL, IN, IS, JP, KE, KG, KP, KR, KZ, LC, LK, LR, LS, LT, LU, LV, MA, MD, MG, MK, MN, MW, MX, MZ, NO, NZ, OM, PH, PL, PT, RO, RU, SD, SE, SG, SI, SK, SL, TJ, TM, TR, TT, TZ, UA, UG, US, UZ, VN, YU, ZA, ZM, ZW.

(84) Designated States *(regional)*: ARIPO patent (GH, GM, KE, LS, MW, MZ, SD, SL, SZ, TZ, UG, ZM, ZW), Eurasian patent (AM, AZ, BY, KG, KZ, MD, RU, TJ, TM), European patent (AT, BE, CH, CY, DE, DK, ES, FI, FR, GB, GR, IE, IT, LU, MC, NL, PT, SE, TR), OAPI patent

[Continued on next page]

(54) Title: PLASMA REDUCTION PROCESSING OF MATERIALS

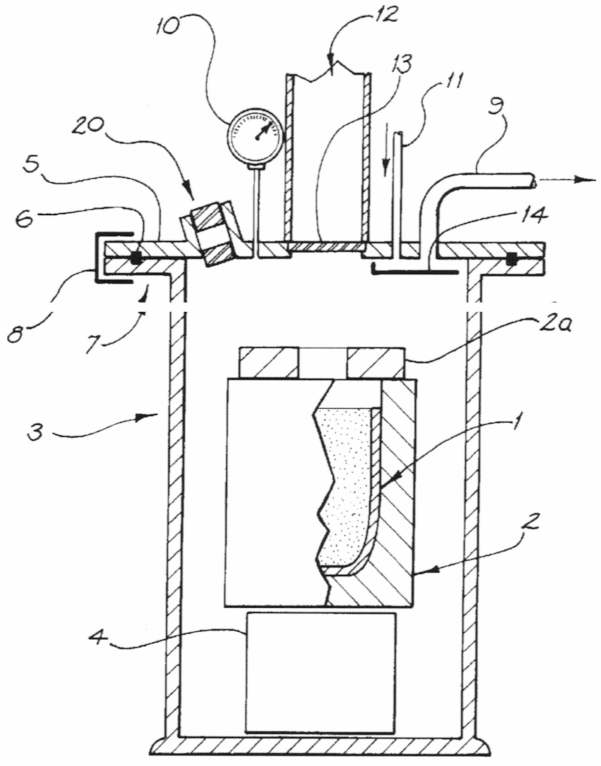

(57) Abstract: In a process for the reduction of a metalliferous ore or concentrate the ore or concentrate is first prepared into a particulate form. A reaction chamber (3, 103, 203, 301, 401, 503, 603, 702) is then charged with ore or concentrate, a reductant and an input gas. The reaction chamber (3, 103, 203, 301, 401, 503, 603, 702) is irradiated with electromagnetic radiation within a frequency range of 30 MHz to 300 GHz until a non-equilibrium plasma is initiated. The plasma is sustained and controlled with the radiation until the ore or concentrate is reduced to form reduction product.

WO 02/46482 A1